The compatible solutes ectoine and 5-hydroxyectoine: Catabolism and regulatory mechanisms

Dissertation

- kumulativ -

Zur Erlangung des Grades eines
Doktor der Naturwissenschaften
(Dr. rer. nat.)

des Fachbereichs Biologie der
Philipps-Universität Marburg

Vorgelegt von

Lucas Hermann

aus Dierdorf

Marburg (Lahn), 2022

Die Arbeit zur vorliegenden Dissertation wurde von Oktober 2017 bis Februar 2022 unter der Betreuung von Herrn Prof. Dr. Erhard Bremer an der Philipps-Universität Marburg in der Arbeitsgruppe Molekulare Mikrobiologie angefertigt.

Vom Fachbereich Biologie der Philipps-Universität Marburg (Hochschulkennziffer 1180) als Dissertation angenommen am 17.03.2022

Erstgutachter: Prof. Dr. Erhard Bremer
Zweitgutachter: Prof. Dr. Tobias Erb

Tag der Disputation: 09.06.2022

Declaration of authorship

I hereby declare that this dissertation "The compatible solutes ectoine and 5-hydroxyectoine: Catabolism and regulatory mechanisms" is entirely of my own and to the best of my knowledge has not been submitted for a dissertation at this or any other educational institution. Quotes and paraphrased material are clearly acknowledged, and all sources are referenced.

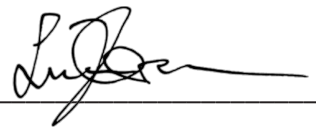

Lucas Hermann, Marburg, March 2022

Erklärung

Hiermit versichere ich, dass ich meine Dissertation mit dem Titel: "The compatible solutes ectoine and 5-hydroxyectoine: Catabolism and regulatory mechanisms" selbstständig ohne unerlaubte Hilfe angefertigt und mich dabei keiner anderen als der von mir ausdrücklich bezeichneten Quellen und Hilfsmittel bedient habe.

Diese Dissertation wurde weder in der jetzigen noch einer ähnlichen Form bei einer Hochschule eingereicht.

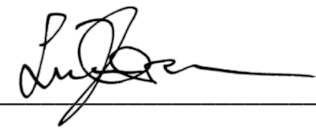

Lucas Hermann, Marburg, März 2022

The world is changing. I feel it in the water. I feel it in the earth. I smell it in the air. Much that once was is lost, for none now live who remember it.

J. R. R. Tolkien, The Lord of the Rings

1 List of publications

In association with my thesis, the following original publications, review articles, or manuscripts have been put together. Asterisks (*) indicate co-first authorship.

Original paper with peer-review process (published)

1) Schulz, A., Hermann, L., Freibert, S. A., Bönig, T., Hoffmann, T., Riclea, R., Dickschat, J. S., Heider, J. & Bremer, E. (2017). Transcriptional regulation of ectoine catabolism in response to multiple metabolic and environmental cues. *Environ Microbiol*, 19(11), 4599-4619.

2) Mais, C. N.*, Hermann, L.*, Altegoer, F., Seubert, A., Richter, A. A., Wernersbach, I., Czech, L., Bremer, E. & Bange, G. (2020). Degradation of the microbial stress protectants and chemical chaperones ectoine and hydroxyectoine by a bacterial hydrolase-deacetylase complex. *J Biol Chem,* 295(27), 9087-9104.

3) Hermann, L., Dempwolff, F., Steinchen, W., Freibert, S. A., Smits, S., Seubert, A., Bremer, E. (2021) The GabR/MocR ectoine catabolism regulator EnuR: Inducer and DNA binding. *Front Microbiol,* 12:764731.

Publication with minor contribution

1) von Borzyskowski, L. S., Severi, F., Krüger, K., Hermann, L., Gilardet, A., Sippel, F., Pommerenke, B., Claus, P., Cortina, N. S., Glatter, T., Zauner, S., Zarzycki, J., Fuchs, B., M., Bremer, E., Maier, U. G., Amann, R. I. & Erb, T. J. (2019). Marine *Proteobacteria* metabolize glycolate via the β-hydroxyaspartate cycle. *Nature*, 575(7783), 500-504.

Unpublished manuscript

1) Hermann, L. (2022) Ectoine metabolism: A diverse field with differing modes.

Review articles with peer-review process

1) Czech, L., Hermann, L., Stöveken, N., Richter, A. A., Höppner, A., Smits, S. H., Heider, J. & Bremer, E. (2018). Role of the extremolytes ectoine and hydroxyectoine as stress protectants and nutrients: genetics, phylogenomics, biochemistry, and structural analysis. *Genes*, 9(4), 177.

2) Hermann, L.*, Mais, C. N.*, Czech, L.*, Smits, S. H., Bange, G., & Bremer, E. (2020). The ups and downs of ectoine: structural enzymology of a major microbial stress protectant and versatile nutrient. *Biol Chem*, 401(12), 1443-1468.

2 Zusammenfassung

Um osmotischem Stress zu begegnen, nutzen viele Mikroorganismen die Anhäufung von niedermolekularen, osmotisch aktiven, organischen Verbindungen, die so genannten kompatiblen Solute. Beispiele für besonders effektive Vertreter dieser Stoffklasse sind die Tetrahydropyrimidine Ectoin und sein Derivat 5-Hydroxyectoin. Diese beiden Moleküle werden von vielen Mikroorganismen nicht nur gegen osmotischen Stress, sondern beispielsweise auch gegen thermischen Stress verwendet. Der Biosyntheseweg, um beide Stoffe zu synthetisieren, ist bereits weitgehend erforscht und die verwendeten Enzyme sind sowohl strukturell als auch biochemisch gut charakterisiert. Jedoch ist mit der reinen Synthese die Geschichte der Ectoine bei weitem noch nicht ausgezählt. Unausweichlich werden sie regelmäßig in die Umgebung abgegeben. Nicht nur können sie von dort wieder durch Aufnahme einer cytoprotektiven Rolle zugeführt werden, auch kann eine beachtlich große Gruppe von Bakterien diese stickstoffhaltigen Verbindungen recyceln. Insbesondere in besonders kompetitiven Habitaten wie den oberen Schichten der Weltmeere haben sich einige Bakterien auf eine solche Nische spezialisiert. Der Modellorganismus, der in dieser Arbeit verwendet wird, ist einer dieser Vertreter. Das marine Bakterium *Ruegeria pomeroyi* DSS-3 gehört zur Gruppe der *Roseobacter*, heterotroph lebende Proteobakterien, die sowohl in Symbiose mit Phytoplankton leben können als auch diesen den „Krieg“ erklären können, um an wertvolle Nährstoffe zu gelangen.

Ectoine können von *Ruegeria pomeroyi* DSS-3 durch ein hoch-affines Transportsystem aufgenommen werden und dienen dann sowohl als Energie- wie auch als Stickstoff- und Kohlenstoffquelle. Hierzu werden beide Ectoine von der Hydrolase EutD gespalten und anschließend von der Deacetylase EutE deacetyliert. Die so entstandenen DABA und Hydroxy-DABA können dann nach einigen weiteren Schritten dem zentralen Stoffwechsel zugeführt werden. Die Rolle und Funktionsweise der zusammenarbeitenden EutD- und EutE-Enzyme ist ein zentraler Aspekt der vorliegenden Arbeit. Beide Enzyme wurden biochemisch und strukturell charakterisiert und der Aufbau des Stoffwechselweges konnte teilweise aufgeklärt werden. Die zuerst entstehenden Moleküle α-ADABA (aus Ectoin) und Hydroxy-α-ADABA (aus Hydroxyectoin) sind nämlich nicht nur zentral im Ectoin-Katabolismus selbst, sondern auch im damit verbundenen Regulationsmechanismus. Beide Moleküle dienen als Induktoren des zentralen Regulatorproteins dieses Stoffwechselweges, dem MocR-/GabR-Typ Regulatorprotein EnuR. Im Rahmen der vorliegenden Arbeit konnten die molekularen Details aufgeklärt werden, die es dem Repressormolekül EnuR ermöglichen, beide Moleküle hochaffin zu sensieren und darauf aufbauend die Gene des Ectoin-Stoffwechsels zu induzieren.

3 Summary

To cope with osmotic stress many microorganisms make use of short, osmotically active, organic compounds, the so-called compatible solutes. Examples for especially effective members of this type of molecules are the tetrahydropyrimidines ectoine and 5-hydroxyectoine. Both molecules are produced by a large number of microorganisms, not only to fend-off osmotic stress, but also for example low and high temperature challenges. The biosynthetic pathway used by these organisms to synthesize ectoines has already been studied intensively and the enzymes used therein are characterized quite well, both biochemically as well as structurally. However, synthesis of ectoines is only half the story. Inevitably, ectoines are frequently released from the producer cells in different environmental settings. Especially in highly competitive habitats like the upper ocean layers some bacteria specialized on a niche like this. The model organism used in this work is such a species. It is the marine bacterium *Ruegeria pomeroyi* DSS-3 which belongs to the *Roseobacter*-clade. *Roseobacter* species are heterotrophic *Proteobacteria* which can live in symbiosis with phytoplankton as well as turning against them in a bacterial warfare fashion to scavenge valuable nutrients.

Ectoines can be imported by *R. pomeroyi* DSS-3 in a high-affinity fashion and be used as energy- as well as carbon- and nitrogen-sources. To achieve this, both ectoines rings are degraded by the hydrolase EutD and deacetylated by the deacetylase EutE. The first hydrolysis products α-ADABA (from ectoine) and hydroxy-α-ADABA (from hydroxyectoine) are deacetylated to DABA and hydroxy-DABA which are in additional biochemical reactions transformed to aspartate to fuel the cell's central metabolism. The role and functioning of the EutDE enzymes which work in a concerted fashion are a central aspect of this work. Both enzymes could be biochemically and structurally characterized, and the architecture of the metabolic pathway could be illuminated. α-ADABA and hydroxy-α-ADABA are not only central to ectoine catabolism, but also to the regulatory mechanisms associated with it. Both molecules serve as inducers of the central regulatory protein of this pathway, the MocR-/GabR-type regulator protein EnuR. In the framework of this dissertation molecular details could be clarified which enable the EnuR repressor molecule to sense both molecules with high affinity to subsequently de-repress the genes for the import and catabolism of ectoines.

4 Table Of Content

5 Introduction

5.1 The interplay of water management and nutrients in the physiology of life

One of the major constrains of life is the availability of water. The essentiality of water for life is deeply rooted in the properties of the molecule H_2O. The polarity of the water molecule makes it an excellent solvent for salts, polar molecules and is a prerequisite for any biochemical reaction, making it the "active matrix of life" (Wiggins, 1990; Ball, 2017).Water was essential in the first steps of evolution of life as we know it and allowed the self-assembly of the first semi-permeable membranes (Chandler, 2005). Cells were in their discovery by Robert Hooke defined by their boundaries (Mazzarello, 1999) especially their cell wall, which most prokaryotes (Margolin, 2009) [with a few exceptions (Friis, 1975; Kloda and Martinac, 2001; Young, 2006)] and eukaryotes with the exception of animals (Vellai *et al.*, 1998) possess in varying compositions (Bartnicki-Garcia, 1968; Grabber, 2005; Romaniuk and Cegelski, 2015). This hydrophobic barrier allows not only compartmentalization and provides a confined space for the copying of the genetic material [at first presumably RNA (Crick, 1968; Gilbert, 1986; Sankaran, 2016)]. A key factor is that the cell wall also enables the cell to build-up an electrostatic potential and therefore lays the fundamentals of metabolism (Ray *et al.*, 2016).

Although the differences in the architecture of their cell wall can be tremendous in bacteria, in addition to a plasma membrane made of lipids, they all possess a rigid peptidoglycan layer. In cells with a cell wall the accumulation of ions, small molecules, and macromolecules increases the osmolarity of the cytoplasm (Wood, 2011; van den Berg *et al.*, 2017). An increased osmolarity of the cytoplasm leads to an influx of water, decreasing the intracellular osmolarity again, but increasing the internal pressure of the cell, the turgor. The turgor is seen as a major force in cellular growth, making its regulation vital for a physiological concerted growth, especially in microbial cells (Rojas *et al.*, 2017; Rojas and Huang, 2018). One key feature of microbes is their adaptability to changing habitats, ecological niches, and physiological constrains. As changing osmotic circumstances have direct impact on the turgor of microbial cells, osmoadaptation is thus a facet of microbial life in nearly all habitats.

When microbial cells face hypoosmotic conditions (e.g. soil microbes after a rainfall) water molecules following the osmotic gradient are entering the cell, the turgor increases to non-physiological levels and cells could finally burst (Levina *et al.*, 1999; Hoffmann *et al.*, 2008; Reuter *et al.*, 2014). In the other extreme case, under hyperosmotic conditions (e.g. in dry environments) water leaves the cell and the remaining molecules may be subject of molecular crowding with negative effects on the functionality of the cell's enzymes and metabolic pathways (van den Berg *et al.*, 2017). As the turgor decreases the cell also faces the most danger of collapsing (Bremer and Krämer, 2000; Wood, 2011). The dramatic effects of increased salt concentrations can be seen in many aspects of life. Salting is one of the earliest food-preservation methods used by humans as it drastically decreases

bacteria, fungi, and other pathogens, for example in codfish, dried herring, salt-cured-meat, or vegetables like cabbage in the form of Sauerkraut or Kimchi (Mheen and Kwon, 1984). Salt has been used as a weapon by mankind to devastate its most perilous enemies. The legend that the city of Carthage was sown with salt after its sacking by the Roman Republic remains in historic accounts after more than two millennia (Ridley, 1986). Nowadays weeds (Widmer and Stadtherr, 1961) and snails (Roda *et al.*, 2018) are subject to salt-attacks by gardeners.

As destructive as these processes may be, life eventually finds its way. High salinity environments such as the Dead Sea (Galinski and Oren, 1991), hypersaline lakes in Antarctica (Williams *et al.*, 2014) or the Tibetan plateau (Jiang *et al.*, 2007) are all habitats of microorganisms perfectly adapted to these environments. Viable halophilic microorganisms are even found in salt mines, completely separated from the environment for 220 million years (Megaw *et al.*, 2019; Thompson *et al.*, 2021). To cope with these extreme circumstances, many living cells possess aquaporins, membrane proteins that increase the water permeability of the plasma membrane, to regulate water flux across the plasma membrane (Walz *et al.*, 1997; Calamita, 2000; Hill *et al.*, 2004). Nevertheless, no microorganism is able to transport water actively (e.g. as an energy-dependent process) and directly across its membrane (Tanghe *et al.*, 2006; Tong *et al.*, 2019). To keep the cytoplasm properly hydrated and the turgor in physiological scale, they employ the accumulation or extrusion of osmotically active molecules. These molecules can either be ions [most prominently K^+ (Whatmore and Reed, 1990)] or small organic compounds (Bremer and Krämer, 2000) and lead to two principal adaptation mechanisms which are both energetically costly, although to varying degrees.

5.2 The adaptation mechanisms of osmotically stressed cells

When facing increased osmolarity, the first response of all microorganisms is the import and accumulation of K^+- and Cl^--ions from the environment to reduce the osmotic gradient across the cell membrane (Whatmore and Reed, 1990; Oren, 2013). The more abundant Na^+-ions are used rather scarcely for this task (Oren *et al.*, 1997), as the accumulation of Na^+-ions would have cytotoxic effects on cells and therefore the Na^+-concentration is consequently kept in close boundaries (Lo *et al.*, 2006) (Lee *et al.*, 2013). Adverse effects of accumulated Na^+-ions include the collapse of the cytoplasmic potential (Castle *et al.*, 1986), interference with Na^+/H^+- antiporters (Paulino and Kuhlbrandt, 2014) and adverse effects on protein complexes such as the bacterial flagellum (Takekawa *et al.*, 2020) or protein-protein complexes (Dumetz *et al.*, 2007). Elevated concentrations of K^+-ions are the energetically cheapest way to deal with increased osmolarity, but they interfere with the central metabolism of many microbes, as they negatively influence enzymatic activities (Oren, 1999, 2011). Nevertheless, many microbes living in environments with permanently increased osmolarity are able to use this “salt-in” strategy and are adapted to the high intracellular K^+-concentrations

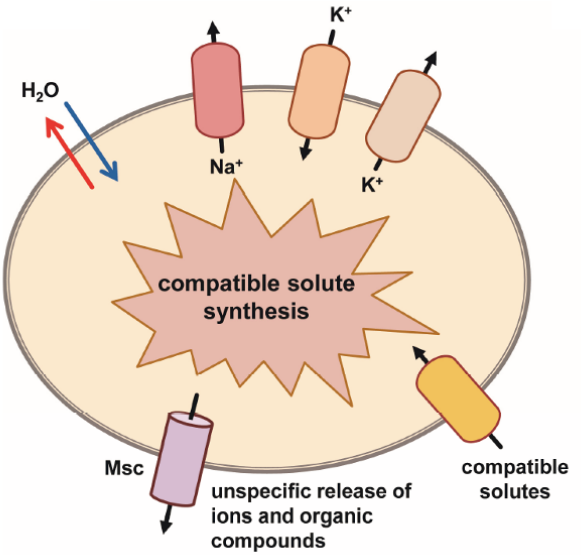

Figure 1: Schematic illustration of the salt-out strategy used by microorganisms to adapt to osmotic stress. Illustration taken from (Czech *et al.*, 2018b).

(Galinski and Truper, 1994; Oren, 2013). This adaptation is possible due to a change of the amino acids exposed on the surfaces of proteins (Galinski and Truper, 1994). In halophilic organisms like *Halorhodospira halophila* the usage of hydrophobic amino acids on the protein surfaces is reduced and the proteomes of these microorganisms exhibit an overall acidic signature (Tadeo *et al.*, 2009; Coquelle *et al.*, 2010; Talon *et al.*, 2014), although there seem to be exceptions from this model (Deole *et al.*, 2013). As the high internal salt concentration exhibits various negative physiological side-effects, most microorganisms (and even some halophilic microorganisms like *H. halochloris* and members of the *Halobacteriales*) use another adaptation mechanism, the "salt-out" strategy (Figure 1). These organisms use low molecular mass organic molecules to decrease the osmotic gradient over the cytoplasmic membrane (Becker *et al.*, 2014; Youssef *et al.*, 2014; Vaidya *et al.*, 2018). These osmotically active substances can be accumulated by cells to extraordinarily high, up to molar concentrations (Dotsch *et al.*, 2008; Pastor *et al.*, 2010; Kunte *et al.*, 2014), without impairing essential cellular functions, an aspect which earned them the term "compatible solutes" (Brown, 1976). Although synthesis of this class of osmolytes is energetically more costly compared to the uptake of K^+-ions (Oren, 1999), these molecules are frequently used in all three domains of life (Archaea, Bacteria and Eukarya) to counteract the negative effects of increased external osmolarity on cellular hydration and cell volume (Arakawa and Timasheff, 1985; Kempf and Bremer, 1998; Bolen and Baskakov, 2001; Roesser and Müller, 2001; Street *et al.*, 2006; Auton *et al.*, 2011). However, they do not only balance the osmotic gradient, but also exhibit cytoprotective characteristics that protect cells from challenges imposed by a number of detrimental conditions like extreme temperatures (Yancey, 2005), hydrostatic pressure, freezing, desiccation and the denaturation of macromolecules by ions and urea (Caldas *et*

al., 1999; Diamant *et al.*, 2001; Holtmann and Bremer, 2004; Yancey, 2005; Hoffmann and Bremer, 2011).

Compatible solutes interact with the cell's macromolecules, especially proteins and membranes in an uncommon way. The strong polarity exhibited by most compatible solutes prohibits interactions with the backbone of proteins, which leads to their exclusion from the immediate hydration shell of proteins (Bolen and Baskakov, 2001; Street *et al.*, 2006; Auton *et al.*, 2011). This "preferential exclusion" effect (Arakawa and Timasheff, 1985) leads to an uneven distribution of compatible solutes in the cell-water which shifts the thermodynamic equilibrium of proteins to a more globular form, which in most cases is identical with a correctly folded variant of the protein. Therefore, especially higher intracellular concentrations of compatible solutes do not disturb the fold of macromolecules but rather promote the functionality of proteins. Altogether, these function promoting traits led to their reference as "chemical chaperones" (Tatzelt *et al.*, 1996; Diamant *et al.*, 2001) describing their protecting role for proteins and entire cells (Lippert and Galinski, 1992; Knapp *et al.*, 1999; Manzanera *et al.*, 2002; Manzanera *et al.*, 2004). These properties are a reason for the evolutionary success story of compatible solutes (Kempf and Bremer, 1998; Roesser and Müller, 2001; Yancey, 2005; Burg and Ferraris, 2008), as well as for their medical, pharmaceutical, and economical potential that has arisen in the past decades (Lentzen and Schwarz, 2006; Graf *et al.*, 2008; Pastor *et al.*, 2010; Kunte *et al.*, 2014; Jorge *et al.*, 2016). Compatible solutes stem from a variety of groups of chemical compounds which can act in different ways, and for example either promote the stability or the solubility of proteins.

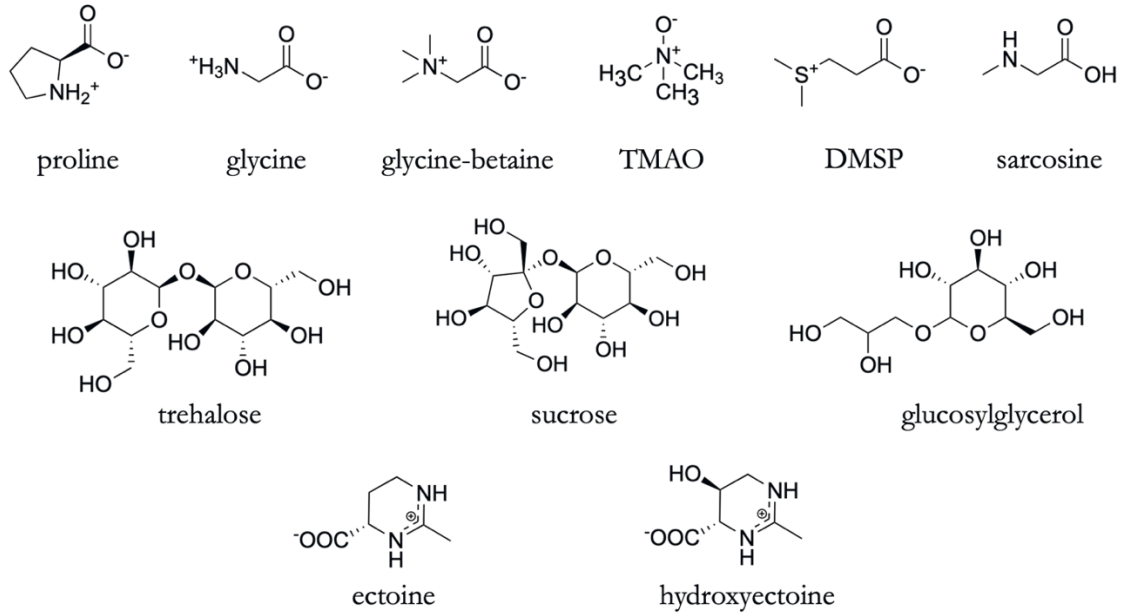

Figure 2: Chemical structures of important and widely used compatible solutes from various chemical backgrounds.

Compatible solutes can either be amino-acids, sugars, polyols, betaines, and derivatives of all these compounds, as well as modified peptides (da Costa *et al.*, 1998). Some of the most prominent and widely used compatible solutes are the amino acids proline and glutamate, the betaines glycine-betaine and trimethylammonium-*N*-oxide (TMAO), the sugars trehalose and sucrose, the heteroside glucosylglycerol, and the amino acid derivatives dimethylsulfoniopropionate (DMSP) and sarcosine (Figure 2). The spectrum of compatible solutes used in all domains of live has been reviewed in-depth in the literature (Csonka, 1989; da Costa *et al.*, 1998) (Roesser and Müller, 2001; Santos and da Costa, 2002; Roberts, 2004). The focus of this dissertation is on the amino acid derivatives ectoine and 5-hydroxyectoine (Figure 2) which are widely used as compatible solutes by members of the Bacteria and Archaea (Pastor *et al.*, 2010; Czech *et al.*, 2018b; Hermann *et al.*, 2020).

The individual chemical attributes of compatible solutes are a reason why the usage of different compatible solutes can even change depending on the specific task at hand and the environmental parameters an organism faces. Not only are compatible solutes energetically more expansive than the import of potassium ions, but the synthesis of different compatible solutes can have varying energetic costs (Oren, 1999). So, it is not unexpected that some organisms employ a mixture of osmolytes and are able to change the concentrations of different osmolytes in this mixture (Auton *et al.*, 2011). This phenomenon has been termed “osmolyte switching” and may affect the temporal dynamics of ectoine production. *Halobacillus halophilus*, for example uses a hybrid osmostress adjustment strategy. Initially, it uses L-glutamate in combination with Cl^- as its primary osmolyte and upon increased external salinity it switches to the synthesis of L-proline and in the transition from exponential to stationary phase even changes to ectoine as its preferred osmolyte (Saum and Muller, 2007, 2008). In a similar fashion *Virgibacillus pantothenticus* changes from synthesizing L-proline at moderate external salinity to ectoine at increased external salinity (Kuhlmann *et al.*, 2008a). As natural abundance ^{13}C-NMR-spectroscopy shows, different members of the *Bacilli* produce different osmolytes and here again, the most salt-stress-tolerant *Bacilli* are capable of producing ectoine and additionally 5-hydroxyectoine (Kuhlmann and Bremer, 2002; Bursy *et al.*, 2007). There seem to be differences in the effectiveness of different compatible solutes and ectoines may be ideally fitted for tougher environmental circumstances (Cayley *et al.*, 1992; Held *et al.*, 2010; Diehl *et al.*, 2013; Cheng *et al.*, 2016).

5.3 Ectoine, 5-hydroxyectoine, their way of function and their biosynthetic genes

The physiological mechanisms which allow some microorganisms to cope with extremely halophilic conditions, in addition to the salt-in strategy, were a mystery to microbiologists for a long time. First steps to illuminate the theme were made in 1985, when Galinski *et al.* investigated the purple sulfur bacterium *Ectothiorhodospira halochloris* (now: *Halorhodospira halochloris*) using ^{13}C-NMR

spectroscopy. Under increased osmolarity, they found high intracellular levels of a novel compound which they identified as (4*S*)-2-methyl-1,4,5,6-tetrahydropyrimidine-4-carboxylic acid and named ectoine (Galinski *et al.*, 1985). The hydroxylated derivative of ectoine, 5-hydroxyectoine, was found in the following by Inbar and Lapidot in the Gram-positive soil bacterium *Streptomyces parvulus* (Inbar and Lapidot, 1988). Ectoine and 5-hydroxyectoine are heterocyclic derivatives of the amino acid aspartate and belong to the class of partially hydrogenated pyrimidines (Galinski *et al.*, 1985; Inbar and Lapidot, 1988). In a pH-neutral setting, the pyrimidine ring structure possesses a delocalized positive charge, while the attached carboxylate group is negatively charged. Due to this polarity and the formation of seven and nine hydrogen bonds with water, respectively (Smiatek *et al.*, 2012), both zwitterions ectoine and 5-hydroxyectoine are strong water binders. This not only results in a high solubility of ectoine in water (about 4 mol L^{-1} at 20° C) (Zaccai *et al.*, 2016), but also has effects on the binding of ions and the local water structure (Smiatek *et al.*, 2012; Smiatek, 2014; Eiberweiser *et al.*, 2015; Hahn *et al.*, 2015). The differences between ectoine and 5-hydroxyectoine in the number of water bonds they can form due to the hydroxy-group of 5-hydroxyectoine (seven and nine, respectively), make 5-hydroxyectoine an even better desiccation protectant (Manzanera *et al.*, 2002; Manzanera *et al.*, 2004). The features supporting the compatibility of ectoines with cellular processes and molecules are the ones previously described for compatible solutes in general, i.e. their polarity, their preferential exclusion, and high number of hydrogen bonds. The exclusion of ectoine from the hydration shell of proteins and the interface of membranes with their liquid environment have also been shown experimentally (Harishchandra *et al.*, 2010; Zaccai *et al.*, 2016). Interestingly for the osmostress adaptation, these effects also prove true under increased salt concentrations (Smiatek *et al.*, 2013). Therefore, ectoines do not only allow an equilization of the osmotic gradient of osmotically stressed cells and provide hydration of the cytoplasm, but also have diverse effects on the conformation and functionality of proteins, membranes, DNA, macromolecules in general, and their interactions with each other (Lippert and Galinski, 1992; Knapp *et al.*, 1999; Barth *et al.*, 2000; Kurz, 2008; Hahn *et al.*, 2015; Zaccai *et al.*, 2016). Due to these properties, ectoines are not only used in microbial responses to osmotic stress but also to fend off the detrimental effects of a variety of stressors. Ectoines have been found in stress responses of microorganisms against cold-stress, heat-stress, oxidative stress, and stress factors related to transition of exponential growth into the stationary phase. Furthermore, ectoine protects DNA against the induction of single strand breaks by ionizing radiation and serves as a scavenger for hydroxyl radicals (Hahn *et al.*, 2017; Meyer *et al.*, 2017; Schroter *et al.*, 2017). There are also reports proposing the usage of ectoine as a piezolyte, a cytoprotectant against hydrostatic pressure, as observed in *Alcalivorax borkumensis*, a marine *Proteobacterium* which is predominant in crude-oil containing seawater (Scoma and Boon, 2016).

Ectoines were first, and at first exclusively, discovered in halophilic bacteria. Therefore, the general assumption was that they are a rare osmolyte, only used by salt-adapted microorganisms for osmoadaptation (Galinski *et al.*, 1985; Peters *et al.*, 1990; Severin *et al.*, 1992). In one of these salt-adapted microbes, the halophilic firmicute *Marinococcus halophilus* isolated from salted mackerels (Venkataraman and Sreenivasan, 1954), the biosynthetic genes *ectABC*, involved in the production of ectoine, were first identified (Peters *et al.*, 1990). This genetic information, combined with HPLC analysis and especially ^{13}C-natural abundance NMR spectroscopy in a wide variety of microbial isolates, changed the assumption that ectoines are exclusively used by true halophiles. In the following years, a plethora of microorganisms representing all three domains of life were identified to be capable of using ectoine [e.g., (Iorio *et al.*, 2021; Kum and Ince, 2021; Tanveer *et al.*, 2021)]. When investigating the *ectABC*-genes of *Streptomyces chrysomallus*, an adjacent gene was found and termed *ectD*. It could be shown that the corresponding enzyme is involved in the production of 5-hydroxyectoine (Prabhu *et al.*, 2004). Bioinformatical genetic assessments found the *ectD* gene to be present in many ectoine-synthesizing microorganisms. Although the genetic organization of the *ectABC* genes is rather conserved (Pastor *et al.*, 2010; Reshetnikov *et al.*, 2011b; Widderich *et al.*, 2014; Widderich *et al.*, 2016c), the presence of *ectD* in this context can vary, even between closely related species and especially in terms of its locus on the chromosome (Garcia-Estepa *et al.*, 2006a; Bursy *et al.*, 2007). Microbes capable of synthesizing both ectoine and 5-hydroxyectoine are frequently shown to possess a mixture of both ectoines, a presumably effective way to harness the positive effects of both substances. As an example, *Streptomyces coelicolor* is best protected against osmotic and heat stress when provided with a 1:1 mixture (0.5 mM each) of ectoine and 5-hydroxyectoine in the growth medium (Bursy *et al.*, 2008).

Some bacteria produce almost exclusively 5-hydroxyectoine during osmotic stress and different growth phases of the culture (Seip *et al.*, 2011; Stöveken *et al.*, 2011), especially upon entering the enter stationary phase (Tao *et al.*, 2016). This observation implies that the hydroxylated derivative of ectoine possesses stress-relieving properties that will allow the cell to better cope with the multitude of challenges imposed by stationary phase (Klauck *et al.*, 2007). This attribute might stem from the frequently observed superior function-preserving properties of 5-hydroxyectoine when tested either *in vivo* (Garcia-Estepa *et al.*, 2006a; Bursy *et al.*, 2008) or *in vitro* (Lippert and Galinski, 1992; Knapp *et al.*, 1999; Borges *et al.*, 2002; Manzanera *et al.*, 2002; Manzanera *et al.*, 2004; Kurz, 2008; Van-Thuoc *et al.*, 2013; Tanne *et al.*, 2014). Biosynthesis and external application of 5-hydroxyectoine can thus be exploited for synthetic anhydrobiotic engineering (Tanne *et al.*, 2014; Hoffmann and Bremer, 2016, 2017). Ectoines have also pronounced effects on the melting temperature of DNA but ectoine and 5-hydroxyectoine differ in this regard. While ectoine lowers the melting temperature, 5-hydroxyectoine increases it (Kurz, 2008).

The excellent function-preserving attributes of ectoines attracted considerable attention to exploit them in the fields of biotechnology, skin care, and medicine (Lentzen and Schwarz, 2006; Graf *et al.*, 2008; Pastor *et al.*, 2010; Kunte *et al.*, 2014; Jorge *et al.*, 2016). This demand of ectoines for practical purposes led to an industrial-scale production process that exploits the highly salt-tolerant γ-*Proteobacterium Halomonas elongata* as a natural and engineered cell factory (Pastor *et al.*, 2010; Kunte *et al.*, 2014) delivering ectoines on the scale of about 20 tons per annum (Strong *et al.*, 2016; Cantera *et al.*, 2020; Pérez *et al.*, 2021). Ectoine is a high-value natural product with an estimated sales value of 600 € up to 1 000 € per kg (Pérez *et al.*, 2021). Insightful reviews covering these topics have been published (Lentzen and Schwarz, 2006; Graf *et al.*, 2008; Pastor *et al.*, 2010; Kunte *et al.*, 2014) and recent reports summarize the current status of efforts to improve the productivity of natural and synthetic microbial cell factories for ectoines (Seip *et al.*, 2011; Becker *et al.*, 2013; Rodriguez-Moya *et al.*, 2013; Chen *et al.*, 2015; Czech *et al.*, 2016; Ning *et al.*, 2016; Perez-Garcia *et al.*, 2017; Chen *et al.*, 2018; Czech *et al.*, 2018b). From the extremolytes currently considered for practical applications (Jorge *et al.*, 2016), ectoine and 5-hydroxyectoine have certainly the greatest potential for sustained commercial exploitation (Lentzen and Schwarz, 2006; Pastor *et al.*, 2010; Kunte *et al.*, 2014). Biotechnologically interesting stress-protective and function-preserving properties might also be derived from synthetic ectoines with reduced or expanded ring sizes (Schnoor *et al.*, 2004) or by chemical modifications that provide a hydrophobic anchor (e.g. lauryl-ectoine) to the otherwise highly water-soluble ectoine molecule (Wedeking *et al.*, 2014).

5.4 Biosynthesis of ectoines

The biosynthetic route of ectoine-/5-hydroxyectoine biosynthesis was first postulated in 1990 (Peters *et al.*, 1990). After the identification and characterization of the ectoine biosynthetic genes *ectABC* in *M. halophilus* (Louis and Galinski, 1997) and the *ectD* gene involved in the production of 5-hydroxyectoine in *S. chrysomallus* (Prabhu *et al.*, 2004), knowledge on the biosynthesis of ectoines rapidly grew. Today, ectoine biosynthesis is quite well understood, both from a functional as well as structural point of view. All enzymes involved in ectoine biosynthesis were biochemically characterized, crystal structures were obtained, and the genes were used in microbial cell-factories to produce ectoine. In recent years also intriguing aspects of the regulation of ectoine biosynthesis could be illuminated.

Looking at ectoine synthesis, not only the direct pathway is of importance, but also the provision of its biosynthetic precursors. Ectoine synthesis starts from the precursor L-aspartate-β-semialdehyde, a microbial metabolite of special importance in the synthesis of lysine, isoleucine, aromatic amino acids, dipicolinate and therefore also cell wall and antibiotic synthesis (Lo *et al.*, 2009). Although it is a frequent and important microbial metabolite, many ectoine producing microorganisms possess special

enzymes to refill their L-aspartate-β-semialdehyde pool during ectoine synthesis. L-aspartate-β-semialdehyde is synthesized through the sequential enzymatic reactions of an aspartokinase (Ask; EC 2.7.2.4) and a L-aspartate-semialdehyde-dehydrogenase (Asd; EC 1.2.1.11). The Ask enzyme synthesizes aspartyl-β-phosphate via an ATP-dependent phosphorylation of L-aspartate, which is subsequently reduced to L-aspartate-β-semialdehyde by the Asd enzyme in an NADPH-dependent reaction (Figure 3). To avoid a wasteful production of the energy-rich intermediate β-aspartyl-phosphate, the enzymatic activities of aspartokinases are usually regulated by feedback inhibition and the expression of the corresponding *ask* gene is also often subjected to sophisticated transcriptional regulation (Lo *et al.*, 2009). Because the feedback-control of Ask enzyme activity could potentially lead to a bottleneck in ectoine biosynthesis (Bestvater *et al.*, 2008), the report of Reshetnikov *et al*.

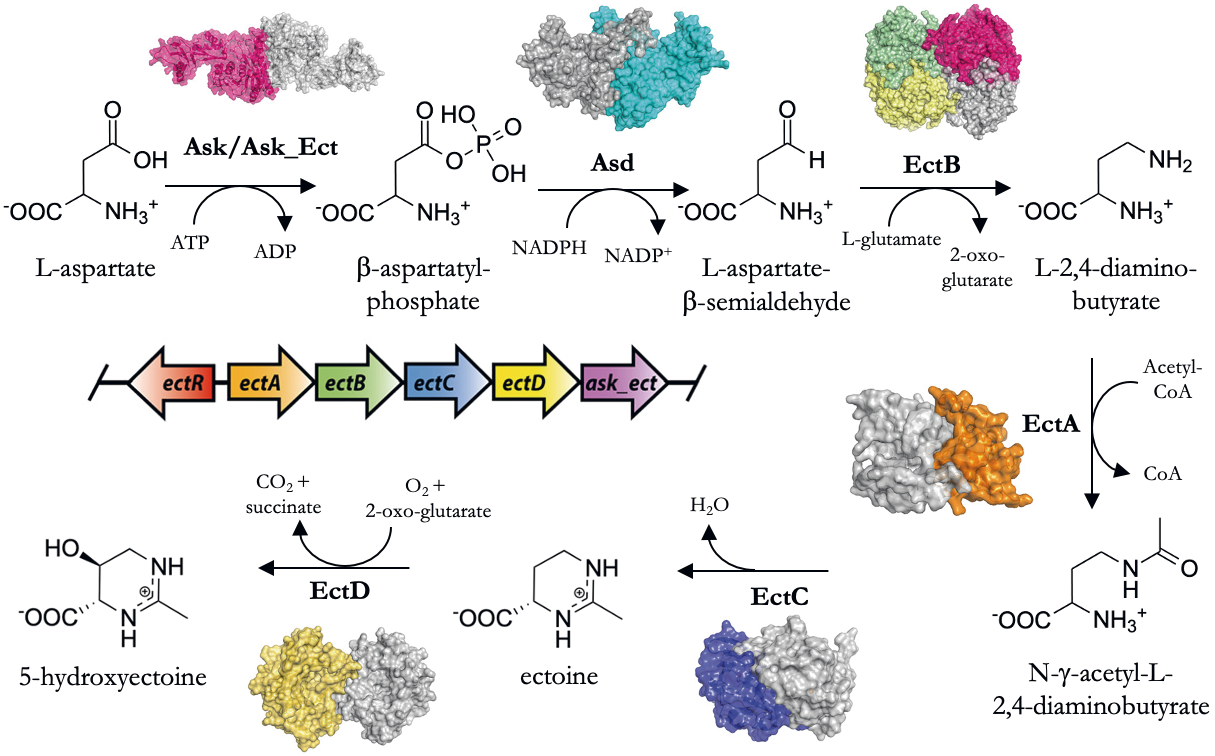

Figure 3: Biosynthesis of ectoine and 5-hydroxyectoine. Shown is the exemplary *ect* gene cluster from the acidophilic *Acidiphilium cryptum* (Moritz *et al.*, 2015), biochemical reaction schemes, and crystal structures (or models) of the involved enzymes. The depicted enzymes which are represented by structural models are the specialized aspartokinase (Ask_Ect) from *Kytococcus sedentarius* [modelled on ask from *Synechocystis* sp. PCC 6803 (PDB: 3L76) (Robin *et al.*, 2010)] and the aspartate semialdehyde dehydrogenase (Asd) of *K. sedentarius* [modeled on the Asd from *Mycobacterium tuberculosis* (PDB: 3TZ6) (Vyas *et al.*, 2012)]. For the central enzymes of ectoine-/5-hydroxyectoine-biosynthesis crystal structures could be solved. The depicted structures are from *Paenibacillus lautus* in the case of the DABA-acetyltransferase EctA (PDB: 6SLL) (Richter *et al.*, 2020) and the ectoine synthase EctC (PDB: 5ONM) (Czech *et al.*, 2019), the crystal structure of the DABA aminotransferase EctB (PDB: 6RL5) (Hillier *et al.*, 2020) stems from *Chromohalobacter salexigens* and the depicted ectoine hydxroxylase EctD (PDB:4Q5O) (Hoeppner *et al.*, 2014) is from *Sphingopyxis alaskensis*. Details on the features of the biochemistry are given in the main text. The illustration is taken and adapted from (Hermann *et al.*, 2020).

(Reshetnikov *et al.*, 2006) that the osmotically inducible ectoine biosynthetic gene cluster of *M. alcaliphilum* was co-transcribed with a gene encoding an aspartokinase, was of considerable interest. This finding indicated that the enzyme encoded by this particular *ask* gene could play a specialized role in ectoine biosynthesis. Indeed, it was observed in subsequent studies (Widderich *et al.*, 2014) that a considerable number of ectoine/5- hydroxyectoine biosynthetic gene clusters include an additional paralogous *ask* gene (referred to in the following as *ask_ect*) (Reshetnikov *et al.*, 2006; Stöveken *et al.*, 2011; Widderich *et al.*, 2014). Its biochemical properties were studied by Stöveken *et al*. (Stöveken *et al.*, 2011) using the Ask_Ect enzyme from *Pseudomonas stutzeri* A1501 and by Reshetnikov *et al*. (Reshetnikov *et al.*, 2011b) using the corresponding enzyme from *Methylobacterium extorquens* AM1. These studies found the Ask_Ect enzymes to be a distinct sub-group of aspartokinases with a reduced or even abrogated allosteric control of their enzymatic activity. To achieve this, the Ask_Ect enzymes accumulated crucial changes in residues implicated in participating in the feedback control of various Ask enzymes (Lo *et al.*, 2009).

Initiating from L-aspartate-β-semialdehyde, three enzymes are involved in ectoine synthesis: L-2,4-diaminobutyrate transaminase (EctB; EC 2.6.1.76), L-2,4-diaminobutyrate (DABA) acetyltransferase (EctA; EC 2.3.1.178), and ectoine synthase (EctC; EC 4.2.1.108). Organisms capable of producing 5-hydroxyectoine do this through a position- and stereospecific hydroxylation of ectoine, an enzymatic reaction catalyzed by the ectoine hydroxylase (EctD; EC 1.14.11.55) (Figure 3). The ectoine biosynthetic route was originally illuminated by Peters *et al*. through an analysis of enzyme activities present in cell-free extracts of *E. halochloris* and *H. elongata* (Peters *et al.*, 1990). Subsequently, Ono *et al*. used purified EctABC enzymes from *H. elongata* to study the properties of the three ectoine biosynthetic enzymes and could verify the postulated biosynthetic route (Ono *et al.*, 1999). Bursy et al. were able to illuminate the biochemistry of the ectoine hydroxylase (Bursy *et al.*, 2007).

The core of the ectoine biosynthetic pathway starts with the transamination of the precursor L-aspartate-β-semialdehyde, a reaction catalyzed by the L-2,4-diaminobutyrate-2-oxoglutarate transaminase EctB. EctB is a pyridoxal-5´-phosphate (PLP)-dependent aminotransferase, using L-glutamate as the amino donor to form 2-oxoglutarate and diamino-butyric acid (DABA). Several EctB-enzymes from *H. elongata* (Ono *et al.*, 1999), *Methylomicrobium alcaliphilum* (Reshetnikov *et al.*, 2006; Reshetnikov *et al.*, 2011b), *Chromohalobacter salexigens* (Hillier *et al.*, 2020) and *Paenibacillus lautus* (Richter *et al.*, 2019) have been biochemically characterized and the closest relatives to EctB-type enzymes, the γ-aminobutyrate transaminases are functionally quite well understood (Bruce *et al.*, 2012; Richter *et al.*, 2019). The *P. lautus* EctB even possesses the catalytic function of a γ-aminobutyrate transaminase (Richter *et al.*, 2019), although it is unclear whether that is true for all EctB-enzymes. The biochemical studies on EctB enzymes also lead to questions regarding different

findings concerning their structural conformation and specificities regarding their biochemical attributes. So, Ono *et al.* and Reshetnikov *et al.* found EctB to form hexamers, while Richter *et al.* and Hillier et al. observed tetramers of EctB. Ono *et al.* found the *H. elongata*-EctB to be heavily K^+ dependent while Richter et al. did not see this feature for the *P. lautus* EctB. Although biochemical analysis as well as modelling and docking analysis were performed on EctB (Richter *et al.*, 2019) and a crystal structure of EctB has been published (PDB:6RL5) (Hillier *et al.*, 2020), EctB it is the least understood enzyme of the ectoine-biosynthetic pathway, especially, as crystal structures in complex with the substrates (L-glutamate as the amino donor and L-aspartate-β-semialdehyde as the amino acceptor) are still lacking.

The EctB-product DABA is subsequently acetylated at its primary amino group to *N*-γ-acetyl-2,4-diaminobutyrate (γ-ADABA) by the acetyltransferase EctA. This enzyme belongs to the superfamily of GCN5-related-*N*-acetyltransferases (GNAT) which uses acetyl-coenzyme A as a co-substrate and acetyl-donor (Vetting *et al.*, 2005). Ono *et al*. (Ono *et al.*, 1999) were first who reported on the enzymatic properties of an EctA ortholog isolated from *H. elongata*. Three further EctA orthologs from methanotrophic bacteria (*M. alcaliphilum*, *Methylophaga thalassica*, and *Methylophaga alcalica*) were subsequently biochemically characterized by Trotsenko and co-workers (Reshetnikov *et al.*, 2006; Mustakhimov *et al.*, 2008; Reshetnikov *et al.*, 2011a). Their properties reflect the different physiologies of the methanotrophic host species from which they were isolated. After an initial report of a crystal structure of the homo dimeric EctA protein from the human pathogen *Bordetella parapertussis* (PDB: 3D3S), Richter *et al.* were able to provide crystal structures of the *P. lautus* EctA in the apo form as well as in states with the ligands CoA, DABA, CoA and DABA, and the product γ-ADABA (Richter *et al.*, 2020). These later structures proved the DABA positioning in the dimeric interface as indicated by the *B. parapertussis* EctA-structure (PDB: 3D3S) to be a crystallization artifact. In combination with biochemical and mutational data, the EctA structures reported by Richter *et al.* could rather pinpoint the active site in close distance to a longer CoA-binding-tunnel and a DABA binding-pocket (Richter *et al.*, 2020). The produced γ-ADABA can itself act as a compatible solute and protein stabilizer (Cánovas *et al.*, 1997; Canovas *et al.*, 1999; Garcia-Estepa *et al.*, 2006b).

The central enzyme in the ectoine biosynthetic pathway is the ectoine synthase EctC (EC 4.2.1.108), a head-to-tail dimer from the cupin super-family of enzymes. This carbon-oxygen hydrolyase catalyzes the ring closure of γ-ADABA to ectoine by the elimination rection of a water molecule and the generation of an intramolecular imino bond. The *H. elongata*-EctC was first biochemically investigated by Ono *et al*. (Ono *et al.*, 1999), which could establish the reaction mechanism. The cyclization of the linear γ-ADABA is facilitated by a nucleophilic attack in the amino-group at the terminal carbonyl group (Ono *et al.*, 1999; Witt *et al.*, 2011; Czech *et al.*, 2019). This nucleophilic attack is executed by an iron atom coordinated inside the cavity of this barrel-like reaction

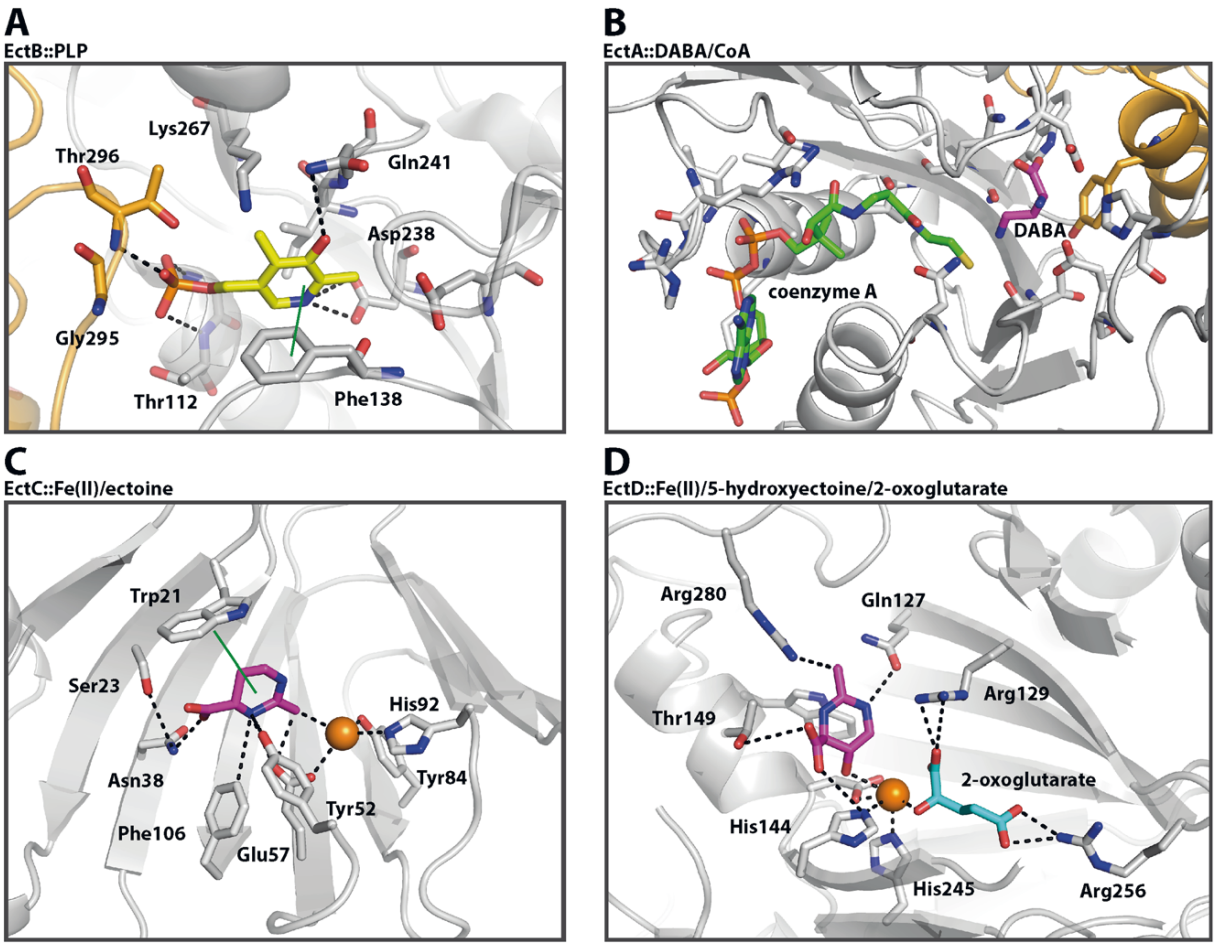

Figure 4: Structural views of the active sites of ectoine/5-hydroxyectoine biosynthetic enzymes. (A) The crystal structure of the dimeric EctB enzyme from *Chromohalobacter salexigens* in complex with the cofactor PLP (yellow sticks) which is coordinated by amino acid residues from both EctB-monomers (orange/grey) (PDB: 6RL5) (Hillier *et al.*, 2020). (B) An overlay of the structures of the dimeric EctA enzyme from *Paenibacillus lautus* in complex with DABA (pink) (PDB: 6SL8) and CoA (green) (PDB: 6SK1). A Tyr-residue from the second monomer (orange) is involved in DABA coordination (Richter *et al.*, 2020). (C) The dimeric ectoine synthase EctC from *P. lautus* in with ectoine (pink) (PDB: 5ONO) (Czech *et al.*, 2019). (D) The ectoine hydroxylase EctD, from *Sphingopyxis alaskensis* in complex with the reaction product 5-hydroxyectoine (pink) and the co-substrate 2-oxoglutarate (blue) (PDB: 4Q5O) (Hoeppner *et al.*, 2014). Amino acids involved in ligand binding are shown as sticks if iron is used as a catalyst it is depicted as an orange sphere. Figure taken from (Hermann *et al.*, 2020).

chamber (Widderich *et al.*, 2016a; Czech *et al.*, 2019). For members of the cupin super-family, coordinating a transition state metal (e.g. iron, copper, zinc, manganese, cobalt, nickel) is a common way to achieve the potential of a diversity of chemical reactions (Dunwell *et al.*, 2004). Biochemical studies on ectoine synthases (Ono *et al.*, 1999; Moritz *et al.*, 2015) were crucial for clarifying the catalytic mechanism of the EctC enzyme. But determination of the crystal structures of the EctC enzyme from the cold-adapted bacterium *Sphingopyxis alaskensis* (Widderich *et al.*, 2016b) and especially the thermotolerant bacterium *P. lautus* (Czech *et al.*, 2019) in its iron-bound, iron- and substrate (γ-ADABA)-bound, and in the presence of its reaction product ectoine, illuminated the

molecular principles of this reaction (Figure 4). The condensation reaction of γ-ADABA seems to be nearly irreversible. Neither Ono et al., nor Witt et al. could observe the reverse reaction from ectoine to γ-ADABA to be catalyzed by EctC at significant rates (Ono *et al.*, 1999; Witt *et al.*, 2011). This could be a possible advantage of ectoine over γ-ADABA in their comparison as compatible solutes, as the synthesis of γ-ADABA from DABA is a reversible reaction.

As the residues critical for co-factor and ligand coordination are evolutionary conserved and their mutation leads to EctC variants with only residual catalytic activity (Czech *et al.*, 2019). Hence, the EctC catalyzed reaction seems to be γ-ADABA specific. Nevertheless, Witt *et al*. (Witt *et al.*, 2011) found L-glutamine to be also cyclized by the *H*. *elongata* EctC enzyme, although at a very low rate. The synthetic product of this reaction is 5-amino-3,4-dihydro-2H-pyrrole-2-carboxylate (ADPC), another compatible solute (Witt *et al.*, 2011) that could hint at the biotechnological potential still lying in ectoine-synthetic enzymes. Also, in contrast to ectoine, the *H*. *elongata* EctC enzyme is able to hydrolyze the synthetic ectoine analogs homoectoine [(*S*)-4,5,6,7-tetrahydro-2-methyl-1H-(1,3)-diazepine-4-carboxylic acid], and DL-DHMICA [(*RS*)-4,5-dihydro-2-methyl-imidazole-4-carboxylic acid] (Schnoor *et al.*, 2004). Hence, ectoine synthases seem to vary in their catalytic profile.

As the ectoine synthase is the only enzyme in the ectoine biosynthetic pathway with no direct homologs of other function (in contrast to EctB and EctA), the *ectC*-gene can be used in bioinformatic assessments to discriminate ectoine-producing from non-ectoine-producing organisms (Widderich *et al.*, 2016c; Czech *et al.*, 2018b; Hermann *et al.*, 2020). However, these assessments must be performed carefully, as so called "orphan *ectC*" genes exist. Whether the corresponding enzymes are actually produced, and the degree of their actual ectoine-producing potential are not clear. The respective orphan *ectC*-genes make up 25% of all *ectC* genes found in the analysis performed by Czech *et al.*, accumulating to 145 "orphan *ectCs"*, neither origin nor functional role have been unraveled yet (Czech *et al.*, 2018b; Czech *et al.*, 2019).

Although ectoine is quite an effective compatible solute by itself, many ectoine producers additionally convert ectoine to 5-hydroxyectoine (Bursy *et al.*, 2007; Widderich *et al.*, 2014; Widderich *et al.*, 2016c). 5-Hydroxyectoine was known since 1988 (Inbar and Lapidot, 1988), and its stereo-chemical configuration was illuminated subsequently from samples of *Streptomyces parvulus* (Inbar *et al.*, 1993), yet the biochemical basis for its formation was unknown for a long time. In the recent years however, this reaction has attracted a lot of research. It became clear that the hydroxylation of ectoine is a position- and stereo-specific reaction performed by the ectoine hydroxylase EctD (EC 1.14.11.55) (Bursy *et al.*, 2007; Bursy *et al.*, 2008), a member of the superfamily of non-heme Fe(II)-containing and 2-oxoglutarate-dependent dioxygenases (Dunwell *et al.*, 2004; Clifton *et al.*, 2006; Aik *et al.*, 2012; Hangasky *et al.*, 2013; Islam *et al.*, 2018). The biochemical underpinnings of the EctD enzyme and its reaction mechanism have been investigated in nine microorganisms (the bacteria *Virgibacillus*

salexigens, Streptomyces coelicolor, Sphyngopyxis alaskensis, Paenibacillus lautus, Pseudomonas stutzeri, Alkalilimnicola ehrlichii, Acidiphilium cryptum, and *H. elongata*, as well as the archaeon *Nitrosopumilus maritimus* SCM1) (Reuter *et al.*, 2010; Widderich *et al.*, 2014; Widderich *et al.*, 2016a).

The hydroxylation of ectoine is achieved by the oxidative dexarboxylation of 2-oxoglutarate to succinate and CO_2. This reaction is oxygen-dependent (Reuter *et al.*, 2010) and so the molecular oxygen has to be activated by a catalyst, in this case an iron-cofactor (Widderich *et al.*, 2014). In most iron-containing proteins this iron-cofactor is coordinated by a heme-group, a paradigm not true in this group of enzymes. Various crystal structures of the EctD enzyme from *V. salexigens* and *S. alaskensis* in its apo-form and with various ligands could show how the iron catalyst is coordinated. Its substrates and the reaction product 5-hydroxyectoine are coordinated in the active site in a way typical for non-heme Fe(II)-containing and 2-oxoglutarate-dependent dioxygenases (Reuter *et al.*, 2010; Hoeppner *et al.*, 2014; Widderich *et al.*, 2014). The overall-fold is that of swapped "head-to-tail" arranged homodimers and each monomer possesses a cupin fold which is made of double-stranded β-sheets (Aik *et al.*, 2012; Hangasky *et al.*, 2013; Islam *et al.*, 2018). These antiparallel β-sheets are surrounded and stabilized by several α-helices and the two monomers in the EctD dimer interact via amino acid residues located in extended loop areas (Hoeppner *et al.*, 2014). Of special importance for EctD-type enzymes is a segment of 23 amino acids on one side of the cupin-barrel (Hoeppner *et al.*, 2014), of which 17 amino acids are highly conserved. This amino acid string contains five residues involved in the binding of the iron catalyst, the co-substrate 2-oxoglutarate, and the reaction-product 5-hydroxyectoine and can be seen as a signature sequence to distinguish EctD-type proteins from other members of the non-heme Fe(II)-containing and 2-oxoglutarate-dependent dioxygenases superfamily (Reuter *et al.*, 2010).

Interestingly, although the investigated EctD-enzymes stem from microorganisms from a variety of different habitats and environmental circumstances, the biochemical properties found for these enzymes in in vitro assays are quite similar and the affinities towards ectoine are moderate (Reuter *et al.*, 2010; Widderich *et al.*, 2014; Widderich *et al.*, 2016b). On the other hand, when expressed in *E. coli*, substantially different levels of hydroxyectoine could be achieved in vivo (Czech *et al.*, 2016). The moderate affinities for their substrate ectoine could relate to the fact that the accumulation of ectoine to a substantial intracellular level via *de novo* synthesis typically precedes the production of 5-hydroxyectoine (Bursy *et al.*, 2007; Bursy *et al.*, 2008; Seip *et al.*, 2011; Stöveken *et al.*, 2011). An important factor for the synthesis of 5-hydroxyectoine from ectoine seem to be the reaction conditions, presumably also in the microbial cell, as an optimization of these conditions is crucial for the 5-hydroxyectoine synthesis in vitro (Czech *et al.*, 2016).

Nowadays, the biosynthetic pathway for ectoine and 5-hydroxyectoine is understood up to a molecular level and proposed alternative biochemical ways to these compounds are not backed by

molecular or biochemical evidence. In earlier years, the hypothesis of hydroxylating not ectoine but rather γ-ADABA as the entry point for hydroxyectoine biosynthesis was discussed (Canovas *et al.*, 1997; Canovas *et al.*, 1999; Vargas *et al.*, 2008; Pastor *et al.*, 2010). Most likely, this pathway either stays only a hypothesis or is taken up in the field of synthetic microbiology, as neither the γ-ADABA-hydroxylation product 3-hydroxy-γ-acetyl-2,4-diaminobutyrate, nor the enzyme needed for the cyclization of this compound were found. Especially, that no such enzyme could be found makes this hypothetical pathway very unlikely to play any ecological role.

After the description of the *ectABC* genes in *Marinococcus halophilus* (Louis and Galinski, 1997), and that of the *ectABCD* locus in *Streptomyces chrysomallus* (Prabhu *et al.*, 2004) not only their wide distribution, but also variability in their genomic context could be shown (Pastor *et al.*, 2010; Reshetnikov *et al.*, 2011b) (Widderich *et al.*, 2014) (Widderich *et al.*, 2016c; Czech *et al.*, 2018b; Hermann *et al.*, 2020). In most cases, the *ectABC* and *ectABCD* gene clusters build a backbone, to which a variety of genes can added. Nevertheless, there can be rearrangements of individual genes within the *ect* cluster, individual *ect* genes can be separated from each other, or multiple copies of the same gene can be present at various location within the genome. The previously mentioned the specialized aspartokinase (*ask_ect*) (Reshetnikov *et al.*, 2006; Mustakhimov *et al.*, 2010; Stöveken *et al.*, 2011) and more rarely the L-aspartate-β-semialdehyde-dehydrogenase (*asd*) are associated with the ectoine biosynthetic genes, although only in the case of the marine Gram-positive *Kytococcus sedentarius* (Sims *et al.*, 2009) both genes are jointly present (Widderich *et al.*, 2014; Czech *et al.*, 2018b; Hermann *et al.*, 2020). Of importance in the ectoine-context are also a gene encoding the MarR-type regulator EctR as well as genes encoding for transporter systems.

5.5 Regulation of ectoine biosynthesis

As the main function of ectoine and 5-hydroxyectoine is to protect cells from the detrimental effects of osmotic stress and these compounds can be accumulated up to molar concentrations (Pastor *et al.*, 2010) (Kunte *et al.*, 2014), it is of no wonder that the transcription of the genes for the biosynthesis of ectoines is fast and strongly up-regulated when cells face osmotic stress. This feature can be observed in the case of sudden or permanently increased osmolarity (Pastor *et al.*, 2010; Kunte *et al.*, 2014). On the other hand, the production of compatible solutes and the biosynthetic enzymes must be tightly controlled in order to avoid the waste of energy. The synthesis of ectoines depletes the nitrogen accumulated via the glutamine synthetase pathway and central metabolism of the cell, as it drains TCA-cycle intermediates like oxaloacetate and acetyl-CoA (Pastor *et al.*, 2013; Kindzierski *et al.*, 2017; Piubeli *et al.*, 2018). Consequently, anaplerotic routes must be engaged to replenish the TCA cycle for

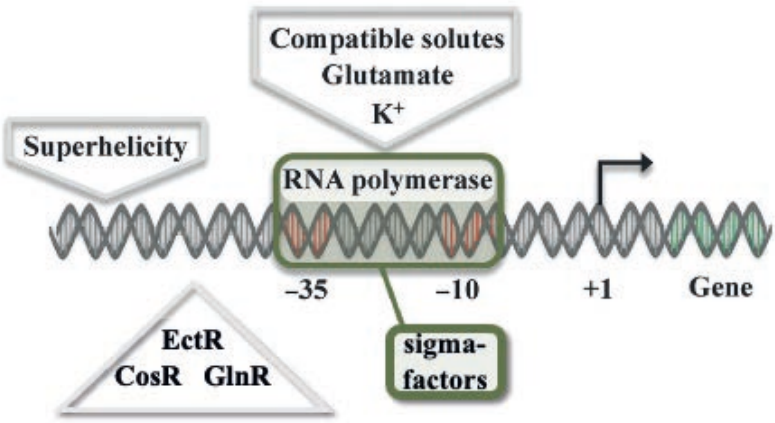

Figure 5: Schematic drawing of factors potentially influencing gene expression under high salinity stress conditions. The illustration is taken and adapted from (Hoffmann and Bremer, 2016).

routine central carbon metabolism and at the same time an increased flux of metabolites into the ectoine/5-hydroxyectoine biosynthetic pathway must be ensured (Salar-Garcia *et al.*, 2017). Compatible solutes and especially ectoines are expensive molecules for the cell, not only as their synthesis uses large amounts of carbon and nitrogen, but the synthesis is quite costly by itself. Taking all starting materials in account, heterotrophic bacteria growing on glucose needs to invest approximately 40 ATP molecules to produce one molecule of ectoine. For bacteria growing autotrophically on CO_2, ectoine-synthesis can cost up to 55 ATP equivalents, as these organisms have to invest more energy to produce the starting materials (Oren, 1999). To avoid these costs when ectoines are not needed, regulation of the transcriptional activity of the *ect*-genes is of critical importance for microorganisms.

The ways to translate the increased osmolarity/salinity of the environment into a transcriptional response are manifold and interwoven, making it difficult for researchers to disentangle the various mechanisms. Nevertheless, several factors could be determined in recent years (Figure 5). The first response of microorganisms to an increase in osmolarity is the import of K^+-ions, and these in combination with glutamate seem to have direct effect on the interaction of the RNA-polymerase with promoters, which differ in their response to salt stress (Sutherland *et al.*, 1986; Rajkumari *et al.*, 1996; Gralla and Vargas, 2006). Up to date, five different regulatory proteins have been found to be involved in the transcriptional regulation of ectoine biosynthesis. These are the MarR-type regulators EctR (first identified in *M. alcaliphilum*) (Mustakhimov *et al.*, 2009; Mustakhimov *et al.*, 2010) and CosR (first identified in *Vibrio cholera*) (Shikuma *et al.*, 2013; Gregory *et al.*, 2019; Gregory *et al.*, 2020), the quorum sensing factors AphA and OpaR (both also from (*Vibrio cholera*) (Gregory *et al.*, 2019) and GlnR, the global regulator for nitrogen metabolism (from *S. coelicolor*) (Shao *et al.*, 2015). While the involvements of AphA, OpaR and GlnR in ectoine regulation are linked to quorum sensing and the synthesis of the nitrogen-rich ectoines, CosR and EctR might be involved int the transfer of a signal

derived from osmotic stress. For CosR, ionic strength has been proposed as the key factor determining its DNA-binding activity (Shikuma *et al.*, 2013). It has been speculated, that EctR might act by a similar sensory mechanism as the closely related MarR-type regulators CosR (Shikuma *et al.*, 2013) and BusR which is a regulator for the uptake of glycine betaine uptake (Romeo *et al.*, 2003; Romeo *et al.*, 2007), although no real evidence has yet been provided for this hypothesis (Czech, 2019). Other ways to achieve osmotically responsive gene expression of the *ect*-genes might be through changes in the promoter regions of *ect*-genes from consensus sequences as has been shown for other compatible solutes (Fischer and Bremer, 2012; Hoffmann *et al.*, 2018). These changes might be seen in a similar context as changes in DNA superhelicity, which has also been reported to be involved in sensing osmotic signals (Higgins *et al.*, 1988; Graeme-Cook *et al.*, 1989; Nagarajavel *et al.*, 2007). An interrelation might also be given with cyclic small messenger molecules like cAMP and c-di-AMP, as these compounds exhibit changing concentrations under different osmotic concentrations and direct correlations with osmostress-responses have been proposed (Xu and Johnson, 1997; Schuster *et al.*, 2016; Hoffmann and Bremer, 2017; Commichau *et al.*, 2018; Gundlach *et al.*, 2018). Inherent features of the promoter elements, the spacer, and flanking regions, definitely play a role, as Czech *et al.* (2018) could show (Czech *et al.*, 2018a). In this study the *ect* promoter from the plant roots-associated bacterium *Pseudomonas stutzeri* A1501 was heterologously expressed in the non-ectoine producing host *E. coli*. Although no ectoine-regulating proteins a should be present in this bacterium, and even after extensive site-directed mutagenesis of the promoter region, the *ect*-promoter still preserved its osmotic inducibility (Czech *et al.*, 2018a). Despite all these intriguing findings, the way true osmotic stress is recognized by the bacterial cell and the way this information is processed is still only understood in a rudimentary fashion.

5.6 Import of ectoines and the involved transporter systems

As discussed above (5.5), the biochemical synthesis of ectoines is a relative expensive procedure for microorganisms. In contrast, the import of ectoine from an environmental source is far cheaper (Oren, 1999). An ABC-transporter for example only requires the hydrolysis of two ATP molecules per imported ectoine molecule, while in contrast ectoine biosynthesis might cost 40/55 ATP molecules. In the context of the bioinformatical analysis of *ect* gene clusters a large group of putative ectoine producers (318 of 539 microbes) was shown to harbor genes encoding potential transporters in the neighborhood of the ectoine/5-hydroxyectoine biosynthetic gene clusters (Czech *et al.*, 2018b). Osmotically induced uptake systems for ectoine and 5-hydroxyectoine have been described in numerous bacterial species and these transporters belong to four different families: TRAP-, MFS-, BCCT-, and ABC-, transport systems. All those systems as well as mechanosensitive channels were found to be co-located with the

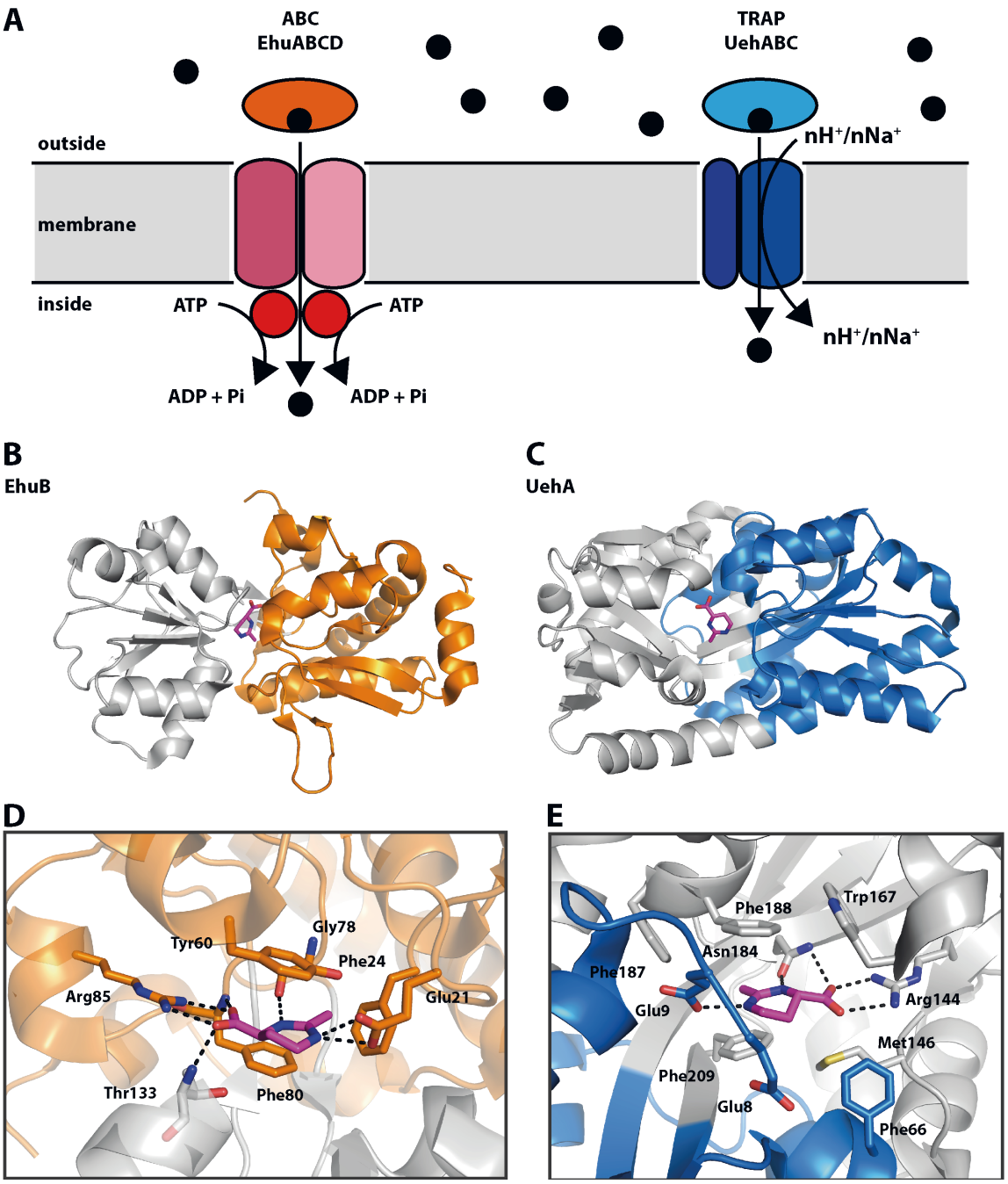

Figure 6: ABC- and TRAP-type transporters used for the import of ectoines. The EhuABCD system from *S. meliloti* is an ATP-binding-cassette (ABC) type transporter (Jebbar *et al.*, 2005) while the UehABC system from *R. pomeroyi* is a member of the Tripartite ATP-independent periplasmic (TRAP) transporter family (Lecher *et al.*, 2009). The EhuB and UehA proteins are the extracellular substrate-binding proteins of these transporters crystalized in the presence of ectoine (Hanekop *et al.*, 2007; Lecher *et al.*, 2009). (A) Schematic overview on the subunit composition of the EhuABCD and UehABC system. The transport activity of the Ehu transporter is fueled by ATP-hydrolysis, while that of the Ueh system is energized either by a proton (H^+) or a sodium (Na^+) gradient. (B and C) Overall fold of the EhuB [PDB: 2Q88] (Hanekop *et al.*, 2007) and UehA [PDB: 3FXB] (Lecher *et al.*, 2009) substrate binding proteins crystalized in the presence of ectoine. The two domains in EhuB and UehA are highlighted in grey/orange (B) and grey/blue (C), respectively. The bound ectoine ligand is shown as pink sticks.

(D, E) Zoom into the ligand-binding site of EhuB (D) and UehA (E) and. All residues involved in ectoine binding are depicted as sticks and ectoine is shown in pink. Figure taken from (Hermann *et al.*, 2020).

ect genes in various microorganisms and function by a variety of mechanisms (Czech *et al.*, 2018b). These transport systems differ in composition as well as their source of energy.

TRAP-transporter (Tripartite-ATP independent Periplasmic transporter) are energized by proton or sodium gradients. Especially TeaABC from *H. elongata* and UehABC from *R. pomeroyi* are well charactized TRAP-transporter systems, for which biochemical data as well as crystal structures of their corresponding extracellular substrate-binding proteins were presented (Kuhlmann *et al.*, 2008b; Lecher *et al.*, 2009; Schweikhard *et al.*, 2010). MFS (Major facilitator superfamily) transport systems like ProP from *E. coli* are dependent on the proton motif force to facilitate transport (Jebbar *et al.*, 1992; Gouesbet *et al.*, 1996; Culham *et al.*, 2018). Members of the BCCT family (Betaine-Choline-Carnithine Transporters) are energized either by proton or sodium gradients (Steger *et al.*, 2004; Ziegler *et al.*, 2010). ABC-type transporters (ATP-Binding Cassette) like EhuABCD from *Sinorhizobium meliloti* are dependent on ATP- and a specific substrate binding protein and have been described to transport various compatible solutes in different organisms (Higgins, 1992; Jebbar *et al.*, 2005; Bursy *et al.*, 2008; Kuhlmann *et al.*, 2008b). Not only microorganisms able to synthesize ectoines have transport systems for ectoine. The non-ectoine-producer *E. coli* demonstrates this, as it possesses the osmoprotectant uptake systems ProP and ProU which are able to transport ectoines among other compatible solutes (Jebbar *et al.*, 1992; Lamark *et al.*, 1992; Lucht and Bremer, 1994).

Interestingly, it has been shown in *H. elongata*, that the cells producing ectoine, also release it and subsequently reimport it through the ectoine specific uptake system TeaABC. A *teaABC* deletion strain is no longer able to reimport the osmoprotectant and so accumulates ectoine outside the cells. Hypothetically, microorganisms might fine-tune the solute concentrations within their cytoplasm through the activity of export-reimport-cycles (Grammann *et al.*, 2002). The mechanism for newly synthesized ectoines to be excluded from the cell might be either leakage or active excretion from the producer cells (Grammann *et al.*, 2002). Extrusion of ectoines has been shown to be facilitated by mechanosensitive channels, which are sometimes found in direct vicinity or even in *ect*-gene clusters (Czech *et al.*, 2018b). These channels transiently open during osmotic down-shock and release molecules in an unspecific manner from the cytoplasm into the environment (Booth *et al.*, 2007b; Booth *et al.*, 2007a). But microorganism even came up with more specific ways to export ectoines to finetune their osmotic response as exemplified by the MFS-exporter EctE (Czech, 2019).

Microorganisms do not only import ectoines from environmental sources via high affinity transport systems for their protection against salt stress and extremes in temperature, but also for their acquisition as nutrients (Jebbar *et al.*, 2005), a process facilitated by either the EhuABCD- or UehABC-transport systems (Hanekop *et al.*, 2007; Lecher *et al.*, 2009). Although the Ehu and Ueh

systems belong to different transporter families (ABC- and TRAP-transporters, respectively), they are both dependent on a periplasmic substrate-binding protein (EhuB and UehA, respectively, Figure 6) (Hanekop *et al.*, 2007; Lecher *et al.*, 2009). These binding proteins trap ectoines that passed the outer membrane via passive diffusion (probably via general porins) with high affinity in the periplasm and deliver them to the core components of the Ehu and Ueh transporters present in the inner membrane for energy-dependent translocation into the cytoplasm. Ligand-binding studies with the purified EhuB and UehA proteins revealed their high affinity for ectoine and 5-hydroxyectoine; EhuB has a K_d values of 1.6 μM for ectoine and 0.5 μM for 5-hydroxyectoine (Jebbar *et al.*, 2005; Hanekop *et al.*, 2007), while UehA exhibits K_d values of 1.4 μM for ectoine and 1.1 μM for 5-hydroxyectoine (Lecher *et al.*, 2009), respectively. Crystallographic studies of the EhuB (PDB accession code 2Q88 and 2Q89) (Hanekop *et al.*, 2007) and UehA (PDB accession code 3FXB) (Lecher *et al.*, 2009) proteins in complex with ectoines revealed the details of the architecture of a ligand-binding site for these compatible solutes, thereby providing further insights into the structural principles of substrate recognition and binding of organic osmolytes that are otherwise preferentially excluded from protein surfaces (Bolen and Baskakov, 2001; Street *et al.*, 2006; Auton *et al.*, 2011).

Similar design principles for trapping the ectoine ligand were observed in the crystal structure of the binding protein (TeaA) of the TeaABC TRAP transporter from *H. elongata* (Kuhlmann *et al.*, 2008b), a system that primarily served for the acquisition of ectoines when they are used as osmostress protectants (Grammann *et al.*, 2002). Crystal structures of the TeaA protein in complex with either ectoine (PDB accession code 2VPN) or 5-hydroxyectoine (PDB accession code 2VPO) have been determined (Kuhlmann *et al.*, 2008b). This protein has K_d values of 0.2 μM^{-1} for ectoine and 3.8 μM^{-1} for 5-hydroxyectoine, respectively (Kuhlmann *et al.*, 2008b). Interestingly, the crystal structures of the UehA and TeaA ligand-binding sites are virtually superimposable (Kuhlmann *et al.*, 2008b; Lecher *et al.*, 2009), despite the fact that the TeaABC and UehABC transporters serve different physiological functions. The genes for the same transporter system are also subject of different types of gene regulation, either osmoadapative or substrate inducible regulatory mechanisms.

5.7 Ectoines as nutrients

In addition to their tremendous adaptability, another feature guaranteeing the evolutionary success of bacteria and other microorganisms is their metabolic potential. Everything that is synthesized by microorganisms will eventually also be catabolized by microorganisms, either by the producer cell itself or by other microorganisms living in the same habitat. This also holds true for compatible solutes, and in this case the nitrogen-rich ectoine/5-hydroxyectoine molecules make no exception. After their synthesis, for example upon osmotic stress, ectoines will eventually either recycled by the producer

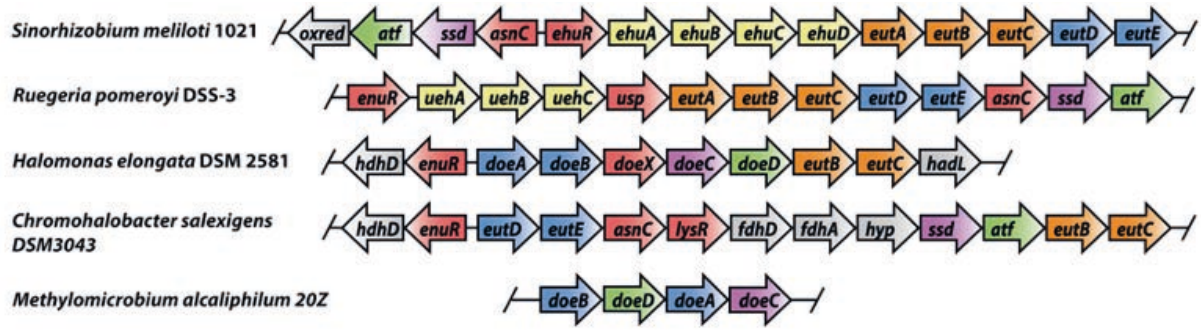

Figure 7: Catabolic gene clusters for ectoines. Schematic illustration of the ectoine catabolic gene clusters from *S. meliloti* (Jebbar *et al.*, 2005), *R. pomeroyi* (Schulz *et al.*, 2017a), *H. elongata* (Schwibbert *et al.*, 2011), *C. salexigens* (Vargas *et al.*, 2006), and *M. alcaliphilum* (Reshetnikov *et al.*, 2020). In addition to the transporter and catabolic genes discussed in the main text, some of these gene clusters contain genes with yet undefined roles in ectoine catabolism. Their gene products have bioinformatically predicted functions as alcohol dehydrogenase (*adh*), hydroxyacid dehydrogenase (*hdhD*), formate dehydrogenases (*fdhD, fdhA*), haloacid dehalogenase (*hadL*), transcriptional regulator (l*ysR*) and a hypothetical protein (*hyp).* Figure taken from (Hermann *et al.*, 2020).

cell itself, or as this might take too long upon an osmotic-down-shock, be excreted into the environment. As discussed in the previous chapter, this can either occur via mechanosensitive channels or direct exporters for compatible solutes. Ectoines might also be set free after cellular lysis, a fate that can overcome bacteria in several ways. Noteworthy are the attacks of phages (the tremendous number of phages in the oceans is a smoking gun), toxins, predatory microorganisms, eukaryotic cells, or just harsh environmental conditions. Environmental ectoines have been detected in different ecosystems (Mosier *et al.*, 2013; Warren, 2013, 2014; Bouskill *et al.*, 2016b; Bouskill *et al.*, 2016a; Warren, 2016) and their presence provides new opportunities for microbial ectoine consumers living in habitats that are also populated by ectoine producers. Different microbial species have been shown to use both ectoine as sole carbon, nitrogen, and energy sources (Galinski and Herzog, 1990; Manzanera *et al.*, 2002; Jebbar *et al.*, 2005; Vargas *et al.*, 2006; Rodriguez-Moya *et al.*, 2010; Schwibbert *et al.*, 2011; Schulz *et al.*, 2017b; Schulz *et al.*, 2017a).

Ectoine-catabolizing microorganisms can scavenge these valuable compounds from the environment through high-affinity, substrate-induced transport systems such as the ABC-system EhuABCD or the TRAP transporter UehABC (Jebbar *et al.*, 2005; Hanekop *et al.*, 2007; Lecher *et al.*, 2009; Schulz *et al.*, 2017a). While use of ectoines as nutrients has been known for quite some time (Galinski and Herzog, 1990; Manzanera *et al.*, 2002; Jebbar *et al.*, 2005; Vargas *et al.*, 2006; Schulz *et al.*, 2017a), a molecular and biochemical understanding of ectoine/5-hydroxyectoine catabolism is still shaping up. A proteomics approach first identified proteins induced in cells of the symbiotic plant-root-associated soil bacterium *Sinorhizobium meliloti* grown in the presence of ectoine. The protein products of eight ectoine-induced genes were identified by mass-spectrometry, and their genes could

be localized in one gene cluster (Figure 7) (Jebbar *et al.*, 2005). Four of the nine ectoine-inducible genes encode the components of a binding-protein-dependent ABC-transporter EhuABCD and five additional genes *eutABCDE* are predicted to encode enzymes for ectoine/5-hydroxyectoine catabolism. The entire *ehuABCD-eutABCDE* gene cluster is preceded by a regulatory gene known as *enuR* encoding a member of the GntR superfamily of transcriptional regulators (Jebbar *et al.*, 2005; Schulz *et al.*, 2017b). Divergently oriented from the *S. meliloti* ectoine degradation operon was an additional regulatory gene (*asnC*) encoding a member of the AsnC/Lrp family of the *feast-and-famine* DNA-binding proteins (Yokoyama *et al.*, 2006; Shrivastava and Ramachandran, 2007; Kumarevel *et al.*, 2008) and three ectoine-inducible genes functionally annotated as an aminotransferase, an oxidoreductase, and a succinate semialdehyde dehydrogenase (Jebbar *et al.*, 2005). Building on these findings in *S. meliloti* (Jebbar *et al.*, 2005), related ectoine/5-hydroxyectoine import and catabolic gene clusters were identified in *C. salexigens* (Vargas *et al.*, 2006), *H. elongata* (Schwibbert *et al.*, 2011) and the marine bacterium *Ruegeria pomeroyi* DSS-3 (Schulz *et al.*, 2017a).

Schwibbert *et al*. (Schwibbert *et al.*, 2011) made the first proposal and biochemical analysis for the degradation pathway of ectoine using the blueprint of the *H. elongata* genome sequence. These authors introduced a new nomenclature for ectoine-catabolic genes and used the term *doe* (**d**egradation **o**f **e**ctoines) rather than the prior used *eut* (**e**ctoine **ut**ilization) nomenclature. As there are no obvious reasons for this change of nomenclature, in the framework of this dissertation,

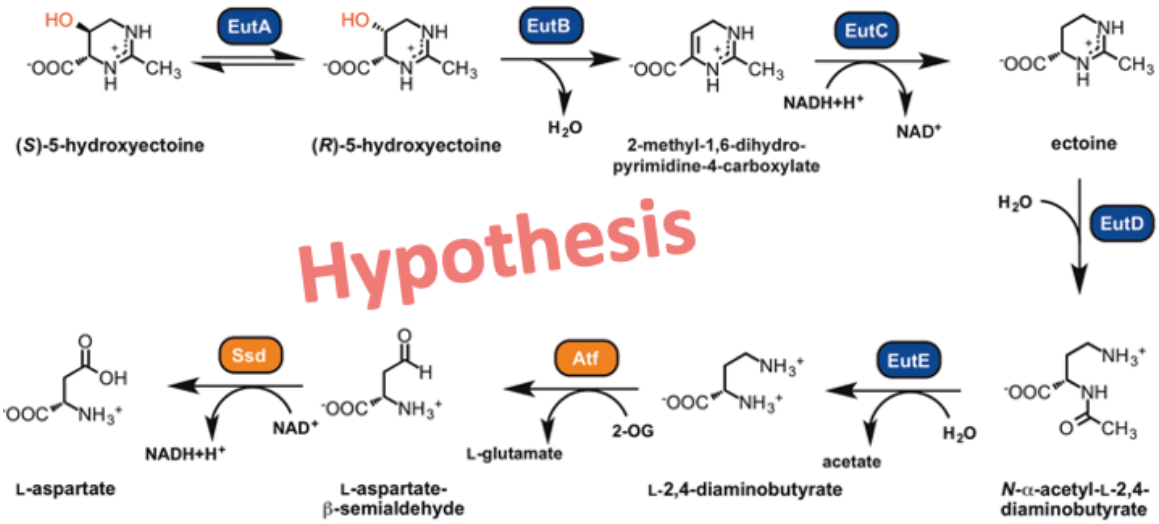

Figure 8: Hypothesis of the biochemical pathway of ectoine/5-hydroxyectoine degradation. Predicted pathway for the catabolism of ectoine and its derivative 5-hydroxyectoine in R. pomeroyi DSS-3. The EutABC-enzymes are predicted to convert 5-hydroxyectoine in a three-step reaction into ectoine. The ectoine ring is subsequently hydrolyzed by the EutD enzyme, resulting in the production of α-ADABA, an intermediate, which is then further catabolized to L-aspartate by the EutE, Atf and Ssd enzymes. Illustration taken and modified from (Czech *et al.*, 2018b).

I will use the original nomenclature introduced by Jebbar et al. (2005). According to their proposal, ectoine degradation begins with the enzymatic opening of the ectoine ring by the ectoine hydrolase EutD (EC 3.5.4.44) to form *N*-α-acetyl-L-2,4-diaminobutyrate (α-ADABA), which is subsequently catabolized by the *N*-α-acetyl-L-2,4-diaminobutyrate deacetylase EutE (EC 3.5.1.125) to acetate and DABA. An acetyl-ornithine-aminotransferase (Atf) then converts DABA to L-aspartate-β-semi-aldehyde and L-glutamate via a transamination reaction. A succinate semialdehyde dehydrogenase (Ssd) then further oxidizes the L-aspartate semi-aldehyde formed by the Atf enzyme to L-aspartate.

This proposed route for the ectoine catabolism (Figure 8) (Schwibbert *et al.*, 2011; Schulz *et al.*, 2017a) resembles a reverse ectoine-biosynthetic route. The types of enzymes involved in the anabolic and catabolic routes are obviously different, but an apparently small difference between both routes can induce an immense effect. The biosynthetic route for ectoines uses exclusively γ-ADABA as the building-block for ectoine, while the biodegradation route for ectoines commences via α-ADABA and hydroxy-α-ADABA. Whether the biodegradation route also exclusively uses these intermediates is of interest for a complete understanding of ectoine catabolism. Schwibbert *et al.* (2011) measured the degradation of ectoine towards a 2:1 mixture of α-ADABA and γ-ADABA, when they heterologously expressed the *H. elongata* EutD-enzyme in *E. coli* (Schwibbert *et al.*, 2011). As they also found that the EutE-enzyme can only deacetylate α-ADABA, this leaves a problematic question: What happens with the residual γ-ADABA in particular in those microorganisms unable to synthesize ectoine?

H. elongata possesses both, the ectoine biosynthetic and degradative pathways and could therefore use the γ-ADABA to form new ectoine, yet it is unknown whether this is feasible, as upon catabolism of ectoine it seems unlikely that the genes for ectoine biosynthesis are induced. Although this could potentially allow the *H. elongata* cells to physiologically navigate osmotic downshifts, in such a circumstance the osmolarity would have to reduce very slowly. Otherwise, mechanosensitive channels will transiently open upon a drop in osmolarity and the ectoine pool will be reduced rapidly (Booth, 2014). The downside of this scenario would be, that *H. elongata* would establish a futile cycle of simultaneous synthesis and degradation of ectoine. This would burden the *H. elongata* under already challenged osmotic conditions with the costs of two additional ATP molecules per turn of ectoine synthesis. As many bacteria capable of both ectoine catabolism are also able to synthesize ectoine (Schulz *et al.*, 2017b) it seems unlikely that they can all still compete despite this metabolic burden.

Examining the ectoine/5-hydroxyectoine catabolic pathway in *R. pomeroyi* DSS-3, Schulz *et al*. (Schulz *et al.*, 2017a) agreed with the proposal by Schwibbert *et al*. with respect to the degradation route of ectoine to L-aspartate. Additionally, they made a proposal for the conversion of 5-hydroxyectoine into ectoine. These authors envisioned the removal of the 5-hydroxyl group from the ectoine ring as a three-step enzymatic process that involves the EutABC proteins. In this scenario, the

racemase EutA, converts (*S*)-5-hydroxyectoine to its (*R*)-5-hydroxyectoine enantiomer. This (*R*)-5-hydroxyectoine would then undergo a dehydration reaction performed by EutB, a pyridoxal-5'-phosphate (PLP) dependent threonine dehydratase. The predicted reaction product 2-methyl-1,6-dihydropyrimidine-4-carboxylate is then proposed to be reduced to ectoine by the EutC enzyme in a NADH-dependent reduction (Schulz *et al.*, 2017a). Neither the conversion of 5-hydroxectoine to ectoine nor its further catabolism to L-aspartate as suggested by Schwibbert *et al*. (Schwibbert *et al.*, 2011) and Schulz *et al*. (Schulz *et al.*, 2017a) were experimentally tested, with the exception of the preliminary assessment of the opening of the ectoine ring by the ectoine hydrolase from *H. elongata* in cells of a heterologous host bacterium (Schwibbert *et al.*, 2011).

The hypothesis of 5-hydroxyectoine catabolism as proposed by Schulz *et al.* (2017a) was refuted by experimental data included in this dissertation (Mais *et al.*, 2020). Mais and colleagues were able to show in vitro and in vivo, that the 5-hydroxyectoine molecule is directly opened by the EutDE enzyme bi-module. The hydrolase EutD produces the 5-hydroxyectoine intermediate hydroxy-α-ADABA which is subsequently deacetylated to hydroxy-DABA by the EutE enzyme. As the involvement of the EutABC enzymes in 5-hydroxyectoine catabolism was shown by Schulz *et al.* (Schulz *et al.*, 2017b), this hydroxy-DABA is the most likely point, the EutABC enzymes engage in the degradation pathway of 5-hydroxyectoine (Mais *et al.*, 2020).

5.8 Regulation of ectoine-catabolism

Environmental ectoines have been detected in different ecosystems (Mosier *et al.*, 2013; Warren, 2013, 2014; Bouskill *et al.*, 2016b; Bouskill *et al.*, 2016a; Warren, 2016) and many *Proteobacteria* can use these substances as carbon, nitrogen, and energy sources (Jebbar *et al.*, 2005; Schwibbert *et al.*, 2011; Schulz *et al.*, 2017b; Schulz *et al.*, 2017a). As the concentrations of ectoines in the environment are quite low, the ectoine/5-hydroxyectoine importer and catabolic genes need to be under a tight transcriptional control. The transcription of the ectoine catabolic genes is strongly upregulated when ectoines are present in the growth medium (Jebbar *et al.*, 2005; Schulz *et al.*, 2017b; Yu *et al.*, 2017).

Many ectoine/5-hydroxyectoine catabolic gene clusters also contain a gene (asnC/doeX) for a member of the feast and famine family of transcriptional regulators (Yokoyama *et al.*, 2006; Schwibbert *et al.*, 2011; Schulz *et al.*, 2017b). These types of proteins can wrap DNA into nucleosome-like structures and frequently respond in their DNA-binding activity to low-molecular weight effector molecules (e.g. amino acids) (Shrivastava *et al.*, 2004; Shrivastava and Ramachandran, 2007; Kumarevel *et al.*, 2008; Dey *et al.*, 2016). Schwibbert *et al.* (2011) showed that such an AsnC-type protein (referred to by these authors as DeoX) targets DNA sequences located at or in the vicinity of the promoter for the *H. elongata* ectoine/5-hydroxyectoine catabolic gene cluster (Schwibbert *et al.*, 2011). Notably, AsnC serves as an activator for the *R. pomeroyi* import and catabolic gene cluster and

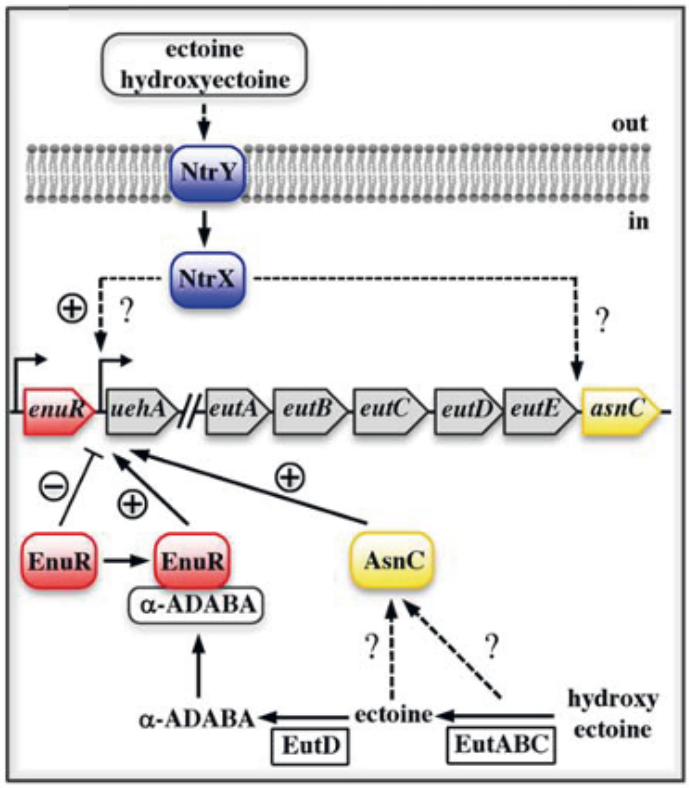

Figure 9: Working model for the genetic control of hydroxyectoine/ectoine uptake and catabolic genes in *R. pomeroyi.* Picture taken from (Schulz *et al.*, 2017b).

its loss abolished the use of ectoine as sole carbon but not as sole nitrogen source (Schulz *et al.*, 2017b). Transposon mutagenesis also revealed another regulatory system involved in the regulation of ectoine catabolism, the two-component system NtrYX (Schulz *et al.*, 2017b). This close relative of the NtrBC two component systems (Ishida *et al.*, 2002; Bonato *et al.*, 2016) also has the effect of a transcriptional activator, as *R. pomeroyi* mutants of *ntrYX* are no longer able to catabolize ectoines.

However, the most important regulator of ectoine catabolism is the MocR/GabR type regulator EhuR/EnuR. Most of the investigated ectoine/5-hydroxyectoine catabolic gene clusters contain a gene encoding a member of this family of transcriptional regulators (Tramonti *et al.*, 2018). Members of this protein family typically consist of a N-terminal winged-helix-turn-helix DNA-reading head connected via a long and highly flexible linker to a C-terminal aminotransferase domain of fold I (Edayathumangalam *et al.*, 2013; Tramonti *et al.*, 2018). In their aminotransferase domain, MocR/GabR-type regulators possess a covalently bound PLP, that is not used for an enzymatic function, but triggers a conformational change of the protein affecting DNA binding and therefore transcription (Edayathumangalam *et al.*, 2013; Wu *et al.*, 2017; Tramonti *et al.*, 2018; Frezzini *et al.*, 2020). As a free amino group of the ligand molecule is needed to achieve an interaction with the covalently bound PLP, both ectoines can be discarded as direct inducers of EnuR. Detailed studies on the EhuR/EnuR regulatory proteins from *S. meliloti* and *R. pomeroyi* rather identified the degradation

intermediates α-ADABA and DABA as system-specific inducers and ligands for EhuR/EnuR (Schulz *et al.*, 2017b; Yu *et al.*, 2017).

In EnuR, the PLP cofactor is covalently bound to Lys-302 forming an internal aldimine. The formation of the intermediate of ectoine degradation α-ADABA in cells catabolizing ectoine results in the binding of α-ADABA, or DABA, to PLP thereby forming an external aldimine (Schulz *et al.*, 2017b). These chemical reactions trigger a conformational change of the EnuR regulator, and concurrently relieves the transcriptional repression of the ectoine/5-hydroxyectoine catabolic gene cluster. The replacement of Lys-302 with an amino acid residue (His) to which PLP cannot covalently attach to, transforms this mutant EnuR protein into a super-repressor that no longer responds to its ectoine-derived internal inducers genes (Schulz *et al.*, 2017b). Physiologically important is the fact that in contrast to the specific ectoine metabolite α-ADABA, γ-ADABA, the major substrate of the ectoine synthase EctC (Czech, 2019; Czech *et al.*, 2019), does not serve as an inducer of the catabolic genes (Schulz *et al.*, 2017b). Remarkably, externally provided 5-hydroxyectoine is a much stronger inducer of the *R. pomeroyi* ectoine/ 5-hydroxyectoine catabolic genes than ectoine (Schulz *et al.*, 2017b) and the reason for this conundrum will be confronted in this dissertation.

6 Publications

6.1 Original paper with peer-review process (published)

6.1.1 Transcriptional regulation of ectoine catabolism in response to multiple metabolic and environmental cues (2017)

Environ Microbiol 2019; 19(11), 4599-4619 doi:10.1111/1462-2920.13924

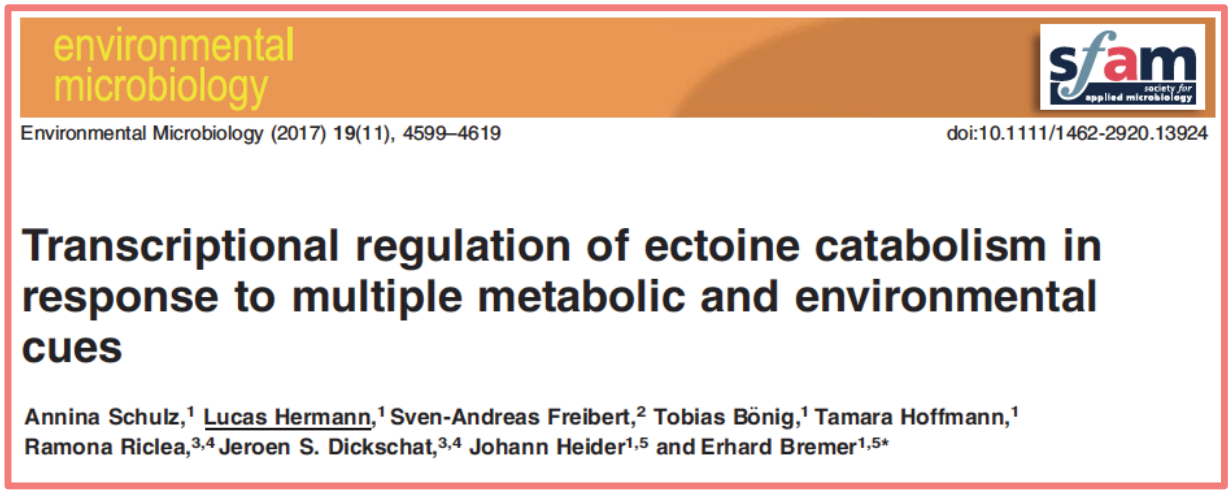

The following research article “Transcriptional regulation of ectoine catabolism in response to multiple metabolic and environmental cues” was published in Environmental Microbiology in 2019 after a peer-reviewing process. My contribution to this publication were the bioinformatic assessment of the EnuR binding site, Electrophoretic mobility shift assays, growth experiments of *Ruegeria pomeroyi* strains on agar plates and figure preparation. T. Bönig performed the transposon mutagenesis, A. Schulz performed all other experiments with input from S. A. Freibert for the microscale thermophoresis. R. Riclea and J. S. Dickschat synthesized γ-ADABA and α-ADABA. T. Hoffmann helped preparing the figures. J. Heider was involved in proposing the catabolic pathway for ectoine and 5-hydroxyectoine. E. Bremer planned experiments, analyzed data, and supervised the project. E. Bremer, A. Schulz and I wrote the manuscript, with contributions from all other authors.

environmental microbiology

Environmental Microbiology (2017) **19**(11), 4599–4619 doi:10.1111/1462-2920.13924

Transcriptional regulation of ectoine catabolism in response to multiple metabolic and environmental cues

Annina Schulz,[1] Lucas Hermann,[1] Sven-Andreas Freibert,[2] Tobias Bönig,[1] Tamara Hoffmann,[1] Ramona Riclea,[3,4] Jeroen S. Dickschat,[3,4] Johann Heider[1,5] and Erhard Bremer[1,5]*

[1]*Department of Biology, Laboratory for Microbiology, Philipps-University Marburg, Karl-von-Frisch-Str. 8, D-35043 Marburg, Germany.*

[2]*Department of Medicine, Institute for Cytobiology and Cytopathology, Philipps-University Marburg, Robert-Koch Str. 6, D-35032 Marburg, Germany.*

[3]*Institute of Organic Chemistry, Technical University Braunschweig, D-38106 Braunschweig, Germany.*

[4]*Kekulé-Institute for Organic Chemistry and Biochemistry, Friedrich-Wilhelms-Universität Bonn, D-53121 Bonn, Germany.*

[5]*LOEWE-Center for Synthetic Microbiology, Philipps-University Marburg, Hans-Meerwein Str. 6, D-35043 Marburg, Germany.*

Summary

Ectoine and hydroxyectoine are effective microbial osmostress protectants, but can also serve as versatile nutrients for bacteria. We have studied the genetic regulation of ectoine and hydroxyectoine import and catabolism in the marine *Roseobacter* species *Ruegeria pomeroyi* and identified three transcriptional regulators involved in these processes: the GabR/MocR-type repressor EnuR, the feast and famine-type regulator AsnC and the two-component system NtrYX. The corresponding genes are widely associated with ectoine and hydroxyectoine uptake and catabolic gene clusters (*enuR*, *asnC*), and with microorganisms predicted to consume ectoines (*ntrYX*). EnuR contains a covalently bound pyridoxal-5'-phosphate as a co-factor and the chemistry underlying the functioning of MocR/GabR-type regulators typically requires a system-specific low molecular mass effector molecule. Through ligand binding studies with purified EnuR, we identified *N*-(alpha)-L-acetyl-2,4-diaminobutyric acid and L-2,4-diaminobutyric acid as inducers for EnuR that are generated through ectoine catabolism. AsnC/Lrp-type proteins can wrap DNA into nucleosome-like structures, and we found that the *asnC* gene was essential for use of ectoines as nutrients. Furthermore, we discovered through transposon mutagenesis that the NtrYX two-component system is required for their catabolism. Database searches suggest that our findings have important ramifications for an understanding of the molecular biology of most microbial consumers of ectoines.

Received 25 June, 2017; revised 29 August, 2017; accepted 31 August, 2017. *For correspondence. E-mail: bremer@staff.uni-marburg.de; Tel. (+49)-6421-2821529; Fax (+49)-6421-2828979.

Introduction

Ectoine and its derivative 5-hydroxyectoine (Pastor *et al.*, 2010; Kunte *et al.*, 2014) are members of a selected group of organic osmolytes, the compatible solutes. Many *Bacteria* and some *Archaea* use these types of compounds to fend off the detrimental effects of high osmolarity/salinity on cellular physiology and growth (Kempf and Bremer, 1998; Roesser and Müller, 2001). Their accumulation promotes the hydration of the cytoplasm under osmotically unfavourable environmental conditions, and thereby allows maintaining vital turgor within physiologically acceptable boundaries (Bremer and Krämer, 2000; Wood, 2011; Booth, 2014). The physicochemical attributes of ectoines make them highly compliant with cellular physiology, biochemistry and the functionality of macromolecular structures and assemblies (Lippert and Galinski, 1992; Manzanera *et al.*, 2002; Harishchandra *et al.*, 2010; Tanne *et al.*, 2014; Zaccai *et al.*, 2016). As a result, these compounds can be accumulated by high osmolarity challenged cells to exceedingly high cellular levels, either through transport or synthesis (Kuhlmann and Bremer, 2002; Kuhlmann *et al.*, 2011). The ability to synthesize ectoines as osmotic stress protectants is an ecophysiologically important trait for many microorganisms that populate marine, terrestrial, or plant-associated habitats (Widderich *et al.*, 2014; 2016b). The biosynthetic routes for ectoine

and hydroxyectoine are genetically and biochemically rather well understood. They rely on the EctABC enzymes to produce ectoine from aspartate-β-semialdehyde, a central intermediate in amino acid metabolism and cell wall synthesis, and on the EctD enzyme to further convert it to 5-hydroxyectoine (Pastor *et al.*, 2010; Kunte *et al.*, 2014) (Fig. 1).

Ectoines also serve as carbon, nitrogen and energy sources for different microbial species (Galinski and Herzog, 1990; Manzanera *et al.*, 2002; Jebbar *et al.*, 2005; Vargas *et al.*, 2006; Rodriguez-Moya *et al.*, 2010; Schwibbert *et al.*, 2011; Schulz *et al.*, 2017). These compounds are released into the environment from producer microorganisms either through the transient opening of mechanosensitive channels as a consequence of osmotic down-shocks, through secretion, or on cellular decomposition (Welsh, 2000; Grammann *et al.*, 2002; Booth, 2014; Widderich *et al.*, 2016b). Given the wide occurrence of microorganisms capable of synthesizing ectoines (Widderich *et al.*, 2014; 2016b), it does not come as a surprise that these compounds have been detected in different ecosystems (Mosier *et al.*, 2013; Warren, 2014; 2016).

In contrast to the wide taxonomic affiliation of hydroxyectoine/ectoine producers (Widderich *et al.*, 2014; 2016b), all currently known, or predicted, microbial consumers of ectoines are members of the *Proteobacteria* (Schulz *et al.*, 2017). Building on previous data (Jebbar *et al.*, 2005; Schwibbert *et al.*, 2011), we have recently proposed a pathway for the complete route of hydroxyectoine/ectoine uptake and catabolism (Schulz *et al.*, 2017) (Fig. 1) in the marine bacterium *Ruegeria pomeroyi* DSS-3 (Moran *et al.*, 2004), a member of the widely distributed and metabolically versatile *Roseobacter* clade (Wagner-Döbler and Biebl, 2006; Luo and Moran, 2014; Simon *et al.*, 2017). In this bacterium, import of ectoines is mediated by a high affinity binding-protein-dependent and substrate-inducible TRAP-type transport system (UehABC) (Lecher *et al.*, 2009; Mulligan *et al.*, 2011) (Fig. 1). Once imported, the catabolism of ectoines can be broken down to three functional modules: (i) three enzymes (EutABC) convert hydroxyectoine to ectoine, (ii) the ectoine ring is then hydrolytically opened by the ectoine hydrolase EutD to form *N*-(α)-L-acetyl-2,4-diaminobutyric acid [*N*-(α)-ADABA] and (iii) this intermediate is subsequently further metabolized to L-aspartate via the EutE-Atf-Ssd enzymes (Schulz *et al.*, 2017) (Fig. 1).

The hydroxyectoine/ectoine uptake and catabolic genes of *R. pomeroyi* DSS-3 are genetically organized in a 13.5-Kbp operon whose expression is mediated by two promoters, one of which is located upstream of *enuR* and the other is present in front of *uehA*. The *enuR* gene encodes a major regulatory gene for the hydroxyectoine/ectoine uptake and catabolic gene cluster (Schulz *et al.*, 2017) (Fig. 1). Its promoter operates constitutively at a low transcriptional level, whereas the promoter positioned upstream of *uehA* directs the expression of the transport and catabolic genes; its transcriptional activity is strongly enhanced by the presence of ectoines in the growth medium. As a result, a robust substrate induction of hydroxyectoine/ectoine uptake and catabolic activities is observed in *R. pomeroyi* DSS-3 (Lecher *et al.*, 2009; Schulz *et al.*, 2017).

A bioinformatics assessment of the genome context of the hydroxyectoine/ectoine catabolic gene clusters in a substantial number of bacteria (Schulz *et al.*, 2017) revealed a strong correlation with a gene coding for a member of the GabR/MocR family of regulatory proteins, a sub-group of the GntR super-family of transcriptional regulators (Rigali *et al.*, 2002; Bramucci *et al.*, 2011; Suvorova and Rodionov, 2016). The name chosen by us for this gene stands for **e**ctoine **n**utrient **u**tilization **r**egulator (*enuR*) but orthologues of the same type of gene have been referred to in the literature either as *ehuR* or as *eutR* (Suvorova and Rodionov, 2016; Yu *et al.*, 2017). EnuR serves as a repressor of the hydroxyectoine/ectoine uptake and catabolic genes, both in *R. pomeroyi* DSS-3 (Schulz *et al.*, 2017) and in *Sinorhizobium meliloti* (Yu *et al.*, 2017), a plant-root associated bacterium in which molecular details of ectoine import and catabolism were initially described through a proteomic approach and crystallographic analysis of the ligand binding protein of a hydroxyectoine/ectoine-specific ABC-type importer (EhuABCD) (Jebbar *et al.*, 2005; Lecher *et al.*, 2009).

MocR/GabR-type regulators are widely distributed in Gram-positive and Gram-negative bacteria but only a few of them have been functionally characterized (Belitsky and Sonenshein, 2002; Wiethaus *et al.*, 2008; Belitsky, 2014; Okuda *et al.*, 2015b; Takenaka *et al.*, 2015; Tramonti *et al.*, 2017). They possess a conserved structural organization with an N-terminal DNA-reading head containing a winged helix-turn-helix DNA-binding motif that is connected via a flexible linker region to a large carboxy-terminal effector-binding/dimerization domain. This latter domain is structurally related to aminotransferases of type-I fold (Edayathumangalam *et al.*, 2013; Milano *et al.*, 2015; Suvorova and Rodionov, 2016). It frequently contains a covalently bound pyridoxal-5'-phosphate (PLP) co-factor (attached to a Lys-residue) but MocR/GabR-type regulators do not perform a full aminotransferase enzyme reaction (Edayathumangalam *et al.*, 2013; Okuda *et al.*, 2015a,b; Takenaka *et al.*, 2015; Park *et al.*, 2017; Wu *et al.*, 2017). Instead, a partial aminotransferase reaction occurs that initially involves the covalent binding of a system-specific low molecular mass effector molecule to the protein-bound PLP co-factor (the internal aldimine) and the subsequent formation of an external aldimine between PLP and the effector molecule. These chemical reactions are transduced into a conformational change of the entire

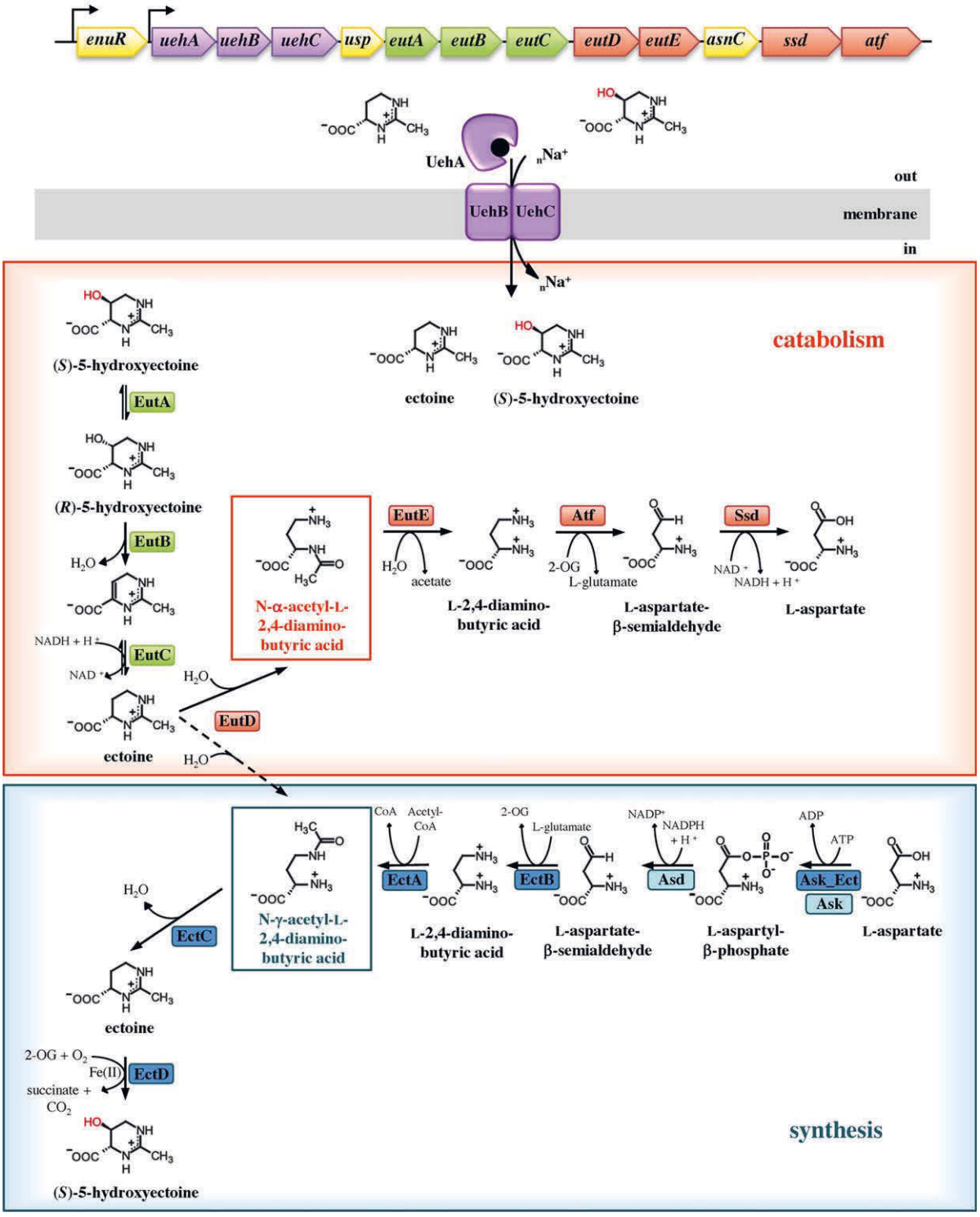

Fig. 1. Anabolic and catabolic routes for ectoines. The genetic organization of the hydroxyectoine/ectoine catabolic gene cluster present in the *R. pomeroyi* DSS-3 genome is shown (Moran *et al.*, 2004; Schulz *et al.*, 2017). The sketches for the synthesis route for ectoine and hydroxyectoine (Ono *et al.*, 1999; Bursy *et al.*, 2007; Stöveken *et al.*, 2011) and that for their catabolism (Schwibbert *et al.*, 2011; Schulz *et al.*, 2017) are based on previously published data. All enzymes involved in ectoine and hydroxyectoine biosynthesis have been enzymatically studied (Ono *et al.*, 1999; Bursy *et al.*, 2007; Stöveken *et al.*, 2011), while EutD (DeoA) is the only enzyme from the catabolic route whose function has been experimentally assessed. The information on the generation of both *N*-(α)-ADABA and *N*-(γ)-ADABA by the recombinant EutD (DoeA) enzyme from *H. elongata* is based on data reported by Schwibbert *et al.* (Schwibbert *et al.*, 2011).

regulatory protein, which then dictates the DNA-binding and functional properties of MocR/GabR-type proteins to function either as activators or repressors (or both) of gene transcription (Belitsky and Sonenshein, 2002; Wiethaus *et al.*, 2008; Edayathumangalam *et al.*, 2013; Okuda *et al.*, 2015a,b; Takenaka *et al.*, 2015; Park *et al.*, 2017; Tramonti *et al.*, 2017; Wu *et al.*, 2017). EnuR possesses such a covalently bound PLP molecule, and Lys-302 present in its carboxy-terminal aminotransferase domain has been identified through *in silico* modelling and mutant studies as the residue to which the co-factor is attached (Schulz *et al.*, 2017).

Although an exogenous supply of ectoines triggers a strong induction of the transcription of the hydroxyectoine/ectoine uptake and catabolic genes in *R. pomeroyi* DSS-3 (Lecher *et al.*, 2009; Schulz *et al.*, 2017), they cannot be the true inducer molecules because the chemistry underlying the interaction of the system-specific effector molecule with the Lys-bound PLP co-factor requires a primary amino group (Bramucci *et al.*, 2011; Edayathumangalam *et al.*, 2013; Okuda *et al.*, 2015a,b; Takenaka *et al.*, 2015; Suvorova and Rodionov, 2016; Park *et al.*, 2017; Wu *et al.*, 2017). Since free amino groups are only generated after the first step of ectoine degradation (Fig. 1), it seemed plausible that catabolic intermediates would function as internal inducer(s) for the EnuR repressor protein. Indeed, based on DNA binding studies with the EnuR orthologue (EhuR) from *S. meliloti* (Jebbar *et al.*, 2005), 2,4-diaminobutyric acid (DABA) (Fig. 1) has been proposed as a potential inducer for hydroxyectoine/ectoine uptake and utilization genes but direct binding studies between EhuR and DABA have not been reported (Yu *et al.*, 2017).

Since DABA is also produced in microbial pathways not involved in ectoine catabolism (Ikai and Yamamoto, 1997; Du *et al.*, 2013; Fidalgo *et al.*, 2016), we set out to genetically and biochemically define the physiologically most relevant system-specific inducer for EnuR. We identify it here as *N*-(α)-ADABA, a highly specific intermediate of ectoine catabolism (Schwibbert *et al.*, 2011; Schulz *et al.*, 2017) (Fig. 1). The hydroxyectoine/ectoine import and catabolic gene cluster of *R. pomeroyi* DSS-3 contains a gene (*asnC*) (Fig. 1) encoding a member of the *feast-and-famine* class of transcriptional regulators (Yokoyama *et al.*, 2006). We found that the AsnC protein is essential for the ability of *R. pomeroyi* DSS-3 to use ectoine as a carbon source. Finally, the tetrahydropyrimidines ectoine and hydroxyectoine contain two nitrogen atoms (Fig. 1), and thus are particularly valuable compounds in nutrient-deprived ecosystems (Lidbury *et al.*, 2014; 2015; Taubert *et al.*, 2017). We discovered through transposon mutagenesis that the two-component NtrYX regulatory system (Fernandez *et al.*, 2017) is a key player in the use of ectoines as nutrients by *R. pomeroyi* DSS-3. In conjunction with extensive database searches, the physiological and molecular data reported here for the model system *R. pomeroyi* DSS-3 have important implications for an understanding of the consumption of ectoines in general, and paint a rather complex picture of the genetic control of this ecophysiologically relevant catabolic process.

Results

Ectoine- and hydroxyectoine-mediated induction of import and catabolic genes

To study the expression of the hydroxyectoine/ectoine uptake and catabolic genes (Fig. 1), we used three previously constructed transcriptional *lacZ* reporter fusions (Schulz *et al.*, 2017). Plasmid pBAS19 carries the promoter present in front of *enuR*, while plasmid pBAS21 carries the promoter present in front of the *uehA* transporter gene. Plasmid pBAS20 carries the same *uehA-lacZ* operon fusion as plasmid pBAS21 but harbours, in addition, an intact *enuR* gene that is expressed from its native promoter (Fig. 2A). These three reporter plasmids were introduced via conjugation into the *R. pomeroyi* strain J470 (Supporting Information Table S1), a rifampicin-resistant derivative of the wild-type isolate DSS-3 (Moran *et al.*, 2004; Todd *et al.*, 2012) and used them to evaluate the influence of an external supply of ectoines on the transcriptional activity of the *enuR* and *uehA* promoters. Growth of the cells in a glucose and ammonium based minimal medium resulted only in very low expression levels (approximately 20 Miller Units) of either the *enuR-lacZ* and *uehA-lacZ* reporter fusions (Fig. 2B). We observed that the promoter in front of *enuR* was not responsive to the presence of ectoines, while the transcriptional activity of the *uehA* promoter was strongly substrate inducible (Fig. 2B). Ectoine induced the expression of the *uehA-lacZ* reporter fusion present on plasmid pBAS21 30-fold, and adding hydroxyectoine to the growth medium led to a 64-fold increased expression level. The corresponding values for the induction of *uehA-lacZ* gene expression in a strain carrying the reporter plasmid pBAS20 (*enuR*$^+$) are 41-fold (for ectoine) and 95-fold (for hydroxyectoine), respectively (Fig. 2B). Hence, hydroxyectoine seems to be a more potent inducer of *uehA-lacZ* transcription. This phenomenon was particularly notable when these cells carried the *enuR*$^+$ plasmid pBAS20 (Fig. 2B).

We, and others, have recently shown that EnuR (= EhuR) serves as a repressor for ectoine catabolism (Schulz *et al.*, 2017; Yu *et al.*, 2017). Therefore, it came somewhat as a surprise that the *uehA-lacZ* reporter fusion present on the *enuR*$^+$ plasmid pBAS20 exhibited higher induction levels in response to ectoines in comparison with plasmid pBAS21 that lacks an intact *enuR* regulatory gene (Fig. 2A and B). Furthermore, *R. pomeroyi* J470 that was used as a background strain for the *lacZ* reporter fusion experiments carries itself an intact chromosomal copy of

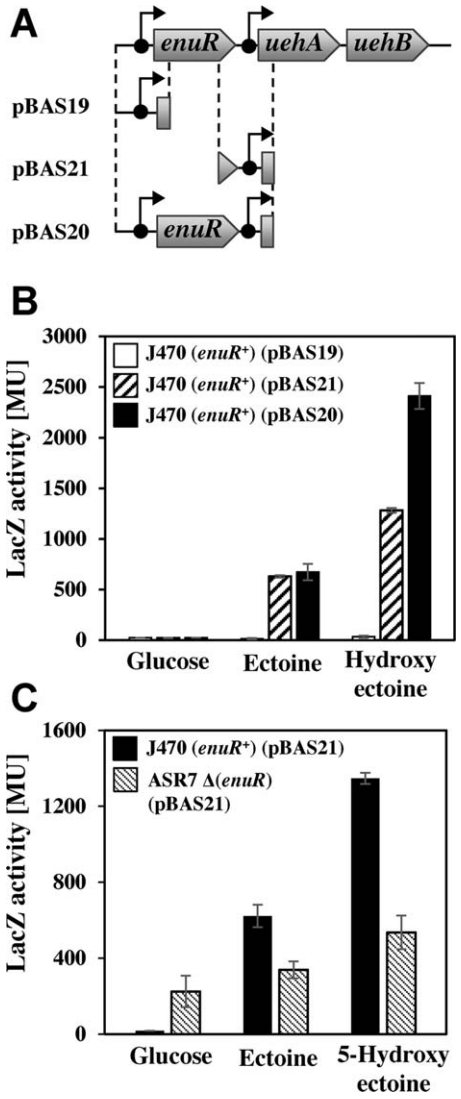

Fig. 2. Substrate induction of *uehA-lacZ* expression and role of EnuR. (A) Genetic make-up of the DNA fragments used to construct *enuR-lacZ* and *uehA-lacZ* gene fusions using the *lacZ* reporter plasmid pBIO1878 (Todd *et al*., 2012). The approximate positions of the so-far unidentified promoters present in front of *enuR* and *uehA* (Schulz *et al*., 2017) are indicated by the arrows. (B) Transcriptional activity of *enuR-lacZ* and *uehA-lacZ* reporter fusions in response to ectoine or hydroxyectoine availability in the growth medium in the *enuR*$^{+}$ wild-type strain J470, a Rif^{R}-derivative of *R. pomeroyi* DSS3. (C) Comparison of *uehA-lacZ* reporter fusion activity in the wild-type strain J470 and its Δ(*enuR*) mutant derivative strain ASR7.

the *enuR* gene. Hence, either EnuR possesses both repressor and activator functions as previously reported for GabR (Belitsky and Sonenshein, 2002; Belitsky, 2004; Edayathumangalam *et al*., 2013), or alternatively, DNA-sequences located upstream of *uehA* required for full genetic control of the *uehA* promoter were removed during construction of plasmid pBAS21 (Fig. 2A).

We also assessed the influence of the chromosomal *enuR* gene on the activity of the *uehA-lacZ* reporter construct present on plasmid pBAS21 that itself does not harbour an intact *enuR* gene (Fig. 2A). When the *enuR* gene was disrupted (strain ASR7) in the chromosome of *R. pomeroyi*, the activity of the *uehA-lacZ* reporter fusion was high in cells grown in the absence of ectoines, a 13-fold increase over its isogenic *enuR*$^{+}$ parent strain J470 grown in the same glucose- and ammonium-based basal minimal medium (Fig. 2C). This is consistent with the notion that EnuR acts genetically as a repressor (Schulz *et al*., 2017; Yu *et al*., 2017). Induction of the reporter fusion by either ectoine or hydroxyectoine in a chromosomal *enuR* deletion strain was less prominent, but was not completely eliminated (Fig. 2C). This latter finding indicates that in addition to EnuR, other regulatory proteins might contribute to substrate induction of the *uehA-lacZ* reporter fusion expression.

Substrate-mediated induction of ectoine catabolism depends on a PLP co-factor covalently bound to EnuR

When EnuR is produced in *E. coli* as a recombinant protein, the affinity-purified EnuR has a strong yellow colour and possesses spectroscopic properties typical for PLP-containing proteins (Phillips, 2015; Schulz *et al*., 2017). The substitution of Lys-302, the residue to which the PLP molecule is attached, with a His residue resulted in a mutant protein (K302/H; EnuR*) that had lost its yellow colour and the characteristic spectroscopic properties of the wild-type protein (Schulz *et al*., 2017). We tested the influence of the K302/H amino acid substitution mutation on the regulatory properties of EnuR to assess the role played by the covalently attached PLP molecule for the substrate-mediated induction of the hydroxyectoine/ectoine transport and catabolic gene cluster.

To this end, we introduced the wild-type *enuR* gene (present on plasmid pBAS20) and its mutant *enuR** derivative (present on plasmid pBAS23) (Fig. 3A) into *R. pomeroyi* strains that either lacked or carried an intact chromosomal copy of the *enuR* gene. The *enuR*$^{+}$ gene present on pBAS20 was able to repress the elevated level of *uehA-lacZ* transcription observed in *enuR* mutant cells grown with glucose and ammonium (Fig. 2C) and allowed induction of promoter activity in response to the availability of ectoines (Fig. 3B). Not surprisingly, the same pattern of transcription was found in a strain carrying an additional intact chromosomal copy of *enuR*. In contrast, the presence of the *enuR** mutation on plasmid pBAS23 no longer allowed substrate induction, regardless of whether the chromosomal *enuR* gene was intact or not (Fig. 3B). The EnuR* protein thus behaves genetically as a dominant negative repressor and, unlike its EnuR wild-type counterpart, was unable to respond to the availability of ectoines

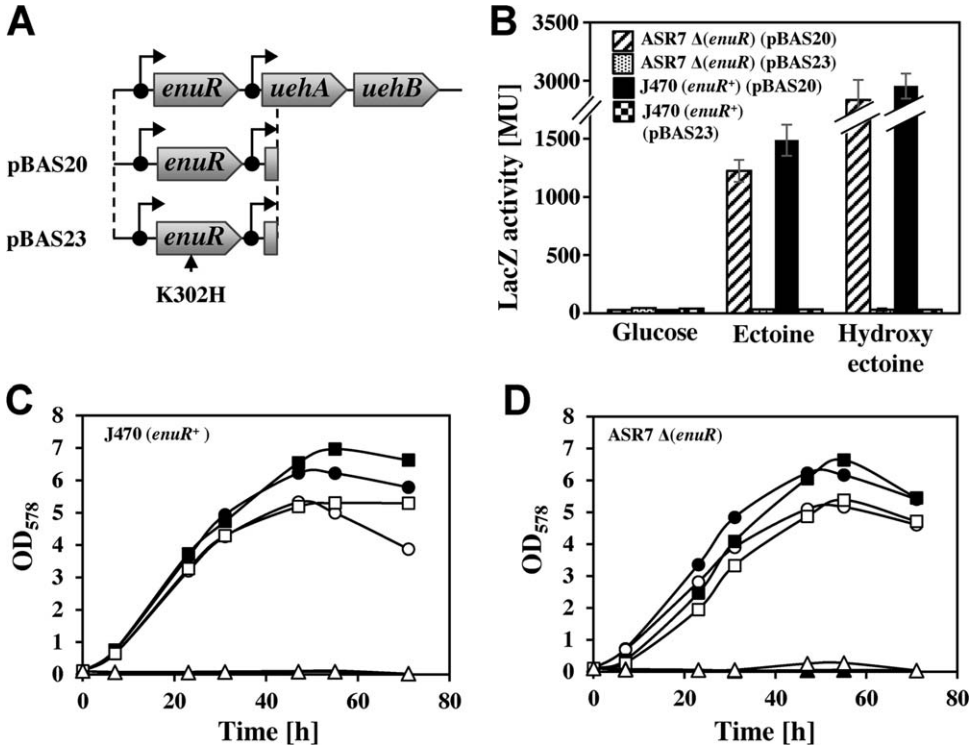

Fig. 3. Substrate induction of *uehA-lacZ* expression and the role of the mutant EnuR* protein on *uehA-lacZ* expression. (A) Genetic make-up of the DNA-fragments used to construct *uehA-lacZ* gene fusions using the *lacZ* reporter plasmid pBIO1878. Plasmid pBAS20 carries the wild-type *enuR* gene, whereas plasmid pBAS23 carries the Lys-302 to His *enuR** substitution mutation. (B) Transcriptional activity of *uehA-lacZ* reporter fusions in response to ectoine or hydroxyectoine availability in the growth medium in the wild-type strain J470 (*enuR*$^+$) or its Δ(*enuR*) mutant derivative strain ASR7 carrying plasmids with either an intact (pBAS20) or mutant (*enuR**) (pBAS23) *enuR* gene. (C) Growth of the *enuR*$^+$ *R. pomeroyi* wild-type strain J472 in basal minimal medium with either ectoine (black symbols) or hydroxyectoine (open symbols) carrying either the empty fusion vector pBIO1878 (open and closed circles), the *enuR*$^+$ plasmid pBAS20 (open and closed squares), or the *enuR** plasmid (open and closed triangles). (D) The same growth conditions and plasmid-bearing strains were used as described in (C), except that the genetic background of the host strain ASR7 carries a chromosomal Δ(*enuR*) mutation.

in the growth medium (Fig. 3B). The properties of EnuR* to act as a dominant negative repressor were also manifested when we analysed the effects of the *enuR** mutation on the growth of both *enuR*$^+$ and *enuR* mutant *R. pomeroyi* cells harbouring either plasmid pBAS20 (*enuR*$^+$) or pBAS23 (*enuR**). In both genetic backgrounds, use of ectoines as joint carbon and nitrogen sources was no longer possible when the cells carried pBAS23 (*enuR**) while the presence of the *enuR*$^+$ plasmid pBAS20 permitted growth of *R. pomeroyi* cultures to high optical densities (OD_{574} values between approximately 5 and 7) (Fig. 3C and D).

Identification of internal inducers of the EnuR regulatory protein

MocR/GabR-type regulators (Suvorova and Rodionov, 2016) that possess a covalently attached PLP molecule depend on a system-specific effector molecule to alter their regulatory properties; e.g., GABA for GabR, taurine (or derivatives of it) for TauR, and a dipeptide for DdlR (Wiethaus *et al.*, 2008; Takenaka *et al.*, 2015; Park *et al.*, 2017; Wu *et al.*, 2017). We set out to identify the system-specific effector molecule for EnuR. To detect and quantify ligand binding by the purified EnuR protein, we used microscale thermophoresis (MST), a method that traces the movement of fluorescently labelled proteins in a temperature gradient in response to the presence of a ligand (Duhr and Braun, 2006; Wienken *et al.*, 2010).

The chemistry underlying the formation of the internal and external aldimine depends on the presence of a primary amino group in the system-specific effector molecule (Takenaka *et al.*, 2015; Suvorova and Rodionov, 2016; Park *et al.*, 2017; Wu *et al.*, 2017). Neither ectoine nor hydroxyectoine possess such a primary amino group (Fig. 1) and consequently, neither one of them bound to the purified EnuR protein when we tested concentrations up to 10 mM in MST experiments (Supporting Information Fig. S1). Inspection of the hydroxyectoine/ectoine catabolic route revealed that the cleavage of the ectoine ring by the EutD hydrolase generates *N*-(α)-acetyl-2,4-diaminobutyric acid [*N*-(α)-ADABA], the first metabolite possessing a

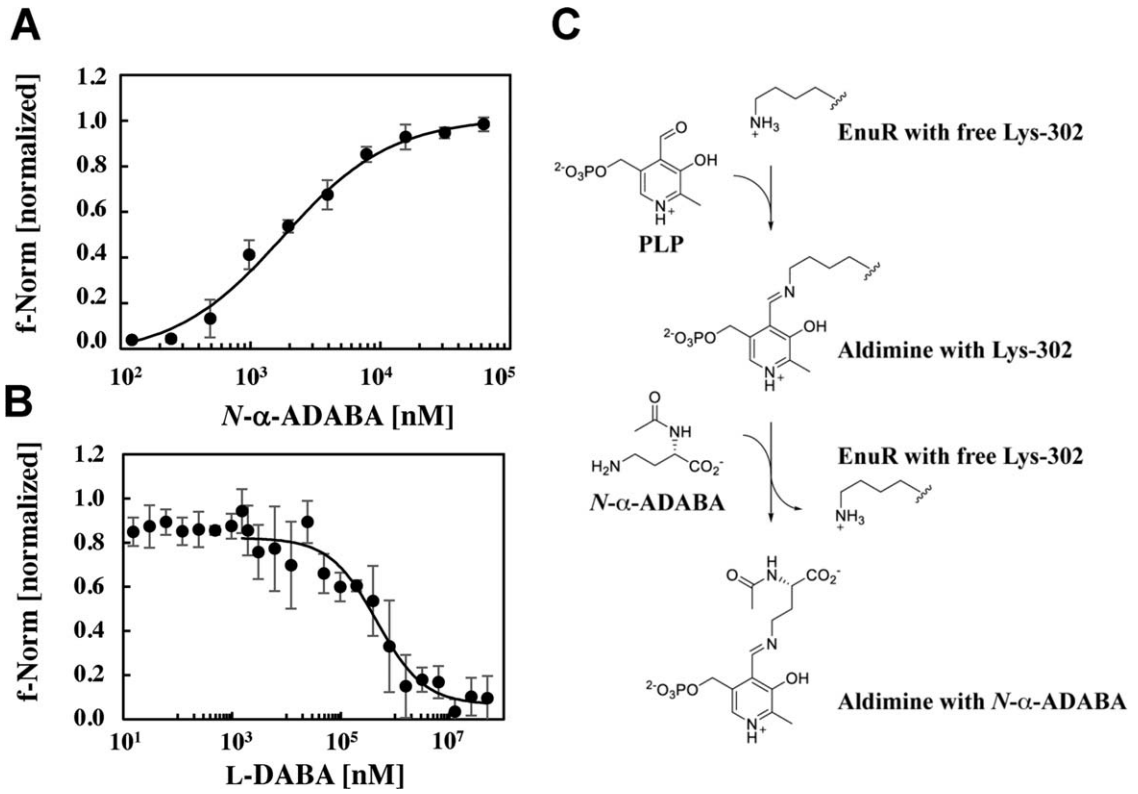

Fig. 4. Ligand binding by the wild-type EnuR protein. Purified EnuR protein (200 nM) was incubated with increasing concentrations of (A) *N*-(α)-ADABA, or (B) DABA, and the ability of these compounds to bind to the EnuR was assessed by microscale thermophoresis. (C) Proposal for the PLP-dependent and *N*-(α)-ADABA-triggered formation of initially the internal and subsequently the external aldimine in EnuR. PLP is initially bound in this sequence of chemical reactions by the side-chain of Lys-302 present in the carboxy-terminal aminotransferase domain of EnuR (Schulz *et al.*, 2017). This scheme was adapted from data reported for the MocR/GabR-type regulators GabR and DdlR that respond to the availability of GABA and a di-peptide (D-alanyl-D-alanine), respectively (Edayathumangalam *et al.*, 2013; Okuda *et al.*, 2015a,b; Takenaka *et al.*, 2015; Park *et al.*, 2017; Wu *et al.*, 2017).

primary amino group (Fig. 1). To the best of our knowledge, *N*-(α)-ADABA is exclusively generated during ectoine catabolism, making this compound an interesting candidate as system-specific effector molecule for EnuR. Indeed, ligand-binding measurements in MST experiments revealed strong binding of this metabolite by EnuR with a K_d of 1.7 ± 0.3 μM (Fig. 4A). Importantly, the EnuR* mutant protein was unable to bind *N*-(α)-ADABA, even at a concentration of 1 mM (Supporting Information Fig. S1).

The isomer of the high affinity EnuR ligand *N*-(α)-ADABA, *N*-(γ)-ADABA, is an intermediate in ectoine biosynthesis (Fig. 1) and serves as the main substrate for the ectoine synthase (EctC) (Ono *et al.*, 1999; Widderich *et al.*, 2016a). In some ectoine consumers (e.g., *Halomonas elongata*), *N*-(γ)-ADABA can apparently also be generated through the ectoine hydrolase (EutD/DoeA) as a by-product of the main chemical reaction (Fig. 1) (Schwibbert *et al.*, 2011). However, it is not clear so far whether this is only the case in the sub-group of hydroxyectoine/ectoine consumers that also synthesize ectoines as osmostress protectants; e.g., *H. elongata* (Schulz *et al.*, 2017). Given the close chemical relatedness of *N*-(α)-ADABA and *N*-(γ)-ADABA (Fig. 1), we also tested binding of *N*-(γ)-ADABA to EnuR by MST but detected no binding up to the highest concentration (1 mM) tested (Supporting Information Fig. S1).

Another intermediate of ectoine catabolism is L-2,4-diaminobutyric acid (DABA) (Fig. 1) which has been suggested to function as an inducer for the EnuR orthologue EhuR from *S. meliloti* (Yu *et al.*, 2017). We found that DABA is also recognized by the *R. pomeroyi* EnuR protein and determined a K_d of ligand binding of 457 ± 1 μM via MST (Fig. 4B), an approximately 230-fold reduction in ligand binding with respect to *N*-(α)-ADABA. Taken together, these ligand binding data identify *N*-(α)-ADABA (highly efficient) and DABA (moderately effective) as internal inducers for the EnuR regulatory protein, both of which are generated during ectoine catabolism (Fig. 1).

In silico and experimental analysis of the uehA regulatory region

Using comparative genomics and metabolic reconstruction, Suvorova and Rodionov (2016) recently analysed the

distribution of MocR/GabR-type regulators in a non-redundant set of 390 microbial genomes representing 43 diverse lineages of *Bacteria*. They predicted the putative operator binding sites of various sub-groups of this family of transcriptional regulators through bioinformatics. These authors also focused on EnuR-type proteins (referred to in their study as EutR) and suggested that they recognize a conserved inverted repeat DNA sequence as their operator sequences DNA-binding motif (Suvorova and Rodionov, 2016). We searched the 433 bp DNA-fragment (Fig. 5A) carried by the EnuR-responsive *uehA-lacZ* operon fusion plasmid pBAS21 for the presence of DNA sequences resembling the EutR consensus sequence proposed by Suvorova and Rodionov (2016). We found two possible operator binding sites for EnuR in the 97 bp intergenic region between the 3'-end of the *enuR* gene and the 5'-end of *uehA* (Fig. 5A). One of these putative operators (16 bp) adheres closely to the proposed consensus sequence. The five outermost base-pairs in each of the corresponding inverted repeat sequences match perfectly to the most conserved base-pairs in the consensus EutR-type operator sequence proposed by Suvorova and Rodionov (2016) by inspecting 69 microbial genome sequences (Fig. 5B). Six base-pairs downstream of this putative EnuR operator site, a second copy of a sequence resembling the consensus operator proposed by Suvorova and Rodionov (2016) is present, but it is two base-pairs longer (Fig. 5A and B). This second putative operator sequence contains an inverted repeat as well, where the five-outermost base-pairs in each of the inverted repeat structures match again perfectly to the most conserved base-pairs in the EutR consensus sequence (Fig. 5B).

DNase I footprinting analysis conducted to determine the binding site of the EnuR orthologue (EhuR) of the *S. meliloti ehuABCD-eutABCDE* promoter have also identified two operator sequences (Fig. 5B), one of which overlaps the putative −35 region of the promoter present in front of the *S. meliloti ehuA* gene (Yu *et al.*, 2017). These two EhuR operator sequences resemble each other closely and fit to the EutR-type consensus sequence defined by Suvorova and Rodionov (2016) from the analysis of 15 genome sequences of *Rhizobiales* (Suvorova and Rodionov, 2016) (Fig. 5B). Although not specifically mentioned in their report on ectoine utilization by *H. elongata* (Schwibbert *et al.*, 2011), this bacterium actually possesses an EnuR-related protein (34% sequence identity to EnuR from *R. pomeroyi*) whose structural gene is positioned next to the catabolic gene cluster. These authors mapped the transcriptional start site of the ectoine catabolic gene cluster (Schwibbert *et al.*, 2011) and we found through DNA-sequence inspection a putative EnuR binding site in its vicinity (Fig. 5B).

To provide further evidence that the intergenic region between the *enuR* and *uehA* genes of *R. pomeroyi* contains the operator(s) for EnuR, we carried out DNA-band-shift assays with affinity-chromatography-purified EnuR. The heterologous produced protein contained PLP, as judged by its intense yellow colour (Schulz *et al.*, 2017).

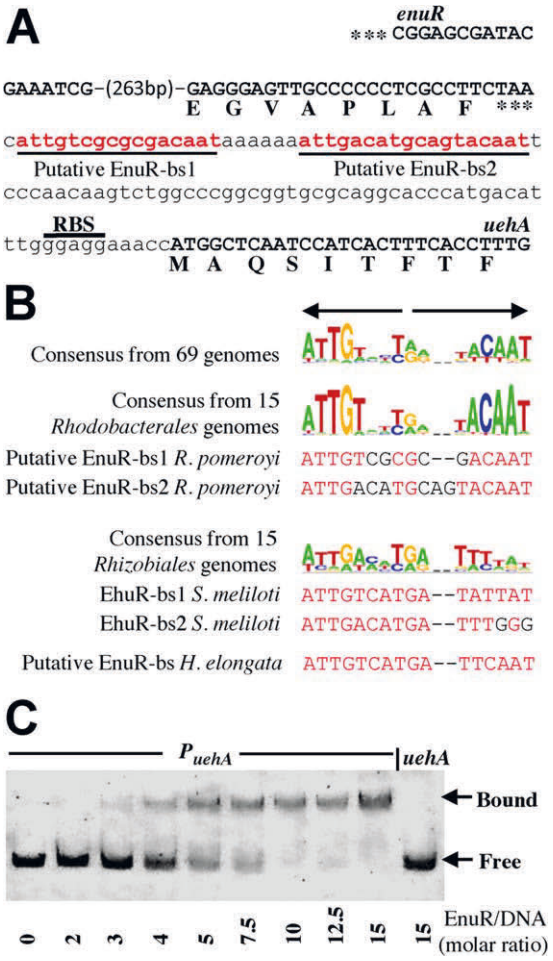

Fig. 5. *In silico* analysis of putative EnuR binding sites and interactions of EnuR with DNA. (A) DNA sequence of the 3'-end of the *enuR* gene, the *enuR-uehA* intergenic region and the beginning of the *uehA* gene. The end of the shown *uehA* DNA sequence corresponds to the *uehA/lacZ* junction present in the transcriptional *lacZ* reporter gene fusion plasmids pBAS20, pBAS21 and pBAS23. The predicted two EnuR binding sites and the ribosome-binding site (RBS) of the *uehA* gene are indicated. (B) DNA sequence logos of *in silico* predicted EutR-type binding-sites (Suvorova and Rodionov, 2016) and those for EnuR (this study), the EhuR protein from *S. meliloti* as determined by DNase I footprinting analysis (Yu *et al.*, 2017), and as identified by us from previously reported promoter-mapping experiments of the ectoine catabolic gene cluster of *H. elongata* (Schwibbert *et al.*, 2011). (C) Electrophoretic DNA-band-shift assays of a 251-bp DNA fragment with affinity-purified EnuR protein. 0.5 pmol of the fluorescently labelled DNA fragment carrying the *enuR-uehA* intragenic region was incubated with increasing concentrations of affinity-purified EnuR protein; subsequently, the DNA fragment incubated in the absence of EnuR and the formed DNA:EnuR complexes were electrophoretically separated and visualized by imaging. A 278-bp DNA fragment derived from the coding region of *uehA* that should not contain any EnuR binding sites was used as a control.

To this end, we incubated increasing EnuR concentrations with 0.5 pmol of a 251 bp DNA fragment that carries part of the 3'-end of the *enuR* gene, the 97 bp *enuR-uehA* intergenic region, and 14 codons of *uehA* and visualized the formed DNA:EnuR complexes after non-denaturing gel electrophoresis. DNA:EnuR complexes began to form with a concentration of EnuR as little as 75 nM (Fig. 5C). These interactions were specific, because there was no DNA mobility shift of a 0.5 pmol DNA fragment (278 bp) derived from the *uehA* coding region (Fig. 5C).

Influence of hydroxyectoine and ectoine importer and catabolic genes on uehA-lacZ reporter gene expression

The above reported data show that internal inducers, *N*-(α)-ADABA and DABA, for the EnuR regulatory protein are generated through the catabolism of ectoines. To study this issue further, we used a set of strains in which the hydroxyectoine/ectoine UehABC transporter system (Lecher *et al.*, 2009) or various catabolic genes (Schulz *et al.*, 2017) were defective and employed the transcriptional activity of the *uehA-lacZ* reporter fusion present on pBAS20 as a read-out for these experiments. First, we tested a strain (ASR6) in which the entire hydroxyectoine/ectoine importer and catabolic cluster was deleted and found that induction of *uehA-lacZ* expression in response to the presence of either ectoine or hydroxyectoine was no longer possible (Fig. 6A).

In a strain (ASR12) in which the *uehABC* transporter genes are intact but those for the catabolism of ectoines are deleted, reasonably good induction of gene expression by ectoine (8.6-fold in the mutant versus 14-fold in the wild-type) can be observed, whereas that afforded by hydroxyectoine is greatly diminished (8.3-fold in the mutant versus 64-fold in the wild-type) (Fig. 6B). A similar pattern of induction of *uehA-lacZ* expression was observed when only the *eutABC* genes were deleted; these genes are required for the growth of *R. pomeroyi* on 5-hydroxyectoine but not on ectoine (Supporting Information Fig. S2). The loss of the EutABC enzymes had a major impact on the induction of *uehA-lacZ* expression in response to the availability of hydroxyectoine whereas that afforded by the presence of ectoine was only moderately affected (Fig. 6C). When *eutD* was deleted (strain ASR8), a mutation that abolishes the use of both ectoines as nutrients (Supporting Information Fig. S2), induction of *uehA-lacZ* expression in response to ectoine occurred at a substantially reduced level (7.7-fold in the mutant versus 15.2-fold in the wild-type) but the strong induction of transcription afforded by hydroxyectoine (60-fold) was unaffected (Fig. 6D).

These findings are both surprising and informative in several aspects when one considers that the EutD enzyme is required to generate the internal inducers *N*-(α)-ADABA and DABA for EnuR (Figs. 1 and 4A and B). First, our observation that induction of gene expression (at least to some extent) in response to ectoine can still occur in an *eutD* mutant (Fig. 6D) and in a mutant in which all catabolic genes are deleted but in which those for the UehABC transporter were intact (Fig. 6B) indicates that genetic and

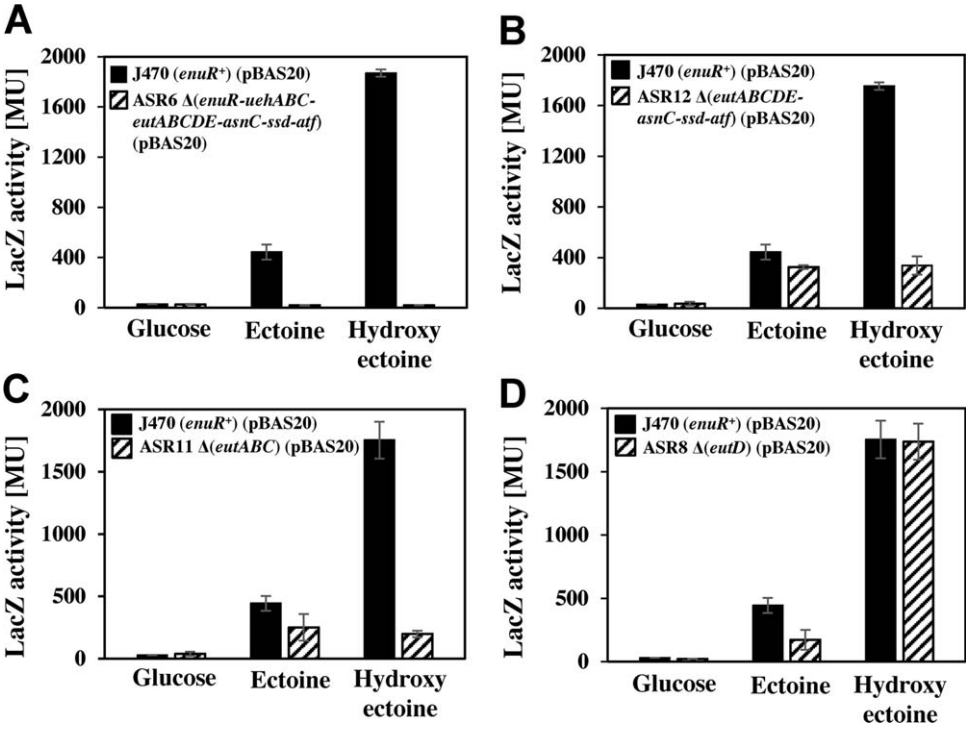

Fig. 6. Substrate induction of *uehA-lacZ* expression in response to hydroxyectoine and ectoine availability and the influence of various chromosomal mutations. The pattern of substrate induction of the *uehA-lacZ* reporter fusion present on plasmid pBAS20 by either hydroxyectoine or ectoine was assessed in strains carrying either (A) a complete deletion of the hydroxyectoine/ectoine importer and catabolic genes (strain ASR6), (B) the *ehuABC*$^{+}$*-eutABCDE-asnC-ssd-atf strain* ASR12, (C) the Δ(*eutABC*) mutant strain ASR11 and (D) the Δ(*eutD*) mutant strain ASR8.

physiological input into the regulatory system occurs beyond the generation of the internal inducers *N*-(α)-ADABA and DABA through ectoine catabolism. Second, our finding that induction of gene expression in response to hydroxyectoine occurs unabated in an *eutD* mutant, while that by ectoine is negatively affected (Fig. 6D), suggests that an internal inducer other than *N*-(α)-ADABA and DABA is generated through the break-down of hydroxyectoine. Indeed, loss of the *eutABC* gene not only abolished use of hydroxyectoine as a nutrient (Supporting Information Fig. S2) but simultaneously severely affected transcription of the *uehA-lacZ* reporter fusion as well (Fig. 6C). All these complex regulatory effects depend on the import of ectoine or hydroxyectoine (Fig. 6A and B).

The feast-and-famine regulator AsnC has a major influence on the expression of the importer and catabolic gene cluster

In most (494 out of the 539) of the importer and catabolic gene clusters of previously predicted microbial hydroxyectoine/ectoine consumers, a gene for the *feast-and-famine* type regulator AsnC is present (Schulz *et al.*, 2017) (Supporting Information Fig. S3). These types of proteins can form octamers wrapping their target DNA around them into a high-ordered tertiary nucleosome-like complex, and their DNA-binding properties are dictated through interactions with low-molecular-mass effector molecules, often amino acids (Yokoyama *et al.*, 2006; Shrivastava and Ramachandran, 2007; Kumarevel *et al.*, 2008; Kamensek *et al.*, 2015; Dey *et al.*, 2016). We have previously demonstrated that the deletion of the last two genes (*ssd-atf*) in the hydroxyectoine/ectoine catabolic operon (Fig. 1) is functionally substituted by other genes from *R. pomeroyi*, and has in essence no effect on the use of ectoines as nutrients (Fig. 7C). In contrast, the simultaneous deletion of the *asnC-ssd-atf* genes abolishes consumption of ectoine when it was provided as joint carbon and nitrogen source (Schulz *et al.*, 2017). We now found that AsnC was required for use of ectoine as sole carbon source but was dispensable for its use as sole nitrogen source (Fig. 7C). Collectively, these growth data imply an important regulatory role for the AsnC protein encoded in the *R. pomeroyi* 5-hydroxyectoine/ectoine importer and catabolic gene cluster.

Consistent with the previously reported growth data (Schulz *et al.*, 2017), we found that ectoine- or hydroxyectoine-mediated induction of *uehA-lacZ* expression in an *asnC*$^+$-Δ(*ssd-atf*) strain (ASR14) still reached about 66% (for ectoine) and 75% (for hydroxyectoine), respectively, of the level observed in a wild-type strain (Fig. 7A). In striking contrast, induction of *uehA-lacZ* expression in the Δ(*asnC-ssd-atf*) strain ASR10 by either ectoine or hydroxyectoine was reduced substantially further, reaching approximately 50% of the wild-type level with ectoine, and only 16% with hydroxyectoine (Fig. 7B). This strong positive influence of the AsnC regulatory protein on transcription of the importer and catabolic gene cluster is reflected by the inability of the *asnC* mutant to exploit ectoine as sole carbon source (Fig. 7C).

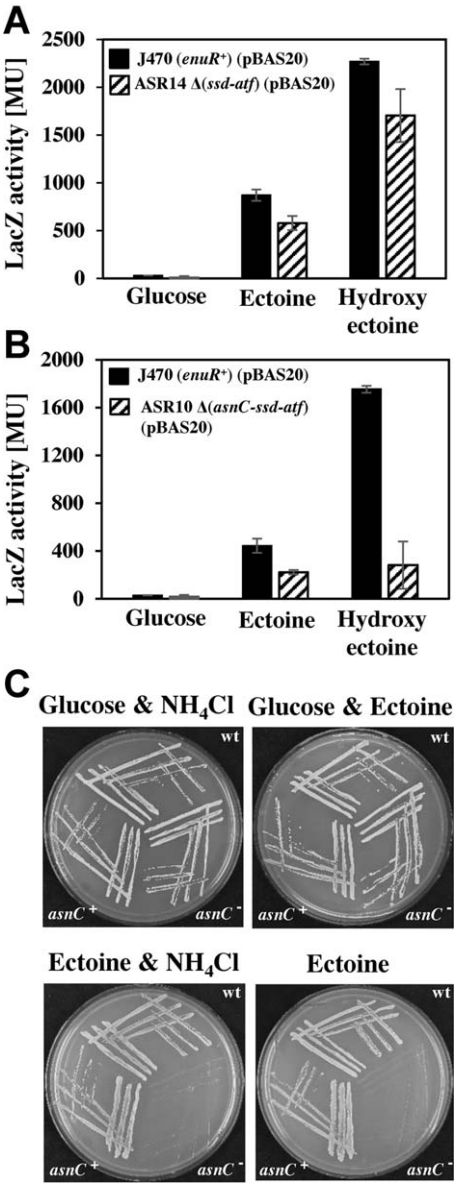

Fig. 7. Role of the AsnC regulator for substrate-mediated induction of *uehA-lacZ* expression and the use of ectoine as a nutrient. The pattern of substrate induction of the *uehA-lacZ* reporter fusion present on plasmid pBAS20 by hydroxyectoine or ectoine was assessed in strains carrying either a chromosomal (A) Δ(*ssd-atf*) mutation (strain ASR14) or (B) a strain (ASR10) in which the *asnC* gene was additionally deleted [Δ(*asnC-ssd-atf*)]. (C) Use of ectoine as nutrient by the *R. pomeroyi* wild-type strain J470 (WT), strain ASR14 [*asnC*$^+$-Δ(*ssd-atf*)] (*asnC*$^+$) and strain ASR10 [Δ(*asnC-ssd-atf*)] (*asnC*$^-$).

Regulatory input of the nitrogen-sensing NtrYX two-component system into the genetic control of import and catabolism of ectoines

The tetrahydropyrimidines hydroxyectoine and ectoine are nitrogen-containing compounds (Fig. 1) and can be used by *R. pomeroyi* as sole sources of this essential element (Schulz *et al.*, 2017) (Fig. 7C). We, therefore, wondered if the expression of the hydroxyectoine and ectoine import and catabolic gene cluster would be under the genetic control of sensory systems monitoring the availability of nitrogen-containing compounds in the environment. To search for such regulatory systems, we carried out a transposon mutagenesis of *R. pomeroyi* DSS-3 using the EZ-Tn*5*^{TM} transposition system (Epicenter, Madison, USA) (Goryshin and Reznikoff, 1998) and searched the resulting EZ-Tn*5*^{TM} transposon insertion collection for mutant strains unable to use ectoine as a nutrient on agar plates where ectoine was the sole available carbon and nitrogen source. From approximately 21 000 colonies that were inspected, we identified three colonies with a defect in ectoine utilization. Molecular analysis showed that these three strains contained the EZ-Tn*5* transposon at the same position in codon 189 of the *ntrY* gene (Fig. 8A). The recovered *ntrY*::EZ-Tn*5* insertion mutants thus either are siblings or result from a hot-spot of Tn*5* integration into the *R. pomeroyi* chromosome. The *ntrY* gene encodes a 762-amino-acid-comprising integral membrane protein that serves as the sensor-kinase for a two-component regulatory system (NtrYX) implicated, among several other cellular processes, in the catabolism of nitrogen-containing compounds (Fernandez *et al.*, 2017). On further molecular analysis, we found that the *ntrY*::EZ-Tn*5* insertion mutant strains obtained in the above described genetic screen contained multiple EZ-Tn*5* copies, making it impossible to employ these strains for clean genetic and physiological studies.

Taking the data from the transposon mutagenesis as a lead, we constructed a genetically precisely defined chromosomal deletion/insertion mutation (strain ASR9) destroying the NtrYX system entirely [Δ(*ntrYX::Gm*^{R})1] through recombinant DNA techniques. We found that this engineered mutation abolished the use of ectoine as sole carbon source but still permitted the use of ectoine as sole nitrogen source (Fig. 8B). We introduced the *uehA-lacZ* reporter fusion plasmid pBAS20 into the [Δ(*ntrYX::Gm*^{R})1] mutant strain ASR9 and studied the influence of this gene disruption mutation on the transcriptional activity of the *uehA* promoter in response to the availability of ectoines. The transcriptional profile of strain ASR9 (pBAS20) differed significantly from that of the wild-type strain. Loss of the NtrYX two-component regulatory system allowed only a reduced level of induction of gene expression, with the inducing effects of hydroxyectoine being the most strongly affected (Fig. 8C). We note, that the remaining level of transcription of these genes in the absence of the NtrYX system (Fig. 8C) was insufficient to allow *R. pomeroyi* the use of ectoines as the sole carbon source (Fig. 8B).

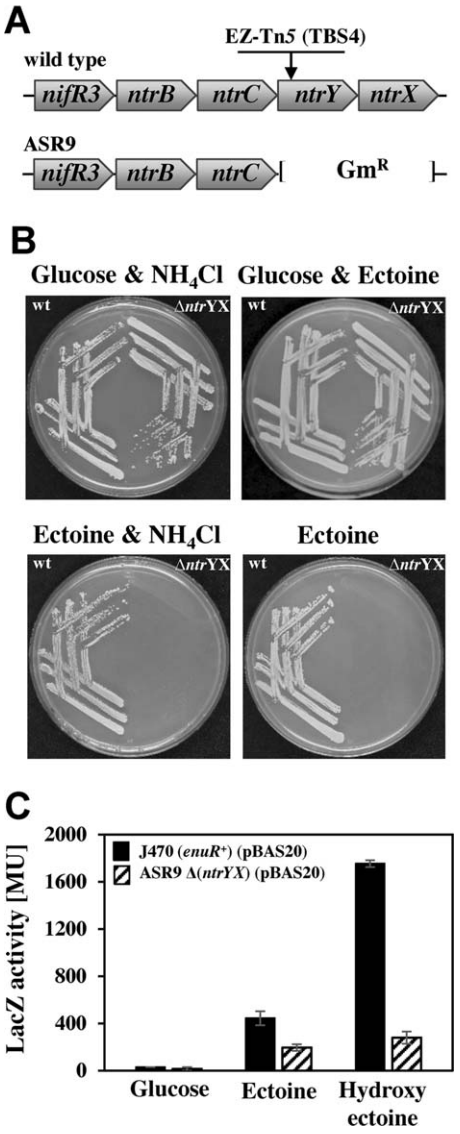

Fig. 8. Role of the NtrXY two-component regulatory system for growth of *R. pomeroyi* on ectoine and substrate-mediated induction of *uehA-lacZ* expression. (A) Genetic organization of the *nifR3-ntrB-ntrC-ntrY-ntrX* region of the *R. pomeroyi* genome (Moran *et al.*, 2004), the position of the *ntrY*::EZ-Tn*5* insertion in strains unable to use ectoine as nutrients, and the *in vitro* constructed Δ(*ntrYX::Gm*^{R}) deletion mutation in strain ASR9. (B) Growth of the *R. pomeroyi* wild-type strain J470 and its Δ(*ntrYX::Gm*^{R}) mutant derivative (strain ASR9) on basal minimal medium agar plates containing 28 mM ectoine when used either as sole carbon or nitrogen source. When the use of ectoine as joint carbon and nitrogen sources was tested, the plates contained 56 mM ectoine. (C) The pattern of substrate induction of the *uehA-lacZ* reporter fusion present on plasmid pBAS20 by either hydroxyectoine or ectoine was assessed either in the wild-type strain J470 or in its Δ(*ntrYX::Gm*^{R}) mutant derivative strain ASR9.

R. pomeroyi can exploit the osmolytes glycine betaine and choline as nutrients (Lidbury *et al.*, 2015). We found that the disruption of the NtrYX system has no influence on the use of these nitrogen-containing compounds when they were tested either as sole carbon or nitrogen sources (Supporting Information Fig. S4).

Discussion

The co-occurrence of microbial hydroxyectoine/ectoine producers and consumers in the same habitat (Schwibbert *et al.*, 2011; Widderich *et al.*, 2014; 2016b; Schulz *et al.*, 2017) drives ecophysiological relevant networks of synthesis, release and catabolism of compounds that are produced in abundance by many osmotically stressed bacterial cells (Pastor *et al.*, 2010; Kunte *et al.*, 2014; Widderich *et al.*, 2014). For the exploitation of externally provided ectoines as nutrients, it is essential that the consumers can sensitively detect the presence of these compounds in their surroundings (Welsh, 2000; Mosier *et al.*, 2013; Warren, 2014; 2016), so that they can trigger enhanced expression of those genes whose products mediate import and catabolism of ectoines (Jebbar *et al.*, 2005; Lecher *et al.*, 2009; Schwibbert *et al.*, 2011; Schulz *et al.*, 2017; Yu *et al.*, 2017).

The data presented here address this issue in the metabolically versatile marine bacterium *R. pomeroyi* DSS-3 (Luo and Moran, 2014) and identify three regulators that contribute to the transcriptional control of hydroxyectoine/ectoine import and catabolism: the GabR/MocR-type repressor EnuR, the *feast-and-famine*-type regulator AsnC, and the two-component regulatory system NtrYX (Fig. 9A). In Supporting Information Fig. S3, we have projected onto a EutD-based phylogenetic tree (Schulz *et al.*, 2017) the distribution of these three regulators among 539 proteobacterial potential consumers of ectoines. There is considerable overlap between the distribution of *enuR*, *asnC* and *ntrYX* genes in the genomes of ectoine-consuming microorganisms (Fig. 9B), and notably, a very substantial group (about 45%) of them possesses all three regulators (EnuR, AsnC, NtrYX). While the *enuR* and *asnC* genes are widely distributed among all branches of ectoine-degrading *Proteobacteria*, the *ntrYX* genes are notably restricted to all ectoine-consuming members of the *Alphaproteobacteria* (Supporting Information Fig. S3). However, it appears from additional database searches that the presence of the NtrYX system is a common trait in *Alphaproteobacteria* and this includes also species unable to catabolize ectoines.

Our genetic and molecular data identify EnuR as a key regulator for the use of ectoines as nutrients. Not only is the *enuR* gene commonly (85%) associated with hydroxyectoine/ectoine catabolic gene clusters (Fig. 9 and Supporting Information Fig. S3), its regulatory function

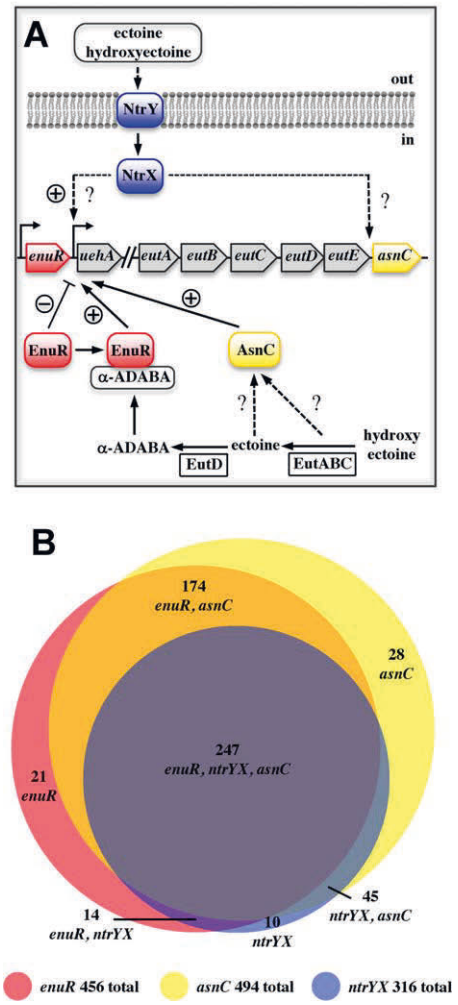

Fig. 9. Distribution of *enuR*, *asnC* and *ntrXY* genes in predicted hydroxyectoine/ectoine consumers and a working model for genetic regulation of hydroxyectoine/ectoine uptake and catabolic genes. (A) Working model for the genetic control of hydroxyectoine/ectoine uptake and catabolic genes in *R. pomeroyi*. (B) A previously assembled dataset of 539 predicted hydroxyectoine/ectoine consumers, all of which belong to the *Proteobacteria* (Schulz *et al.*, 2017) (Supporting Information Fig. S3), were inspected for the presence of *enuR*-type genes in the vicinity of the hydroxyectoine/ectoine uptake and catabolic gene clusters, for the presence of *asnC*-type genes within these gene clusters, and for the presence of *ntrXY*-type genes elsewhere in the genome sequences of this group of microorganisms.

also depends on an effector molecule [*N*-(α)-ADABA] that is exclusively generated during ectoine catabolism (Fig. 1). EnuR is a member of the widely distributed family of MocR/GabR-type transcriptional regulators (Bramucci *et al.*, 2011; Suvorova and Rodionov, 2016), and like other members of this family contains a covalently attached PLP co-factor in its carboxy-terminal aminotransferase domain (Schulz *et al.*, 2017). We found that the bound PLP is indispensable for the recognition of the *N*-(α)-ADABA effector molecule (Fig. 4A and Supporting Information Fig. S1) and

for the ability of this internal inducer to relieve EnuR-mediated repression of transcription (Fig 3B). Not surprisingly, the residue to which the PLP co-factor is attached (corresponding to K302 in the *R. pomeroyi* EnuR protein) is strictly conserved in an alignment of 456 EnuR-type proteins. Consistent with data reported for the EnuR orthologue of *S. meliloti* (Yu *et al*., 2017), DABA serves also as an inducer for the EnuR protein of *R. pomeroyi*. However, the binding affinities of EnuR for DABA are substantially reduced (about 230-fold) in comparison with *N*-(α)-ADABA (Fig. 4A and B). *N*-(α)-ADABA can thus be regarded as the primary internal inducer for hydroxyectoine/ectoine uptake and catabolism.

Apart from the high affinity of EnuR for *N*-(α)-ADABA, this compound has the additional advantage of being a specific ectoine-derived metabolite (Fig. 1), whereas DABA occurs also as an intermediate in other metabolic and biosynthetic processes in microorganisms (Ikai and Yamamoto, 1997; Du *et al*., 2013; Fidalgo *et al*., 2016), including the biosynthesis of ectoine (Ono *et al*., 1999) (Fig. 1). In the K302/H substitution variant of EnuR (EnuR*), the covalent attachment of the PLP molecule is no longer possible (Schulz *et al*., 2017). As shown here, this turns the EnuR* mutant protein into a negative dominant super-repressor unable to respond to externally provided ectoines (Fig 3B). EnuR* apparently binds to DNA *in vivo* so tightly that the use of ectoines as nutrients is abolished (Fig. 3C and D). The pairing of the EnuR repressor with the attached PLP co-factor and ectoine-derived metabolites [*N*-(α)-ADABA and DABA] establishes a sensitive intracellular trigger to relieve EnuR-mediated repression. In contrast to *N*-(α)-ADABA, its isomer *N*-(γ)-ADABA is not bound by EnuR (Supporting Information Fig. S1C). This is a significant finding as *N*-(γ)-ADABA is an intermediate in ectoine biosynthesis (Fig. 1) (Ono *et al*., 1999; Widderich *et al*., 2016a). This discovery is particularly relevant for the substantial group of microorganisms that are capable of both ectoine synthesis and catabolism (Schwibbert *et al*., 2011; Schulz *et al*., 2017).

Recent detailed biochemical and structural studies with the PLP-containing and GABA-responsive GabR regulatory protein from *B. subtilis* (Edayathumangalam *et al*., 2013) have significantly enhanced our understanding of the roles played by the PLP molecule and the respective system-specific inducer of MocR/GabR-type regulators (Okuda *et al*., 2015a,b; Park *et al*., 2017; Wu *et al*., 2017). The side chain of K312 of GabR forms an internal aldimine with PLP and further chemical reactions of the system-specific inducer GABA with the bound PLP molecule leads to a formation of a PLP-GABA adduct (the external aldimine) with the concomitant release of PLP from the side chain of K312. This sequence of events triggers a structural transition in the entire regulatory protein affording a change in GabR-mediated regulation of transcription (Park *et al*., 2017; Wu *et al*., 2017). The GabR protein is a head-to-tail dimer (Edayathumangalam *et al*., 2013) and the structural transitions caused by the formation of the external aldimine have recently been captured in the crystal structure of the GabR carboxy-terminal effector binding/oligomerization domain where one of the monomers contains the internal aldimine and the other subunit harbours the external aldimine (Park *et al*., 2017).

Based on the extensive studies of PLP-mediated inducer binding by GabR, and related studies with the D-alanyl-D-alanine-responsive MocR/GabR-type regulator DdlR from *Bacillus brevis* (Takenaka *et al*., 2015), we propose here that the basal form of EnuR containing the internal aldimine between K302 and PLP changes to an external aldimine form when *N*-(α)-ADABA is produced through ectoine catabolism and binds to the K302-attached PLP co-factor. The ensuing conformational change of EnuR will then trigger changes in the DNA-binding properties of this regulatory protein, thereby causing an increase in transcription of the hydroxyectoine/ectoine uptake and catabolic gene cluster (Fig. 4C). A similar reaction scheme can readily be envisioned for the secondary internal inducer of EnuR, DABA, as well (Fig. 1).

Without the proper functioning of the *eutD*-encoded ectoine hydrolase, the internal inducers *N*-(α)-ADABA and DABA cannot be formed through the catabolism of ectoine. The catabolism of hydroxyectoine is envisioned to proceed through the transient formation of ectoine (Fig. 1). It follows from the proposal of this catabolic route (Schulz *et al*., 2017) that an external supply of hydroxyectoine should no longer lead to the expression of the *ueh-lacZ* reporter gene fusion if its inducing effect is also dependent on EnuR and the EutD-generated formation of *N*-(α)-ADABA and DABA. However, in contrast to expectations, there is strong induction of *ueh-lacZ* transcription in response to hydroxyectoine in a *eutD* mutant strain (Fig. 6D). Interestingly, induction by hydroxyectoine is largely abolished in a strain lacking the *eutABC* genes (Fig. 6C), which encode the enzymes required for conversion of hydroxyectoine to ectoine and growth of *R. pomeroyi* on hydroxyectoine as the sole carbon, nitrogen and energy source (Supporting Information Fig. S2). In agreement with the proposed overall route for the catabolism of ectoines (Schulz *et al*., 2017) (Fig. 1), loss of the EutABC enzymes still permits utilization of ectoine as a nutrient (Supporting Information Fig. S2). Ectoine also still triggers the induction of *uehA-lacZ* reporter gene expression in the corresponding mutant strain, albeit at a somewhat reduced level (Fig. 6C), a phenomenon that might be caused by a partially polar effect of the *eutABC::Gm*^{R} deletion/insertion mutation on the transcription of the down-stream located ectoine catabolic genes (Fig. 1).

The internal inducer generated from the catabolism of hydroxyectoine through the enzymatic activities of the

EutABC proteins is substantially more potent than the EnuR ligands *N*-(α)-ADABA and DABA (Figs. 2B, C, and 6A). Notably, induction of *ueh-lacZ* reporter gene expression by hydroxyectoine is greatly reduced in a Δ(*asnC-ssd-atf*) mutant strain (Fig. 7B), while an external supply of this compound triggers a very strong induction of the reporter fusion in a *asnC*$^{+}$-Δ(*ssd-atf*) strain (Fig. 7A). Combined with our finding that induction of *ueh-lacZ* expression is dependent on the activity of the EutABC enzymes (Fig. 6C), we are left with the conclusion that the metabolism of hydroxyectoine generates a compound(s) that might serve as an effector molecule for AsnC (Fig. 9B). Ligand binding assays with AsnC are required to verify or refute this genetically derived hypothesis, experiments not easy to conduct since none of the predicted intermediates in hydroxyectoine catabolism to ectoine (Fig. 1) are commercially available.

AsnC exerts a clear activating influence on the expression of the *R. pomeroyi* hydroxyectoine/ectoine-importer and catabolic gene cluster. AsnC/Lrp-type proteins wrap DNA into nucleosome-like structures and frequently respond in their DNA-binding properties to low-molecular-mass effector molecules that are generated through metabolism (e.g., amino acids) (Shrivastava and Ramachandran, 2007; Kumarevel *et al*., 2008; Dey *et al*., 2016). In many cases, these proteins respond to *feast-and-famine* situations and thereby permit the efficient exploitation of sudden burst in the supply of a particular nutrient in fluctuating environmental settings (Yokoyama *et al*., 2006). Interestingly, Landa *et al*. (2017) recently reported a major remodelling of the *R. pomeroyi* DSS 3 transcriptome, depending whether this bacterium was co-cultivated with the dinoflagellate *Alexandrium tamarense* or the diatom *Thalassosira pseudonana*. Depending on which phytoplankton species dominated the co-culture, the ectoine uptake and catabolic genes were differentially expressed; the presence of the diatom triggered enhanced transcription of these genes, hinting to a *T. pseudonana*-derived source of ectoine for use as a nutrient by *R. pomeroyi* DSS 3 (Landa *et al*., 2017).

Initial DNA-binding studies with an AsnC orthologue (referred to as DeoX) of *H. elongata* revealed interaction(s) with the presumed regulatory region of the ectoine catabolic gene cluster (Schwibbert *et al*., 2011). Relevant to a discussion about the role of hydroxyectoine/ectoine catabolism associated AsnC-type proteins is the fact that AsnC/Lrp-type proteins can also work in concert with other types of regulators (Kamensek *et al*., 2015), a facet in gene regulation that probably becomes highly relevant for the large group of microbial ectoine consumers that possesses both EnuR and AsnC (about 85% in our data-set) (Fig. 9B). Nevertheless, 73 of 494 AsnC-containing representatives lack EnuR (Fig. 9B and Supporting Information Fig. S3), indicating that the regulatory roles played by EnuR and AsnC are not necessarily mutually interdependent.

The data presented here also identify a novel player (NtrYX) in the genetic control of hydroxyectoine/ectoine-catabolism by *R. pomeroyi* where this two-component regulatory system serves as a positive regulator of gene expression. Two-component regulatory systems such as NtrYX serve as major signalling devices of microorganisms through which information about changes in the environment are detected, processed and then transmitted to the transcriptional apparatus of the cell (Zschiedrich *et al*., 2016). The NtrYX system (Fig. 9A) has been implicated in a number of biologically rather varied cellular processes in *Alphaproteobacteria* [for a recent description of the NtrYX system and additional references see (Fernandez *et al*., 2017)], notably also in the metabolism and assimilation of nitrogen-containing compounds (Pawlowski *et al*., 1991; Carrica Mdel *et al*., 2012; Cheng *et al*., 2014; Bonato *et al*., 2016; Calatrava-Morales *et al*., 2017). Our data now subscribe a function to the NtrYX system of *R. pomeroyi* with respect to the catabolism of ectoine when it is used as sole carbon source while still allowing its use as sole nitrogen source (Fig. 8B). These differences in the use of ectoine as a nutrient by the *R. pomeroyi ntrYX* mutant might be caused by the facts that (i) more carbon than nitrogen units are required for growth and (ii) that a *ntrYX* deletion mutant is not completely deficient in the induction of the hydroxyectoine/ectoine import and catabolic gene cluster in response to both ectoines (Fig. 8C). We do not know yet whether the influence of the NtrYX system on the utilization of ectoines by *R. pomeroyi* are mediated through direct interactions of the unusual NtrC-type NtrX response regulator (Zschiedrich *et al*., 2016; Fernandez *et al*., 2017) with the regulatory region present in front of the *R. pomeroyi* hydroxyectoine/ectoine-uptake and catabolic gene cluster (Fig. 9A), or whether they are mediated indirectly through a so far undisclosed regulatory circuit (e.g., by controlling the expression of *asnC* or AsnC activity).

With the exception of the deletion that removes the hydroxyectoine/ectoine-importer and metabolic genes altogether, none of the single *enuR*, *asnC* and *ntrYX* gene disruption mutations abolishes hydroxyectoine/ectoine-responsive *uehA-lacZ* reporter gene expression entirely. These hints to multiple levels of input of ectoines into the signal perception and transduction process and the data reported here paint a rather complex picture of the finely tuned genetic control of hydroxyectoine/ectoine import and catabolism. In Fig. 9A, we present a regulatory scheme that is consistent with our experimental data and formulates experimentally testable hypothesis. The physical organization and the precise gene content of hydroxyectoine/ectoine uptake and catabolic gene clusters vary (Schwibbert *et al*., 2011; Schulz *et al*., 2017), indicating that alternatives to our proposal (Fig. 1) for the catabolism

of hydroxyectoine to ectoine likely exist in microorganisms (Schulz *et al*., 2017). The data and consideration we present here indicate that their transcriptional regulation probably entails variations of a common theme as well.

Experimental procedures

Chemicals

Ectoine was kindly provided by the bitop AG (Witten, Germany) and hydroxyectoine was purchased from Santa Cruz Biotechnology (Heidelberg, Germany). Anhydrotetracycline hydrochloride (AHT), desthiobiotin and Strep-Tactin Superflow chromatography material were obtained from IBA GmbH (Göttingen, Germany). The β-galactosidase substrate, o-nitrophenyl-β-*D*-galactopyranosid (ONPG), and the antibiotics gentamycin, spectinomycin, rifampicin and kanamycin were obtained from Serva (Heidelberg, Germany). Ampicillin was purchased from Carl Roth GmbH (Karlsruhe, Germany). The α- and γ-isomers of *N*-acetyl-L-2,4-diaminobutyric acid (ADABA) were prepared through alkaline hydrolysis of ectoine (Kunte *et al*., 1993) and their separation was accomplished through repeated chromatography on a silica gel column (Merck silica gel 60). The identity and purity of these compounds was established by thin-layer chromatography and nuclear magnetic resonance (^{1}H-NMR and ^{13}C-NMR) spectroscopy as detailed previously (Widderich *et al*., 2016a).

Media and growth conditions

Ruegeria pomeroyi strains (Supporting Information Table S1) were maintained on half-strength YTSS agar. When required, gentamycin was added to the agar plates. For all growth experiments, strains of *R. pomeroyi* were cultivated in defined basal minimal medium (Baumann *et al*., 1971). This medium had the following composition: 50 mM MOPS (pH 7.5), 200 mM NaCl, 10 mM KCl, 330 μM K_2HPO_4, 10 mM $CaCl_2$, 50 mM $MgSO_4$ and 100 μM $FeSO_4$. To this basal medium we added a stock solution (200-fold concentrated) of vitamin mixture A and vitamin mixture B. The final concentrations of the vitamins were for mixture A 39 μg l^{-1} biotin, 78 μg l^{-1} nicotinic acid, 78 μg l^{-1} lipoic acid and 78 μg l^{-1} folic acid and for mixture B 78 μg l^{-1} pantothenic acid, 78 μg l^{-1} pyridoxine, 78 μg l^{-1} thiamine, 78 μg l^{-1} 4-aminobenzoic acid and 1.6 μg l^{-1} cobalamin. We also added 0.1 mM methionine, 0.1 mM serine and 0.1 mM glutamate to the growth medium since, according to our experience, these amino acids significantly improved the growth of *R. pomeroyi* strains. Glucose (28 mM) and NH_4Cl (200 mM) were routinely used as the carbon and nitrogen sources for *R. pomeroyi* DSS-3 in liquid medium. When either ectoine or hydroxyectoine were used as combined carbon and nitrogen sources in liquid cultures, NH_4Cl and glucose were left out of the medium and ectoines were provided at a final concentration of 28 mM. When *R. pomeroyi* cells were plated on basal medium agar plates, glucose (28 mM) and NH_4Cl (56 mM) were used as carbon and nitrogen sources. When ectoine was tested as a carbon or nitrogen source on such agar plates, ectoine was used at a concentration of 28 mM as a substitute for glucose or NH_4Cl, and when it was simultaneously used as carbon and nitrogen source, we added 56 mM to growth media. When the use of choline or glycine betaine was tested as sole carbon or nitrogen sources, they were added to basal medium agar plates at a final concentration of 28 mM (when tested as sole carbon sources), at 56 mM (when tested as sole nitrogen sources), and at 84 mM (when tested as joint carbon and nitrogen sources). When applicable, the antibiotics gentamycin, spectinomycin, rifampicin, or kanamycin were added to liquid and solid media at concentrations of 20, 150, 20 and 80 μg ml^{-1} respectively. Liquid cultures of *R. pomeroyi* and agar plates streaked with this microorganism were grown at 30°C.

Plasmids containing the *enuR*$^{+}$ or *enuR** genes were routinely maintained in the *Escherichia coli* strain DH5α (Invitrogen, Karlsruhe, Germany) on LB agar plates containing ampicillin (100 μg ml^{-1}). Minimal Medium A (MMA) (Miller, 1972) containing 0.5% (w/v) glucose as the carbon source, 0.5% (w/v) casamino acids (0.5%), 1 mM $MgSO_4$ and 3 mM thiamine was used for cultivation of the *E. coli* B strain BL21 carrying plasmids pBAS3 (*enuR*$^{+}$) or pBAS17 (*enuR**) (Supporting Information Table S2) for the overproduction of the EnuR protein and its EnuR* mutant derivative (a K302/H amino acid substitution) (Schulz *et al*., 2017).

Bacterial strains and plasmids

The *E. coli* strain DH5α was used for routine cloning purposes and the *E. coli* B strain BL21 (DE3) (Stratagene, La Jolla, CA) was employed for the overexpression of the *R. pomeroyi enuR* gene and its mutant *enuR** derivative. The *R. pomeroyi* strain DSS-3 (Moran *et al*., 2004) was obtained from the German Collection of Microorganisms (DSMZ; Braunschweig, Germany), and a rifampicin-resistant (Rif^{R}) derivative of this isolate (strain J470) (Todd *et al*., 2012) was kindly provided by J. Todd and A. Johnston (University of East Anglia, United Kingdom). *E. coli* DH5α strains carrying the helper plasmid pRK2013 [Kan^{R}] (Figurski and Helinski, 1979) for conjugation experiments between *E. coli* and *R. pomeroyi*, and the *lacZ* reporter fusion plasmid pBIO1878 [Spc^{R}] (Todd *et al*., 2012) were also provided by these colleagues.

Recombinant DNA techniques and construction of plasmids

Chromosomal DNA of *R. pomeroyi* DSS-3 was isolated as described (Schulz *et al*., 2017). The High Pure Plasmid Isolation Kit (Roche, Mannheim, Germany) was used to isolate plasmid DNA from *E. coli* strains. Restriction endonucleases and DNA ligase were obtained from ThermoScientific (St. Leon-Rot, Germany) and used as suggested by the manufacturer. Chemically competent cells of *E. coli* were prepared and transformed as reported previously (Sambrook *et al*., 1989). To construct a *uehA-lacZ* reporter gene fusion that also carried the intact *enuR* gene, a 2.6-kb chromosomal DNA fragment from strain DSS-3 was amplified by PCR using Phusion DNA polymerase (Life Technologies, Darmstadt, Germany) and the custom-synthesized DNA primers LacZenuR_up_for and LacZuehA_PstI_rev (Supporting Information Table S3). After purification of this DNA fragment using the QIA Quick PCR Purification Kit (Qiagen, Hilden, Germany), it was digested with EcoR1 and Pst1 and ligated into the linearized broad-host-range *lacZ*-fusion vector pBIO1878 (Todd

et al., 2012) that had also been cut with these enzymes. This yielded the *enuR*$^{+}$*-uehA-lacZ* reporter plasmid pBAS20; it encompasses the complete *enuR* gene, the 97-bp *enuR-uehA* intergenic region and 28 bp of the *uehA* coding sequence. A variant of pBAS20 carrying a mutation [AAA/CAT] that leads to the substitution of K302 of EnuR by a H residue (EnuR*) was constructed through site-directed mutagenesis using the Q5 kit (New England Biolabs; USA) and custom-synthesized primers (Supporting Information Table S3); the resulting plasmid was pBAS23. The presence of the desired codon change and absence of other undesired alterations in the 2.6-kb genomic region present in pBAS23 was verified by DNA sequence analysis.

To construct a deletion of the *R. pomeroyi* chromosomal *ntrYX* gene cluster, 600-bp fragments located upstream and downstream of the respective genomic area (Fig. 8A) were amplified by PCR using custom synthesized primers (Supporting Information Table S3). A DNA fragment encompassing a gentamycin resistance cassette was amplified from plasmid p34S_Gm (Dennis and Zylstra, 1998). Using the Gibson assembly procedure (Gibson *et al.*, 2009), the three DNA fragments were cloned into the linearized (by cutting with EcoRI and XbaI) suicide vector pK18mobsacB (Kvitko and Collmer, 2011), which confers resistance to kanamycin. The resulting plasmid was pBAS41 and carries the Δ(*ntrXY::Gm*)1 mutation.

Construction of R. pomeroyi chromosomal gene disruption mutants

Plasmid pBAS41 [Δ(*ntrYX::Gm*)1] was conjugated via triparental mating by mixing the *E. coli* strain PRK2015 (pRK2013) [Kan^{R}] (Figurski and Helinski, 1979), and DH5α (pBAS41) [Kan^{R} Gm^{R}] and the Rif^{R} *R. pomeroyi* recipient strain J470 as detained previously (Schulz *et al.*, 2017). *R. pomeroyi* J470 trans-conjugants that had received plasmid pBAS41 were selected on 1/2 YTSS agar plates containing the antibiotics rifampicin and gentamycin; the integration of the Δ(*ntrYX::Gm*)1 gene disruption mutation into the chromosome via a double homologous recombination event was selected for by including 10% saccharose into the agar plates (Schulz *et al.*, 2017). The resulting Kan^{S} Gm^{R} trans-conjugates were evaluated via PCR for the presence of the chromosomal Δ(*ntrYX::Gm*) deletion/insertion mutation and loss of the wild-type *ntrYX* genes using chromosomal DNA as the template and DNA primers listed in Supporting Information Table S3; these hybridize to genomic regions flanking the *ntrYX* gene cluster. The Δ(*ntrYX::Gm*)1 mutation removes the overlapping genes *ntrX* and *ntrY* (3.695 bp) from the genome of *R. pomeroyi* strain J470 (Fig. 8A), with one deletion endpoint beginning at the GTG start codon of *ntrY* and the second deletion junction ending with the TAA stop codon of *ntrX*. This strain was named ASR9 (Supporting Information Table S1).

Mutagenesis with the EZ-Tn5 transposon and DNA-sequence analysis of specific chromosomal insertion sites

We used the EZ-Tn*5* [R6Kγori/KAN-2] transposition system (Epicentre, Madison, USA) to mutagenize *R. pomeroyi* DSS-3. All reagents required for these experiments were contained in the kit provided by the supplier. The EZ-Tn*5* [R6Kγori/KAN-2] transposon, along with a hyperactive Tn*5* transposase and a type I restriction enzyme inhibitor (both purchased from Epicentre) were electroporated into *R. pomeroyi* DSS-3 cells (puls: 1.6 kV, 200 Ω and 25 μF) using the Gene Pulser Xcell system (Biorad, Munich, Germany). The transformed cells were then carefully re-suspended (at 30°C) into 1 ml prewarmed basal minimal medium and incubated for 3 h at 30°C on a shaker. Portions of 20-μl cell suspension were subsequently plated on basal medium agar plates containing 120 μg ml^{-1} of kanamycin to select for chromosomal EZ-Tn*5* [R6Kγori/KAN-2] transposition insertions; the selective agar plates were incubated at 30°C for 7–14 days. To search for transposon insertions affecting the use of ectoine as a nutrient, colonies that had grown on the selection plates were replica plated onto basal medium agar plates containing 15 mM ectoine as sole carbon and nitrogen source and onto basal medium agar plates containing glucose (28 mM) and NH_4Cl (56 mM) as carbon and nitrogen sources. These replica plates were then incubated for 10 days at 30°C. From a collection of about 21 000 colonies with EZ-Tn*5* [R6Kγori/KAN-2] transposon insertions, three candidates with a growth defect in the use of ectoine were identified. These were purified by re-streaking on basal medium agar plates containing glucose, NH_4Cl and kanamycin and were subsequently tested for their inability to exploit ectoine as a nutrient on basal medium agar plates. The insertion site of the Tn*5* [R6Kγori/KAN-2] transposon in these strains was then determined either by RACE PCR with primers (purchased from Epicentre) listed in Supporting Information Table S3 or via rescue cloning. For this latter approach, chromosomal DNA from the Tn*5* [R6Kγori/KAN-2] transposon insertion strains was prepared, cleaved with EcoR1, re-ligated, and transformed into TransforMax™ EC100D™ *pir*$^{+}$ *E. coli* cells (Epicentre). The only plasmid able to replicate in these cells from the entire restriction/ligation mixture is the Tn*5* [R6Kγori/KAN-2] transposon along with its flanking genomic DNA sequences since the mini-transposon carries the R6Kγori region that is only functional in a *pir*$^{+}$ strain (e.g., not in *R. pomeroyi*). It establishes itself in the TransforMax™ EC100D™ *pir*$^{+}$ *E. coli* cells as a low-copy-number plasmid that can be selected for by plating the transformed cells on LB-agar plates containing 120 μg ml^{-1} kanamycin. DNA of these plasmids were prepared and the *R. pomeroyi* DNA sequences flanking the Tn*5* [R6Kγori/KAN-2] transposon insertion site were determined using primers (Supporting Information Table S3) provided in the EZ-Tn*5* [R6Kγori/KAN-2] transposition kit (Epicentre).

β-galactosidase enzyme activity measurements

R. pomeroyi strains carrying plasmids containing *lacZ* reporter genes were grown overnight in a basal medium containing glucose (28 mM) and NH_4Cl (200 mM) as the carbon and nitrogen source. These precultures were then used to inoculate (with maximally 500 μl) the main culture (25-ml) to an optical density (OD_{578}) of about 0.1. When ectoine or hydroxyectoine was used as sole carbon- or nitrogen sources by *R. pomeroyi*, they were separately provided at a concentration of 28 mM. The cultures were grown at 30°C until they had reached an OD_{578} of about 1. The cells were collected by

centrifugation (13 000 rpm for 10 min), and processed for β-galactosidase activity assays with ONPG as the chromogenic substrate (Miller, 1972). β-galactosidase enzyme activity is expressed as Miller Units (MU). A strain harbouring the promoterless *lacZ* fusion vector pBIO1878 (Todd *et al*., 2012) that was used to construct the reporter fusions used in this study yields ß-galactosidase background values between 2 and 5 MU (Schulz *et al*., 2017).

Overproduction, purification and ligand-binding assays with EnuR

For overproduction of EnuR-*Strep*-tag-II and EnuR*-*Strep*-tag-II recombinant proteins, cells of the *E. coli* B strain BL21 (DE3) were transformed with the appropriate overproduction plasmids [pBAS3 (*enuR*$^{+}$; pBAS17 (*enuR**)] (Supporting Information Table S2) that allow the expression of the *enuR* gene under the control of the *tet* promoter, a system (IBA, Germany) that is controlled by the anhydrotetracycline (AHT)-responsive TetR repressor (Schulz *et al*., 2017). The plasmid-containing *E. coli* cells were grown at 37°C in MMA containing 0.5% casamino acids until the OD_{578} reached 0.6 and the *tet*-promoter/TetR mediated overexpression of plasmid-encoded *enuR/enuR** genes was triggered by adding the TetR inducer AHT (final concentration: 0.2 μg ml^{-1}) to the growth medium. The growth temperature of the cultures was reduced to 35°C and they were subsequently incubated for additional two hours to allow overproduction of the recombinant EnuR and EnuR* proteins. Cells were then harvested by centrifugation, lysed and the EnuR and EnuR* proteins were purified from the cell extracts via affinity chromatography on a Strep-Tactin Superflow column as described (Schulz *et al*., 2017).

Ligand binding assays with the purified EnuR and EnuR* proteins were carried out by microscale thermophoresis (MST) (Duhr and Braun, 2006; Wienken *et al*., 2010). All experiments were performed on a Monolith NT.115 (NanoTemper Technologies GmbH, Munich, Germany) at 21°C (red LED power was set to 80% and infrared laser power to 70%). The buffer of the purified EnuR and EnuR* [in 100 mM Tris- HCl (pH 7.5), 150 mM NaCl] was first exchanged with the labelling buffer of the Monolith NTTM Protein Labeling Kit RED (NanoTemper) to avoid interference of the labelling reactions with free amines in the buffer solution. Subsequent to labelling of EnuR and EnuR* (20 μM each) with the dye NT 647 (according to the suppliers reaction protocol), the EnuR/EnuR* proteins were re-buffered into a solution buffer containing 10 mM Tris-HCl (pH 7.5), 150 mM NaCl and 0.2% Tween. 200 nM EnuR or EnuR* was titrated with ectoine or hydroxyectoine starting from a concentration of 10 mM. Both proteins were also titrated with *N*-(α)-ADABA or *N*-(γ)-ADABA (starting from 65 μM and 1 mM, respectively). Additionally, 200 nM EnuR was titrated with DABA with a starting concentration of 50 mM. At least six independent MST experiments per ligand and type of EnuR protein were recorded at 680 nm and analysed using NanoTemper Analysis 1.2.009 and Origin8G software suits.

Electrophoretic mobility shift assays

Fluorescently labelled DNA fragments for electrophoretic mobility shift assays (EMSA) were generated by PCR from genomic DNA of *R. pomeroyi* DSS-3. For the *uehA* regulatory region, primers L1_rev-dye and L2_fw (Supporting Information Table S3) were used to generate a 251-bp fragment containing the putative *uehA* promoter. A 278-bp fragment of the *uehA*-coding region was generated using primers L5_rev_dye and L4_fw (Supporting Information Table S3). The DNA primers L1_rev_dye and L5_rev_dye were 5'-labelled with the Dyomics 781 fluorescent dye (Microsynth AG, Balgach, Switzerland). Binding reactions between the DNA fragments (0.5 pmol) and various concentrations of the purified EnuR protein were performed in buffer A (20 mM phosphate [pH 7.0], 1 mM dithiothreitol, 5 mM $MgCl_2$, 50 mM KCl, 15 μg/ml bovine serum albumin, 50 μg/ml salmon sperm DNA, and 5% [vol/vol] glycerol, 0.1% Tween20) in a total volume of 20 μl. After incubation of the reaction mixture, the samples were loaded onto a native 5% polyacrylamide gel and electorphoretically separated at 110 V for 45 min. EnuR:DNA-interactions were detected using an Odyssey FC Imaging System (LI-COR Biosciences, Linoln, USA).

Database searches for potential microbial ectoine consumers and phylogenetic analysis of the EnuR, AsnC and NtrYX regulatory proteins

Searches for orthologues of the *R. pomeroyi* DSS-3 EutD protein (accession number: AAV94440.1) (Moran *et al*., 2004) had previously been conducted via the Web-server of the genome portal of the Department of Energy Joint Genome Institute (http://genome.jgi.doe.gov/) (JGI) (Nordberg *et al*., 2013) using the BLAST algorithm (Altschul *et al*., 1990). The taxonomic affiliation of the potential hydroxyectoine/ectoine consumers had been analysed and visualized via the Interactive Tree of Life iTOL web-tool (http://itol.embl.de/) (Letunic and Bork, 2011). This curated dataset comprised 539 entries and 456 of these possessed a *enuR*-related gene in the immediate vicinity of the hydroxyectoine/ectoine import and catabolic gene cluster (Schulz *et al*., 2017). This data set was newly further searched for the presence of an *asnC*-type gene positioned within the hydroxyectoine/ectoine import and catabolic gene clusters. Furthermore, the genome sequences of the 539 potential hydroxyectoine/ectoine consumers were again queried through a BLAST search for the presence of NtrXY-type two-component regulatory systems. Along with EnuR, the presence of AsnC and NtrXY proteins was then projected onto the previously reported EutD-derived phylogenetic tree (Schulz *et al*., 2017) (Supporting Information Fig. S3).

Acknowledgements

The authors are grateful to A. Johnston and J. Todd for generously providing molecular tools for strain constructions and *lacZ* reporter plasmids. We thank our colleague Roland Lill for his interest in and support of this project. The kind help of Vickie Koogle in the language editing of our manuscript is greatly appreciated. We are thankful to the bitop AG (Witten, Germany) for kind gifts of ectoines. We gratefully acknowledge the expert technical support of the Core Facility 'Protein Spectroscopy and Protein Biochemistry' of the Medical School of the Philipps University Marburg for our work. The German Research Foundation (DFG) in the framework of the

Collaborative Research Center (SFB) 987 (to E.B., J.H. and Roland Lill) and the Collaborative Research Center Transregio (TRR 51) (to J.D.) provided funding for this study. Additional funds were made available through the LOEWE Program of the State of Hessen (via the Centre for Synthetic Microbiology; Synmicro, Marburg) (to E.B., J.H. and Roland Lill). A.S. gratefully acknowledges the receipt of a fellowship from the Christiane Nüsslein-Vollhard-Stiftung to support her PhD studies.

CONFLICT OF INTEREST

The authors declare that they have no financial conflict of interest with regard to the data presented in this study.

References

Altschul, S.F., Gish, W., Miller, W., Myers, E.W., and Lipman, D.J. (1990) Basic local alignment search tool. *J Mol Biol* **215:** 403–410.

Baumann, P., Baumann, L., and Mandel, M. (1971) Taxonomy of marine bacteria: the genus *Beneckea*. *J Bacteriol* **107:** 268–294.

Belitsky, B.R. (2004) *Bacillus subtilis* GabR, a protein with DNA-binding and aminotransferase domains, is a PLP-dependent transcriptional regulator. *J Mol Biol* **340:** 655–664.

Belitsky, B.R. (2014) Role of PdxR in the activation of vitamin B6 biosynthesis in *Listeria monocytogenes*. *Mol Microbiol* **92:** 1113–1128.

Belitsky, B.R., and Sonenshein, A.L. (2002) GabR, a member of a novel protein family, regulates the utilization of gamma-aminobutyrate in *Bacillus subtilis*. *Mol Microbiol* **45:** 569–583.

Bonato, P., Alves, L.R., Osaki, J.H., Rigo, L.U., Pedrosa, F.O., Souza, E.M., *et al*. (2016) The NtrY-NtrX two-component system is involved in controlling nitrate assimilation in *Herbaspirillum seropedicae* strain SmR1. *FEBS J* **283:** 3919–3930.

Booth, I.R. (2014) Bacterial mechanosensitive channels: progress towards an understanding of their roles in cell physiology. *Curr Opin Microbiol* **18:** 16–22.

Bramucci, E., Milano, T., and Pascarella, S. (2011) Genomic distribution and heterogeneity of MocR-like transcriptional factors containing a domain belonging to the superfamily of the pyridoxal-5'-phosphate dependent enzymes of fold type I. *Biochem Biophys Res Commun* **415:** 88–93.

Bremer, E., and Krämer, R. (2000) Coping with osmotic challenges: osmoregulation through accumulation and release of compatible solutes. In *Bacterial Stress Responses*. Storz, G., Hengge-Aronis, R. (eds). Washington DC: ASM Press, pp. 79–97.

Bursy, J., Pierik, A.J., Pica, N., and Bremer, E. (2007) Osmotically induced synthesis of the compatible solute hydroxyectoine is mediated by an evolutionarily conserved ectoine hydroxylase. *J Biol Chem* **282:** 31147–31155.

Calatrava-Morales, N., Nogales, J., Ameztoy, K., van Steenbergen, B., and Soto, M.J. (2017) The NtrY/NtrX system of *Sinorhizobium meliloti* GR4 regulates motility, EPS I production and nitrogen metabolism but is dispensable for symbiotic nitrogen fixation. *Mol Plant Microbe Interact* **30:** 566–577.

Carrica Mdel, C., Fernandez, I., Marti, M.A., Paris, G., and Goldbaum, F.A. (2012) The NtrY/X two-component system of *Brucella* spp. acts as a redox sensor and regulates the expression of nitrogen respiration enzymes. *Mol Microbiol* **85:** 39–50.

Cheng, Z., Lin, M., and Rikihisa, Y. (2014) *Ehrlichia chaffeensis* proliferation begins with NtrY/NtrX and PutA/GlnA upregulation and CtrA degradation induced by proline and glutamine uptake. *mBio* **5:** e02141.

Dennis, J.J., and Zylstra, G.J. (1998) Plasposons: modular self-cloning minitransposon derivatives for rapid genetic analysis of gram-negative bacterial genomes. *Appl Environ Microbiol* **64:** 2710–2715.

Dey, A., Shree, S., Pandey, S.K., Tripathi, R.P., and Ramachandran, R. (2016) Crystal structure of *Mycobacterium tuberculosis* H37Rv AldR (rv2779c), a regulator of the *ald* gene: DNA-binding, and identification of small-molecule inhibitors. *J Biol Chem* 11967–11980.

Du, Y.L., Dalisay, D.S., Andersen, R.J., and Ryan, K.S. (2013) N-carbamoylation of 2,4-diaminobutyrate reroutes the outcome in padanamide biosynthesis. *Chem Biol* **20:** 1002–1011.

Duhr, S., and Braun, D. (2006) Why molecules move along a temperature gradient. *Proc Natl Acad Sci USA* **103:** 19678–19682.

Edayathumangalam, R., Wu, R., Garcia, R., Wang, Y., Wang, W., Kreinbring, C.A., *et al*. (2013) Crystal structure of *Bacillus subtilis* GabR, an autorepressor and transcriptional activator of *gabT*. *Proc Natl Acad Sci USA* **110:** 17820–17825.

Fernandez, I., Cornaciu, I., Carrica, M.D., Uchikawa, E., Hoffmann, G., Sieira, R., *et al*. (2017) Three-dimensional structure of full-length NtrX, an unusual member of the NtrC family of response regulators. *J Mol Biol* **429:** 1192–1212.

Fidalgo, C., Riesco, R., Henriques, I., Trujillo, M.E., and Alves, A. (2016) *Microbacterium diaminobutyricum* sp. nov., isolated from *Halimione portulacoides*, which contains diaminobutyric acid in its cell wall, and emended description of the genus *Microbacterium*. *Int J Syst Evol Microbiol* **66:** 4492–4500.

Figurski, D.H., and Helinski, D.R. (1979) Replication of an origin-containing derivative of plasmid RK2 dependent on a plasmid function provided in trans. *Proc Natl Acad Sci USA* **76:** 1648–1652.

Galinski, E.A., and Herzog, R.M. (1990) The role of trehalose as a substitute for nitrogen-containing compatible solutes (*Ectothiorhodospira halochloris*). *Arch Microbiol* **153:** 607–613.

Gibson, D.G., Young, L., Chuang, R.Y., Venter, J.C., Hutchison, C.A., 3rd., and Smith, H.O. (2009) Enzymatic assembly of DNA molecules up to several hundred kilobases. *Nat Methods* **6:** 343–345.

Goryshin, I.Y., and Reznikoff, W.S. (1998) Tn*5* in vitro transposition. *J Biol Chem* **273:** 7367–7374.

Grammann, K., Volke, A., and Kunte, H.J. (2002) New type of osmoregulated solute transporter identified in halophilic members of the bacteria domain: TRAP transporter TeaABC mediates uptake of ectoine and hydroxyectoine in *Halomonas elongata* DSM 2581(T). *J Bacteriol* **184:** 3078–3085.

Harishchandra, R.K., Wulff, S., Lentzen, G., Neuhaus, T., and Galla, H.J. (2010) The effect of compatible solute ectoines

on the structural organization of lipid monolayer and bilayer membranes. *Biophys Chem* **150:** 37–46.

Ikai, H., and Yamamoto, S. (1997) Identification and analysis of a gene encoding L-2,4-diaminobutyrate:2-ketoglutarate 4-aminotransferase involved in the 1,3-diaminopropane production pathway in *Acinetobacter baumannii*. *J Bacteriol* **179:** 5118–5125.

Jebbar, M., Sohn-Bösser, L., Bremer, E., Bernard, T., and Blanco, C. (2005) Ectoine-induced proteins in *Sinorhizobium meliloti* include an ectoine ABC-type transporter involved in osmoprotection and ectoine catabolism. *J Bacteriol* **187:** 1293–1304.

Kamensek, S., Browning, D.F., Podlesek, Z., Busby, S.J., Zgur-Bertok, D., and Butala, M. (2015) Silencing of DNase colicin E8 gene expression by a complex nucleoprotein assembly ensures timely colicin Induction. *PLoS Genet* **11:** e1005354.

Kempf, B., and Bremer, E. (1998) Uptake and synthesis of compatible solutes as microbial stress responses to high osmolality environments. *Arch Microbiol* **170:** 319–330.

Kuhlmann, A.U., and Bremer, E. (2002) Osmotically regulated synthesis of the compatible solute ectoine in *Bacillus pasteurii* and related *Bacillus* spp. *Appl Environ Microbiol* **68:** 772–783.

Kuhlmann, A.U., Hoffmann, T., Bursy, J., Jebbar, M., and Bremer, E. (2011) Ectoine and hydroxyectoine as protectants against osmotic and cold stress: uptake through the SigB-controlled betaine-choline-carnitine transporter-type carrier EctT from *Virgibacillus pantothenticus*. *J Bacteriol* **193:** 4699–4708.

Kumarevel, T., Nakano, N., Ponnuraj, K., Gopinath, S.C., Sakamoto, K., Shinkai, A., *et al*. (2008) Crystal structure of glutamine receptor protein from *Sulfolobus tokodaii* strain 7 in complex with its effector L-glutamine: implications of effector binding in molecular association and DNA binding. *Nucleic Acids Res* **36:** 4808–4820.

Kunte, H.J., Galinski, E.A., and Trüper, G.H. (1993) A modified FMOC-method for the detection of amino acid-type osmolytes and tetrahydropyrimidines (ectoines). *J Microbiol Meth* **17:** 129–136.

Kunte, H.J., Lentzen, G., and Galinski, E. (2014) Industrial production of the cell protectant ectoine: protection, mechanisms, processes, and products. *Cur Biotechnol* **3:** 10–25.

Kvitko, B.H., and Collmer, A. (2011) Construction of *Pseudomonas syringae* pv. tomato DC3000 mutant and polymutant strains. *Meth Mol Biol* **712:** 109–128.

Landa, M., Burns, A.S., Roth, S.J., and Moran, M.A. (2017) Bacterial transcriptome remodelling during sequential co-culture with a marine dinoflagellate and diatom. *ISME J* (in press) doi:10.1038/ismej.2017.117

Lecher, J., Pittelkow, M., Zobel, S., Bursy, J., Bönig, T., Smits, S.H., *et al*. (2009) The crystal structure of UehA in complex with ectoine-A comparison with other TRAP-T binding proteins. *J Mol Biol* **389:** 58–73.

Letunic, I., and Bork, P. (2011) Interactive Tree Of Life v2: online annotation and display of phylogenetic trees made easy. *Nucleic Acids Res* **39:** W475–W478.

Lidbury, I., Murrell, J.C., and Chen, Y. (2014) Trimethylamine N-oxide metabolism by abundant marine heterotrophic bacteria. *Proc Natl Acad Sci USA* **111:** 2710–2715.

Lidbury, I., Kimberley, G., Scanlan, D.J., Murrell, J.C., and Chen, Y. (2015) Comparative genomics and mutagenesis analyses of choline metabolism in the marine *Roseobacter* clade. *Environ Microbiol* **17:** 5048–5062.

Lippert, K., and Galinski, E.A. (1992) Enzyme stabilization by ectoine-type compatible solutes: protection against heating, freezing and drying. *Appl Microbiol Biotechnol* **37:** 61–65.

Luo, H., and Moran, M.A. (2014) Evolutionary ecology of the marine *Roseobacter* clade. *Microbiol Mol Biol Rev* **78:** 573–587.

Manzanera, M., Garcia de Castro, A., Tondervik, A., Rayner-Brandes, M., Strom, A.R., and Tunnacliffe, A. (2002) Hydroxyectoine is superior to trehalose for anhydrobiotic engineering of *Pseudomonas putida* KT2440. *Appl Environ Microbiol* **68:** 4328–4333.

Milano, T., Contestabile, R., Lo Presti, A., Ciccozzi, M., and Pascarella, S. (2015) The aspartate aminotransferase-like domain of *Firmicutes* MocR transcriptional regulators. *Comput Biol Chem* **58:** 55–61.

Miller, J.H. (1972) *Experiments in Molecular Genetics*. New York: Cold Spring Harbor Laboratory.

Moran, M.A., Buchan, A., Gonzalez, J.M., Heidelberg, J.F., Whitman, W.B., Kiene, R.P., *et al*. (2004) Genome sequence of *Silicibacter pomeroyi* reveals adaptations to the marine environment. *Nature* **432:** 910–913.

Mosier, A.C., Justice, N.B., Bowen, B.P., Baran, R., Thomas, B.C., Northen, T.R., and Banfield, J.F. (2013) Metabolites associated with adaptation of microorganisms to an acidophilic, metal-rich environment identified by stable-isotope-enabled metabolomics. *mBio* **4:** e00484–e00412.

Mulligan, C., Fischer, M., and Thomas, G.H. (2011) Tripartite ATP-independent periplasmic (TRAP) transporters in bacteria and archaea. *FEMS Microbiol Rev* **35:** 68–86.

Nordberg, H., Cantor, M., Dusheyko, S., Hua, S., Poliakov, A., Shabalov, I., *et al*. (2013) The genome portal of the Department of Energy Joint Genome Institute: 2014 updates. *Nucleic Acids Res* **42:** D26–D31.

Okuda, K., Ito, T., Goto, M., Takenaka, T., Hemmi, H., and Yoshimura, T. (2015a) Domain characterization of *Bacillus subtilis* GabR, a pyridoxal 5'-phosphate-dependent transcriptional regulator. *J Biochem* **158:** 225–234.

Okuda, K., Kato, S., Ito, T., Shiraki, S., Kawase, Y., Goto, M., *et al*. (2015b) Role of the aminotransferase domain in *Bacillus subtilis* GabR, a pyridoxal 5'-phosphate-dependent transcriptional regulator. *Mol Microbiol* **95:** 245–257.

Ono, H., Sawada, K., Khunajakr, N., Tao, T., Yamamoto, M., Hiramoto, M., *et al*. (1999) Characterization of biosynthetic enzymes for ectoine as a compatible solute in a moderately halophilic eubacterium, *Halomonas elongata*. *J Bacteriol* **181:** 91–99.

Park, S.A., Park, Y.S., and Lee, K.S. (2017) Crystal structure of the C-terminal domain of *Bacillus subtilis* GabR reveals a closed conformation by gamma-aminobutyric acid binding, inducing transcriptional activation. *Biochem Biophys Res Commun* **487:** 287–291.

Pastor, J.M., Salvador, M., Argandona, M., Bernal, V., Reina-Bueno, M., Csonka, L.N., *et al*. (2010) Ectoines in cell stress protection: uses and biotechnological production. *Biotechnol Adv* **28:** 782–801.

Pawlowski, K., Klosse, U., and de Bruijn, F.J. (1991) Characterization of a novel *Azorhizobium caulinodans* ORS571 two-

component regulatory system, NtrY/NtrX, involved in nitrogen fixation and metabolism. *Mol Gen Genet* **231:** 124–138.
Phillips, R.S. (2015) Chemistry and diversity of pyridoxal-5'-phosphate dependent enzymes. *Biochim Biophys Acta* **1854:** 1167–1174.
Rigali, S., Derouaux, A., Giannotta, F., and Dusart, J. (2002) Subdivision of the helix-turn-helix GntR family of bacterial regulators in the FadR, HutC, MocR, and YtrA subfamilies. *J Biol Chem* **277:** 12507–12515.
Rodriguez-Moya, J., Argandona, M., Reina-Bueno, M., Nieto, J.J., Iglesias-Guerra, F., Jebbar, M., and Vargas, C. (2010) Involvement of EupR, a response regulator of the NarL/FixJ family, in the control of the uptake of the compatible solutes ectoines by the halophilic bacterium *Chromohalobacter salexigens*. *BMC Microbiol* **10:** 256.
Roesser, M., and Müller, V. (2001) Osmoadaptation in bacteria and archaea: common principles and differences. *Environ Microbiol* **3:** 743–754.
Sambrook, J., Fritsch, E.F., and Maniatis, T.E. (1989) *Molecular Cloning. A Laboratory Manual*. New York: Cold Spring Harbor Laboratory, Cold Spring Harbor.
Schulz, A., Stöveken, N., Binzen, I.M., Hoffmann, T., Heider, J., and Bremer, E. (2017) Feeding on compatible solutes: a substrate-induced pathway for uptake and catabolism of ectoines and its genetic control by EnuR. *Environ Microbiol* **19:** 926–946.
Schwibbert, K., Marin-Sanguino, A., Bagyan, I., Heidrich, G., Lentzen, G., Seitz, H., *et al*. (2011) A blueprint of ectoine metabolism from the genome of the industrial producer *Halomonas elongata* DSM 2581 T. *Environ Microbiol* **13:** 1973–1994.
Shrivastava, T., and Ramachandran, R. (2007) Mechanistic insights from the crystal structures of a feast/famine regulatory protein from *Mycobacterium tuberculosis* H37Rv. *Nucleic Acids Res* **35:** 7324–7335.
Simon, M., Scheuner, C., Meier-Kolthoff, J.P., Brinkhoff, T., Wagner-Döbler, I., Ulbrich, M., *et al*. (2017) Phylogenomics of *Rhodobacteraceae* reveals evolutionary adaptation to marine and non-marine habitats. *ISME J* **11:** 1483–1499.
Stöveken, N., Pittelkow, M., Sinner, T., Jensen, R.A., Heider, J., and Bremer, E. (2011) A specialized aspartokinase enhances the biosynthesis of the osmoprotectants ectoine and hydroxyectoine in *Pseudomonas stutzeri* A1501. *J Bacteriol* **193:** 4456–4468.
Suvorova, I., and Rodionov, D. (2016) Comparative genomics of pyridoxal 5'-phosphate-dependent transcription factor regulons in *Bacteria*. *MGen* **2:** e000047.
Takenaka, T., Ito, T., Miyahara, I., Hemmi, H., and Yoshimura, T. (2015) A new member of MocR/GabR-type PLP-binding regulator of D-alanyl-D-alanine ligase in *Brevibacillus brevis*. *FEBS J* **282:** 4201–4217.
Tanne, C., Golovina, E.A., Hoekstra, F.A., Meffert, A., and Galinski, E.A. (2014) Glass-forming property of hydroxyectoine is the cause of its superior function as a dessication protectant. *Front Microbiol* **5:** 150.
Taubert, M., Grob, C., Howat, A.M., Burns, O.J., Pratscher, J., Jehmlich, N., *et al*. (2017) Methylamine as a nitrogen source for microorganisms from a coastal marine environment. *Environ Microbiol* **19:** 2246–2257.
Todd, J.D., Kirkwood, M., Newton-Payne, S., and Johnston, A.W. (2012) DddW, a third DMSP lyase in a model *Roseobacter* marine bacterium, *Ruegeria pomeroyi* DSS-3. *ISME J* **6:** 223–226.
Tramonti, A., Milano, T., Nardella, C., di Salvo, M.L., Pascarella, S., and Contestabile, R. (2017) *Salmonella typhimurium* PtsJ is a novel MocR-like transcriptional repressor involved in regulating the vitamin B6 salvage pathway. *FEBS J* **284:** 466–484.
Vargas, C., Jebbar, M., Carrasco, R., Blanco, C., Calderon, M.I., Iglesias-Guerra, F., and Nieto, J.J. (2006) Ectoines as compatible solutes and carbon and energy sources for the halophilic bacterium *Chromohalobacter salexigens*. *J Appl Microbiol* **100:** 98–107.
Wagner-Döbler, I., and Biebl, H. (2006) Environmental biology of the marine *Roseobacter* lineage. *Annu Rev Microbiol* **60:** 255–280.
Warren, C. (2016) Do microbial osmolytes or extracellular depolymerization products accumulate as soil dries? *Soil Biology & Biochemistry* **98:** 54–63.
Warren, C.R. (2014) Response of osmolytes in soil to drying and rewetting. *Soil Biol Biochem* **70:** 22–32.
Welsh, D.T. (2000) Ecological significance of compatible solute accumulation by micro-organisms: from single cells to global climate. *FEMS Microbiol Rev* **24:** 263–290.
Widderich, N., Höppner, A., Pittelkow, M., Heider, J., Smits, S.H., and Bremer, E. (2014) Biochemical properties of ectoine hydroxylases from extremophiles and their wider taxonomic distribution among microorganisms. *PLoS One* **9:** e93809.
Widderich, N., Kobus, S., Höppner, A., Ricela, R., Seubert, A., Dickschat, J.S., *et al*. (2016a) Biochemistry and crystal structure of the ectoine synthase: a metal-containing member of the cupin superfamily. *PLoS One* **11:** e0151285.
Widderich, N., Czech, L., Elling, F.J., Könneke, M., Stöveken, N., Pittelkow, M., *et al*. (2016b) Strangers in the archaeal world: osmostress-responsive biosynthesis of ectoine and hydroxyectoine by the marine thaumarchaeon *Nitrosopumilus maritimus*. *Environ Microbiol* **18:** 1227–1248.
Wienken, C.J., Baaske, P., Rothbauer, U., Braun, D., and Duhr, S. (2010) Protein-binding assays in biological liquids using microscale thermophoresis. *Nat Commun* **1:** 100.
Wiethaus, J., Schubert, B., Pfander, Y., Narberhaus, F., and Masepohl, B. (2008) The GntR-like regulator TauR activates expression of taurine utilization genes in *Rhodobacter capsulatus*. *J Bacteriol* **190:** 487–493.
Wood, J.M. (2011) Bacterial osmoregulation: a paradigm for the study of cellular homeostasis. *Annu Rev Microbiol* **65:** 215–238.
Wu, R., Sanishvili, R., Belitsky, B.R., Juncosa, J.I., Le, H.V., Lehrer, H.J., *et al*. (2017) PLP and GABA trigger GabR-mediated transcription regulation in *Bacillus subtilis* via external aldimine formation. *Proc Natl Acad Sci USA* **114:** 3891–3896.
Yokoyama, K., Ishijima, S.A., Clowney, L., Koike, H., Aramaki, H., Tanaka, C., *et al*. (2006) Feast/famine regulatory proteins (FFRPs): *Escherichia coli* Lrp, AsnC and related archaeal transcription factors. *FEMS Microbiol Rev* **30:** 89–108.
Yu, Q., Cai, H., Zhang, Y., He, Y., Chen, L., Merritt, J., *et al*. (2017) Negative regulation of ectoine uptake and catabolism in *Sinorhizobium meliloti*: characterization of the EhuR gene. *J Bacteriol* **199:** e00119–e00116.

Zaccai, G., Bagyan, I., Combet, J., Cuello, G.J., Deme, B., Fichou, Y., *et al*. (2016) Neutrons describe ectoine effects on water H-bonding and hydration around a soluble protein and a cell membrane. *Sci Rep* **6:** 31434.

Zschiedrich, C.P., Keidel, V., and Szurmant, H. (2016) Molecular mechanisms of two-component signal transduction. *J Mol Biol* **428:** 3752–3775.

Supporting information

Additional supporting information may be found in the online version of this article at the publisher's web-site.

Table S1. *Ruegeria pomeroyi* strains used in this study.
Table S2. Plasmids used in this study.
Table S3. Primers used in this study.
Fig. S1. Ligand binding by the wild-type EnuR protein and its mutant EnuR* derivative as assessed by microscale thermophoresis. Purified EnuR protein (200 nM) was titrated with increasing concentrations of (A) ectoine, (B) hydroxyectoine, and (C) γ-L-ADABA. (D) Purified mutant EnuR* protein (200 nM) was titrated with increasing concentrations of α-L-ADABA.
Fig. S2. Growth curves of rifampicin-resistant *R. pomeroyi* J470 mutant derivatives defective in various ectoine catabolic genes. Cultures were grown in basal minimal media containing either ectoine (squares) or hydroxyectoine (circles) as the sole carbon and nitrogen source, or glucose and NH_4Cl (rhombi) as carbon and nitrogen source respectively. Ectoine, hydroxyectoine, and glucose were present in these cultures at a concentration of 28 mM. NH_4Cl was added to a final concentration of 200 mM. (A) Growth of the *R. pomeryi* strain ASR8 [Δ(*eutD::Gm*)1] (B) Growth of the *R. pomeryi* strain ASR11 [Δ(*eutABC::Gm*)1].
Fig. S3. Taxonomic distribution of *enuR*, *asnC*, and *ntrYX* genes among microorganisms predicted to consume ectoines. An alignment of 539 amino acid sequences homologous to the EutD protein from *Ruegeria pomeroyi* DSS-3 has previously been used to construct a phylogenetic tree of presumed consumers of ectoines. The color code outlines the distribution of EutD-type proteins among the classes of the *Proteobacteria*. The presence of *enuR* or *asnC* genes in the direct vicinity (for *enuR*) or within (for *asnC*) hydroxyectoine/ectoine-transport and catabolic gene clusters are indicated by a pink pentagon and a purple circle respectively. The presence of a gene cluster (*ntrXY*) encoding the two-component NtrYX regulatory system in the genome sequences of the predicted consumers of ectoines is indicated by orange pentagons.
Fig. S4. Growth of rifampicin-resistant *R. pomeroyi* wild type J470 and its mutant derivative ASR9 which carries a deletionfor *ntrXY* (Δ*ntrXY*). Cells were grown on basal minimal medium agar plates containing ectoine, glycine betaine or choline either as a sole carbon, as a sole nitrogen or as a combined carbon and nitrogen source as indicated.

Supporting Information

Transcriptional regulation of ectoine catabolism in response to multiple metabolic and environmental cues

Annina Schulz[1,¶], Lucas Hermann[1,¶], Sven-Andreas Freibert[2], Tobias Bönig[1], Tamara Hoffmann[1], Ramona Riclea[3,4], Jeroen S. Dickschat[3,4], Johann Heider[1,5], and Erhard Bremer[1,5]*

[1]Department of Biology, Laboratory for Microbiology, Philipps-University Marburg, Karl-von-Frisch-Str. 8, D-35043Marburg, Germany

[2]Department of Medicine, Institute for Cytobiology and Cytopathology, Philipps-University Marburg, Robert-Koch Str. 6, D-35032Marburg, Germany

[3]Institute of Organic Chemistry, Technical University Braunschweig, D-38106 Braunschweig, Germany

[4]Kekulé-Institute for Organic Chemistry and Biochemistry, Friedrich-Wilhelms-Universität Bonn, D-53121Bonn, Germany

[5]LOEWE-Center for Synthetic Microbiology, Philipps-University Marburg, Hans-Meerwein Str. 6, D-35043 Marburg, Germany

[¶]Both authors contributed equally to this study

Running title: Genetic control of ectoine and hydroxyectoine catabolism

*For correspondence:

Dr. Erhard Bremer, Philipps-University Marburg, Dept. of Biology, Laboratory for Microbiology, Karl-von-Frisch-Str. 8, D-35043 Marburg, Germany. Phone: (+49)-6421-2821529. Fax: (+49)-6421-2828979. E-Mail: bremer@staff.uni-marburg.de.

Table S1. *Ruegeria pomeroyi* strains used in this study.

Strains	Relevant genotype	Reference/source
DSS-3	Wild type	(Moran et al., 2004)
J470	DSS-3 Rif^R (wild type)	(Todd et al., 2011)
ASR6	J470 Δ(*enuR-uehABC-usp-eutABCDE-asnC-ssd-atf*::*Gm*)1	(Schulz et al., 2017)
ASR7	J470 Δ(*enuR*::*Gm*)1	(Schulz et al., 2017)
ASR8	J470 Δ(*eutD*::*Gm*)1	(Schulz et al., 2017)
TBS3[a]	DSS-3 (*ntrY*::EZ-Tn*5*)1	This study
ASR9	J470 Δ(*ntrXY*::*Gm*)2	This study
ASR10	J470 Δ(*asnC-ssd-atf*::*Gm*)1	(Schulz et al., 2017)
ASR11	J470 Δ(*eutABC*::*Gm*)1	(Schulz et al., 2017)
ASR12	J470 Δ(*eutABCDE-asnC-ssd-atf*::*Gm*)1	(Schulz et al., 2017)
ASR14	J470 Δ(*ssd-atf*::*Gm*)1	(Schulz et al., 2017)

[a]This strain contains insertions of the EZ-Tn*5* mini-transposon at multiple chromosomal locations.

Table S2. Plasmids used in this study.

Plasmid	Description	Reference/source
pK18mobsacB	Suicide vector for *R. pomeroyi*, Kan^R	(Kvitko and Collmer, 2011)
pBIO1878	Vector with *lacZ* reporter gene, Spc^R	(Todd et al., 2012)
p34S_Gm	Plasmid carrying a gentamicin (Gm^R) resistance cassette	(Dennis and Zylstra, 1998)
pRK2013	Helper plasmid for tri-parental mating, Kan^R	(Figurski and Helinski, 1979)
pBAS3	pASG-IBA3 with synthetic, codon-optimized *enuR* gene[a]	(Schulz et al., 2017)
pBAS17	pBAS3 with codon exchange mutation (AAA/CAT) in *enuR* leading to the replacement of Lys-302 with a His residue	(Schulz et al., 2017)
pBAS19	pBIO1878 with 1100 bp upstream of *enuR*, Spc^R	(Schulz et al., 2017)
pBAS20	pBIO1878 with 2617 bp upstream of *uehA*, Spc^R	This study
pBAS21	pBIO1878 with 433 bp upstream of *uehA*, Spc^R	(Schulz et al., 2017)
pBAS41	pK18mobsacB with flanking regions of the *ntrXY*-gene cluster interrupted with a Gm^R cassette, Kan^R	This study
pTB3	Construct from plasmid rescue with chromosomal DNA from *R. pomeroyi* strainTBS3 (*ntrY*::Tn*5*, ori_{pir})	This study

[a]The DNA-sequence of the codon-optimized *enuR* gene from *Ruegeria pomeroyi* has been deposited in GenBank under accession number KU891821.

.

Table S3. Primers used in this study.

Primer	Description	Reference/source
LacZenuR_up_for	GCGAATTCCTTCATGTTCAGCGCCCTC	construction of pBAS19 and pBAS2(
LacZenuR_PstI_rev	GCCTGCAGGATCGGGCAGCCAATTTG	construction of pBAS19
LacZuehA_PstI_rev	GCCTGCAGCAAAGGTGAAAGTGATGGATTGAG	construction of pBAS20 and pBAS2
LacZuehA_EcoRI_for	GCGAATTCCGGAGCGATACGAAATCG	construction of pBAS21
EnuR_His/Ala_rev:	GTGAGGTAAATCGTCCGC	site-directed mutagenesis of pBAS20 [Lys-302/His; AAA/CAT]
EnuR_His_for:	GACTTTTACAcatTGCACCGTTTCC	site-directed mutagenesis of pBAS20 [Lys-302/His; AAA/CAT]
deltantrXY_up_for	CACACAGGAAACAGCTATGACATGATTACGCGG GTCGACGATATCCCG	construction of pBAS41
deltantrXY_up_rev	CAGGCTTATGTCAATTCGAGCTGGTTGCCACCT GCTGCC	construction of pBAS41
Gentamycin_ntrXY_for	GGCACATCAGGATGAGGGCAGCAGGTGGCAACC AGCTCGAATTGACATAAGCCTG	construction of pBAS41 (amplification of the Gm^R gene from p34S_Gm)
Gentamycin_ntrXY_rev	CCCGCAGGCTAGGGGCGCAACGCCTTCTTACTC TTAGGTGGCGGTACTTGGG	construction of pBAS41 (amplification of the Gm^R gene from p34S_Gm)
deltantrXY_down_for	CACTTTGATATCGACCCAAGTACCGCCACCTAA GAGTAAGAAGGCGTTGCGC	construction of pBAS41
deltantrXY_down_rev	CCAAGCTTGCATGCCTGCAGGTCGACTCTAGGA TGATGACCTTCATTCCCTGG	construction of pBAS41
deltantrXY_rev_for	GGCGGTAAGCCGCGTTAGCGGCA	construction of chromosomal (*ntrXY::Gm*)1 deletion mutant
deltantrXY_rev_for	GCCCGCAGGCTAGGGGCGCAAC	construction of chromosomal (*ntrXY::Gm*)1 deletion mutant
L1_rev_dye[a]	GGCAGCGACGGCCCCAAAGG	amplification of *uehA* promoter fragment for EMSA analysis
L2_fw	CCGCATCTCGCTGGGCAGCG	amplification of *uehA* promoter fragment for EMSA analysis
L5_rev_dye[a]	CCAGCAGCGGATTGGTCATCACCCG	amplification of *uehA* internal fragment for EMSA analysis
L4_fw	CGTCGACCAGTCGCCGGGCT	amplification of *uehA* internal fragment for EMSA analysis
EZ-Tn5 PCR for	GCAAAGCAAAAGTTCAAAATCACC	RATE-PCR
EZ-Tn5 PCR rev	GGATCTGCATCGCAGGATGC	RATE-PCR
KAN-2-FP-1	ACCTACAACAAAGCTCTCATCAACC	EZ-Tn*5* sequencing primer
R6KAN-2 RP-1	CTACCCTGTGGAACACCTACATCT	EZ-Tn*5* sequencing primer

[a]These primers carry the fluorescence label dyomics781 (Microsynth, Balgach, Switzerland) at their 5´end.

Figure S1

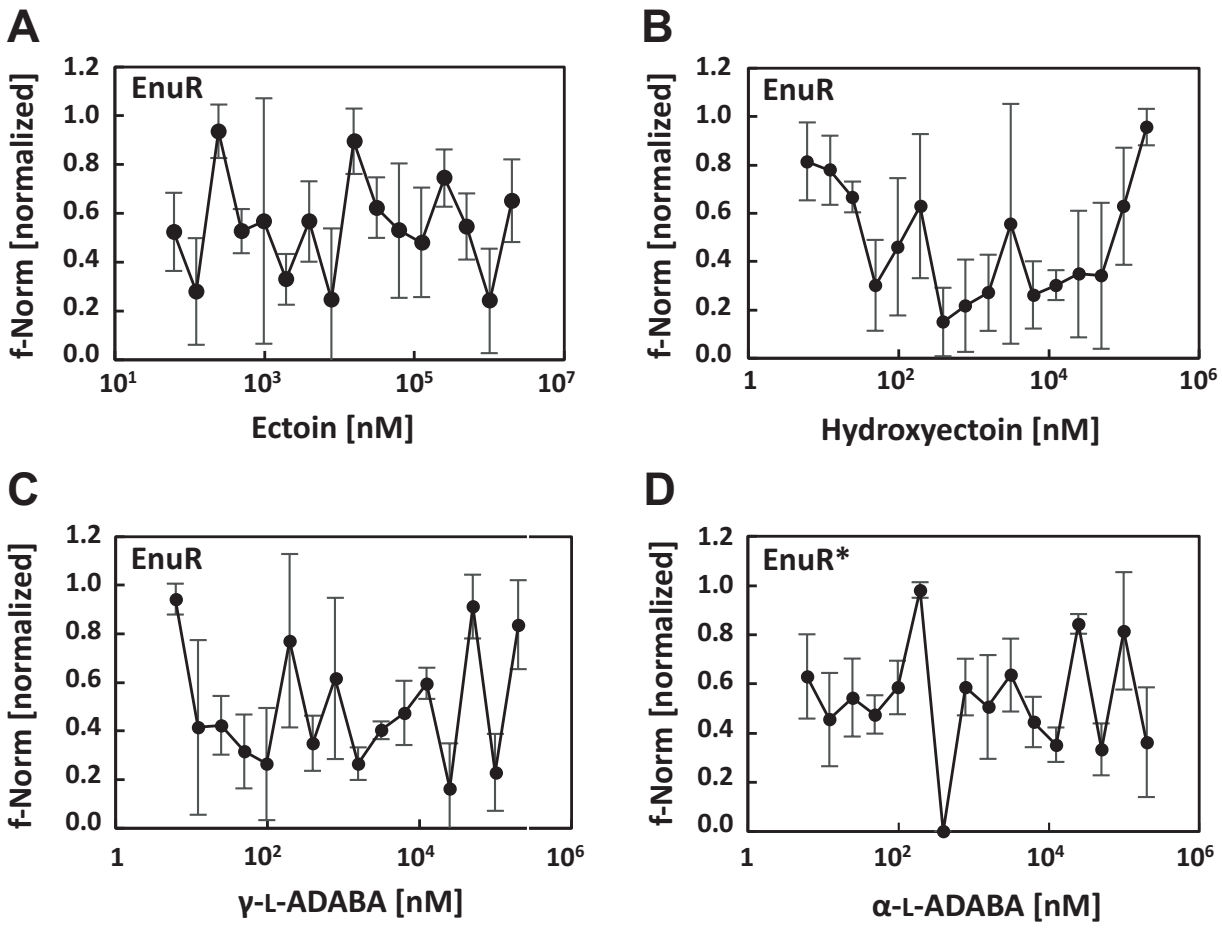

Fig. S1. Ligand binding by the wild-type EnuR protein and its mutant EnuR* derivative as assessed by microscale thermophoresis. Purified EnuR protein (200 nM) was titrated with increasing concentrations of (A) ectoine, (B) hydroxyectoine, and (C) γ-L-ADABA. (D) Purified mutant EnuR* protein (200 nM) was titrated with increasing concentrations of α-L-ADABA.

Figure S2

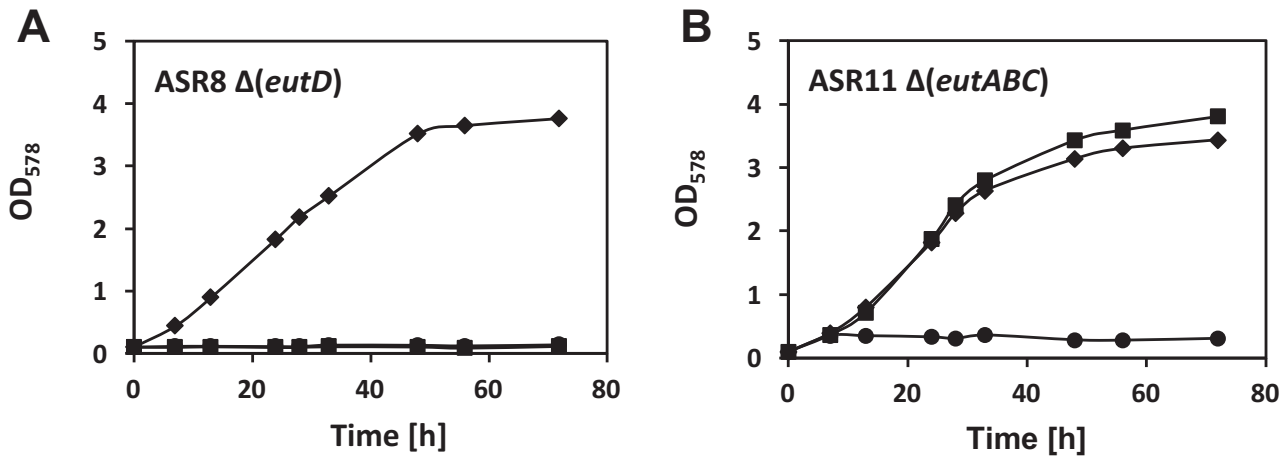

Fig. S2. Growth curves of rifampicin-resistant *R. pomeroyi* J470 mutant derivatives defective in various ectoine catabolic genes. Cultures were grown in basal minimal media containing either ectoine (squares) or hydroxyectoine (circles) as the sole carbon and nitrogen source, or glucose and NH_4Cl (rhombi) as carbon and nitrogen source respectively. Ectoine, hydroxyectoine, and glucose were present in these cultures at a concentration of 28 mM. NH_4Cl was added to a final concentration of 200 mM. (A) Growth of the *R. pomeryi* strain ASR8 [Δ(*eutD::Gm*)1] (B) Growth of the *R. pomeryi* strain ASR11 [Δ(*eutABC::Gm*)1].

Figure S3

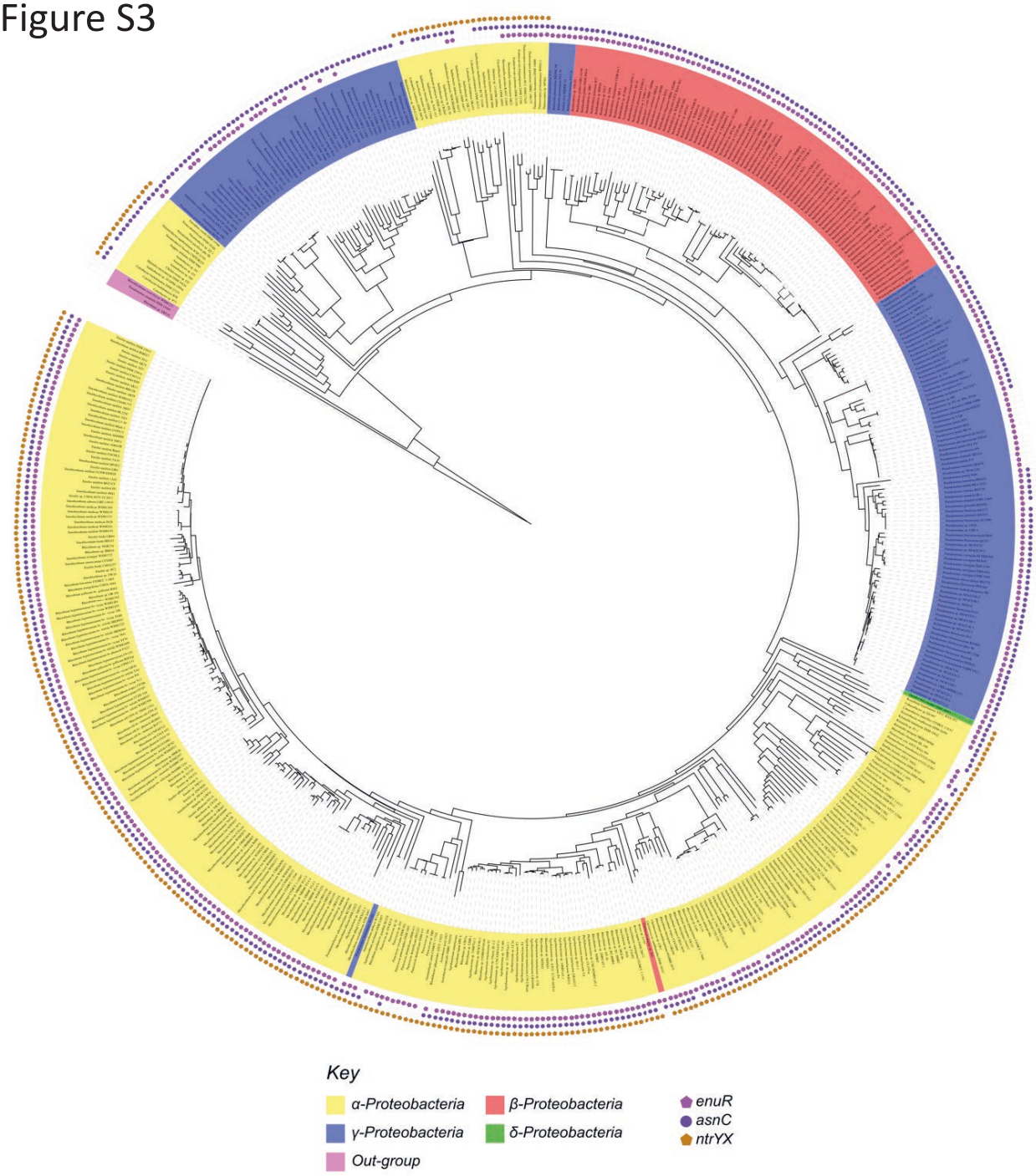

Fig. S3. Taxonomic distribution of *enuR*, *asnC*, and *ntrYX* genes among microorganisms predicted to consume ectoines. An alignment of 539 amino acid sequences homologous to the EutD protein from *Ruegeria pomeroyi* DSS-3 has previously been used to construct a phylogenetic tree of presumed consumers of ectoines. The color code outlines the distribution of EutD-type proteins among the classes of the *Proteobacteria*. The presence of *enuR* or *asnC* genes in the direct vicinity (for *enuR*) or within (for *asnC*) hydroxyectoine/ectoine-transport and catabolic gene clusters are indicated by a pink pentagon and a purple circle respectively. The presence of a gene cluster (*ntrXY*) encoding the two-component NtrYX regulatory system in the genome sequences of the predicted consumers of ectoines is indicated by orange pentagons.

Figure S4

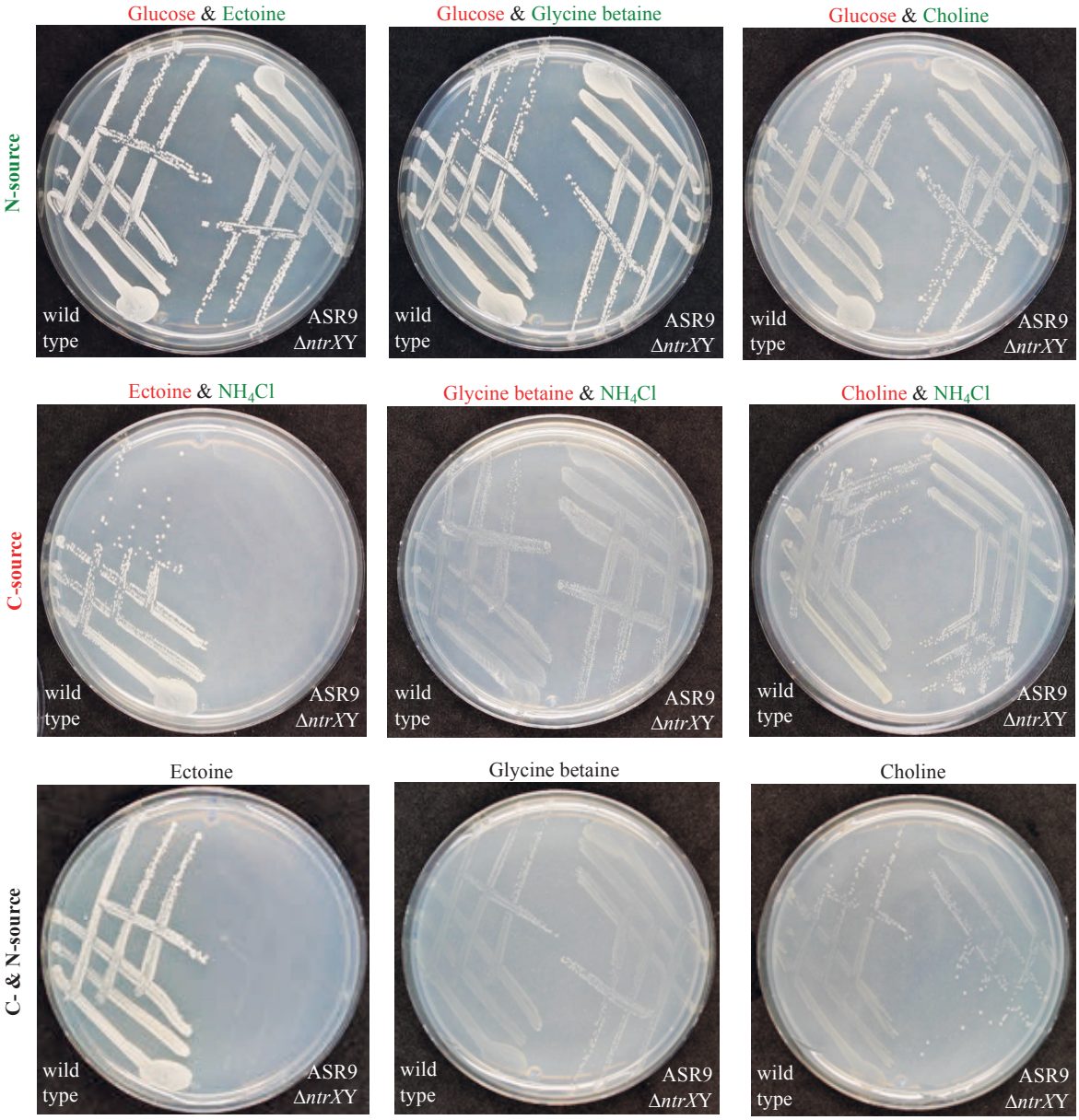

Fig. S4. Growth of rifampicin-resistant *R. pomeroyi* wild type J470 and its mutant derivative ASR9 which carries a deletionfor *ntrXY* (Δ*ntrXY*). Cells were grown on basal minimal medium agar plates containing ectoine, glycine betaine or choline either as a sole carbon, as a sole nitrogen or as a combined carbon and nitrogen source as indicated.

References

Dennis, J.J., and Zylstra, G.J. (1998) Plasposons: modular self-cloning minitransposon derivatives for rapid genetic analysis of gram-negative bacterial genomes. *Appl Environ Microbiol* **64**: 2710-2715.

Figurski, D.H., and Helinski, D.R. (1979) Replication of an origin-containing derivative of plasmid RK2 dependent on a plasmid function provided in trans. *Proc Natl Acad Sci U S A* **76**: 1648-1652.

Kvitko, B.H., and Collmer, A. (2011) Construction of *Pseudomonas syringae* pv. tomato DC3000 mutant and polymutant strains. *Methods Mol Biol* **712**: 109-128.

Moran, M.A., Buchan, A., Gonzalez, J.M., Heidelberg, J.F., Whitman, W.B., Kiene, R.P. et al. (2004) Genome sequence of *Silicibacter pomeroyi* reveals adaptations to the marine environment. *Nature* **432**: 910-913.

Schulz, A., Stöveken, N., Binzen, I.M., Hoffmann, T., Heider, J., and Bremer, E. (2017) Feeding on compatible solutes: a substrate-induced pathway for uptake and catabolism of ectoines and its genetic control by EnuR. *Environ Microbiol* **19**: 926-946.

Todd, J.D., Kirkwood, M., Newton-Payne, S., and Johnston, A.W. (2012) DddW, a third DMSP lyase in a model Roseobacter marine bacterium, *Ruegeria pomeroyi* DSS-3. *ISME J* **6**: 223-226.

Todd, J.D., Curson, A.R., Kirkwood, M., Sullivan, M.J., Green, R.T., and Johnston, A.W. (2011) DddQ, a novel, cupin-containing, dimethylsulfoniopropionate lyase in marine roseobacters and in uncultured marine bacteria. *Environ Microbiol* **13**: 427-438.

6.1.2 Degradation of the microbial stress protectants and chemical chaperones ectoine and hydroxyectoine by a bacterial hydrolase-deacetylase complex (2020)

J Biol Chem 2020; 295(27), 9087-9104 doi: 10.1074/jbc.RA120.012722

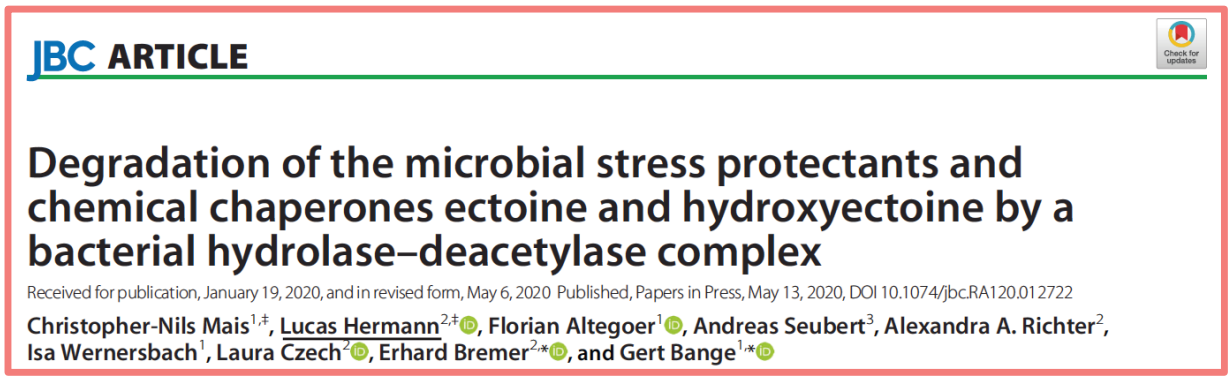

JBC ARTICLE

Degradation of the microbial stress protectants and chemical chaperones ectoine and hydroxyectoine by a bacterial hydrolase–deacetylase complex

Received for publication, January 19, 2020, and in revised form, May 6, 2020 Published, Papers in Press, May 13, 2020, DOI 10.1074/jbc.RA120.012722

Christopher-Nils Mais[1,‡], Lucas Hermann[2,‡], Florian Altegoer[1], Andreas Seubert[3], Alexandra A. Richter[2], Isa Wernersbach[1], Laura Czech[2], Erhard Bremer[2,*], and Gert Bange[1,*]

The following research article “Degradation of the microbial stress protectants and chemical chaperones ectoine and hydroxyectoine by a bacterial hydrolase-deacetylase complex” was published in the Journal of Biological Chemistry in 2020 after a peer-reviewing process. The Journal of Biological Chemistry also chose this article as the cover figure of the corresponding printed issue. My contribution to this publication were the bioinformatic analysis for ectoine consumers, figure preparation, enzymatic assays, and analysis via HPLC as well as the *in vivo* experiments in *Escherichia coli* and their analysis via HPLC. C. N. Mais prepared figures and produced, purified, characterized, crystallized, and determined the structure of the EutD and EutE proteins, with the help of F. Altegoer and I. Wernersbach. A. Seubert isolated α-ADABA. A. A. Richter performed the acetate assays. L. Czech performed the bioinformatic analysis for ectoine producers. E. Bremer and G. Bange conceptualized and supervised the project. C. N. Mais, E. Bremer, G. Bange and I wrote the manuscript with contributions from all authors.


JBC
JOURNAL OF BIOLOGICAL CHEMISTRY
JULY 3, 2020 | VOLUME 295 | NUMBER 27
EctD
Ectoine
EctC
γ-ADABA
CoA
Acetyl-CoA
EutD
α-ADABA
EutABC
EutE
Acetate
Hydroxy-α-ADABA
Hydroxy-DABA
Atf
β-sem..aldehyde
Ssd
L-Aspa...
ASBMB PUBLICATIONS

Degradation of the microbial stress protectants and chemical chaperones ectoine and hydroxyectoine by a bacterial hydrolase–deacetylase complex

Received for publication, January 19, 2020, and in revised form, May 6, 2020 Published, Papers in Press, May 13, 2020, DOI 10.1074/jbc.RA120.012722

Christopher-Nils Mais[1,‡], Lucas Hermann[2,‡], Florian Altegoer[1], Andreas Seubert[3], Alexandra A. Richter[2], Isa Wernersbach[1], Laura Czech[2], Erhard Bremer[2,*], and Gert Bange[1,*]

From the [1]Philipps-University Marburg, Center for Synthetic Microbiology (SYNMIKRO) & Faculty of Chemistry, Marburg, Germany, the [2]Philipps-University Marburg, Center for Synthetic Microbiology (SYNMIKRO) & Faculty of Biology, Marburg, and the [3]Philipps-University Marburg, Faculty of Chemistry, Marburg, Germany

Edited by Ruma Banerjee

When faced with increased osmolarity in the environment, many bacterial cells accumulate the compatible solute ectoine and its derivative 5-hydroxyectoine. Both compounds are not only potent osmostress protectants, but also serve as effective chemical chaperones stabilizing protein functionality. Ectoines are energy-rich nitrogen and carbon sources that have an ecological impact that shapes microbial communities. Although the biochemistry of ectoine and 5-hydroxyectoine biosynthesis is well understood, our understanding of their catabolism is only rudimentary. Here, we combined biochemical and structural approaches to unravel the core of ectoine and 5-hydroxyectoine catabolisms. We show that a conserved enzyme bimodule consisting of the EutD ectoine/5-hydroxyectoine hydrolase and the EutE deacetylase degrades both ectoines. We determined the high-resolution crystal structures of both enzymes, derived from the salt-tolerant bacteria *Ruegeria pomeroyi* and *Halomonas elongata*. These structures, either in their apoforms or in forms capturing substrates or intermediates, provided detailed insights into the catalytic cores of the EutD and EutE enzymes. The combined biochemical and structural results indicate that the EutD homodimer opens the pyrimidine ring of ectoine through an unusual covalent intermediate, *N*-α-2 acetyl-L-2,4-diaminobutyrate (α-ADABA). We found that α-ADABA is then deacetylated by the zinc-dependent EutE monomer into diaminobutyric acid (DABA), which is further catabolized to L-aspartate. We observed that the EutD–EutE bimodule synthesizes exclusively the α-, but not the γ-isomers of ADABA or hydroxy–ADABA. Of note, α-ADABA is known to induce the MocR/GabR-type repressor EnuR, which controls the expression of many ectoine catabolic genes clusters. We conclude that hydroxy–α-ADABA might serve a similar function.

Many members of the three domains of life use compatible solutes as cytoprotectants (1–4). These highly water-soluble organic compounds are compliant with the physiology of both prokaryotic and eukaryotic cells and can thus be accumulated to very high intracellular concentrations. The function-preserving attributes of compatible solutes for proteins and other cellular components are reflected in their description as chemical chaperones (5–7). Microorganisms have widely adopted these solutes as stress protectants against the detrimental effects of high environmental osmolarity and salinity (4, 8). The degree of osmotic stress imposed onto the bacterial cell sensitively determines the size of the cytoplasmic compatible solute pool. Consequently, high osmolarity instigated water efflux, drop of vital turgor, and an undue increase in molecular crowding are counteracted by the accumulation of these organic osmolytes (9, 10). Microorganisms exploit compatible solutes not only as osmostress protectants but also in their cellular defense against extremes in both high and low growth temperatures (11–13), desiccation (14, 15), and oxidative stress (16). Bacteria and Archaea can synthesize a considerable variety of compatible solutes (*e.g.* glycine betaine, L-proline, and trehalose) (2, 4, 8). Also, they can import many of them via osmotically regulated transport systems (9, 10). By these means, severely osmotically stressed cells can accumulate compatible solutes in concentrations of up to several hundred millimolars (1).

The tetrahydropyrimidines ectoine (17) and its derivative 5-hydroxyectoine (18) (Fig. 1*A*) are prominent members of compatible solutes synthesized or imported by microorganisms (19). Like other compatible solutes, ectoines are preferentially excluded from the immediate hydration shell of proteins (20), a property hindering protein aggregation and preserving macromolecular functionality (5, 6, 21). These attributes of ectoines, and their water-binding and anti-inflammatory nature, led to various commercial applications, in particular in the area of skin care. Using *Halomonas elongata* as a cell factory, an industrial scale biotechnological production process for ectoines can deliver these valuable natural products on the scale of tons annually (21, 22).

Reflecting the function of ectoines as osmostress protectants, transcription of their biosynthetic genes (*ectABC*/*ectD*) is up-regulated in response to increases in environmental osmolarity (23). Biosynthesis of ectoines is now a rather well biochemically and structurally understood process (23–26). Biosynthesis begins with the central microbial metabolite L-aspartate-β-semialdehyde, and involves the ectoine biosynthetic enzymes L-2,4-diaminobutyrate transaminase EctB

This article contains supporting information.
‡These authors contributed equally to this work.
*For correspondence: Erhard Bremer, bremer@staff.uni-marburg.de; Gert Bange, gert.bange@synmikro.uni-marburg.de.

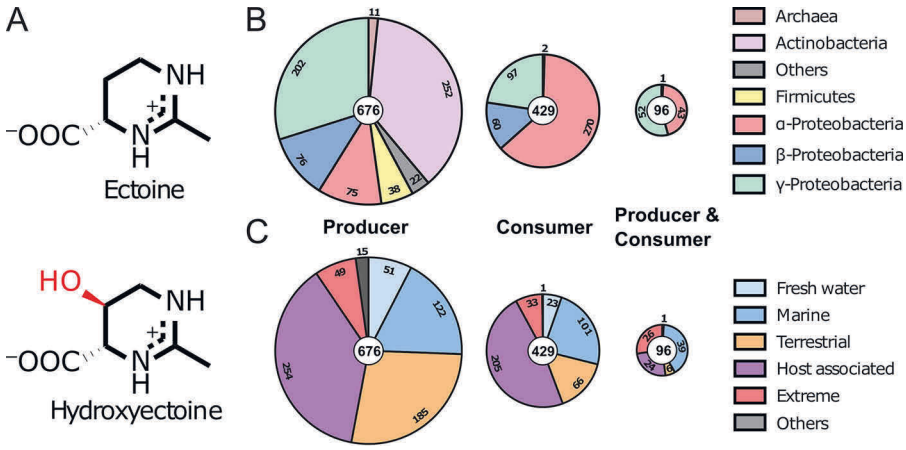

Figure 1. Eco-physiology of the ectoines. *A,* chemical structure of ectoine ((*S*)-2-methyl-1,4,5,6-tetrahydropyrimidine-4-carboxylic acid) and its derivative 5-hydroxyectoine ((4*S*,5*S*)-5-hydroxy-2-methyl-1,4,5,6-tetrahydropyrimidine-4-carboxylic acid). The 5-hydroxyl moiety of 5-hydroxyectoine is shown in *red*. *B,* distribution of microorganisms capable of ectoine production and/or degradation among different phyla. *C,* distribution of organisms capable of ectoine production and/or degradation among different habitats.

(EC 2.6.1.76) (27, 28), L-2,4-diaminobutyrate acetyltransferase EctA (EC 2.3.1.178) (25), and ectoine synthase EctC (EC 4.2.1.108) (29), with L-2,4-diaminobutyrate (DABA) and *N*-γ-acetyl-L-2,4-diaminobutyrate (γ-ADABA) as the respective intermediates (24, 29). In a substantial subgroup of ectoine producers, ectoine can be further transformed into 5-hydroxyectoine through a regio- and stereospecific reaction catalyzed by the ectoine hydroxylase EctD (EC 1.14.11.55) (30, 31). Like compatible solute production in general (32), *de novo* synthesis of ectoine is costly. When the entire biosynthetic process is considered, cells growing heterotrophically in a minimal medium with glucose as the sole carbon source need to spend ~40 ATP equivalents to produce just a single ectoine molecule (32).

In addition to their stress-protective and function-preserving properties, the nitrogen- and carbon-rich ectoine and 5-hydroxyectoine molecules (Fig. 1*A*) have found uses as nutrients for microorganisms (33–37). Ectoines are released into the environment from microbial producer cells through the transient opening of mechano-sensitive channels upon sudden osmotic down-shock (38), or simply when cells disintegrate. Environmental ectoines can then be re-captured by members of the microbial community either for re-use as osmostress protectants or recycled as nutrients (10, 23). Ectoine catabolism might also be triggered when cells capable of both ectoine synthesis and consumption are slowly shifted from high to lower environmental osmolarities (37).

A pioneering proteomics study by Jebbar *et al.* (35) focusing on the plant root-associated bacterium *Sinorhizobium meliloti* identified a substrate-inducible ABC-type transport system for the import of ectoines and several enzymes required for their catabolism. This study promoted the identification of orthologous genes in other species such as the highly salt-tolerant bacterium *H. elongata* (37) and the marine proteobacterium *Ruegeria pomeroyi* (39). Although *R. pomeroyi* is only an ectoine consumer (36), *H. elongata* can both synthesize and degrade ectoine (37). In contrast to the genes for ectoine/5-hydroxyectoine biosynthesis that are mostly contained in an evolutionarily conserved operon structure (23), the operons for the catabolism of ectoines are more varied, both with respect to gene order and content (36, 37). However, a common denominator of the catabolic gene cluster is the presence of a EutD/EutE (Eut: ectoine utilization) enzyme bi-module, regarded as central for ectoine utilization as a nutrient.

It is thought that ectoine degradation begins with the opening of the pyrimidine ring by the ectoine hydrolase EutD (DoeA) (EC 3.5.4.44) to form *N*-acetyl-diaminobutyrate (ADABA), which is then catabolized by the *N*-acetly-L-2,4-diaminobutyrate deacetylase EutE (DoeB) (EC 3.5.1.125) to acetate and diaminobutyrate (DABA) (36, 37). The Atf aminotransferase and the Ssd dehydrogenase subsequently transform DABA into L-aspartate with L-aspartate-β-semialdehyde as the intermediate (36, 37).

An initial *in vivo* characterization of the *H. elongata* DoeA (EutD) protein heterologously produced in *Escherichia coli* by Schwibbert *et al.* (37) suggests that this enzyme can form both the α- and γ-ADABA isomers from imported ectoine. Mutant studies in *H. elongata* also revealed that DoeB (EutE) specifically de-acetylates the α-ADABA isomer, whereas the DoeA (EutD)-formed γ-ADABA molecule was suggested to be recycled into ectoine via the EctC ectoine synthase (37). Moreover, the EutABC enzymes were speculated by Schulz *et al.* (36) to initially convert 5-hydroxyectoine into ectoine for further metabolism by the EutD/EutE bi-module. This proposal was primarily based on bioinformatics and the observation that a *eutABC* deletion mutant of *R. pomeroyi* was unable to metabolize 5-hydroxyectoine but retained the ability to utilze ectoine as a nutrient (23, 36).

Overall, most of the steps of the proposed ectoine and 5-hydroxyectoine degradation routes have not been experimentally challenged to date at any level of detail. Here, we clarify the catalytic mechanisms underlying the central steps in the catabolism of ectoine and 5-hydroxyectoine through an in-depth biochemical and structural analysis of the conserved EutD/EutE enzyme bi-module. Our study shows that the EutD and EutE enzymes from *R. pomeroyi* act in concert. The EutD hydrolase opens the pyrimidine ring of ectoine via an unusual covalent intermediate involving a conserved glutamate to generate α-ADABA, but not γ-ADABA. This is an important

finding, as α-ADABA, but not γ-ADABA, serves as the internal inducer of the MocR/GabR-type repressor EnuR controlling the expression of the majority of ectoine/5-hydroxyectoine catabolic gene clusters (39, 40). Following α-ADABA synthesis by EutD, the zinc-dependent diaminobutyrate deacetylase EutE hydrolyzes this intermediate to produce acetate and the L-aspartate precursor DABA. Contrary to the previous proposal by Schulz *et al.* (36), we observed that the EutD protein also hydrolyzes 5-hydroxyectoine to form hydroxy–α-ADABA, a finding that requires a rethinking of the overall organization of the ectoine/5-hydroxyectoine degradation route.

Results

Phylogenomics and ecology of ectoine production and consumption

To study the phylogenomics of ectoine synthesis and metabolism, we analyzed all fully sequenced and annotated bacterial and archaeal genomes available in the IMG/M database (41). We used the amino acid sequence of the EctC ectoine synthase from *Paenibacillus lautus* (29), and that of the EutD ectoine hydrolase from *R. pomeroyi* (36) as search queries as markers for ectoine production and consumption, respectively. At the time of the search (November 2019) 8,850 fully sequenced prokaryotic genome sequences were represented in the IMG/M database. We found 676 predicted ectoine producers in these data set (7.5%) (665 originate from Bacteria and 11 from Archaea). 429 Ectoine consumers were found (4.8%); none was a member of the Archaea (Fig. 1*B*; Fig. S1). 96 Microbial species possessed both ectoine synthesis and degradation genes (less than 1%) (Fig. 1*B*); with respect to the total number of ectoine producers, this group of microorganisms rises to 14.2%.

Ectoine producers and consumers are found in most ecological niches ranging from freshwater, saltwater, and terrestrial, to extreme environments. They are also present in host-associated species including pathogens of animals, humans, and plants (Fig. 1*C*). Ectoine producers are found among the α-, β-, and γ-proteobacteria, actinobacteria, firmicutes, and some archaea (overall 12 phyla), whereas ectoine consumers are primarily found among the α-, β-, and γ-proteobacteria (Fig. 1*B*). In particular, both catabolic and anabolic ectoine genes were present in a restricted group of α- and γ-proteobacteria (Fig. 1*B*). These are primarily found in members of the Oceanospirallales, Vibrionales, and Rhodobacteriales (Fig. S1).

EutD and EutE cooperate to degrade ectoine

The wide distribution of bacteria able to consume ectoine prompted us to investigate the degradation route in mechanistic detail. We focused on the EutD/EutE enzyme bi-module as it is considered central for the catabolism of ectoine and 5-hydroxyectoine (36, 37). To dissect the molecular mechanism of ectoine degradation, we chose the marine bacterium *R. Pomeroyi* (*Rp*) as our model system, a bacterium that can only consume ectoine and in which the genetics and physiology of ectoine/5-hydroxyectoine degradation has already been studied to some extent (36, 39). Recombinantly produced in *E. coli* BL21(DE3), the *Rp*EutD and *Rp*EutE proteins were purified by a nickel-ion-affinity followed by size exclusion chromatography (Fig. S2, *A* and *B*). With the purified enzymes in hand, we qualitatively analyzed their ability to degrade 1 mM ectoine within 20 min by HPLC. Neither *Rp*EutD nor *Rp*EutE were capable of degrading ectoine (Fig. 2*A*). However, when both enzymes were present in the assay, substantial ectoine degradation was observed (Fig. 2*A*). These findings suggest that both enzymes cooperate for ectoine degradation. Next, we aimed at a better enzyme-kinetic understanding of the *Rp*EutD/*Rp*EutE enzyme pair. To this end, we employed a commercially available kit allowing the online detection of acetate, which together with DABA is a plausible reaction product of the EutD/EutE-catalyzed ectoine degradation pathway (Fig. 2*B*). Only when EutD and EutE were present together, did efficient acetate production occur (Fig. S2*C*), yielding apparent k_M and V_{max} values of 0.6 mM and 1.2 mmol/min/g, respectively (Fig. 2*C*). Our data indicate that the degradation of ectoine requires a complex of the EutD and EutE enzymes, which we tried to detect by size exclusion chromatography, isothermal calorimetry, and pull-down experiments. We were not able to visualize the complex by these methods arguing for its short-lived nature. Taken together, EutD and EutE cooperate for efficient ectoine degradation likely through a transient complex.

Degradation of ectoine proceeds via α-ADABA

EutD catalyzed opening of the ectoine pyrimidine ring should yield ADABA, which can exist in the constitutional isomers α-ADABA and γ-ADABA (Fig. 2*B*). We prepared both ADABAs by alkaline hydrolysis of ectoine and subsequent separation by anion chromatography and then analyzed their use as substrates in the enzyme assays (Fig. S3). We analyzed the ability of *Rp*EutE to degrade α- and γ-ADABA (Fig. 2*B*). *Rp*EutE exclusively degraded α-ADABA with k_M and V_{max} values of 0.1 mM and 2.2 mmol/min/g, respectively (Fig. 2*D*). Thus, ectoine degradation by the *R. pomeroyi* enzymes exclusively proceeds via α-ADABA, a finding that is consistent with data obtained for the corresponding *H. elongata* enzymes (37). Our kinetic analysis also suggests that the EutD-mediated generation of α-ADABA is slower than the EutE-catalyzed degradation of α-ADABA, possibly making EutD the rate-limiting step (Fig. 2, *C* and *D*).

To show that ectoine degradation proceeds via α-ADABA also *in vivo*, we produced *Rp*EutD, *Rp*EutE, and both proteins together in *E. coli* strain MC4100 grown on minimal medium supplemented with 1 mM ectoine and 0.3 M NaCl to trigger ectoine import by the ProP and ProU transporters (42). Consistent with our *in vitro* analysis, neither α- nor γ-ADABA was detected when only either EutD or EutE was present (Fig. 2*E*). Surprisingly, when both enzymes were produced together exclusively α-ADABA was detected (Fig. 2*E*) but we could not find the expected reaction product of the EutD/EutE bi-module, DABA, by HPLC analysis. We have no explanation why α-ADABA is formed when EutD/EutE are co-produced, but EutE is unable to convert α-ADABA to DABA. It is important to keep in mind that both proteins are being produced in a recombinant background that might allow the EutD/EutE-dependent conversion of ectoine into α-ADABA, but somehow impairs the conversion of the latter into DABA. It might also be

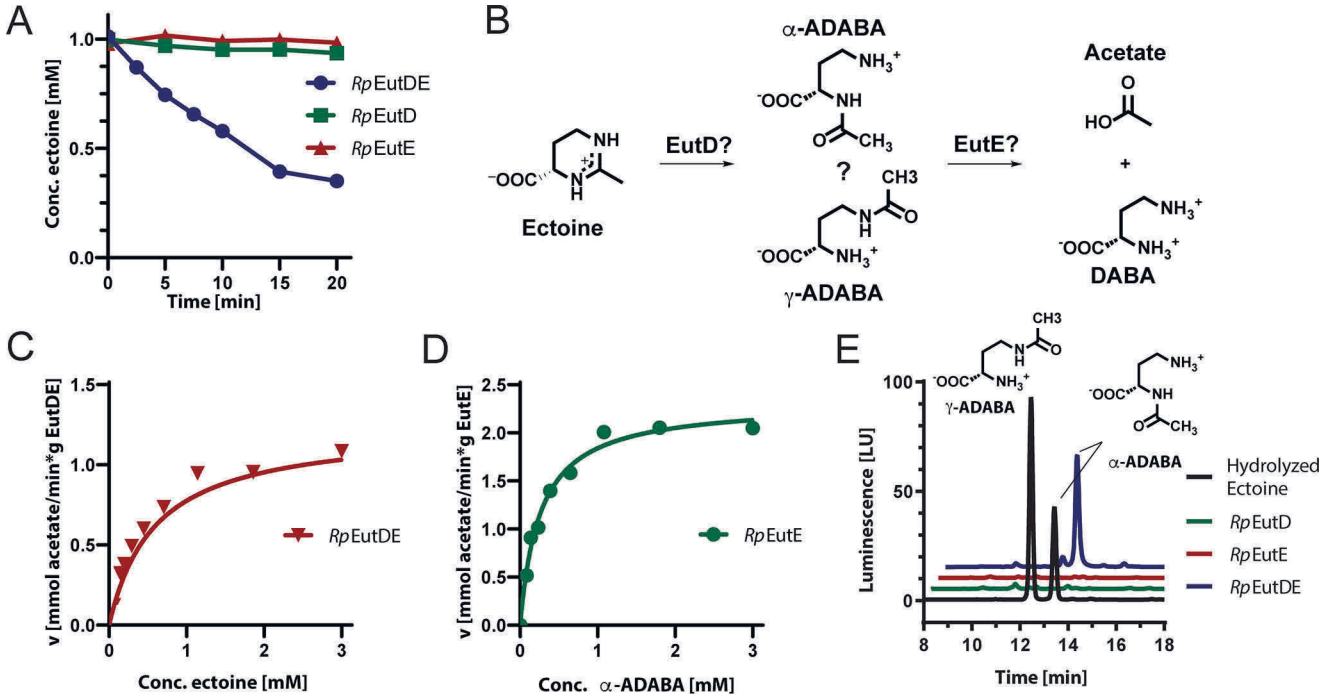

Figure 2. Ectoine degradation by EutD and EutE. *A,* degradation of ectoine by *Rp*EutD (*green*), *Rp*EutE (*red*), and both enzymes together (*blue*), as monitored by HPLC. *B,* proposed pathway of ectoine degradation. EutD opens the pyrimidine ring of ectoine to generate ADABA, which can exist in the α- and γ-ADABA isomers. In the next step, EutE deacetylates ADABA into DABA and acetate. *C,* Michaelis-Menten plot of the enzyme pair *Rp*EutD/EutE degrading ectoine. The product acetate was quantified via a commercially available absorption-based assay. k_M = 0.6 mM; V_{max} = 1.2 mmol/min/g. *D,* Michaelis-Menten plot of *Rp*EutE degrading α-ADABA into DABA and acetate. k_M = 0.2 mM; V_{max} = 2.2 mmol/min/g. *E,* analysis of α-ADABA and γ-ADABA in *E. coli* cells expressing EutD, EutE, and both grown on ectoine containing minimal medium with glucose as the sole carbon source. HPLC analysis detects α-ADABA when both enzymes are present (*blue*). ADABA is not detected in cells expressing either *Rp*EutD or *Rp*EutE (*green* and *red*, respectively). The α-ADABA and γ-ADABA standards are shown in *black*.

that EutE is inhibited by or limited for a yet unknown compound of the *E. coli* cytoplasm (*e.g.* zinc; see below). Whatever the precise reason might be, the co-expression of *eutD/eutE* allowed us to conclude that (i) the hydrolysis of ectoine by EutD exclusively proceeds via α-ADABA as the intermediate and that (ii) both EutD and EutE need to be present to achieve hydrolysis of ectoine. We note, however, that for the corresponding *H. elongata* enzymes, somewhat different data were reported since production of solitary recombinant DoeA (EutD) protein in *E. coli* yielded both ADABA isomers. However, these were produced at very low amounts despite the fact that 1 mM ectoine was fed to the recombinant cells (37).

EutD lacks the metal-binding site of M24-type aminopeptidases

Next, we wanted to determine the crystal structure of *Rp*EutD. Unfortunately, the obtained *Rp*EutD crystals were only of poor diffraction quality. However, the closely related EutD (DoeA) protein from *H. elongata* (*He*), which shares 62.5% sequence identity with *Rp*EutD, produced well diffracting crystals (Table 1). The structure of the apo-state of *He*EutD was determined to a resolution of 2.15 Å by molecular replacement employing the structure of *E. coli* (*Ec*) PepP as search model. *Ec*PepP and *He*EutD share 25.6% sequence identity.

The crystal structure of *He*EutD shows a highly intertwined homodimer (Fig. 3*A*). Homodimerization of *He*EutD in solution was supported by multiangle light scattering experiments (Fig. S2*A*). EutD is closely related in structure and amino acid sequence to the M24-family of aminopeptidases, which usually require two metal ions for activity (Fig. S4, *A* and *B*). This could suggest that EutD operates in a metal-dependent manner. However, closer inspection of the active site architecture reveals that this cannot be the case. Aminopeptidases, such as *Ec*PepP, typically coordinate two metal ions (*e.g.* manganese or zinc) within their active sites that are critical for catalyzing cleavage of the peptide bond (reviewed in Ref. 43). In these zinc-dependent proteases, both metals are coordinated by five amino acids (*i.e.* His-354, Asp-271, Asp-260, Glu-406, and Glu-383 in the case of *Ec*PepP) (Fig. S4*C*). In EutD, however, the majority of the amino acids required for the metal ion coordination are not present, and instead were replaced by amino acids unfavorable for metal ion coordination (*i.e.* Pro-266, Tyr-329, Met-363, and Thr-376) (Fig. S4*C*). The only exception is Glu-255 of *He*EutD, which is conserved between EutD enzymes and the M24-type aminopeptidases (Fig. S4*C*). These findings suggest that EutD operates in a metal-independent manner.

Ectoine ring cleavage proceeds via a covalent α-ADABA–Glu-255 adduct

To gain further insights into the catalytic mechanism of the ectoine hydrolase, we determined the structure of *He*EutD in the presence of ectoine at a resolution of 2.25 Å (Table 1). Inspection of one active site (AS I) of the EutD homodimer revealed electron densities that could be unambiguously attributed to ectoine (Fig. 4*A*, Fig. S5*A*). The ectoine is kept in place by a hydrogen bond between Arg-326 and the carboxyl moiety

Table 1
Data collection and refinement statistics
Data were collected on ID30A-1 (MASSIF-1, ESRF), ID23-2 (ESRF), and MX14.2 (BESSY).

	*He*EutD	*He*EutD ectoine	*Rp*EutE	*Rp*EutE ADABA	*He*EutD ADABA
Data collection					
Space group	*C*2	$P4_12_12$	$P6_322$	$P2_1$	P 4_12_12
Cell dimensions					
a, *b*, *c* (Å)	120.37, 123.14, 61.49	158.2, 158.2, 122.32	99.19, 99.19, 134.62	76.667, 145.949, 164.116	157.073, 157.073, 124.072
α, β, γ (°)	90 97.184 90	90 90 90	90 90 120	90 92.30 90	90 90 90
Wavelength (Å)	0.966	0.873	0.972	0.918	0.9814
Resolution (Å)[a]	43.34–2.15 (2.22–2.15)	43.88–2.25 (2.33–2.25)	46.54–1.99 (2.06–1.99)	46.46–2.5 (2.59–2.5)	19.39–2.4 (2.48–2.4)
R_{merge}	0.0869 (0.621)	0.1474 (1.243)	0.0626 (4.804)	0.213 (1.27)	0.1901 (1.852)
$I/\sigma I$	8.96 (1.58)	10.69 (1.96)	23.00 (0.60)	5.69 (0.97)	$12.O_2$ (1.38)
Completeness (%)	98.26 (96.67)	99.96 (99.97)	99.48 (98.86)	98.59 (99.67)	99.14 (95.57)
Redundancy	3.0 (2.9)	8.9 (9.3)	21.0 (20.2)	3.9 (4.0)	14.6 (14.6)
CC1/2	0.995 (0.659)	0.997 (0.657)	1 (0.551)	0.984 (0.421)	0.998 (0.766)
Refinement					
Resolution (Å)	43.34–2.15	43.88–2.25	42.95–2.00	46.46–2.5	19.39–2.4
No. reflections	47,539 (4,593)	73,757 (7,290)	27,066 (2,612)	122,999 (12,342)	60,636 (5,766)
R_{work}/R_{free}	0.23/0.26	0.16/0.19	0.24/0.29	0.20/0.26	0.18/0.21
No. atoms	6,432	6,847	2,331	30,865	6,658
Protein	6,158	6,273	2,327	29,396	6,291
Ligand/ion	0	30	0	22	29
Water	274	544	14	1447	338
B-factors	41.42	$40.O_2$	80.66	49.99	52.27
Protein	41.30	39.29	80.76	50.46	52.25
Ligand/ion	0	72.17	0	97.10	63.62
Water	44.10	46.66	64.35	39.67	51.73
Root mean square deviations					
Bond lengths (Å)	0.005	0.003	0.031	0.003	0.008
Bond angles (°)	0.77	0.60	1.67	0.75	0.94
Ramachandran					
Favored (%)	97.66	97.71	98.36	97.92	97.22
Allowed (%)	2.34	2.16	1.32	2.08	2.53
Outliers (%)	0.00	0.13	0.00	0.00	0.25

[a] Values in parentheses are for highest-resolution shell.

of the ligand (Fig. 3*B*). Moreover, a water molecule (with a B-factor of 45) is hydrogen-bonded by His-238 (Figs. 3*B* and 4*A*). Approximately 4 Å away from this water, Glu-255, the N5-nitrogen of the pyrimidine ring of ectoine, and Tyr-52 from the N-terminal domain of the opposing EutD chain can be found (Figs. 3*B* and 4*A*). Being 4.0 Å away from the C4 carbon of ectoine, this water might be ideally suited to provide the attacking hydroxyl anion for nucleophilic cleavage of the pyrimidine ring (Fig. 3*B*). Changing Glu-255 into aspartate, and Tyr-52 and His-238 into alanine residues yielded catalytically inactive EutD variants in our acetate assay, supporting their catalytic relevance (Table S1).

In the other active site (AS II) of the EutD homodimer, however, we did not observe electron densities corresponding to ectoine. Instead, a tubular density connected to Glu-255 was visible, which we assigned as α-ADABA with its C4 carbon linked to the carboxyl moiety of Glu-255 (Figs. 3*C* and 4*B*, and Fig. S5*B*). Thus, Glu-255 serves as electron donor forming a covalent adduct with α-ADABA upon opening of the pyrimidine ring (Fig. 3*C*). The correct distance of the Glu-255 carboxyl moiety and the ectoine substrate is essential. A E255D variant is unable to perform the catalytic reaction as monitored in the *in vitro* acetate assay, presumably because the side chain of aspartate is one methylene group shorter than that of glutamate (Table S1). Thus, the opening of the ectoine ring proceeds via a covalent α-ADABA-EutD adduct, which relies on Glu-255 (Fig. 3*D*).

Release of α-ADABA from EutD requires cleavage of its orthoester-like bond with Glu-255 accompanied with the abstraction of a proton. Glu-374 and His-361 localize in reasonable proximity to serve as possible proton-acceptors (Fig. S5*E*). The E374D and H361S variants decreased EutD activity to 20 and 5%, respectively (Table S1). Thus, His-361 could be the proton acceptor allowing α-ADABA release from Glu-255. However, His-361 might also be part of a proton exchange chain together with Glu-374. Taken together, we show that EutD opens the pyrimidine ring of ectoine in a metal-independent manner through the α-ADABA intermediate, which is transiently bound to Glu-255 (Fig. 3*D*).

EutD allows back-cyclization of α-ADABA into ectoine

Our data suggest that EutD only cleaves the ectoine ring in an efficient manner when EutE is present. Moreover, our structural data suggest that the covalently bound α-ADABA intermediate could be able to cycle back into the ectoine ring structure. To test whether a back-cyclization would indeed be possible, we exposed purified *Rp*EutD to mixtures of α- and γ-ADABA and analyzed whether any of the two isomers would be converted back into ectoine. Our experiments clearly show that exclusively α-ADABA disappeared and ectoine was formed from it (Fig. 5, *A* and *B*). Thus, we conclude that *Rp*EutD is able to perform the backward reaction from α-ADABA to ectoine.

To consolidate these findings at the structural level, we co-crystallized *He*EutD in the presence of 1 mM α-ADABA to a resolution of 2.4 Å (Table 1). The crystal structure shows the *He*EutD homodimer. A closer inspection of the two active sites revealed the α-ADABA product in one and the covalently bound α-ADABA–Glu-255 intermediate in the other active site (Figs. 4, *C* and *D*, 5, *C* and *D*; Fig. S5, *C* and *D*). The carboxyl

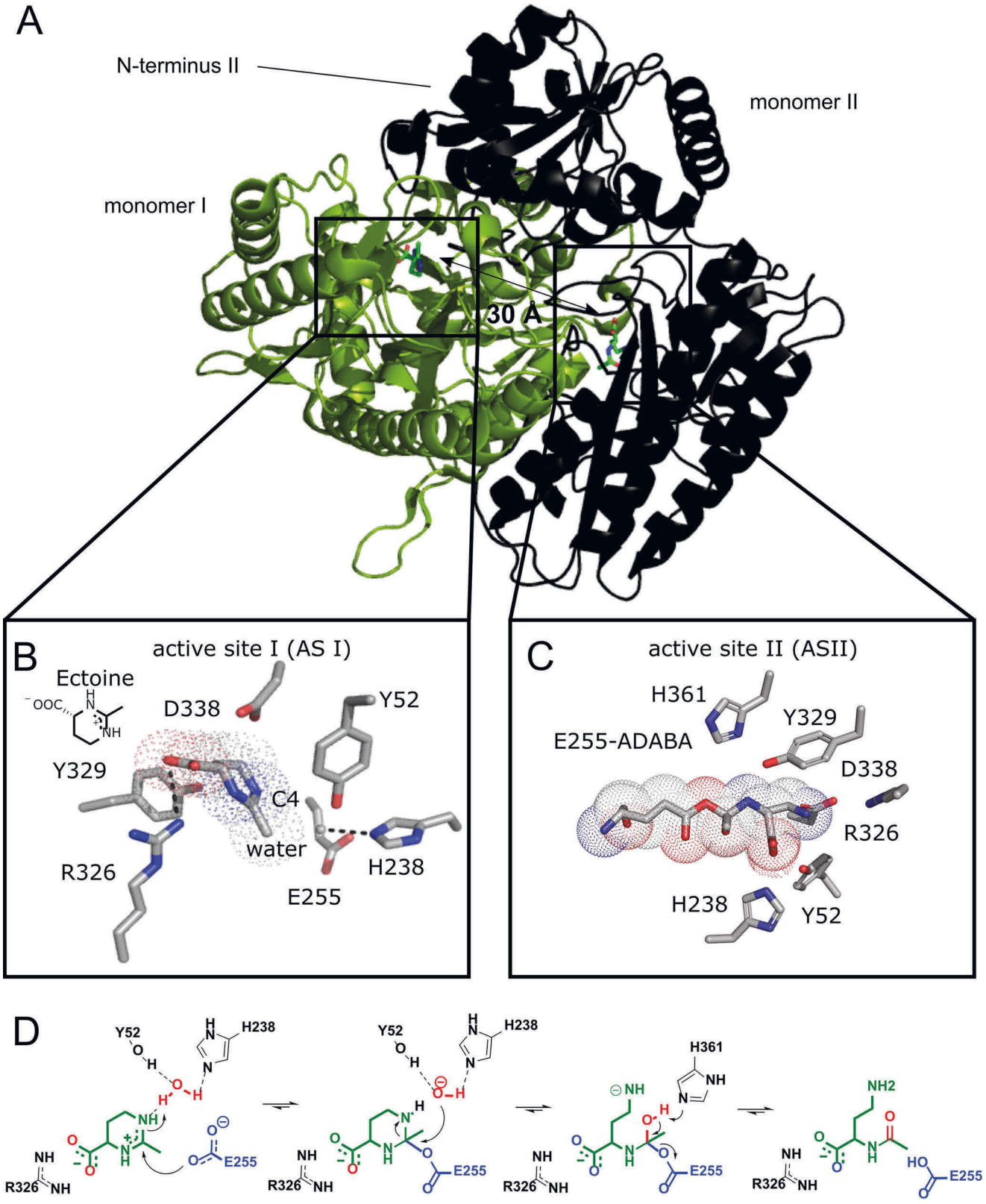

Figure 3. Crystal structure and mechanism of EutD. *A,* crystal structure of the EutD homodimer with one monomer shown as *green cartoon* and surface and the other as *black cartoon* indicating secondary structure. The localization of both actives sites is depicted. *B,* coordination of ectoine (surrounded by a *dotted outline*) and the putative catalytic water in the active site of *He*EutD. Ectoine is coordinated by hydrogen bonds to Arg-326. The attacking water is hydrogen-bonded by His-238. Glu-255 and Tyr-52 can be observed in proximity. *C, He*EutD active site with the α-ADABA intermediate covalently bound to Glu-255 (surrounded by a *dotted outline*). Further hydrogen bonds by His-238, Tyr-52, and Asp-338 keep the molecule in place. *D,* catalytic mechanism of ectoine hydrolysis by EutD. Ectoine, the catalytic water and Glu-255 are shown in *green*, *red*, and *blue*, respectively.

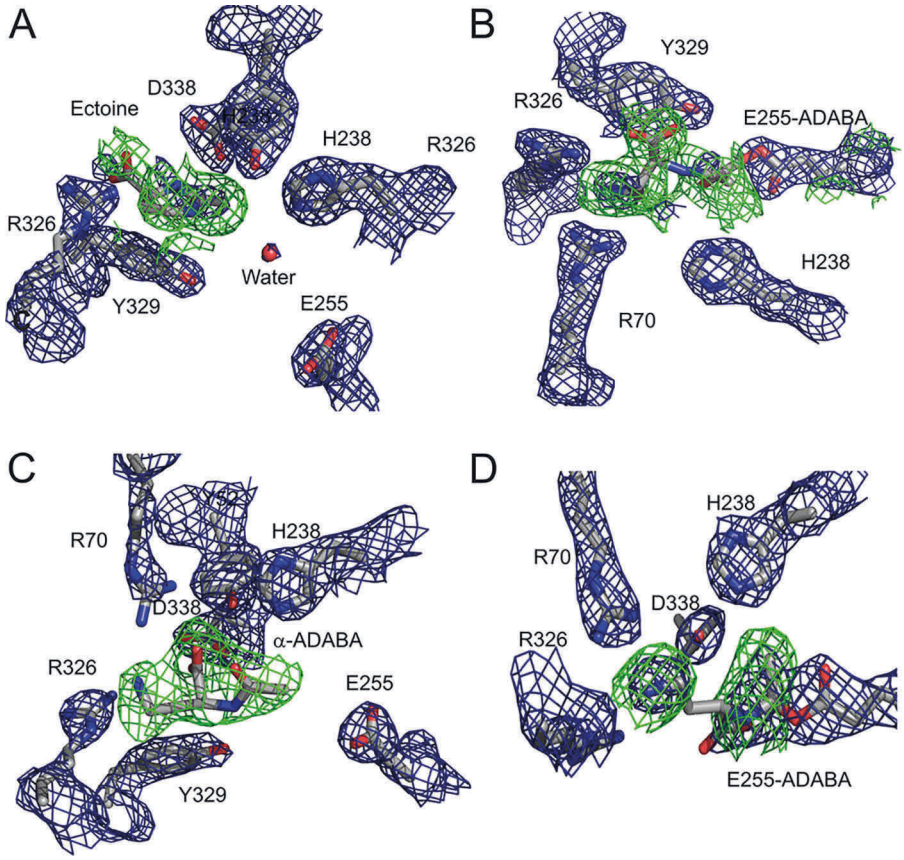

Figure 4. Unbiased electron densities of EutD ligands. *A,* unbiased $F_{obs} - F_{calc}$ difference electron density of ectoine at 3σ shown as a *green mesh*. Bias was removed by refinement prior to incorporation of the ligand. Applies to all following unbiased densities (PDB ID 6TWK). *B,* unbiased $F_{obs} - F_{calc}$ difference electron density of α-ADABA covalently linked to glutamate 255 at 3σ shown as a *green mesh*. The refined $2F_{obs} - F_{calc}$ electron density around glutamate 255 is shown as a *blue mesh* at 1.5 σ (PDB ID 6TWK). *C,* unbiased $F_{obs} - F_{calc}$ difference electron density of α-ADABA at 3σ shown as a *green mesh* (PDB ID 6YO9). *D,* unbiased $F_{obs} - F_{calc}$ difference electron density of α-ADABA covalently linked to glutamate 255 at 3σ shown as a *green mesh*. The refined $2F_{obs} - F_{calc}$ electron density around glutamate 255 is shown as a *blue mesh* at 1.5σ (PDB ID 6YO9).

moiety of the α-ADABA product interacts via hydrogen bonds with Arg-70 and Tyr-52 from the N terminus of the opposing monomer (Figs. 5*D* and 4*C*). The α-ADABA–Glu-255 intermediate in the other active site appears identical to its counterpart observed in the EutD structure obtained in the presence of 1 mM ectoine (see above) (Fig. 5*C* and 4*D*). Notably, the flexible amine group of the intermediate now points more toward Arg-326 rather than Asp-338, which could be explained by the flexible nature of the α-ADABA moiety. Taken together, our structural and biochemical analysis shows that EutD is able to form the covalent α-ADABA–Glu-255 intermediate also from the α-ADABA product, and allow the back-cyclization of α-ADABA into ectoine. Thus, the EutD-mediated cleavage of ectoine is reversible.

Cooperation between the active sites in the EutD homodimer

Our crystal structure shows a homodimer of EutD in which the ectoine substrate is present in one and the α-ADABA intermediate is found in the other active site. This indicates that both active sites, which are ~30 Å away from each other (Fig. 3*A*), are able to cooperate with each other so that one active site "knows" the catalytic state of the other active site. Closer inspection of our structure shows that Tyr-52 of one monomer reaches into the other active site of the other monomer and vice versa. This tyrosine either locates in close proximity (4 Å) to the putative catalytic water in AS I or the α-ADABA–Glu-255 intermediate in AS II (Fig. 3). Moreover, it forms a hydrogen bond with the carboxyl moiety of the α-ADABA product (Fig. 5*D*). Therefore, Tyr-52 is an ideal candidate to sense the catalytic status of one active site and communicate to the other or vice versa. Superimposition of ASs I and II further reveals a significant movement of the loop harboring Tyr-52 when the reaction proceeds (Fig. 5*E*). This in turn leads to three major conformation changes in the N-terminal domain by moving two helices closer to the C-terminal domain as well as opening a loop region in the backside of the N-terminal domain (Fig. 5*F*). These topological changes directly affect the C-terminal domain, which is harboring the respective other active site, establishing the before-mentioned communication. It can be imagined that in this way the catalytic sites communicate with each other to establish their cooperativity.

To solidify this idea, we also employed the pK_a prediction tool H++ (44) to analyze pK_a differences of Glu-255 and thus its potential protonation state between AS I and AS II (substrate- *versus* intermediate-bound site). In the ectoine-bound AS I, Glu-255 is predicted to be completely deprotonated (p$K_a < 0$), allowing the nucleophilic attack required for ectoine ring cleavage (Fig. 3*D*). In the intermediate-bound AS

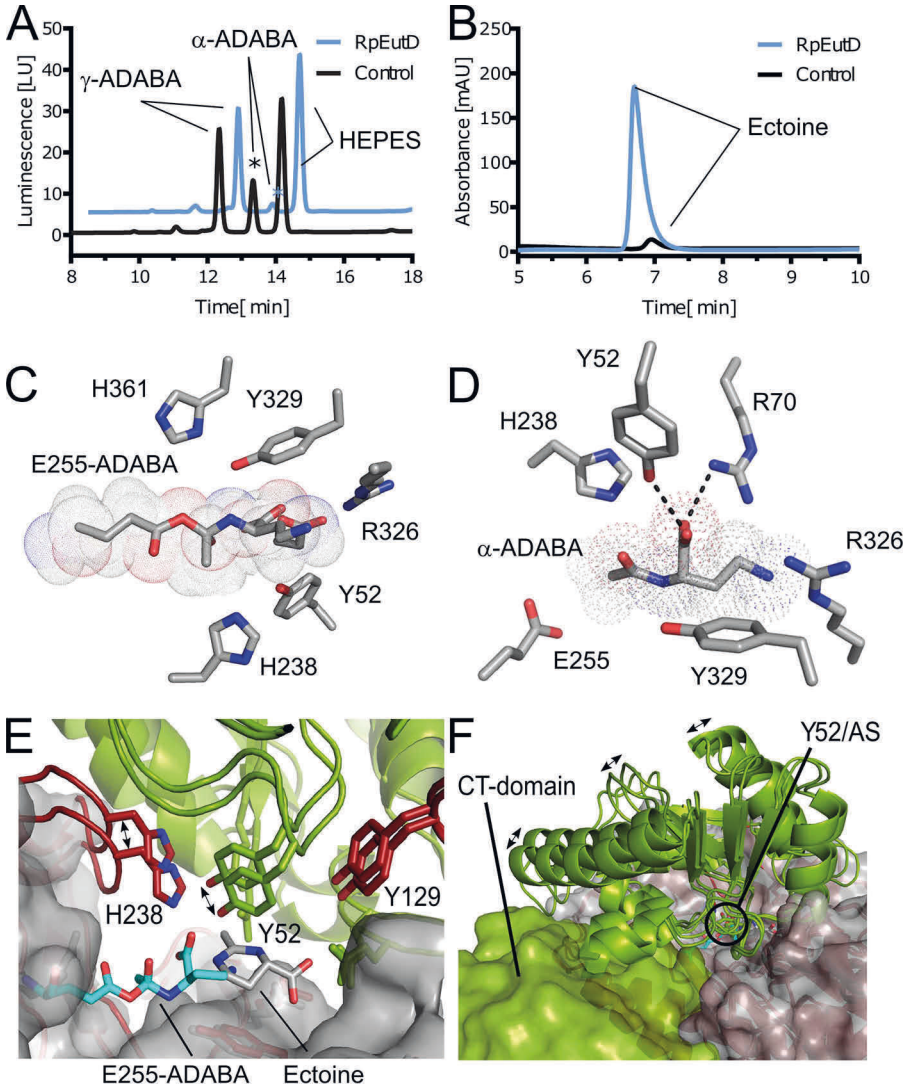

Figure 5. Reverse reaction and half-site cooperativity of EutD. *A,* ADABA isomers present in ectoine hydrolysate (*black*) and upon the addition of *Rp*EutD (*blue*). In the absence of *Rp*EutD three distinct peaks for α-ADABA, γ-ADABA, and a peak derived from the HEPES buffer were detected in this order. The size of the α-ADABA peak differing upon addition of *Rp*EutD is marked with an *asterisk*. *B,* the remaining ectoine present in the ectoine hydrolysate (*black*) and formed ectoine upon addition of *Rp*EutD (*blue*). *C, He*EutD active site (*AS*) with the α-ADABA intermediate covalently bound to Glu-255 (surrounded by a *dotted outline*), as obtained from co-crystallization with α-ADABA. *D,* AS of *Rp*EutD containing the product α-ADABA. The molecule is held in place by hydrogen bonds to Tyr-52, Asp-338, and Arg-326. *E,* superimposition of AS I and AS II, revealing distinct movements by His-238 and Tyr-52. In the intermediate bound state, this leads to a significant narrowing of the active site. *F,* comparison of the N-terminal architecture between AS I and AS II. Originating from conformational changes of Tyr-52, two helices and a loop region reposition themselves, potentially providing a topological signal.

II, however, the calculated pK_a of Glu-255 in its not α-ADABA–bound state would be 5.1. This pK_a value would in principle allow the protonation of the α-ADABA–Glu-255 adduct to enable release of the α-ADABA product. Unfortunately, the prediction of the pK_a value of the α-ADABA–Glu-255 intermediate with the H++ program is not straightforward due to its uncommon chemical nature. Thus, further studies need to address this issue in greater detail. Moreover, our *in silico* analysis also suggests that the pK_a differences of Glu-255 between AS I and AS II are not caused by a single residue, but seem to be the consequence of an overall narrowing of AS II compared with AS I. A notable consequence of the AS II narrowing is that the catalytically relevant histidines 238 and 361 (Table S1) appear in closer proximity to the α-ADABA–Glu-255 intermediate. Again, since prediction of the pK_a value of the α-ADABA–Glu-255 in this context is difficult, a definite statement cannot be made at this point. Taken together, our structural analysis suggests that the two catalytic half-sites of EutD cooperate in a highly synchronous manner via an intricate network of interactions.

EutE deacetylates α-ADABA in a zinc-dependent manner

To complete the catalytic picture of ectoine degradation, we grew crystals of *Rp*EutE in the presence of α-ADABA and determined the structure to a resolution of 2.5 Å by molecular replacement employing the structure of aspartoacylase (AAC) from *Rhodobacter sphaeroides* (PDB ID 3CDX; sequence identity 39.2%) (Table 1). *Rp*EutE consists of two subdomains that appear in an extended crescent-like shape (Fig. 6*A*). It shares structural homology to the universally

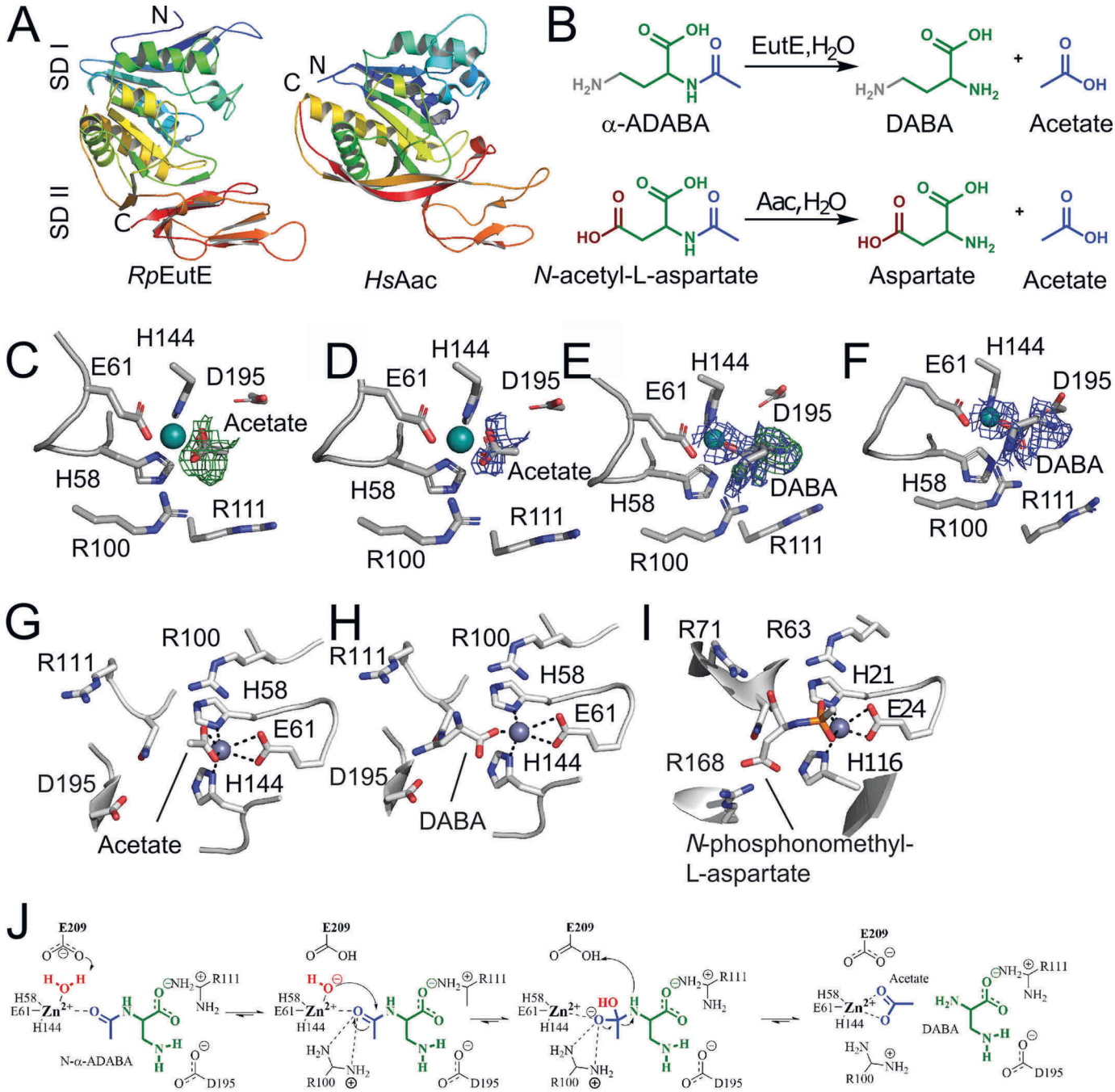

Figure 6. EutE deacetylates α-ADABA in a zinc-dependent manner. *A,* the crystal structure of *Rp*EutE (*left*) shows that it is structurally related to AACs. Both structures are shown as cartoon in *rainbow colors* from their N to C termini. The two subdomains (*SD*) are indicated as SD I and SD II. *B,* deacetylation reactions of α-ADABA and *N*-acetyl-L-aspartate carried out by EutE and AACs, respectively. Note: α-ADABA and *N*-acetyl-L-aspartate only differ in their terminal amine and carboxyl groups, respectively. *C,* unbiased $F_{obs} - F_{calc}$ difference electron density of acetate at 3σ shown as a *green mesh* (PDB 6TWM). *D,* the $2F_{obs} - F_{calc}$ after final refinement with acetate is shown as a *blue mesh* at 1.5 σ (PDB 6TWM). *E,* unbiased $F_{obs} - F_{calc}$ difference electron density of DABA at 3σ shown as a *green mesh*. 2 $F_{obs} - F_{calc}$ in the area is shown as a *blue mesh* at 1.5 σ (PDB 6TWM). *F,* the $2F_{obs} - F_{calc}$ after final refinement with DABA is shown as a *blue mesh* at 1.5 σ (PDB 6TWM). *G,* coordination of the reaction product acetate. *H,* coordination of DABA in the active site of *Rp*EutE. Both products remain coordinated to the catalytically active zinc ion, which is itself coordinated by His-58, His-144, and Glu-61. *I,* active site of a human AAC bound to an acetylaspartate mimic, depicting the likely substrate/transition state coordination in AACs (46). *J,* catalytic mechanism of EutE.

conserved AACs (reviewed in Ref. 45), including the zinc-binding site formed by His-58, His-144, and Glu-61 at the concave side of *Rp*EutE (Fig. 6*A*). Alanine substitutions of His-58, His-144, and Glu-61 completely inactivated EutE proving its metal-dependence (Table S1). The *Rp*EutE crystals grown in the presence of α-ADABA contained 12 EutE monomers within their asymmetric unit. Investigation of their active sites revealed unambiguous electron densities for three acetate/zinc products (Fig. 6, *C* and *D*) and seven DABA/zinc (Fig. 6, *E* and *F*), leaving two proteins within the asymmetric unit with empty active sites. Although acetate coordinates with zinc via its carboxyl moiety in a bi-dentate

manner, DABA coordinates with the metal ion via one of its carboxyl oxygens in a uni-dentate way (Fig. 6, *G* and *H*).

To detail the catalytic mechanism of EutE, we compared our DABA-product state of EutE with that of the human AAC bound to the substrate mimetic *N*-phosphonomethyl-L-aspartate (46) (Fig. 6*I*). AACs convert acetyl-aspartate (A-Asp) into aspartate and acetate, whereas EutE converts α-ADABA into DABA and acetate (Fig. 6*B*). The substrates of EutE and AAC only differ in their terminal moieties not involved in the deacetylation reaction (Fig. 6*B*). Comparing EutE with AAC identified Arg-111 of EutE to be involved in coordinating the carboxyl group of α-ADABA in an equivalent manner as in the AACs (Fig. 6, *G–I*; Table S1). Moreover, our comparison of EutE and AAC shows that Arg-100 coordinates the transition state of the EutE-catalyzed α-ADABA cleavage reaction similar to what has been observed for AACs (Fig. 6, *G–I*; Table S1).

The substrates of EutE and AAC differ in their terminal amino and carboxyl moieties, respectively (Fig. 6*B*). Thus, both enzymes must also differ to compensate these substrate specialties. Indeed, the terminal amine of the DABA product, which is also present in α-ADABA, hydrogen bonds with Asp-195 (Fig. 6*H*). An D195R variant is incapable of degrading α-ADABA, supporting a role of Asp-195 in substrate recognition (Table S1). Taken together, we show that EutE operates highly reminiscent to AACs (Fig. 6*J*). Substrate binding critically relies on Arg-111 and Asp-195, both forming hydrogen bonds to the carboxyl group and the amine of α-ADABA, respectively (Fig. 6*J*). The zinc ion further coordinates the carbonyl-oxygen of the α-ADABA peptide bond. The deacetylation reaction begins with water deprotonation promoted by the zinc ion and Glu-209 (Fig. 6*J*). The so-formed hydroxyl anion attacks the carbonyl-carbon of α-ADABA in a nucleophilic manner leading to the tetrahedral transition state, whose electron-negative character is compensated by the guanidinium moiety of Arg-100. Subsequently, Glu-209 promotes protonation and allows release of DABA and acetate (Fig. 6*J*).

RpEutD/EutE degrades 5-hydroxyectoine but less efficient than ectoine

Next, we wondered whether *Rp*EutD/EutE would also be able to degrade 5-hydroxyectoine (Fig. 1*A*). As for ectoine (Fig. 2*A*), degradation of 5-hydroxyectoine was only observed by HPLC analysis when the *Rp*EutD and *Rp*EutE enzymes were present together in the *in vitro* assay (Fig. 7*A*; Fig. S2*D*). Using the acetate assay 5-hydroxectoine degradation by the *Rp*EutD/EutE bi-module was also detected. However, no Michaelis-Menten–like behavior for the degradation of 5-hydroxyectoine could be observed (Fig. 7*B*). This finding suggests that one or both enzymes are not ideally suited for the degradation of 5-hydroxyectoine.

Inspection of the EutD structure suggests the extra hydroxyl moiety of hydroxyectoine could well be accommodated within the active site of the enzyme, which was also true for the putative Glu-255–bound hydroxy–α-ADABA intermediate (Fig. S5*G*). However, analysis of the EutE structure suggests that Glu-187 provides steric hindrance for the hydroxyl moiety of the hydroxy–α-ADABA substrate (Fig. S5). To challenge this idea, we prepared both hydroxy–ADABA isomers with purities >95% by alkaline hydrolysis of 5-hydroxyectoine and subsequent separation by anion exchange chromatography (Fig. S3, *lower panel*). Although *Rp*EutE was unable to degrade hydroxy–γ-ADABA, hydroxy–α-ADABA was converted into acetate albeit with significantly lower reaction velocity and a drastically increased k_M value (Fig. 7*C*). To investigate the degradation of 5-hydroxyectoine *in vivo*, we produced *Rp*EutD, *Rp*EutE, and *Rp*EutD/EutE in *E. coli* strain MC4100 grown on minimal medium supplemented with 1 mM 5-hydroxyectoine and 0.3 M NaCl (see above). Only when both enzymes were present was hydroxy–α-ADABA exclusively detected (Fig. 7*D*). The identity of this predicted reaction product of the *Rp*EutD enzyme as hydroxy–α-ADABA was ascertained by NMR spectroscopy (Fig. S3). Collectively, we conclude from these *in vitro* and *in vivo* experiments that the EutD/EutE enzyme bi-module can degrade 5-hydroxyectoine via hydroxy–α-ADABA into acetate and hydroxy–DABA, albeit with lesser efficiency than ectoine.

As we were able to observe that *Rp*EutD can catalyze the reverse reaction of ectoine degradation, we set out to test this for hydroxyectoine as well. To do so, we subjected a mixture of hydroxy–α- and hydroxy–γ-ADABA to *Rp*EutD and monitored via HPLC analysis which of these compounds disappeared from the assay solution and if 5-hydroxyectoine would be formed. In this case, *Rp*EutD used exclusively hydroxy–α-ADABA as the substrate for the backward reactions and formed the corresponding hydroxyectoine (Fig. S6).

Discussion

Ecophysiology of ectoine and 5-hydroxyectoine consumption

Like other compatible solutes, osmotically stimulated high-level production of ectoines requires the expenditure of considerable biosynthetic and energetic resources (32). It is therefore not surprising that microorganisms have found ways to exploit compatible solutes in general, and ectoine in particular, as nutrients, when they are no longer needed as osmostress protectants (47). A prime example for the utilization of compatible solutes as nutrients is the algal osmolyte dimethylsulfoniopropionate (DMSP) (48, 49). It is produced on a scale of millions of tons annually in marine habitats. Released into the water column, DMSP can be scavenged by microorganisms and exploited as carbon and sulfur source. Its metabolism drives the global sulfur cycle and the produced volatile dimethylsulfide (DMS) is considered as a contributor to global warming.

Another ecophysiological important process related to compatible solutes is the catabolism of the osmostress protectant choline in the gastrointestinal tracts of humans. This trimethylammonium compound can be catabolized by gut microbiota under anaerobic conditions to trimethylamine (TMA), a metabolite that can be further converted to trimethylamine-*N*-oxide (TMAO) in the human liver (50). Notably, several human diseases are associated with gut microbial production of TMA, and its derived metabolite TMAO (50).

Although certainly not as abundant in the biosphere as DMSP, choline, and glycine betaine (3), free ectoines have been detected in various ecosytems (23). Even if one considers only

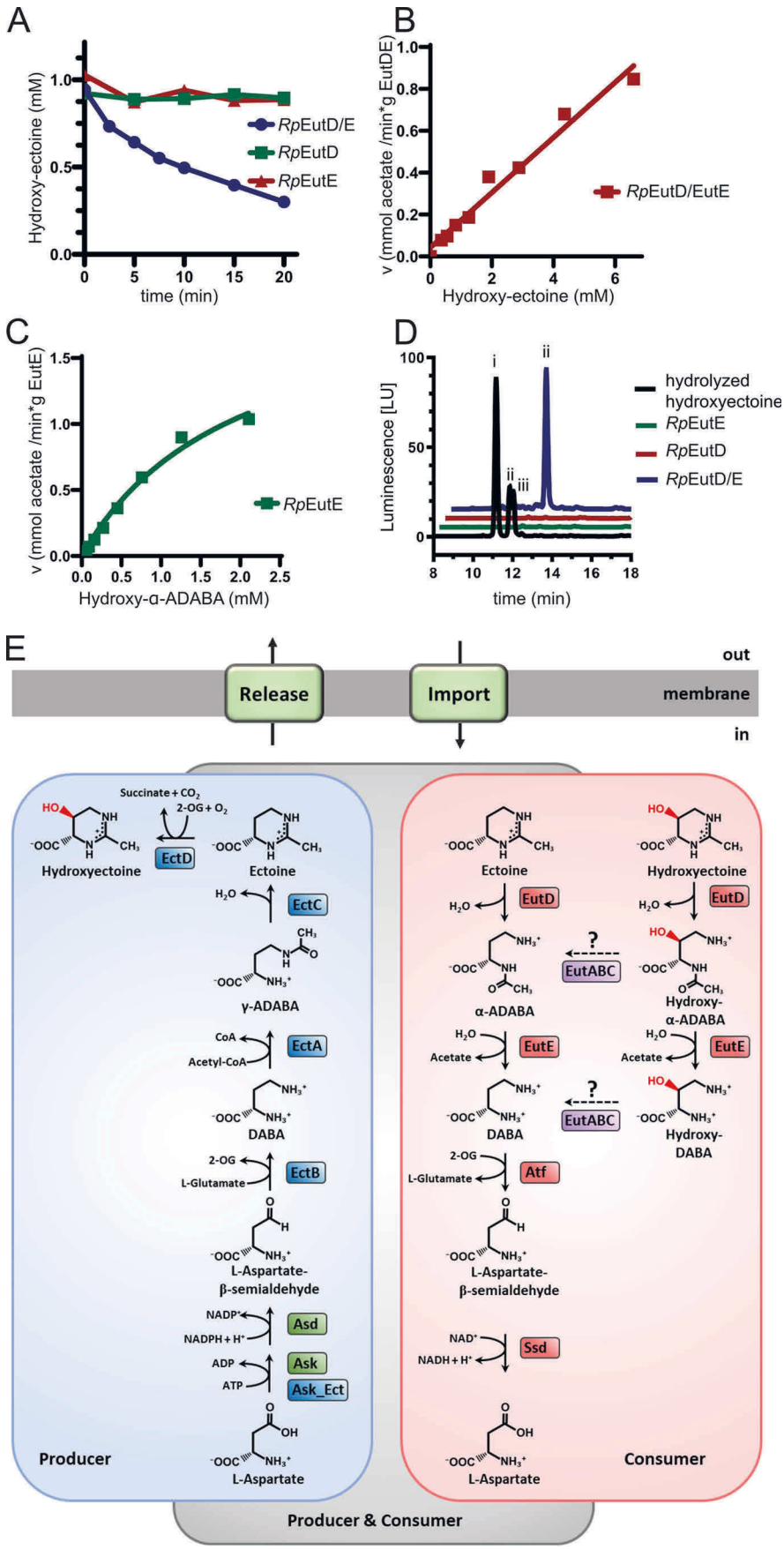
A
Hydroxy-ectoine (mM)
time (min)
RpEutD/E
RpEutD
RpEutE
B
v (mmol acetate /min*g EutDE)
Hydroxy-ectoine (mM)
RpEutD/EutE
C
v (mmol acetate /min*g EutE)
Hydroxy-α-ADABA (mM)
RpEutE
D
Luminescence [LU]
time (min)
hydrolyzed hydroxyectoine
RpEutE
RpEutD
RpEutD/E
E
out
membrane
in
Release
Import
Succinate + CO2
2-OG + O2
EctD
Hydroxyectoine
Ectoine
EctC
γ-ADABA
CoA
Acetyl-CoA
EctA
DABA
2-OG
L-Glutamate
EctB
L-Aspartate-β-semialdehyde
NADP+
NADPH + H+
Asd
ADP
ATP
Ask
Ask_Ect
L-Aspartate
Producer
EutD
EutABC
α-ADABA
Hydroxy-α-ADABA
EutE
Acetate
Hydroxy-DABA
Atf
NAD+
NADH + H+
Ssd
Consumer
Producer & Consumer

fully sequenced microbial genomes, ectoine biosynthetic genes can be found in about 7.5% of all species and strains currently represented in the IMG/M database. The widespread production of ectoine as an osmostress protectant likely provided an evolutionarily incentive to develop pathways for its catabolism. This event occurred primarily in the large phylum of the Proteobacteria (Fig. 1*B*; Fig. S1). Microorganisms populating marine, terrestrial, and plant-associated ecosystems are dominantly represented among the ectoine consumers (Fig. 1*C*). Most of the ectoine/5-hydroxyectoine using microorganisms can either exclusively synthesize or catabolize these nitrogen-rich compounds (Fig. 1*B*) but there is also an interesting group of bacteria that can do both. However, these are limited in number and their occurrence is restricted to particular subgroups of the α- and γ-Proteobacteria (Fig. 1*B*, Fig. S1).

The gene clusters for ectoine degradation often vary with respect to gene order and content (23, 36, 37). However, the vast majority encode the ectoine hydrolase EutD (EC 3.5.4.44) and the deacetylase EutE (EC 3.5.1.125) (Fig. S1). Here, we provide a comprehensive structural and biochemical analysis unraveling the molecular mechanism of the EutD/EutE enzymes, a bi-module positioned at the core of the ectoine/5-hydroxyectoine catabolic pathways, as it is required for opening of the pyrimidine ring of ectoines for their further degradation (Fig. 7*E*).

Catalytic mechanism for ectoine degradation

Our structural analysis shows that EutD enzymes share close structural and sequence conservation to the M24-family aminopeptidases, which rely on two highly coordinated metal ions for their activity (43). Despite this high overall structural similarity, EutD lacks most residues required for metal ion binding except for Glu-255. Instead, the metal ion site seen in the M24 aminopeptidase is changed in EutD to create a cavity well-suited to accommodate ectoine. Our study thus shows how the conserved enzyme fold of the M24-aminopeptidases was adapted in EutD to enable a new function in ectoine degradation. Generally spoken, the M24-aminopeptidase fold seems well-suited as a template to evolve new function. For instance, the ribosome-biogenesis factor Ebp1 (also Arx1) represents an ancient M24-aminopeptidase in which the substrate-binding pocket is maintained, but the zinc-ion–binding site was destroyed to evolve a ribosome-biogenesis factor (51) (Fig. S4*C*).

Only one of the metal-coordinating residues present in *Ec*PepP remained preserved in EutDs, which is Glu-255. This residue plays several central roles in the catalytic reaction executed by EutD. Although it is not directly involved in ectoine binding, Glu-255 contributes to the coordination of a water molecule, which should be catalytically relevant by providing the attacking hydroxyl ion required for opening of the ectoine ring. Moreover, Glu-255 was found to be the "anchor" of the α-ADABA intermediate, which is covalently attached to this residue via an orthoester-like bond. Although covalently bonded reaction intermediates with cysteines or lysines are rather frequently described (52), this is to our knowledge, the first covalent intermediate involving a glutamate. Cleavage of this chemically labile orthoester-like bond requires the presence of a proton, which is in all likelihood provided by His-361, eventually being part of a proton exchange chain (Fig. 3*D*).

Both active sites of EutD homodimer operate in a concerted manner as clearly evidenced by the simultaneous presence of ectoine in one active site and the α-ADABA/Glu-255 adduct in the other. As efficient ectoine degradation only occurs when EutD and EutE are present, this suggests that EutE supports the α-ADABA release from EutD through transient interactions. But how could EutE then discriminate an α-ADABA–loaded active site of EutD from one that is either empty or has the substrate ectoine bound? Structural comparison of the EutD monomers harboring either ectoine or α-ADABA revealed a mobile loop (signal loop) adjacent to the center of the active sites (Fig. S5*F*). The position of this loop differs by 2.6 Å depending on whether substrate or intermediate is present. Therefore, we speculate that the signal loop provides a topological signal, guiding EutE to an α-ADABA–loaded AS of EutD. However, further experiments are required to challenge this idea.

EutE itself degrades α-ADABA into DABA and acetate. The enzyme shares high structural and sequence similarity to the AAC family, which is conserved across all kingdoms of life (45). Our study shows that EutE operates by a highly similar mechanism as AAC enzymes. Prior to the reaction, the substrate is coordinated by Arg-111, which is forming a hydrogen bond to the carboxyl group, as well as by Asp-195, which forms hydrogen bonds to the amine of α-ADABA (Fig. 6, *G–I*). The carbonyl-oxygen of the α-ADABA peptide bond coordinates the zinc ion, which contributes to further substrate binding. The deacetylation reaction starts with the deprotonation of a water molecule that is coordinated by the zinc ion and Glu-209. The newly formed hydroxyl anion performs a nucleophilic attack on the carbonyl-carbon of the α-ADABA, thereby forming the negatively charged, tetrahedral transition state, which is stabilized by the positive charge of the guanidinium moiety of the adjacent Arg-100. Release of the products of the EutE-catalyzed reaction, DABA and acetate, involves Glu-209, which promotes protonation of the transition state (Fig. 6*J*).

Rethinking the degradation scheme of 5-hydroxyectoine

Our study shows that EutD/EutE constitute the enzymatic core sufficient to degrade both ectoine and 5-hydroxyectoine

Figure 7. Microbial ectoine degradation. *A,* degradation of 5-hydroxyectoine by *Rp*EutD (*green*), *Rp*EutE (*red*), and both enzymes together (*blue*), as monitored by HPLC. *B,* the velocity of acetate production as a function of 5-hydroxyectoine concentration was measured by the acetate assay. The enzymes do not exhibit a Michaelis-Menten–like behavior, suggesting that one or both enzymes are not ideally suited for degradation of 5-hydroxyectoine. *C,* Michaelis-Menten plot of *Rp*EutE degrading α-ADABA into DABA and acetate. Estimated k_M and V_{max} values are 3 mM and 2 mmol/min/g, respectively. *D,* analysis of hydroxy–α-ADABA and hydroxy–γ-ADABA in *E. coli* cells producing EutD, EutE, or both proteins grown on hydroxyectoine containing minimal medium with glucose as the sole carbon source. HPLC analysis detects hydroxy–α-ADABA when both enzymes are present (*blue*). No hydroxy–ADABA is detected in cells expressing either *Rp*EutD or *Rp*EutE (*green* and *red*, respectively). A chemically hydrolyzed hydroxyectoine standard (*black*) shows three peaks for (i) hydroxy–γ-ADABA, (ii) hydroxy–α-ADABA, and (iii) a mixture of both isomers. *E,* ectoine degradation (*red box*) can be thought as opposite of its biosynthesis pathway (*blue* box). Both pathways separate at the respective ADABAs isomers.

(Fig. 7*E*). Whether further enzymes increase efficiency of 5-hydroxyectoine degradation remains to be shown (Fig. 7*E*). Our study also suggests that a previous proposal by Schulz *et al.* (36) in which 5-hydroxyectoine degradation would begin with the EutABC-mediated removal of its 5-hydroxyl moiety seems not to be valid (23). This proposal was primarily based on bioinformatics and on the observation that deletion of the *eutABC* genes abolishes growth of *R. pomeroyi* on 5-hydroxyectoine, whereas leaving growth on ectoine unaffected (36). In light of our data, the EutABC enzymes might contribute to degradation of 5-hydroxyectoine at the level of hydroxy–α-ADABA (Fig. 7*E*). Because EutB shares significant homology to the PLP-dependent group of threonine dehydratases, it is plausible that it removes the hydroxyl moiety of hydroxy–α-ADABA (Fig. 7*E*). Subsequently, EutC could reduce the resulting product into α-ADABA in a NADPH-dependent manner. The so-generated α-ADABA would then serve as a *bona fide* substrate of EutE.

Interestingly, a pair of functionally related enzymes operates in the widely distributed β-hydroxyasparte pathway (53). BhcB, the β-hydroxyasparte dehydratase, catalyzes a water elimination of its substrate to form iminosuccinate, an intermediate that is further reduced in an NADH-dependent reaction by the BhcD imminosuccinate reductase to produce L-aspartate (53). The role of EutA remains uncertain in such a scenario, because closer inspection of many genomes shows that *eutA* only sporadically appears in the context of the *eutD/eutE* gene cluster (Fig. S1). We cannot exclude that the EutABC enzymes could play a role in converting hydroxy–α-DABA to DABA for further catabolism to L-aspartate (Fig. 7*E*). Hence, future biochemical and structural studies are clearly required to challenge these ideas.

Regulation of bacterial ectoine metabolism

Ectoine degradation can be thought as the opposite of the ectoine biosynthetic route (Fig. 7*E*). We show that EutD/EutE-mediated ectoine degradation in *R. pomeroyi* proceeds via α-ADABA, but not γ-ADABA. This could nicely explain how producer/degrader cells can prevent futile ectoine production and consumption. Although the ectoine synthetase EctC primarily relies on γ-ADABA as the substrate (29), EutD selectively produces α-ADABA.

The ectoine biosynthetic genes are osmotically induced (19, 23), whereas those for ectoine/5-hydroxyectoine degradation are substrate inducible when ectoines are added to the growth medium (35, 36, 39). However, ectoine is not the true inducer; instead α-ADABA, and to a much lesser extend also the intermediate DABA, serve as internal inducers for the EnuR repressor (39, 40). This PLP-dependent MocR/GabR-type regulator (54) controls transcription of the ectoine/5-hydroxyectoine import and catabolic gene cluster of *R. pomeroyi*, and most likely, also in many other bacteria capable to degrade ectoines (23). Notably, γ-ADABA, the substrate of the ectoine synthase EctC does not serve as inducer for EnuR (39). In this way, ectoine biosynthesis and degradation are elegantly separated through the chemical uniqueness of the γ-ADABA and α-ADABA isomers. Since we found that EutD is able to convert 5-hydroxyectoine into hydroxy–α-ADABA, the possibility is raised that this compound also serves as an internal inducer for EnuR as well.

The genetic regulatory circuits controlling the expression of the genes for ectoine biosynthesis as an osmostress protectant and use of ectoine as a nutrient are clearly targeted for the physiological task at hand. However, for those microorganisms that can both synthesize and degrade ectoine, the situation can become complex due to intermediates shared in both pathways. For instance, Schwibbert *et al.* (37) reported that the EutD (DoeA) ectoine hydrolase from *H. elongata*, a microorganism capable of both ectoine production and catabolism, synthesizes both α-ADABA and γ-ADABA. Although α-ADABA is funneled to EutE (DoeB) for further catabolism, γ-ADABA is thought to serve as an intermediate in a new round of ectoine production (37). Conditions in natural settings that would require the simultaneous production and degradation of ectoine are not immediately obvious to us. Nevertheless, it should be noted that inactivation of the catabolic genes led to higher intracellular ectoine titers in the *H. elongata* industrial production host (37).

Concluding remarks

Use of compatible solutes as nutrients is an important aspect for the functioning of microbial ecosystems (47). Ectoine and 5-hydroxyectoine are among the most widely synthesized osmostress protectants in the microbial world. Severely osmotically stressed microorganisms synthesize and accumulate ectoines to cellular concentrations as high as hundreds of micromolar. The recent exiting discovery of ectoine production and uptake by halophilic protists and marine microalgae (55–57) raises the possibility for ectoines to function in microbial interactions with these eukaryotic cells. Similarly to the catabolism of the compatible solutes DMSP, choline, and glycine betaine, their environmental release can shape architecture and composition of microbial communities (57, 58).

Taken together, our study unravels the structure-based mechanism of the enzyme core essential for the catabolism of the stress protectants ectoine and 5-hydroxyectoine. The presented data clarify the key mechanism for ectoine consumption, an eco-physiologically relevant process preventing microbial ecosystems from losing valuable resources.

Materials and methods

Chemicals

Ectoine was kindly provided by bitop AG (Witten, Germany) and hydroxyectoine was purchased from Merck (Darmstadt, Germany). Ampicillin was purchased from Carl Roth GmbH (Karlsruhe, Germany). The γ-isomer of γ-ADABA was purchased from Chem-Impex International Inc. (Wood Dale, IL, USA). Ectoine and hydroxyectoine were hydrolyzed via alkaline hydrolysis as described for ectoine (59) and hydroxyectoine (60). The α-isomer of ADABA was separated from the hydrolysis product of ectoine by repeated chromatography on a silica gel column (Merck Silica Gel 60).

Database searches for ectoine producing and consuming microorganisms

For the phylogenomic analysis of ectoine biosynthetic and catabolic genes, we used the IMG/M database of the Joint Genome Institute and considered for our analysis only fully sequenced microbial genomes (41). At the time of the search (November 2019) 8,850 prokaryotic genomes were available; 8,557 were from members of the Bacteria, and 293 represented archaeal genomes. We used the amino acid sequence of the EctC ectoine synthase (29) from the Gram-positive bacterium *Paenibacillus lautus* as the search query for ectoine producers (61). EctC is the signature enzyme for the ectoine biosynthetic route, but a group of microorganisms exists that possesses a solitary EctC-type protein whose enzymatic function is unclear (23, 62). We therefore considered only EctC-type proteins as *bona fide* ectoine synthases when the inspected genome sequence also possessed genes for the two other enzymes (EctA–EctB) required for ectoine biosynthesis (23).

To identify ectoine consuming microorganisms, we used the amino acid sequence of the EutD ectoine hydrolase for the marine bacterium *R. pomeroyi* as the search query, as this enzyme is key for ectoine consumption. As the amino acid sequence of the EutD protein is related to other types of hydrolases (in particular to peptidases), we considered only EutD-type proteins as *bona fide* ectoine hydrolases when the *eutD* gene was part of a gene cluster containing other known ectoine-catabolizing genes. We then used the resulting 429 EutD-type proteins to construct a phylogenetic protein tree using software resources provided by the IMG/M website. Subsequently, the iTOL software suit (63) was used to visualize the EutD tree. Onto this tree, we projected information on the presence of ectoine biosynthetic genes in the microorganism under consideration derived from the above described EctC search. Furthermore, data on the habitat of ectoine-producing and consuming microorganisms were collected from information deposited in the IMG/M database or derived from literature searches. In the case of ectoine-consuming microorganisms, this information was incorporated into the iTOL-derived EutD protein tree. Similarly, information on the taxonomic affiliation of microorganisms was projected onto the tree; this information was derived from the IMG/M database. Amino acid sequence identities of EutD-type proteins relative to EutD protein from *R. pomeroyi* (used as the original search query) and that of the EutD (DoeA) protein from *H. elongata* were calculated using Clustal O (64). The amino acid sequence identity of ectoine hydrolases ranged between 41.88% (for *Rhodobacter sphaeroides* ATCC 17025) and 95.95% (for *Leisingera* sp. *NJS204*) when the *R. pomeroyi* EutD protein was used for the search and ranged between 39.56% (for *Mycobacterium tuberculosis* H37Ra) and 97.24% (for *Halomonas beimenensis* NTU-111) when the *H. elongata* EutD protein was used for the search.

Protein production, purification, and characterization

The genes encoding for the *He*EutD, *Rp*EutD, and *Rp*EutE proteins were amplified by PCR and cloned into pET24d (Novagen) via the NcoI and XhoI restriction sites. All proteins contained an N-terminal His_6 tag. Proteins were produced in *E. coli* BL21(DE3) (Novagen). Cells were lysed by a Microfluidizer (M110-L, Microfluidics). Cell debris after lysis was removed by high-speed centrifugation. All proteins were purified by nickel-ion affinity and size exclusion chromatography, as described previously (65). The SEC buffer consisted of 20 mM HEPES-Na (pH 7.5), 200 mM NaCl, 20 mM KCl, and 20 mM $MgCl_2$.

For the analytical size exclusion chromatography (SEC) with multiangle light scattering (SEC-MALS), a sample (100 μl) of the purified EutD and EutE protein concentrations of 100 μM were injected at 4 °C on to a pre-equilibrated S200 300/10 GL analytical size exclusion column (GE Healthcare, München, Germany). The buffer at pH 7.5 contained 20 mM HEPES, 200 mM NaCl, 20 mM $MgCl_2$, and 20 mM KCl. For the MALS-RI experiments, a multiangle light scattering and a differential refractive index detector (Postnova Analytics, Landsberg am Lech, Germany) was attached to the column.

Crystallization and structure determination

Crystallization was performed by the sitting-drop method at 20 °C in 600-nl drops consisting of equal parts of protein and precipitation solutions. Protein solutions of 300 μM (*He*EutD) and 1 mM (*Rp*EutE) were prepared in buffer described for SEC purification. For the crystals containing substrates, 1 mM (final concentration) ectoine or α-ADABA, respectively, were added and incubated at room temperature for 10 min. Crystallization conditions were: *He*EutD with ectoine (0.2 M trisodium citrate, 20% (w/v) PEG 3350); *Rp*EutE with α-ADABA (0.1 M Bicine (pH 9.0), 20% (v/v) PEG 6000). Prior to data collection, crystals were flash-frozen in liquid nitrogen using a cryo-solution that consisted of mother liquor supplemented with 20% (v/v) glycerol. Data were collected under cryogenic conditions at the European Synchrotron Radiation Facility (Grenoble, France) beamlines ID23-1 (66), ID23-2 and MASSIF-1 (67), and at beamline MX14.2 at BESSY II (Berlin, Germany) (68).

Data were processed with XDS and scaled with XSCALE (69). All structures were determined by molecular replacement with PHASER (70), manually built in COOT (71), and refined with PHENIX (72). The search model for the *He*EutD-Apo structure was the *E. coli* aminopeptidase P (PDB ID 2BWS, sequence identity is 25.6%). The search model for all other EutD structures was the *He*EutD-Apo structure (this study).

The search model for the *Rp*EutE structure was the aspartoacylase from *R. sphaeroides* (PDB ID 3CDX, sequence identity is 39.2%). The search model for all other EutE structures was the *Rp*EutE-Apo structure (this study).

For all ligand-bound structures of *He*EutD and *Rp*EutE, first the protein model was manually built to completeness and refined without placing waters or any other ligands. After completion of the protein model, the respective ligand was placed into the unbiased density (when present) and refined. In the last step, the water molecules were modeled. Final validation of the structures was carried out with the validation server of the PDB (73). Figures were prepared with PyMOL (RRID:SCR_000305).

Isolation of pure α-ADABA

A mixture of approximately 25% α-ADABA and 75% γ-ADABA made from chemically hydrolyzed ectoine was separated into the pure ADABA species by preparative anion exchange chromatography. A Metrohm Carb2 column (250 × 4 mm inner diameter) operated with a 90 mM $(NH_4)_2CO_3$ eluent adjusted to pH 9.25 at 1 ml/min was used for the separation. Sample loading was 100 μl of a 50 mM solution of the ADABA mixture. The obtained separation factor for α-ADABA and γ-ADABA was 1.9 under these preparative conditions. The fractions of each ADABA species were collected, unified, and the eluent was removed using a vacuum drying oven at 40 °C overnight. The purity of the resulting α-ADABA sample was determined to 90% by HPLC.

HPLC-based assay

Ectoine and hydroxyectoine were detected by high pressure liquid chromatography (HPLC) using the 1260 Infinity system (Agilent Technologies, Walsbronn, Germany) with a GromSil Amino-1 PR, 3 μm column (125 × 4 mm) (Dr. Maisch GmbH, Ammerbruch, Germany) and a diode array detecting module (Agilent Technologies, Walsbronn, Germany) using a wavelength of 210 nm. The mobile phase consisted of 80% (v/v) acetonitrile (MeCN, HPLC grade) and 20% (v/v) H_2O. The separation was performed, after injecting 10 μl of the sample, by an isocratic measurement over 15 min with a flow rate of 1 ml/min at 20 °C.

The ectoine degradation assay for HPLC-based analysis were performed in 200-μl assays containing 20 mM HEPES-Na (pH 7.5), 200 mM NaCl, 20 mM $MgCl_2$, 20 mM KCl, 1 mM ectoine or hydroxyectoine, and 40 μg of purified EutD and/or EutE at a temperature of 30 °C. After 0, 5, 10, 15, and 20 min, a sample of 30 μl was taken and added to 30 μl of MeCN to stop the reaction. Before injecting 10 μl each into the HPLC system, the samples were centrifuged (13,300 rpm for 10 min at 4 °C) to remove the denatured enzymes.

Acetate assay

For the assays the commercially available kit from Sigma-Aldrich, named "Acetate Colorimetric Assay Kit" (catalog number MAK086) was used and applied according to the manufacturer's manual. In short, 1 nmol (final concentration = 10 μM) of the respective enzyme were mixed with acetate buffer from the kit to a total volume of 10 μl in the reaction well of a flat-bottom 96-well plate. The substrates, α-ADABA and ectoine, respectively, were prepared in a total of 15 μl of acetate buffer for final concentrations of 3, 1.8, 1.08, 0.65, 0.38, 0.23, 0.13, and 0.08 mM. The enzyme and substrate mixture of the kit were mixed accordingly to the instructions and added to the substrates. This mixture was then transferred to the prepared enzymes, in turn starting the reaction. The 450 nm absorption of each well was monitored for 15 min in 11-s intervals.

EutD-mediated synthesis of ectoines in its backward enzyme reaction

Assays were performed in 200-μl volumes containing 20 mM HEPES-Na (pH 7.5), 200 mM NaCl, 20 mM $MgCl_2$, 20 mM KCl, and either 1 mM hydrolyzate of ectoine or hydroxyectoine. 40 μg of purified EutD were added to start the assay, which was performed at a temperature of 30 °C. After 1 h a sample of 30 μl was taken and added to 30 μl of MeCN to stop the reaction. The samples were centrifuged (13,300 rpm for 10 min at 4 °C) to remove the denatured enzymes before assessing the content of ectoines and ADABA-isomers in the samples, employing the HPLC-based detection methods described above.

Cultivation of recombinant E. coli strains for the hydrolysis of ectoine and hydroxyectoine

To determine the hydrolytic activity of EutD, EutE, and EutD/EutE on ectoine and hydroxyectoine, *E. coli* strain MC4100 (74) harboring plasmids pLH48, pLH49, pLH50, or the empty expression vector pTrc99a were grown in MMA (75) with 0.5% (w/v) glucose as a carbon source and ampicillin (100 μg ml^{-1}) as an antibiotic. Growth took place in 100-ml Erlenmeyer flasks in a water bath set to 220 rpm at 37 °C. MMA precultures were used to inoculate MMA supplemented with 0.3 M NaCl and 1 mM ectoine or hydroxyectoine to an OD_{578} of 0.1, and after growth to an OD_{578} of 0.5, 1 mM isopropyl 1-thio-β-D-galactopyranoside was added to the media to induce expression. 2-ml probes were sampled by centrifugation (5 min, 13,000 rpm, room temperature) directly before induction, 2 h, and 4 h after induction and the cell pellets and supernatants were separated and stored at −20 °C until further analysis.

In vivo detection of ectoine and hydroxyectoine degradation

To extract ectoine degradation products from *E. coli*, 1 ml of 20% (v/v) ethanol was added to the cell pellets and the probes were rigorously shaken for 1 h and subsequently centrifuged (30 min, 13,000 rpm, 4 °C). The supernatant was dried at 50 °C for 20 h. 100 μl of distilled water was added to the samples, which were then centrifuged for 30 min. 2 μl of the supernatant was derivatized using 3 μl of 9-fluorenylmethoxy carbonyl (FMOC) (25 mg/ml in acetonitrile), excessive FMOC was removed by addition of 6 μl of ADAM (7.6 mg/ml in 50% (w/v) borate buffer, 0.5 mol $liter^{-1}$ (pH 7.7), and 50% (v/v) acetone). 489 μl of distilled water was added to the solution and the samples were centrifuged (15 min, 13,000 rpm at room temperature), before they were analyzed by isocratic HPLC. These measurements were performed with an Agilent 1260 Infinity LC system (Agilent, Waldbronn, Germany) and a Gemini 5-μm C_{18} 110- Å column (Phenomenex, Torrance, CA, USA). The flow rate of the system was set to 1 ml min^{-1} and the Gemini column was operated at 40 °C. The following gradient of solvent A (80% (w/v) acetate buffer, 50 mmol $liter^{-1}$, pH 4.2, 20% (v/v) acetonitrile, 0.5% (w/v) THF) and solvent B (20% acetate buffer, 50 mmol $liter^{-1}$, pH 4.2, 80% (v/v) acetonitrile) was applied: 0 min, 0% solvent B; 2 min, 0% solvent B; 8 min, 20% solvent B; 16 min, 27% solvent B; 18 min, 54% solvent B; 20 min, 100% solvent B; 25 min, 100% solvent B; 26 min, 0% solvent B; 29 min, 0% solvent B. Samples were analyzed with the OpenLAB software suite (Agilent) and visualized with GraphPad Prism (GraphPad Software, Inc.).

Data availability

The atomic coordinates have been deposited in the Protein Data Bank under accession codes 6TWJ (Apo-*He*EutD), 6TWK (*He*EutD bound to ectoine and α-ADABA–Glu-255), 6YO9 (*He*EutD bound to α-ADABA and α-ADABA–Glu-255), 6TWL (Apo-*Rp*EutE) and 6TWM (product-bound state of *Rp*EutE). The authors declare that all other data supporting the findings of this study are available within the article and its supplementary information files.

Acknowledgments—We thank the BESSYII (Berlin, Germany) and the European Synchrotron Radiation Facility (ESRF, Grenoble, France) for excellent support.

Author contributions—C.-N. M., L. H., F. A., and G. B. formal analysis; C.-N. M., L. H., F. A., A. A. R., I. W., L. C., and E. B. investigation; C.-N. M., L. H., F. A., L. C., E. B., and G. B. visualization; C.-N. M., L. H., and A. S. methodology; C.-N. M., L. H., E. B., and G. B. writing-original draft; F. A., E. B., and G. B. supervision; A. S. and G. B. resources; E. B. and G. B. conceptualization; E. B. and G. B. project administration; G. B. funding acquisition; G. B. validation; G. B. writing-review and editing.

Funding and additional information—This work was supported by a grant from the Deutsche Forschungsgemeinschaft (DFG) Collaborative Research Center (CRC) 987 "Microbial Diversity in Environmental Signal Response" (to G. B. and E. B.) and a Ph.D. fellowship from the International Max Planck Research School for Environmental, Cellular and Molecular Microbiology (IMPRS-Mic; Marburg) (to L. C.).

Conflict of interest—The authors declare no conflict of interest.

Abbreviations—The abbreviations used are: EctA, L-2,4-diaminobutyrate acetyltransferase; EctB, L-2,4-diaminobutyrate transaminase; EctC, ectoine synthase; EctD, ectoine hydroxylase; Eut, ectoine utilization; Doe, degradation of ectoines; *N*-γ-ADABA, *N*-γ-acetyl-L-2,4-diaminobutyrate; *N*-α-ADABA, *N*-α-acetyl-L-2,4-diaminobutyrate; DABA, L-2,4-diaminobutyrate; DMSP, dimethylsulfoniopropionate; DMS, dimethyl-sulfide; TMA, trimethlyamine; TMAO, trimethlyamine-*N*-oxide; FMOC, fluorenylmethyloxycarbonyl; SEC, size exclusion chromatography; MALS, multiangle light scattering; PDB, Protein Data Bank; AC, active site; AAC, aspartoacylase; Bicine, *N*,*N*-bis(2-hydroxyethyl)glycine; ADAM, 1-adamantylamine hydrochloride; MMA, Minimal Medium A.

References

1. Gunde-Cimerman, N., Plemenitaš, A., and Oren, A. (2018) Strategies of adaptation of microorganisms of the three domains of life to high salt concentrations. *FEMS Microbiol. Rev.* **42,** 353–375 CrossRef Medline
2. Roesser, M., and Müller, V. (2001) Osmoadaptation in bacteria and archaea: common principles and differences. *Environ. Microbiol.* **3,** 743–754 CrossRef Medline
3. Yancey, P. H. (2005) Organic osmolytes as compatible, metabolic and counteracting cytoprotectants in high osmolarity and other stresses. *J. Exp. Biol.* **208,** 2819–2830 CrossRef Medline
4. Kempf, B., and Bremer, E. (1998) Uptake and synthesis of compatible solutes as microbial stress responses to high-osmolality environments. *Arch. Microbiol.* **170,** 319–330 CrossRef Medline
5. Bolen, D. W., and Baskakov, I. V. (2001) The osmophobic effect: natural selection of a thermodynamic force in protein folding. *J. Mol. Biol.* **310,** 955–963 CrossRef Medline
6. Stadmiller, S. S., Gorensek-Benitez, A. H., Guseman, A. J., and Pielak, G. J. (2017) Osmotic shock induced protein destabilization in living cells and its reversal by glycine betaine. *J. Mol. Biol.* **429,** 1155–1161 CrossRef Medline
7. Diamant, S., Eliahu, N., Rosenthal, D., and Goloubinoff, P. (2001) Chemical chaperones regulate molecular chaperones in vitro and in cells under combined salt and heat stresses. *J. Biol. Chem.* **276,** 39586–39591 CrossRef Medline
8. da Costa, M. S., Santos, H., and Galinski, E. A. (1998) An overview of the role and diversity of compatible solutes in Bacteria and Archaea. *Adv. Biochem. Eng. Biotechnol.* **61,** 117–153 CrossRef Medline
9. Wood, J. M. (2011) Bacterial osmoregulation: a paradigm for the study of cellular homeostasis. *Annu. Rev. Microbiol.* **65,** 215–238 CrossRef Medline
10. Bremer, E., and Krämer, R. (2019) Responses of microorganisms to osmotic stress. *Annu. Rev. Microbiol.* **73,** 313–334 CrossRef Medline
11. García-Estepa, R., Argandoña, M., Reina-Bueno, M., Capote, N., Iglesias-Guerra, F., Nieto, J. J., and Vargas, C. (2006) The *ectD* gene, which is involved in the synthesis of the compatible solute hydroxyectoine, is essential for thermoprotection of the halophilic bacterium *Chromohalobacter salexigens*. *J. Bacteriol.* **188,** 3774–3784 CrossRef Medline
12. Kuhlmann, A. U., Hoffmann, T., Bursy, J., Jebbar, M., and Bremer, E. (2011) Ectoine and hydroxyectoine as protectants against osmotic and cold stress: uptake through the SigB-controlled betaine-choline- carnitine transporter-type carrier EctT from *Virgibacillus pantothenticus*. *J. Bacteriol.* **193,** 4699–4708 CrossRef Medline
13. Hoffmann, T., and Bremer, E. (2011) Protection of *Bacillus subtilis* against cold stress via compatible-solute acquisition. *J. Bacteriol.* **193,** 1552–1562 CrossRef Medline
14. Tanne, C., Golovina, E. A., Hoekstra, F. A., Meffert, A., and Galinski, E. A. (2014) Glass-forming property of hydroxyectoine is the cause of its superior function as a desiccation protectant. *Front. Microbiol.* **5,** 150 CrossRef Medline
15. Manzanera, M., García de Castro, A., Tøndervik, A., Rayner-Brandes, M., Strøm, A. R., and Tunnacliffe, A. (2002) Hydroxyectoine is superior to trehalose for anhydrobiotic engineering of *Pseudomonas putida* KT2440. *Appl. Environ. Microbiol.* **68,** 4328–4333 CrossRef Medline
16. Brands, S., Schein, P., Castro-Ochoa, K. F., and Galinski, E. A. (2019) Hydroxyl radical scavenging of the compatible solute ectoine generates two *N*-acetimides. *Arch. Biochem. Biophys.* **674,** 108097 CrossRef Medline
17. Galinski, E. A., Pfeiffer, H. P., and Truper, H. G. (1985) 1,4,5,6-Tetrahydro-2-methyl-4-pyrimidinecarboxylic acid: a novel cyclic amino acid from halophilic phototrophic bacteria of the genus Ectothiorhodospira. *Eur. J. Biochem.* **149,** 135–139 CrossRef Medline
18. Inbar, L., and Lapidot, A. (1988) The structure and biosynthesis of new tetrahydropyrimidine derivatives in actinomycin D producer *Streptomyces parvulus*: use of ^{13}C- and ^{15}N-labeled L-glutamate and ^{13}C and ^{15}N NMR spectroscopy. *J. Biol. Chem.* **263,** 16014–16022 Medline
19. Pastor, J. M., Salvador, M., Argandoña, M., Bernal, V., Reina-Bueno, M., Csonka, L. N., Iborra, J. L., Vargas, C., Nieto, J. J., and Cánovas, M. (2010) Ectoines in cell stress protection: uses and biotechnological production. *Biotechnol. Adv.* **28,** 782–801 CrossRef Medline
20. Zaccai, G., Bagyan, I., Combet, J., Cuello, G. J., Demé, B., Fichou, Y., Gallat, F. X., Galvan Josa, V. M., von Gronau, S., Haertlein, M., Martel, A., Moulin, M., Neumann, M., Weik, M., and Oesterhelt, D. (2016) Neutrons describe ectoine effects on water H-bonding and hydration around a soluble protein and a cell membrane. *Sci. Rep.* **6,** 31434 CrossRef Medline
21. Kunte, H., Lentzen, G., and Galinski, E. (2014) Industrial production of the cell protectant ectoine: protection mechanisms, processes, and products. *Curr. Biotechnol.* **3,** 10–25 CrossRef
22. Becker, J., and Wittmann, C. (2020) Microbial production of extremolytes: high-value active ingredients for nutrition, health care, and well-being. *Curr. Opin. Biotechnol.* **65,** 118–128 CrossRef Medline
23. Czech, L., Hermann, L., Stoveken, N., Richter, A. A., Hoppner, A., Smits, S. H. J., Heider, J., and Bremer, E. (2018) Role of the extremolytes ectoine and hydroxyectoine as stress protectants and nutrients: genetics,

phylogenomics, biochemistry, and structural analysis. *Genes (Basel)* **9,** 177 CrossRef

24. Ono, H., Sawada, K., Khunajakr, N., Tao, T., Yamamoto, M., Hiramoto, M., Shinmyo, A., Takano, M., and Murooka, Y. (1999) Characterization of biosynthetic enzymes for ectoine as a compatible solute in a moderately halophilic eubacterium, *Halomonas elongata*. *J. Bacteriol.* **181,** 91–99 CrossRef Medline
25. Richter, A. A., Kobus, S., Czech, L., Hoeppner, A., Zarzycki, J., Erb, T. J., Lauterbach, L., Dickschat, J. S., Bremer, E., and Smits, S. H. J. (2020) The architecture of the diaminobutyrate acetyltransferase active site provides mechanistic insight into the biosynthesis of the chemical chaperone ectoine. *J. Biol. Chem.* **295,** 2822–2838 CrossRef Medline
26. Peters, P., Galinski, E. A., and Trüper, H. G. (1990) The biosynthesis of ectoine. *FEMS Microbiol. Lett.* **71,** 157–162 CrossRef Medline
27. Richter, A. A., Mais, C. N., Czech, L., Geyer, K., Hoeppner, A., Smits, S. H. J., Erb, T. J., Bange, G., and Bremer, E. (2019) Biosynthesis of the stress-protectant and chemical chaperon ectoine: biochemistry of the transaminase EctB. *Front. Microbiol.* **10,** 2811 CrossRef Medline
28. Hillier, H. T., Altermark, B., and Leiros, I. (2020) The crystal structure of the tetrameric DABA-aminotransferase EctB, a rate-limiting enzyme in the ectoine biosynthesis pathway. *FEBS J.* doi: 10.1111/febs.15265 CrossRef
29. Czech, L., Höppner, A., Kobus, S., Seubert, A., Riclea, R., Dickschat, J. S., Heider, J., Smits, S. H. J., and Bremer, E. (2019) Illuminating the catalytic core of ectoine synthase through structural and biochemical analysis. *Sci. Rep.* **9,** 364 CrossRef Medline
30. Bursy, J., Pierik, A. J., Pica, N., and Bremer, E. (2007) Osmotically induced synthesis of the compatible solute hydroxyectoine is mediated by an evolutionarily conserved ectoine hydroxylase. *J. Biol. Chem.* **282,** 31147–31155 CrossRef Medline
31. Hoppner, A., Widderich, N., Lenders, M., Bremer, E., and Smits, S. H. (2014) Crystal structure of the ectoine hydroxylase, a snapshot of the active site. *J. Biol. Chem.* **289,** 29570–29583 CrossRef Medline
32. Oren, A. (1999) Bioenergetic aspects of halophilism. *Microbiol. Mol. Biol. Rev.* **63,** 334–348 CrossRef Medline
33. Grammann, K., Volke, A., and Kunte, H. J. (2002) New type of osmoregulated solute transporter identified in halophilic members of the bacteria domain: TRAP transporter TeaABC mediates uptake of ectoine and hydroxyectoine in *Halomonas elongata* DSM 2581(T). *J. Bacteriol.* **184,** 3078–3085 CrossRef Medline
34. Vargas, C., Jebbar, M., Carrasco, R., Blanco, C., Calderon, M. I., Iglesias-Guerra, F., and Nieto, J. J. (2006) Ectoines as compatible solutes and carbon and energy sources for the halophilic bacterium *Chromohalobacter salexigens*. *J. Appl. Microbiol.* **100,** 98–107 CrossRef Medline
35. Jebbar, M., Sohn-Bösser, L., Bremer, E., Bernard, T., and Blanco, C. (2005) Ectoine-induced proteins in *Sinorhizobium meliloti* include an ectoine ABC-type transporter involved in osmoprotection and ectoine catabolism. *J. Bacteriol.* **187,** 1293–1304 CrossRef Medline
36. Schulz, A., Stöveken, N., Binzen, I. M., Hoffmann, T., Heider, J., and Bremer, E. (2017) Feeding on compatible solutes: a substrate-induced pathway for uptake and catabolism of ectoines and its genetic control by EnuR. *Environ. Microbiol.* **19,** 926–946 CrossRef Medline
37. Schwibbert, K., Marin-Sanguino, A., Bagyan, I., Heidrich, G., Lentzen, G., Seitz, H., Rampp, M., Schuster, S. C., Klenk, H. P., Pfeiffer, F., Oesterhelt, D., and Kunte, H. J. (2011) A blueprint of ectoine metabolism from the genome of the industrial producer *Halomonas elongata* DSM 2581 T. *Environ. Microbiol.* **13,** 1973–1994 CrossRef Medline
38. Booth, I. R., and Blount, P. (2012) The MscS and MscL families of mechanosensitive channels act as microbial emergency release valves. *J. Bacteriol.* **194,** 4802–4809 CrossRef Medline
39. Schulz, A., Hermann, L., Freibert, S. A., Bönig, T., Hoffmann, T., Riclea, R., Dickschat, J. S., Heider, J., and Bremer, E. (2017) Transcriptional regulation of ectoine catabolism in response to multiple metabolic and environmental cues. *Environ. Microbiol.* **19,** 4599–4619 CrossRef Medline
40. Yu, Q., Cai, H., Zhang, Y., He, Y., Chen, L., Merritt, J., Zhang, S., and Dong, Z. (2017) Negative regulation of ectoine uptake and catabolism in *Sinorhizobium meliloti*: characterization of the EhuR gene. *J. Bacteriol.* **199,** e00119-16 CrossRef Medline
41. Chen, I. A., Chu, K., Palaniappan, K., Pillay, M., Ratner, A., Huang, J., Huntemann, M., Varghese, N., White, J. R., Seshadri, R., Smirnova, T., Kirton, E., Jungbluth, S. P., Woyke, T., Eloe-Fadrosh, E. A., *et al.* (2019) IMG/M v.5.0: an integrated data management and comparative analysis system for microbial genomes and microbiomes. *Nucleic Acids Res* **47,** D666–D677 CrossRef Medline
42. Jebbar, M., Talibart, R., Gloux, K., Bernard, T., and Blanco, C. (1992) Osmoprotection of *Escherichia coli* by ectoine: uptake and accumulation characteristics. *J. Bacteriol.* **174,** 5027–5035 CrossRef Medline
43. Rawlings, N. D., and Barrett, A. J. (1993) Evolutionary families of peptidases. *Biochem. J.* **290,** 205–218 CrossRef Medline
44. Gordon, J. C., Myers, J. B., Folta, T., Shoja, V., Heath, L. S., and Onufriev, A. (2005) H++: a server for estimating p*Ka*s and adding missing hydrogens to macromolecules. *Nucleic Acids Res.* **33,** W368–W371 CrossRef Medline
45. Makarova, K. S., Aravind, L., and Koonin, E. V. (1999) A superfamily of archaeal, bacterial, and eukaryotic proteins homologous to animal transglutaminases. *Protein Sci.* **8,** 1714–1719 CrossRef Medline
46. Le Coq, J., Pavlovsky, A., Malik, R., Sanishvili, R., Xu, C., and Viola, R. E. (2008) Examination of the mechanism of human brain aspartoacylase through the binding of an intermediate analogue. *Biochemistry* **47,** 3484–3492 CrossRef Medline
47. Welsh, D. T. (2000) Ecological significance of compatible solute accumulation by micro-organisms: from single cells to global climate. *FEMS Microbiol. Rev.* **24,** 263–290 CrossRef Medline
48. Curson, A. R., Todd, J. D., Sullivan, M. J., and Johnston, A. W. (2011) Catabolism of dimethylsulphoniopropionate: microorganisms, enzymes and genes. *Nat. Rev. Microbiol.* **9,** 849–859 CrossRef Medline
49. Moran, M. A., Reisch, C. R., Kiene, R. P., and Whitman, W. B. (2012) Genomic insights into bacterial DMSP transformations. *Ann. Rev. Mar. Sci.* **4,** 523–542 CrossRef Medline
50. Xu, H., Wang, X., Feng, W., Liu, Q., Zhou, S., Liu, Q., and Cai, L. (2020) The gut microbiota and its interactions with cardiovascular disease. *Microb. Biotechnol.* **13,** 637–656 CrossRef Medline
51. Kowalinski, E., Bange, G., Bradatsch, B., Hurt, E., Wild, K., and Sinning, I. (2007) The crystal structure of Ebp1 reveals a methionine aminopeptidase fold as binding platform for multiple interactions. *FEBS Lett.* **581,** 4450–4454 CrossRef Medline
52. Heine, A., DeSantis, G., Luz, J. G., Mitchell, M., Wong, C. H., and Wilson, I. A. (2001) Observation of covalent intermediates in an enzyme mechanism at atomic resolution. *Science* **294,** 369–374 CrossRef Medline
53. Schada von Borzyskowski, L., Severi, F., Krüger, K., Hermann, L., Gilardet, A., Sippel, F., Pommerenke, B., Claus, P., Cortina, N. S., Glatter, T., Zauner, S., Zarzycki, J., Fuchs, B. M., Bremer, E., Maier, U. G., *et al.* (2019) Marine Proteobacteria metabolize glycolate via the β-hydroxyaspartate cycle. *Nature* **575,** 500–504 CrossRef Medline
54. Tramonti, A., Nardella, C., di Salvo, M. L., Pascarella, S., and Contestabile, R. (2018) The MocR-like transcription factors: pyridoxal 5′-phosphate-dependent regulators of bacterial metabolism. *FEBS J.* **285,** 3925–3944 CrossRef Medline
55. Harding, T., Brown, M. W., Simpson, A. G., and Roger, A. J. (2016) Osmoadaptative strategy and its molecular signature in obligately halophilic heterotrophic protists. *Genome Biol. Evol.* **8,** 2241–2258 CrossRef Medline
56. Weinisch, L., Kirchner, I., Grimm, M., Kuhner, S., Pierik, A. J., Rosselló-Móra, R., and Filker, S. (2019) Glycine betaine and ectoine are the major compatible solutes used by four different halophilic heterotrophic ciliates. *Microb. Ecol.* **77,** 317–331 CrossRef Medline
57. Fenizia, S., Thume, K., Wirgenings, M., and Pohnert, G. (2020) Ectoine from bacterial and algal origin is a compatible solute in microalgae. *Mar. Drugs* **18,** 42 CrossRef
58. Landa, M., Burns, A. S., Roth, S. J., and Moran, M. A. (2017) Bacterial transcriptome remodeling during sequential co-culture with a marine dinoflagellate and diatom. *ISME J.* **11,** 2677–2690 CrossRef Medline
59. Kunte, H. J., Galinski, E. A., and Trüper, H. G. (1993) A modified FMOC-method for the detection of amino acid-type osmolytes and tetrahydropyrimidines (ectoines). *J. Microbiol. Meth.* **17,** 129–136 CrossRef

60. Sarciaux, M., Pantel, L., Midrier, C., Serri, M., Gerber, C., Marcia de Figueiredo, R., Campagne, J. M., Villain-Guillot, P., Gualtieri, M., and Racine, E. (2018) Total synthesis and structure-activity relationships study of odilorhabdins, a new class of peptides showing potent antibacterial activity. *J. Med. Chem.* **61,** 7814–7826 CrossRef Medline
61. Mead, D. A., Lucas, S., Copeland, A., Lapidus, A., Cheng, J. F., Bruce, D. C., Goodwin, L. A., Pitluck, S., Chertkov, O., Zhang, X., Detter, J. C., Han, C. S., Tapia, R., Land, M., Hauser, L. J., *et al.* (2012) Complete genome sequence of *Paenibacillus* strain Y4.12MC10, a novel *Paenibacillus lautus* strain isolated from Obsidian Hot Spring in Yellowstone National Park. *Stand. Genomic Sci.* **6,** 381–400 CrossRef Medline
62. Kurz, M., Burch, A. Y., Seip, B., Lindow, S. E., and Gross, H. (2010) Genome-driven investigation of compatible solute biosynthesis pathways of *Pseudomonas syringae* pv. *syringae* and their contribution to water stress tolerance. *Appl. Environ. Microbiol.* **76,** 5452–5462 CrossRef Medline
63. Letunic, I., and Bork, P. (2011) Interactive Tree Of Life v2: online annotation and display of phylogenetic trees made easy. *Nucleic Acids Res.* **39,** W475–W478 CrossRef Medline
64. Sievers, F., Wilm, A., Dineen, D., Gibson, T. J., Karplus, K., Li, W., Lopez, R., McWilliam, H., Remmert, M., Soding, J., Thompson, J. D., and Higgins, D. G. (2011) Fast, scalable generation of high-quality protein multiple sequence alignments using Clustal Omega. *Mol. Syst. Biol.* **7,** 539 CrossRef Medline
65. Han, X., Altegoer, F., Steinchen, W., Binnebesel, L., Schuhmacher, J., Glatter, T., Giammarinaro, P. I., Djamei, A., Rensing, S. A., Reissmann, S., Kahmann, R., and Bange, G. (2019) A kiwellin disarms the metabolic activity of a secreted fungal virulence factor. *Nature* **565,** 650–653 CrossRef Medline
66. Nurizzo, D., Mairs, T., Guijarro, M., Rey, V., Meyer, J., Fajardo, P., Chavanne, J., Biasci, J. C., McSweeney, S., and Mitchell, E. (2006) The ID23-1 structural biology beamline at the ESRF. *J Synchrotron Radiat.* **13,** 227–238 CrossRef Medline
67. Svensson, O., Malbet-Monaco, S., Popov, A., Nurizzo, D., and Bowler, M. W. (2015) Fully automatic characterization and data collection from crystals of biological macromolecules. *Acta Crystallogr. D Biol. Crystallogr.* **71,** 1757–1767 CrossRef Medline
68. Mueller, U., Darowski, N., Fuchs, M. R., Förster, R., Hellmig, M., Paithankar, K. S., Pühringer, S., Steffien, M., Zocher, G., and Weiss, M. S. (2012) Facilities for macromolecular crystallography at the Helmholtz-Zentrum Berlin. *J. Synchrotron Radiat.* **19,** 442–449 CrossRef Medline
69. Kabsch, W. (2010) Xds. *Acta Crystallogr. D Biol. Crystallogr.* **66,** 125–132 CrossRef Medline
70. McCoy, A. J., Grosse-Kunstleve, R. W., Adams, P. D., Winn, M. D., Storoni, L. C., and Read, R. J. (2007) Phaser crystallographic software. *J. Appl. Crystallogr.* **40,** 658–674 CrossRef Medline
71. Emsley, P., and Cowtan, K. (2004) Coot: model-building tools for molecular graphics. *Acta Crystallogr. D Biol. Crystallogr.* **60,** 2126–2132 CrossRef Medline
72. Adams, P. D., Afonine, P. V., Bunkóczi, G., Chen, V. B., Davis, I. W., Echols, N., Headd, J. J., Hung, L. W., Kapral, G. J., Grosse-Kunstleve, R. W., McCoy, A. J., Moriarty, N. W., Oeffner, R., Read, R. J., Richardson, D. C., *et al.* (2010) PHENIX: a comprehensive Python-based system for macromolecular structure solution. *Acta Crystallogr. D Biol. Crystallogr.* **66,** 213–221 CrossRef Medline
73. Gore, S., Sanz Garcia, E., Hendrickx, P. M. S., Gutmanas, A., Westbrook, J. D., Yang, H., Feng, Z., Baskaran, K., Berrisford, J. M., Hudson, B. P., Ikegawa, Y., Kobayashi, N., Lawson, C. L., Mading, S., Mak, L., *et al.* (2017) Validation of structures in the Protein Data Bank. *Structure* **25,** 1916–1927 CrossRef Medline
74. Casadaban, M. J. (1976) Transposition and fusion of the *lac* genes to selected promoters in *Escherichia coli* using bacteriophage λ and Mu. *J. Mol. Biol.* **104,** 541–555 CrossRef Medline
75. Miller, J. H. (1972) Experiments in molecular genetics, Cold Spring Harbor Laboratory, Cold Spring Harbor, New York

Catalytic mechanism for the degradation of microbial stress protectants and chemical chaperones ectoine and hydroxyectoine

Running title:

Microbial degradation of ectoine and hydroxyectoine by the EutD and EutE enzymes

Christopher-Nils Mais[1,5], Lucas Hermann[2,5], Florian Altegoer[1], Andreas Seubert[3], Alexandra A. Richter[2], Isa Wernersbach[1], Laura Czech[2], Erhard Bremer[2,4], Gert Bange[1,4]

[1]Philipps-University Marburg, Center for Synthetic Microbiology (SYNMIKRO) & Faculty of Chemistry, Hans-Meerwein-Strasse 6, C07, 35043, Marburg, Germany
[2]Philipps-University Marburg, Center for Synthetic Microbiology (SYNMIKRO) & Faculty of Biology, Karl-von-Frisch-Strasse 8, 35043, Marburg, Germany
[3]Philipps-University Marburg, Faculty of Chemistry, Hans-Meerwein-Strasse 4, 35043, Marburg, Germany
[4]Correspondence: gert.bange@synmikro.uni-marburg.de and bremer@biologie.uni-marburg.de

[5]These authors contributed equally to this work.

To whom correspondence may be addressed: Erhard Bremer, Faculty of Biology, Laboratory for Microbiology, Philipps-University Marburg, Karl-von-Frisch Strasse 8, D-35043 Marburg, Germany. Phone: (+49)-6421-2821529. Fax: (+49)-6421-2828979. E-mail: bremer@staff.uni-marburg.de

To whom correspondence may be addressed: Gert Bange, Philipps-University Marburg, Center for Synthetic Microbiology (SYNMIKRO) & Faculty of Chemistry, Hans-Meerwein-Strasse 6, C07, 35043, Marburg, Germany. Phone: (+49)-6421-2823361. E-mail: gert.bange@synmikro.uni-marburg.de

---

Please direct all correspondence concerning this manuscript **during the reviewing, editorial and printing process to Dr. Gert Bange.** Philipps-University Marburg, Center for Synthetic Microbiology (SYNMIKRO) & Faculty of Chemistry, Hans-Meerwein-Strasse 6, C07, 35043, Marburg, Germany. Phone: (+49)-6421-2823361 E-Mail: gert.bange@synmikro.uni-marburg.de

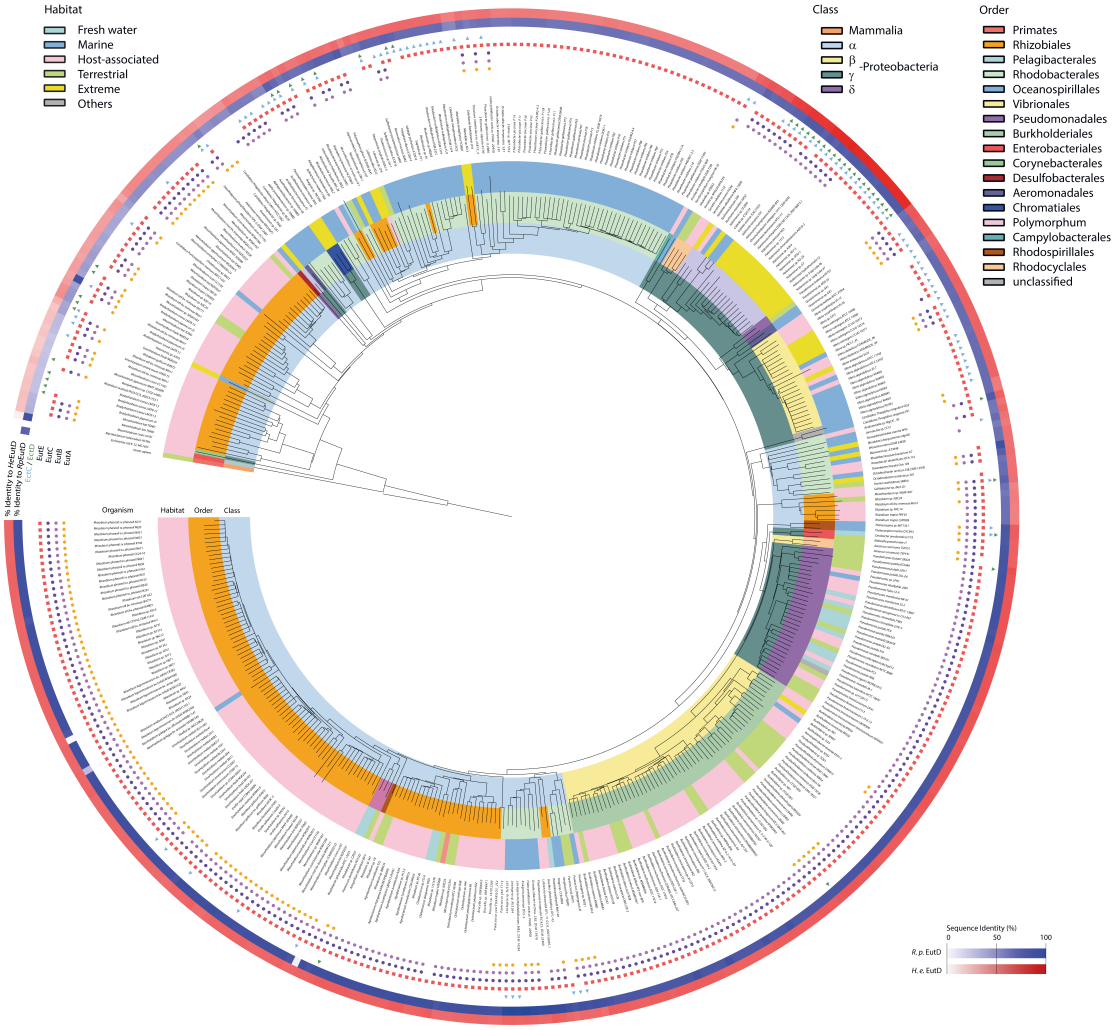

Supplementary Fig. S1. Phylogenic tree of organisms possessing the ectoine/hydroxyectoine hydrolase EutD. EutD can be found in a large variety of microorganisms populating different ecosystems. Almost all microorganisms containing EutD also posse EutE. The description EctC/EctD represents those microorganisms capable to synthesize ectoine (EctC) or ectoine and hydroxyectoine (EctC/EctD). The genes encoding the EutD/EutE bi-module co-occure very frequently, while the gene encoding the EutA protein occurs more rarely in the analyzed dataset.

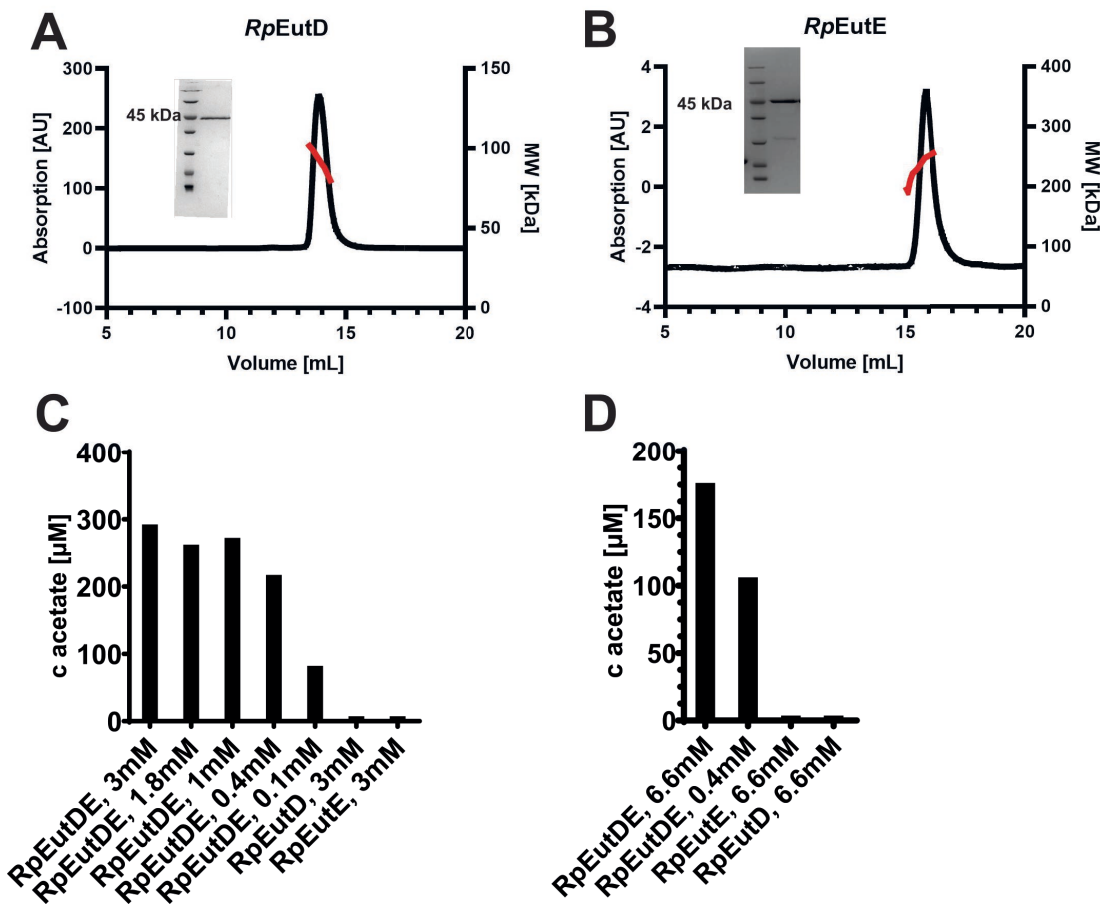

Supplementary Fig. S2. Purification and initial characterization of *Rp*EutD and *Rp*EutE. Analytical size exclusion chromatography of (**A**) *Rp*EutD and (**B**) *Rp*EutE. The red line displays the molecular weight determined by MALS-RI, averaging to ≈ 90 kDa for EutD, the expected molecular weight of a dimer and 200 kDa for EutE. **(C)** Acetate production was measured 3 min after addition of the depicted concentrations of ectoine. The RpEutD/RpEutE enzymes are only active when both are present in the enzyme assays. **(D)** Acetate production by *Rp*EutD and *Rp*EutE together 10 min after addition of depicted concentrations of hydroxyectoine.

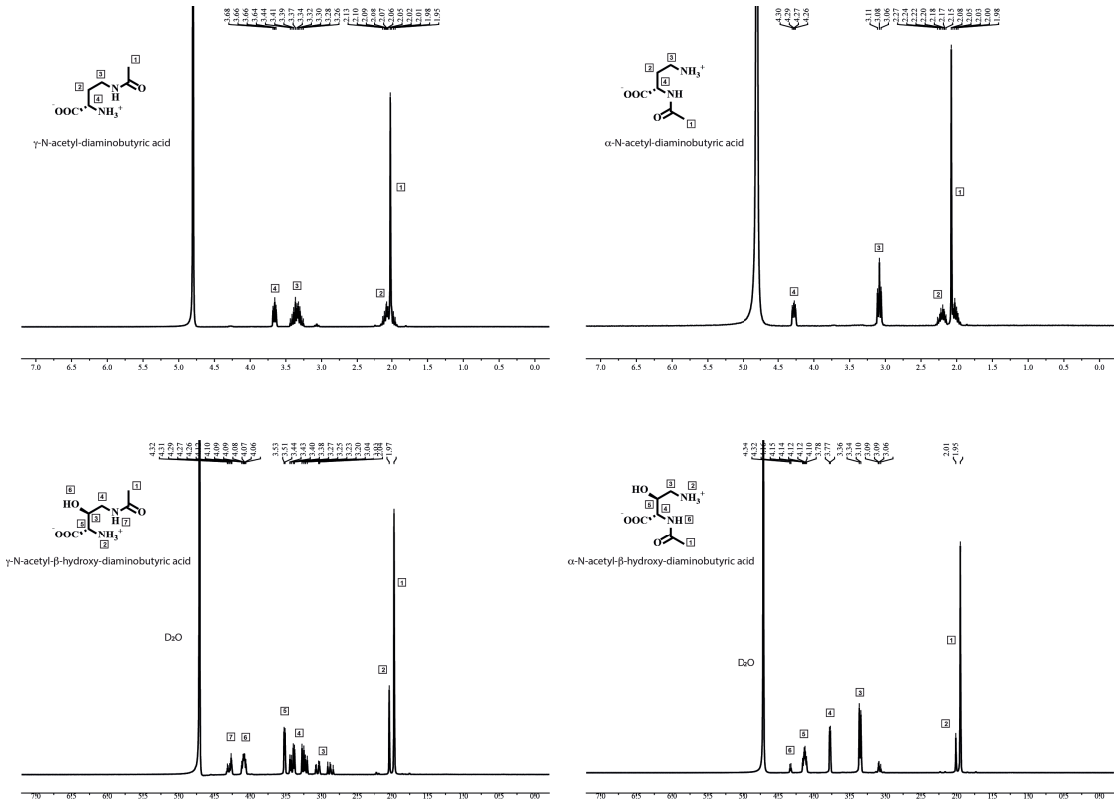

Supplementary Fig. S3. NMR analysis of different ADABA isomers. All isomers were prepared by alkaline hydrolysis of ectoine or hydroxyectoine and were subsequently purified by anion chromatography (see main text). Upper panel: NMR spectra of α- and γ-ADABA obtained from alkaline hydrolysis of ectoine. Lower panel: NMR spectra of α- and γ-hydroxy-ADABA obtained from alkaline hydrolysis of hydroxyectoine.

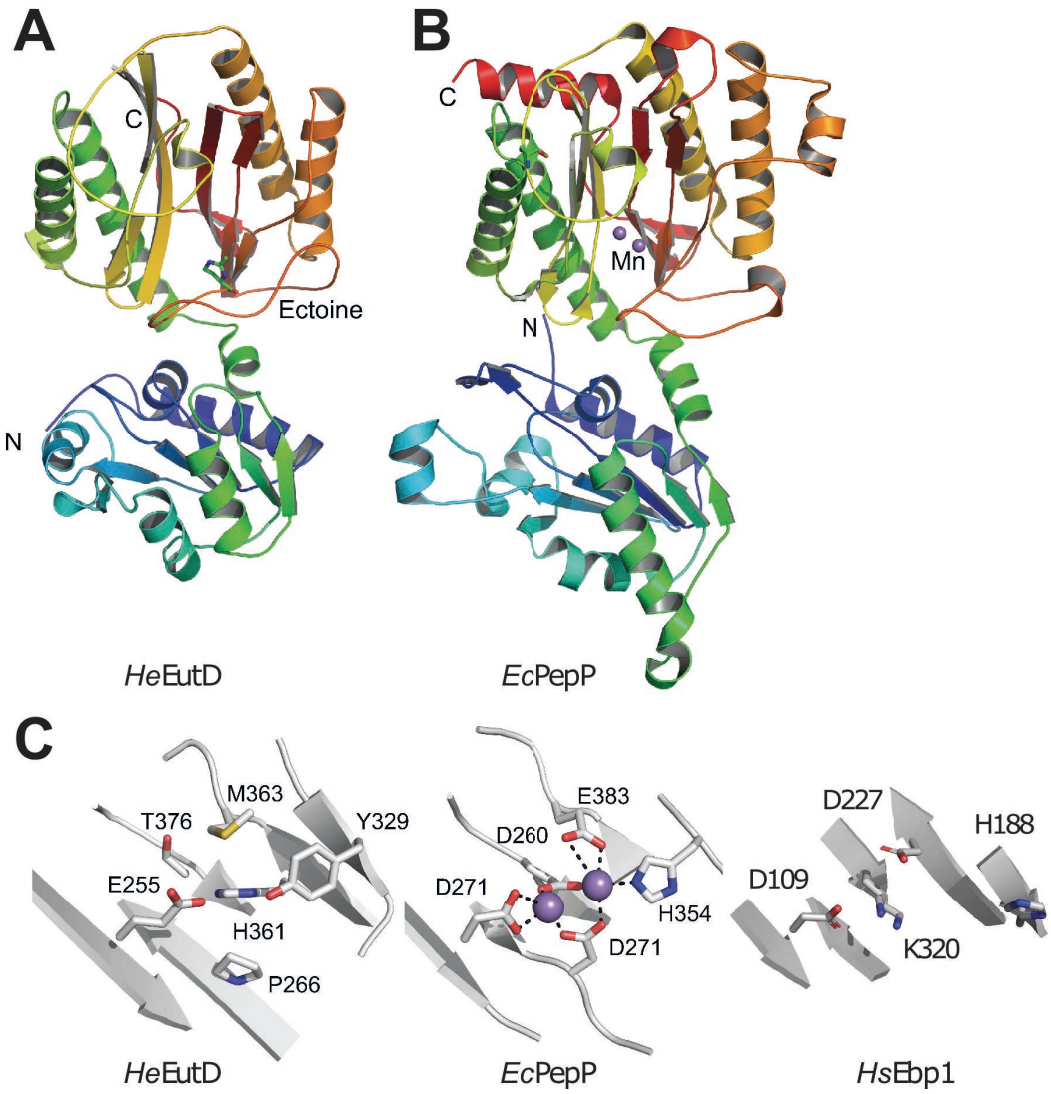

Supplementary Fig. S4. EutD shares a conserved pita-bread fold with M24-aminopeptidases. Side-by-side view of the superimposed cartoon representations of a *He*EutD monomer (**A**; *this study*) and the *E. coli* proline peptidase PepP (**B**, PDB-ID: 2BWS). Proteins are colored in rainbow from their N- to their C-termini. **(C)** Side-by-side view on the superimposed active sites of *He*EutD (*left*; this study), *E. coli* PepP (*left;* PDB-ID: 2BWS) and *H. sapiens* Ebp1 (*right*; PDB-ID: 2Q8K).

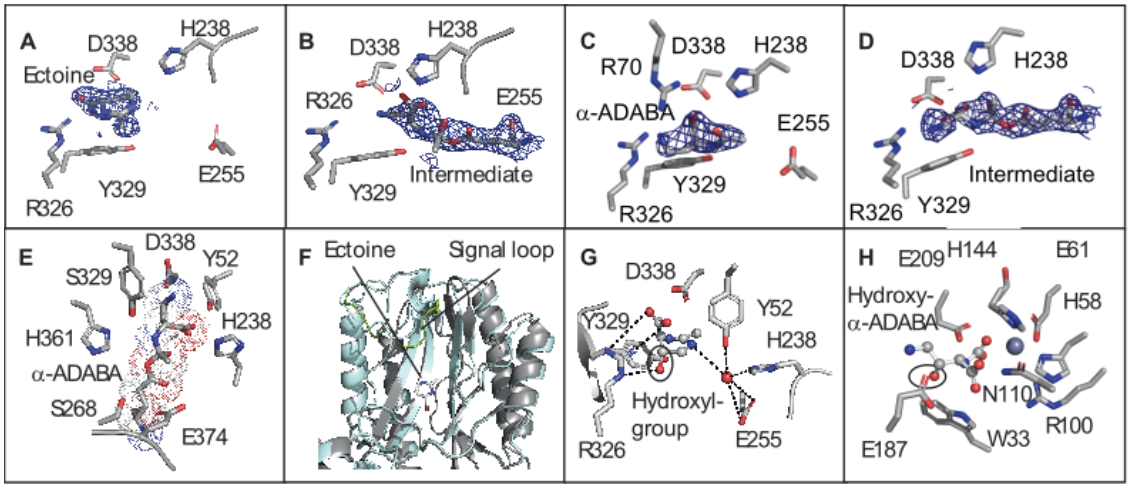

Supplementary Fig. S5. Substrate coordination in EutD and EutE. (A) The $2F_{obs}$-F_{calc} after final refinement with ectoine is shown as a blue mesh at 1.5 σ. (PDB: 6TWK). **(B)** The $2F_{obs}$-F_{calc} after final refinement with the covalently linked α-ADABA in place is shown as a blue mesh at 1.5 σ. (PDB: 6TWK). **(C)** The $2F_{obs}$-F_{calc} after final refinement with α-ADABA is shown as a blue mesh at 1.5 σ. (PDB:6YO9). **(D)** The $2F_{obs}$-F_{calc} after final refinement with the covalently linked α-ADABA in place is shown as a blue mesh at 1.5 σ. (PDB:6YO9). **(E)** Close to the covalent bond between α-ADABA and glutamate 255 two residues, histidine 361 and serine 268, can be observed. These are presumably involved in the protonation of the orthoester-like bond during the release of α-ADABA. **(F)** Comparison of apo and substrate bound *He*EutD revealing a singal loop undergoing conformational changes during the reaction. **(G)** Modeling of hydroxyectoine into the active site of EutD reveals no sterical clashes with any residues, hinting EutD takes ectoine as well as hydroxyectoine as substrate for the ring opening reaction. **(H)** Model of hydroxy-α-ADABA in the active site of *Rp*EutE. The black circle depicts the clash of the hydroxyl moiety with glutamate 187.

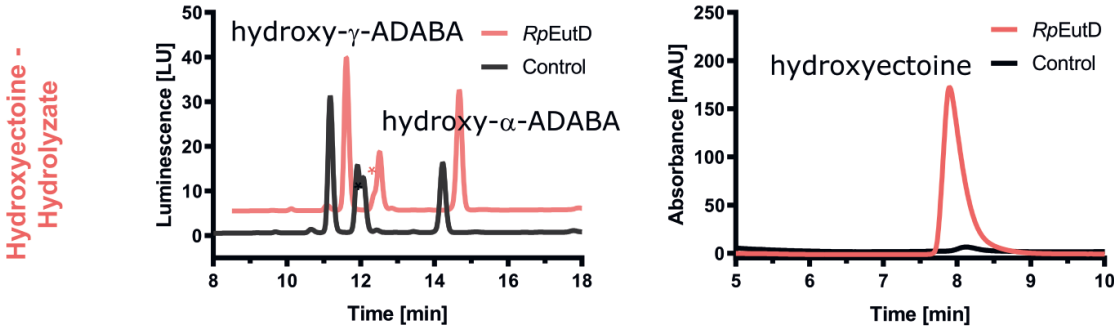

Supplementary Fig. S6. Recyclization of hydroxy-α-ADABA into 5-hydroxyectoine. HPLC analysis of derivatized 5-hydroxyectoine hydrolysate (left) without addition of *Rp*EutD (black) shows four peaks representing (from left to right) hydroxy-γ-ADABA hydroxy-α-ADABA, a mixture of both isomers, and an unspecified component of the HEPES-buffer. When hydroxyectoine hydrolysate is incubated with *Rp*EutD for 1 h (red) the disappearance of hydroxy-α-ADABA can be observed. When both samples are applied to HPLC analysis detecting ectoines (right), the formation of 5-hydroxyectoine can be observed when the hydrolysate (black) is incubated with RpEutD for 1 h (red).

Supplementary Table S1. Activity of EutD and EutE variants.

Halomonas elongata	Activity	k_M [mM]	V_{max} [mol/min*g]
EutD+ EutE WT	100%	1.2	1.3
EutE WT	100%	0.1	1.6
EutD E255D + EutE	0%	-	-
EutD H238A + EutE	5%	-	-
EutD Y52A + EutE	2%	-	-
EutD R326D + EutE	0%	-	-
EutD Y329A + EutE	130%	-	-
EutD E374D + EutE	20%	-	-
EutD S268A+ EutE	70%	-	-
EutD H361S+ EutE	5%	-	-

Ruegeria pomeroyi	Activity	k_M [mM]	V_{max} [mol/min*g]
EutD + EutE WT	100%	0.6	1.2
EutE WT	100%	0.1	2.2
EutE E61A	0%	-	-
EutE E209A	20%	-	-
EutE W33A	78%	-	-
EutE R100A	8%	-	-
EutE R111D	7%	-	-
EutE D195R	7%	-	-

6.1.3 The MocR/GabR ectoine catabolism regulator EnuR: Inducer and DNA binding (2021)

Front Microbiol 12:764731 doi: 10.3389/fmicb.2021.764731

The MocR/GabR Ectoine and Hydroxyectoine Catabolism Regulator EnuR: Inducer and DNA Binding

Lucas Hermann[1,2†], Felix Dempwolff[3†], Wieland Steinchen[3†], Sven-Andreas Freibert[4†], Sander H. J. Smits[5,6†], Andreas Seubert[7†] and Erhard Bremer[1,3†]*

The following chapter encompasses the manuscript “The MocR/GabR ectoine catabolism regulator EnuR: Inducer and DNA binding” published by Frontiers in Microbiology in Dezember 2021. E. Bremer and I planned the study and discussed data. I constructed the bacterial strains and plasmids used in this study, purified, and characterized enzymes, performed Electrophoretic Mobility Shift Assays, reporter gene assays, and microscale thermophoresis assays. The bioinformatic assessments for this study and all figures were produced by me. F. Dempwolff performed growth experiments and prepared cell extracts for targeted metabolomics. W. Steinchen purified the enzymes used in mass spectrometry and performed these experiments. A. Freibert helped with the microscale thermophoresis assays and their analysis. S. H. J. Smits performed the docking experiments. A. Seubert isolated the ligands α-ADABA and hydroxy-α-ADABA and measured the intracellular concentrations of ectoine catabolites. E. Bremer and I wrote the manuscript with input from all authors.

frontiers in Microbiology

ORIGINAL RESEARCH
published: 24 December 2021
doi: 10.3389/fmicb.2021.764731

The MocR/GabR Ectoine and Hydroxyectoine Catabolism Regulator EnuR: Inducer and DNA Binding

Lucas Hermann[1,2†], Felix Dempwolff[3†], Wieland Steinchen[3†], Sven-Andreas Freibert[4†], Sander H. J. Smits[5,6†], Andreas Seubert[7†] and Erhard Bremer[1,3†]*

[1] Faculty of Biology, Philipps-University Marburg, Marburg, Germany, [2] Department of Biochemistry and Synthetic Metabolism, Max-Planck-Institute for Terrestrial Microbiology, Marburg, Germany, [3] SYNMIKRO Research Center, Philipps-University Marburg, Marburg, Germany, [4] Department of Medicine, Institute for Cytobiology and Cytopathology, and SYNMIKRO Research Center, Philipps-University Marburg, Marburg, Germany, [5] Institute of Biochemistry, Heinrich-Heine-University, Düsseldorf, Germany, [6] Center for Structural Studies (CSS), Faculty of Biochemistry, Heinrich-Heine-University, Düsseldorf, Germany, [7] Faculty of Chemistry, Philipps-University Marburg, Marburg, Germany

The compatible solutes ectoine and 5-hydroxyectoine are widely synthesized by bacteria as osmostress protectants. These nitrogen-rich tetrahydropyrimidines can also be exploited as nutrients by microorganisms. Many ectoine/5-hydroxyectoine catabolic gene clusters are associated with a regulatory gene (*enuR*: ectoine nutrient utilization regulator) encoding a repressor protein belonging to the MocR/GabR sub-family of GntR-type transcription factors. Focusing on EnuR from the marine bacterium *Ruegeria pomeroyi*, we show that the dimerization of EnuR is mediated by its aminotransferase domain. This domain can fold independently from its amino-terminal DNA reading head and can incorporate pyridoxal-5′-phosphate (PLP) as cofactor. The covalent attachment of PLP to residue Lys302 of EnuR was proven by mass-spectrometry. PLP interacts with system-specific, ectoine and 5-hydroxyectoine-derived inducers: alpha-acetyldiaminobutyric acid (alpha-ADABA), and hydroxy-alpha-acetyldiaminobutyric acid (hydroxy-alpha-ADABA), respectively. These inducers are generated in cells actively growing with ectoines as sole carbon and nitrogen sources, by the EutD hydrolase and targeted metabolic analysis allowed their detection. EnuR binds these effector molecules with affinities in the low micro-molar range. Studies addressing the evolutionary conservation of EnuR, modelling of the EnuR structure, and docking experiments with the inducers provide an initial view into the cofactor and effector binding cavity. In this cavity, the two high-affinity inducers for EnuR, alpha-ADABA and hydroxy-alpha-ADABA, are positioned such that their respective primary nitrogen group can chemically interact with PLP. Purified EnuR bound with micro-molar affinity to a 48 base pair DNA fragment containing the sigma-70 type substrate-inducible promoter for the ectoine/5-hydroxyectoine importer and catabolic gene cluster. Consistent with

Edited by:
Jörg Stülke,
University of Göttingen, Germany

Reviewed by:
Boris Belitsky,
Tufts University School of Medicine, United States
Michael Bott,
Institute for Bio and Earth Sciences Biotechnology (IBG-1), Germany

***Correspondence:**
Erhard Bremer
bremer@staff.uni-marburg.de

†ORCID:
Lucas Hermann
orcid.org/0000-0001-6684-1644
Felix Dempwolff
orcid.org/0000-0002-7788-8445
Wieland Steinchen
orcid.org/0000-0003-2990-3660
Sven-Andreas Freibert
orcid.org/0000-0002-8521-2963
Sander H. J. Smits
orcid.org/0000-0003-0780-9251
Andreas Seubert
orcid.org/0000-0002-7398-363X
Erhard Bremer
orcid.org/0000-0002-2225-7005

Specialty section:
This article was submitted to Microbial Physiology and Metabolism, a section of the journal Frontiers in Microbiology

Received: *25 August 2021*
Accepted: *01 December 2021*
Published: *24 December 2021*

Citation:
Hermann L, Dempwolff F, Steinchen W, Freibert S-A, Smits SHJ, Seubert A and Bremer E (2021) The MocR/GabR Ectoine and Hydroxyectoine Catabolism Regulator EnuR: Inducer and DNA Binding. Front. Microbiol. 12:764731. doi: 10.3389/fmicb.2021.764731

the function of EnuR as a repressor, the core elements of the promoter overlap with two predicted EnuR operators. Our data lend themselves to a straightforward regulatory model for the initial encounter of EnuR-possessing ectoine/5-hydroxyectoine consumers with environmental ectoines and for the situation when the external supply of these compounds has been exhausted by catabolism.

Keywords: ectoine, hydroxyectoine, GntR transcription factor, repressor, inducer, PLP

INTRODUCTION

One cornerstone of the evolutionary success of microorganisms is their enormous metabolic potential, a trait which allows them to take advantage of a wide spectrum of nutrients present in their varied ecological niches. To preserve precious energetic and biosynthetic resources, microorganisms exert a tight control over the expression of genes encoding nutrient uptake and utilization systems. In this process, activator or repressor proteins affecting transcription play a key role (Bervoets and Charlier, 2019). One of these are GntR-type transcription factors (Rigali et al., 2002; Jain, 2015; Vigouroux et al., 2021).

GntR family proteins possess a common domain-based architecture with an N-terminal DNA-reading head that typically contains a winged helix-turn-helix operator binding motif and a C-terminal oligomerization and effector-binding domain. Depending on the type and fold of the C-terminal domain, GntR-type transcription factors can be divided into several sub-families (Rigali et al., 2002; Jain, 2015); one of them is formed by MocR/GabR-type proteins (Rossbach et al., 1994; Bramucci et al., 2011; Suvorova and Rodionov, 2016; Tramonti et al., 2018; Pascarella, 2019). The genetically, biochemically, and structurally best characterized member of this sub-family is the GabR protein from *Bacillus subtilis*, a regulatory protein involved in the utilization of γ-amino-butyric acid (GABA) as a nitrogen source (Belitsky and Sonenshein, 2002; Belitsky, 2004; Edayathumangalam et al., 2013; Wu et al., 2017; Nardella et al., 2020).

The C-terminal effector-binding and oligomerization domains of MocR/GabR-type proteins resemble in their fold that of aminotransferases of type I, enzymes that depend on the cofactor pyridoxal-5′-phosphate (PLP, vitamin B6) for their activity (Percudani and Peracchi, 2003; Belitsky, 2004; Suvorova and Rodionov, 2016; Tramonti et al., 2018; Richts et al., 2019). However, the aminotransferase domain (ATD) of these regulatory proteins does not possess enzymatic activity; instead it is used as a sensory domain to affect DNA-binding in response to environmental or cellular cues (Percudani and Peracchi, 2003; Okuda et al., 2015b; Wu et al., 2017; Tramonti et al., 2018).

In some MocR/GabR regulators, in particular those that are involved in the synthesis of vitamin B6, a PLP molecule serves as the sole effector molecule (Belitsky, 2014; Richts et al., 2019). In other MocR/GabR-type regulators, the covalently bound PLP interacts chemically with system-specific low molecular mass inducer molecules (Edayathumangalam et al., 2013; Okuda et al., 2015b; Tramonti et al., 2018). Stemming from this interaction, internal and external aldimines are formed, thereby triggering a conformational change that affects the DNA-binding properties of the transcription factor (Edayathumangalam et al., 2013; Okuda et al., 2015b; Wu et al., 2017; Tramonti et al., 2018; Frezzini et al., 2020). The term internal aldimine refers to a PLP molecule covalently bound via a Schiff-base to the side chain of a lysine residue. This aldimine bond is hydrolyzed upon the chemical interaction of a low molecular mass inducer with the bound PLP molecule, a reaction that leads to the formation of a PLP: inducer adduct, the external aldimine (Tramonti et al., 2018).

Ectoine nutrient utilization regulator (EnuR) [also referred to as EhuR (Yu et al., 2017), or EutR (Suvorova and Rodionov, 2016)] is a member of the MocR/GabR family (Suvorova and Rodionov, 2016; Pascarella, 2019) and serves as a repressor protein involved in the transcriptional control of ectoine/5-hydroxyectoine catabolic gene clusters (Jebbar et al., 2005; Schulz et al., 2017a,b; **Figure 1A**). The tetrahydropyrimidines ectoine and 5-hydroxyectoine (Galinski et al., 1985; Inbar and Lapidot, 1988) are among the most widely synthesized compatible solutes by members of the *Bacteria* (da Costa et al., 1998; Pastor et al., 2010; Czech et al., 2018; Hermann et al., 2020; Imhoff et al., 2020). Their accumulation is used by microorganisms to fend off the detrimental consequences of high osmolarity on cellular hydration and extremes in temperatures on growth (Pastor et al., 2010; Czech et al., 2018; Kunte et al., 2020).

The nitrogen-rich ectoines can also be used by microorganisms as nutrients (Galinski and Herzog, 1990; Onraedt et al., 2004; Jebbar et al., 2005; Vargas et al., 2006; Schwibbert et al., 2011; Landa et al., 2017; Schulz et al., 2017b; Reshetnikov et al., 2020; Nowinski and Moran, 2021). As ectoines are present in the environment in low concentrations (Mosier et al., 2013; Warren, 2014; Bouskill et al., 2016), their uptake requires high-aÿnity transport systems (Grammann et al., 2002; Jebbar et al., 2005; Hanekop et al., 2007; Kuhlmann et al., 2008; Lecher et al., 2009; Kuhlmann et al., 2011). Once imported, the tetrahydropyrimidine rings of ectoine and 5-hydroxyectoine are opened by the ectoine/5-hydroxyectoine hydrolase EutD (EC 3.5.4.44) to form α-acetyldiaminobutyric acid (α-ADABA) from ectoine and hydroxy-α-acetyldiaminobutyric acid (hydroxy-α-ADABA) from 5-hydroxyectoine. These metabolites are then further processed by the *N*-acetyl-L-2,4-diaminobutyric acid

Abbreviations: ATD, aminotransferase domain; K_d, dissociation constant; ABC transporter, ATP binding cassette transporter; TRAP transporter, tripartite ATP-independent periplasmic transporter; PLP, pyridoxal-5′-phosphate; DABA, diaminobutyric acid; α-ADABA, α-acetyldiaminobutyric acid; hydroxy-α-ADABA, hydroxy-α-acetyldiaminobutyric acid; EnuR, ectoine nutrient utilization regulator.

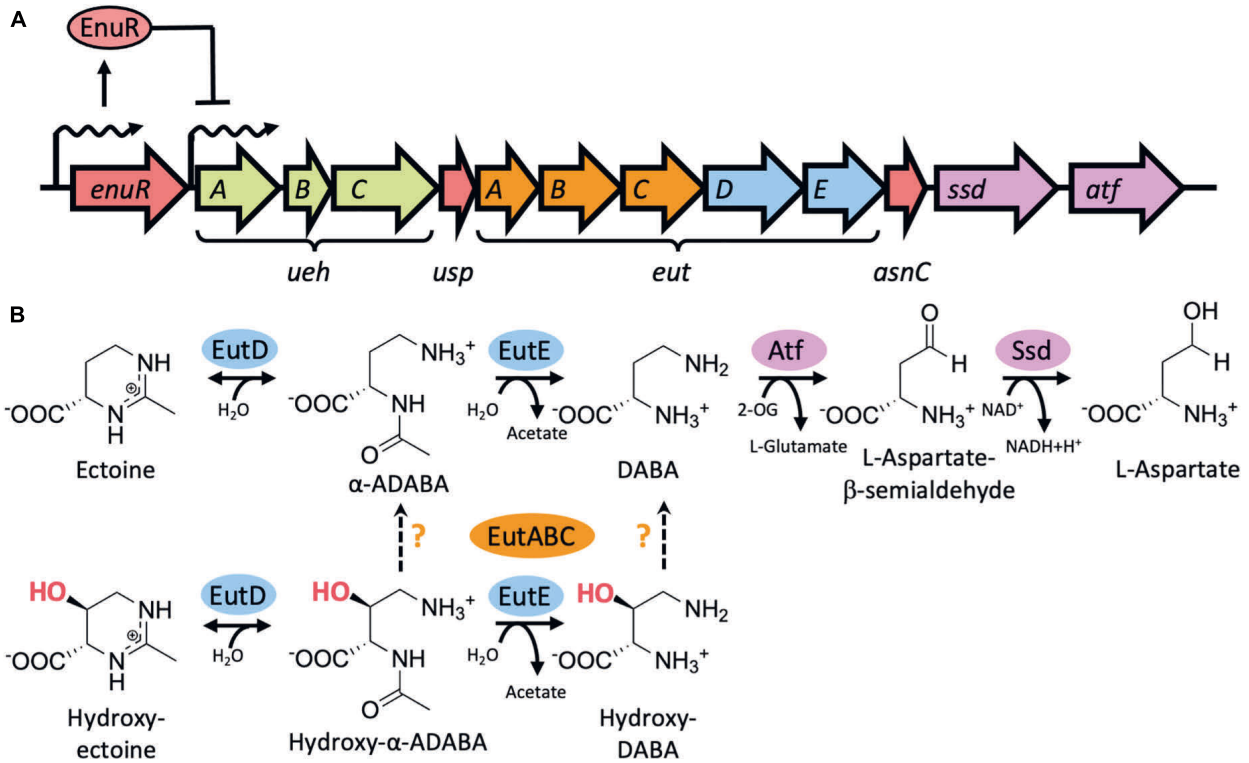

FIGURE 1 | Genetic organization of the ectoine/5-hydroxyectoine importer and catabolic gene cluster from *Ruegeria pomeroyi* DSS-3, EutD/EutE-mediated catabolism of ectoine and 5-hydroxyectoine, and transcriptional induction of the ectoine/5-hydroxyectoine importer and catabolic genes. **(A)** Schematic overview of the ectoine/5-hydroxyectoine catabolic operon that is expressed from a substrate-inducible and EnuR regulated promoter positioned upstream of the first gene in the operon, *uehA* (Schulz et al., 2017b). The gene cluster encodes an ectoine/5-hydroxyectoine specific binding-protein-dependent TRAP transporter (UehABC) (Lecher et al., 2009), genes for enzymes hydrolyzing the ectoine and 5-hydroxyectoine ring to form α-ADABA/hydroxy-α-ADABA (EutD), to deacetylate these metabolites forming DABA and hydroxy-DABA (EutE), and enzymes (Ssd, Atf) mediating the catabolism of DABA to L-aspartate (Mais et al., 2020). The metabolism of 5-hydroxyectoine requires the function of the EutABC enzymes for its use as a nutrient by *R. pomeroyi* DSS-3 (Schulz et al., 2017b) but their precise enzymatic activities are unknown. The catabolic ectoine/5-hydroxyectoine gene cluster also contains two putative regulatory genes with experimentally untested functions: *usp* encodes a member of the universal stress proteins (Schweikhard et al., 2010), and *asnC* [also referred to as *deoX* (Schwibbert et al., 2011)] encodes a member of the feast and famine regulatory proteins (Yokoyama et al., 2006). **(B)** Biochemistry of the catalytic core of the ectoine/5-hydroxyectoine degradation route (Mais et al., 2020) as described in (A) and in the main text. The precise steps catalyzed by the EutABC enzymes in the catabolism of 5-hydroxyectoine (Schulz et al., 2017a) are uncertain. 2-OG: 2-oxoglutarate.

deacetylase EutE (EC 3.5.1.125) to diaminobutyric acid (DABA) in the case of ectoine, and possibly to hydroxy-DABA in the case of 5-hydroxyectoine (**Figure 1B**; Schwibbert et al., 2011; Mais et al., 2020). The presence of both EutD and EutE is needed to eÿciently degrade ectoine and 5-hydroxyectoine. In this enzyme bimodule, EutE presumably supports the release of α-ADABA from the EutD active site through transient interactions (Mais et al., 2020). Eventually, the metabolites generated through the joint EutD/EutE enzyme activities are converted by additional enzymes encoded in ectoine/5-hydroxyectoine catabolic gene clusters, or elsewhere in the genome sequence, to L-aspartate to fuel the TCA-cycle (Schwibbert et al., 2011; Hermann et al., 2020; Mais et al., 2020). It should be noted in this context that the gene content of ectoine/5-hydroxyectoine catabolic clusters are variable (Schwibbert et al., 2011; Schulz et al., 2017b; Hermann et al., 2020; Reshetnikov et al., 2020), and consequently, the complete degradation route(s) of ectoines are not fully understood.

In contrast to the expression of ectoine/5-hydroxyectoine biosynthetic gene clusters that are typically induced in response to osmotic stress, the transcription of those for ectoine/5-hydroxyectoine catabolic operons is substrate inducible (Jebbar et al., 2005; Schulz et al., 2017b; Yu et al., 2017). However, externally provided ectoines are not the true inducers. Instead, the ectoine-derived metabolites α-ADABA and DABA serve this function by reacting with the PLP molecule covalently attached to the ATD of EnuR (Schulz et al., 2017a,b; Yu et al., 2017). Ectoine/5-hydroxyectoine importer and catabolic gene clusters are often juxtapositioned to a gene (*enuR*) encoding EnuR-type proteins (Schulz et al., 2017a; Hermann et al., 2020). This genetic arrangement implies a wider role for the EnuR repressor in controlling the use of ectoines as nutrients.

We use the marine α-proteobacterium *Ruegeria pomeroyi* DSS-3, a member of the widely distributed and ecophysiologically important *Roseobacter* clade (Moran et al., 2004), as our model system for the analysis of the catabolism of ectoines

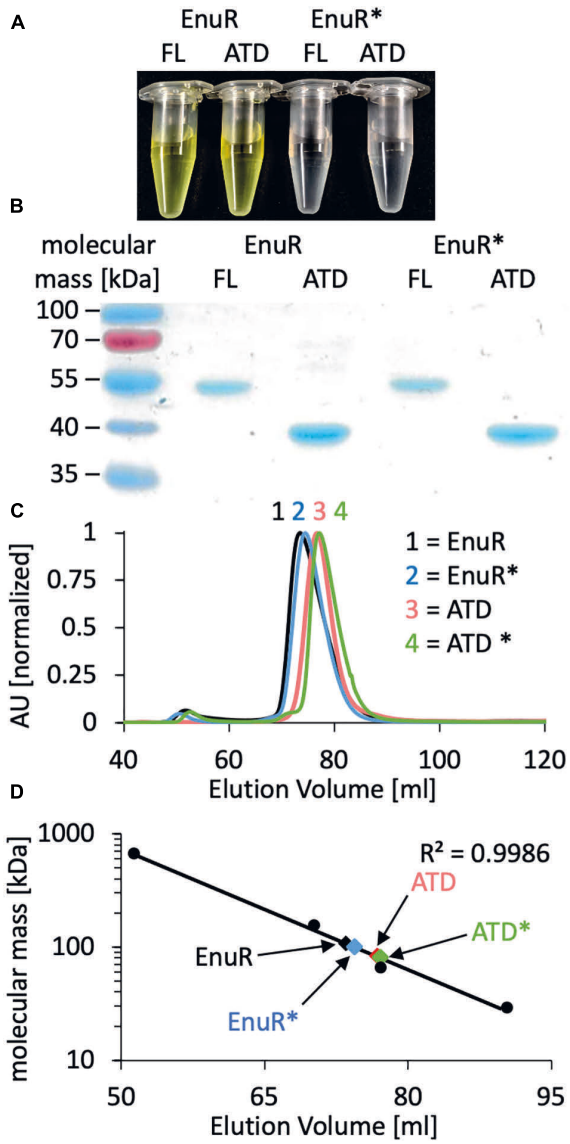

FIGURE 2 | Biochemical analysis of EnuR. **(A)** The full-length (FL) wild-type EnuR protein from *R. pomeroyi* DSS-3, the EnuR* mutant (Lys302His) derivative unable to bind PLP (Schulz et al., 2017a) and the corresponding ATDs from both proteins were purified via affinity chromatography. The protein concentration in each sample was set to 50 μM and the yellow color of samples indicates the presence of a covalently bound PLP molecule. **(B)** The purity of the isolated proteins was analyzed by SDS-PAGE (12% polyacrylamide). Proteins were visualized by staining the gel with Instant*Blue*. **(C)** Analysis of the quaternary assembly of the full-length and ATD proteins of the wild-type EnuR protein and its EnuR*-mutant derivative by size exclusion chromatography (SEC) on a HiLoad 16/600 Superdex 200 pg column. The positions at which these protein species eluted from the SEC-column were as follows: EnuR = 73.50 ml; EnuR* = 74.42 ml; ATD = 76.75 ml, and ATD* = 77.12 ml. AU: absorbance unit at a wavelength of 280 nm. **(D)** Comparison of the elution volumes of EnuR and ATD-proteins and their respective Lys302His derivatives with respect to the chromatographic behavior of marker proteins (thyroglobulin, 669 kDa; alcohol dehydrogenase, 150 kDa; bovine albumin, 66 kDa; carbonic anhydrase, 29 kDa). From this chromatographic behavior the following molecular masses were estimated: EnuR = 109 kDa; ATD = 83 kDa; EnuR* = 101 kDa and ATD* = 81 kDa, indicating that each of these proteins forms dimers in solution. The calculated molecular masses of the studied proteins fused to a *Strep*-tag II affinity peptide are: EnuR = 104 kDa; ATD = 80 Da; EnuR* = 104 kDa, and of the ATD* = 80 kDa.

(Continued)

(Schulz et al., 2017a,b; Hermann et al., 2020; Mais et al., 2020). In contrast to other members of the *Roseobacter* clade (Simon et al., 2017), *R. pomeroyi* DSS-3 cannot synthesize ectoines (Schulz et al., 2017b). The ectoine/5-hydroxyectoine importer and catabolic operon of *R. pomeroyi* DSS-3 comprises 12 genes that are transcribed as a 12 kbp poly-cistronic mRNA (**Figure 1A**). The substrate-mediated induction of the transcription of this operon is carried out by a predicted sigma-70-type promoter, while the expression of the *enuR* gene, juxtapositioned to the importer and catabolic genes, occurs constitutively at a low level (Schulz et al., 2017b).

The external supply of 5-hydroxyectoine triggers a substantially stronger induction of expression of the ectoine/5-hydroxyectoine catabolic gene cluster in comparison with that afforded by ectoine (about 4-fold) (Schulz et al., 2017a). Binding of ectoine-derived α-ADABA to the purified EnuR protein has been demonstrated (K_d of about 1.7 μM) (Schulz et al., 2017a) but it is unclear if the initial hydrolysis product of 5-hydroxyectoine, hydroxy-α-ADABA (Mais et al., 2020), will also interact with EnuR to serve as a metabolically derived internal inducer. Here, we address this question through biochemical and bioinformatical analysis of the EnuR protein from *R. pomeroyi* DSS-3. We show through mass spectrometry that the ATD of EnuR contains a covalently bound PLP and that the initial hydrolysis products of ectoine and 5-hydroxyectoine, α-ADABA and hydroxy-α-ADABA, can be found in cells catabolizing ectoines. These metabolites serve as high-aÿnity ligands for EnuR with dissociation constants (K_d) in the low micromolar range. We used molecular modelling and docking experiments to provide a view into the cofactor and inducer binding site of this transcription factor. Putative EnuR binding sites overlap core elements of the substrate-inducible sigma-70 type promoter of the catabolic gene cluster and the EnuR repressor protein binds to a 48 bp DNA fragment containing the corresponding promoter/regulatory region with a K_d-value of about 2 μM.

RESULTS

Purification and Biochemical Assessment of Ectoine Nutrient Utilization Regulator and Its Separate Aminotransferase Domain

To biochemically characterize EnuR from *R. pomeroyi* DSS-3 further, we expressed a full-length recombinant EnuR-*Step*-Tag-II protein heterologously in *E. coli* and purified it to apparent homogeneity via aÿnity chromatography on a Streptactin column. We also separately expressed and purified the C-terminal ATD of the wild-type protein as a *Strep*-Tag-II fusion protein. In addition, we carried out similar types of

production and aÿnity purification experiments with a variant of the *R. pomeroyi* DSS-3 EnuR protein in which the Lys residue to which the PLP cofactor is presumably covalently attached is replaced by a His residue (EnuR*; Lys302His). As a result of this amino acid substitution, PLP cannot be covalently bound, leading to the loss of the characteristic PLP-dependent yellow color of the full-length wild-type EnuR protein solutions (Schulz et al., 2017b; **Figures 2A,B**). Incorporation of the PLP cofactor also occurred during the heterologous production of the ATD from the wild-type protein but not into the ATD derived from the EnuR* protein (**Figure 2A**).

The GabR protein from *B. subtilis* is a homodimer where the monomers are arranged in a head to tail configuration (Edayathumangalam et al., 2013) and where the isolated ATD can form homodimers as well (Okuda et al., 2015a). In a similar vein, we found that the purified EnuR protein and its separately produced ATD also assemble into homo-dimers in solution. These proteins eluted from a size exclusion column as corresponding to 109 kDa and 83 kDa molecular mass species, respectively (**Figures 2C,D**). The calculated molecular mass of the *R. pomeroyi* DSS-3 monomeric EnuR protein is 51 kDa, while that of its ATD is 40 kDa. The EnuR* protein and its isolated ATD* behaved in these chromatography experiments identical to that of the corresponding wild-type proteins (**Figures 2C,D**). Taken together, these biochemical experiments show that (i) dimer-formation of EnuR depends on its ATD, regardless whether the ATD carries a covalently attached PLP or not, and (ii) that the PLP cofactor can be attached to the ATD even when the N-terminal DNA-reading head of EnuR is missing.

Verification of Bound Pyridoxal-5′-Phosphate in Ectoine Nutrient Utilization Regulator and Its ATD by Mass Spectrometry

In order to probe whether the PLP co-purifying with EnuR is covalently attached to Lys302 or just coordinated by this residue, we subjected the EnuR and EnuR-ATD proteins to mass spectrometric (MS) analysis. Due to the lability of the aldimine group that would be formed between the ε-amino group of the lysine side chain and the PLP cofactor, the purified proteins were reduced with $NaBH_4$ prior to tryptic digestion. In the subsequent MS analysis, we retrieved peptides spanning amino acid residues 294-302 of both the EnuR and EnuR-ATD proteins that exhibited a mass-to-charge (m/z) ratio of 1,318.63305 (theoretical mass-to-charge ratio of $M + H^+$ of 1,087.60339), corresponding to a mass shift of 231.02966 Da, a value in excellent agreement with the presence of a covalently attached PLP (theoretical difference of 231.029662 Da). Further MS/MS fragmentation of these peptides corroborates that Lys302 is the site of attachment for PLP (**Figures 3A,B**). This consolidates the previous suggestion that EnuR binds PLP, similar to type I aminotransferases and MocR/GabR-type regulators (Tramonti et al., 2018), through the formation of an aldimine between an evolutionary conserved lysine residue (Lys302 in EnuR) and the cofactor (Schulz et al., 2017a).

Inducer-Binding by the Purified Ectoine Nutrient Utilization Regulator Protein and Its Isolated ATD

Micro-scale thermophoresis is a sensitive method that traces the movement of fluorescently labelled proteins in a temperature gradient in response to a ligand (Wienken et al., 2010). We used this method to determine the dissociation constant (K_d) (**Figure 4**) for the binding of the known ectoine-derived inducer α-ADABA (Schulz et al., 2017a) and that of the presumed 5-hydroxyectoine-derived inducer hydroxy-α-ADABA (**Figure 1B**; Mais et al., 2020). Both compounds were obtained via chemical synthesis through alkaline-mediated hydrolysis of the tetrahydropyrimidine ring of either ectoine (Kunte et al., 1993) or 5-hydroxyectoine. They were purified by repeated chromatography on silica columns to apparent homogeneity as assessed by NMR-spectroscopy (Mais et al., 2020).

Ectoine nutrient utilization regulator bound α-ADABA with a K_d of 2.55 ± 0.5 μM (**Figure 4A**), a value that fits well with a previous measured K_d-value of 1.7 ± 0.3 μM for this ligand (Schulz et al., 2017a). The full length EnuR protein exhibited a K_d-value of 0.43 ± 0.2 μM for hydroxy-α-ADABA (**Figure 4B**). We also assessed the binding of α-ADABA to the PLP-bound ATD of the wild-type EnuR protein in a micro-scale thermophoresis ligand-binding experiment. We found that this domain bound this ectoine metabolite with approximately the same K_d-value (1.98 ± 0.45 μM) (**Figure 4C**) as the full length EnuR protein (K_d of 2.55 ± 0.5 μM).

Modeling the Overall Fold of Ectoine Nutrient Utilization Regulator and Phylogenomic Conservation of This Repressor Protein

Since we wanted to further understand the molecular determinants for inducer binding by EnuR, we generated a structural model of its monomer. The EnuR model was fashioned on the crystal structure of the *B. subtilis* GabR protein (Edayathumangalam et al., 2013), the only GabR/MocR-type regulatory protein whose crystal structure is known. Our EnuR model (**Figure 5A**) was generated using Phyre[2] (Kelley et al., 2015) set in the extensive mode[1]. An overlay of the GabR protein and of the EnuR model revealed a root mean square deviation (RMSD) of just 0.86 Å (over 390 amino acids), indicating that the overall fold of these two MocR/GabR-type regulatory proteins is most likely closely related.

In addition to the modelling of the putative EnuR structure, we also assessed the phylogenomic conservation of this regulatory protein. For this analysis, we relied on a recently reported manually curated dataset assessing the presence of ectoine/5-hydroxyectoine catabolic gene clusters in 8 850 microbial genome sequences (Mais et al., 2020). The identification of putative ectoine/5-hydroxyectoine catabolic gene clusters was based upon a direct juxtaposition of the *eutD* and *eutE* genes. 363 microbial genome sequences contained *eutD/eutE* pairs. We found that 76% (278 out of 363) of the corresponding ectoine/5-hydroxyectoine

[1]http://www.sbg.bio.ic.ac.uk/˜phyre2/

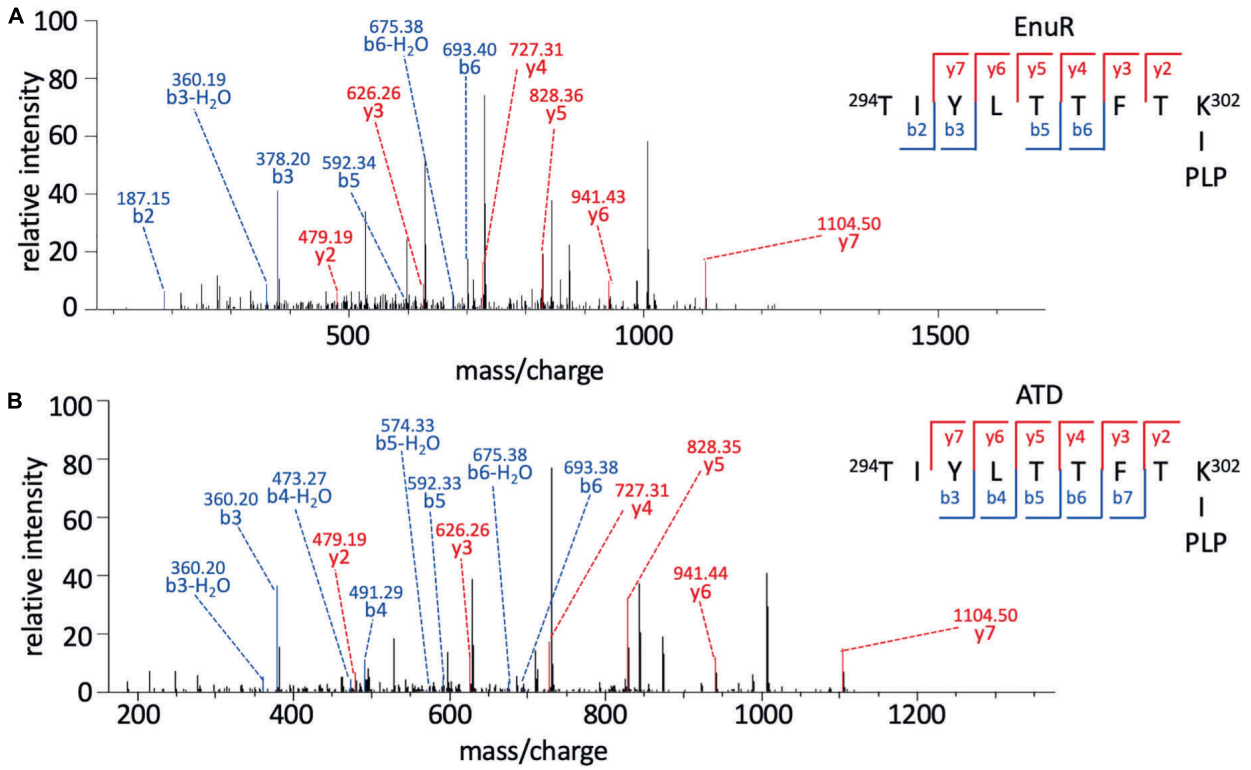

FIGURE 3 | Pyridoxal-5′-phosphate is covalently bound to Lys302 (K302) of EnuR. MS/MS spectrum of the PLP-containing peptide spanning residues 294-302 (TIYLTTFTK∼PLP) of **(A)** full-length EnuR and **(B)** EnuR-ATD. EnuR and EnuR-ATD were reduced with $NaBH_4$ before tryptic digestion of the proteins to stabilize the otherwise acid-labile aldimine. These tryptic digests were subjected to analysis by mass spectrometry. The peptide ^{294}TIYLTTFTK^{302} exhibited a mass-to-charge ratio (m/z) of 1,318.63305 ($M + H^+$ ion), although its theoretical mass-to-charge ratio is only 1,087.60339 ($M + H^+$ ion); the difference of 231.02966 is in good agreement with the mass of a PLP. To narrow down the position of PLP attachment in the ^{294}TIYLTTFTK^{302} peptide ion, this precursor ion was further fragmented by MS/MS resulting in breaks of the precursor ion at the peptide bonds, giving rise to b-ions (*N*-terminal ion, blue) and y-ions (C-terminal, red), respectively. The detected b-ions correspond to the theoretical masses of the unmodified amino acids contained therein; however, all y-ions show the difference in mass corresponding to PLP, e.g., the y2 ion has a theoretical mass of 248.16187 but exhibits 479.19387 experimentally in this MS/MS (difference of 231.03200). As residue Thr301 is unable to covalently bind PLP, this consolidates amino acid Lys302 of EnuR as the PLP-binding residue.

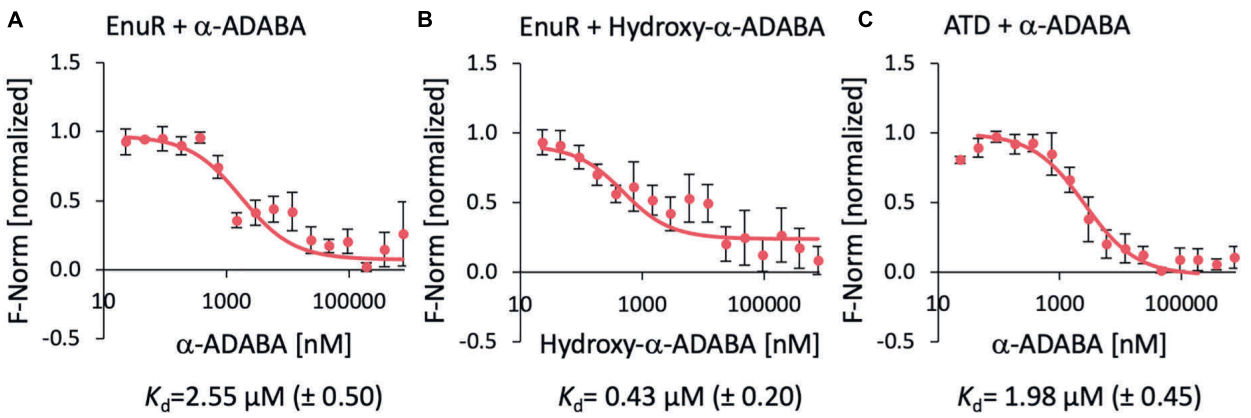

FIGURE 4 | Ligand binding by the wild-type EnuR protein and its isolated ATD as assessed by microscale thermophoresis. Purified EnuR protein (200 nM) was incubated with increasing concentrations of α-ADABA **(A)**, Hydroxy-α-ADABA **(B)**, and the C-terminal ATD of EnuR was incubated with α-ADABA **(C)**. The ability of these compounds to bind to the EnuR protein **(A,B)** or its isolated ATD **(C)** was measured by microscale thermophoresis. The ligands were titrated to a constant amount (200 nM) of purified and PLP-containing EnuR protein, or its PLP-containing ATD. Error bars show the standard deviation; the ligand-binding experiments were repeated six times with independently purified and fluorescently labeled EnuR/ATD preparations. F-norm refers to the thermophoretic behavior of these tested proteins in a ligand gradient.

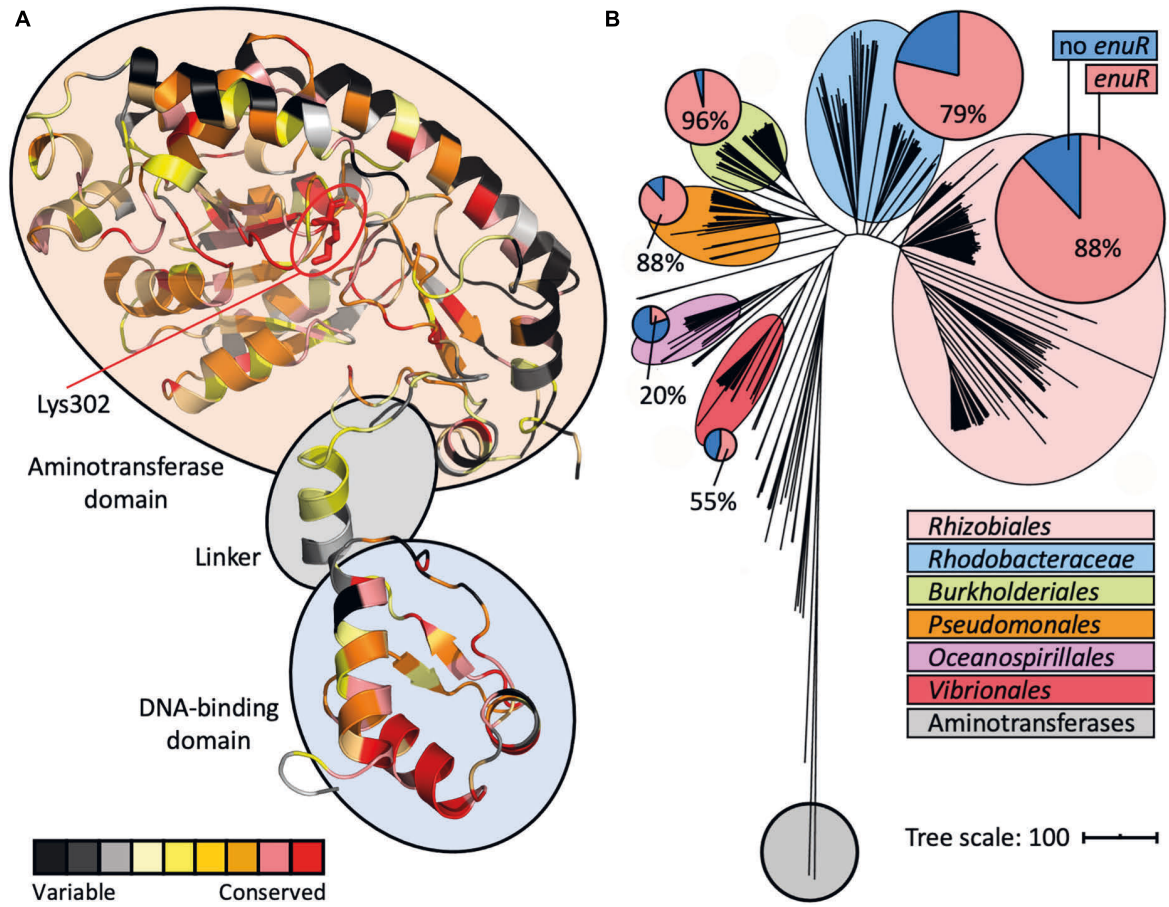

FIGURE 5 | A model of the structure of a EnuR monomer and phylogenomic distribution of *enuR*-type genes in bacteria encoding EutD/EutE ectoine/5-hydroxyectoine degrading enzymes. **(A)** A model of the *R. pomeroyi* DSS-3 EnuR protein was established using the Phyre[2] protein structure prediction server (Kelley et al., 2015) that is based on the crystal structure of the *B. subtilis* GabR protein (Edayathumangalam et al., 2013). Each amino acid in this model is color coded by its degree of conservation in EnuR-type proteins as assessed with the ConSurf algorithm (Berezin et al., 2004). An amino acid sequence alignment of 278 EnuR-type proteins was used to calculate the conservation at each position of the protein chain. The predicted domain-organization of EnuR with its N-terminal DNA-reading head containing a winged-helix-turn-helix motif, the flexible linker region, and the C-terminal ATD containing the Lys residue (Lys302) to which the PLP cofactor is covalently attached, is indicated. **(B)** iTol (Letunic and Bork, 2019) generated tree of the ectoine/5-hydroxyectoine hydrolase EutD representing 363 EutD-type proteins (Mais et al., 2020). The EutD protein-based tree was rooted with *E. coli* and *Homo sapiens* aminopeptidases (Bradshaw et al., 1998; Wilce et al., 1998). All microorganisms possessing EutD-type ectoine/5-hydroxyectoine hydrolases were analyzed for the presence of *enuR*-type genes juxtapositioned to ectoine/5-hydroxyectoine catabolic gene clusters; larger phylogenetic groups possessing such genetic arrangements are highlighted. In the circles, the red segments represent the number of microorganisms within a given phylogenetic group that possess *enuR*-type genes, while the blue segment represents the number of those bacteria that lack it.

catabolic gene clusters contained a juxtapositioned *enuR* gene (**Figure 5B**). We then used the information gleaned from this bioinformatic approach (**Supplementary Figure 1**) to assess the degree of amino acid conservation at each position in the EnuR protein chain (**Supplementary Figure 2**). Subsequently, we projected these data onto our EnuR model by using the ConSurf algorithm (Berezin et al., 2004; **Figure 5A**).

In an alignment of the 278 retrieved EnuR-type proteins, we found that the degree of amino acid sequence identity ranged between 82% (for the EnuR protein from *Leisingeria* sp. NJS201) and 40% (for the EnuR protein from *Salipiger pacificus* YSBP01) when the *R. pomeroyi* DSS-3 EnuR protein was used as the search query. As expected, those amino acid residues forming the N-terminally positioned winged-helix-turn-helix DNA reading head are particularly well conserved, as are central segments of the ATD (**Figure 5A** and **Supplementary Figure 2**). Notably, the Lys residue in the ATD to which the PLP molecule is covalently attached in EnuR (Lys302 in the *R. pomeroyi* DSS3 EnuR protein) (Schulz et al., 2017b), is completely conserved among the 278 inspected EnuR-type proteins (**Supplementary Figure 2**).

Among those 363 genome sequences that contain *eutD/eutE* pairs, six major microbial orders are represented (**Figure 5B**), all of which belong to the proteobacteria (**Supplementary Table 1**). Using computational tools provided via the IMG/M web-server (Chen et al., 2021), a phylogenetic tree was calculated for the 363 EutD-type proteins using aminotransferases from *Escherichia coli* (Wilce et al., 1998) and *Homo sapiens* (Bradshaw et al., 1998) as outgroups. The EutD-derived tree

was visualized using the iTOL software suit (Letunic and Bork, 2019), and the presence of 278 *enuR*-type genes was then projected onto this tree (**Figure 5B**; **Supplementary Figure 1**). *enuR*-type genes are dominantly represented among *Rhizobiales, Rhodobacterales, Burkholderiales, Pseudomonales, Oceanospirillales,* and *Vibrionales* predicted to use ectoines as nutrients (**Figure 5B**).

Molecular Docking of α-ADABA, hydroxy-α-ADABA, γ-ADABA, and DABA Into the ATD of Ectoine Nutrient Utilization Regulator Reveals the Likely Molecular Determinants for Inducer-Binding

The crystal structure of the dimeric full-length *B. subtilis* GabR protein contained in the cofactor and inducer binding site of one of its monomers a PLP molecule covalently bound to a Lys residue (**Figure 6A**). In the second monomer, a free PLP molecule was found that was chemically ligated to γ-ethynyl-GABA, a substrate-mimic of GABA (**Figure 6B**), thereby revealing the structure of the external aldimine (Edayathumangalam et al., 2013). In addition, a crystal structure of the isolated dimeric ATD of GabR captured the GABA-mediated structural transition catalyzed by the conversion of the internal aldimine to the external aldimine (Park et al., 2017). Collectively, these crystal structures guided our docking experiments of the high aÿnity inducers α-ADABA and hydroxy-α-ADABA into the presumed ligand-binding site of EnuR. The docking experiments were carried out using AutoDock Vina (Trott and Olson, 2010).

In our EnuR model, hydroxy-α-ADABA is bound in close proximity to the PLP molecule with which it interacts via its free amino group. Nine interactions of the inducer molecule with the EnuR protein are observed (**Figure 6C**). The oxygen of PLP interacts with the hydroxyl-oxygen of hydroxy-α-ADABA as well as with the primary amino group of this molecule. This nitrogen atom is also bound by the O-1 atom of Asn244. Additionally, hydroxy-α-ADABA is stabilized by interactions with the N-2 atom of Asn244 and through interactions with Thr245, Phe417, Ser431, Ser104 (**Figure 6C**). Collectively, these nine interactions are the foundation for the high aÿnity of EnuR for hydroxy-α-ADABA (**Figure 4B**); they thereby establish the orientation of this 5-hydroxyectoine-derived metabolite in the inducer binding site of EnuR. A more detailed description of the energetics of these interactions are summarized in **Supplementary Table 2**.

Compared to hydroxy-α-ADABA, α-ADABA appears to be a slightly more linear molecule due to the lack of the hydroxy group. Consequently, it is positioned in the predicted inducer binding site of EnuR in a slightly different orientation (**Figure 6D**). Like hydroxy-α-ADABA, the primary amino group of α-ADABA interacts with the oxygen atom of PLP. A second interaction of the primary amino group of α-ADABA is found with the side chain of Ser104, a configuration different from that predicted for hydroxy-α-ADABA (**Figures 6C,D**). As observed for hydroxy-α-ADABA, the carboxyl group of α-ADABA interacts with the nitrogen atom present in the side chain of Asn244. The secondary nitrogen atom of α-ADABA interacts with the oxygen atom of Ser431. In total five interactions of EnuR with α-ADABA are predicted (**Figure 6D** and **Supplementary Table 2**), suggesting that this compound will be bound with a somewhat lower aÿnity by EnuR in comparison with hydroxy-α-ADABA. This is precisely what we observed in our *in vitro* ligand binding experiments where the aÿnity of EnuR for hydroxy-α-ADABA was about five times higher than that for α-ADABA (K_d of about 0.43 μM versus 2.55 μM for hydroxy-α-ADABA and α-ADABA, respectively) (**Figures 4A,B**).

The amino acid sequence alignment of 278 EnuR-type proteins revealed a high degree of conservation of the amino acids predicted to be involved in hydroxy-α-ADABA and α-ADABA binding by our docking studies (**Figures 6C,D**). Especially Ser104, Asn244, Lys302, Phe417, and Arg429 are either strictly or highly conserved (**Supplementary Table 3**). Slight deviations can be observed for the position of Ser431; however, this amino acid is mainly exchanged to a Cys residue (135/278). In our model of the EnuR ligand binding cavity, the sulfur atom of Ser431 interacts directly with both inducer molecules and it is thus a reasonable assumption that the sulfur atom of the Cys side chain will adopt the same interaction. The positions Ala412 and Thr245, more peripheral residues in the ligand binding site (**Figures 6C,D**), seem to be less important for the binding of the hydroxy-α-ADABA and α-ADABA molecules. Ala412 is frequently substituted by a Leu residue (123/278), while a great variety of residues can assume the position of Thr245 in EnuR-type proteins (**Supplementary Table 3**). A visualization of the EnuR binding site for the PLP cofactor and the inducer α-ADABA is rendered in **Figure 6F**.

The ectoine metabolite diaminobutyric acid (DABA) (**Figure 1B**) also serves as an inducer for EnuR (Schulz et al., 2017a; Yu et al., 2017). A K_d-value of about 460 μM has been reported for the EnuR protein from *R. pomeroyi* DSS-3 (Schulz et al., 2017a). Hence, there is a substantial difference in aÿnity between DABA on one hand and α-ADABA and hydroxy-α-ADABA on the other hand for EnuR (**Figures 4A,B**). As a consequence of the low binding aÿnity of DABA for EnuR, we observed multiple positions for the DABA molecule within the presumed inducer binding site of EnuR in the first round of docking experiments. Optimization and refinement of these positions was diÿcult and only two interactions of DABA were observed that hinted at a possible binding state (**Supplementary Table 2**). However, in contrast to α-ADABA and hydroxy-α-ADABA (**Figures 6C,D**), this would position DABA too far away from the PLP molecule (**Figure 6E**; Tramonti et al., 2018) in order to serve its function as an inducer for EnuR. While the distances between the primary nitrogen group of α-ADABA and hydroxy-α-ADABA to the PLP cofactor in our EnuR model are 2.6 Å and 3 Å, respectively, the distance of the corresponding nitrogen group of DABA is about 7 Å. Consequently, the actual position of the low-aÿnity EnuR ligand DABA cannot be reliably predicted by our docking experiments.

The isomer of α-ADABA, γ-ADABA, is the substrate for the ectoine synthase EctC (Czech et al., 2019), the key enzyme for the production of ectoine (Peters et al., 1990; Ono et al., 1999; Hermann et al., 2020). We wondered if interactions of γ-ADABA

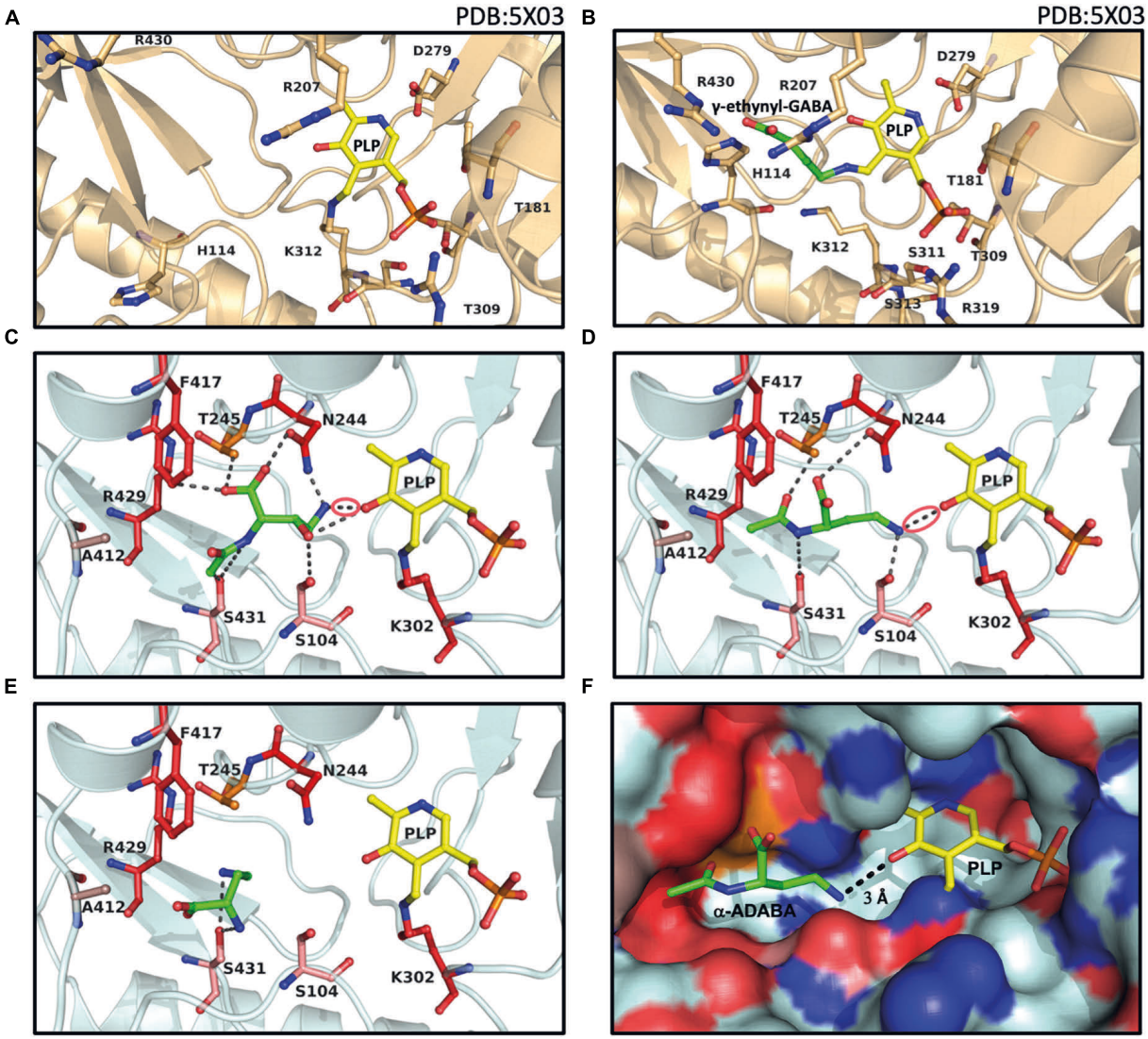

FIGURE 6 | Structural views into the presumed inducer binding sites of GabR and EnuR. The crystal structure of the dimeric *B. subtilis* GabR protein (PDB accession code: 5XO3) (Edayathumangalam et al., 2013) contains **(A)** in one monomer a PLP molecule covalently attached to a the side-chain of Lys312 and in the second monomer **(B)** a PLP molecule ligated to γ-ethynyl-GABA (a mimic of GABA). Docking models of the ectoine/5-hydroxyectoine derived inducers (green) **(C)** hydroxy-α-ADABA, **(D)** α-ADABA, and **(E)** DABA docked into the presumed EnuR ligand binding cavity. The ligands and EnuR amino acid residues predicted to be involved in inducer-binding are displayed as sticks. The protein backbone is shown in gold for the GabR protein **(A,B)**, cyan for the EnuR protein **(C,D,E)**, and the PLP cofactor covalently attached to the side-chain of Lys302 in EnuR is depicted in yellow. The aldimine bonds formed by the chemical interaction of the inducers and PLP in the process of the external aldimine formation (Tramonti et al., 2018) are indicated by red circles in **(C,D)**. **(F)** Surface representation of the EnuR ligand and PLP cofactor binding cavity with the predicted position of the α-ADABA molecule. Positively and negatively charged segments of the binding cavity are labeled in blue and red, respectively. The graphical representation of the ligand binding sites in each of the shown panels was rendered with PyMol (Delano, 2002).

with EnuR could be found in docking experiments but no stable binding was observed. This was mainly due to steric clashes with amino acid residues whose side chains protrude into the inducer binding site of EnuR. This result is fully consistent with previous experiments in which no binding of γ-ADABA to purified EnuR from *R. pomeroyi* DSS-3 could be measured (Schulz et al., 2017a). The failure to dock the non-inducer γ-ADABA into the EnuR binding site can be considered as an internal control for the successful docking experiments with its isomer α-ADABA, a high-aÿnity ligand for EnuR (**Figure 4A**).

Targeted Metabolic Analysis of Ectoine- and 5-Hydroxyectoine-Derived Metabolites

Since α-ADABA, hydroxy-α-ADABA, DABA, and possibly also hydroxy-DABA can interact with EnuR and serve as inducers, we wondered if these compounds can be found in cells of *R. pomeroyi* DSS-3 actively catabolizing ectoines. We therefore performed targeted metabolic analysis of ectoine- and 5-hydroxyectoine-derived metabolites in cells that were grown with either ectoine

or 5-hydroxyectoine as sole carbon, energy and nitrogen sources. The metabolic profile of these cultures was compared with that of cells using glucose as carbon and energy source and NH_4Cl as nitrogen source in a chemically fully defined minimal medium. The analyzed samples contained substantial amounts of either ectoine or 5-hydroxyectoine, but these values represent in all likelihood not only intracellular pools of these compounds but probably also reflect incomplete removal during the harvesting and washing of the cells (**Figure 7A**).

Substantial amounts of α-ADABA were found in the extracts of cells grown in the presence of ectoine, while hydroxy-α-ADABA was found in cells grown in the presence of 5-hydroxyectoine (**Figure 7B**). Interestingly, DABA was found under both cultivation conditions, regardless whether the cells were grown in the presence of ectoine or of 5-hydroxyectoine. The pool of hydroxy-DABA in cells that received 5-hydroxyectoine as their sole carbon and nitrogen sources was very low and, as expected, not detectable in cells that were exposed to ectoine (**Figure 7B**). A rather surprising finding was the detection of substantial amounts of γ-ADABA in cells that were grown in the presence of ectoine, while γ-ADABA was present only in very low amounts in cells grown in the presence of 5-hydroxyectoine (**Figure 7B**).

Binding of Ectoine Nutrient Utilization Regulator to the Promoter Region

Using comparative genomics and metabolic reconstruction, Suvorova and Rodionov (2016) have previously analyzed putative EnuR (EutR) operator binding sites in 69 microbial genomes. This analysis suggested a consensus operator sequence for EnuR (EutR)-type proteins that consists of an inverted repeat of five base pairs separated by six base pairs [ATTGTnnnnnnACAAT] (Suvorova and Rodionov, 2016). However, depending on the microbial species under study, variations on this theme exist (Schulz et al., 2017a; Yu et al., 2017).

In *R. pomeroyi* DSS-3, two closely spaced potential EnuR binding sites in the intergenic region between the 3′-end of *enuR* and the beginning of the ectoine/5-hydroxyectoine catabolic operon (**Figure 1A**) can be observed. They overlap with core elements (−10 and −35 sequences separated by 17 bp) of the predicted sigma-70 type promoter (Feklistov et al., 2014; **Figure 8A**) for the ectoine/5-hydroxyectoine catabolic gene cluster. DNA band-shift assays have previously shown that EnuR can specifically bind *in vitro* to a 278 bp DNA fragment carrying both predicted operators (Schulz et al., 2017a). The putative binding site one is a perfect repeat with eight bp in each of the half-sites, while the second putative binding site has an overall length of 18 bp and only the outermost four bp are a perfect inverted repeat (**Figure 8A**). It is currently unknown if both of the *in silico* predicted EnuR binding sites (Suvorova and Rodionov, 2016) are biological relevant to control the ectoine/5-hydroxyectoine importer and catabolic gene cluster from *R. pomeroyi* DSS-3.

Since no quantitative data for the interaction of the *R. pomeroyi* DSS-3 EnuR protein with its presumed operator(s) have been reported, we carried out DNA-binding assays with the purified full-length and PLP-containing EnuR protein with a labeled 48 bp DNA fragment containing both presumed EnuR binding sites using microscale thermophoresis. We measured a K_d-value of 1.9 μM (**Figure 8B**). This is a higher yet physiologically relevant K_d-value than the K_d-value (9.14 nM) reported for the promoter/operator interaction of EnuR with its two established operators for the *S. meliloti* ectoine/5-hydroxyectoine catabolic gene cluster (Yu et al., 2017).

DISCUSSION

A computational classification of MocR/GabR-type regulators has previously shown that EnuR/EhuR-type proteins form a clade well separated from other sub-groups of MocR/GabR-type transcription factors (Pascarella, 2019). As studied in detail for the *B. subtilis* GabR protein, the PLP-dependent chemistry driving the transition of an internal to an external aldimine, and hence the ensuing interconversion of the DNA-binding status of MocR/GabR-type regulators, requires the formation of an aldimine bond between a previously covalently bound PLP with a primary nitrogen group present in a system-specific inducer molecule (e.g., GABA) (Edayathumangalam et al., 2013; Okuda et al., 2015a,b; Park et al., 2017; Wu et al., 2017; Tramonti et al., 2018). Spectroscopic and mutagenesis studies have previously suggested that the EnuR repressor from *R. pomeroyi* DSS-3 contains PLP as a cofactor that is covalently attached to the side chain of Lys302 (Schulz et al., 2017a). The mass-spectrometry data reported here (**Figure 3**) corroborate these previous reports. The presence of the Lys302-bound PLP cofactor is crucial for the induction process, as a mutant (Lys302His) (EnuR*) unable to incorporate PLP into EnuR functions as a constitutive repressor leading to the inability of *R. pomeroyi* DSS3 to use ectoines as nutrients (Schulz et al., 2017a). The central role of this residue for the proper functioning of the EnuR repressor from *R. pomeroyi* DSS-3 is reflected in the strict conservation of the corresponding lysine residue in each of the 278 EnuR-type proteins that we have inspected (**Figure 5A**).

Despite being strong inducers of their catabolic importer and degradative gene cluster in *R. pomeroyi* DSS-3 (Schulz et al., 2017a,b), externally provided ectoines cannot directly serve such a regulatory function as these tetrahydropyrimidines lack a primary amino group that would allow them to chemically interact with the covalently bound PLP cofactor present in EnuR (**Figure 1B**). Such a primary amino group is, however, present in each of the initial hydrolysis products of ectoine and 5-hydroxyectoine, α-ADABA and hydroxy-α-ADABA, respectively, metabolites formed by the EutD enzyme, and in their deacetylated derivatives, DABA and hydroxy-DABA, respectively, formed by the EutE enzyme (**Figure 1B**; Schwibbert et al., 2011; Hermann et al., 2020; Mais et al., 2020). Collectively, our data suggest that these four metabolically derived compounds of ectoine/5-hydroxyectoine serve as internal inducers for the EnuR repressor. Although likely, we cannot be certain of such a role for hydroxy-DABA as this compound is currently not available in amounts required for ligand binding experiments.

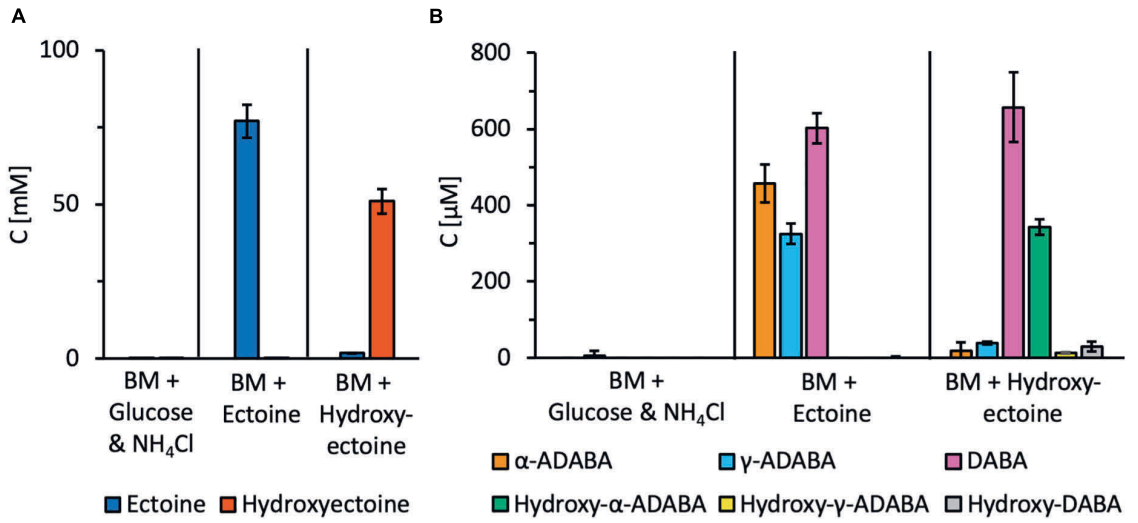

FIGURE 7 | Targeted metabolic analysis of ectoine and 5-hydroxyectoine-derived metabolites. *R. Pomeroyi* DSS-3 cultures were grown in basal medium (BM) either in the presence of glucose and NH_4Cl, or ectoines as sole carbon, energy, and nitrogen sources. Cultures were grown to an OD_{578} of about one, centrifuged, and the cells were washed once in BM. Subsequently, metabolites were extracted with 20% ethanol. Ectoine and 5-hydroxyectoine-derived metabolites were analyzed by HPLC-ESI-MS. For these experiments, four independent cultures were grown and a sample prepared from each of them was assayed twice. The indicated error bars show the standard deviation. **(A)** Presumed intracellular pools of the growth substrates ectoine and 5-hydroxyectoine, and **(B)** intracellular pools of ectoine and 5-hydroxyectoine derived metabolites.

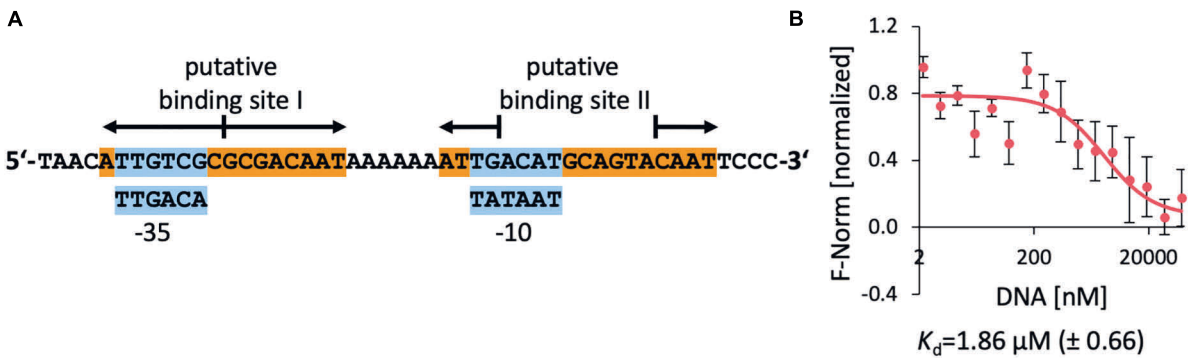

FIGURE 8 | DNA-binding of EnuR to the promoter and regulatory region of the ectoine/5-hydroxyectoine catabolic gene cluster of *R. pomeroyi* DSS-3. **(A)** A 48 bp DNA fragment was used for the DNA-binding assays. Putative –35 and –10 regions (in blue boxes) of a sigma-70-type promoter (Feklistov et al., 2014) are indicated and predicted EnuR binding sites (Suvorova and Rodionov, 2016; Schulz et al., 2017a) are marked. **(B)** DNA binding activity of the *R. pomeroyi* DSS-3 purified EnuR protein containing PLP to the promoter region was assessed by microscale thermophoresis. The double-stranded 48 bp DNA regulatory fragment was titrated to a constant amount (200 nM) of purified and PLP containing EnuR protein. Error bars shows the standard deviation; the DNA binding experiment was repeated six times with independently purified and fluorescently labeled EnuR preparations. F-norm refers to the thermophoretic behavior of the tested protein in a ligand (= DNA) gradient.

α-ADABA and DABA have already been shown to serve as ligands for the *R. pomeroyi* DSS-3 EnuR protein (Schulz et al., 2017a). DABA has also been shown to serve such a role for the related protein from *S. meliloti*, although the aÿnity of the corresponding EnuR repressor for this ligand is unknown (Yu et al., 2017). We show here that hydroxy-α-ADABA interacts in a high aÿnity process with EnuR. EnuR bound hydroxy-α-ADABA with a K_d-value of 0.43 ± 0.2 µM, an about five-fold improved aÿnity compared with α-ADABA (K_d of 2.55 ± 0.5 µM) (**Figure 4**). On the other hand, the *R. pomeroyi* DSS-3 EnuR protein binds DABA with a K_d-value of about 460 µM (Schulz et al., 2017a). Hence, the aÿnitie s of EnuR for the primary, EutD-mediated hydrolysis products of ectoine and 5-hydroxyectoine, are about 180- and 1,000-fold higher than those for DABA.

The central ectoine/5-hydroxyectoine catabolic enzymes, the hydrolase EutD and the deacetylase EutE, operate as a bi-module in the sense that both enzymes have to be present to eÿciently degrade ectoines (**Supplementary Figure 3**), although a stable EutD/EutE protein complex has yet to be observed *in vitro* (Mais et al., 2020). This raises the question whether the two high-aÿnity inducers of EnuR, α-ADABA

and hydroxy-α-ADABA, are actually present in the cell and are not immediately deacetylated to produce the medium-aÿnity inducers DABA and hydroxy-DABA (**Figure 1B**). Through targeted metabolic analysis of cultures grown either in the presence of ectoine or 5-hydroxyectoine, we detected considerable amounts of α-ADABA and hydroxy-α-ADABA, respectively, in the cells (**Figure 7B**), so that these compounds will readily be able to interact with EnuR. Sizable amounts of the inducer DABA were also detected in cells grown in the presence of either ectoine or 5-hydroxyectoine, while hydroxy-DABA was found only in rather low concentrations and, as expected, only in cells grown on 5-hydroxyectoine (**Figure 7B**). The substantial amounts of DABA in the cytoplasm of cells of these latter cultures indicate that hydroxy-DABA is rapidly converted into DABA, a finding that needs to be taken into account for further studies on the enzymology of the ectoine/5-hydroxyectoine catabolic route (**Figure 1B**; Schwibbert et al., 2011; Hermann et al., 2020; Mais et al., 2020; Reshetnikov et al., 2020).

Our docking experiments with EnuR involving α-ADABA and hydroxy-α-ADABA as ligands (**Figures 6C,D,F**) do not capture the chemical interconversion of the internal to the external aldimine crucial for the change in the DNA-binding properties of MocR/GabR-type regulators (Edayathumangalam et al., 2013; Okuda et al., 2015b; Park et al., 2017; Wu et al., 2017; Tramonti et al., 2018). Despite this limitation, our *in silico* experiments should provide a solid structure-based view into the cofactor and inducer binding site of the EnuR repressor (**Figures 6C,D,F**). This conclusion is supported by the fact that our unconstrained docking experiments position the primary nitrogen group present in both inducers in close distance, 3 Å for hydroxy-α-ADABA and 2.6 Å for α-ADABA, to the PLP cofactor with whom they have to interact. These distances are well suited for a chemical reaction between the bound PLP and the inducers (**Figures 6C,D,F**). Most of the EnuR residues predicted by our modeling studies to interact with hydroxy-α-ADABA or α-ADABA are either completely or functionally conserved in the 278 EnuR-type proteins onto which our analysis relied (**Figure 5A**) (**Supplementary Figure 1** and **Supplementary Table 3**).

The isomer of α-ADABA, γ-ADABA, is enzymatically generated during ectoine biosynthesis and serves as the substrate for the ectoine synthase EctC (Czech et al., 2019). It does not serve as an inducer for EnuR (Schulz et al., 2017a). Consistent with previous ligand-binding experiments, we were unable to place γ-ADABA into the presumed inducer-binding site of EnuR in our docking experiments. Assuming that the core of the γ-ADABA molecule would localize in the same manner in the EnuR ligand-binding cavity as its isomer α-ADABA so that its primary amino group would be positioned toward the PLP cofactor, then the carboxyl moiety of γ-ADABA would be placed in close proximity to the side chain of Asn244 (**Figure 6D**). This would lead, in all likelihood, to a sterical clash, and binding of γ-ADABA should thereby be prevented, or at least strongly disfavored (**Figures 6D,F**). Collectively, these are physiologically important findings as the central intermediate in ectoine synthesis, γ-ADABA, can consequently not trigger ectoine catabolism in those microorganisms capable to both synthesize and degrade ectoines (Schwibbert et al., 2011; Czech et al., 2018; Hermann et al., 2020; Mais et al., 2020).

The detection of γ-ADABA in cells grown in the presence of ectoine (**Figure 7B**) comes as a true surprise as *R. pomeroyi* DSS-3 cannot synthesize ectoine (Moran et al., 2004; Schulz et al., 2017b). Previous *in vivo* and *in vitro* experiments of recombinant EutD and EutE enzymes prepared in *E. coli* indicated that γ-ADABA did not play any role in the catabolism of ectoines by *R. pomeroyi* DSS-3 (Mais et al., 2020). However, in *H. elongata*, a bacterium that can both degrade and synthesize ectoine, γ-ADABA was an intermediate in ectoine catabolism, potentially re-used for ectoine biosynthesis (Schwibbert et al., 2011). This is not possible in the marine bacterium *R. pomeroyi* DSS-3. Our detection of γ-ADABA raises the question if this ectoine biosynthetic precursor is a dead-end by-product of ectoine catabolism in *R. pomeroyi* DSS-3, or alternatively, which physiological function it might serve. Notable, no γ-ADABA was detected in cells of halotolerant methylotrophs metabolizing ectoine (Reshetnikov et al., 2020).

The data reported here for hydroxy-α-ADABA, and those that were previously provided for the binding of α-ADABA and DABA to EnuR (Schulz et al., 2017a,b; Yu et al., 2017), lend themselves to a straight-forward regulatory model for the encounter of microbial ectoine/5-hydroxyectoine consumers with environmental ectoines (Mosier et al., 2013; Warren, 2014; Bouskill et al., 2016). In the absence of ectoines, the *R. pomeroyi* DSS-3 importer and catabolic gene cluster is expressed at a very low level (Schulz et al., 2017a). Nevertheless, this basal level of transcription is suÿcient to allow import of trace amounts of ectoines via the high aÿnity TRAP-type UehABC uptake system from *R. pomeroyi* DSS-3 (Lecher et al., 2009). Subsequent to the initial import of ectoines, their catabolism will set in at a low level, thereby forming limited pools of the high-aÿnity EnuR inducers α-ADABA and hydroxy-α-ADABA, and the medium aÿnity inducers DABA (and potentially hydroxy-DABA as well). Their interactions with the covalently bound PLP cofactor will relieve EnuR-mediated repression of the transcriptional activity of the substrate-inducible promoter (**Figures 1A**, **8A**). Consequently, enhanced and subsequently sustained increased expression of the ectoine/5-hydroxyectoine importer and catabolic gene cluster will ensue, thereby promoting increased import and catabolism of ectoines. As the inducers α-ADABA, hydroxy-α-ADABA, DABA and hydroxy-DABA are early intermediates in the catabolism of ectoines (Schwibbert et al., 2011; Yu et al., 2017; Hermann et al., 2020; Mais et al., 2020; **Figure 1B**), they will inevitably disappear from the cell when the environmental supply of ectoines has been exhausted. EnuR will consequently resume its repressor function.

Depending on the procedure to assess the phylogenomic occurrence of ectoine/5-hydroxyectoine catabolic gene clusters (Schulz et al., 2017b; Hermann et al., 2020; Mais et al., 2020), the corresponding bacteria possess between 77 and 85% juxtapositioned *enuR*-type genes. Hence, the wide-spread existence of EnuR transcriptional regulators highlights the importance of the genetic regulatory circuit that we outlined above for the transcriptional control of ectoine/5-hydroxyectoine catabolism in bacteria. At the same time, these numbers sharply pose the question how microorganisms that lack EnuR

(**Figure 5B**) might induce and genetically control this complex metabolic pathway.

MATERIALS AND METHODS

Chemicals and Reagents

The antibiotics gentamycin, rifampicin, and kanamycin were obtained from Serva (Heidelberg, Germany); ampicillin was purchased from Carl Roth GmbH (Karlsruhe, Germany). Anhydrotetracycline hydrochloride, desthiobiotin, and Strep-Tactin Superflow chromatography material were obtained from IBA GmbH (Göttingen, Germany). Marker proteins for size exclusion chromatography experiments were purchased from Sigma-Aldrich (Taufkirchen, Germany). Restriction endonucleases and DNA ligase were obtained from ThermoScientific (St. Leon-Rot, Germany) and used as suggested by the manufacturer. Ectoine was a kind gift from the bitop AG (Witten, Germany) and 5-hydroxyectoine was purchased from Merck (Darmstadt, Germany). γ-ADABA was purchased from abcr GmbH (Karlsruhe, Germany).

Media and Growth Conditions

Ruegeria pomeroyi strains (**Supplementary Table 4**) were maintained on half-strength YTSS agar. For all growth experiments, the strains were cultivated in defined basal minimal medium (Baumann et al., 1971). Both media were prepared as described previously (Schulz et al., 2017b). When applicable, the antibiotics gentamycin and rifampicin, were added to liquid and solid media at a concentration of 20 $\mu g\ ml^{-1}$. When the use of ectoine or 5-hydroxyectoine as combined carbon and nitrogen sources by *R. pomeroyi* strains was tested on basal minimal medium agar plates, the plates were supplemented with 28 mM ectoine or 28 mM 5-hydroxyectoine as sole carbon, energy and nitrogen sources. Agar plates with streaked *R. pomeroyi* strains were typically incubated at 30°C for five days.

The IBA-Stargate plasmids containing either the *enuR* (pBAS3), the *enuR** (pBAS17), *enuR* wild-type C-terminal aminotransferase (ATD) domain (pLH17), or the *enuR** C-terminal aminotransferase domain (pLH17) genes, were routinely maintained in the *E. coli* K-12 DH5α (Invitrogen, Karlsruhe, Germany) on LB agar plates containing ampicillin (100 $\mu g\ mL^{-1}$). Minimal Medium A (MMA) (Miller, 1972) containing 0.5% (w/v) glucose as the carbon source, 0.5% (w/v) casamino acids (0.5%), 1 mM MgSO4, and 3 mM thiamine was used for cultivation of the *E. coli* B strain BL21 carrying plasmids pBAS3 (*enuR*$^+$), pBAS17 (*enuR**), pLH17 (*enuR*-ATD) or pLH26 (*enuR**-ATD) (**Supplementary Table 5**) for the overproduction of the EnuR protein and its mutant derivatives (Schulz et al., 2017a,b).

Chemical Synthesis, Purification of Ectoine Nutrient Utilization Regulator Inducers, and Metabolic Analysis

The cyclic ectoine and 5-hydroxyectoine molecules were linearized through alkaline hydrolysis as previously described (Kunte et al., 1993; Mais et al., 2020). Subsequently, the α- and γ-isomers of *N*-acetyl-L-2,4-diaminobutyric acid (α-ADABA and γ-ADABA) and hydroxy-α-ADABA were separated from other hydrolysis products of ectoine and 5-hydroxyectoine by repeated chromatography on a silica gel column (Merck silica gel 60) (Mais et al., 2020). The purity of the isolated α-ADABA and hydroxy-α-ADABA samples was at least 90% as determined by HPLC analysis. The identity and purity of these compounds was assessed by NMR spectroscopy as described by Mais et al. (2020), although we cannot exclude that minor impurities resulting from the alkaline hydrolysis of ectoines are still present in the preparations that we used for our experiments (Mais et al., 2020).

To identify metabolites derived from ectoines in *R. pomeroyi* DSS-3 cells growing in the presence if either ectoine or 5-hydroxyectoine, we carried out targeted metabolic analysis. In one set of experiments, we grew the cells in basal minimal medium with glucose (28 mM) as a carbon source and NH_4Cl (56 mM) as a nitrogen source in the absence of ectoines (control culture). In the second set of experiments, we grew the cells in an basal medium in the absence of glucose and NH_4Cl and provided either ectoine (56 mM) or 5-hydroxyectoine (56 mM) as sole and combined source of carbon, energy and nitrogen to the cells. In both sets of experiments, the cells were grown at 30°C in orbital shaker (20 ml culture volume in a 100 ml Erlenmeyer Flask) until the *R. pomeroyi* DSS-3 cultures reached an OD_{578} of about 1. The cells were pelleted by centrifugation, resuspended in basal medium and were then re-centrifuged. For the extraction of ectoine/5-hydroxyectoine-derived metabolites, one ml of 20% ethanol was added to the cells and they were vigorously shaken at room temperature for 30 min; cellular debris was then removed by centrifugation in table top Eppendorf centrifuge (13 000 rpm for 30 min at 4°C). The supernatant was evaporated at 50°C for at least 24 hours and the formed dry residue was re-suspended in 500 µl of double distilled water. After another centrifugation step, the supernatant was analyzed, and intracellular concentrations were estimated by assuming a volume of 0.5 µl of the cytoplasm of 1 ml *R. pomeroyi* DSS-3 cells at an OD_{578} of 1.

Separation and quantification of ectoine, 5-hydroxyectoine and its metabolites DABA, α-ADABA, γ-ADABA, hydroxy-DABA, hydroxy-α-ADABA and hydroxy-γ-ADABA in ethanolic cell extracts were conducted on a HPLC-ESI-MS system (Agilent 1,100 system with MSD1946D) using 100 mM NH_4HCO_3 in 90% H_20/10% acetonitrile as eluent. The separation column was a 250 × 2 mm i.d. Metrohm Carb 2 strong anion exchanger operated at 0.2 ml/min. The analytes were detected in selected ion modus as their positively charged H^+ adducts. Possible interference of aspartic acid on hydroxy-DABA were checked and discarded. Calibration was performed using commercially available γ-ADABA samples. For all measurements, four independently grown *R. pomeroyi* DSS-3 cultures were used and form each of them two ethanolic extracts were prepared.

Previously Constructed Bacterial Strains and Plasmids

The *R. pomeroyi* strain DSS-3 (Moran et al., 2004) was obtained from the German Collection of Microorganisms

(DSMZ; Braunschweig, Germany), and a rifampicin-resistant [Rif^R] derivative of this isolate (strain J470) (Todd et al., 2012) was kindly provided by J. Todd and A. Johnston (University of East Anglia, United Kingdom). *E. coli* K-12 DH5α carrying the helper plasmid pRK2013 [Kan^R] (Figurski and Helinski, 1979) for conjugation experiments between *E. coli* and *R. pomeroyi* were also provided by these colleagues. The construction of the *R. pomeroyi eutD* mutant (ASR8) and the complete operon deletion strain ASR6 [Δ(*enuR-atf*:Gm^R)] were described previously (Schulz et al., 2017a,b), as were plasmids pBAS3 (*enuR*$^+$; wild-type) and pBAS17 (*enuR**; Lys302His) (Schulz et al., 2017a). These plasmids are derivatives of the expression vector pASG-IBA3 (IBA GmbH, Göttingen, Germany) and express *enuR* genes under the control of the anhydrotetracycline hydrochloride (AHT) responsive TetR controlled *tet* promoter carried by pASG-IBA3 and its recombinant derivatives. Both the wild-type EnuR protein and its Lys302His mutant (EnuR*) carry a *Strep*-TAG-II peptide fused to their C-termini to allow aÿnity purification of the recombinant EnuR and EnuR* proteins from cell extracts of the *E. coli* B strain BL21 (DE3) (Schulz et al., 2017a,b).

Newly Constructed Bacterial Strains and Plasmids

To construct a deletion of the *R. pomeroyi* chromosomal *eutE* gene, 500 bp fragments located upstream and downstream of the respective genomic region (Moran et al., 2004) were amplified by PCR using custom synthesized primers (**Supplementary Table 6**). A DNA fragment encompassing a gentamycin resistance cassette (Gm^R) was amplified from plasmid p34S_Gm (Dennis and Zylstra, 1998). Using the Gibson assembly procedure (Gibson et al., 2009), the three DNA fragments were cloned into the linearized (with *Eco*RI) and dephosphorylated suicide vector pK18mobsacB (Kvitko and Collmer, 2011), which confers resistance to kanamycin. The resulting plasmid was pLH72 and carries the Δ(*eutE*:Gm^R)1 deletion mutation (**Supplementary Table 5**).

Plasmids for the overproduction of the aminotransferase domains of EnuR and its Lys302His mutant derivative EnuR* were constructed via the IBA-Stargate cloning procedure as described by the manufacturer (IBA GmbH, Göttingen, Germany). Custom designed primers (**Supplementary Table 6**) (Microsynth AG, Balgach, Switzerland) were used to amplify the 1,110 bp aminotransferase domains (ATD) for the *enuR* and *enuR** genes from the respective plasmids pBAS3 (*enuR*$^+$) and pBAS17 (*enuR**), and were then inserted into the expression plasmid pASG-IBA3 so that recombinant proteins with a *Strep*-TAG-II aÿnity peptide at their carboxy-termini were produced. The resulting plasmids were pLH17 (*enuR*-CTD) and pLH26 (*enuR**-CTD), respectively (**Supplementary Table 5**).

Chromosomal DNA of *R. pomeroyi* strain DSS-3 was isolated as described (Marmur, 1961). The High Pure Plasmid Isolation Kit (Roche, Mannheim, Germany) was used to isolate plasmid DNA from *E. coli* strains. Chemically competent *E. coli* cells were prepared and transformed with plasmid DNA as reported (Sambrook et al., 1989). All recombinant DNA methods were carried out via routine procedures (Sambrook et al., 1989).

Construction of a *Ruegeria pomeroyi* Chromosomal *eutE* Gene Disruption Mutant

Plasmid pLH73 [Δ(*eutE*:Gm^R)1] (**Supplementary Table 5**) was conjugated by tri-parental mating into *R. pomeroyi* by mixing the *E. coli* strain PRK2015 (pRK2013 [Kan^R]) (Figurski and Helinski, 1979), DH5α (pLH73) [Kan^R and Gm^R] and the Rif^R *R. pomeroyi* recipient strain J470. *R. pomeroyi* J470 transconjugants that had received plasmid pLH73 were selected on 1/2 YTSS agar plates containing the antibiotics rifampicin and gentamycin and 10% saccharose as described (Schulz et al., 2017b). The resulting colonies were tested for their antibiotic resistance profile and Kan^S Gm^R strains were then evaluated for the presence of the chromosomal Δ(*eutE*:Gm) deletion/insertion mutation via PCR using chromosomal DNA as the template and DNA primers listed in **Supplementary Table 6** that hybridize to genomic regions flanking the *eutE* gene. The resulting *R. pomeroyi* J470-derived strain was named LHR7 [Δ(*eutE*:Gm^R)1] (**Supplementary Table 4**).

Overproduction and Purification of Ectoine Nutrient Utilization Regulator and Its Mutant Derivatives

For overproduction of the EnuR-Strep-tag-II and EnuR*-Strep-tag-II recombinant proteins, cells of the *E. coli* B strain BL21 (DE3) were transformed with the appropriate overproduction plasmids pBAS3 (*enuR*$^+$) or pBAS17 (*enuR**) (**Supplementary Table 5**).These plasmids allow the expression of the *enuR*$^+$ and *enuR** genes under the control of the *tet* promoter, a system that is controlled by the anhydrotetracycline (AHT) responsive TetR repressor whose structural gene is present on the expression plasmids (Schulz et al., 2017b). The same type of overproduction system was used to produce either the ATD from the wild-type EnuR protein (plasmid pLH17), or of the ATD from the mutant EnuR* protein (plasmid pLH26) (**Supplementary Table 5**). The plasmid-containing *E. coli* cells were grown at 37°C in MMA containing 0.5% casamino acids until the cultures reached an OD_{578} of about 0.5. *tet*-promoter/TetR-mediated overexpression of the various plasmid-encoded genes was triggered by adding the inducer AHT (final concentration: 0.2 mg l^{-1}) to the cultures. The growth temperature of the cultures was then reduced to room temperature (about 25°C) and the cultures were subsequently incubated for additional two hours to allow overproduction of the recombinant proteins. Cells were harvested by centrifugation, resuspended in purification buffer (100 mM Tris-HCl (pH 7.5), 150 mM NaCl), lysed by passing them three to five-times through a French Pressure Cell (Aminco, Urbana, Il, United States) at 900 psi, and a cleared cell extract was obtained by centrifugation at 35,000 × *g* for 1 h at 4°C. The recombinant proteins marked with a *Strep*-TAG-II peptide were purified from the cleared cell extracts via aÿnity chromatography on a Strep-Tactin Superflow column as described (Schulz et al., 2017b). Strep-Tactin purified proteins were analyzed and further purified via Size-Exclusion-Chromatography (SEC) on a HiLoad 16/600 Superdex 200 pg column (GE Healthcare Europe, Freiburg, Germany), using either a buffer containing 10 mM Tris-HCl (pH 7.5) and 150 mM

NaCl when the proteins were subsequently used in ligand-binding assays. The purity of all isolated proteins was assessed by sodium-dodecylsulfate (SDS) polyacrylamide gel electrophoresis (12% acrylamide). Proteins were stained and visualized with Instant*Blue* (Expedion, Cambridgeshire, United Kingdom).

Examination of Pyridoxal-5′-Phosphate Binding to Ectoine Nutrient Utilization Regulator and Its ATD by Mass Spectrometry

Ectoine Nutrient Utilization Regulator and EnuR-ATD proteins were purified as described above. The buffer used for these preparations was 20 mM HEPES-Na pH 7.5, 115 mM NaCl, 1.2 mM $CaCl_2$, 1.2 mM $MgCl_2$, 2.4 mM K_2HPO_4. 25 μl (10 μM) of aÿnity purified full-length EnuR, or EnuR-ATD were treated with 10 mM $NaBH_4$ (1 μl of 250 mM stock prepared freshly in 0.1 M NaOH) and incubated at room temperature for 30 min to reduce the aldimine. The $NaBH_4$ reduction was quenched by acidification of the solution to pH of 5-6 with HCl and neutralized to approximately pH 7 with NaOH (Hoegl et al., 2018). These samples were immediately supplemented with 6 μl of SDS loading dye (300 mM Tris-Cl pH 6.8, 10% (w/v) SDS, 25% (v/v) β-mercaptoethanol, 25% (v/v) glycerol, 0.05% (w/v) bromo phenol blue) followed by mixing and heat treatment at 95°C for 5 min. Samples were loaded and separated on 15% polyacrylamide SDS-PAGE gels at 200 V. Gels were stained with Coomassie brilliant blue R250 [0.36% (w/v) Coomassie R250 dissolved in 46% (v/v) ethanol supplemented with 9% (v/v) glacial acetic acid] and destained with 30% (v/v) ethanol supplemented with 10% (v/v) glacial acetic acid. After destaining the protein bands corresponding to full-length EnuR, or EnuR-ATD were excised out of the gel and digested in gel by the addition of Sequencing Grade Modified Trypsin (Serva) at 37°C for 45 min, after which the supernatant was removed and further incubated at 37°C overnight. Peptides were desalted and concentrated using Chromabond C18WP spin columns (Macherey-Nagel). Finally, Peptides were dissolved in 5% (v/v) acetonitrile supplemented with 0.1% (v/v) formic acid.

Mass spectrometric analysis of the tryptic digests was performed using a timsTOF Pro mass spectrometer (Bruker Daltonic). A nanoElute HPLC system (Bruker Daltonics), equipped with an Aurora column (25 cm × 75 μm) C18 RP column filled with 1.7 μm beads (IonOpticks), was connected online to the mass spectrometer. Sample loading was performed at a constant pressure of 800 bar, and 2 μl of a 1:3 dilution of the tryptic digests in double-distilled water injected directly on the separation column. Separation was conducted at 50°C column temperature with the following gradient of water + 0.1% (v/v) formic acid (solvent A) and acetonitrile + 0.1%(v/v) formic acid (solvent B) at a flow rate of 400 nl/min: A linear increase from 2% solvent B to 17% solvent B within 60 min was followed by a linear gradient to 25% solvent B within 30 min and a linear increase to 37% solvent B in additional 10 min. Finally, solvent B was increased to 95% within 10 min and held for additional 10 min. The built-in "DDA PASEF-standard_1.1sec_cycletime" method developed by Bruker Daltonics was used for mass spectrometric measurement. Data analysis was performed using Proteome Discoverer 2.4 (ThermoScientific) with SEQUEST search engine and Byonic version 3.7.4 (Protein Metrics) using the amino acid sequences of full-length EnuR, trypsin, and keratin, as database.

Ligand-Binding Assays With Ectoine Nutrient Utilization Regulator and Its ATD

Ligand binding assays with the purified EnuR and EnuR-ATD proteins were carried out by microscale thermophoresis (MST) (Wienken et al., 2010). All experiments were performed on a Monolith NT.115 (NanoTemper Technologies GmbH, Munich, Germany) at 21°C (red LED power was set to 80% and infrared laser power to 70%). The buffer of the purified EnuR and EnuR-ATD [in 10mM Tris- HCl (pH 7.5), 150 mM NaCl] was first exchanged with the labeling buffer of the Monolith NTTM Protein Labeling Kit RED (NanoTemper) to avoid interference of the labeling reactions with free amines in the buffer solution. Subsequent to the labeling of either EnuR, or EnuR-ATD (20 μM each) with the NT 647 dye (according to the supplier's reaction scheme), the proteins were re-buffered into a solution buffer containing 10 mM Tris-HCl (pH 7.5), 150 mM NaCl and 0.07% Tween20. EnuR (200 nM) was titrated with α-ADABA and hydroxy-α-ADABA (starting from a ligand concentration of 1 mM). Likewise, the EnuR-ATD protein was also titrated with α-ADABA (starting from a ligand concentration of 1 mM). To determine the DNA-binding properties of EnuR, the protein was treated in the same manner and titrated with buffer containing a DNA-fragment (48 bp) harboring the presumed EnuR operator site(s) and the promoter region of the *R. pomeroyi* DSS-3 ectoine/5-hydroxyectoine importer and catabolic gene cluster (**Supplementary Table 6** and **Figure 8A**). At least six independent MST experiments per ligand of the EnuR protein were recorded at 680 nm and analyzed using NanoTemper Analysis 1.2.009 and Origin8G software suits.

Bioinformatic Analysis

To analyze the phylogenomic distribution of *enuR*-type genes, a recently compiled and manually curated dataset of 363 bacterial ectoine/5-hydroxyectoine catabolic gene clusters was used as a starting point (Mais et al., 2020). In this dataset, only microorganisms harboring *eutD/eutE*-genes in direct genetic neighborhood were included, as both proteins are needed to degrade ectoines (Mais et al., 2020). Accordingly, this analysis does not include ectoine/5-hydroxyectoine degradation gene clusters in which the *eutD* and *eutE* catabolic genes are not juxtapositioned [e.g., from *M. alcaliphilum* (Reshetnikov et al., 2020)]. The 363 EutD-protein sequences represented in the dataset reported by Mais et al. (2020) was retrieved from the IMG/M database (Chen et al., 2021) and represented in a tree-format visualized using the iTOL software (Letunic and Bork, 2019). Onto this EutD-protein based tree, we projected the presence of *enuR*-type genes (278 representatives) that were positioned in the immediate vicinity of ectoine/5-hydroxyectoine degradation gene clusters. Alignments of EnuR-type proteins that were obtained through IMG/JGI Web resources, were visualized with Jalview (Waterhouse et al., 2009).

A model of the presumed EnuR structure was created using the crystal structure of the *B. subtilis* GabR protein as the template (Edayathumangalam et al., 2013) and by employing the Phyre[2] software (Kelley et al., 2015) set in the extensive mode (see Text Footnote 1). An overlay of the GabR protein and the EnuR model revealed a root mean square deviation (RMSD) of 0.86 Å (over 390 amino acids). *In silico* modelling and docking experiments for EnuR and its various ligands were carried out using Chimera (Pettersen et al., 2004) and AutoDock Vina (Trott and Olson, 2010). The definition files for the ligands α-ADABA, hydroxy-α-ADABA, γ-ADABA and DABA were created using the Schrödinger Meastro package (Release, 2017). Initial docking was performed using a wide grid setting and by allowing the positioning of the ligand all around the EnuR protein. The best solution was further optimized by multiple cycles of AutoDock Vina (Trott and Olson, 2010). Final assessment was performed by manual inspection of the interactions of each ligand within the predicted EnuR ligand binding site.

DATA AVAILABILITY STATEMENT

The original contributions presented in the study are included in the article/**Supplementary Material**, further inquiries can be directed to the corresponding author/s.

AUTHOR CONTRIBUTIONS

EB designed and supervised the study. LH planned and performed most of the experiments. LH and S-AF jointly conducted the microscale thermophoresis studies. FD performed growth experiments and extraction of metabolites. SHJS performed the *in silico* modelling and docking experiments. WS conducted the mass spectrometic analysis of EnuR proteins. AS synthesized and purified α-ADABA and hydroxy-α-ADABA and performed analysis of ectoine/5-hydroxyectoine metabolites. EB and LH wrote the manuscript with input from the other authors. All authors contributed to the article and approved the submitted version.

FUNDING

Financial support for this study was provided to EB by the German Research foundation (Deutsche Forschungsgemeinschaft; DFG) in the framework of the Collaborative Research Center SFB 987. The Center of Structural studies at the University of Düsseldorf is funded by the Deutsche Forschungsgemeinschaft as well (grant no. 417919780). The funding agencies had no role in study design, in the collection, analysis and interpretation of data, the writing of the manuscript, and in the decision to submit the article for publication.

ACKNOWLEDGMENTS

We thank Jochen Sohn for expert technical assistance during protein purification and greatly appreciate the kind help of Vickie Koogle in the language editing of our manuscript. LH thanks Tobias Erb (MPI for Terrestrial Microbiology Marburg) for financial support. We thank our colleagues Roland Lill (Department of Medicine, Philipps-University Marburg) and Gert Bange (SYNMIKRO, Philipps-University Marburg) for their interest and support of this project. We gratefully acknowledge access to the core facility *Protein Spectroscopy and Protein Biochemistry* of the Medical School of the Philipps-University Marburg for our studies. We also thank Tina Krieg and Uwe Linne from the core facility for mass spectrometry at the Department of Chemistry of the Philipps-University Marburg for their advice and assistance. We are indebted to Tamara Hoffmann for her kind help in preparing some of the figures. We greatly appreciate the kind gift of bacterial strains and plasmids by J. Todd and A. Johnston (University of East Anglia, United Kingdom).

SUPPLEMENTARY MATERIAL

The Supplementary Material for this article can be found online at: https://www.frontiersin.org/articles/10.3389/fmicb.2021.764731/full#supplementary-material

REFERENCES

Baumann, P., Baumann, L., and Mandel, M. (1971). Taxonomy of marine bacteria: the genus *Beneckea*. *J. Bacteriol.* 107, 268–294. doi: 10.1128/jb.107.1.268-294.1971

Belitsky, B. R. (2004). *Bacillus subtilis* GabR, a protein with DNA-binding and aminotransferase domains, is a PLP-dependent transcriptional regulator. *J. Mol. Biol.* 340, 655–664. doi: 10.1016/j.jmb.2004.05.020

Belitsky, B. R. (2014). Role of PdxR in the activation of vitamin B6 biosynthesis in *Listeria monocytogenes*. *Mol. Microbiol.* 92, 1113–1128. doi: 10.1111/mmi.12618

Belitsky, B. R., and Sonenshein, A. L. (2002). GabR, a member of a novel protein family, regulates the utilization of gamma-aminobutyrate in *Bacillus subtilis*. *Mol. Microbiol.* 45, 569–583. doi: 10.1046/j.1365-2958.2002.03036.x

Berezin, C., Glaser, F., Rosenberg, J., Paz, I., Pupko, T., Fariselli, P., et al. (2004). ConSeq: the identification of functionally and structurally important residues in protein sequences. *Bioinformatics* 20, 1322–1324. doi: 10.1093/bioinformatics/bth070

Bervoets, I., and Charlier, D. (2019). Diversity, versatility and complexity of bacterial gene regulation mechanisms: opportunities and drawbacks for applications in synthetic biology. *FEMS Microbiol. Rev.* 43, 304–339. doi: 10.1093/femsre/fuz001

Bouskill, N. J., Wood, T. E., Baran, R., Ye, Z., Bowen, B. P., Lim, H., et al. (2016). Belowground response to drought in a tropical forest soil. I. changes in microbial functional potential and metabolism. *Front. Microbiol.* 7:525. doi: 10.3389/fmicb.2016.00525

Bradshaw, R. A., Brickey, W. W., and Walker, K. W. (1998). N-terminal processing: the methionine aminopeptidase and N alpha-acetyl transferase families. *Trends Biochem. Sci.* 23, 263–267.

Bramucci, E., Milano, T., and Pascarella, S. (2011). Genomic distribution and heterogeneity of MocR-like transcriptional factors containing a domain belonging to the superfamily of the pyridoxal-5′-phosphate dependent enzymes of fold type I. *Biochem. Biophys. Res. Commun.* 415, 88–93. doi: 10.1016/j.bbrc.2011.10.017

Chen, I. A., Chu, K., Palaniappan, K., Ratner, A., Huang, J., Huntemann, M., et al. (2021). The IMG/M data management and analysis system v.6.0: new tools

and advanced capabilities. *Nucleic Acids Res.* 49, D751–D763. doi: 10.1093/nar/gkaa939

Czech, L., Hermann, L., Stöveken, N., Richter, A. A., Höppner, A., Smits, S. H. J., et al. (2018). Role of the extremolytes ectoine and hydroxyectoine as stress protectants and nutrients: genetics, phylogenomics, biochemistry, and structural analysis. *Genes* 9:177. doi: 10.3390/genes9040177

Czech, L., Höppner, A., Kobus, S., Seubert, A., Riclea, R., Dickschat, J. S., et al. (2019). Illuminating the catalytic core of ectoine synthase through structural and biochemical analysis. *Sci. Rep.* 9:364. doi: 10.1038/s41598-018-36247-w

da Costa, M. S., Santos, H., and Galinski, E. A. (1998). An overview of the role and diversity of compatible solutes in Bacteria and Archaea. *Adv. Biochem. Eng. Biotechnol.* 61, 117–153. doi: 10.1007/BFb0102291

Delano, W. L. (2002). *The PyMol Molecular Graphics System*. San Carlos, CA: Delano Scientific.

Dennis, J. J., and Zylstra, G. J. (1998). Improved antibiotic-resistance cassettes through restriction site elimination using Pfu DNA polymerase PCR. *Biotechniques* 25, 772–774, 776. doi: 10.2144/98255bm04

Edayathumangalam, R., Wu, R., Garcia, R., Wang, Y., Wang, W., Kreinbring, C. A., et al. (2013). Crystal structure of *Bacillus subtilis* GabR, an autorepressor and transcriptional activator of *gabT*. *Proc. Natl. Acad. Sci. U.S.A.* 110, 17820–17825. doi: 10.1073/pnas.1315887110

Feklistov, A., Sharon, B. D., Darst, S. A., and Gross, C. A. (2014). Bacterial sigma factors: a historical, structural, and genomic perspective. *Annu. Rev. Microbiol.* 68, 357–376. doi: 10.1146/annurev-micro-092412-155737

Figurski, D. H., and Helinski, D. R. (1979). Replication of an origin-containing derivative of plasmid RK2 dependent on a plasmid function provided in trans. *Proc. Natl. Acad. Sci. U.S.A.* 76, 1648–1652. doi: 10.1073/pnas.76.4.1648

Frezzini, M., Narzi, D., Sciolari, A. M., Guidoni, L., and Pascarella, S. (2020). Molecular dynamics of an asymmetric form of GabR, a bacterial transcriptional regulator. *Biophys. Chem.* 262:106380. doi: 10.1016/j.bpc.2020.106380

Galinski, E. A., and Herzog, R. M. (1990). The role of trehalose as a substitute for nitrogen-containing compatible solutes (*Ectothiorhodospira halochloris*). *Arch. Microbiol.* 153, 607–613. doi: 10.1007/bf00245273

Galinski, E. A., Pfeiffer, H. P., and Trüper, H. G. (1985). 1,4,5,6-Tetrahydro-2-methyl-4-pyrimidinecarboxylic acid. A novel cyclic amino acid from halophilic phototrophic bacteria of the genus *Ectothiorhodospira*. *Eur. J. Biochem.* 149, 135–139. doi: 10.1111/j.1432-1033.1985.tb08903.x

Gibson, D. G., Young, L., Chuang, R. Y., Venter, J. C., Hutchison, C. A. III, and Smith, H. O. (2009). Enzymatic assembly of DNA molecules up to several hundred kilobases. *Nat. Methods* 6, 343–345. doi: 10.1038/nmeth.1318

Grammann, K., Volke, A., and Kunte, H. J. (2002). New type of osmoregulated solute transporter identified in halophilic members of the bacteria domain: TRAP transporter TeaABC mediates uptake of ectoine and hydroxyectoine in *Halomonas elongata* DSM 2581(T). *J. Bacteriol.* 184, 3078–3085. doi: 10.1128/JB.184.11.3078-3085.2002

Hanekop, N., Höing, M., Sohn-Bösser, L., Jebbar, M., Schmitt, L., and Bremer, E. (2007). Crystal structure of the ligand-binding protein EhuB from *Sinorhizobium meliloti* reveals substrate recognition of the compatible solutes ectoine and hydroxyectoine. *J. Mol. Biol.* 374, 1237–1250. doi: 10.1016/j.jmb.2007.09.071

Hermann, L., Mais, C. N., Czech, L., Smits, S. H. J., Bange, G., and Bremer, E. (2020). The ups and downs of ectoine: structural enzymology of a major microbial stress protectant and versatile nutrient. *Biol. Chem.* 401, 1443–1468. doi: 10.1515/hsz-2020-0223

Hoegl, A., Nodwell, M. B., Kirsch, V. C., Bach, N. C., Pfanzelt, M., Stahl, M., et al. (2018). Mining the cellular inventory of pyridoxal phosphate-dependent enzymes with functionalized cofactor mimics. *Nat. Chem.* 10, 1234–1245. doi: 10.1038/s41557-018-0144-2

Imhoff, J. F., Rahn, T., Kunzel, S., Keller, A., and Neulinger, S. C. (2020). Osmotic adaptation and compatible solute biosynthesis of phototrophic bacteria as revealed from genome analyses. *Microorganisms* 9:46. doi: 10.3390/microorganisms9010046

Inbar, L., and Lapidot, A. (1988). The structure and biosynthesis of new tetrahydropyrimidine derivatives in actinomycin D producer Streptomyces parvulus. Use of 13C- and 15N-labeled L-glutamate and 13C and 15N NMR spectroscopy. *J. Biol. Chem.* 263, 16014–16022. doi: 10.1016/s0021-9258(18)37550-1

Jain, D. (2015). Allosteric control of transcription in GntR family of transcription regulators: a structural overview. *IUBMB Life* 67, 556–563. doi: 10.1002/iub.1401

Jebbar, M., Sohn-Bösser, L., Bremer, E., Bernard, T., and Blanco, C. (2005). Ectoine-induced proteins in *Sinorhizobium meliloti* include an ectoine ABC-type transporter involved in osmoprotection and ectoine catabolism. *J. Bacteriol.* 187, 1293–1304. doi: 10.1128/JB.187.4.1293-1304.2005

Kelley, L. A., Mezulis, S., Yates, C. M., Wass, M. N., and Sternberg, M. J. (2015). The Phyre2 web portal for protein modeling, prediction and analysis. *Nat. Protoc.* 10, 845–858. doi: 10.1038/nprot.2015.053

Kuhlmann, A. U., Hoffmann, T., Bursy, J., Jebbar, M., and Bremer, E. (2011). Ectoine and hydroxyectoine as protectants against osmotic and cold stress: uptake through the SigB-controlled betaine-choline- carnitine transporter-type carrier EctT from *Virgibacillus pantothenticus*. *J. Bacteriol.* 193, 4699–4708. doi: 10.1128/JB.05270-11

Kuhlmann, S. I., Terwisscha Van Scheltinga, A. C., Bienert, R., Kunte, H. J., and Ziegler, C. (2008). 1.55 A structure of the ectoine binding protein TeaA of the osmoregulated TRAP-transporter TeaABC from *Halomonas elongata*. *Biochemistry* 47, 9475–9485. doi: 10.1021/bi8006719

Kunte, H. J., Galinski, E. A., and Trüper, G. H. (1993). A modified FMOC-method for the detection of amino acid-type osmolytes and tetrahydropyrimidines (ectoines). *J. Microbiol. Methods* 17, 129–136. doi: 10.1016/0167-7012(93)90006-4

Kunte, H. J., Schwarz, T., and Galinski, E. A. (2020). "The compatible solute ectoine: protection mechanisms, strain developmnet, and industrial production," in *Biotechnological Applications of Extremophilic Microorganisms*, ed. N. Lee (Berlin: De Gruyter), 121–152.

Kvitko, B. H., and Collmer, A. (2011). Construction of *Pseudomonas syringae* pv. *tomato* DC3000 mutant and polymutant strains. *Methods Mol. Biol.* 712, 109–128. doi: 10.1007/978-1-61737-998-7_10

Landa, M., Burns, A. S., Roth, S. J., and Moran, M. A. (2017). Bacterial transcriptome remodeling during sequential co-culture with a marine dinoflagellate and diatom. *ISME J.* 11, 2677–2690. doi: 10.1038/ismej.2017.117

Lecher, J., Pittelkow, M., Zobel, S., Bursy, J., Bönig, T., Smits, S. H., et al. (2009). The crystal structure of UehA in complex with ectoine - A comparison with other TRAP-T binding proteins. *J. Mol. Biol.* 389, 58–73. doi: 10.1016/j.jmb.2009.03.077

Letunic, I., and Bork, P. (2019). Interactive Tree Of Life (iTOL) v4: recent updates and new developments. *Nucleic Acids Res.* 47, W256–W259. doi: 10.1093/nar/gkz239

Mais, C.-N., Hermann, L., Altegoer, F., Seubert, A., Richter, A. A., Wernersbach, I., et al. (2020). Degradation of the microbial stress protectants and chemical chaperones ectoine and hydroxyectoine by a bacterial hydrolase-deacetylase complex. *J. Biol. Chem.* 295, 9087–9104. doi: 10.1074/jbc.RA120.012722

Marmur, J. (1961). Procedure for isolation of dioxyribonucleic acid from micrroganism. *J. Mol. Biol.* 3, 208–218.

Miller, J. H. (1972). *Experiments in Molecular Genetics*. Cold Spring Harbor New York, NY: Cold Spring Harbor Laboratory.

Moran, M. A., Buchan, A., Gonzalez, J. M., Heidelberg, J. F., Whitman, W. B., Kiene, R. P., et al. (2004). Genome sequence of *Silicibacter pomeroyi* reveals adaptations to the marine environment. *Nature* 432, 910–913. doi: 10.1038/nature03170

Mosier, A. C., Justice, N. B., Bowen, B. P., Baran, R., Thomas, B. C., Northen, T. R., et al. (2013). Metabolites associated with adaptation of microorganisms to an acidophilic, metal-rich environment identified by stable-isotope-enabled metabolomics. *mBio* 4:e00484-12. doi: 10.1128/mBio.00484-12

Nardella, C., Barile, A., Di Salvo, M. L., Milano, T., Pascarella, S., Tramonti, A., et al. (2020). Interaction of *Bacillus subtilis* GabR with the *gabTD* promoter: role of repeated sequences and effect of GABA in transcriptional activation. *FEBS J.* 287, 4952–4970. doi: 10.1111/febs.15286

Nowinski, B., and Moran, M. A. (2021). Niche dimensions of a marine bacterium are identified using invasion studies in coastal seawater. *Nat. Microbiol.* 6, 524–532. doi: 10.1038/s41564-020-00851-2

Okuda, K., Kato, S., Ito, T., Shiraki, S., Kawase, Y., Goto, M., et al. (2015b). Role of the aminotransferase domain in *Bacillus subtilis* GabR, a pyridoxal 5′-phosphate-dependent transcriptional regulator. *Mol. Microbiol.* 95, 245–257. doi: 10.1111/mmi.12861

Okuda, K., Ito, T., Goto, M., Takenaka, T., Hemmi, H., and Yoshimura, T. (2015a). Domain characterization of *Bacillus subtilis* GabR, a pyridoxal 5′-phosphate-dependent transcriptional regulator. *J. Biochem.* 158, 225–234. doi: 10.1093/jb/mvv040

Ono, H., Sawada, K., Khunajakr, N., Tao, T., Yamamoto, M., Hiramoto, M., et al. (1999). Characterization of biosynthetic enzymes for ectoine as a compatible solute in a moderately halophilic eubacterium, *Halomonas elongata*. *J. Bacteriol.* 181, 91–99. doi: 10.1128/JB.181.1.91-99.1999

Onraedt, A., De Muynck, C., Walcarius, B., Soetaert, W., and Vandamme, E. (2004). Ectoine accumulation in *Brevibacterium epidermis*. *Biotechnol. Lett.* 26, 1481–1485. doi: 10.1023/b:bile.0000044448.86907.e4

Park, S. A., Park, Y. S., and Lee, K. S. (2017). Crystal structure of the C-terminal domain of *Bacillus subtilis* GabR reveals a closed conformation by gamma-aminobutyric acid binding, inducing transcriptional activation. *Biochem. Biophys. Res. Commun.* 487, 287–291. doi: 10.1016/j.bbrc.2017.04.052

Pascarella, S. (2019). Computational classification of MocR transcriptional regulators into subgroups as a support for experimental and functional characterization. *Bioinformation* 15, 151–159. doi: 10.6026/97320630015151

Pastor, J. M., Salvador, M., Argandona, M., Bernal, V., Reina-Bueno, M., Csonka, L. N., et al. (2010). Ectoines in cell stress protection: uses and biotechnological production. *Biotechnol. Adv.* 28, 782–801. doi: 10.1016/j.biotechadv.2010.06.005

Percudani, R., and Peracchi, A. (2003). A genomic overview of pyridoxal-phosphate-dependent enzymes. *EMBO Rep.* 4, 850–854. doi: 10.1038/sj.embor.embor914

Peters, P., Galinski, E. A., and Trüper, H. G. (1990). The biosyntheis of ectoine. *FEMS Microbiol. Lett.* 71, 157–162.

Pettersen, E. F., Goddard, T. D., Huang, C. C., Couch, G. S., Greenblatt, D. M., Meng, E. C., et al. (2004). UCSF Chimera—a visualization system for exploratory research and analysis. *J. Comput. Chem.* 25, 1605–1612. doi: 10.1002/jcc.20084

Release, S. (2017). *1: Maestro*. New York, NY: Schrödinger, LLC.

Reshetnikov, A. S., Rozova, O. N., Trotsenko, Y. A., But, S. Y., Khmelenina, V. N., and Mustakhimov, I. I. (2020). Ectoine degradation pathway in halotolerant methylotrophs. *PLoS One* 15:e0232244. doi: 10.1371/journal.pone.0232244

Richts, B., Rosenberg, J., and Commichau, F. M. (2019). A survey of pyridoxal 5′-phosphate-dependent proteins in the Gram-positive model bacterium *Bacillus subtilis*. *Front. Mol. Biosci.* 6:32. doi: 10.3389/fmolb.2019.00032

Rigali, S., Derouaux, A., Giannotta, F., and Dusart, J. (2002). Subdivision of the helix-turn-helix GntR family of bacterial regulators in the FadR, HutC, MocR, and YtrA subfamilies. *J. Biol. Chem.* 277, 12507–12515. doi: 10.1074/jbc.M110968200

Rossbach, S., Kulpa, D. A., Rossbach, U., and De Bruijn, F. J. (1994). Molecular and genetic characterization of the rhizopine catabolism (*mocABRC*) genes of *Rhizobium meliloti* L5-30. *Mol. Gen. Genet.* 245, 11–24.

Sambrook, J., Fritsch, E. F., and Maniatis, T. E. (1989). *Molecular Cloning. A Laboratory Manual*. Cold Spring Harbor, NY: Cold Spring Harbor Laboratory.

Schulz, A., Hermann, L., Freibert, S.-A., Bönig, T., Hoffmann, T., Riclea, R., et al. (2017a). Transcriptional regulation of ectoine catabolism in response to multiple metabolic and environmental cues. *Environ. Microbiol.* 19, 4599–4619. doi: 10.1111/1462-2920.13924

Schulz, A., Stöveken, N., Binzen, I. M., Hoffmann, T., Heider, J., and Bremer, E. (2017b). Feeding on compatible solutes: a substrate-induced pathway for uptake and catabolism of ectoines and its genetic control by EnuR. *Environ. Microbiol.* 19, 926–946. doi: 10.1111/1462-2920.13414

Schweikhard, E. S., Kuhlmann, S. I., Kunte, H. J., Grammann, K., and Ziegler, C. M. (2010). Structure and function of the universal stress protein TeaD and its role in regulating the ectoine transporter TeaABC of *Halomonas elongata* DSM 2581T. *Biochemistry* 49, 2194–2204. doi: 10.1021/bi9017522

Schwibbert, K., Marin-Sanguino, A., Bagyan, I., Heidrich, G., Lentzen, G., Seitz, H., et al. (2011). A blueprint of ectoine metabolism from the genome of the industrial producer *Halomonas elongata* DSM 2581T. *Environ. Microbiol.* 13, 1973–1994. doi: 10.1111/j.1462-2920.2010.02336.x

Simon, M., Scheuner, C., Meier-Kolthoff, J. P., Brinkhoff, T., Wagner-Döbler, I., Ulbrich, M., et al. (2017). Phylogenomics of Rhodobacteraceae reveals evolutionary adaptation to marine and non-marine habitats. *ISME J.* 11, 1483–1499. doi: 10.1038/ismej.2016.198

Suvorova, I., and Rodionov, D. (2016). Comparative genomics of pyridoxal 5′-phosphate-dependent transcription factor regulons in *Bacteria*. *Microb. Genom.* 2:e000047. doi: 10.1099/mgen.0.000047

Todd, J. D., Kirkwood, M., Newton-Payne, S., and Johnston, A. W. (2012). DddW, a third DMSP lyase in a model *Roseobacter* marine bacterium, *Ruegeria pomeroyi* DSS-3. *ISME J.* 6, 223–226. doi: 10.1038/ismej.2011.79

Tramonti, A., Nardella, C., Di Salvo, M. L., Pascarella, S., and Contestabile, R. (2018). The MocR-like transcription factors: pyridoxal 5′-phosphate-dependent regulators of bacterial metabolism. *FEBS J.* 285, 3925–3944. doi: 10.1111/febs.14599

Trott, O., and Olson, A. J. (2010). AutoDock Vina: improving the speed and accuracy of docking with a new scoring function, eÿcient optimization, and multithreading. *J. Comput. Chem.* 31, 455–461. doi: 10.1002/jcc.21334

Vargas, C., Jebbar, M., Carrasco, R., Blanco, C., Calderon, M. I., Iglesias-Guerra, F., et al. (2006). Ectoines as compatible solutes and carbon and energy sources for the halophilic bacterium *Chromohalobacter salexigens*. *J. Appl. Microbiol.* 100, 98–107. doi: 10.1111/j.1365-2672.2005.02757.x

Vigouroux, A., Meyer, T., Naretto, A., Legrand, P., Aumont-Nicaise, M., Di Cicco, A., et al. (2021). Characterization of the first tetrameric transcription factor of the GntR superfamily with allosteric regulation from the bacterial pathogen *Agrobacterium fabrum*. *Nucleic Acids Res.* 49, 529–546. doi: 10.1093/nar/gkaa1181

Warren, C. R. (2014). Response of osmolytes in soil to drying and rewetting. *Soil Biol. Biochem.* 70, 22–32. doi: 10.1016/j.soilbio.2013.12.008

Waterhouse, A. M., Procter, J. B., Martin, D. M., Clamp, M., and Barton, G. J. (2009). Jalview Version 2–a multiple sequence alignment editor and analysis workbench. *Bioinformatics* 25, 1189–1191. doi: 10.1093/bioinformatics/btp033

Wienken, C. J., Baaske, P., Rothbauer, U., Braun, D., and Duhr, S. (2010). Protein-binding assays in biological liquids using microscale thermophoresis. *Nat. Commun.* 1:100. doi: 10.1038/ncomms1093

Wilce, M. C., Bond, C. S., Dixon, N. E., Freeman, H. C., Guss, J. M., Lilley, P. E., et al. (1998). Structure and mechanism of a proline-specific aminopeptidase from *Escherichia coli*. *Proc. Natl. Acad. Sci. U.S.A.* 95, 3472–3477. doi: 10.1073/pnas.95.7.3472

Wu, R., Sanishvili, R., Belitsky, B. R., Juncosa, J. I., Le, H. V., Lehrer, H. J., et al. (2017). PLP and GABA trigger GabR-mediated transcription regulation in *Bacillus subtilis* via external aldimine formation. *Proc. Natl. Acad. Sci. U.S.A.* 114, 3891–3896. doi: 10.1073/pnas.1703019114

Yokoyama, K., Ishijima, S. A., Clowney, L., Koike, H., Aramaki, H., Tanaka, C., et al. (2006). Feast/famine regulatory proteins (FFRPs): *Escherichia coli* Lrp, AsnC and related archaeal transcription factors. *FEMS Microbiol. Rev.* 30, 89–108. doi: 10.1111/j.1574-6976.2005.00005.x

Yu, Q., Cai, H., Zhang, Y., He, Y., Chen, L., Merritt, J., et al. (2017). Negative regulation of ectoine uptake and catabolism in *Sinorhizobium meliloti*: characterization of the EhuR gene. *J. Bacteriol.* 199:e00119-16. doi: 10.1128/JB.00119-16

Conflict of Interest: The authors declare that the research was conducted in the absence of any commercial or financial relationships that could be construed as a potential conflict of interest.

The MocR/GabR ectoine and hydroxyectoine catabolism regulator EnuR: Inducer and DNA binding

Lucas Hermann[1,2], Felix Dempwolff[3], Wieland Steinchen[3], Sven-Andreas Freibert[4], Sander H.J. Smits[5,6], Andreas Seubert[7], Erhard Bremer[1,3]

[1]Philipps-University Marburg, Faculty of Biology, Karl-von-Frisch Strasse 8, 35043, Marburg, Germany.
[2]Max-Planck-Institute for Terrestrial Microbiology, Department of Biochemistry and Synthetic Metabolism, Karl-von-Frisch Strasse 10, 35043, Marburg, Germany
[3]Philipps-University Marburg, SYNMIKRO Research Center, Karl-von-Frisch Strasse 14, 35043, Marburg, Germany.
[4]Philipps-University Marburg, Department of Medicine, Institute for Cytobiology and Cytopathology, and SYNMIKRO Research Center, Karl-von-Frisch Strasse 14, 35043, Marburg, Marburg, Germany.
[5]Heinrich-Heine-University, Institute of Biochemistry, Universitäts Strasse 1, 40225 Düsseldorf, Germany
[6]Heinrich-Heine-University Düsseldorf, Center for Structural Studies (CSS), Faculty of Biochemistry, Universitäts Strasse 1, 40225, Düsseldorf, Germany.
[7]Philipps-University Marburg, Faculty of Chemistry, Hans-Meerwein Strasse 4, 35043, Marburg, Germany.

Running title: Genetic control of ectoine/hydroxyectoine utilization

ORCID

Lucas Hermann: https://orcid-org/0000-0001-6684-1644
Felix Dempwolff: https://orcid-org/0000-0002-7788-8445
Wieland Steinchen: https://orcid-org/0000-0003-2990-3660
Sven-Andreas Freibert: https://orcid-org/0000-0002-8521-2963
Sander H.J. Smits: https://orcid-org/0000-0003-0780-9251
Andreas Seubert: https://orcid-org/0000-0002-7398-363x
Erhard Bremer: https://orcid-org/0000-0002-2225-7005

For correspondence:

Dr. Erhard Bremer, Philipps-University Marburg, SYNMIKRO Research Center, Karl-von-Frisch Strasse 14, 35043, Marburg, Germany. Phone: (+49)-6421-2821529; Fax: (+49)-6421-2822229; E-Mail: bremer@staff.uni-marburg.de

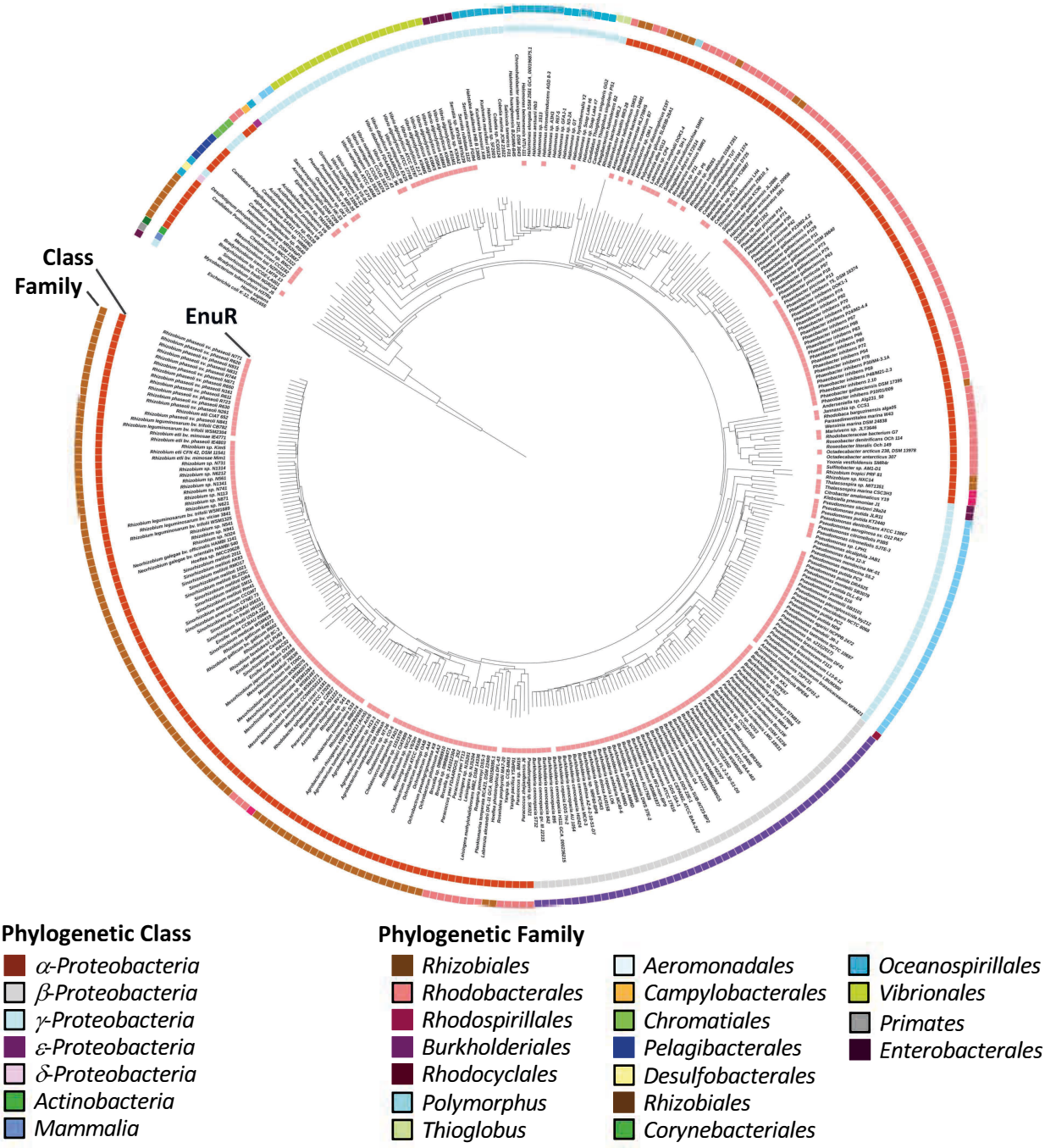

Supplementary Figure S1. Phylogenomics of EnuR-type proteins.

A phylogenetic tree of the ectoine/-5-hydroxyectoine hydrolase EutD was established using the iTol server (Letunic and Bork, 2019). The tree of 364 EutD-type proteins (Mais et al., 2020) is rooted with *Escherichia coli* and *Homo sapiens* aminopeptidases (Bradshaw et al., 1998;Wilce et al., 1998). The phylogenetic groups of microorganisms possessing EutD-type ectoine/5-hydroxyectoine hydrolases are highlighted in the two outer circles and the ectoine/5-hydroxyectoine catabolic gene clusters were analyzed for the presence of EnuR homologues in their vicinity as indicated in the inner circle.

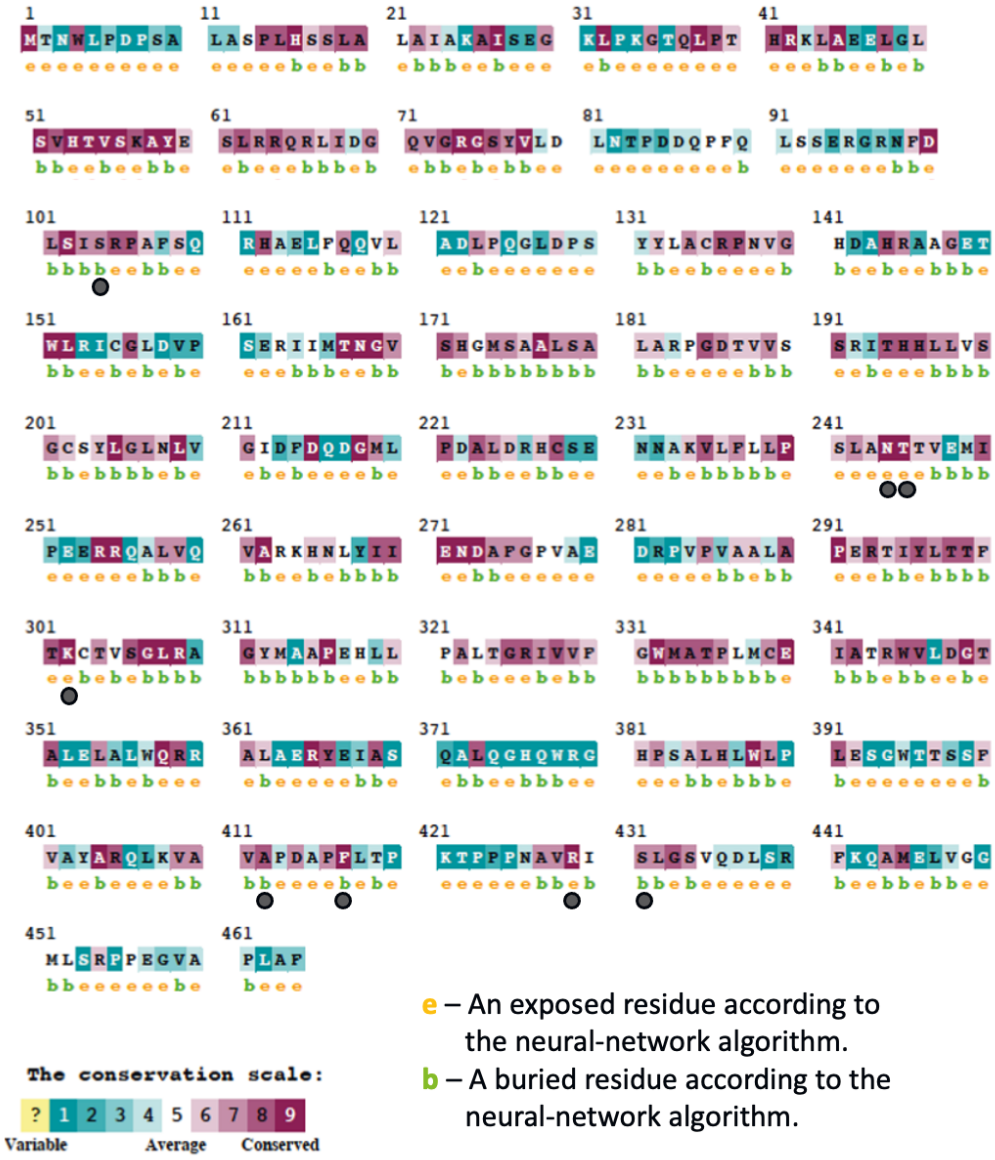

Supplementary Figure S2. Evolutionary conservation of EnuR-type proteins.

The degree of amino acid conservation of individual amino acids of the EnuR protein of *Ruegeria pomeroyi* DSS-3 using the ConSurf server (Berezin et al., 2004). The amino acid sequences of 278 EnuR-like proteins were used in an alignment to derive a conservation matrix. The amino acid sequence of the EnuR *R. pomeroyi* DSS-3 query protein (SPO1148) (Moran et al., 2004) is displayed with the degree of evolutionary conservation at position in the protein chain. Each site is color-coded according to the degree of conservation. The first row below the sequence lists the predicted burial status of the site (see legend) (Berezin et al., 2004). Black dots mark the amino-acids determined in the *in-silico* modelling and docking experiments to be crucial for ligand-binding.

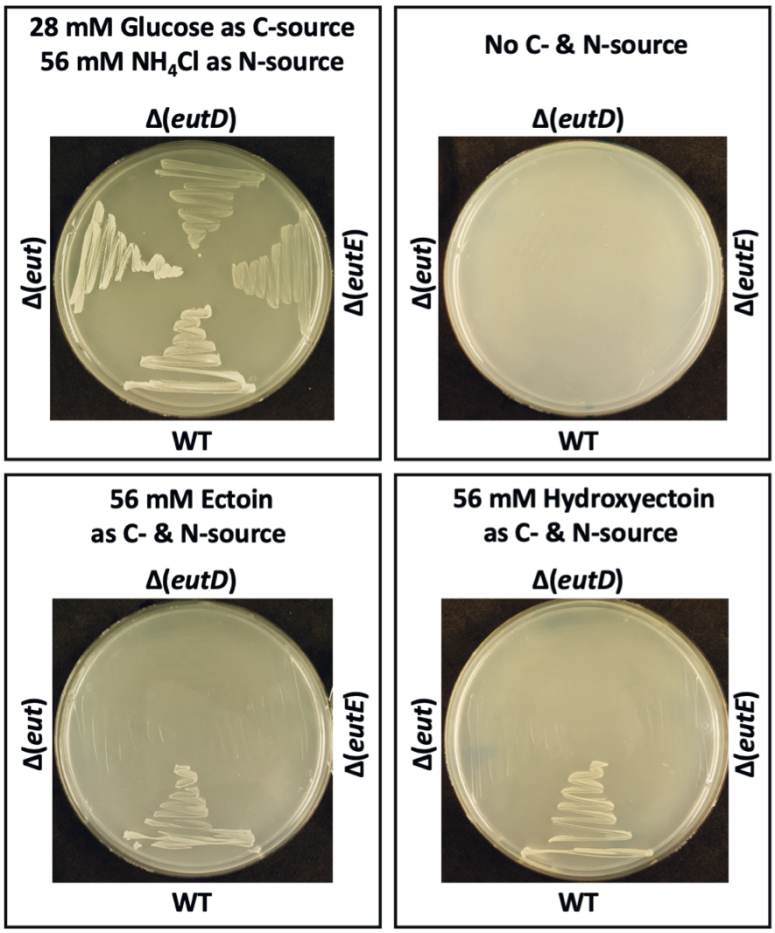

Supplementary Figure S3. Utilization of ectoines by *R. pomeroyi* DSS-3 as nutrients.

Growth of the *R. pomeroyi* wild-type strain J470 and its mutant derivatives [ASR6 D(*eut::gm*^{R}), ASR8 D(*eutD*::*gm*^{R}), and LHR7 D(*eutE*::*Gm*^{R})] on basal minimal medium agar plates containing 28 mM ectoine or 5-hydroxyectoine when used either as sole carbon or nitrogen source. The D(*eut::gm*^{R}) allele removes the entire ectoine/5-hydroxyectoine importer and catabolic gene cluster (from *enuR to atf*; see **Figure 1A**). Colonies were picked from basal medium agar plates containing glucose and NH_4Cl as carbon and nitrogen sources and streaked onto basal minimal agar plates containing the indicated carbon and nitrogen sources. The agar plates were incubated at 30° C for five days.

Supplementary Table S1. Phylogenetic groups of ectoine-consumers and distribution of EnuR-like proteins.

Phylogenetic group	Number of organisms	Organisms possessing EnuR like proteins	Percentage of organisms possessing EnuR [%]
Rhizobiales	117	103	88.0
Rhodobacteraceae	89	70	78.7
Burkholderiales	52	50	96.2
Pseudomonales	33	29	87.9
Oceanospirillales	25	5	20.0
Vibrionales	22	12	54.5
Minor groups	25	9	34.6
Total	363	278	76.6

Using computational tools provided via the IMG/M web-server (Chen et al., 2021), 363 microbial genome sequences (out of 8 850 inspected genome sequences) contained juxtapositioned *eutD/eutE* pairs in their ectoine/5-hydroxyectoine catabolic gene clusters (Mais et al., 2020). The taxonomic association of the corresponding microorganisms were assessed and the presence of *enuR*-type genes in the immediate vicinity of the ectoine/5-hydroxyectoine catabolic gene clusters was tabulated.

Supplementary Table S2. Docking of inducers into the presumed effector binding site of EnuR.

Inducer molecule	Binding energy (kCal/ mol)	Residues involved in hydrogen bonding
Hydroxy-α-ADABA	-7.3	Asn244, Thr245, Phe417, Ser431, Ser104
α-ADABA	-5.9	Asn244, Ser104, Ser431, Thr245
DABA	-3.8	Ser431

Results of the docking studied using AutoDock Vina (Trott and Olson, 2010) showing the predicted free energy change upon ligand-binding by the *R. pomeroyi* DSS-3 EnuR protein, and tabulation of the amino acids predicted to be involved in inducer-binding.

Supplementary Table S3. Conservation of amino acids of EnuR predicted to be involved in α-ADABA and hydroxy-α-ADABA binding.

Residue	Conservation	Functional replacement
Ser104	274/278	3 Thr; 1 Ala
Asn244	260/278	1 Ser; 12 Gly; 5 Ala
Thr245	196/278	2 Tyr; 2 Gln; 4 Arg; 4 Asn; 57 Met; 4 Leu; 3 Lys; 2 His; 4 Phe
Lys302	278/278	
Ala412	148/278	123 Leu; 3 Met; 4 Cys
Phe417	278/278	
Arg429	278/278	
Ser431	133/278	7 Ala; 135 Cys; 3 Asn

The amino acid sequences of 278 EnuR-type proteins were aligned with Jalview (Waterhouse et al., 2009) and the conservation of those amino acids implicated by our modelling and docking studies for the binding of the inducer molecules α-ADABA and hydroxy-α-ADABA were assessed.

Supplementary Table S4. Strains used in this study.

Strain	Genotype or description	Source or reference
Escherichia coli DH5a	Used for routine cloning purposes	Invitrogen, Karlsruhe, Germany
Escherichia coli BL21 (DE3)	Strain, used for overexpression	Stratagene, La Jolla, CA
Ruegeria pomeroyi DSS-3	Wild-type strain	(Moran et al., 2004)
Ruegeria pomeroyi J470[a]	Rif^R derivative of the wild-type strain	(Todd et al., 2012)
Ruegeria pomeroyi ASR6[b]	*R. pomeroyi* J470 Δ(*enuR-atf::gm*)1	(Schulz et al., 2017a)
Ruegeria pomeroyi ASR8[b]	*R. pomeroyi* J470 Δ(*eutD::gm*)1	(Schulz et al., 2017a)
Ruegeria pomeroyi LHR7[b]	*R. pomeroyi* J470 Δ(*eutE::gm*)1	This study

[a]Rif^R: Resistant against the antibiotic rifampicin.

[b]*gm*: Genetic determinant conferring resistance against the antibiotic gentamycin.

Supplementary Table S5. Plasmids used in this study.

Plasmid	Genotype or description	Source or reference
pRK2013[a]	Helper plasmid for tri-parental mating, Kan^R	(Figurski and Helinski, 1979)
pK18mobsacB	Suicide vector for *R. pomeroyi*, Kan^R	(Kvitko and Collmer, 2011)
p34S-*gm*[c]	Plasmid carrying a gentamicin (Gm^R) resistance cassette	(Dennis and Zylstra, 1998)
pLH73	pK18mobsacB with flanking regions of the *eutE*-gene, interrupted with a Gm^R cassette, Kan^R	This study
pEntry51	Cloning vector for IBA-Stargate cloning	IBA GmbH, Göttingen, Germany
pASG-IBA3	*E. coli* expression vector carrying a TetR-controlled and anhydrotetracyclin-responsive *tet* promoter	IBA GmbH, Göttingen, Germany
pBAS3[d]	pASG-IBA3 with synthetic, codon optimized *enuR* gene	(Schulz et al., 2017b)
pBAS17[d]	pBAS3 with codon exchange mutation (AAA/CAT) in the codon-optimized *enuR* leading to the replacement of Lys-302 with a His residue	(Schulz et al., 2017a)
pLH17[d]	pASG-IBA3 with synthetic, codon optimized sole aminotransferase domain of the *enuR* gene	This study
pLH26[d]	pLH17 with codon exchange mutation (AAA/CAT) in the codon-optimized *enuR* gene leading to the replacement of Lys-302 with a His residue	This study

[a]Kan^R: Resistant against the antibiotic kanamycin.

[b]*gm*: Genetic determinant conferring resistance against the antibiotic gentamycin.

[c]The *R. pomeroyi* DSS-3 *enuR* gene (or a segment thereof) carried by these plasmids was codon-optimized for enhanced expression in *E. coli* (Schulz et al., 2017b). The DNA-sequence of this synthetic gene is available in GenBank under accession number KU891821.

Supplementary Table S6. Oligonucleotides used in this study.

Primer	Sequence	Reference, description
ATD_pEntry_fw	AAGCTCTTCAATGCGTAATTTTGATCTGAGCATTAGCCG	IBA-Stargate cloning of the ATD of *Ruegeria pomeroyi* EnuR
ATD_pEntry_rev	AAGCGGCTCTTCTCCCAAGCTCTTCACCCAAATGCCAG	IBA-Stargate cloning of the ATD of *Ruegeria pomeroyi* EnuR
L263_fw	GGTCGGCGGCATGCTG	EMSA-fragments for the *uehA*-operator region
L229_rev_dye	GGTTTCCTCCCAAATGTCATGGG	EMSA-fragments for the *uehA*-operator region
Δ*eutE*_F1_fw	ACAGCTATGACATGATTACGCGCATCTGACCTGGGACGAT	Construction of plasmid pLH73
Δ*eutE*_F1_rev	ttcgagctcgAGTCCTTCACGAACATCTTGCGCGG	Construction of plasmid pLH73
Δ*eutE*_gm_fw	GTGAAGGACTcgagctcgaattgacataagcctgtt	Construction of plasmid pLH73
Δ*eutE_gm*_rev	GGTCCGCCTCtgttaggtggcggtacttgggt	Construction of plasmid pLH73
Δ*eutE*_F2_fw	ccacctaacaGAGGCGGACCCATGCA	Construction of plasmid pLH73
Δ*eutE*_F2_rev	ATCCCCGGGTACCGAGCTCGGCTGGCGCCGTCACT	Construction of plasmid pLH73
MST BS WT fw	TAACATTGTCGCGCGACAATAAAAAAATTGACATGCAGTACAATTCCC	Fragment for MST[a]
MST BS WT rev	GGGAATTGTACTGCATGTCAATTTTTTTATTGTCGCGCGACAATGTTA	Fragment for MST[a]

[a]MST: micoscale thermophoresis

References

Berezin, C., Glaser, F., Rosenberg, J., Paz, I., Pupko, T., Fariselli, P., Casadio, R., and Ben-Tal, N. (2004). ConSeq: the identification of functionally and structurally important residues in protein sequences. *Bioinformatics* 20**,** 1322-1324.

Bradshaw, R.A., Brickey, W.W., and Walker, K.W. (1998). N-terminal processing: the methionine aminopeptidase and N alpha-acetyl transferase families. *Trends Biochem. Sci.* 23**,** 263-267.

Chen, I.A., Chu, K., Palaniappan, K., Ratner, A., Huang, J., Huntemann, M., Hajek, P., Ritter, S., Varghese, N., Seshadri, R., Roux, S., Woyke, T., Eloe-Fadrosh, E.A., Ivanova, N.N., and Kyrpides, N.C. (2021). The IMG/M data management and analysis system v.6.0: new tools and advanced capabilities. *Nucleic Acids Res.* 49**,** D751-D763.

Dennis, J.J., and Zylstra, G.J. (1998). Improved antibiotic-resistance cassettes through restriction site elimination using Pfu DNA polymerase PCR. *Biotechniques* 25**,** 772-774, 776.

Figurski, D.H., and Helinski, D.R. (1979). Replication of an origin-containing derivative of plasmid RK2 dependent on a plasmid function provided in trans. *Proc. Natl. Acad. Sci U S A* 76**,** 1648-1652.

Kvitko, B.H., and Collmer, A. (2011). Construction of *Pseudomonas syringae* pv. tomato DC3000 mutant and polymutant strains. *Methods Mo.l Biol.* 712**,** 109-128.

Letunic, I., and Bork, P. (2019). Interactive Tree Of Life (iTOL) v4: recent updates and new developments. *Nucleic Acids Res.* 47**,** W256-W259.

Mais, C.-N., Hermann, L., Altegoer, F., Seubert, A., Richter, A.A., Wernersbach, I., Czech, L., Bremer, E., and Bange, G. (2020). Degradation of the microbial stress protectants and chemical chaperones ectoine and hydroxyectoine by a bacterial hydrolase-deacetylase complex. *J. Biol. Chem.* 295**,** 9087-9104.

Moran, M.A., Buchan, A., Gonzalez, J.M., Heidelberg, J.F., Whitman, W.B., Kiene, R.P., Henriksen, J.R., King, G.M., Belas, R., Fuqua, C., Brinkac, L., Lewis, M., Johri, S., Weaver, B., Pai, G., Eisen, J.A., Rahe, E., Sheldon, W.M., Ye, W., Miller, T.R., Carlton, J., Rasko, D.A., Paulsen, I.T., Ren, Q., Daugherty, S.C., Deboy, R.T., Dodson, R.J., Durkin, A.S., Madupu, R., Nelson, W.C., Sullivan, S.A., Rosovitz, M.J., Haft, D.H., Selengut, J., and Ward, N. (2004). Genome sequence of *Silicibacter pomeroyi* reveals adaptations to the marine environment. *Nature* 432**,** 910-913.

Schulz, A., Hermann, L., Freibert, S.-A., Bönig, T., Hoffmann, T., Riclea, R., Dickschat, J.S., Heider, J., and Bremer, E. (2017a). Transcriptional regulation of ectoine catabolism in response to multiple metabolic and environmental cues. *Env. Microbiol.* 19**,** 4599-4619.

Schulz, A., Stöveken, N., Binzen, I.M., Hoffmann, T., Heider, J., and Bremer, E. (2017b). Feeding on compatible solutes: a substrate-induced pathway for uptake and catabolism of ectoines and its genetic control by EnuR. *Environ. Microbiol.* 19**,** 926-946.

Todd, J.D., Kirkwood, M., Newton-Payne, S., and Johnston, A.W. (2012). DddW, a third DMSP lyase in a model Roseobacter marine bacterium, *Ruegeria pomeroyi* DSS-3. *ISME J* 6**,** 223-226.

Trott, O., and Olson, A.J. (2010). AutoDock Vina: improving the speed and accuracy of docking with a new scoring function, efficient optimization, and multithreading. *J. Comput. Chem.* 31**,** 455-461.

Waterhouse, A.M., Procter, J.B., Martin, D.M., Clamp, M., and Barton, G.J. (2009). Jalview Version 2--a multiple sequence alignment editor and analysis workbench. *Bioinformatics* 25**,** 1189-1191.

Wilce, M.C., Bond, C.S., Dixon, N.E., Freeman, H.C., Guss, J.M., Lilley, P.E., and Wilce, J.A. (1998). Structure and mechanism of a proline-specific aminopeptidase from *Escherichia coli*. *Proc Natl Acad Sci U S A* 95**,** 3472-3477.

6.2 Publication with minor contribution

6.2.1 Marine *Proteobacteria* metabolize glycolate via the β-hydroxyaspartate cycle (2019)

Nature 2019; 57587783:500-504. doi: 10.1038/s41586-019-1748-4

Article

Marine Proteobacteria metabolize glycolate via the β-hydroxyaspartate cycle

https://doi.org/10.1038/s41586-019-1748-4
Received: 29 March 2019
Accepted: 20 September 2019
Published online: 13 November 2019

Lennart Schada von Borzyskowski[1]*, Francesca Severi[1], Karen Krüger[2], Lucas Hermann[3], Alexandre Gilardet[1], Felix Sippel[1], Bianca Pommerenke[1], Peter Claus[1], Niña Socorro Cortina[1], Timo Glatter[4], Stefan Zauner[5], Jan Zarzycki[1], Bernhard M. Fuchs[2], Erhard Bremer[3,6], Uwe G. Maier[5,6], Rudolf I. Amann[2] & Tobias J. Erb[1,6]*

The following publication "Marine *Proteobacteria* metabolize glycolate via the β-hydroxyaspartate cycle." was published in Nature in 2019 after a peer-reviewing process. My contribution to this publication were the planning, performance, and analysis of Electric Mobility Shift Assays with the regulatory protein BhcR. L. Schada von Borzyskowski identified the *bhc* gene cluster, purified proteins, performed enzyme kinetic analysis, qPCR, phylogenetic analysis, and analysis of Tara Oceans metagenomes, generated and characterized mutant *Paracoccus denitrificans* strains and measured glycolate uptake rates. F. Severi performed enzyme kinetic analysis, crystallization of BhcD and enzyme assays in *P. denitrificans* cell-free extracts. K. Krüger performed phylogenetic analysis and analysis of Helgoland metagenomes. A.Gilardet performed crystallization of BhcC. F. Sippel performed enzyme kinetic analysis. B. Pommerenke generated mutant *P. denitrificans* strains. P. Claus and N. Socorro Cortina performed small-molecule mass spectrometry. T. Glatter performed mass spectrometry for proteomics. J. Zarzycki collected X-ray datasets, solved, refined, and analysed crystal structures. B. M. Fuchs and R. I. Amann planned and supervised fieldwork at Helgoland and provided reagents. L. Schada von Borzyskowski, E. Bremer, S. Zauner, U. G. Maier, R. I. Amann and T. J. Erb planned experiments, analysed data, and supervised the project. L. Schada von Borzyskowski and T. J. Erb wrote the manuscript, with contributions from all other authors.

Marine Proteobacteria metabolize glycolate via the β-hydroxyaspartate cycle

https://doi.org/10.1038/s41586-019-1748-4

Received: 29 March 2019

Accepted: 20 September 2019

Published online: 13 November 2019

Lennart Schada von Borzyskowski[1]*, Francesca Severi[1], Karen Krüger[2], Lucas Hermann[3], Alexandre Gilardet[1], Felix Sippel[1], Bianca Pommerenke[1], Peter Claus[1], Niña Socorro Cortina[1], Timo Glatter[4], Stefan Zauner[5], Jan Zarzycki[1], Bernhard M. Fuchs[2], Erhard Bremer[3,6], Uwe G. Maier[5,6], Rudolf I. Amann[2] & Tobias J. Erb[1,6]*

One of the most abundant sources of organic carbon in the ocean is glycolate, the secretion of which by marine phytoplankton results in an estimated annual flux of one petagram of glycolate in marine environments[1]. Although it is generally accepted that glycolate is oxidized to glyoxylate by marine bacteria[2–4], the further fate of this C_2 metabolite is not well understood. Here we show that ubiquitous marine Proteobacteria are able to assimilate glyoxylate via the β-hydroxyaspartate cycle (BHAC) that was originally proposed 56 years ago[5]. We elucidate the biochemistry of the BHAC and describe the structure of its key enzymes, including a previously unknown primary imine reductase. Overall, the BHAC enables the direct production of oxaloacetate from glyoxylate through only four enzymatic steps, representing—to our knowledge—the most efficient glyoxylate assimilation route described to date. Analysis of marine metagenomes shows that the BHAC is globally distributed and on average 20-fold more abundant than the glycerate pathway, the only other known pathway for net glyoxylate assimilation. In a field study of a phytoplankton bloom, we show that glycolate is present in high nanomolar concentrations and taken up by prokaryotes at rates that allow a full turnover of the glycolate pool within one week. During the bloom, genes that encode BHAC key enzymes are present in up to 1.5% of the bacterial community and actively transcribed, supporting the role of the BHAC in glycolate assimilation and suggesting a previously undescribed trophic interaction between autotrophic phytoplankton and heterotrophic bacterioplankton.

Global net primary production has been estimated to be approximately 100 petagrams of carbon per year, equal parts of which are produced in terrestrial and marine habitats[6]. In the oceans, more than a third of primary production can be released into the water column by phytoplankton as dissolved organic carbon[7], generating a plethora of substrates for heterotrophic bacterioplankton. An abundant component of the pool of dissolved organic carbon is the carboxylic acid glycolate, which is released as a photorespiratory waste product of marine autotrophs[3,8,9]. Concentrations of glycolate in the nanomolar-to-low micromolar range have been measured in different marine habitats[1,2,10,11] (Extended Data Fig. 1), and the compound is readily taken up by bacterioplankton[12]. The first step in glycolate metabolism is its oxidation to glyoxylate, which is catalysed by the enzyme glycolate oxidase. The abundance and transcription of the *glcD* gene, which encodes a subunit of glycolate oxidase, has previously been used to investigate bacterial groups that are capable of glycolate utilization[4,13]. However, it has been assumed that glycolate is the subject of bacterial oxidation mainly to conserve energy[2–4]; the further fate of glyoxylate has not been described in detail. For SAR11 bacteria, it has been shown that glyoxylate can be used to replace the obligate glycine requirement[14]. In SAR11 and other bacteria, glyoxylate can be co-assimilated by malate synthase into the tricarboxylic acid cycle[14–16] or directly assimilated into central carbon metabolism through the well-studied glycerate pathway[17,18]. An alternative solution is the BHAC[5,19], which has been previously proposed to operate in the Alphaproteobacterium *Paracoccus denitrificans*[20,21]. However, the complete reaction sequence and the proteins comprising this pathway and their detailed biochemistry have remained unknown for the past 56 years.

On the basis of the sequence of a putative β-hydroxyaspartate aldolase gene (*dhaa*; GenBank accession number AB075600) from *P. denitrificans* IFO 13301[22], we identified a homologue in the genome of *P. denitrificans* DSM413 (BLT64_RS06500), annotated as a DSD1 family pyridoxal 5-phosphate (PLP)-dependent enzyme. This gene is part of a gene cluster, which consists of four structural genes and a putative transcriptional regulator that we termed *bhcABCD* and *bhcR* (Fig. 1a). In addition to the gene for the putative β-hydroxyaspartate aldolase (*bhcC*), the cluster comprises the open reading frames that encode a putative PLP-dependent aminotransferase (BLT64_RS06510, *bhcA*), a putative serine/threonine dehydratase (BLT64_RS06505, *bhcB*) and a putative ornithine cyclodeaminase (BLT64_RS06495, *bhcD*). The

[1]Department of Biochemistry & Synthetic Metabolism, Max Planck Institute for Terrestrial Microbiology, Marburg, Germany. [2]Department of Microbial Ecology, Max Planck Institute for Marine Microbiology, Bremen, Germany. [3]Laboratory for Molecular Microbiology, Department of Biology, Philipps-University Marburg, Marburg, Germany. [4]Facility for Mass Spectrometry and Proteomics, Max Planck Institute for Terrestrial Microbiology, Marburg, Germany. [5]Laboratory for Cell Biology, Department of Biology, Philipps-University Marburg, Marburg, Germany. [6]LOEWE-Center for Synthetic Microbiology, Philipps-University Marburg, Marburg, Germany. *e-mail: schada@mpi-marburg.mpg.de; toerb@mpi-marburg.mpg.de

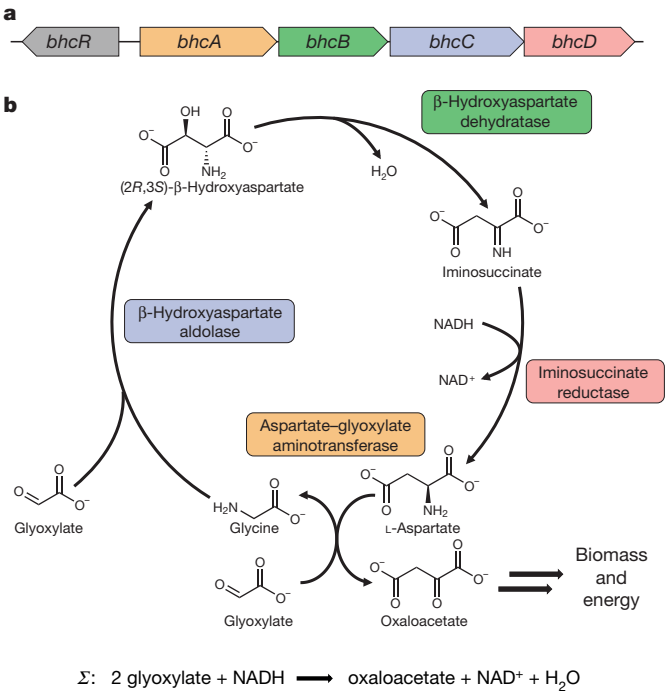

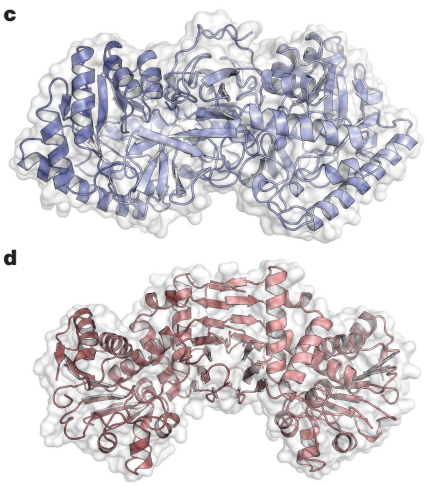

Fig. 1 | The BHAC. a, Genetic structure of the bhc gene cluster in *P. denitrificans* DSM 413. **b**, Reaction sequence and net balance of the BHAC. **c**, Cartoon representation of the β-hydroxyaspartate aldolase (BhcC) homodimer with superimposed protein surface (PDB 6QKB). **d**, Cartoon representation of the iminosuccinate reductase (BhcD) homodimer with superimposed protein surface (PDB 6RQA).

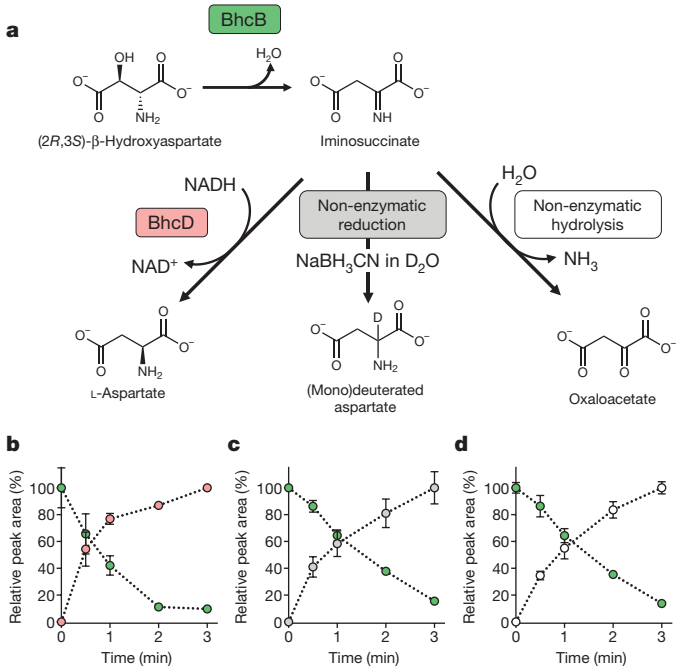

Fig. 2 | Reaction sequence catalysed by β-hydroxyaspartate dehydratase (BhcB) and iminosuccinate reductase (BhcD). a, Overview of the relevant reactions. **b**, Production of L-aspartate (red) from (2*R*, 3*S*)-β-hydroxyaspartate (green) by BhcB and reduction of iminosuccinate by BhcD. **c**, Production of (mono)deuterated aspartate (grey) from (2*R*, 3*S*)-β-hydroxyaspartate (green) by BhcB and reduction of iminosuccinate via $NaBH_3CN$ in D_2O. The data represent the formation of monodeuterated aspartate; owing to proton exchange, di- and trideuterated aspartate can also be formed in small quantities. **d**, Production of oxaloacetate (white) from (2*R*, 3*S*)-β-hydroxyaspartate (green) by BhcB and subsequent hydrolysis of iminosuccinate when neither BhcD nor $NaBH_3CN$ are added. **b**–**d**, Data are mean ± s.d.; $n = 3$ independent experiments.

putative transcriptional regulator (BLT64_RS06515), annotated as IclR-family regulator, is located in the opposite orientation to the four structural genes.

We expressed and characterized the four enzymes that are encoded in the gene cluster. BhcA is a PLP-dependent aminotransferase that transaminates glyoxylate into glycine using aspartate as the preferred amino group donor. BhcB functions as a β-hydroxyaspartate dehydratase. BhcC is a β-hydroxyaspartate aldolase, the key enzyme of the BHAC that catalyses the condensation of glyoxylate and glycine into β-hydroxyaspartate. This enzyme is closely related to D-threonine aldolases (Extended Data Fig. 2). The crystal structure of β-hydroxyaspartate aldolase that we solved at 1.7 Å (Protein Data Bank (PDB) 6QKB) shows that the three amino acids A160, A195 and S313 distinguish the active site of BhcC from that of D-threonine aldolases, providing a signature sequence for this enzyme family (Fig. 1c, Extended Data Fig. 2 and Extended Data Table 1). When combined, the BhcABC proteins were sufficient to reconstruct a reaction sequence from aspartate and two molecules of glyoxylate to two molecules of oxaloacetate and free ammonia. However, this left us puzzled about the function of the fourth open reading frame, the putative ornithine cyclodeaminase (*bhcD*).

When we tested BhcD in combination with BhcB, we discovered that it functions as an imine reductase (IRED) that accepts a labile iminosuccinate intermediate[23] formed by the latter enzyme (Fig. 2a, b). We used sodium cyanoborohydride trapping to demonstrate that BhcB produces iminosuccinate (Fig. 2c). Although this compound spontaneously decays into free ammonia and oxaloacetate in solution (Fig. 2d), iminosuccinate is reduced to L-aspartate in the presence of BhcD, thereby regenerating the amino group donor for the first step of the BHAC. IREDs are extensively investigated owing to their biotechnological potential[24]. Almost all IREDs described to date act on secondary imines, whereas the reduction of a free primary imine—as catalysed by BhcD—has not previously been described. The enzymatic reduction of primary imines is known only as part of the reaction sequence in glutamate dehydrogenase[25] and as part of a non-physiological side reaction of ketimine reductases[26]. The crystal structure of BhcD, which we solved to a resolution of 2.6 Å (PDB 6RQA), shows major differences in the active site compared to L-alanine dehydrogenase from *Archaeoglobus fulgidus* (PDB 1OMO), the closest structural homologue within the ornithine cyclodeaminase/μ-crystalline enzyme superfamily (Fig. 1d, Extended Data Fig. 3 and Extended Data Table 1). Phylogenetic analysis supports these active site differences and reveals that BhcD and its homologues constitute a novel family of primary IREDs within the ornithine cyclodeaminase/μ-crystalline superfamily (Extended Data Fig. 3).

Table 1 | Kinetic parameters of the four enzymes of the BHAC

Enzyme	Substrate	k_{cat} (s^{-1})	App. K_M (mM)	k_{cat}/K_M ($M^{-1} s^{-1}$)
Aspartate–glyoxylate aminotransferase (BhcA)	Glyoxylate	58 ± 1	0.43 ± 0.02	1.34×10^5
	L-Aspartate	56 ± 1	2.51 ± 0.10	2.25×10^4
	Glycine	0.76 ± 0.01	9.52 ± 0.40	7.97×10^1
	Oxaloacetate	0.76 ± 0.02	2.90 ± 0.27	2.62×10^2
	L-Serine	8.8 ± 0.3	2.10 ± 0.24	4.20×10^3
	L-Glutamate	5.0 ± 0.3	20.62 ± 2.33	2.44×10^2
β-Hydroxyaspartate dehydratase (BhcB)	(2*R*, 3*S*)-β-Hydroxyaspartate	35 ± 1	0.20 ± 0.02	1.75×10^5
β-Hydroxyaspartate aldolase (BhcC)	Glyoxylate	86 ± 4	0.23 ± 0.03	3.72×10^5
	Glycine	91 ± 2	4.31 ± 0.34	2.11×10^4
	(2*R*, 3*S*)-β-Hydroxyaspartate	33 ± 1	0.28 ± 0.03	1.18×10^5
	D-Threonine	76 ± 2	9.24 ± 0.86	8.25×10^3
Iminosuccinate reductase (BhcD)	Iminosuccinate	201 ± 10	0.09 ± 0.01	2.29×10^6
	NADH	–	0.02 ± 0.003	–
	NADPH	–	0.33 ± 0.05	–

Data are mean ± s.d., as determined from nonlinear fits of 18 data points with GraphPad Prism 8. Michaelis–Menten fits of enzyme kinetics and an SDS–PAGE gel showing purified proteins are provided in Extended Data Fig. 4 and Supplementary Fig. 1, respectively. For BhcA, kinetics for glyoxylate and L-aspartate were measured with 20 mM L-aspartate and 5 mM glyoxylate, respectively, and kinetics for glycine and oxaloacetate were measured with 20 mM oxaloacetate and 30 mM glycine, respectively. Kinetics for L-serine and L-glutamate were measured with 5 mM glyoxylate. For BhcC, kinetics for glycine and glyoxylate were measured with 5 mM glyoxylate and 20 mM glycine, respectively.

The kinetic parameters of all enzymes of the BHAC are reported in Table 1. The complete reaction sequence of the pathway is shown in Fig. 1b. The cycle extends the originally proposed reaction sequence[5] by the IRED reaction. Overall, the BHAC converts two molecules of glyoxylate (C_2) into oxaloacetate (C_4) without the loss of carbon as CO_2, under consumption of just one reducing equivalent and regeneration of the catalytic amino donor, which makes it one of the most efficient glyoxylate assimilation pathways described to date (Supplementary Table 1). Oxaloacetate formed in the BHAC can directly enter the tricarboxylic acid cycle or serve as substrate for anabolic reactions. The pathway is essential for the growth of *P. denitrificans* in the presence of glycolate and glyoxylate, and its enzymes are highly expressed and active in cells grown in the presence of glycolate (Extended Data Fig. 5). Glyoxylate negatively affected the interaction of the transcriptional regulator BhcR with the promoter region of the bhc gene cluster (Extended Data Fig. 5).

We next studied the phylogenetic distribution of the BHAC. The bhc gene cluster is widespread among the Rhizobiales and Rhodobacterales orders of the Alphaproteobacteria, and is also found in several gammaproteobacterial orders (Extended Data Fig. 6). Most of these bacteria were isolated from marine habitats, and the *Roseobacter* group within the Rhodobacterales is one of the three major bacterial groups responding to phytoplankton blooms[27]; *Roseobacter*-group bacteria can constitute up to 15% of the bacterial community in these blooms[28]. Notably, 94% of the isolates with the bhc gene cluster also encode glycolate oxidase in their genomes, enabling them to oxidize glycolate to glyoxylate for subsequent assimilation by the BHAC (Supplementary Data 1). BhcC is also ubiquitously present in marine metagenomes collected on the *Tara* Oceans expedition (Extended Data Fig. 7 and Supplementary Data 2), suggesting that the BHAC functions in glycolate assimilation in marine environments worldwide. Notably, the BHAC (represented by BhcC) is on average 20-fold more abundant than the glycerate pathway (represented by Gcl) in these datasets (Extended Data Fig. 7d).

To investigate the ecological importance of the BHAC, we focused our analyses on Helgoland (Extended Data Fig. 8a, b), an island in the North Sea that has already been used extensively as a study site to investigate the succession of bacterial populations during algal blooms[28,29]. We analysed metagenomes from seawater samples collected between 2010 and 2012 at Helgoland and detected the bhc gene cluster in all years at intermediate abundances (up to 3 reads per kilobase per million reads (RPKM), corresponding to roughly 1.5% of all cells[28]) (Extended Data Fig. 8c–e and Supplementary Data 3). To further investigate the role of the BHAC in situ, we monitored the spring phytoplankton bloom at Helgoland from March to May 2018. We determined chlorophyll *a* (Chl *a*) fluorescence as proxy for phytoplankton biomass and total microbial cell counts for each working day. Glycolate concentrations in the seawater were determined weekly.

The 2018 spring bloom was dominated by pennate diatoms and consisted of two peaks in phytoplankton growth in late April and late May (Fig. 3a). We determined a background concentration of glycolate in the seawater of 300 nM before the bloom, which is in line with previous measurements[1,2,4,9–11,30–39] (600 ± 340 nM) (Extended Data Fig. 1). During the bloom, from early March to late May, glycolate concentrations increased by approximately 350 nM (Fig. 3b), indicating the accumulation of phytoplankton-derived glycolate. At three time points in April and May, before and during the algal bloom, we determined bulk uptake rates of glycolate in the sea water. Glycolate uptake rates were in line with previously reported values[12] and increased more than threefold from 1.46 nM h^{-1} to 4.68 nM h^{-1} between the first and the last measurement (Fig. 3b), indicating that the capacity for glycolate uptake had multiplied at the same factor as the total microbial cell counts. Notably, these rates are comparable to uptake and consumption rates for dimethylsulfoniopropionate in the open ocean[40] and would enable a turnover of the total glycolate pool at our sampling site every 5–10 days. The bhc gene cluster was prevalent during the progression of the phytoplankton bloom. *bhcC* genes were detected at all of the time points, with the highest abundance per cell (around 1.5%) during the peaks of the phytoplankton bloom in April and May (Fig. 3c, Extended Data Fig. 9 and Supplementary Data 4). Transcription of *bhcC* was confirmed before and during the spring bloom (Fig. 3d, e), indicating that the BHAC is an active route for glycolate assimilation in the ocean.

In summary, our study provides the full reaction sequence and genetic basis of the BHAC. We demonstrate the biochemistry of the pathway, which involves a previously unknown family of IREDs, and provide support for its ecological importance in the assimilation of phytoplankton-derived dissolved organic carbon. The discovery of the BHAC as a ubiquitous pathway in marine environments adds a new

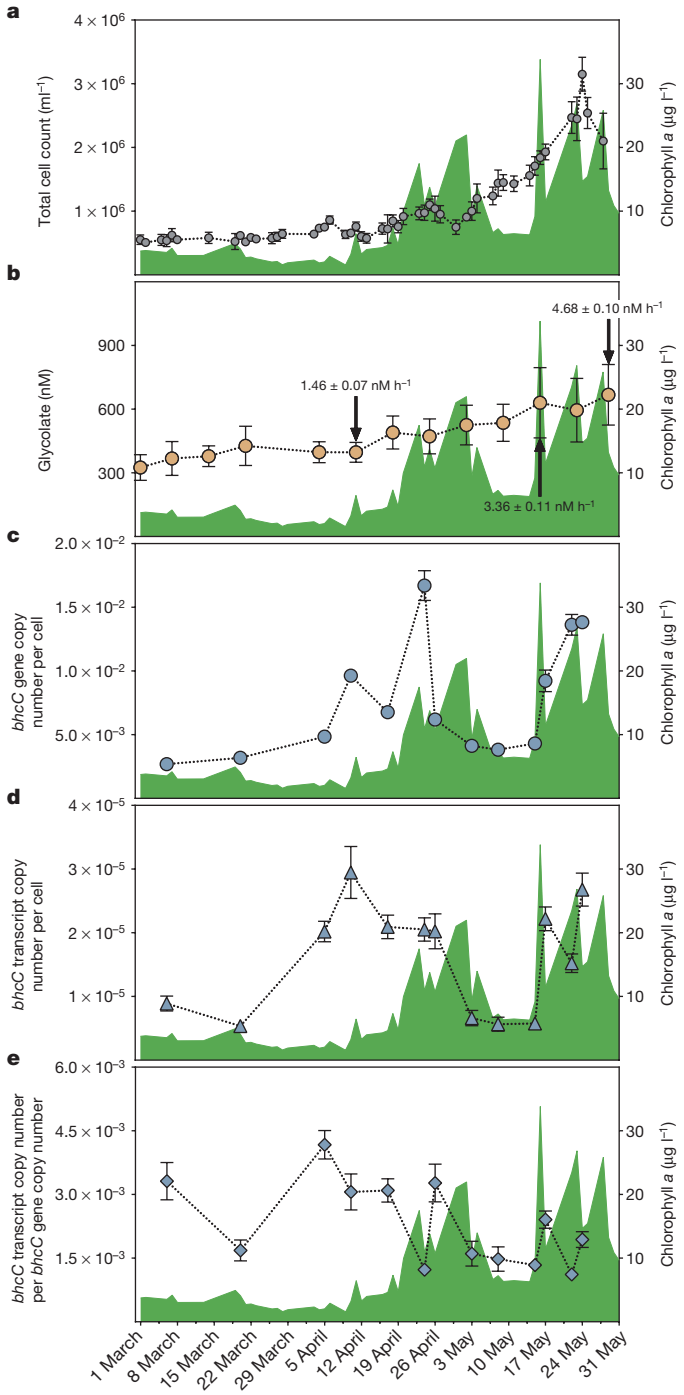

Fig. 3 | The BHAC during the spring phytoplankton bloom 2018 at Helgoland. a, From 1 March to 31 May, total microbial cell counts (grey) and Chl *a* concentrations (green) were determined each working day ($n = 1$). **b**, The concentration of glycolate (light brown) was determined once per week using liquid chromatography with mass spectrometry and increased from approximately 300 nM to around 650 nM. The uptake rate of bulk glycolate was determined at three time points through ^{14}C-glycolate incorporation and uptake rates are indicated. Data are the mean ± s.d. of $n = 5$ seawater samples for glycolate concentrations, and of $n = 4$ seawater samples for glycolate uptake rates. **c**, The *bhcC* gene copy number per cell (blue circles) was determined using qPCR. **d**, The *bhcC* transcript copy number per cell (blue triangles) was determined via cDNA synthesis followed by qPCR. **e**, *bhcC* transcript copy number divided by *bhcC* gene copy number (blue diamonds). **c**–**e**, Data are mean ± s.d.; $n = 3$ independent experiments.

dimension to the biochemical cycle of glycolate, an abundant organic acid in the global oceans. As the BHAC requires only one reducing equivalent and enables carbon-conserving glycolate assimilation, it may confer an advantage compared to the glycerate pathway, which releases CO_2. This may explain the high prevalence of the BHAC in marine Proteobacteria and could provide a starting point for future studies that investigate carbon fluxes from phytoplankton to heterotrophic bacterioplankton.

Online content

Any methods, additional references, Nature Research reporting summaries, source data, extended data, supplementary information, acknowledgements, peer review information; details of author contributions and competing interests; and statements of data and code availability are available at https://doi.org/10.1038/s41586-019-1748-4.

1. Wright, R. T. & Shah, N. M. Trophic role of glycolic acid in coastal seawater. II. Seasonal changes in concentration and heterotrophic use in Ipswich Bay, Massachusetts, USA. *Mar. Biol.* **43**, 257–263 (1977).
2. Wright, R. T. & Shah, N. M. Trophic role of glycolic acid in coastal seawater. I. Heterotrophic metabolism in seawater and bacterial cultures. *Mar. Biol.* **33**, 175–183 (1975).
3. Fogg, G. E. The ecological significance of extracellular products of phytoplankton photosynthesis. *Bot. Mar.* **26**, 3–14 (1983).
4. Lau, W. W., Keil, R. G. & Armbrust, E. V. Succession and diel transcriptional response of the glycolate-utilizing component of the bacterial community during a spring phytoplankton bloom. *Appl. Environ. Microbiol.* **73**, 2440–2450 (2007).
5. Kornberg, H. L. & Morris, J. G. β-Hydroxyaspartate pathway: a new route for biosyntheses from glyoxylate. *Nature* **197**, 456–457 (1963).
6. Field, C. B., Behrenfeld, M. J., Randerson, J. T. & Falkowski, P. Primary production of the biosphere: integrating terrestrial and oceanic components. *Science* **281**, 237–240 (1998).
7. Duarte, C. M. & Cebrian, J. The fate of marine autotrophic production. *Limnol. Oceanogr.* **41**, 1758–1766 (1996).
8. Hellebust, J. A. Excretion of some organic compounds by marine phytoplankton. *Limnol. Oceanogr.* **10**, 192–206 (1965).
9. Tolbert, N. E. & Zill, L. P. Excretion of glycolic acid by algae during photosynthesis. *J. Biol. Chem.* **222**, 895–906 (1956).
10. Leboulanger, C., Descolasgros, C. & Jupin, H. HPLC determination of glycolic acid in seawater. An estimation of phytoplankton photorespiration in the Gulf of Lions, western Mediterranean Sea. *J. Plankton Res.* **16**, 897–903 (1994).
11. Leboulanger, C., Oriol, L., Jupin, H. & Descolas-Gros, C. Diel variability of glycolate in the eastern tropical Atlantic Ocean. *Deep Sea Res. Part I Oceanogr. Res. Pap.* **44**, 2131–2139 (1997).
12. Casey, J. R., Ferrón, S. & Karl, D. M. Light-enhanced microbial organic carbon yield. *Front. Microbiol.* **8**, 2157 (2017).
13. Lau, W. W. & Armbrust, E. V. Detection of glycolate oxidase gene *glcD* diversity among cultured and environmental marine bacteria. *Environ. Microbiol.* **8**, 1688–1702 (2006).
14. Carini, P., Steindler, L., Beszteri, S. & Giovannoni, S. J. Nutrient requirements for growth of the extreme oligotroph 'Candidatus *Pelagibacter ubique*' HTCC1062 on a defined medium. *ISME J.* **7**, 592–602 (2013).
15. Eiler, A. et al. Tuning fresh: radiation through rewiring of central metabolism in streamlined bacteria. *ISME J.* **10**, 1902–1914 (2016).
16. Tripp, H. J. et al. Unique glycine-activated riboswitch linked to glycine–serine auxotrophy in SAR11. *Environ. Microbiol.* **11**, 230–238 (2009).
17. Krakow, G. & Barkulis, S. S. Conversion of glyoxylate to hydroxypyruvate by extracts of *Escherichia coli*. *Biochim. Biophys. Acta* **21**, 593–594 (1956).
18. Hansen, R. W. & Hayashi, J. A. Glycolate metabolism in *Escherichia coli*. *J. Bacteriol.* **83**, 679–687 (1962).
19. Kornberg, H. L. & Morris, J. G. The utilization of glycollate by *Micrococcus denitrificans*: the β-hydroxyaspartate pathway. *Biochem. J.* **95**, 577–586 (1965).
20. Gibbs, R. G. & Morris, J. G. Assay and properties of β-hydroxyaspartate aldolase from *Micrococcus denitrificans*. *Biochim. Biophys. Acta* **85**, 501–503 (1964).
21. Gibbs, R. G. & Morris, J. G. Purification and properties of *erythro*-β-hydroxyaspartate dehydratase from *Micrococcus denitrificans*. *Biochem. J.* **97**, 547–554 (1965).
22. Liu, J. Q., Dairi, T., Itoh, N., Kataoka, M. & Shimizu, S. A novel enzyme, d-3-hydroxyaspartate aldolase from *Paracoccus denitrificans* IFO 13301: purification, characterization, and gene cloning. *Appl. Microbiol. Biotechnol.* **62**, 53–60 (2003).
23. Mortarino, M. et al. l-Aspartate oxidase from *Escherichia coli*. I. Characterization of coenzyme binding and product inhibition. *Eur. J. Biochem.* **239**, 418–426 (1996).
24. Lenz, M., Borlinghaus, N., Weinmann, L. & Nestl, B. M. Recent advances in imine reductase-catalyzed reactions. *World J. Microbiol. Biotechnol.* **33**, 199 (2017).
25. Hochreiter, M. C. & Schellenberg, K. A. α-Iminoglutarate formation by beef liver l-glutamate dehydrogenase. Detection by borohydride or dithionite reduction to glutamate. *J. Am. Chem. Soc.* **91**, 6530–6531 (1969).
26. Hallen, A., Cooper, A. J., Smith, J. R., Jamie, J. F. & Karuso, P. Ketimine reductase/CRYM catalyzes reductive alkylamination of α-keto acids, confirming its function as an imine reductase. *Amino Acids* **47**, 2457–2461 (2015).

27. Buchan, A., LeCleir, G. R., Gulvik, C. A. & González, J. M. Master recyclers: features and functions of bacteria associated with phytoplankton blooms. *Nat. Rev. Microbiol*. **12**, 686–698 (2014).
28. Teeling, H. et al. Recurring patterns in bacterioplankton dynamics during coastal spring algae blooms. *eLife* **5**, e11888 (2016).
29. Teeling, H. et al. Substrate-controlled succession of marine bacterioplankton populations induced by a phytoplankton bloom. *Science* **336**, 608–611 (2012).
30. Shah, N. M. & Wright, R. T. Occurrence of glycolic acid in coastal sea-water. *Mar. Biol*. **24**, 121–124 (1974).
31. Fogg, G. E., Burton, N. F. & Coughlan, S. J. The occurrence of glycollic acid in Antarctic waters. *Br. Antarct. Surv. Bull*. **41 & 42**, 193–195 (1975).
32. Hasan-Al, R. H., Coughlan, S. J., Pant, A. & Fogg, G. E. Seasonal variations in phytoplankton and glycollate concentrations in the Menai Straits, Anglesey. *J. Mar. Biol. Assoc. U.K*. **55**, 557–565 (1975).
33. Edenborn, H. M. & Litchfield, C. D. Glycolate turnover in the water column of the New York Bight apex. *Mar. Biol*. **95**, 459–467 (1987).
34. Leboulanger, C., Serve, L., Comellas, L. & Jupin, H. Determination of glycolic acid released from marine phytoplankton by post-derivatization gas chromatography mass spectrometry. *Phytochem. Anal*. **9**, 5–9 (1998).
35. Lord, J. M., Codd, G. A. & Merrett, M. J. The effect of light quality on glycolate formation and excretion in algae. *Plant Physiol*. **46**, 855–856 (1970).
36. Smith, W. O. Extracellular release of glycolic acid by a marine diatom. *J. Phycol*. **10**, 30–33 (1974).
37. Leboulanger, C., Martin-Jezequel, V., Descolas-Gros, C., Sciandra, A. & Jupin, H. J. Photorespiration in continuous culture of *Dunaliella tertiolecta* (Chlorophyta): relationships between serine, glycine, and extracellular glycolate. *J. Phycol*. **34**, 651–654 (1998).
38. Schnitzler Parker, M., Armbrust, E. V., Piovia-Scott, J. & Keil, R. G. Induction of photorespiration by light in the centric diatom *Thalassiosira weissflogii* (*Bacillariophyceae*): molecular characterization and physiological consequences. *J. Phycol*. **40**, 557–567 (2004).
39. Bertilsson, S., Berglund, O., Pullin, M. J. & Chisholm, S. W. Release of dissolved organic matter by *Prochlorococcus*. *Vie Milieu* **55**, 225–231 (2005).
40. Simó, R. & Pedrós-Alió, C. Short-term variability in the open ocean cycle of dimethylsulfide. *Glob. Biogeochem. Cycles* **13**, 1173–1181 (1999).

Methods

Data reporting

No statistical methods were used to predetermine sample size. The experiments were not randomized and the investigators were not blinded to allocation during experiments and outcome assessment.

Chemicals and reagents

Unless otherwise stated, all chemicals and reagents were acquired from Sigma-Aldrich and were of the highest purity available.

Strains, medium and cultivation conditions

All strains used in this study are listed in Supplementary Table 2. *Escherichia coli* TOP10 (for genetic work), ST18 (for plasmid conjugation) and BL21 AI (for protein expression) were grown at 37 °C in lysogeny broth (LB)[41].

P. denitrificans DSM 413[42] and its derivatives were grown at 30 °C in LB or in mineral salt medium with TE3-Zn trace elements[43] supplemented with various carbon sources. To monitor growth, the optical density at 600 nm (OD_{600}) of culture samples was determined on a photospectrometer (Merck Chemicals).

Vector construction

The genes encoding the four enzymes of the BHAC (*bhcABCD*) as well as the *bhcR* gene encoding the transcriptional regulator were cloned into the standard expression vector pET16b (Merck Chemicals). To this end, the respective genes were amplified from genomic DNA of *P. denitrificans* DSM 413 with the primers provided in Supplementary Table 3. The resulting PCR products were digested with suitable restriction endonucleases (Thermo Fisher Scientific) as given in Supplementary Table 3 and ligated into the expression vector pET16b that had been digested with the same enzymes to create a vector for heterologous expression of the respective protein. Successful cloning of the desired open reading frames was verified by DNA sequencing (Eurofins Genomics). All plasmids used in this study are listed in Supplementary Table 2.

Expression and purification of recombinant proteins

For heterologous overexpression of the BhcA, BhcB, BhcC and BhcD enzymes, the corresponding plasmid encoding the respective enzyme was first transformed into chemically competent *E. coli* BL21 AI cells. The cells were then grown on LB agar plates containing 100 μg ml^{-1} ampicillin at 37 °C overnight. A starter culture in selective LB medium was inoculated from a single colony on the next day and left to grow overnight at 37 °C in a shaking incubator. The starter culture was used on the next day to inoculate an expression culture in selective terrific broth (TB) medium at a 1:100 dilution. The expression culture was grown at 37 °C in a shaking incubator to an OD_{600} of 0.5–0.7, induced with 0.5 mM isopropyl-β-D-thiogalactoside (IPTG) and 0.2% L-arabinose and subsequently grown overnight at 18 °C in a shaking incubator. Cells were collected at 6,000*g* for 15 min at 4 °C and cell pellets were stored at −20 °C until purification of enzymes. Cell pellets were resuspended in twice their volume in buffer A (300 mM NaCl, 25 mM Tris-HCl pH 8.0, 15 mM imidazole, 1 mM β-mercaptoethanol, 0.1 mM $MgCl_2$, 0.01 mM PLP and one tablet of SIGMAFAST protease inhibitor cocktail, EDTA-free per litre). The cell suspension was treated with a Sonopuls GM200 sonicator (BANDELIN Electronic) at an amplitude of 50% to lyse the cells and subsequently centrifuged at 50,000*g* and 4 °C for 1 h. The filtered supernatant (0.45-μm filter; Sarstedt) was loaded onto Protino Ni-NTA Agarose (Macherey-Nagel) in a gravity column, which had previously been equilibrated with 5 column volumes of buffer A. The column was washed with 20 column volumes of buffer A and 5 column volumes of 85% buffer A and 15% buffer B and the His-tagged protein was eluted with buffer B (buffer A with 500 mM imidazole). The eluate was desalted using PD-10 desalting columns (GE Healthcare) and buffer C (100 mM NaCl, 25 mM Tris-HCl pH 8.0, 1 mM $MgCl_2$, 0.01 mM PLP, 0.1 mM dithiothreitol (DTT)). This was followed by purification on a size-exclusion column (Superdex 200 pg, HiLoad 16/600; GE Healthcare) connected to an ÄKTA Pure system (GE Healthcare) using buffer C. The concentrated protein solution (2 ml) was injected, and the flow was kept constant at 1 ml min^{-1}. Elution fractions containing pure protein were determined via SDS–PAGE analysis[44] on 12.5% gels. Purified enzymes in buffer C were used for crystallization or stored at −20 °C in buffer C containing 50% glycerol for later use in enzymatic assays.

BhcR was expressed and purified in the same way, except that buffer A contained 100 mM KCl, 20 mM HEPES-KOH pH 7.5, 10 mM $MgCl_2$, 4 mM β-mercaptoethanol, 5% glycerol and one tablet of SIGMAFAST protease inhibitor cocktail, EDTA-free per litre. Buffer C contained 100 mM KCl, 20 mM HEPES-KOH pH 7.5, 10 mM $MgCl_2$, 5% glycerol and 1 mM DTT.

NADH-dependent malate dehydrogenase (Mdh) and NADPH-dependent glyoxylate reductase (GhrA) from *E. coli* were overexpressed using the respective strains from the ASKA collection[45]. A starter culture in selective LB medium (34 μg ml^{-1} chloramphenicol) was inoculated from a single colony and left to grow overnight at 37 °C in a shaking incubator. The starter culture was used on the next day to inoculate an expression culture in selective TB medium at a 1:100 dilution. The expression culture was grown at 37 °C in a shaking incubator to an OD_{600} of 0.6, induced with 0.5 mM IPTG and grown another 4 h at 37 °C in a shaking incubator. The enzymes were affinity-purified in the same way as described above, except that buffer A contained 200 mM NaCl, 50 mM potassium phosphate pH 7.0, 15 mM imidazole, 1 mM β-mercaptoethanol and one tablet of SIGMAFAST protease inhibitor cocktail, EDTA-free per litre. Buffer C contained 100 mM NaCl, 50 mM potassium phosphate pH 7.0 and 0.1 mM DTT. The purified enzyme was stored at −20 °C in buffer C containing 50% glycerol.

Enzyme activity assays

For all enzyme assays, the oxidation of NADH or NADPH was followed at 340 nm or 360 nm on a Cary 60 UV-Vis photospectrometer (Agilent) in quartz cuvettes with a path length of 1 mm or 10 mm (Hellma Optik).

The enzyme assay to determine the kinetic parameters of BhcA with glyoxylate and L-aspartate as substrates was performed at 30 °C in a total volume of 300 μl. The reaction mixture contained 100 mM potassium phosphate buffer pH 7.5, 0.1 mM PLP, 0.2 mM NADH, different amounts of the respective substrates and 32 nM BhcA. Five hundred nanomolar Mdh was added as a coupling enzyme to convert oxaloacetate into malate. Kinetics for glyoxylate were measured with 20 mM L-aspartate; kinetics for L-aspartate were measured with 5 mM glyoxylate. To determine the kinetic parameters with oxaloacetate and glycine as substrates, the same assay mixture was used and 3 μM GhrA was added as a coupling enzyme to convert glyoxylate into glycolate. Kinetics for glycine were measured with 20 mM oxaloacetate; kinetics for oxaloacetate were measured with 30 mM glycine. To determine the kinetic parameters with L-serine or L-glutamate and glyoxylate as substrates, the same assay mixture was used and BhcB (3 μM), BhcC (1 μM) and Mdh (500 nM) were added as coupling enzymes. Kinetics for L-serine and L-glutamate were measured with 5 mM glyoxylate.

The enzyme assay to determine the kinetic parameters of BhcB was performed at 30 °C in a total volume of 300 μl. The reaction mixture contained 100 mM potassium phosphate buffer pH 7.5, 0.1 mM PLP, 0.2 mM NADH, different amounts of the substrate (2*R*, 3*S*)-β-hydroxyaspartate and 29 nM BhcB. Five hundred and eighty nanomolar BhcD was added as a coupling enzyme to convert iminosuccinate into L-aspartate. (2*R*, 3*S*)-β-Hydroxyaspartate was custom-synthesized by NewChem and was determined to be >95% pure by NMR analysis.

The enzyme assay to determine the kinetic parameters of BhcC with glyoxylate and glycine as substrates was performed at 30 °C in a total volume of 300 μl. The reaction mixture contained 100 mM potassium phosphate buffer pH 7.5, 0.1 mM PLP, 0.2 mM NADH, 0.5 mM $MgCl_2$, different amounts of the respective substrates and 4 nM BhcC. BhcB (200 nM) and BhcD (2 μM) were added as coupling enzymes. Kinetics

for glycine were measured with 5 mM glyoxylate; kinetics for glyoxylate were measured with 20 mM glycine. To determine the kinetic parameters with (2*R*, 3*S*)-β-hydroxyaspartate as substrate, the same assay mixture was used and 3 µM GhrA was added as a coupling enzyme to convert glyoxylate into glycolate. To determine the kinetic parameters with D-threonine as substrate, the same assay mixture was used and 3 µM alcohol dehydrogenase from *Saccharomyces cerevisiae* (Sigma-Aldrich) was added as coupling enzyme to convert acetaldehyde into ethanol.

The enzyme assay to determine the apparent kinetic parameters of BhcD was performed at 30 °C in a total volume of 250 µl. The reaction mixture contained 100 mM potassium phosphate buffer pH 7.5, 0.2 mM NADH, 0.1 mM PLP, different amounts of (2*R*, 3*S*)-β-hydroxyaspartate, and appropriate amounts of the enzymes BhcB and BhcD. Kinetics for iminosuccinate were measured with 15 nM BhcD, different amounts of (2*R*, 3*S*)-β-hydroxyaspartate and BhcB. To a given amount of (2*R*, 3*S*)-β-hydroxyaspartate, a tenfold molar excess of BhcB was added to start the reaction and completely and almost instantly convert the substrate pool into iminosuccinate. The initial reaction velocity of BhcD was determined after a mixing period of 3 s and the apparent concentration of iminosuccinate at this point in time was calculated on the basis of previously published values[23]. Kinetics for NADH and NADPH were measured with 2 mM (2*R*, 3*S*)-β-hydroxyaspartate, 214 nM BhcB, 28 nM BhcD and different amounts of the respective cofactor. No activity was measurable in a reaction mixture containing 100 mM potassium phosphate buffer pH 7.5, 0.2 mM NADH, 0.1 mM PLP and 3 mM oxaloacetate as well as 9 mM ammonium as putative substrates for BhcD.

The enzyme assay to generate iminosuccinate from (2*R*, 3*S*)-β-hydroxyaspartate (catalysed by BhcB) and further chemical reduction of iminosuccinate to L-aspartate with the reducing agent $NaBH_3CN$[46] was performed at 30 °C in a total volume of 1 ml. The reaction mixture contained 50 mM Tris pH 7.5, 1 mM (2*R*, 3*S*)-β-hydroxyaspartate, 0.1 mM PLP, 1 mM $MgCl_2$, 214 nM BhcB and 1 mM $NaBH_3CN$. The reaction was carried out in D_2O. Aliquots of 180 µl were taken after 0, 0.5, 1, 2 and 3 min and the reaction was immediately stopped by quenching with formic acid (4% final concentration). The samples were centrifuged at 17,000*g* and 4 °C for 15 min and the supernatant diluted 1:4 in double-distilled water for liquid chromatography–mass spectrometry (LC–MS) analysis. In negative control experiments, $NaBH_3CN$ was omitted from the reaction mixture. The same experiment was performed with added BhcD instead of $NaBH_3CN$ to enzymatically reduce iminosuccinate to L-aspartate. The reaction mixture contained 50 mM Tris pH 7.5, 1 mM (2*R*, 3*S*)-β-hydroxyaspartate, 2 mM NADH, 0.1 mM PLP, 1 mM $MgCl_2$, 214 nM BhcB and 28 nM BhcD.

LC–MS measurements were performed using an Agilent 6550 iFunnel Q-TOF LC–MS system equipped with an electrospray ionization (ESI) source set to negative ionization mode. LC was carried out as follows. The analytes were separated on an aminopropyl column (30 mm × 2 mm, particle size 3 µm, 100 Å; Luna NH2, Phenomenex) using a mobile phase system consisting of 95:5 20 mM ammonium acetate pH 9.3 (adjusted with ammonium hydroxide to a final concentration of approximately 10 mM): acetonitrile (A) and acetonitrile (B). Chromatographic separation was carried out using the following gradient condition at a flow rate of 250 µl min^{-1}: 0 min, 85% B; 3.5 min, 0% B, 7 min, 0% B; 7.5 min, 85% B; 8 min, 85% B. Column oven and autosampler temperature were maintained at 15 °C. The ESI source was set to the following parameters: capillary voltage was set at 3.5 kV and nitrogen gas was used as nebulizing (20 psig), drying (13 l min^{-1}, 225 °C) and sheath gas (12 l min^{-1}, 400 °C). The Q-TOF mass detector was calibrated before measurement using an ESI-L Low Concentration Tuning Mix (Agilent) with residuals and corrected residuals less than 2 ppm and 1 ppm, respectively. MS data were acquired with a scan range of 50–600 *m/z*. Autorecalibration was carried out using 113 *m/z* as reference mass. Subsequent peak integration of all analytes was performed using eMZed 2.29.4.0[47].

Enzyme activity assays in *P. denitrificans* cell extracts

P. denitrificans cultures were collected during mid-exponential phase (OD_{600} of 0.5–0.7), resuspended in ice-cold 100 mM potassium phosphate buffer (pH 7.2) and lysed by sonication. Cell debris was separated by centrifugation at 35,000*g* and 4 °C for 1 h. Total protein concentrations of the resulting cell-free extracts were determined by Bradford assay[48] using bovine serum albumin as standard. The assays for activity of BhcABCD were performed as described above, except that 100 mM potassium phosphate buffer pH 7.5 was replaced with 100 mM Tris pH 7.5. During BhcD assays, 90 µl samples were taken after 0.5, 1 and 2 min, and the reaction was immediately stopped by quenching with formic acid (4% final concentration). The samples were centrifuged at 17,000*g* and 4 °C for 15 min and the supernatant diluted 1:10 in double-distilled water for LC–MS analysis. L-Malate and L-aspartate in the samples were quantified using a standard curve of each compound ranging from 10 µM to 1,000 µM.

Genetic modification of *P. denitrificans*

The upstream and downstream flanking regions of the *bhcABCD* genes from *P. denitrificans* DSM 413 were cloned into the gene deletion vector pREDSIX[49]. To this end, the flanking regions were amplified from genomic DNA of *P. denitrificans* DSM 413 with the primers given in Supplementary Table 3. The resulting PCR products were used to perform Gibson assembly with the vector pREDSIX, which had been digested with MfeI. Subsequently, the resulting vector was digested with NdeI, and a kanamycin-resistance cassette, which had been cut out of the vector pRGD-Kan with NdeI, was ligated into the cut site to generate the final vectors for gene deletion. For gene deletion of each of the genes *bhcABCD* separately and of the complete bhc gene cluster, the corresponding plasmid was first transformed into chemically competent *E. coli* ST18[50] cells, which were then grown on LB agar plates containing 100 µg ml^{-1} ampicillin, 50 µg ml^{-1} kanamycin and 50 µg ml^{-1} aminolevulinic acid at 37 °C overnight. A culture in selective LB medium was inoculated the next day and left to grow overnight at 37 °C. The cultures were diluted the next morning to an OD_{600} of 0.1. A culture of wild-type *P. denitrificans* DSM 413 in LB medium was inoculated from a glycerol stock and grown at 30 °C. ST18 cultures were collected at an OD_{600} of around 0.7, and the *P. denitrificans* culture was collected at an OD_{600} of about 1.3. All cell pellets were washed once with sterile 10 mM $MgSO_4$ and resuspended to an OD_{600} of approximately 10 in sterile 10 mM $MgSO_4$. Suspensions of ST18 cells and *P. denitrificans* cells were mixed in a 2:1 ratio and spotted on minimal medium agar plates without any carbon source. Plates were incubated at 30 °C overnight. The next morning, spots were removed from the plates, resuspended in LB medium and plated on LB agar plates containing 25 µg ml^{-1} kanamycin. Plates were incubated at 30 °C for 3 days. The respective gene deletion was verified by colony PCR and DNA sequencing (Eurofins Genomics) and the deletion strain was propagated in selective LB medium.

High-throughput growth assays with *P. denitrificans* strains

Cultures of wild-type *P. denitrificans* DSM 413 and gene deletion strains were pre-grown at 30 °C in LB medium containing 25 µg ml^{-1} kanamycin, when necessary. Cells were collected, washed once with minimal medium containing no carbon source and used to inoculate growth cultures of 180 µl minimal medium containing an appropriate carbon source as well as 25 µg ml^{-1} kanamycin for gene deletion strains. Growth in 96-well plates (Thermo Fisher Scientific) was monitored at 30 °C at 600 nm in a Tecan Infinite M200Pro reader (Tecan). The resulting data were evaluated using GraphPad Prism 8.0.0.

Whole-cell shotgun proteomics

To acquire the proteome of *P. denitrificans* growing on different carbon sources, 30 ml cultures were grown to mid-exponential phase (OD_{600} of around 0.4) in minimal medium supplemented with 30 mM succinate

or 60 mM glycolate. Four replicate cultures were grown for each carbon source. Main cultures were inoculated from precultures grown in the same medium at a dilution of 1:1,000. Cultures were collected by centrifugation at 4,000*g* and 4 °C for 15 min. The supernatant was discarded and pellets were washed in 40 ml phosphate-buffered saline (PBS; 137 mM NaCl, 2.7 mM KCl, 10 mM Na_2HPO_4, 1.8 mM KH_2PO_4, pH 7.4). After washing, cell pellets were resuspended in 1 ml PBS, transferred into Eppendorf tubes and centrifuged as described above. Cell pellets in Eppendorf tubes were snap-frozen in liquid nitrogen and stored at −80 °C until they were used for the preparation of samples for LC–MS analysis and label-free quantification.

For protein extraction, bacterial cell pellets were resuspended in 4% SDS and lysed by heating (95 °C, 15 min) and sonication (Hielscher Ultrasonics). Reduction was performed for 15 min at 90 °C in the presence of 5 mM tris(2-carboxyethyl)phosphine followed by alkylation using 10 mM iodoacetamide at 25 °C for 30 min. The protein concentration in each sample was determined using the BCA protein assay kit (Thermo Fisher Scientific) following the manufacturer's instructions. Protein clean-up and tryptic digestion were performed using the SP3 protocol as previously described[51] with minor modifications regarding protein digestion temperature and solid-phase extraction of peptides. SP3 beads were obtained from GE Healthcare. Trypsin (1 µg, Promega) was used to digest 50 µg of total solubilized protein from each sample. Tryptic digestion was performed overnight at 30 °C. Subsequently, all protein digestions were desalted using C18 microspin columns (Harvard Apparatus) according to the manufacturer's instructions.

LC–MS/MS analysis of protein digestions was performed on a Q-Exactive Plus mass spectrometer connected to an electrospray ion source (Thermo Fisher Scientific). Peptide separation was carried out using an Ultimate 3000 nanoLC-system (Thermo Fisher Scientific), equipped with an in-house-packed C18 resin column (Magic C18 AQ 2.4 µm; Dr. Maisch). The peptides were first loaded onto a C18 precolumn (preconcentration set-up) and then eluted in backflush mode with a gradient from 98% solvent A (0.15% formic acid) and 2% solvent B (99.85% acetonitrile and 0.15% formic acid) to 25% solvent B over 105 min, continued from 25% to 35% of solvent B up to 135 min. The flow rate was set to 300 nl min^{-1}. The data acquisition mode for the initial label-free quantification study was set to obtain one high-resolution MS scan at a resolution of 60,000 (*m/z* 200) with a scanning range from 375 to 1,500 *m/z* followed by MS/MS scans of the 10 most intense ions. To increase the efficiency of MS/MS shots, the charged-state screening modus was adjusted to exclude unassigned and singly charged ions. The dynamic exclusion duration was set to 30 s. The ion accumulation time was set to 50 ms (both MS and MS/MS). The automatic gain control was set to 3×10^6 for MS survey scans and 1×10^5 for MS/MS scans. Label-free quantification was performed using Progenesis QI (v.2.0). MS raw files were imported into Progenesis and the output data (MS/MS spectra) were exported in MGF format. MS/MS spectra were then searched using MASCOT (v.2.5) against a database of the predicted proteome from *P. denitrificans* downloaded from the UniProt database (https://www.uniprot.org/; download date 26 January 2017), containing 386 common contaminant and background proteins that were manually added. The following search parameters were used: full tryptic specificity required (cleavage after lysine or arginine residues); two missed cleavages allowed; carbamidomethylation (C) set as a fixed modification; and oxidation (M) set as a variable modification. The mass tolerance was set to 10 ppm for precursor ions and 0.02 Da for fragment ions for high-energy collision dissociation. Results from the database search were imported back into Progenesis, mapping peptide identifications to MS1 features. The peak heights of all MS1 features annotated with the same peptide sequence were summed, and protein abundance was calculated per LC–MS run. Next, the data obtained from Progenesis were evaluated using the SafeQuant R package v.2.2.2[52]. Then, the 1% false-discovery rate of identification and quantification as well as the intensity-based absolute quantification values were calculated.

Electrophoretic mobility shift assays

Fluorescently labelled DNA fragments for electrophoretic mobility shift assays were generated by PCR from genomic DNA of *P. denitrificans* DSM 413. For the *Pbhc* regulatory region, primers Pbhc_fw and Pbhc_rev-dye were used to generate a 238-bp fragment containing the putative *Pbhc* promoter. The primers bhcA_fw and bhcA_rev-dye were used to generate a 255-bp fragment containing a fragment of the *bhcA* gene as negative control. The primers *Pbhc*_rev-dye and *bhcA*_rev-dye were 5′-labelled with the Dyomics 781 fluorescent dye (Microsynth). Binding reactions between the DNA fragments (0.025 pmol), various amounts of the purified protein BhcR (400×, 2,000×, 4,000×, 10,000×, 20,000× and 40,000× molar excess), and various concentrations of glyoxylate (0.01, 0.05, 0.1, 0.2, 0.5 and 1 mM final concentration) were performed in buffer A (20 mM potassium phosphate pH 7.0, 1 mM DTT, 5 mM $MgCl_2$, 50 mM KCl, 15 µg ml^{-1} bovine serum albumin, 50 µg ml^{-1} herring sperm DNA, 5% v/v glycerol, 0.1% Tween-20) in a total volume of 20 µl. After the reaction mixtures were incubated at 37 °C for 20 min, the samples were loaded onto a native 5% polyacrylamide gel and electrophoretically separated at 110 V for 60 min. BhcR–DNA interactions were detected using an Odyssey FC Imaging System (LI-COR Biosciences).

Crystallization and structure determination of BhcC and BhcD

The sitting-drop vapour-diffusion method was used for crystallization at 16 °C. Purified BhcC (10 mg ml^{-1}) was mixed in a 1:1 ratio with solution A containing 20% PEG 3350, 0.2 M ammonium chloride, pH 6.3 (final drop volume 1.4 µl). Reservoirs were filled with 40 µl solution A. Crystals appeared within 14 days. Crystals were briefly soaked in mother liquor supplemented with 40% glycerol for cryoprotection before freezing in liquid nitrogen.

Purified BhcD (10 mg ml^{-1}) was mixed in a 1:1 ratio with solution B containing 20% PEG 3350, 0.2 M $Mg(NO_3)_2$, 5 mM NAD^+ and 5 mM Tb-Xo4, pH 6.4 (final drop volume 4 µl). Various additives were tested to improve crystal quality and size. The best results were achieved with the recently described nucleating and phasing agent Tb-Xo4[53]. Reservoirs were filled with 114 µl of solution B. Crystals appeared within a week. Crystals were briefly soaked in mother liquor supplemented with 40% ethylene glycol for cryoprotection before freezing in liquid nitrogen.

X-ray diffraction data were collected at the beamlines ID29 and ID30B of the ESRF (Grenoble, France) and at beamline P13 of DESY (Hamburg, Germany). The data were processed with the XDS[54] (build 20180126) and CCP4 v.7.0 software packages[55]. The structures were solved by molecular replacement. For BhcC, the structure of a D-threonine aldolase (PDB 4V15)[56] served as search model. For BhcD, a homology model was made based on the structure of L-alanine dehydrogenase (PDB 1OMO)[57] using Swiss-Model[58]. This homology model was then used as search model for the molecular replacement. The molecular replacement was carried out using Phaser of the Phenix software package[59] (v.1.14), built with Phenix.Autobuild and refined with Phenix.Refine. Additional modelling, manual refining and ligand fitting was done in Coot[60] (v.0.8.9). Final positional and B-factor refinements, as well as water picking, were performed using Phenix.Refine. The structure models for BhcC and BhcD were deposited at the Protein Data Bank in Europe (PDBe) under PDB accession numbers 6QKB and 6RQA, respectively. Figures were made using Pymol 1.8.

Analysis of North Sea metagenome data

Searches for the bhc gene cluster in 38 assembled surface seawater metagenomes sampled at the island of Helgoland between 2010 and 2012 were performed using the *Ruegeria pomeroyi* DSS-3 bhc gene cluster proteins as reference (NCBI protein IDs WP_011241924.1 (BhcR), WP_011241925.1 (BhcA), WP_011241926.1 (BhcB), WP_011241927.1 (BhcC), WP_044029519.1 (BhcD)). All identified proteins of the 38 metagenomes were searched against these proteins using DIAMOND[61] BLASTp and post-filtered to those hits for which the entire gene cluster

could be detected on a metagenome contig. These contigs were, if possible, linked to metagenome-assembled genomes (MAGs) binned from the same 38 metagenomes. MAGs were binned as previously described[62] and both the metagenome assemblies and MAGs are accessible under accession PRJEB28156 at the European Nucleotide Archive (ENA). MAG quality was assessed using CheckM v.1.0.7[63]. Abundance estimates of MAGs and the single unbinned contig were calculated based on read mapping as reads per kilobase per million reads (RPKM; 2 RPKM ≈ 1% relative abundance detected by fluorescence in situ hybridization[28]). Read mapping of all 38 metagenomes to MAGs and the single unbinned contig was performed as previously described[62] using BBMap v.35.14 (http://bbtools.jgi.doe.gov).

Phylogenetic analyses

A genome tree of bacterial strains and five MAGs with the bhc gene cluster was calculated using GTDBtk v.0.1.3 with GTDB v.86[64]. GTDBtk uses an alignment of 120 bacterial marker genes to infer taxonomic relationships. The GTDBtk calculated tree was subsampled to the 264 bhc gene cluster containing bacterial strains and the MAGs and visualized using iTOL[65].

Sequences of BhcABCD from 264 bacterial isolates and 6 metagenome contigs (five of which were linked to MAGs) were aligned using MUSCLE[66], manually curated to remove gaps and concatenated. A phylogenetic tree of concatenated sequences of BhcABCD was calculated using raxmlGUI[67] 1.5b2 using the PROTGAMMA model with Le-Gascuel substitution matrix[68], 100 bootstraps and 100 maximum-likelihood resamplings. The resulting tree was visualized using iTOL.

Sequences from the ornithine cyclodeaminase/μ-crystalline superfamily (Conserved Domain accession cl27428) and the type III PLP-dependent enzymes superfamily (Conserved Domain accession cl00261) were downloaded from the NCBI protein database and aligned using MUSCLE. Phylogenetic trees of the aligned sequences were calculated with raxmlGUI 1.5b2 using the PROTGAMMA model with Le-Gascuel substitution matrix, 100 bootstraps and 100 maximum-likelihood resamplings. The resulting trees were visualized using iTOL.

In total, 1,614 protein sequences from the ornithine cyclodeaminase/μ-crystalline superfamily were used for generation of a sequence similarity network (SSN) using the EFI-EST web tool[69] with a cut-off value of 1×10^{-50}. In this SSN, all connected sequences that shared 80% or more identity were grouped into a single node, resulting in 619 meta nodes. The SSN was visualized with Cytoscape 3.7.1 (https://cytoscape.org) and edges between nodes with less than 50% identity were removed.

Analysis of *Tara* Oceans metagenomes

BhcC from *P. denitrificans* DSM 413 (Uniprot A1B8Z1) and Gcl from *Starkeya novella* DSM 506 (Uniprot D7A6R1) were used as queries to search the OM-RGC_v1 database using the Ocean Gene Atlas[70] web tool (http://tara-oceans.mio.osupytheas.fr/ocean-gene-atlas) with a cut-off value of 1×10^{-100}. The resulting hits were inspected and sequences that were deemed to not belong to BhcC or Gcl were removed. The following criteria were used: at least 50% of the query sequence covered; at least two of the three residues A160, A195, S313 present for BhcC sequences; residues V25, V51, L421, L476, L478, I479[71] present for Gcl sequences. The coordinates of sampling sites with positive hits for BhcC in samples from surface water (0.22–3-μm size fraction) were downloaded and visualized using Ocean Data View 5.1.5 (Schlitzer, R., Ocean Data View, odv.awi.de, 2018). Taxonomic assignments of BhcC and Gcl sequences were downloaded and manually converted to GTDB taxonomy. Sequence IDs are listed in Supplementary Data 2.

Environmental sample collection and processing

Sampling was carried out on each working day (Monday–Friday) with the RV *Aade* (https://www.awi.de/en/expedition/ships/more-ships.html) at the research site 'Kabeltonne' (54° 11.3′ N, 7° 54.0′ E) from approximately 1 m water depth in 20 l carboys. The water samples for microbial biomass were subjected to fractionating filtration directly upon arrival in the Biologische Anstalt Helgoland laboratory (typically less than one hour after sampling). Three membrane 142-mm diameter filtration units were operated in parallel to keep filtration times to a minimum. First, samples were pre-filtered through 142-mm diameter 10-μm-pore-size polycarbonate filters (Merck Chemicals) by means of an air-pressure pump to remove large particles and eukaryotic plankton. Then, the water samples were filtered with air-pressure pumps onto 142-mm diameter 3-μm-pore-size polycarbonate filters (Merck Chemicals) to collect predominantly bacteria associated with smaller particles and algae. Afterwards, dedicated aliquots were filtered onto 142-mm diameter 0.2-μm pore-size-polyethersulfone filters (Merck Chemicals) for DNA and RNA extraction. Bacterioplankton dominated this 0.2-μm fraction. The entire filtration process for all fractions was usually finished within 3 h, that is, latest 4 h after the sampling. All filters were stored at −80 °C until further analyses.

Total cell counts

Samples were fixed with 1% formaldehyde and filtered onto polycarbonate membrane filters as described above. Total cell counts were determined from 10 ml fixed seawater samples. One filter section was cut and stained with 4′,6-diamidino-2-phenylindole (DAPI, 1 μg ml^{-1}). The stained filters were analysed manually; the total cell count includes heterotrophic bacteria as well as autofluorescent cyanobacteria, but not picoeukaryotic cells.

Concentration of Chl *a*

The concentration of Chl *a* was determined in subsurface water on each working day (Monday–Friday) as part of the Helgoland Roads LTER time series (https://www.awi.de/en/science/biosciences/shelf-sea-system-ecology/working-groups/long-term-observations-lto.html). The concentration of Chl *a* was assessed from fluorescence data using an algal group analyser (bbe moldaenke).

Determination of glycolate concentrations

Once per week, 5 aliquots of 2 ml each were taken from the filtrate after 0.2-μm filtration and stored at −80 °C until analysis. Glycolate concentrations were measured after derivatization of the samples with 3-nitrophenylhydrazine as previously described[72]. LC–MS analyses were performed on an Agilent 6495B Triple Quad LC–MS system equipped with an electrospray ionization source. The analytes were separated on a RP-18 column (50 mm × 2.1 mm, particle size 1.8 μm, ZORBAX RRHD Eclipse Plus C18; Agilent) kept at 40 °C using a mobile phase system that consisted of 0.1% formic acid in water (A) and acetonitrile (B). The gradient was as follows: 0 min, 5% B; 1 min, 5% B; 6 min, 95% B; 6.5 min, 95% B; 7 min, 5% B at a flow rate of 250 μl min^{-1}. Samples were held at 15 °C and injection volume was 5 μl. MS/MS data were acquired in negative MRM mode. Capillary voltage was set at 3 kV and nitrogen gas was used as nebulizing (25 psig), drying (11 l min^{-1}, 130 °C) and sheath gas (12 l min^{-1}, 400 °C). The dwell time and fragmentor voltage were 20 ms and 380 V, respectively. Optimized collision energy used for the derivatized glycolate (210 $m/z \rightarrow 137$ m/z) was 22 V. LC–MS data were analysed and quantified using MassHunter Qualitative Navigator and QQQ Quantitative Analysis software (Agilent).

Determination of glycolate uptake rates

Samples for glycolate uptake measurements were collected on 10 April, 15 May and 29 May 2018. All samples were used after filtration through a 3-μm filter and divided into 4 live 40 ml subsamples in sterile plastic tubes wrapped in aluminium foil and incubated with 165 nM calcium [1-^{14}C]glycolate (American Radiolabelled Chemicals; 55 mCi $mmol^{-1}$, 0.1 mCi ml^{-1} in sterile water) at 12 °C for 8 h. Controls consisted of four 40 ml subsamples killed in 10% formalin for 1 h before addition of 165 nM calcium [1-^{14}C]glycolate. Glycolate uptake was monitored over time by withdrawing 5 ml aliquots from each subsample, filtering each aliquot

onto a 0.2-µm pore size Nuclepore polycarbonate filter (GE Healthcare), rinsing the filter 3 times with 5 ml of filter-sterilized sea water and measuring the radioactivity with a Tri-Carb 4910 TR liquid scintillation analyser (PerkinElmer) using the Ultima Gold scintillation cocktail (PerkinElmer). Glycolate uptake rates were determined by linear fit of the counts per minute measured on the filters over time. Uptake rates were corrected to account for the presence of non-radioactive glycolate in the samples.

DNA and RNA extraction, cDNA synthesis and qPCR

DNA and RNA was extracted from filters using the AllPrep Bacterial DNA/RNA/Protein Kit (Qiagen) according to the manufacturer's instructions. The RNA samples were treated with the TURBO DNA-free Kit (Thermo Fisher Scientific) according to the manufacturer's instructions to exclude contamination with DNA. DNA and RNA concentrations were determined using the Qubit dsDNA/RNA HS Assay Kit (Thermo Fisher Scientific) according to the manufacturer's instructions. In total, 2 µg of RNA was used for cDNA synthesis with the GoScript Reverse Transcription System (Promega) and random hexamers according to the manufacturer's instructions.

Degenerate primers for the *bhcC* gene were designed using the j-CODEHOP software[73–75] and an alignment of 207 *bhcC* sequences from bacterial strains isolated from marine habitats. Sequences were aligned using MUSCLE. Extracted DNA and cDNA of RNA were quantified using a CFX Connect Real-Time System (Bio-Rad). SYBR Green JumpStart Taq ReadyMix (Sigma-Aldrich) was used for the PCR amplification mixture according to the manufacturer's instructions. Final $MgCl_2$ concentration was 3 mM, and the amplification protocol consisted of an initial enzyme activation step at 95 °C for 5 min, followed by 45 cycles of 95 °C for 30 s, 60 °C for 30 s, and 72 °C for 45 s. Eight standard amounts ranging from 3×10^1 to 3×10^8 copies were run in triplicate for each set of analyses. Regression of all standard curves yielded an r^2 value of at least 0.998. All samples were run in triplicate. The starting copy numbers of *bhcC* in DNA and cDNA were calculated based on regression parameters of standard curves, and gene/transcript copy numbers per cell were calculated based on the volume of sea water filtered, the microbial cell count at the time of sampling, the amount of extracted DNA or RNA, and the volume of DNA or cDNA used per reaction. The degenerate primers were validated with genomic DNA of *P. denitrificans* DSM 413, *Rhodobacter sphaeroides* 2.4.1, and *E. coli* K-12 MG1655 as template using the same qPCR protocol as above. Standards for quantification were created by PCR using genomic DNA of *P. denitrificans* DSM 413 as template. Purified *bhcC* PCR product was quantified using the Qubit dsDNA HS Assay Kit (Thermo Fisher Scientific) according to the manufacturer's instructions.

Reporting summary

Further information on research design is available in the Nature Research Reporting Summary linked to this paper.

Data availability

The coordinates and structure factors of the crystal structures generated from this research are available at the PDB under accession numbers 6QKB and 6RQA. Mass spectrometry proteomics data are available via ProteomeXchange with the identifier PXD013274. MAGs are available under accession PRJEB28156 at the European Nucleotide Archive (ENA). All other relevant data are available in the Article and the Supplementary Information. Source Data for Figs. 2, 3 and Extended Data Fig. 1, 4, 5, 7–9 are provided with the paper.

41. Bertani, G. Studies on lysogenesis. I. The mode of phage liberation by lysogenic *Escherichia coli*. *J. Bacteriol.* **62**, 293–300 (1951).
42. Beijerinck, M. W. & Minkman, D. C. J. Bildung und Verbrauch von Stickoxydul durch Bakterien. *Zentralbl. Bakteriol. Naturwiss.* **25**, 30–63 (1910).
43. Hahnke, S. M., Moosmann, P., Erb, T. J. & Strous, M. An improved medium for the anaerobic growth of *Paracoccus denitrificans* Pd1222. *Front. Microbiol.* **5**, 18 (2014).
44. Laemmli, U. K. Cleavage of structural proteins during the assembly of the head of bacteriophage T4. *Nature* **227**, 680–685 (1970).
45. Kitagawa, M. et al. Complete set of ORF clones of *Escherichia coli* ASKA library (a complete set of *E. coli* K-12 ORF archive): unique resources for biological research. *DNA Res.* **12**, 291–299 (2005).
46. Lane, C. F. Sodium cyanoborohydride — a highly selective reducing agent for organic functional groups. *Synthesis* **1975**, 135–146 (1975).
47. Kiefer, P., Schmitt, U. & Vorholt, J. A. eMZed: an open source framework in Python for rapid and interactive development of LC/MS data analysis workflows. *Bioinformatics* **29**, 963–964 (2013).
48. Bradford, M. M. A rapid and sensitive method for the quantitation of microgram quantities of protein utilizing the principle of protein-dye binding. *Anal. Biochem.* **72**, 248–254 (1976).
49. Ledermann, R., Strebel, S., Kampik, C. & Fischer, H. M. Versatile vectors for efficient mutagenesis of *Bradyrhizobium diazoefficiens* and other Alphaproteobacteria. *Appl. Environ. Microbiol.* **82**, 2791–2799 (2016).
50. Thoma, S. & Schobert, M. An improved *Escherichia coli* donor strain for diparental mating. *FEMS Microbiol. Lett.* **294**, 127–132 (2009).
51. Moggridge, S., Sorensen, P. H., Morin, G. B. & Hughes, C. S. Extending the compatibility of the SP3 paramagnetic bead processing approach for proteomics. *J. Proteome Res.* **17**, 1730–1740 (2018).
52. Glatter, T. et al. Large-scale quantitative assessment of different in-solution protein digestion protocols reveals superior cleavage efficiency of tandem Lys-C/trypsin proteolysis over trypsin digestion. *J. Proteome Res.* **11**, 5145–5156 (2012).
53. Engilberge, S. et al. Crystallophore: a versatile lanthanide complex for protein crystallography combining nucleating effects, phasing properties, and luminescence. *Chem. Sci.* **8**, 5909–5917 (2017).
54. Kabsch, W. XDS. *Acta Crystallogr. D* **66**, 125–132 (2010).
55. Winn, M. D. et al. Overview of the CCP4 suite and current developments. *Acta Crystallogr. D* **67**, 235–242 (2011).
56. Uhl, M. K. et al. The crystal structure of d-threonine aldolase from *Alcaligenes xylosoxidans* provides insight into a metal ion assisted PLP-dependent mechanism. *PLoS ONE* **10**, e0124056 (2015).
57. Gallagher, D. T. et al. Structure of alanine dehydrogenase from *Archaeoglobus*: active site analysis and relation to bacterial cyclodeaminases and mammalian mu crystallin. *J. Mol. Biol.* **342**, 119–130 (2004).
58. Waterhouse, A. et al. SWISS-MODEL: homology modelling of protein structures and complexes. *Nucleic Acids Res.* **46**, W296–W303 (2018).
59. Adams, P. D. et al. PHENIX: a comprehensive Python-based system for macromolecular structure solution. *Acta Crystallogr. D* **66**, 213–221 (2010).
60. Emsley, P. & Cowtan, K. Coot: model-building tools for molecular graphics. *Acta Crystallogr. D* **60**, 2126–2132 (2004).
61. Buchfink, B., Xie, C. & Huson, D. H. Fast and sensitive protein alignment using DIAMOND. *Nat. Methods* **12**, 59–60 (2015).
62. Francis, T. B., Krüger, K., Fuchs, B. M., Teeling, H. & Amann, R. I. *Candidatus* Prosiliicoccus vernus, a spring phytoplankton bloom associated member of the *Flavobacteriaceae*. *Syst. Appl. Microbiol.* **42**, 41–53 (2019).
63. Parks, D. H., Imelfort, M., Skennerton, C. T., Hugenholtz, P. & Tyson, G. W. CheckM: assessing the quality of microbial genomes recovered from isolates, single cells, and metagenomes. *Genome Res.* **25**, 1043–1055 (2015).
64. Parks, D. H. et al. A standardized bacterial taxonomy based on genome phylogeny substantially revises the tree of life. *Nat. Biotechnol.* **36**, 996–1004 (2018).
65. Letunic, I. & Bork, P. Interactive tree of life (iTOL) v3: an online tool for the display and annotation of phylogenetic and other trees. *Nucleic Acids Res.* **44**, W242–W245 (2016).
66. Edgar, R. C. MUSCLE: multiple sequence alignment with high accuracy and high throughput. *Nucleic Acids Res.* **32**, 1792–1797 (2004).
67. Silvestro, D. & Michalak, I. raxmlGUI: a graphical front-end for RAxML. *Org. Divers. Evol.* **12**, 335–337 (2012).
68. Le, S. Q. & Gascuel, O. An improved general amino acid replacement matrix. *Mol. Biol. Evol.* **25**, 1307–1320 (2008).
69. Gerlt, J. A. et al. Enzyme Function Initiative-Enzyme Similarity Tool (EFI-EST): A web tool for generating protein sequence similarity networks. *Biochim. Biophys. Acta* **1854**, 1019–1037 (2015).
70. Villar, E. et al. The Ocean Gene Atlas: exploring the biogeography of plankton genes online. *Nucleic Acids Res.* **46**, W289–W295 (2018).
71. Kaplun, A. et al. Glyoxylate carboligase lacks the canonical active site glutamate of thiamine-dependent enzymes. *Nat. Chem. Biol.* **4**, 113–118 (2008).
72. Han, J., Gagnon, S., Eckle, T. & Borchers, C. H. Metabolomic analysis of key central carbon metabolism carboxylic acids as their 3-nitrophenylhydrazones by UPLC/ESI-MS. *Electrophoresis* **34**, 2891–2900 (2013).
73. Rose, T. M. et al. Consensus-degenerate hybrid oligonucleotide primers for amplification of distantly related sequences. *Nucleic Acids Res.* **26**, 1628–1635 (1998).
74. Rose, T. M., Henikoff, J. G. & Henikoff, S. CODEHOP (consensus-degenerate hybrid oligonucleotide primer) PCR primer design. *Nucleic Acids Res.* **31**, 3763–3766 (2003).
75. Boyce, R., Chilana, P. & Rose, T. M. iCODEHOP: a new interactive program for designing consensus-degenerate hybrid oligonucleotide primers from multiply aligned protein sequences. *Nucleic Acids Res.* **37**, W222–W228 (2009).

Acknowledgements We thank L. Franzmeyer and K.-P. Rücknagel as well as the crew of the *Aade* and the staff at the Biological Station at Helgoland (BAH) for sample collection and processing; K. H. Wiltshire for providing Chl *a* data collected at BAH; S. Vidal-Melgosa, A. Bolte and J.-H. Hehemann for sharing samples; T. Ferdelman for help with radioactive tracer work; B. Vögeli, T. Schwander, G. Stoffel and S. Burgener for helpful discussions. We acknowledge the support from the staff scientists at the European Synchrotron Radiation Facility Grenoble,

France (ESRF, beamlines ID29 & ID30B) as well as at the Deutsches Elektronen-Synchrotron Hamburg, Germany (DESY, beamline P13). Metagenome sequences were obtained within the COGITO (Coastal Microbe Genomic and Taxonomic Observatory) project granted to H. Teeling (MPI Bremen) as a community sequencing project by the Department of Energy's Joint Genome Institute in Walnut Creek, CA, USA (Proposal ID 998; https://doi.org/10.25585/1488076). This study was funded by the Max-Planck-Society (R.I.A. and T.J.E.), FET-Open Grant 686330 (Future Agriculture) and the German Research Foundation (SFB987 'Microbial diversity in environmental signal response' and FOR 2406 'Proteogenomics of marine polysaccharide utilization').

Author contributions L.S.v.B. identified the bhc gene cluster, purified proteins, performed enzyme kinetic analysis, qPCR, phylogenetic analysis and analysis of *Tara* Oceans metagenomes, generated and characterized mutant *P. denitrificans* strains and measured glycolate uptake rates. F. Severi performed enzyme kinetic analysis, crystallization of BhcD and enzyme assays in *P. denitrificans* cell-free extracts. K.K. performed phylogenetic analysis and analysis of Helgoland metagenomes. L.H. performed gel shift assays with BhcR. A.G. performed crystallization of BhcC. F. Sippel performed enzyme kinetic analysis. B.P. generated mutant *P. denitrificans* strains. P.C. and N.S.C. performed small-molecule mass spectrometry. T.G. performed mass spectrometry for proteomics. J.Z. collected X-ray datasets, solved, refined and analysed crystal structures. B.M.F. and R.I.A. planned and supervised fieldwork at Helgoland and provided reagents. L.S.v.B., E.B., S.Z., U.G.M., R.I.A. and T.J.E. planned experiments, analysed data and supervised the project. L.S.v.B. and T.J.E. wrote the manuscript, with contributions from all other authors.

Competing interests The Max-Planck-Gesellschaft zur Förderung der Wissenschaften is the patent applicant for the following three patents. All patent applications are pending. L.S.v.B. and T.J.E. have filed European patent no. EP 19190404.4 for the production of plants with altered photorespiration due to implementation of the BHAC. L.S.v.B., J.Z. and T.J.E. have filed European patent no. EP 18167406.0 for the production of photoautotrophic organisms with altered photorespiration due to implementation of the BHAC. L.S.v.B. and T.J.E. have filed European patent no. 18211454.6 for the enantioselective preparation of primary amine compounds using the enzyme BhcD or its homologues.

Additional information

Supplementary information is available for this paper at https://doi.org/10.1038/s41586-019-1748-4.

Correspondence and requests for materials should be addressed to L.S.v.B. or T.J.E.

a

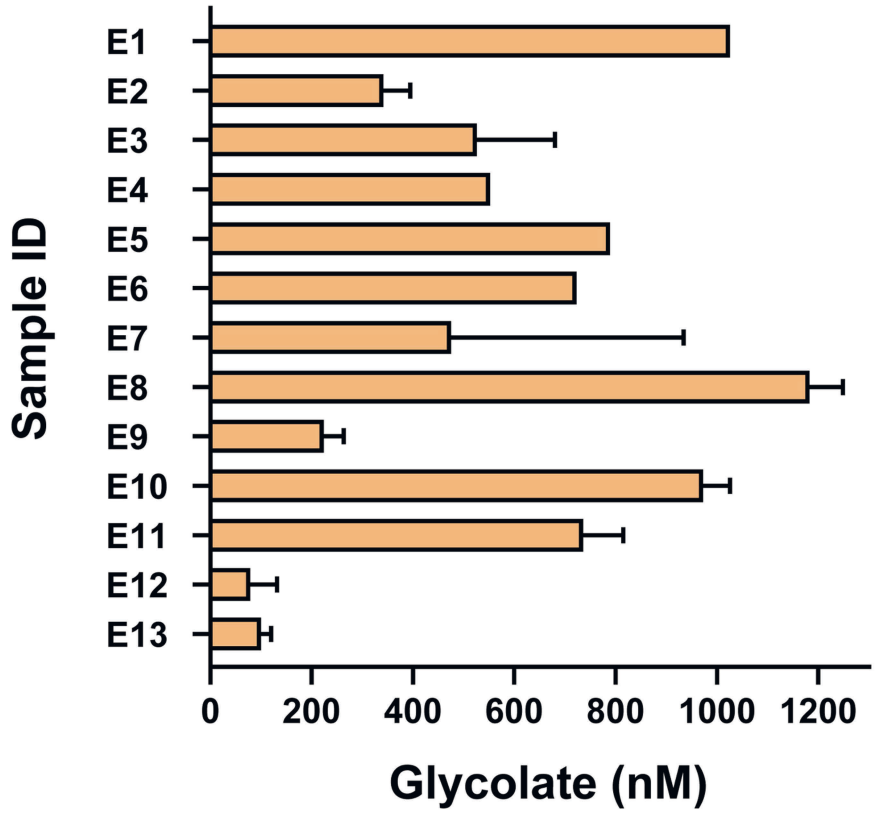

b

Sample ID	Sample	Maximum glycolate concentration [nM]	Analytical method	Reference
E1	Coastal seawater (Ipswich Bay, MA, USA)	1,026	Colorimetry	30
E2	Atlantic Ocean (51°40' S, 57°48' W)	342 ± 53	Colorimetry	31
E3	Antarctic lake (60°42' S, 45°37' W)	526 ± 154		
E4	Coastal seawater (Ipswich Bay, MA, USA)	552	Colorimetry	2
E5	Coastal seawater (Menai Straits, Anglesey, UK)	789	Colorimetry	32
E6	Coastal seawater (Ipswich Bay, MA, USA)	723	Colorimetry	1
E7	Coastal seawater (New York Bight, NY, USA)	475 ± 459	Colorimetry	33
E8	Mediterranean Sea (42°28' N, 30°16' E)	1,183 ± 66	HPLC	10
E9	Atlantic Ocean (oligotrophic waters, 21°01'54" N, 31°09'62" W)	224 ± 39	HPLC	11
E10	Atlantic Ocean (mesotrophic waters, 18°27'22" N, 21°10'18" W)	973 ± 53		
E11	Atlantic Ocean (eutrophic waters, 20°31'49" N, 18°34'39" W)	736 ± 79		
E12	Mediterranean Sea (43°25' N, 7°52' E)	79 ± 53	GC	34
E13	Coastal seawater (Dabob Bay, WA, USA)	100 ± 20	HPLC	4
C1	Culture of *Chlorella*	39,450 – 105,190	^{14}C-tracing	9
C2	Culture of *Euglena gracilis*	591,720	Colorimetry	35
C3	Culture of *Chaetoceros socialis*	240,630	Colorimetry	36
C4	Culture of *Dunaliella tertiolecta*	19,500 ± 1125	HPLC	37
C5	Culture of *Thalassiosira weissflogii*	799	HPLC	38
C6	Culture of *Prochlorococcus* MED4 (phosphorus-limited)	1873 ± 375	HPLC	39
C7	Culture of *Prochlorococcus* MED4 (phosphorus-replete)	2831 ± 458		
C8	Culture of *Prochlorococcus* MIT9312 (phosphorus-limited)	749 ± 916		
C9	Culture of *Prochlorococcus* MIT9312 (phosphorus-replete)	333 ± 125		

Extended Data Fig. 1 | Previously reported glycolate concentrations in environmental samples and cultures of photosynthetic organisms. a, Bar diagram of glycolate concentrations as previously reported in environmental samples. For details on samples, replicates, and analytics see **b** and the literature cited therein. **b**, Table of glycolate concentrations as previously reported in environmental samples (E1, E2 and so on) and cultures of photosynthetic organisms (C1, C2 and so on). When reported in the reference[1,2,4,9–11,30–39], the mean value ± error is given.

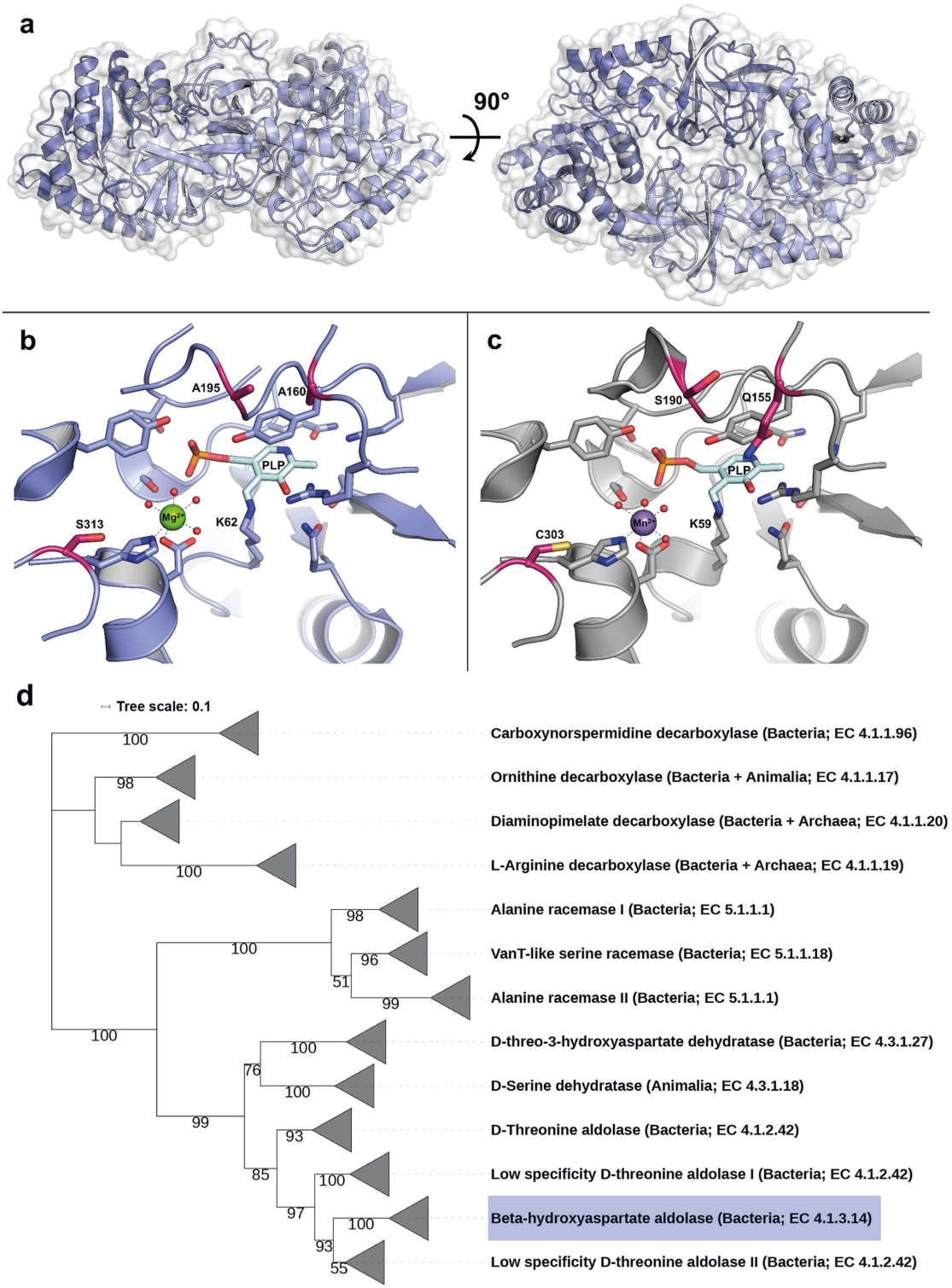

Extended Data Fig. 2 | Crystal structure and phylogenetic analysis of the β-hydroxyaspartate aldolase BhcC. a, Cartoon representation of the β-hydroxyaspartate aldolase homodimer (PDB 6QKB) with superimposed protein surface (left, side view; right, top view). **b**, Active site of β-hydroxyaspartate aldolase with covalently bound PLP (light cyan). Active site residues highlighted in pink (A160, A195 and S313) are completely conserved only among β-hydroxyaspartate aldolases, but differ in D-threonine aldolases. **c**, Active site of D-threonine aldolase (PDB 4V15). The corresponding conserved residues among D-threonine aldolases (Q155, S190 and C303) are highlighted as in **b**. **d**, Maximum likelihood phylogenetic tree of the type III PLP-dependent protein superfamily. Sequences of the β-hydroxyaspartate aldolase BhcC and its homologues form a distinct clade (blue) within the D-threonine aldolase branch of this superfamily. Bootstrap values of at least 50 are given on the respective nodes.

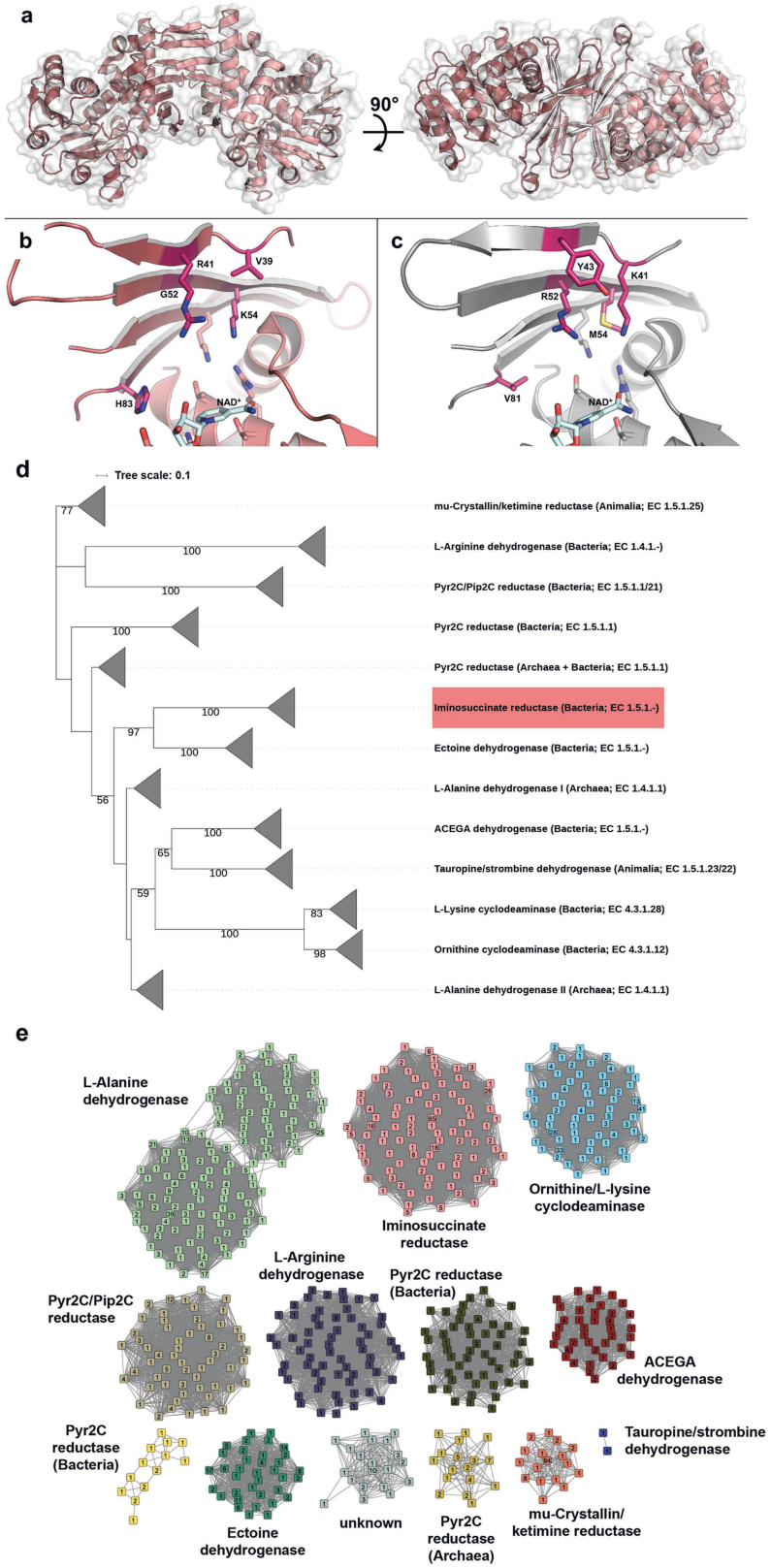

Extended Data Fig. 3 | Crystal structure and phylogenetic analysis of the iminosuccinate reductase BhcD. a, Cartoon representation of the iminosuccinate reductase homodimer (PDB 6RQA) with superimposed protein surface (left, side view; right, top view). **b**, Active site of BhcD with bound NAD^+ (light cyan). Residues highlighted in pink (V39, R41, G52, K54 and H83) may contribute to substrate binding and are conserved among iminosuccinate reductases, but differ in L-alanine dehydrogenases. **c**, Active site of L-alanine dehydrogenase (PDB 1OMO). The corresponding conserved residues among L-alanine dehydrogenases (K41, Y43, R52, M54 and V81) are highlighted as in **b**. **d**, Maximum likelihood phylogenetic tree of the ornithine cyclodeaminase/μ-crystalline protein superfamily. Sequences of the iminosuccinate reductase BhcD and its homologues form a distinct clade (red) within this superfamily. Bootstrap values of at least 50 are given on the respective nodes. **e**, Sequence similarity network of 1,614 sequences from the ornithine cyclodeaminase/μ-crystalline protein superfamily. Connected sequences with more than 80% identity are clustered into nodes. The number in each node gives the number of sequences contained within. Nodes with more than 50% identity are connected by edges. Similar to the phylogenetic analysis shown in **d**, sequences of the iminosuccinate reductase BhcD and its homologues form a distinct clade (red) within this superfamily.

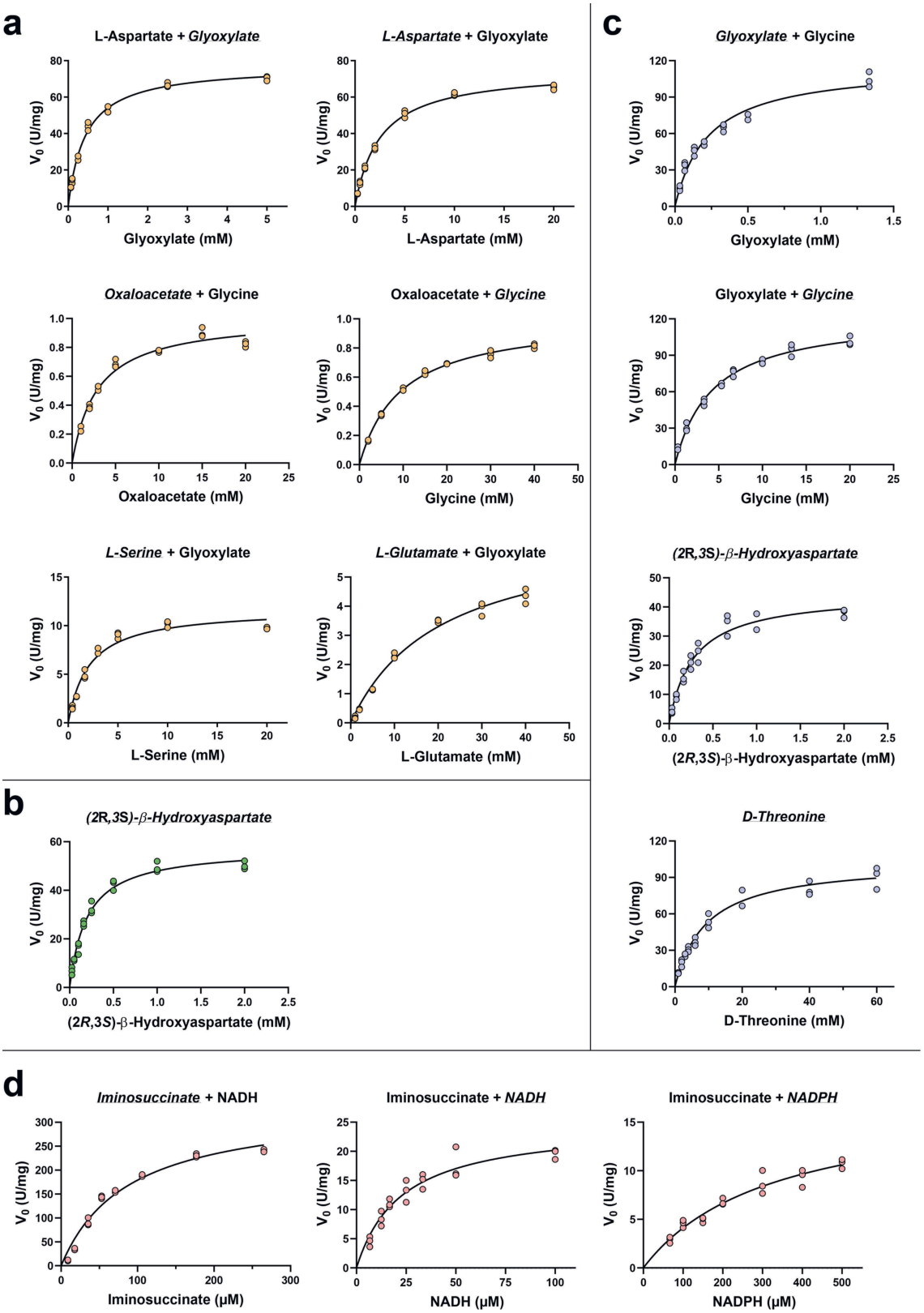

Extended Data Fig. 4 | Michaelis–Menten kinetics of all enzyme reactions characterized in this study. a, Michaelis–Menten kinetics for aspartate–glyoxylate aminotransferase (BhcA). **b**, Michaelis–Menten kinetics for β-hydroxyaspartate dehydratase (BhcB). **c**, Michaelis–Menten kinetics for β-hydroxyaspartate aldolase (BhcC). **d**, Michaelis–Menten kinetics for iminosuccinate reductase (BhcD). **a**–**d**, Data are shown from $n = 3$ independent experiments at different substrate concentrations. The data are summarized in Table 1.

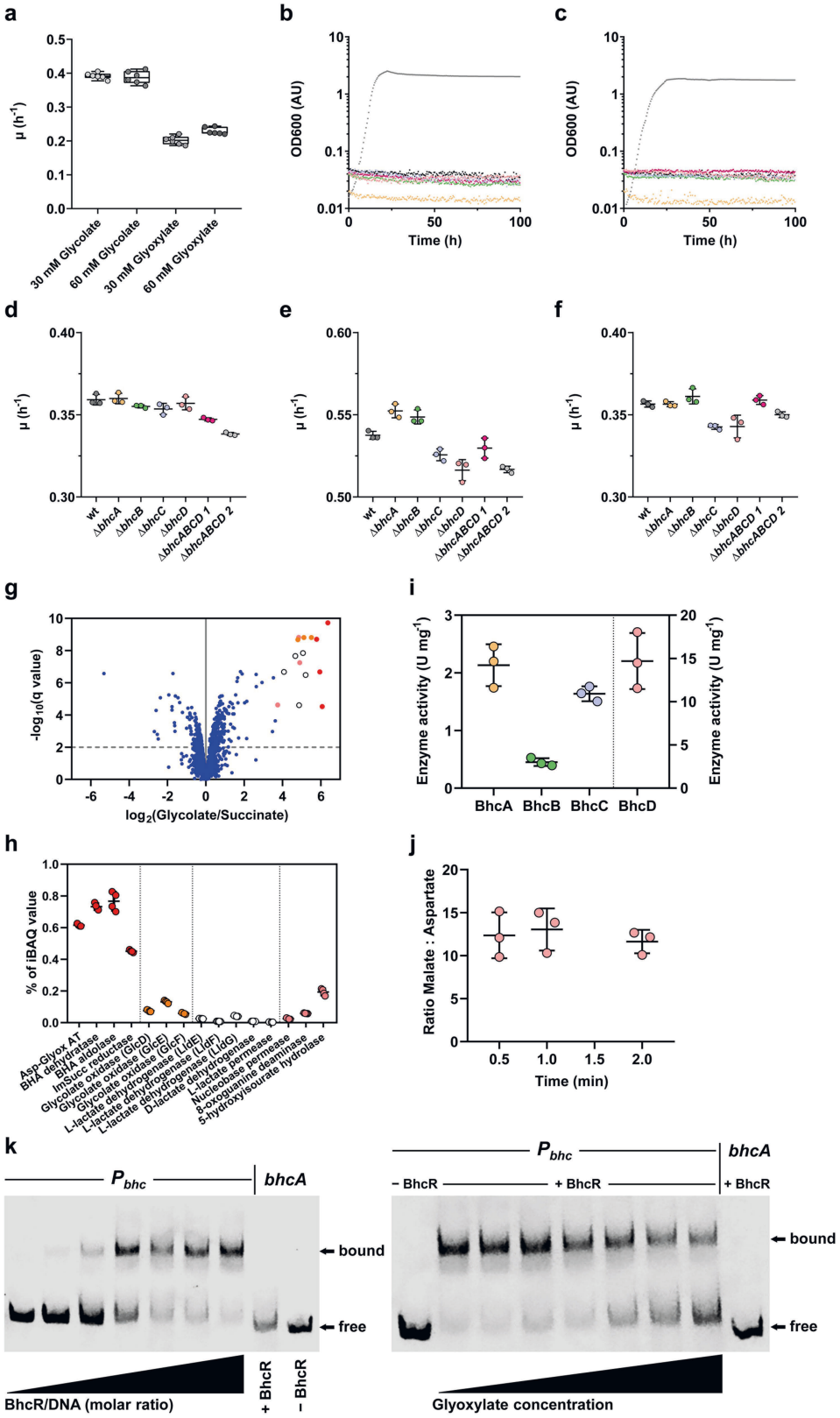

Extended Data Fig. 5 | See next page for caption.

Extended Data Fig. 5 | Physiological role of the BHAC in *P. denitrificans* DSM 413. a, Growth rate of wild-type *P. denitrificans* DSM 413 on the BHAC substrates glycolate and glyoxylate. The middle line and box are the median and interquartile range of $n = 6$ independent experiments and the whiskers indicate the maximum range of the dataset. **b**, **c**, Representative growth curves of wild-type *P. denitrificans* DSM 413 (grey) and bhc deletion strains (coloured) grown in the presence of 60 mM glycolate (**b**) or 60 mM glyoxylate (**c**). Deletion of any single gene in the bhc gene cluster is sufficient to completely abolish growth in the presence of glycolate and glyoxylate. These experiments were repeated three times independently with similar results. **d**–**f**, Growth rates (μ) of wild-type *P. denitrificans* DSM 413 (grey) and BHAC deletion strains (coloured) grown in the presence of 60 mM acetate (**d**), 30 mM succinate (**e**) or 20 mM glucose (**f**). Deletion of any single gene in the bhc gene cluster, or of the whole bhc gene cluster, still permits growth on acetate, succinate or glucose with comparable growth rates as for the wild type. Data are the mean ± s.d. of $n = 3$ independently grown cultures. **g**, Analysis of the proteome of glycolate-grown compared to succinate-grown *P. denitrificans* DSM 413. All proteins that were quantified by at least three unique peptides are shown. The 15 proteins that showed the strongest increase in abundance are marked in the volcano plot. The four enzymes of the BHAC are marked in red, the three subunits of glycolate oxidase in orange, the proteins of a putative operon for lactate utilization in white and the proteins directly downstream of the bhc gene cluster in light red. **h**, The abundance of these proteins, given as the percentage of the intensity-based absolute quantification (iBAQ) value. Data are the mean ± s.d. of $n = 4$ independently grown cultures. **i**, Specific activities of BHAC enzymes in cell-free extracts of glycolate-grown *P. denitrificans* DSM 413, as measured spectrophotometrically. Note that the activity of BhcD is plotted on the right *y* axis and consists of the actual iminosuccinate reductase activity (iminosuccinate to L-aspartate) as well as endogenous malate dehydrogenase activity (oxaloacetate to L-malate). **j**, Ratio of malate to aspartate determined by LC–MS during the enzyme assay for BhcD activity. The ratio remains approximately constant at 12:1, indicating that only approximately 8% of the activity (around 1.3 U mg^{-1}) shown in **i** can be ascribed to iminosuccinate reductase. **i**, **j**, Data are the mean ± s.d. of $n = 3$ independently grown cultures; each data point represents the mean of $n = 3$ technical replicates. **k**, DNA-binding properties of BhcR. Left, a fluorescently labelled DNA fragment carrying the putative promoter region of the bhc gene cluster (P_{bhc}) was incubated with increasing amounts of purified BhcR protein and subsequently separated by electrophoresis to visualize DNA bound to BhcR and free DNA; a DNA fragment derived from the coding region of *bhcA* was used as a negative control. BhcR specifically forms a complex with the DNA fragment containing the putative promoter region of the bhc gene cluster. Right, the P_{bhc}–BhcR complex was incubated with increasing concentrations of glyoxylate and subsequently separated by electrophoresis to assess the effect of glyoxylate on complex formation; the *bhcA* DNA fragment together with BhcR was used as a negative control. Increasing concentrations of glyoxylate decrease the binding of BhcR to the P_{bhc} DNA fragment. For gel source data, see Supplementary Fig. 1.

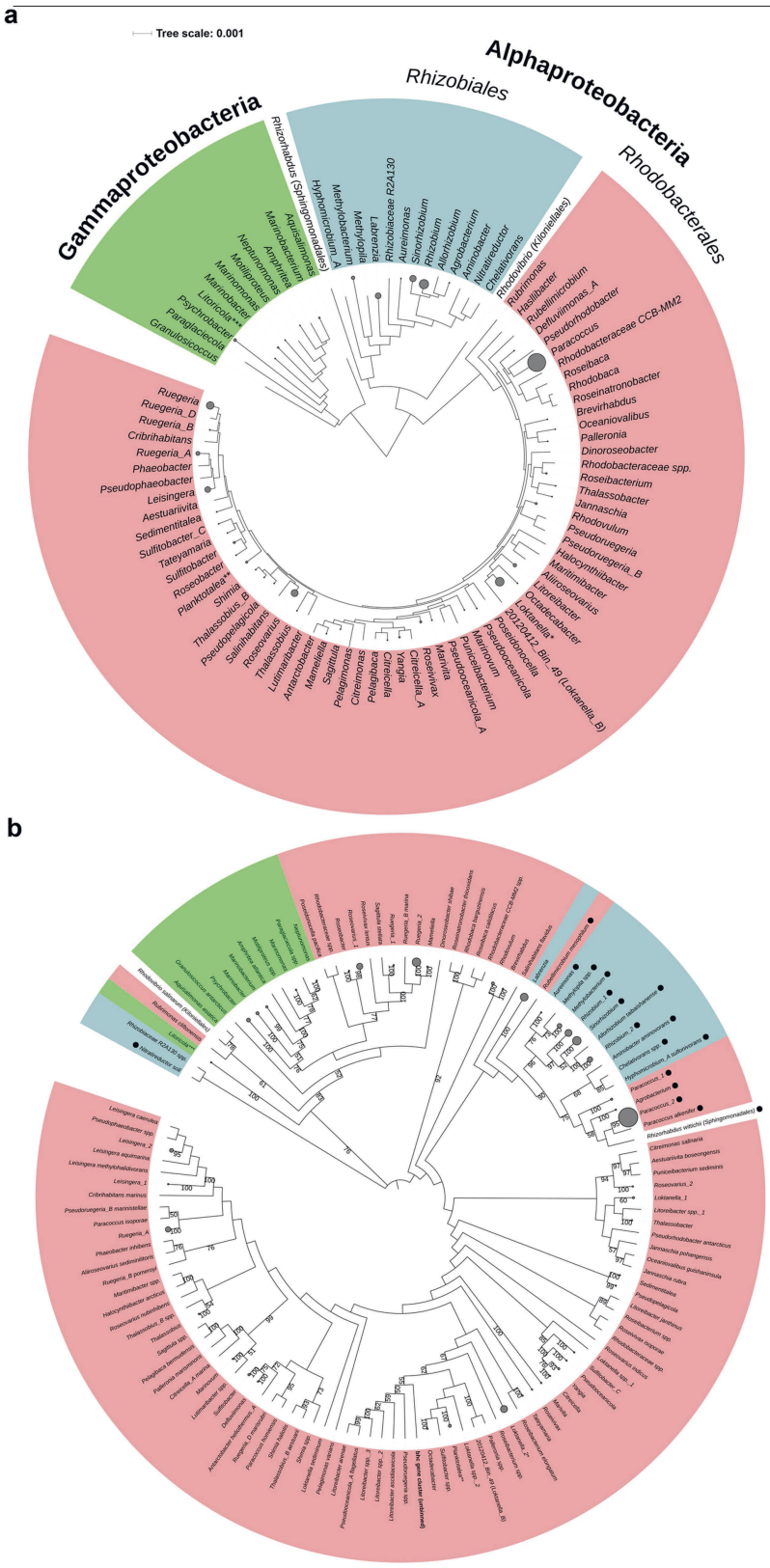

Extended Data Fig. 6 | Phylogenetic analysis of the bhc gene cluster.

a, Genome-based maximum likelihood phylogenetic tree of bacterial strains with the bhc gene cluster. The bhc gene cluster is found in Gammaproteobacteria (green), and in the alphaproteobacterial orders Rhizobiales (blue) and Rhodobacterales (red), as well as in one member each of Sphingomonadales and Kiloniellales. The phylogenetic tree is based on an alignment of 120 bacterial marker genes from 264 publicly available bacterial genomes and 5 MAGs and was calculated using GTDB-Tk[64] (https://github.com/Ecogenomics/GtdbTk). If several strains from the same genus cluster together, nodes are collapsed at the genus level, and the size of the resulting circle corresponds to the respective number of strains. Loktanella*: collapsed node contains the MAGs 20110516_Bin_8_1 and 20110523_Bin_9_1; Planktotalea**: collapsed node contains the MAG 20110523_Bin_97_1; Litoricola***: collapsed node contains the MAG 20110526_Bin_19_1. **b**, Maximum likelihood phylogenetic tree of concatenated BHAC enzyme sequences. Colour code is the same as in **a**. Phylogenetic groups that were mostly isolated from terrestrial or freshwater habitats are marked with a black dot. Comparison with **a** reveals that the sequences of the BHAC enzymes are not phylogenetically representative, as, for example, alpha- and gammaproteobacterial sequences form a common branch and sequences from terrestrial or freshwater Rhizobiales and Rhodobacterales form another common branch. This suggests that the bhc gene cluster might have been subject to horizontal gene transfer between distantly related strains in shared habitats. The environmental bhc gene cluster sequence that could not be binned successfully is marked in bold and clusters together with isolated representatives of *Pseudoruegeria*, *Litoreibacter* and *Pseudooceanicola*. The phylogenetic tree is based on the concatenated alignments of the 4 enzymes (BhcA–BhcD) from 264 publicly available bacterial genomes and from 6 metagenome contigs. It was calculated using raxmlGUI[67]. Bootstrap values of at least 50 are given on the respective nodes; calculated branch lengths of the tree are ignored for the sake of better visualization. If several strains from the same genus cluster together, nodes are collapsed at the genus level, and the size of the resulting circle corresponds to the respective number of strains. If strains from the same genus cluster in more than one node, the respective branches are labelled as Genus_1, Genus_2, and so on, in a clockwise manner. Loktanella_2*: collapsed node contains the MAGs 20110516_Bin_8_1 and 20110523_Bin_9_1; Planktotalea**: collapsed node contains the MAG 20110523_Bin_97_1; Litoricola***: collapsed node contains the MAG 20110526_Bin_19_1. **a**, **b**, Taxonomy is based on GTDB (release 03-RS86; http://gtdb.ecogenomic. org/). All strains contained in the phylogenetic trees are listed in Supplementary Data 1.

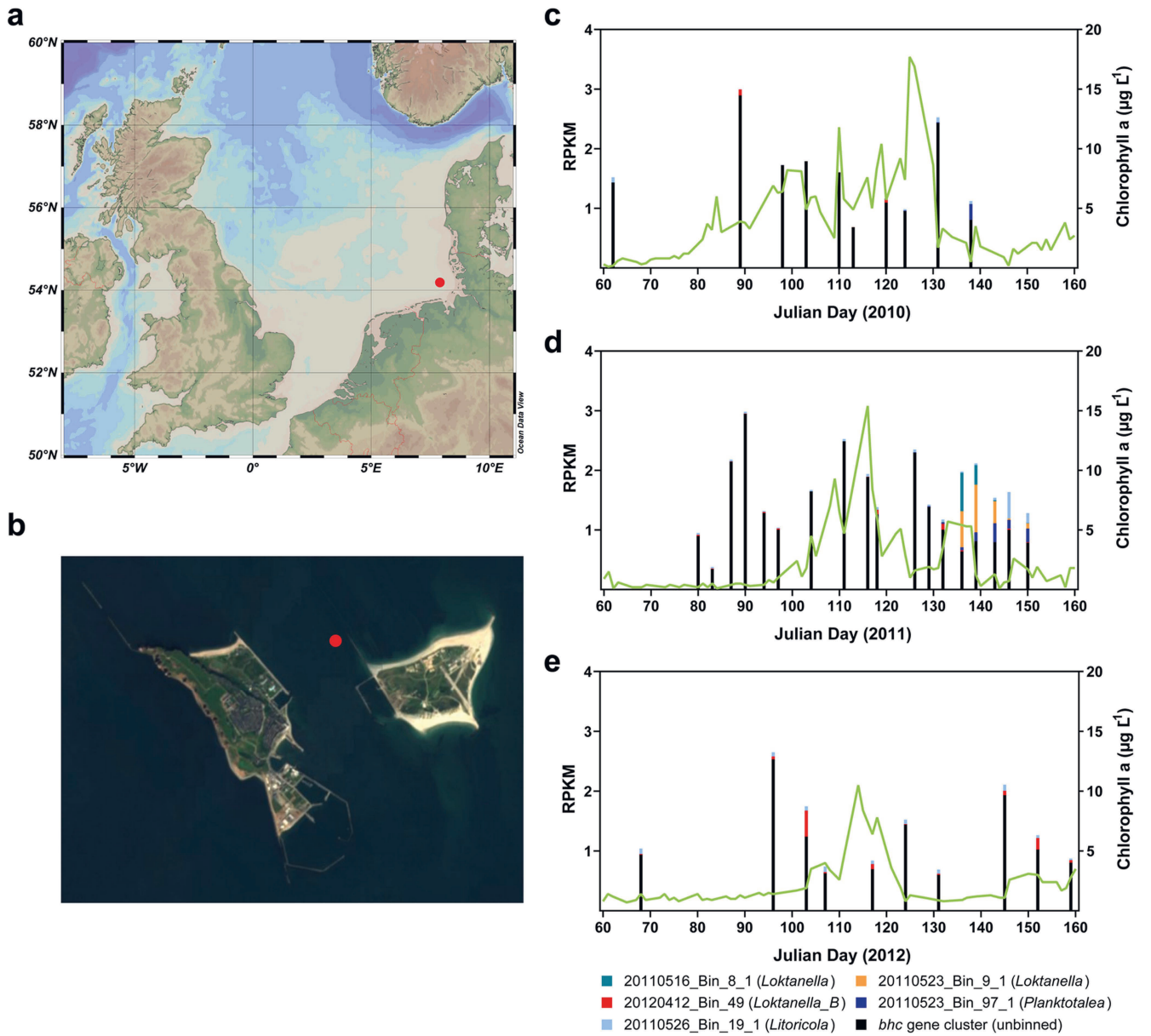

Extended Data Fig. 8 | Abundance of the bhc gene cluster in Helgoland metagenomes. a, The location of Helgoland Island approximately 40 km offshore the northern German coastline in the North Sea is marked with a red dot. The map was made with Ocean Data View 5.1.5 (R. Schlitzer, Ocean Data View, odv.awi.de, 2018). **b**, The long-term ecological research site 'Kabeltonne' (red dot: 54° 11.3′ N, 7° 54.0′ E) is located between Helgoland Island (left) and the small island Düne (right). Satellite image from WorldWind Explorer (B. Schubert, worldwind.earth/explorer, 2016–2018); the image was adapted to indicate the sampling site. **c**–**e**, Abundance of the bhc gene cluster (in RPKM) was calculated in 38 metagenomes from samples collected during the algal spring blooms of 2010 to 2012 in the North Sea close to Helgoland[28]. Six different sequences were investigated, five of which could be assigned to metagenome bins (Extended Data Fig. 6 and Supplementary Data 3), whereas the remaining, most abundant sequence (black) could not be binned successfully.

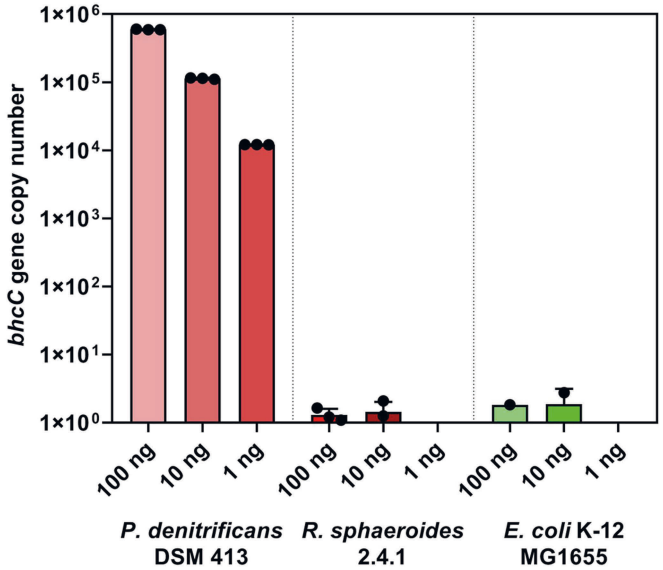

Extended Data Fig. 9 | Validation of degenerate *bhcC* primers. Degenerate primers for *bhcC* were used for qPCR with different amounts of genomic DNA from *P. denitrificans* DSM 413, *Rhodobacter sphaeroides* 2.4.1, and *E. coli* K-12 MG1655 as template. While the *bhcC* gene from *P. denitrificans* DSM 413 is amplified, genomic DNA from organisms that lack the bhc gene cluster does not result in reliable amplification. Data are mean ± s.d.; $n = 3$ independent experiments.

Extended Data Table 1 | X-ray diffraction data collection and model refinement statistics

	β-hydroxyaspartate aldolase with bound pyridoxalphosphate (PDB ID 6QKB)	iminosuccinate reductase with bound NAD^+ (PDB ID 6RQA)
Data collection		
Space group	$P\,2_1\,2_1\,2_1$	$P\,2_1\,2_1\,2_1$
Cell dimensions		
a, *b*, *c* (Å)	66.60, 75.25, 157.31	50.39, 72.41, 164.27
α, β, γ (°)	90.00, 90.00, 90.00	90.00, 90.00, 90.00
Resolution (Å)	29.03 - 1.70 (1.79 - 1.70)	29.40 – 2.56 (2.70 – 2.56)
R_{merge}	0.134 (0.858)	0.097 (0.527)
$I / \sigma I$	10.4 (1.9)	12.6 (3.3)
$CC_{1/2}$ (%)	99.7 (70.8)	99.8 (90.7)
Completeness (%)	99.8 (99.0)	99.9 (100.0)
Redundancy	6.7 (6.5)	6.5 (6.5)
Refinement		
Resolution (Å)	29.03 - 1.70 (1.74 - 1.70)	29.40 – 2.56 (2.70 – 2.56)
No. unique reflections	87194 (5909)	20152 (2893)
R_{work} / R_{free}	0.158 / 0.177	0.176 / 0.225
No. atoms	6671	5027
Protein	5817	4780
Ligands	32	120
Water	822	127
B-factors		
Protein	17.05	52.02
Ligands	23.66	66.03
Water	31.58	47.34
R.m.s. deviations		
Bond lengths (Å)	0.006	0.004
Bond angles (°)	0.84	0.52

Numbers in parentheses indicate statistics for the highest resolution shell. The structures were determined from single crystals.

6.3 Unsubmitted Manuscript

Ectoine metabolism: A diverse field with differing modes

Manuscript

Ectoine metabolism: A diverse field with differing modes

Lucas Hermann[1]

The following draft “Ectoine metabolism: A diverse field with differing modes” is an unpublished manuscript. I performed all bioinformatic analysis experiments included except one protein model alignment performed by Felix Dempwolff in this text and wrote the preliminary manuscript.

Manuscript

Ectoine metabolism: A diverse field with differing modes

Lucas Hermann[1]

[1]Philipps-University Marburg, Faculty of Biology, Karl-von-Frisch Strasse 8, 35043, Marburg, Germany.

INTRODUCTION

To resist changing osmolarities in their environments, microorganisms must adapt the osmotic pressure (turgor) inside their cells. Without this feature, microbes would permanently face the dangers of either dehydrating and collapsing (Bremer and Krämer, 2000; Wood, 2011; van den Berg *et al.*, 2017), or bursting (Levina *et al.*, 1999; Hoffmann *et al.*, 2008; van den Berg *et al.*, 2017), due to the shifting osmotic potential. For this task many microorganisms make use of small, osmotically active organic molecules, the so-called compatible solutes (Kempf and Bremer, 1998). Ectoine and its derivative 5-Hydroxyectoine are compatible solutes used by many microorganisms mainly for this purpose, although ectoines have beneficial functions in numerous circumstances (Pastor *et al.*, 2010; Czech *et al.*, 2018; Hermann *et al.*, 2020). They are for example used as thermoprotectants (Garcia-Estepa *et al.*, 2006) and against some

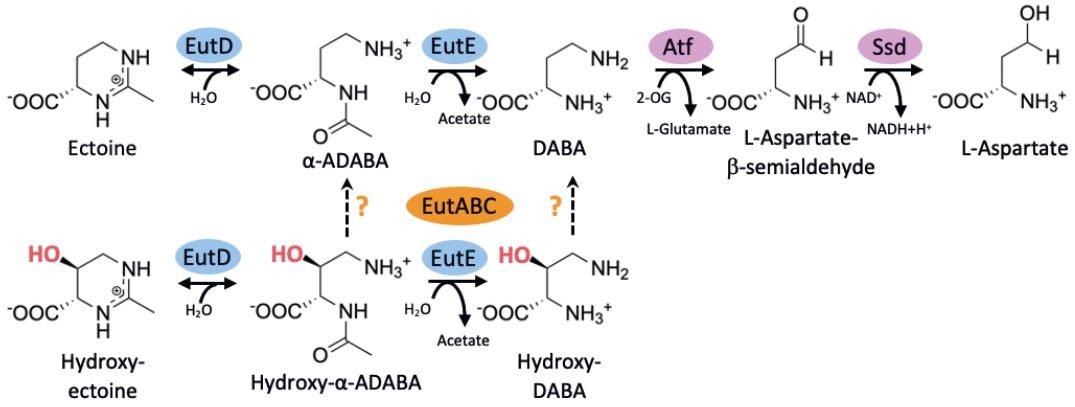

Figure 1: Biochemistry of the catalytic core of the ectoine/5-hydroxyectoine degradation route. Ectoine as well as 5-Hydroxyectoine are hydrolyzed by the aminopeptidase EutD. The so generated α-ADABA and Hydroxy-α-ADABA (which also serve as the inducers of the catabolic gene cluster) are further deacetylated by the EutE deacetylase, forming DABA and hydroxy-DABA. Hydroxy-DABA is presumably converted to DABA by the EutABC enzymes, although their specific function still needs to be found out. DABA is then furtheron metabolized by the Ssd and Atf enzymes to L-Aspartate, which ultimately fuels the TCA-cycle. Figure taken from (Hermann *et al.*, 2021).

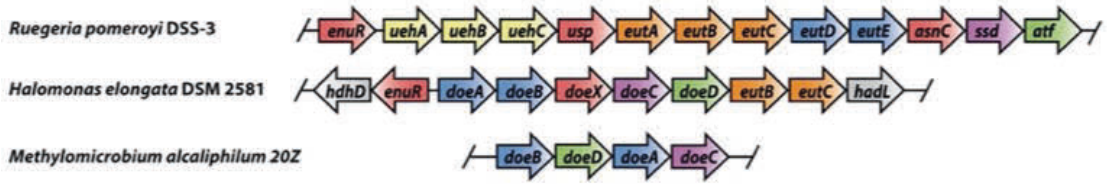

Figure 2: Ectoine catabolic gene clusters from *Ruegeria pomeroyi* DSS-3, *Halomonas elongata* DSM-2581 and *Methylomycrobium alcaliphilum* 20Z. The eut-gene cluster from *R. pomeroyi* possesses 13 genes, either directly involved in the catabolism of ectoine (*eutDE, ssd, atf*), genes for a TRAP-Type transporter (*uehABC*) genes involved in the catabolism of 5-hydroxyectoine (*eutABC*), and three regulatory proteins. *H. elongata* possesses ten genes in its ectoine-catabolic gene cluster, involved in the catabolism of ectoine (*doeAB, doeC and doeD*), two genes involved in 5-hydroxyectoine catabolism (*eutA* is missing), two genes of unknown function (*hadL* and *hdhD*) as well as two regulatory genes. The *Methylomycrobium alcaliphilum* 20Z in contrast can be seen as a minimal version of ectoine catabolic gene clusters. All four genes are directly involved in ectoine catabolism and were previously identified as homologues of the corresponding genes in *H. elongata* and *R. pomeroyi* (*doeB=eutE, doeD=atf, doeA=eutD, doeC=ssd*). Figure taken from (Hermann *et al.*, 2020).

radiative effects which have the potential to damage DNA (Hahn *et al.*, 2017). Regarding the permanent struggle for nutrients by microorganisms, it is of no surprise that some bacterial species can not only re-use the metabolically expensive ectoines as compatible solutes, but some bacteria are also able to recycle ectoines (Hermann *et al.*, 2020).

According to the latest findings in this research field, in a first step of this metabolic pathway, the ectoine ring is opened by the ectoine-hydrolase EutD (Figure 1) (Mais *et al.*, 2020). The so generated α-ADABA and Hydroxy-α-ADABA are subsequently deacetylated by the EutE-enzyme. Conversion of Hydroxy-DABA to DABA is a yet not fully understood segment of this pathway, although the enzymes EutABC are known to play a crucial role here. DABA is converted to L-Aspartate-β-semialdehyde by an aminotransferase (Atf) and a semialdehyde-dehydrogenase (Ssd) converts it finally to L-Aspartate which is subsequently used to fuel the TCA-cycle.

Although ectoine catabolism was first discovered in *Ectothiorhodospira halochloris* (Galinski and Herzog, 1990), other microorganisms were used by other research groups to investigate different aspects of this metabolic pathway. Jebbar *et al.* were able to identify the genes involved in this pathway using the plant-root associated model organism *Sinorhizobium meliloti* (Jebbar *et al.*, 2005). In the past decade research on ectoine metabolism was focused on three microorganisms, the halotolerant γ-proteobacterium *Halomonas elongata* (Schwibbert *et al.*, 2011), the marine α-proteobacterium *Ruegeria pomeroyi* (Schulz *et al.*, 2017b; Schulz *et al.*, 2017a; Hermann *et al.*, 2020; Hermann *et al.*, 2021) and the

methanotrophic γ-proteobacterium *Methylomicrobium alcaliphilum* (now also referred to as *Methylotuvimicrobium alcaliphilum*) (Reshetnikov *et al.*, 2020), which was isolated from an alkaline salt-lake. These organisms possess ectoine catabolic gene clusters of various content (Figure 2). Yet, they only represent a small proportion of microorganisms capable of recycling ectoines. Earlier bioinformatic studies could identify up to 429 proteobacteria able to degrade ectoines (Mais *et al.*, 2020). Yet, as stated at the time, these approaches were biased, as the approach to only use fully sequenced microorganisms and only recognize gene clusters in which the *eutDE* genes were located next to each other as ectoine consumers presumably underestimated the overall significance and distribution of ectoine metabolism, a problem this study is set to address.

RESULTS & DISCUSSION

Comparison of the ADABA-deacetylating enzymes from *Ruegeria pomeroyi* DSS-3 and *Methylotuvimicrobium alcaliphilum* 20Z

At a closer inspection of the ectoine catabolic gene clusters of the model organisms used in this field of research one peculiar discrepancy stood out. The ADABA deacetylase EutE is usually attributed to the Succinylglutamate-desuccinylase-/ Aspartoacylase-family of proteins and this attribution also holds true in the biochemical studies performed with this enzyme from *R*. *pomeroyi* and *H*. *elongata*. Yet, in *M. alcaliphilum* the gene annotated as *doeB* (*eutE*) was identified by an only 22% sequence identity compared with the *H. elongata doeB* (*eutE*) and its product is not attributed to the Succinylglutamate-desuccinylase-/ Aspartoacylase family. This enzyme rather belongs to the protein family of amidohydrolases and is annotated as a putative hippurate hydrolase. Although hippurate hydrolases are also a class of proteins using zinc in their active site to hydrolyze carbon-nitrogen bonds, similar to deacetylases like EutE (Steele *et al.*, 2006), the overall constitution of both proteins differs significantly.

The differences of both type of ADABA-deacetylases are clearly visible in an amino acid alignment (Figure 3). Whereas the EutE-type ADABA-deacetylases from *R. pomeroyi* and *H. elongata* align very good and amino acids involved in ligand binding are highly conserved, this is not true for the HipO-type ADABA-deacetylase from *M. alcaliphilum.* Such a big

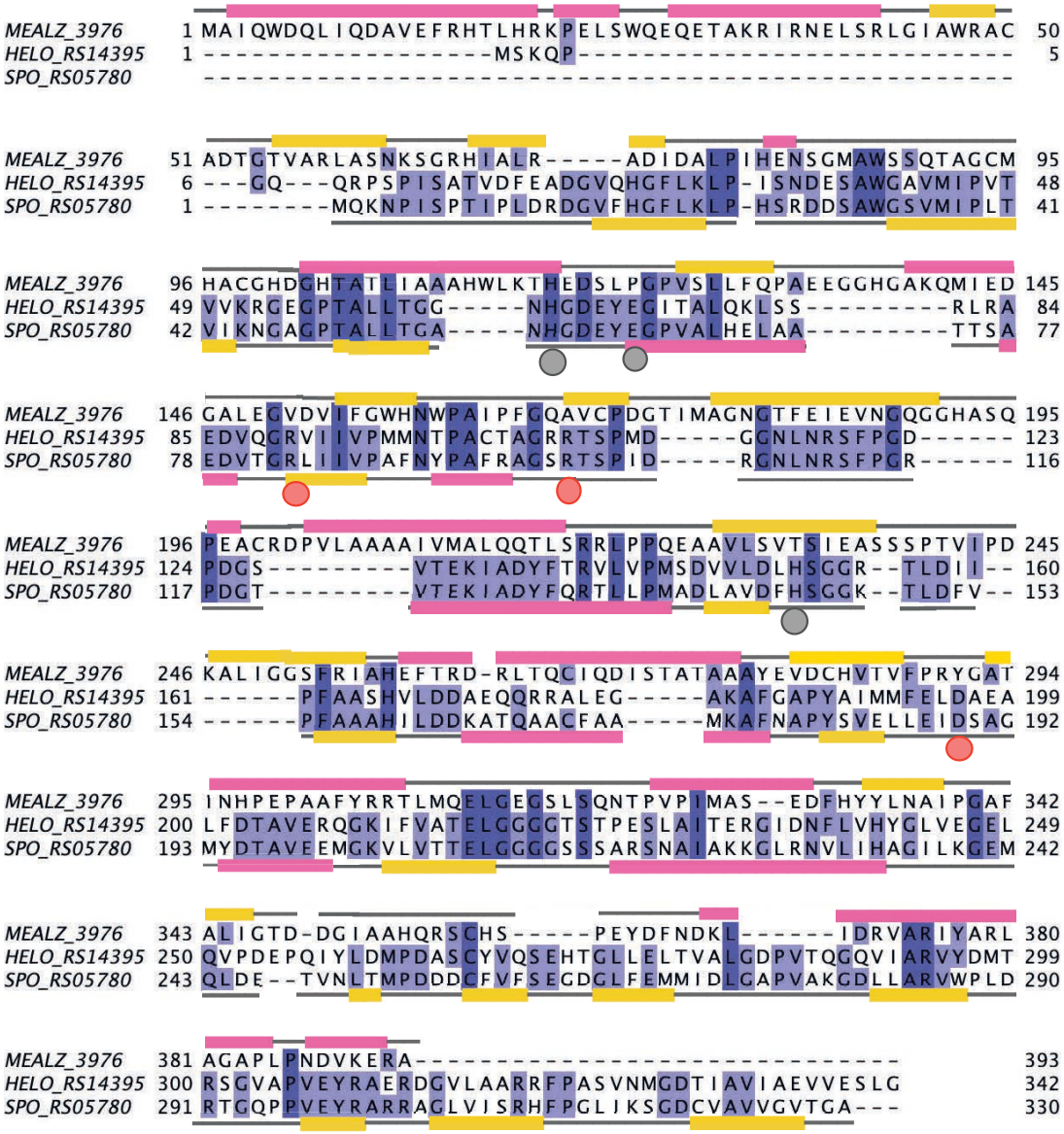

Figure 3: Protein alignements of HipO from *M. alcaliphilum* (MEALZ_3974), EutE from *H. elongata* (HELO_RS14395), and EutE from *R. pomeroyi* (SPO_RS05780). *Rp*EutE amino acids invloved in zinc-coordinating are marked with a grey dot, and DABA coordinating residues with a red dot. PSIPRED (Buchan and Jones, 2019) predicted secondary structures alements are shown above (*M. alcaliphilum*) and below (*R. pomeroyi*) the alignement. Here, pink color indicates α-helices and yellow color indicates β-strands.

difference in amino acid alignments should be clearly reflected in the structural build-up of the protein. Secondary structure prediction using the PSIPRED server (Buchan and Jones, 2019) supports this hypothesis. As to this day no crystal structure of hippurate hydrolases has been solved, alphafold2 protein modelling (Jumper *et al.*, 2021) was used to create a model of the *M. alcaliphilum* HipO protein (Figure 4). The PSIPRED predicted secondary structures of *Ma*HipO and *Rp*EutE proteins are in are consistent with this alphafold2-model as well as the *Rp*EutE crystal structure. When the alphafold2 method was used to predict a protein model

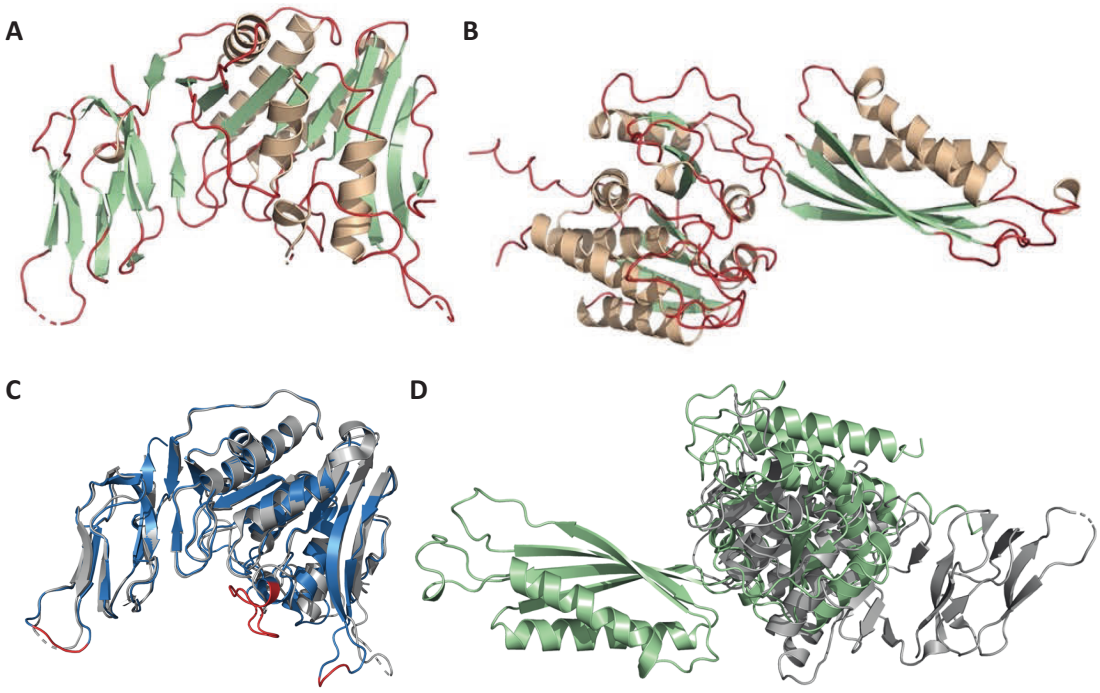

Figure 4: Protein models of EutE from *R. pomeroyi* and HipO from *M. alcaliphilum.* In the crystal structure of EutE from *R. pomeroyi* (PDB: 6TWL) (A) and the Alphafold2 model of HipO from *M. alcaliphilum* (B) secondary structure elements are marked. α-helices are depicted in orange, β-sheets in green and coils in red. Protein model alignements of the alphafold2 models of EutE from *R. pomeroyi* (blue) (C) and HipO from *M. alcaliphilum* (green) (D) against crystal structure of EutE from *R. pomeroyi* (PDB: 6TWL) are shown as well. In panel (C) of the model alignements, amino acid sequences wich could not be aligned using the TopMatch server are highlighted in red.

Table 1: TopMatch similarity prediction of *R. pomeroyi* EutE- and *M. alcaliphilum* HipO- alphafold2-models in comparison with the *R. pomeroyi* EutE crystal structure (PDB: 6TWL).

	Length	Query covered	Target covered	Score	RMSD	Sequence identity
EutE vs 6TWL	306	92.7 %	98.1 %	259.5	1.43 Å	98.7 %
HipO vs 6TWL a	126	40.4 %	32.1 %	84.1	2.61 Å	7.9 %
	48	15.4 %	12.2 %	44.2	2.43 Å	16.7 %
	31	9.9 %	7.9 %	20.8	2.75 Å	16.1 %

Length refers to the number of residue pairs that are structurally equivalent and included in the alignment. Query and target covered refers to the length of either query or target included in this alignment. Score is a measurement of structural similarity, the closer the score value is to the length value, the more the aligned residues match perfectly, the closer the score value is to 0, the more the aligned residues deviate spatially. The RMDS (Root-mean-square deviation) is calculated using all structurally equivalent C-alpha (proteins) atoms and sequence identity in this case means the percentage identity of query and target in the equivalent regions.

of EutE from *R. pomeroyi*, the resulting model aligned in a remarkable way with the solved crystal structure of said protein. The overall RMSD (root-means-square-deviation) of protein and model was calculated to be very low (1.43 Å using the TopMatch-Server (Wiederstein and Sippl, 2020) and 0.57 Å using PyMol (Schrödinger, 2020)), resulting mainly from peripheral amino acid segments not solved in the crystal structure, but modelled by the alphafold2 server. In contrast the HipO-model could not be aligned to the EutE crystal structure in a satisfactory fashion. The calculated RMSDs (2.61 Å, 2.43 Å and 2,75 Å for small segments of the proteins calculated using the TopMatch-Server and 14.55 Å using PyMol) already indicate the major structural differences of both proteins which can be readily seen from the PyMol alignment model (Figure 4) as well as a 2D-topology model of both proteins (Figure 5).

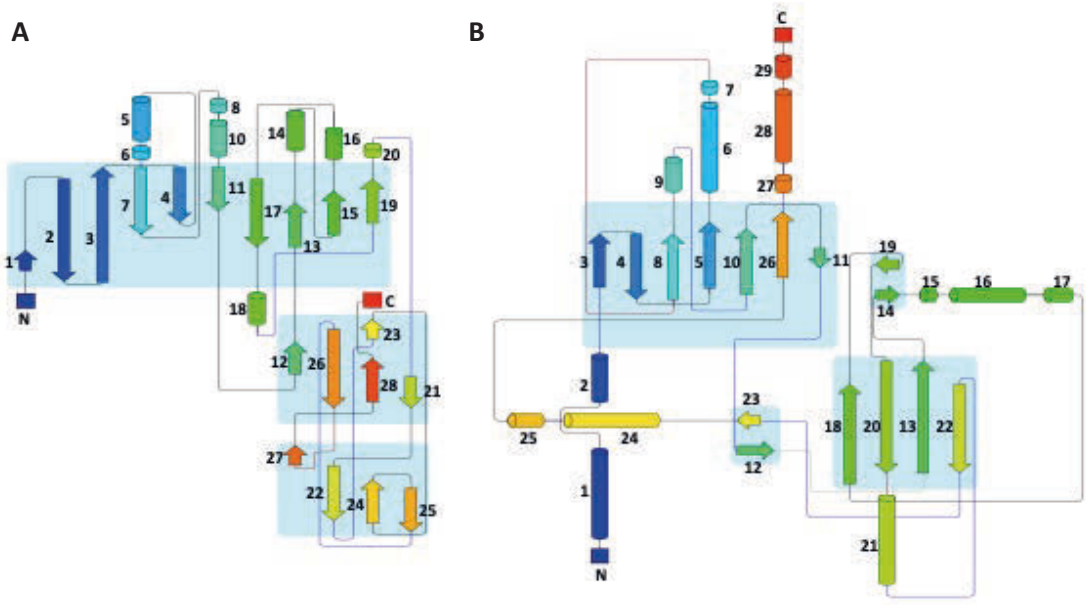

Figure 5: 2D-topology models of *Rp*EutE (A) and *Ma*HipO (B). Helices are depicted as barrels and sheets as arrows. The blue fields mark individual subdomains of both proteins. The 2D-topology models were calculated using Pro-Origami (Stivala *et al.*, 2011).

Due to these large differences between both proteins, one could now just neglect the HipO enzyme as a protein of a completely different function, yet deletion analysis in *M. alcaliphilum* of the corresponding gene resulted in an intracellular accumulation of α-ADABA when cells were set to catabolize ectoine, a process not observed in the *M. alcaliphilum* wild type strain (Reshetnikov *et al.*, 2020). One explanation is therefore, that we are dealing with two different types of proteins carrying out the same catalytical process, another could be that HipO somehow creates a bottleneck in ectoine catabolism which leads to the accumulation of α-ADABA. Yet, hippurate hydrolases are, as well as ectoine-deacetylases, enzymes using zinc atoms in their catalytic center to perform their respective catalytical reactions (Figure 6).

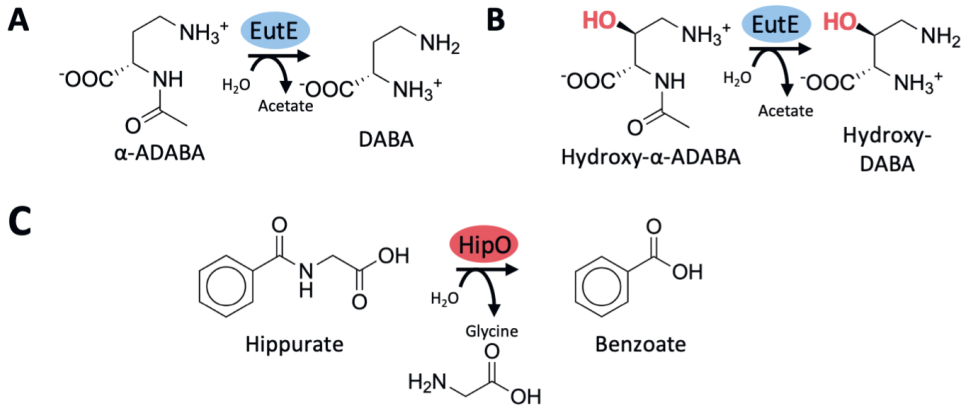

147

148 **Figure 6:** Chemical reactions performed by EutE on α-ADABA (A), hydroxy-α-ADABA (B), and HipO on
149 Hippurate (C). Adapted from (Hermann *et al.*, 2021).

150 Also, a more specific alignment of only fragments of the *R. pomeroyi* EutE crystal structure
151 (PDB: 6TWL) to the *M. alcaliphilum* HipO alphafold2-model produces an alignment in which
152 especially the core elements seem more like each other (Figure 7), whether this alignment is
153 actually feasible and allows the interaction of both HipO monomers as observable for EutE
154 remains to be investigated, probably best using crystal structures.

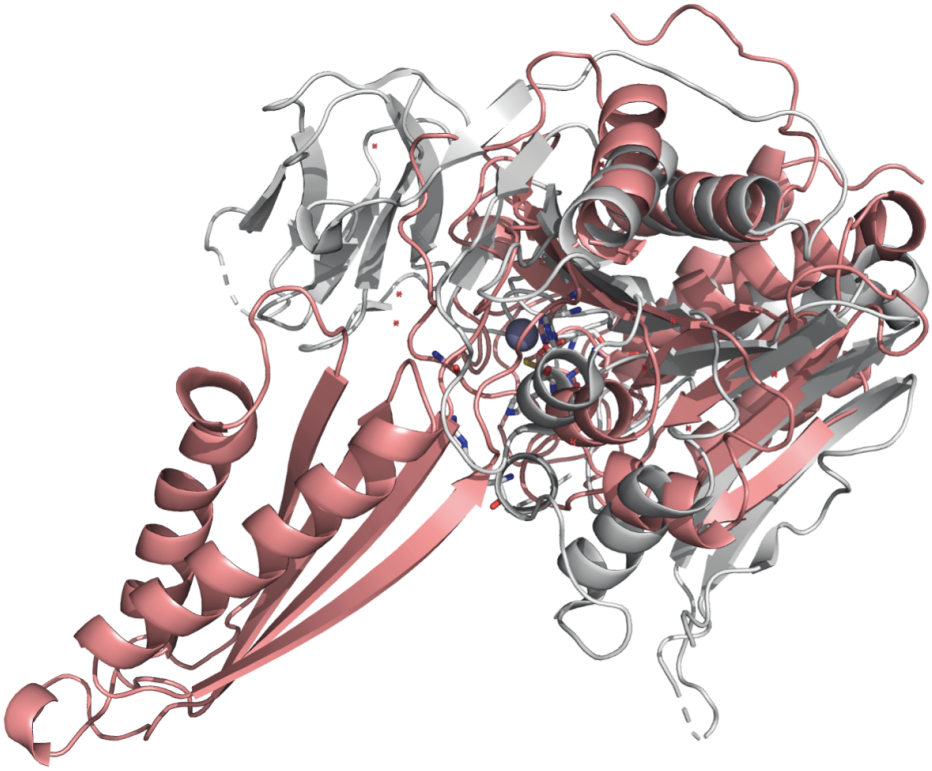

155

156 **Figure 7:** Alignemnt of core fragments of both, the *R. pomeroyi* EutE crystal structure (PDB: 6TWL)
157 (grey), and the *M. alcaliphilum* HipO alphafold2-model (red). Especially the β-sheets near the active site
158 align quite well, also the zinc atom of EutE is at a place where it could also be coordinated in HipO. The
159 figure is adapted from an alignment performed by Dr. Felix Dempwolff.

To find out whether the usage of HipO-type proteins in the context of ectoine metabolism is restricted to a few organisms closely related to *M. alcaliphilum*, or a more widespread modus operandi, a broad bioinformatic analysis was carried out. Using the newly introduced cassette-search method of the JGI IMG/ER-server (Chen *et al.*, 2020), genomes of all organisms included in the IMG/ER database were searched for the presence of ectoine catabolic genes in a genetic neighborhood. This search included 94,000 bacterial, 2,151 archaeal and 710 eukaryotic genomes. As this search-algorithm now allows a far more thorough analysis than previous bioinformatic approaches, also the distribution of the *R. pomeroyi* type ectoine catabolic gene cluster was re-investigated. To carry out the cassette-search method of the JGI IMG/ER-server, the protein families attributed to four central enzymes of ectoine catabolism were used for both types of searches. The protein families attributed to the proteins here were pfam:00557 (metallopeptidase family M24) for EutD, pfam:00202 (aminotransferase class-III) for the aminotransferase and pfam:00171 (aldehyde dehydrogenase) for the semialdehyde dehydrogenase present in both gene cluster types, as well as pfam:04952 (succinylglutamat-desuccinylase) for the EutE-type clusters and pfam:01546 (peptidase M20) for the HipO-type clusters.

For the EutDE type ectoine catabolic gene cluster, 1963 different gene cassettes could be identified containing 2464 EutD-type proteins and belonging to 1771 different bacteria (1.87 %). The EutD-HipO type ectoine catabolic gene cluster could be found in 691 cases from 686 different bacterial genomes (0.72 %), containing 735 EutD-type proteins. For both EutD-protein sets phylogenetic trees were constructed (Figure 8 & 9, and online supplementary material). In these rooted EutD-trees, phylum, class, and order of the microorganism containing the *eutD*-gene are depicted. Dark squares also mark the cases in which several *eutD*-genes exist. The prevalence of *eutD*-genes is also specified in Table 2.

Overall, although the EutDE-type of ectoine catabolism seems to be used by far more individual species, the HipO-EutE-type of ectoine catabolism spans a far wider range of phyla, classes, and orders. Also, in the context of the EutDE-type of ectoine catabolism, far more organisms are found which possess several *eutD*-genes. In HipO-EutD context, 7.1 % of the *eutD*-type genes are accompanied by another eutD-type gene, while in the EutDE context this number increases to 27.4 %. Interestingly, a huge number of these events can be traced back to the Genus *Mesorhizobia*. 189 of the *Mesorhizobia* possessing *eutDE*-type gene clusters overall possess 654 *eutD*-type genes. Although most representatives possess two or three *eutD*-copies, some species stand out. *Mesohizobium erdmanii* possesses 10 *eutD*-type genes, *Mesorhizobium waimense* harbours 11 *eutD*-type genes and

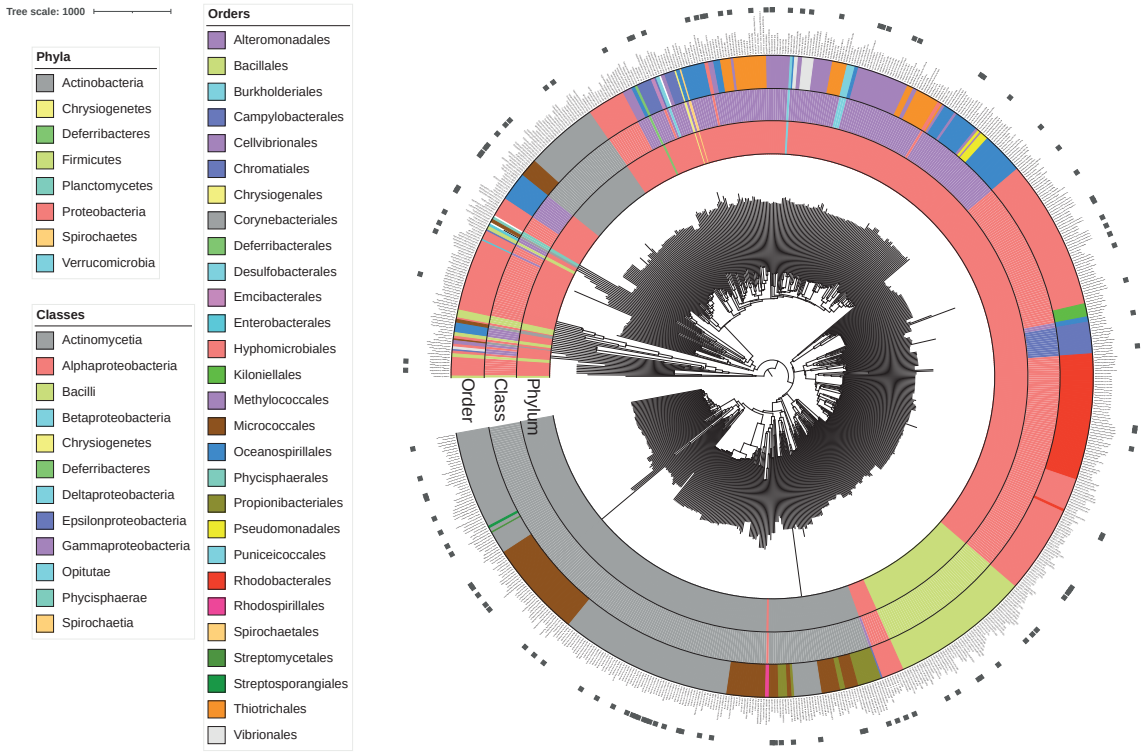

Figure 8: Phylogenetic tree of EutD proteins found in the *hipO-eutD* context. Dark squares mark the cases in which several copies or variants of *eutD*-genes exist in one microorganism. The tree is midpoint-rooted, and the tree scale indicates amino acid changes between the proteins.

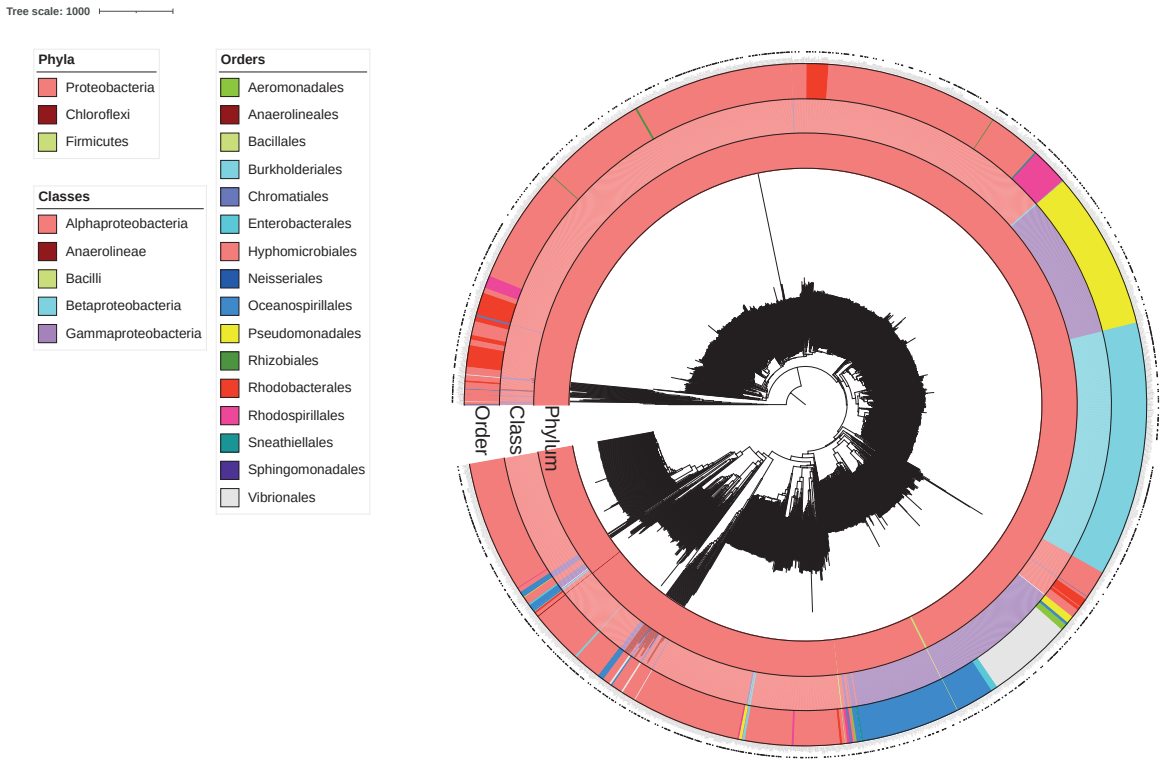

Figure 9: Phylogenetic tree of EutD proteins found in the *eutDE* context. Dark squares (very small) mark the cases in which several copies or variants of *eutD*-genes exist in one microorganism. The tree is midpoint-rooted, and the tree scale indicates amino acid changes between the proteins.

202 **Table 2:** Prevalence of eutD-type genes in microorganisms either possessing the EutDE or the HipO-
203 EutD type of etoine catabolism.

	EutDE-type		HipO-EutD-type	
Group		*eutD*-type genes	Group	*eutD*-type genes
Phylum	*Proteobacteria*	2461	*Actinobacteria*	246
	Firmicutes	2	*Chrysiogenetes*	1
	Chloroflexi	1	*Deferribacteres*	1
			Firmicutes	60
			Planctomycetes	2
			Proteobacteria	423
			Spirochaetes	1
			Verrucomicrobia	1
Class	*Alphaproteobacteria*	1611	*Actinomycetioa*	246
	Anaerolineae	1	*Alphaproteobacteria*	231
	Bacilli	2	*Bacilli*	61
	Betaproteobacteria	313	*Betaproteobacteria*	3
	Gammaproteobacteria	535	*Chrysiogenetes*	1
	unclassified	2	*Deferribacteres*	1
			Deltaproteobacteria	1
			Epsilonproteobacteria	12
			Gammaproteobacteria	178
			Opitutae	1
			Phycisphaerae	2
			Spirochaetia	1
Order	*Aeromonadales*	8	*Alteromonadales*	7
	Anaerolineales	1	*Bacillales*	60
	Bacillales	2	*Burkholderiales*	3
	Burkholderiales	312	*Campylobacterales*	12
	Chromatiales	5	*Cellvibrionales*	40
	Enterobacterales	10	*Chromatiales*	14
	Hyphomicrobiales	1426	*Chrysiogenales*	1
	Neisseriales	1	*Corynebacteriales*	149
	Oceanospirillales	196	*Deferribacterales*	1
	Pseudomonadales	205	*Desulfobacterales*	1
	Rhizobiales	3	*Emcibacterales*	1
	Rhodobacterales	108	*Enterobacterales*	2
	Rhodospirillales	68	*Hyphomicrobiales*	163
	Sneathiellales	6	*Kiloniellales*	11
	Sphingomonadales	1	*Methylococcales*	5
	unclassified	5	*Micrococcales*	6
	Vibrionales	108	*Oceanospirillales*	80
			Phycisphaerales	62
			Propionibacteriales	1
			Pseudomonadales	15
			Puniceicoccales	1
			Rhodobacterales	49
			Rhodospirillales	1
			Spirochaetales	1
			Streptomycetales	1
			Streptosporangiales	1
			Thiotrichales	35
			Vibrionales	6

Mesorhizobium sp. NZP2077 even has 12 copies of *eutD*-like genes. An interesting phenomenon is also the co-occurance of the EutDE and the HipO-EutD type of ectoine catabolism. This phenomenon could be observed in 19 bacteria. All those phenomena, as well as the high variability of ectoine catabolic gene clusters indicates these gene clusters to be subject of constant evolutionary processes. These constant evolutionary processes also become clear when the gene clusters *eutD/hipO* genes are associated with are observed (Figure 10). They are very variable, as are the gene clusters of the original *eutDE* type (Hermann *et al.*, 2020).

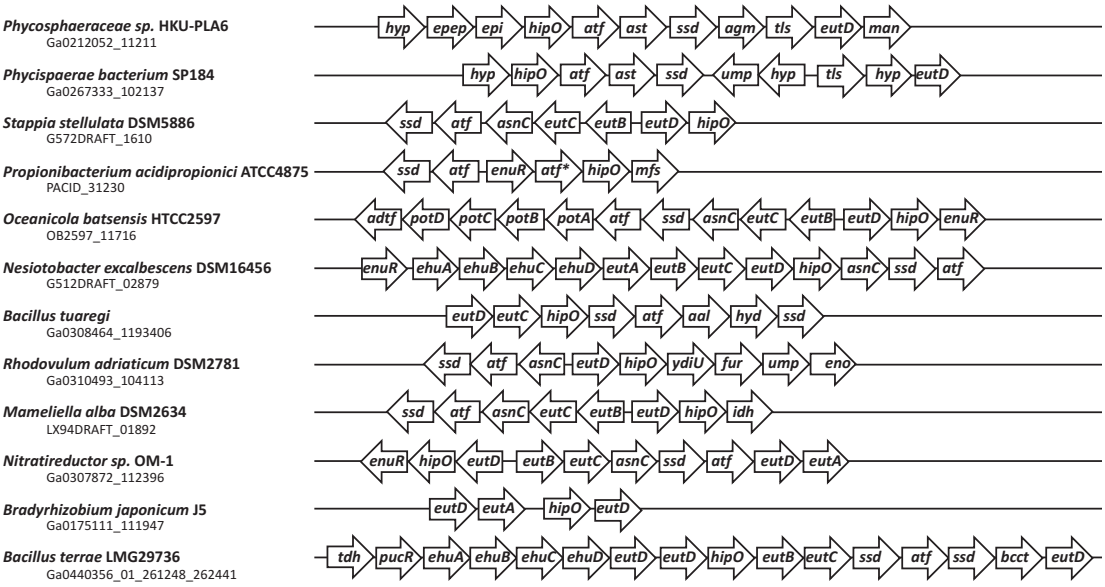

Figure 10: Some examples of *eutD/hipO*-type gene clusters. The names of genes unknown in previous examples of ectoine metabolism are explained in table 3.

Table 3: Nomenclature of genes not previously connected with ectoine catabolism of the gene-clusters depicted in figure 10.

gene	predicted function	gene	predicted function
hyp	hypothetical	*aal*	aspartate ammonia lyase
epep	endopeptidase	*hyd*	hydratase
epi	diaminopimulate epimerase	*ydlU*	adenylyltransferase
ast	arginine-succinyl transferase	*fur*	ferric-uptake regulator
agm	agmatinase	*eno*	enolase
tis	tRNA-lysidine synthase	*idh*	L-idonate-5-dehydrogenase
man	mannosidase	*tdh*	threonine dehydratase
ump	unknown membrane protein	*pucR*	purine catabolism regulator
adtf	adenosyltransferase	*bcct*	Betaine-choline-carnitine-transporter
potABCD	putrescine-spermidine transport system		

The exact biochemical process performed by HipO in ectoine catabolism, and the molecular underpinnings are yet unclear, although the finding that a *M. alcaliphilum* HipO deletion strain accumulates α-ADABA when growing with ectoine (Reshetnikov *et al.*, 2020), is a strong supporter of a second type of ADABA deacetylating mechanisms.

MATERIALS AND METHODS

Protein model prediction and alignment

Secondary structure predictions were performed using PSIPRED (Buchan and Jones, 2019). Protein alignements were performed using ClustalO (Sievers and Higgins, 2014) and visualized in JalView (Waterhouse *et al.*, 2009). The structural models of *R. pomeroyi* EutE and *M. alcaliphilum* HipO were predicted using the combined alphafold2 (Jumper *et al.*, 2021) and RoseTTAFold (Baek *et al.*, 2021) approaches provided by the ColabFold platform (Mirdita *et al.*, 2021). In each case the most likely of the five computated protein models was selected and compared to the crystal structure of EutE from *R. pomeroyi* (PDB: 6TWL). Comparison was carried out using the PyMol software as well as the TopMatch server and visualization was performed with the PyMol software set using the cartoon representation for all proteins.

Phylogenetic analysis of EutDE/EutD-HipO type ectoine catabolic gene clusters

All 94700 bacterial, 2151 archaeal and 710 eukaryotic genomes deposited in the JGI IMG/ER database were investigated of the presence of either EutDE- or EutD-HipO-type gene clusters via the cassette search tool. Both search algorithm used the three identifiers pfam:00557 (metallopeptidase family M24), pfam:00202 (aminotransferase class-III) and pfam:00171 (aldehyde dehydrogenase) accompanied by either pfam:04952 (succinylglutamat-desuccinylase) for the EutDE-type clusters or pfam:01546 (peptidase M20) for the EutD-HipO-type clusters.

For the EutDE type ectoine catabolic gene cluster, 1963 different gene cassettes could be identified containing 2464 EutD-type proteins identified by a at least 30% sequence identity with EutD from *R. pomeroyi* belonging to 1771 different bacteria. The EutD-HipO type ectoine catabolic gene cluster could be found in 691 cases from 683 bacterial genomes, possessing 735 EutD-type proteins identified by a at least 30% sequence identity with EutD from *R. pomeroyi.* For visualization all proteins were aligned using the Clustal Omega service of the EMBL-EBI (Sievers and Higgins, 2014) and phylogenetic trees were calculated with the Jalview (Waterhouse *et al.*, 2009) software using the neighbor joining approach. Phylogenetic trees were rooted and visualized using iTol (Letunic and Bork, 2019).

AUTHOR CONTRIBUTIONS

Up to this state of the manuscript, LH designed, planned, performed the bioinformatic experiments of this study, and wrote the manuscript.

FUNDING

This study was carried out without financial support, so no funding agencies had any role in study design, in the collection, analysis and interpretation of data, the writing of the manuscript.

ACKNOWLEDGEMENTS

I am greatly thankful to Erhard Bremer for discussions on the topic and his support over the past years, as well as Felix Dempwolff for discussion and his efforts for the EutE-HipO alignment.

SUPPLEMENTARY MATERIAL

Figures 8 and 9 at highest resolution can be found online at:
https://drive.google.com/drive/folders/1MGyI6DmWT_GgiJXxke6HtOXeylCa_sgu?usp=sharing

REFERENCES

1. **Baek, M., DiMaio, F., Anishchenko, I., Dauparas, J., Ovchinnikov, S., Lee, G.R., Wang, J., Cong, Q., Kinch, L.N., and Schaeffer, R.D.** (2021) Accurate prediction of protein structures and interactions using a 3-track network. *bioRxiv* 2021.06.14.448402.

2. **Bremer, E., and Krämer, R.** (2000) Coping with osmotic challenges: osmoregulation through accumulation and release of compatible solutes. *In* Bacterial Stress Responses. Storz, G., and Hengge-Aronis, R. (eds). Washington DC, USA: ASM Press, pp.79-97.

3. **Buchan, D.W., and Jones, D.T.** (2019) The PSIPRED protein analysis workbench: 20 years on. *Nucleic Acids Res* 47:W402-W407.

4. **Chen, I.A., Chu, K., Palaniappan, K., Ratner, A., Huang, J., Huntemann, M., Hajek, P., Ritter, S., Varghese, N., Seshadri, R., Roux, S., Woyke, T., Eloe-Fadrosh, E.A., Ivanova, N.N., and Kyrpides, N.C.** (2020) The IMG/M data management and analysis system v.6.0: new tools and advanced capabilities. *Nucleic Acids Res*:doi: 10.1093/nar/gkaa1939.

5. **Czech, L., Hermann, L., Stöveken, N., Richter, A.A., Hoeppner, A., Smits, S.H.J., Heider, J., and Bremer, E.** (2018) Role of the extremolytes ectoine and hydroxyectoine as stress protectants and nutrients: Genetics, phylogenomics, biochemistry, and structural snalysis. *Genes* 9:177.

6. **Galinski, E.A., and Herzog, R.M.** (1990) The role of trehalose as a substitute for nitrogen-containing compatible colutes (*Ectothiorhodospira halochloris*). *Arch Microbiol* 153:607-613.

7. **Garcia-Estepa, R., Argandona, M., Reina-Bueno, M., Capote, N., Iglesias-Guerra, F., Nieto, J.J., and Vargas, C.** (2006) The *ectD* gene, which is involved in the synthesis of the compatible solute hydroxyectoine, is essential for thermoprotection of the halophilic bacterium *Chromohalobacter salexigens*. *J Bacteriol* 188:3774-3784.

8. **Hahn, M.B., Meyer, S., Schröter, M.A., Kunte, H.J., Solomun, T., and Sturm, H.** (2017) DNA protection by ectoine from ionizing radiation: Molecular mechanisms. *Phys Chem Chem Phys* 19:25717-25722.

9. **Hermann, L., Mais, C.N., Czech, L., Smits, S.H.J., Bange, G., and Bremer, E.** (2020) The ups and downs of ectoine: Structural enzymology of a major microbial stress protectant and versatile nutrient. *Biol Chem* 401:1443-1468.

10. **Hermann, L., Dempwolff, F., Steinchen, W., Freibert, S.-A., Smits, S.H.J., Seubert, A., and Bremer, E.** (2021) The MocR/GabR ectoine and hydroxyectoine catabolism regulator EnuR: Inducer and DNA binding. *Front Microbiol* 12.

11. **Hoffmann, T., Boiangiu, C., Moses, S., and Bremer, E.** (2008) Responses of *Bacillus subtilis* to hypotonic challenges: physiological contributions of mechanosensitive channels to cellular survival ▿ . *In* Appl Environ Microbiol, pp.2454-2460.

12. **Jebbar, M., Sohn-Bösser, L., Bremer, E., Bernard, T., and Blanco, C.** (2005) Ectoine-induced proteins in *Sinorhizobium meliloti* include an ectoine ABC-type transporter involved in osmoprotection and ectoine catabolism. *J Bacteriol* 187:1293-1304.

13. **Jumper, J., Evans, R., Pritzel, A., Green, T., Figurnov, M., Ronneberger, O., Tunyasuvunakool, K., Bates, R., Zidek, A., Potapenko, A., Bridgland, A., Meyer, C., Kohl, S.A.A., Ballard, A.J., Cowie, A., Romera-Paredes, B., Nikolov, S., Jain, R., Adler, J., Back, T., Petersen, S., Reiman, D., Clancy, E., Zielinski, M., Steinegger, M., Pacholska, M., Berghammer, T., Bodenstein, S., Silver, D., Vinyals, O., Senior, A.W., Kavukcuoglu, K., Kohli, P., and Hassabis, D.** (2021) Highly accurate protein structure prediction with AlphaFold. *Nature* 596:583-589.

14. **Kempf, B., and Bremer, E.** (1998) Uptake and synthesis of compatible solutes as microbial stress responses to high-osmolality environments. *Arch Microbiol* 170:319-330.

15. **Letunic, I., and Bork, P.** (2019) Interactive Tree Of Life (iTOL) v4: recent updates and new developments. *Nucleic Acids Res* 47:W256-W259.

16. **Levina, N., Totemeyer, S., Stokes, N.R., Louis, P., Jones, M.A., and Booth, I.R.** (1999) Protection of *Escherichia coli* cells against extreme turgor by activation of MscS and MscL mechanosensitive channels: Identification of genes required for MscS activity. *EMBO J* 18:1730-1737.

17. **Mais, C.N., Hermann, L., Altegoer, F., Seubert, A., Richter, A.A., Wernersbach, I., Czech, L., Bremer, E., and Bange, G.** (2020) Degradation of the microbial stress protectants and chemical chaperones ectoine and hydroxyectoine by a bacterial hydrolase-deacetylase complex. *J Biol Chem* 295:9087-9104.

18. **Mirdita, M., Schütze, K., Moriwaki, Y., Heo, L., Ovchinnikov, S., and Steinegger, M.** (2021) ColabFold - making protein folding accessible to all. *bioRxiv*:2021.2008.2015.456425.

19. **Pastor, J.M., Salvador, M., Argandona, M., Bernal, V., Reina-Bueno, M., Csonka, L.N., Iborra, J.L., Vargas, C., Nieto, J.J., and Canovas, M.** (2010) Ectoines in cell stress protection: Uses and biotechnological production. *Biotechnol Adv* 28:782-801.

20. **Reshetnikov, A.S., Rozova, O.N., Trotsenko, Y.A., But, S.Y., Khmelenina, V.N., and Mustakhimov, II** (2020) Ectoine degradation pathway in halotolerant methylotrophs. *PLoS One* 15:e0232244.

21. **Schrödinger, L.** (2020) The PyMOL molecular graphics system, version 2.4. *Version* 1:0.

22. **Schulz, A., Stöveken, N., Binzen, I.M., Hoffmann, T., Heider, J., and Bremer, E.** (2017a) Feeding on compatible solutes: A substrate-induced pathway for uptake and catabolism of ectoines and its genetic control by EnuR. *Environ Microbiol* 19:926-946.

23. **Schulz, A., Hermann, L., Freibert, S.-A., Bönig, T., Hoffmann, T., Riclea, R., Dickschat, J.S., Heider, J., and Bremer, E.** (2017b) Transcriptional regulation of ectoine catabolism in response to multiple metabolic and environmnetal cues. *Env Microbiol* 19:4599-4619.

24. **Schwibbert, K., Marin-Sanguino, A., Bagyan, I., Heidrich, G., Lentzen, G., Seitz, H., Rampp, M., Schuster, S.C., Klenk, H.P., Pfeiffer, F., Oesterhelt, D., and Kunte, H.J.** (2011) A blueprint of ectoine metabolism from the genome of the industrial producer *Halomonas elongata* DSM 2581 T. *Environ Microbiol* 13:1973-1994.

25. **Sievers, F., and Higgins, D.G.** (2014) Clustal omega. *Curr Protoc Bioinformatics* 48:3.13. 11-13.13. 16.

26. **Steele, M., Marcone, M., Gyles, C., Chan, V., and Odumeru, J.** (2006) Enzymatic activity of *Campylobacter jejuni* hippurate hydrolase. *Protein Eng Des Sel* 19:17-25.

27. **Stivala, A., Wybrow, M., Wirth, A., Whisstock, J.C., and Stuckey, P.J.** (2011) Automatic generation of protein structure cartoons with Pro-origami. *Bioinformatics* 27:3315-3316.

28. **van den Berg, J., Boersma, A.J., and Poolman, B.** (2017) Microorganisms maintain crowding homeostasis. *Nat Rev Microbiol* 15:309-318.

29. **Waterhouse, A.M., Procter, J.B., Martin, D.M., Clamp, M., and Barton, G.J.** (2009) Jalview Version 2 - a multiple sequence alignment editor and analysis workbench. *Bioinformatics* 25:1189-1191.

30. **Wiederstein, M., and Sippl, M.J.** (2020) TopMatch-web: pairwise matching of large assemblies of protein and nucleic acid chains in 3D. *Nucleic Acids Res* 48:W31-W35.

371 31. **Wood, J.M.** (2011) Bacterial osmoregulation: A paradigm for the study of cellular
372 homeostasis. *Annu Rev Microbiol* 65:215-238.
373

6.4 Review articles with peer-review process

6.4.1 Role of the extremolytes ectoine and hydroxyectoine as stress protectants and nutrients: genetics, phylogenomics, biochemistry, and structural analysis (2017)

Genes 2018;9:177 doi: 10.3390/genes9040177

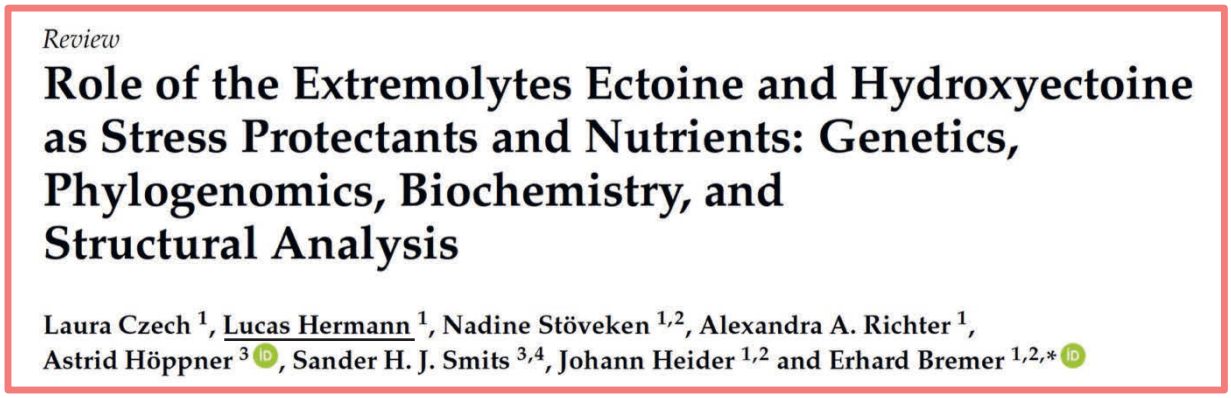

Review

Role of the Extremolytes Ectoine and Hydroxyectoine as Stress Protectants and Nutrients: Genetics, Phylogenomics, Biochemistry, and Structural Analysis

Laura Czech [1], Lucas Hermann [1], Nadine Stöveken [1,2], Alexandra A. Richter [1], Astrid Höppner [3], Sander H. J. Smits [3,4], Johann Heider [1,2] and Erhard Bremer [1,2,*]

The following review article “Role of the extremolytes ectoine and hydroxyectoine as stress protectants and nutrients: genetics, phylogenomics, biochemistry, and structural analysis.” was published in Genes in 2018 after a peer-reviewing process. L. Czech performed the bioinformatic analysis included in this publication. Prof. E. Bremer and L. Czech wrote the text with my contribution to the part of ectoine catabolism. N. Stöveken and J. Heider also contributed and A. A. Richter, A. Höppner, and S. H. J. Smits helped with finalizing the manuscript. Figures in the publication were prepared by L. Czech and by me for the ectoine catabolism part.

genes

MDPI

Review

Role of the Extremolytes Ectoine and Hydroxyectoine as Stress Protectants and Nutrients: Genetics, Phylogenomics, Biochemistry, and Structural Analysis

Laura Czech [1], Lucas Hermann [1], Nadine Stöveken [1,2], Alexandra A. Richter [1], Astrid Höppner [3], Sander H. J. Smits [3,4], Johann Heider [1,2] and Erhard Bremer [1,2,*]

1 Laboratory for Microbiology, Department of Biology, Philipps-University Marburg, Karl-von-Frisch Str. 8, D-35043 Marburg, Germany; lauraczech@hotmail.de (L.C.); lucas.hermann@biologie.uni-marburg.de (L.H.); nadine@stoeveken.com (N.S.); alexandra.richter@biologie.uni-marburg.de (A.A.R.); heider@staff.uni-marburg.de (J.H.)

2 LOEWE—Center for Synthetic Microbiology, Philipps-University Marburg, Hans-Meerwein Str. 6, D-35043 Marburg, Germany

3 Center for Structural Studies, Heinrich-Heine University Düsseldorf, Universitäts Str. 1, D-40225 Düsseldorf, Germany; astrid.hoeppner@uni-duesseldorf.de (A.H.); sander.smits@hhu.de (S.H.J.S.)

4 Institute of Biochemistry, Heinrich-Heine University Düsseldorf, Universitäts Str. 1, D-40225 Düsseldorf, Germany

* Correspondence: bremer@staff.uni-marburg.de; Tel.: +49-6421-282-1529

Received: 10 February 2018; Accepted: 15 March 2018; Published: 22 March 2018

Abstract: Fluctuations in environmental osmolarity are ubiquitous stress factors in many natural habitats of microorganisms, as they inevitably trigger osmotically instigated fluxes of water across the semi-permeable cytoplasmic membrane. Under hyperosmotic conditions, many microorganisms fend off the detrimental effects of water efflux and the ensuing dehydration of the cytoplasm and drop in turgor through the accumulation of a restricted class of organic osmolytes, the compatible solutes. Ectoine and its derivative 5-hydroxyectoine are prominent members of these compounds and are synthesized widely by members of the Bacteria and a few Archaea and Eukarya in response to high salinity/osmolarity and/or growth temperature extremes. Ectoines have excellent function-preserving properties, attributes that have led to their description as chemical chaperones and fostered the development of an industrial-scale biotechnological production process for their exploitation in biotechnology, skin care, and medicine. We review, here, the current knowledge on the biochemistry of the ectoine/hydroxyectoine biosynthetic enzymes and the available crystal structures of some of them, explore the genetics of the underlying biosynthetic genes and their transcriptional regulation, and present an extensive phylogenomic analysis of the ectoine/hydroxyectoine biosynthetic genes. In addition, we address the biochemistry, phylogenomics, and genetic regulation for the alternative use of ectoines as nutrients.

Keywords: osmotic stress; high salinity; growth temperature extremes; enzymes; crystal structures; gene expression; genomics; chemical chaperones; biotechnology

1. Introduction

Microorganisms face myriad stressful conditions and nutrient limitations in their natural habitats; challenging circumstances to which they must react in a timely manner to ensure survival, persistence, and growth. An important parameter that affects essentially all microorganisms is the

osmolarity/salinity of their surroundings [1–6], as increases or decreases in the environmental water activity will inevitably trigger water fluxes across the cytoplasmic membrane.

Water is the active matrix of life [7,8], and the invention of the semi-permeable cytoplasmic membrane was a key event in the evolution of primordial cells. This membrane provided a confined space for the faithful copying of the genetic material, a reaction vessel for biochemical transformations and for the generation of energy to fuel growth. The cytoplasm of microorganisms is a highly crowded compartment caused by large concentrations of nucleic acids, proteins, and metabolites [9]. Together, these compounds generate a considerable osmotic potential [10] and thereby instigate osmotically driven water influx, a process that in turn causes the build-up of a hydrostatic pressure in walled cells, the turgor [2,10–14]. Turgor is considered essential for cell growth in many bacteria [15]. As microbial cells seem to strive to attain crowding homeostasis [9], they maintain turgor within physiologically acceptable boundaries through the accumulation and expulsion of ions and organic solutes [1–6], and they accomplish this even when faced with sudden fluctuations in the external osmolarity, or when they are exposed to persistent high or low osmolarity surroundings.

The development of the cytoplasmic membrane was a prerequisite for the evolution of microbial cells as we know them today; however, its semi-permeable nature makes cells vulnerable to osmotic fluctuations in their surroundings [2,6,10,11]. In extreme cases, the integrity of the cell is threatened by excessive water influx and a concomitant build-up of turgor to non-sustainable levels (under hypo-osmotic conditions) [16–20], or the ability of the cell to perform vital physiological tasks is impaired by the dehydration of the cytoplasm and the ensuing reduction/collapse of turgor when water exits the cell (under hyperosmotic conditions) [2,10]. It is apparent that coordinated cellular stress responses are needed to prevent such catastrophic effects.

Despite the existence of aquaporins in microorganisms that mediate diffusion-driven accelerated water fluxes across the cytoplasmic membrane [21,22], no microorganism can actively pump water (by means of an energy consuming process) into or out of the cell to compensate for water fluxes through this membrane that are instigated by changes in the external osmolarity. Microorganisms can, however, actively influence the direction and scale of water fluxes into or out of the cell by dynamically modulating the osmotic potential of the cytoplasm through the accumulation or expulsion of ions and organic compounds [2,5,10,11,20]. These combined activities allow microbial cells to cope dynamically with increases and decreases in the external osmolarity and are also crucial for their ability to colonize habitats with permanently high salinities/osmolarities [23,24].

When exposed to high-osmolarity environments, microorganisms amass ions and organic osmolytes to increase the osmotic potential of their cytoplasm (Figure 1A). This curbs water efflux and promotes water influx, thereby balancing the vital osmotic gradient across the cytoplasmic membrane under osmotically unfavorable environmental circumstances [4,5,24,25]. An increase in the osmotic potential of the cytoplasm can be accomplished by one of two cellular adjustment strategies. These are to accumulate high levels of either selected salt ions (primarily K^+ and Cl^-) (the *salt-in* strategy) or of physiologically compliant organic osmolytes, the compatible solutes (the *salt-out* strategy) [1,5,25].

While the accumulation of ions and/or organic osmolytes ensures survival and growth of microorganisms under high osmolarity/salinity conditions (Figure 1A), the high intracellular pools of the very same compounds threatens the integrity of the cell when it is suddenly exposed to a drop in the external osmolarity [11,16–18,20]. Such conditions occur, for instance, for soil-dwelling bacteria upon rainfall and by washout into freshwater sources, for microorganisms living in brackish ecosystems, and for enteric bacteria when they exit the intestine of their host. The ensuing osmotic down-shocks require a very rapid cellular adjustment response in order to avoid bursting [11,20,26,27]. For instance, turgor pressure in *Escherichia coli* has been estimated to lie between 0.3 atm and 3 atm [13,14], values that increase practically instantaneously to about 20 atm upon a sudden and severe osmotic down-shift [11]. Such a drastic increase in turgor cannot be restrained by the stress-bearing peptidoglycan sacculus [28,29] of the cell wall alone, and consequently, the cell would burst [11,16–19].

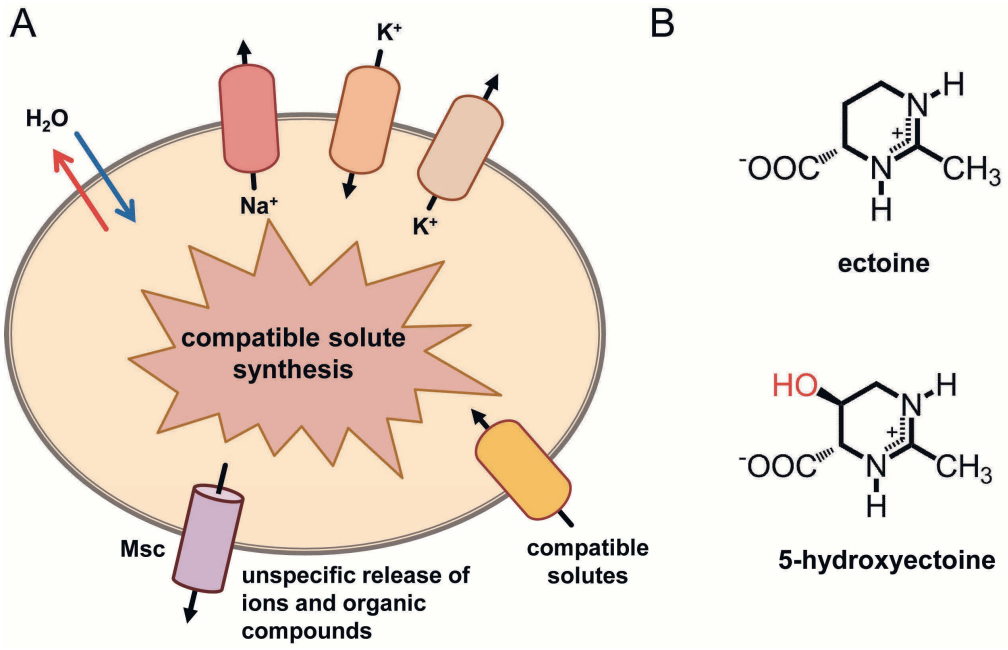

Figure 1. (**A**) General overview of the microbial *salt-out* osmostress adaptation strategy. The components, ion fluxes, and compatible solute pools generated via import and synthesis under hyperosmotic conditions [1,2], and the non-specific release of ions and low molecular weight organic compounds via mechanosensitive channels (Msc) under suddenly imposed hypo-osmotic circumstances are depicted [11,20]. (**B**) Chemical structures of the compatible solutes ectoine and 5-hydroxyectoine.

To avoid rupture under suddenly imposed hypo-osmotic condition, bacteria engage safety valves embedded in the cytoplasmic membrane, the mechanosensitive channels (Figure 1A). An immediate consequence of the osmotically driven water influx upon down-shock is the gating of these channels, a process caused by the increase in the tension of the lateral plain of the cytoplasmic membrane as the consequence of increased turgor. Often, multiple types of mechanosensitive channels [MscM (mini), MscS (small), MscL (large)] are present in a given microbial cell and they possess different pore sizes and gating behaviors [11,20,26,27,30–32]. Their transient opening allows a rapid, non-specific jettison of low-molecular-weight solutes (both ions and organic compounds), whereupon the mechanosensitive channels close again as a result of the reduction in the osmotic potential of the cytoplasm and the ensuring decrease in turgor. Consequently, by relying on the turgor-driven opening and closing of mechanosensitive channels (Figure 1A), the cell can mount a timely and graded response to the severity of the suddenly imposed osmotic imbalance [11,20,30,32]. Mechanosensitive channels are essential for cellular survival under severe osmotic down-shock conditions [11,16–18], but not during steady-state growth at either high or low osmolarity [16,17].

2. The *Salt-In* and *Salt-Out* Strategies for Coping with High Osmolarity Environments

The *salt-in* strategy relies on the massive accumulation of K^+ and Cl^- ions from environmental sources through transport and the active extrusion of cytotoxic Na^+ ions from the cell [24,25]. As a consequence of the permanently high ion content of the cytoplasm, the biochemical properties and the compositions of all proteins have to be adjusted to keep them soluble and functional. On an evolutionary time scale, this has left an acidic signature on the proteome with a narrow distribution of isoelectric points as the consequence of reduced hydrophobicity of proteins and a strong increase in negatively charged amino acids exposed on protein surfaces [33–35]. The *salt-in* strategy is energetically favorable [36,37], and is thus particularly effective in habitats with sustained very high salinity [23–25], but seems less useful in environments in which the salinity/osmolarity fluctuates more often [1,3–5].

A more flexible adjustment to high-osmolarity environments is provided by the *salt-out* strategy, which is therefore used widely in the microbial world [1,5]. This strategy also entails a rapid uptake of potassium ions as an emergency reaction to a sudden challenge by high osmolarity, but part of the initially amassed K^+ pool is subsequently replaced by the cells through types of organic osmolytes that are highly compliant with cellular functions, the compatible solutes (Figure 1A) [1–4]. In this way, the cell attains a level of hydration of the cytoplasm that is appropriate for biochemical processes and simultaneously upholds turgor without concurrently raising the intracellular ionic strength, as this would greatly impair most physiological activities of the cell [2,10]. As an added benefit, the *salt-out* strategy does not require an evolutionary adjustment in the proteome profile. However, the amassing of compatible solutes, either through uptake or synthesis [1,2], is energetically substantially more demanding than the *salt-in* strategy [36,37].

It was thought that the *salt-in* and *salt-out* strategies were mutually exclusive, and that the observation of an acidic proteome was predictive for the use of the *salt-in* strategy. While this is probably correct in general, recent findings require a modification of this long-held view [38,39]. For instance, a group of *Halobacteriales*, halophilic Archaea, was found to combine a high K^+ cytoplasm with the accumulation of the compatible solutes trehalose and 2-sulfotrehalose [38]. Notably, in the extreme halophilic archaeon *Halobacterium salinarum*, even chemotaxis towards the osmoprotectants glycine betaine, carnitine, and choline has been detected [40]. While pathways for the synthesis of compatible solutes in extremely halophilic Archaea seem to be rare, those for the uptake of compatible solutes are prevalent [41]. These observations indicate that some haloarchaea, at least under certain environmental conditions, might combine the *salt-in* and *salt-out* strategies to combat the detrimental effects of high salinity on cellular physiology. It is also noteworthy that in several phylogenetically closely related members of the genus *Halorhodospira*, different osmostress adaptation strategies can be found. For instance, in *Halorhodospira halophila*, a highly acidic proteome is combined with a high K^+/Cl^- pool, while in *Halorhodospira halochloris* this is not the case; instead, this halo-alkaliphilic microorganism is a producer of compatible solutes [24,39,42]. Finally, it was thought that obligate protein halophilicity was the price evolution had to pay for the *salt-in* strategy, but *H. halophila* can substantially reduce its K^+ content from about 2.1 M in cells grown at high salinity to a level (0.4 M) comparable to that of *E. coli* when it is cultivated in media with more moderate salt concentrations (0.21 M) [39]. As stated by A. Oren in his insightful review on intracellular K^+ and acid proteomes [24], the previously clear-cut picture of a correlation between phylogenetic affiliation and mode of salt adaptation, and the correlation between acidic proteomes, accumulation of high K^+ content, and the use of compatible solutes needs a careful re-evaluation. The findings that some microorganisms combine an acidic proteome with the accumulation of compatible solutes [24,38,41,43], and that a substantial reduction in K^+ content can be accomplished in *salt-in* adopters under more moderate salt-stress conditions [39], prompts the exploration of new avenues of research and raises intriguing questions about the role played by protein halophilicity in the evolution of microbial osmostress responses.

3. Compatible Solutes

Stress-Relieving Cytoprotectants Used in All Three Domains of Life

One of the main physiological roles played by compatible solutes in Archaea, Bacteria and Eukarya is to counteract the negative effects of high external osmolarity on cellular hydration and volume [1,5,44–47]. They are therefore amassed by microbial cells with pool sizes that increase in accordance with the degree of the imposed osmotic stress. Compatible solutes are operationally defined as organic osmolytes that can be accumulated by cells to exceedingly high levels without disturbing vital cellular functions [48]. They are also addressed as counteracting [44] or compensatory [49] organic solutes to highlight their cytoprotective effects against challenges in addition to those posed by high osmolarity/salinity; for example, low and high temperate extremes, hydrostatic pressure, freezing, desiccation, and the denaturation of macromolecules by ions and urea. These types of solutes have

physico-chemical properties that distinguish them from other types of organic compounds, and similar types of low-molecular weight compounds have been selected during the course of evolution in all three domains of life to fulfill cellular functions as cytoprotectants [1,5,45–47,50]. One of the most widely distributed compatible solutes on Earth is glycine betaine. This compound, and many other compatible solutes as well, is not only employed as an effective osmostress protectant, but also also provides cytoprotection against challenges posed by extremes in growth temperature and hydrostatic pressure, attributes that lead to the description of particular compatible solutes as thermolytes and piezolytes, respectively [50–58].

A hallmark of compatible solutes is their preferential exclusion from the immediate hydration shell of proteins [59], an effect largely caused by unfavorable interactions between these solutes and the protein backbone [60–62]. This preferential exclusion [59] leads to an uneven distribution of compatible solutes in the cell water and therefore generates a thermodynamic driving force that acts against the denatured and aggregated state of proteins. Hence, proteins are forced to adopt a compact and well-folded state under intracellular unfavorable osmotic and ionic conditions to minimize the number of excluded compatible solute molecules from surfaces [61,62]. Consequently, the accumulation of compatible solutes not only has beneficial effects on cellular hydration and maintenance of turgor, but also promotes the functionality of macromolecules (e.g., in particular, proteins and membranes, and protein:DNA interactions) under otherwise activity-inhibiting conditions [54,63–69].

The function-preserving property of compatible solutes has attracted considerable biotechnological interest, and the term "chemical chaperones" was coined in the literature [54,70,71] to reflect the beneficial effects of these compounds as protein stabilizers and protectants for entire cells [72–75]. The function of compatible solutes as chemical chaperones will certainly contribute to their role as protectants against extremes in either high or low temperatures for microorganisms [51–54,76–81], an underappreciated physiologically important attribute of these types of solutes. For instance, the hyperthermophile *Archaeoglobus fulgidus* cannot grow at 90 °C in a chemically fully defined minimal medium [82], despite the fact that this archaeon synthesizes the extremolyte diglycerol phosphate in response to heat stress, an excellent stabilizer of protein function at high temperature [56,83]. However, the addition of 1 mM glycine betaine to the growth medium and its import via the heat stress inducible ProU ABC transporter efficiently rescued growth of *A. fulgidus* at the extreme temperature of 90 °C [82]. In other words, glycine betaine can act as an effective thermoprotectant for a hyperthermophile. Similarly, a defect in the molecular chaperone DnaK that causes thermo-sensitivity of *E. coli* at 42 °C, can be functionally rescued by an external supply of the compatible solutes L-proline, glycine betaine and by the glycine betaine biosynthetic precursor choline [53,76]. Furthermore, a broad spectrum of compatible solutes serves as thermoprotectants at the cutting upper (about 52 °C) and lower (about 13 °C) temperature boundaries for growth of *Bacillus subtilis* in a chemically defined minimal medium [51,52,84,85].

Although originally coined for unusual compatible solutes produced by microorganisms that live in habitats with extreme temperature, salt and pH profiles [86], the term extremolyte can be applied to these types of solutes in general [5,55,57,86,87]. This is exemplified by the above-cited example of the impressive thermoprotection of *A. fulgidus* by the "ordinary" compatible solute glycine betaine. Within the domain of the Bacteria, important representatives of compatible solutes are the amino acid L-proline, the trimethylammonium compound glycine betaine and its analogue arsenobetaine, proline-betaine, the sugar trehalose, the heteroside glucosylglycerol, the sulfur-containing dimethylsulfoniopropionate (DMSP), and the tetrahydropyrimidines ectoine and 5-hydroxyectoine. We refer readers to several excellent overviews that address the diversity of compatible solutes produced and imported by Bacteria and Archaea [4,5,55,57,87].

Here we focus on the synthesis and import of the compatible solute ectoine and its derivative 5-hydroxyectoine (Figure 1B), their stress-relieving properties, and their alternative function as versatile microbial nutrients.

4. Ectoine and Hydroxyectoine

1. Discovery

Ectoine [(4*S*)-2-methyl-1,4,5,6-tetrahydropyrimidine-4-carboxylic acid] (Figure 1B) was originally discovered in the extremely halophilic phototrophic purple sulfur bacterium *Ectothiorhodospira halochloris* (now taxonomically re-classified as *H. halochloris*) by Galinski et al., in 1985 [88]. This seminal discovery was followed by the detection of a hydroxylated derivative of ectoine, 5-hydroxyectoine [(4*S*,5*S*)-2-methyl-5-hydroxy-1,4,5,6-tetrahydropyrimidine-4-carboxylic acid] by Inbar and Lapidot in 1988 in the Gram-positive soil bacterium *Streptomyces parvulus* [89], a compound that the authors initially referred to as THP (A) [2-methyl-4-carboxy-5-hydroxy-3,4,5,6-tetrahydropyrimidine]. Ectoine and 5-hydroxyectoine (Figure 1B) can chemically be classified as either heterocyclic amino acids or as partially hydrogenated pyrimidine derivatives [88–90]. Both ectoine and 5-hydroxyectoine were initially viewed as rare naturally occurring compatible solutes (e.g., in comparison with the almost universally distributed glycine betaine molecule). However, improved screening procedures using HPLC analysis and, in particular, ^{13}C-natural abundance NMR spectroscopy revealed their widespread synthesis in bacteria in response to high salinity [25,55]. Ectoine producers can be found within a physiologically and taxonomically diverse set of microbial species [91–94]. Today, ectoines are known to be one of the most ubiquitously distributed compatible solutes in the microbial world.

The identification of ectoine biosynthetic genes (*ectABC*) [95] and of the gene coding for the ectoine hydroxylase (*ectD*) [96–98] proved to be a major step forward for an in silico assessment of the distribution of ectoine/5-hydroxyectoine biosynthesis in microorganisms, an approach made possible by the rapid and unabated growth in the number of available genome sequences of Bacteria and Archaea [92,93]. Producers of ectoines are primarily found among members of the domain of the Bacteria [91,93,99] and in a rather restricted number of the Archaea [92]. Surprisingly, ectoine/5-hydroxyectoine biosynthetic genes and production of ectoine have recently also been detected in some bacteriovorus unicellular Eukarya [100–102] that live in permanently high-salinity ecosystems [103]; these protists probably acquired the ectoine/5-hydroxyectoine biosynthetic genes through lateral gene transfer from their food bacteria [100,104].

2. Physico-Chemical Attributes

Like other compatible solutes [61,62], ectoine and 5-hydroxyectoine (Figure 1B) are low-molecular mass compounds that are highly soluble in water (about 4 M at 20 °C) [105], thereby allowing the amassing of these compounds to near molar concentrations in severely osmotically stressed microbial cells [91,94,106]. A variety of biophysical techniques have been used to study the effects of ectoine on the hydration of proteins and cell membranes and on interactions mediated via hydrogen bonding. Collectively, these data showed that ectoine is excluded from the monolayer of dense hydration water around soluble proteins and from the immediate hydration layer at the membrane/liquid interface [66,105]. Ectoine enhances the properties of hydrogen bonds in aqueous solutions and thereby contributes to the dynamics and stabilization of macromolecular structures. Ectoine possesses a negatively charged carboxylate group attached to a ring structure that contains a delocalized positive charge (Figure 1B). The resulting interplay between hydrophilic and hydrophobic forces influences water-water and water-solute interactions [107] and thereby exerts strong effects on the hydration of ectoine itself, the binding of ions and the influence on the local water structure [108–111].

Molecular dynamics simulations have indicated that ectoine and 5-hydroxyectoine are strong water-binders and are able to accumulate seven and nine water molecules, respectively, around them at a distance smaller than 0.6 nm [67]. This results in the formation of a large number of hydrogen bonds at specific functional groups of molecules. Furthermore, these studies indicated that the water-binding behavior of ectoines is not abrogated or perturbed at high salt concentrations [67]. The influence of ectoines on the local water structure also exerts pronounced effects on protein-DNA interactions [109,112–114], a crucial effect that might alter the transcriptional profile of salt-stressed

cells on a genome-wide scale [68]. Collectively, the physico-chemical attributes of ectoines allow a physiologically adequate hydration of the cytoplasm upon their osmostress-responsive accumulation, afford effects on the local water structure, and also exert a major protective influence on the stability of proteins and the functionality of macromolecules [72,73,105,114,115].

4.3. Stress-Protective Properties

Ectoine and 5-hydroxyectoine are produced by microorganisms in response to true osmotic stress, and not just in response to increases in the external salinity [116]. In cases where the build-up of ectoine/5-hydroxyectoine pools has been studied in more detail, there is often a linear relationship between the cellular content of these solutes and the external salinity/osmolarity [116–118]. This finding implies that bacterial cells can perceive incremental increases in the degree of the environmentally imposed osmotic stress, can process this information genetically/physiologically, and can then set its ectoine/5-hydroxyectoine biosynthetic capacity in a finely tuned fashion to relieve the constraints imposed by high-osmolarity on cellular hydration, physiology, and growth [1–4]. As described in greater detail in Section 5.2, high-osmolarity-dictated increases in the cellular ectoine pools are largely accomplished through osmotically-responsive increases in the transcription of the ectoine/5-hydroxyectoine biosynthetic genes, although there might be post-transcriptional effects as well. Attesting to the role of ectoine as a potent osmostress protectant is the finding that the disruption of the *ectABC* biosynthetic genes (see Section 5.1) causes osmotic sensitivity [119,120] and the genetic disruption of the gene (*ectD*) for the ectoine hydroxylase in *Chromohalobacter salexigens* impairs the ability to cope effectively with high growth temperature extremes [97].

In addition, environmental challenges other than high osmolarity also trigger enhanced production of ectoines in some microorganisms, in particular, extremes in either high or low growth temperatures [77,81,97]. Furthermore, the function of ectoines as thermolytes is also manifested when microbial cells acquire these solutes from environmental sources through transport processes [78,79,121]. Although the term chemical chaperone is suggestive of a description of the function-preserving attributes of compatible solutes, it is not truly clear how the thermoprotective effects of ectoines are achieved on a biochemical and molecular level. We find it also important to note in this context that the mechanisms underlying the cytoprotective effects of ectoines at high and low temperature do not necessarily need to be the same. In addition, both processes might be, in their core, different from the cytoprotective effects exerted by ectoines when they act as osmostress protectants.

In microorganisms that are capable of synthesizing both ectoine and 5-hydroxyectoine, a mixture of these two solutes is frequently found. Interestingly, such a 1:1 mixture (0.5 mM each) provided the best salt and heat stress protection to *Streptomyces coelicolor* when it was added to the growth medium [79]. However, there are also microorganisms that seem to produce almost exclusively 5-hydroxyectoine during osmotic stress and different growth phases of the culture [122,123].

An interesting phenomenon that has been dubbed osmolyte switching [124,125], plays an important role in the temporal dynamics of ectoine production in some microorganisms. For instance, *Halobacillus halophilus*, which uses a hybrid osmostress adjustment strategy of Cl^- and compatible solute accumulation [125], initially uses L-glutamate as its primary organic osmolyte and then switches to the synthesis of L-proline when the external salinity is further increased. A second switch in the preferred compatible solute then occurs from L-proline to ectoine at the transition from exponential to stationary phase [124,125]. Similarly, *Virgibacillus pantothenticus* initially relies on the synthesis of L-proline when it is osmotically challenged by moderate increases in the external salinity, and then triggers enhanced ectoine production once the salinity of the growth medium is increased above 0.6 M NaCl [77]. Hence, in microorganisms that produce several organic osmolytes, there seems to be, at least in certain cases, a temporal hierarchy in the type(s) of the dominantly synthesized compatible solute(s). Apparently, when the environmental and cellular circumstances get particularly tough, ectoine is preferentially produced. This notion fits nicely with the results of a study in which the dominantly produced compatible solute(s) in a substantial number of Bacilli were assessed by natural abundance

^{13}C-NMR-spectroscopy [98,117]. Three groups were detected: (i) those that synthesize exclusively L-glutamate, (ii) those that synthesize L-glutamate and L-proline, and (iii) those that synthesize both L-glutamate and ectoine. Some members of this latter group also produce 5-hydroxyectoine. Although not studied in detail, there seems to be a correlation between the type of compatible solute synthesized and the degree of the attained osmostress resistance, with ectoine/5-hydroxyectoine producers being the most salt-stress tolerant Bacilli [98,117]. Presumably, this phenomenon is related to the different physico-chemical attributes of L-glutamate, L-proline, and ectoine and the ensuing effectiveness by which they can than serve as compatible solutes [107,126–128].

As mentioned above, a substantial increase in 5-hydroxyectoine content occurs not only in response to osmotic challenges in some microorganisms, but also when cells enter stationary phase [121,129]. This observation implies that the hydroxylated derivative of ectoine possesses stress-relieving properties that will allow the cell to better cope with the multitude of challenges imposed by stationary phase [130,131]. This attribute might stem from the frequently observed superior function-preserving properties of 5-hydroxyectoine when tested either in vivo [79,97] or in vitro [72–75,114,132–134]. Fourier transform infrared and electron spin resonance studies revealed that 5-hydroxyectoine has a substantially greater glass-forming propensity than ectoine, a trait that stems from stronger intermolecular hydrogen-bonds with the OH group of 5-hydroxyectoine (Figure 1B) [132]. As a consequence of the strongly increased glass transition temperature (87 °C for 5-hydroxyectoine versus 47 °C for ectoine), 5-hydroxyectoine is an excellent desiccation protectant, a characteristic that not only allows the stabilization of individual biomolecules, but the protection of entire cells from anhydrobiotic-induced damage [74,75]. Biosynthesis and external application of 5-hydroxyectoine can thus be exploited for synthetic anhydrobiotic engineering [84,85,132]. In *C. salexigens*, 5-hydroxyectoine has also been found to be a better protectant than ectoine against oxidative stress caused by an excess supply of iron in the growth medium [135].

In *Alcalivorans borkumensis* SK2, a member of a widely distributed genus dominating oil spills worldwide, ectoine has been suggested to function as a piezolyte by protecting the cell against excess hydrostatic pressure [136]. However, a previous study found no evidence for such a function for ectoine by comparing the pressure survival of the piezo-sensitive *E. coli* cell (non-ectoine producer) with that of *C. salexigens* (an ectoine producer) [137]. Ectoines also have pronounced effects on the melting temperature of DNA, but ectoine and 5-hydroxyectoine differ in this regard. While ectoine lowers the melting temperature, 5-hydroxyectoine increases it [114]. Furthermore, ectoine protects DNA against the induction of single-strand breaks by ionizing radiation and serves as a scavenger for hydroxyl radicals [138–140]. Ectoine is also a potent protectant against UV-induced cellular stress [141,142]. Interesting stress-protective and function-preserving properties might also be derived from synthetic ectoines with reduced or expanded ring sizes [143] or by chemical modifications that provide a hydrophobic anchor (e.g., lauryl-ectoine) to the otherwise highly water-soluble ectoine molecule [144].

4.4. Biotechnological Production and Practical Applications of Ectoines

The excellent function-preserving attributes of ectoines have attracted considerable attention to their exploitation in the fields of biotechnology, skin care, and medicine [86,91,94,145–147]. This demand for ectoines for practical purposes has led to an industrial-scale production process that exploits *Halomonas elongata* as a natural and engineered cell factory, delivering ectoines on the scale of tons [86,91,94]. Data reported in the literature [148,149] estimate a worldwide production level of ectoines of about 15,000 tons per annum, which putatively have an estimated sales value of approximately 1000 US Dollars kg^{-1}. However, another study reports a price for ectoine at between about 14,000 and 18,000 Euro kg^{-1} [150]. We are not certain what these numbers are actually based upon, since details pertinent to their calculations are not given in these publications [148–150]. However, there can be no doubt that ectoines are high-value natural products. By consulting catalog prices listed by vendors of laboratory chemicals (and not by the major industrial producer of ectoine; bitop AG, Dortmund, Germany; https://www.bitop.de/), the purchasing costs for one kg of ectoines

ranges between 9000 Euro (Acadechem, Hong Kong, China) and 17,000 Euro (AppliChem, Darmstadt, Germany) kg^{-1} for ectoine, and the sale price for 1 kg of 5-hydroxyectoine is about 17,000 Euro (Merck, Darmstadt, Germany).

Of the extremolytes currently considered for practical applications [146], ectoine and 5-hydroxyectoine certainly have the greatest potential for sustained commercial exploitation [86,91,94,145,147]. It is outside the scope of this overview to address in depth the biotechnological production of ectoines in natural and synthetic microbial cell factories, or to describe in detail the varied practical applications for these compounds. Insightful reviews covering these topics have been published [86,91,94,145], and recent reports have summarized the current status of efforts to improve the productivity of natural and synthetic microbial cell factories for ectoines [116,123,151–157].

Briefly, the industrial-scale production scheme for ectoine relies on the highly salt-tolerant gammaproteobacterium *H. elongata* as a natural cell factory [86,158]. It exploits the massive production of ectoines under high-salinity growth conditions by this bacterium [158] and their non-specific release from the producer cells via the transient opening of mechanosensitive channels upon a severe osmotic down-shock [91,94,159]. Since the gating of mechanosensitive channels prevents cell rupture [11,20,32], the biomass formed during the originally high-cell density fermentation of *H. elongata* under osmotic stress conditions can be re-introduced into the fermentation vessel for a new round of ectoine production and release [91,94,159]. This innovative production process has been fashionably dubbed bacterial milking [159]. During subsequent strain development, the production process was amended by the use of *H. elongata* mutants that lack the TeaABC system, a TRAP-type [160] ectoine/5-hydroxyectoine-specific transporter that can serve as a recycling system for newly synthesized ectoines released, or actively excreted, from the *H. elongata* producer cells [161]. Use of *tea* mutants in the industrial production strain leads to the continuous accumulation of ectoines in the growth medium [94,161]. Ectoines jettisoned during osmotic downshifts of *H. elongata* cells, or released into the growth medium by the *tea* mutant strain, can be recovered from the fermentation medium with high yield and purity by down-stream processes via protein precipitation through acidification, cation exchange chromatography, and evaporation/crystallization [86,91,94,145–147].

A number of commercial applications for ectoines have been developed that rely, in their core, on the ability of ectoine and 5-hydroxyectoine to serve as water-attracting and water-structure-forming compounds [109–111], to stabilize macromolecules and entire cells through their chaperon and glass-forming effects [66,67,86,91,94,105,132,145], to protect DNA from ionizing radiation [138,140], and to prevent UV-induced cell damage of skin cells [141,142,145]. These latter two properties and the moisturizing effects of ectoines have fostered the development of a wide range of products for skin care and cosmetics [145]. Ectoines are used to stabilize enzyme activity in vitro, for promoting protein folding in vivo, for protecting molecules and cells against cycles of freezing and thawing, for promoting their desiccation resistance, for enhancing the resistance of cells and DNA against ionizing radiation and damage elicited by UV, as oxidative and temperature stress protectants, for preventing the impairment of cell membrane functions, for cytoprotection of eukaryotic cells and organs, and they have even been evaluated as protectants against neurodegenerative diseases [86,91,94,145,147].

Compatible solutes have also been explored as beneficial additives to biological waste and wastewater treatment systems to counteract osmotic and other types of environmental stresses [150]. In addition to glycine betaine and trehalose, the effects of ectoine have also been evaluated in this regard. A denitrifying microbial consortium has been used to study the effect of ectoine on denitrification at increased salinity. The addition of ectoine (1 mM) accelerated the de-nitrification process, promoted the almost complete removal of nitrates and nitrites relative to that of control samples in a shorter time frame, and enhanced the activity of key degradative enzymes [162]. The addition of ectoine also stimulated the Anammox process (by about 40%) under conditions of increased salinity [163]. While these pilot studies demonstrate the use of compatible solutes in general, and that of ectoine in particular, for these types of applications [150], it is unlikely that ectoine can ever be used in large-scale biological waste and wastewater treatment systems unless the production costs for ectoine would drop

precipitously and become competitive with the bulk-chemical glycine betaine (196 Euro kg^{-1}) (Merck, Darmstadt, Germany).

5. Ectoine/5-Hydroxyectoine Biosynthetic Routes and Crystal Structures of Selected Enzymes

1. Biosynthetic Pathway: An Overview

Three enzymes are involved in ectoine synthesis: L-2,4-diaminobutyrate (DABA) transaminase (EctB; EC 2.6.1.76), L-2,4-diaminobutyrate acetyltransferase (EctA; EC 2.3.1.178), and ectoine synthase (EctC; EC 4.2.1.108). 5-hydroxyectoine is formed in a subgroup of ectoine producers through a position- and stereo-specific hydroxylation of ectoine, an enzymatic reaction catalyzed by the ectoine hydroxylase (EctD; EC 1.14.11.55) (Figure 2).

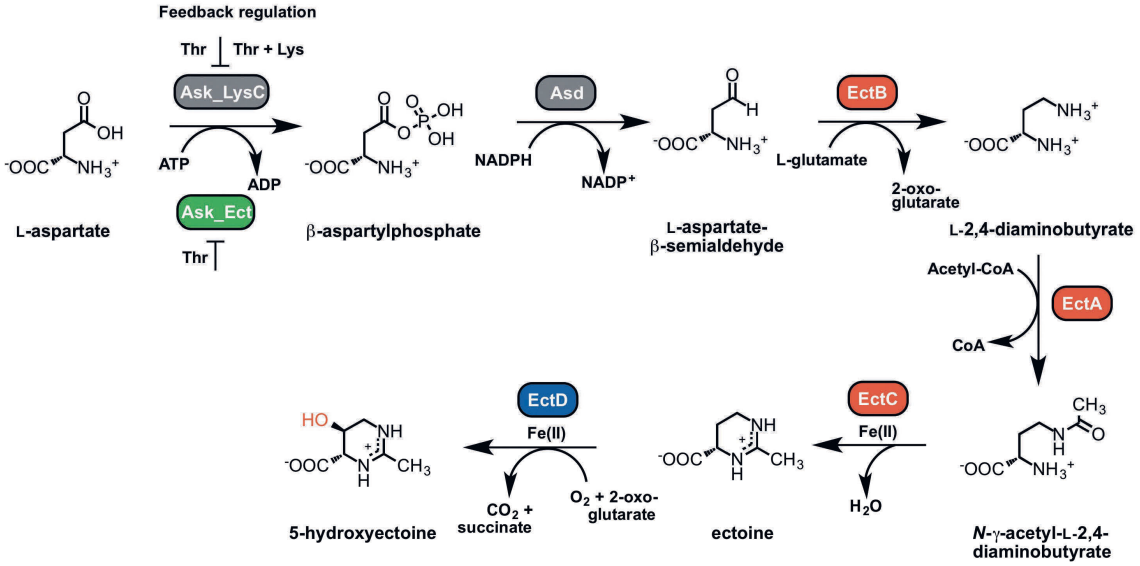

Figure 2. Routes for ectoine and 5-hydroxyectoine biosynthesis.

The ectoine biosynthetic route was originally elucidated by Peters et al. [164] through an analysis of enzyme activities present in cell-free extracts of *E. halochloris* and *H. elongata*. Ono et al. [165] subsequently made major contributions to an understanding of the biochemistry of the ectoine biosynthetic enzymes; these authors used purified EctABC proteins from *H. elongata* to study their enzymatic properties. In addition, biochemical procedures to study these enzymes from various methylotrophic bacteria were summarized by Reshetnikov et al. [166]. The biochemical properties of ectoine hydroxylase from *Salibacillus salexigens* were first determined by Bursy et al. [79,98], and Widderich et al. [92,93] subsequently studied this enzyme from a substantial number of Bacteria and from a single archaeon. Ectoine is synthesized from the precursor L-aspartate-β-semialdehyde (Figure 2), a central intermediate of microbial amino acid metabolism and cell wall and antibiotic synthesis [167]. In a sub-group of ectoine/5-hydroxyectoine producers, the ectoine/5-hydroxyectoine biosynthetic gene cluster contains a gene (*ask_ect*) for a specialized aspartokinase [93,168]. Its biochemical properties were studied by Stöveken et al. [122] using the Ask_Ect enzyme from *Pseudomonas stutzeri* A1501 and by Reshetnikov et al. [166] using the corresponding enzyme from *Methylobacterium extorquens* AM1.

In comparison with the energetic demands to sustain the *salt-in* osmostress adjustment strategy through the import of ions, implementation of the *salt-out* strategy through the production of massive amounts of compatible solutes is energetically very costly for microorganisms [36,37]. This is, of course, also true for the synthesis of ectoine. As calculated by A. Oren, the energy requirements (expressed in ATP equivalents) for the synthesis of a single ectoine molecule by an aerobic heterotroph growing on

glucose corresponds to about 40 ATP equivalents and increases to approximately 55 ATP equivalents when ectoine is synthesized by an autotroph from CO_2 [37]. These values closely resemble those calculated for the synthesis of the compatible solute glycine betaine under these two growth conditions [37] when it is produced either via the sequential methylation of glycine [169] or the through oxidation of choline [170–172]. From an energetic point of view, synthesis of ectoine and glycine betaine are considerable less expensive than that of the compatible solute trehalose, whose production by an aerobic heterotroph growing on glucose requires the expenditure of about 79 ATP equivalents, an energetic cost that rises to about 109 molecules of ATP when this disaccharide is produced by an autotroph from CO_2 [37].

2. Characteristics of the Ectoine/5-Hydroxyectoine Biosynthetic Enzymes

1. L-2,4-Diaminobutyrate Transaminase EctB

Ectoine synthesis starts with the transamination of the precursor L-aspartate-β-semialdehyde, a reaction catalyzed by the L-2,4-diaminobutyrate-2-oxoglutarate transaminase EctB. EctB might be a pyridoxal-5^0-phosphate (PLP)-dependent enzyme [173] similar to other aminotransferases, and requires K^+ for its activity and stability [165]. The EctB enzyme accepts L-aspartate-β-semialdehyde as its substrate and catalyzes the reversible transfer of an amino group from L-glutamate to the aldehyde group of the substrate, thereby forming L-2,4-diaminobutyrate (DABA) and 2-oxoglutarate (Figure 2). Biochemical characterization of EctB was reported for the orthologous enzymes from *H. elongata* [165] and *Methylomicrobium alcaliphilum* [99]. Both enzymes are homo-hexameric proteins and have a strong requirement of K^+ for their enzymatic activity and stability. The preferred amino group donors are L-glutamate for the forward reaction (forming DABA) and DABA or 4-aminobutyrate for the reverse reaction (forming glutamate). Optimal catalytic activities were recorded for the enzyme from *H. elongata* at temperatures of 25 °C, a slightly alkaline pH of 8.6, and KCl concentrations of 0.5 M. Addition of NaCl (0.05–0.5 M) also enhanced the enzyme activity, but the enhancing effect of KCl in the range of 0.01–0.5 M on enzyme activity was much stronger. The apparent K_m values are 9.1 mM for the amino group donor L-glutamate and 4.5 mM for the amino group acceptor L-aspartate-β-semialdehyde [165].

An innovative approach was taken by Chen et al. [156] to identify variants of the *H. elongata* EctB enzyme with substantially enhanced catalytic activity. These authors re-engineered the AraC transcription factor from *E. coli* so that it would preferentially respond in its DNA-binding activity to the *ara* promoter (P_{BAD}) to the cellular ectoine pool, instead of to its natural effector molecule L-arabinose. They then combined the synthetic $AraC^{Ect}$ regulatory protein with a P_{BAD}-ECFP fluorescent reporter system in a strain simultaneously expressing the *H. elongata ectABC* gene cluster on a plasmid. In this way, they were able to identify variants of the *ectABC* gene cluster, generating higher cellular ectoine pools. These strains carried amino acid substitutions in EctB, the enzyme that controls the flux of the precursor L-aspartate-β-semialdehyde into the ectoine biosynthetic route (Figure 2) [165,166]. One of the recovered *ectB* mutants simultaneously carried three mutations, leading to amino acid substitutions D180V/F320Y/Q325R. The encoded mutant EctB enzyme exhibited a notably improved (by about 4.1-fold) catalytic efficiency (K_{cat}/K_m), and thereby concomitantly increased cellular ectoine titers in the heterologous *E. coli* host by about 3.3-fold relative to a strain possessing the wild-type EctB protein [156]. The bio-sensing metabolic engineering approach used by Chen et al. [156] should be generally applicable for improving the biotechnological production of ectoines for practical purposes, both in natural and in synthetic cell factories and might, as evidenced by EctB, yield interesting variants of the ectoine biosynthetic enzymes.

2. L-2,4-Diaminobutyrate Acetyltransferase EctA

The transformation of DABA and the co-substrate acetyl-coenzyme A into *N*-γ-acetyl-2,4-diaminobutyrate (*N*-γ-ADABA) and CoA is catalyzed by the L-2,4-diaminobutyrate acetyltransferase EctA. This enzyme belongs to the large superfamily of GCN5-related-*N*-acetyltransferases (GNAT)

that catalyze the transfer of an acetyl-group from acetyl-coenzyme A as donor to a primary amine as acceptor molecule [174]. Ono et al. [165] were the first to report on the enzymatic properties of an EctA ortholog isolated from *H. elongata*. The partially purified enzyme showed its highest activities at pH 8.2, at temperatures of about 20 °C, and in the presence of 0.4 M NaCl. Gel filtration experiments revealed a native molecular mass of about 45 kDa, which represents a homodimer of the EctA subunit. Three further EctA orthologs from methanotrophic or methylotrophic bacteria (*M. alcaliphilum*, *Methylophaga thalassica*, and *Methylophaga alcalica*) were subsequently biochemically characterized by Trotsenko and co-workers [99,168,175]. Their properties reflect the different physiologies of the host species from which they were isolated. The highest enzyme activities were recorded at a slightly alkaline pH of 8.5 for the enzyme derived from the neutrophilic *M. thalassica* and at a more alkaline pH of 9.5 for the enzymes obtained from the alcaliphiles *M. alcalica* and *M. alcaliphilum*. Interestingly, the activities of the EctA enzymes from the two methylotrophic *Methylophaga* species were inhibited by addition of NaCl or KCl, while the orthologous protein of the methanotrophic *M. alcaliphilum* was activated by these salts with an optimum of salt concentration of about 0.2 M NaCl or 0.25 M KCl [99].

A crystal structure of the homo-dimeric EctA protein from the human pathogen *Bordetella parapertussis* has been solved [Protein Data Bank (PDB) accession code 3D3S]. In this structure, a single molecule of the substrate DABA is bound within the dimer interface (Figure 3A). However, the experimental details of this particular EctA crystal structure or the biochemistry of the enzyme have not been formally published. Hence, nothing is known about the enzymatic properties of the *B. parapertussis* EctA enzyme and whether the unusual position of the substrate within the dimer assembly was experimentally verified through site-directed mutagenesis of residues within the supposed active site.

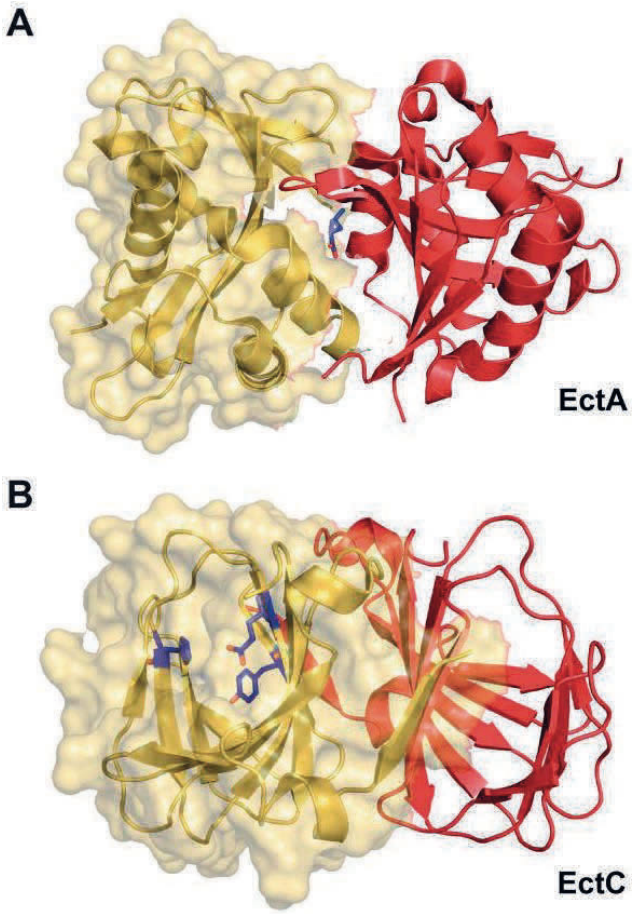

Figure 3. *Cont.*

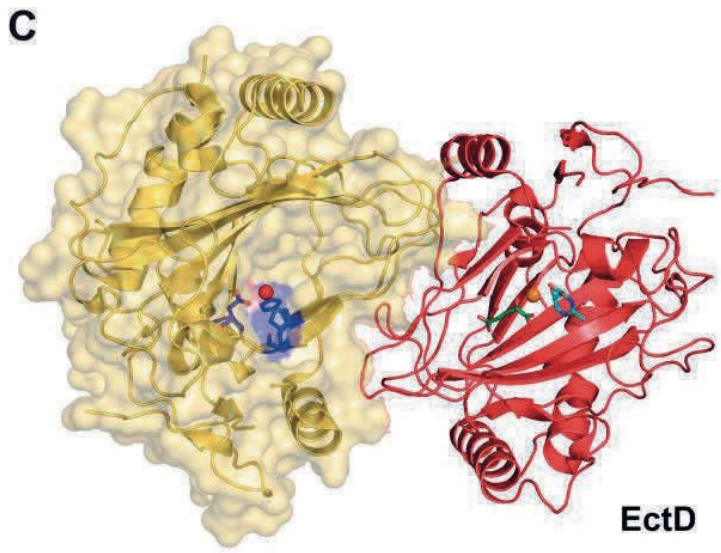

Figure 3. Crystal structures of the EctA and EctC ectoine biosynthetic enzymes and that of the ectoine hydroxylase EctD. Dimers of the L-2,4-diaminobutyrate acetyltransferase (EctA), ectoine synthase (EctC), and ectoine hydroxylase (EctD) are depicted. (**A**) In the crystal structure of the EctA protein from *Bordetella parapertussis* [Protein Data Bank (PDB) accession code 3D3S] a single molecule of the substrate DABA is bound at the dimer interface. (**B**) Crystal structure of the EctC protein from *Sphingopyxis alaskensis* (PDB accession code 5BXX). In one of the dimers, the putative metal-binding residues (Glu^{57}, Tyr^{85}, His^{93}) are highlighted; these protrude into the lumen of the cupin barrel, where the predicted active site of the enzyme is located [176]. (**C**) Crystal structure of the EctD protein from *S. alaskensis* (PDB accession code 4Q5O). In the left monomer of the dimer assembly, the three residues (His^{144}, Asp^{146}, His^{245}) coordinating the catalytically important iron (shown as an orange sphere) are highlighted. In the right monomer of the dimer assembly, the position of the co-substrate for the EctD enzyme, 2-oxoglutarate, and the ectoine-derived product 5-hydroxyectoine are depicted relative to that of the ion catalyst [177].

5.2.3. Ectoine Synthase EctC

The last step in ectoine biosynthesis, the ring closure to form the end product ectoine, consists of an intramolecular condensation reaction catalyzed by the ectoine synthase EctC (EC 4.2.1.108) (Figure 2). As a member of the carbon-oxygen hydro-lyases (EC 4.2.1), EctC catalyzes the ring enclosure of ectoine by the elimination of a water molecule from a carbonyl C=O-bond in the substrate *N*-γ-ADABA and the generation of an intramolecular imino bond.

The ectoine synthase of *H. elongata* [165] shows its highest enzymatic activity at a pH of 8.5–9.0, a temperature of 15 °C, and in the presence of 0.5 M NaCl. The purified enzyme appears to be stabilized in vitro by the presence of high NaCl concentrations since the optimal temperature for the enzyme reaction can be shifted from 15 °C to 30 °C by raising the NaCl concentration from 0.77 M to 3 M. The NaCl concentration also affects the kinetic properties of EctC. The K_m value of the EctC enzyme for its substrate *N*-γ-ADABA is about 11 mM under low salt concentration (0.05 M NaCl), but decreases to 8.4 mM upon addition of 0.77 M NaCl. The studied EctC enzyme from *H. elongata* showed high substrate specificity towards *N*-γ-ADABA, and Ono et al. [165] found no evidence for a reverse hydrolyzing activity of EctC that would convert the cyclic ectoine molecule into the linear *N*-γ-ADABA. *N*-γ-ADABA (Figure 2) can provide osmostress protection to a degree similar to that afforded by ectoine when it is accumulated in an ectoine synthase (EctC)-deficient mutant of *C. salexigens* [120], or when it is externally provided to salt-stressed *Salmonella typhimurium* cells [178]. Since *N*-γ-ADABA can also protect thermolabile proteins from denaturation [179], it possesses properties that are hallmarks of compatible solutes [54,61,62]. It remains to be seen, however, if this intermediate in ectoine biosynthesis

is accumulated in ectoine-producing wild-type strains to cellular levels that would be relevant for notable function-preserving effects.

The biochemically and structurally best-characterized ectoine synthase is that of the cold-adapted marine alphaproteobacterium *Sphingopyxis alaskensis* [177]. Like other EctC orthologs, it is a dimer in solution, and also in the crystal structures. It possesses the following kinetic parameters: a K_m of about 5 mM, V_{max} of about 25 U mg^{-1}, a k_{cat} of about 7 s^{-1}. Reflecting the permanently cold habitat of *S. alaskensis*, the temperature optimum of its ectoine synthase is 15 °C, and the enzyme has a pH optimum of 8.5. The optimum salt concentration for the enzyme is around 0.25 M of either KCl or NaCl, but the *S. alaskensis* EctC protein is highly salt-tolerant, as substantial enzyme activity is observed when high concentrations of KCl (up to 1 M) or NaCl (up to 0.5 M) are present in the assay buffer [176].

The biochemical properties of the ectoine synthase from the acidiphilic alphaproteobacterium *Acidiphilum cryptum* have been studied, as well [180]. Interestingly, the best enzymatic activity of the recombinantly produced EctC protein was observed in the absence of salt. This difference in the enzymatic properties of the *A. cryptum* ectoine synthase with reference to the strong salt-dependence of the *H. elongata* enzyme (pI 4.87) [165] prompted Moritz et al. [180] to calculate the theoretical isoelectric point (pI) of 80 EctC-type proteins. In this dataset, the *A. cryptum* enzyme exhibits one of the least acidic calculated pI's (6.03), a feature that might contribute to the salt-independence of this particular ectoine synthase.

Only a few members of the Archaea are capable of ectoine synthesis (see Section 6.3). One of them is the thaumarchaeon *Nitrosopumilus maritimus* SCM1 [92]. Its ectoine synthase was heterologously produced and biochemically characterized. The enzyme is a dimer in solution and possesses the following kinetic parameters for its natural substrate *N*-γ-ADABA: a K_m of about 7 mM, a V_{max} of about 13 U mg^{-1}, a k_{cat} of about 6 s^{-1}, and a k_{cat}/K_m of about 1 s^{-1} mM^{-1}. Its temperature and pH optima are about 30 °C and 7, respectively [92]. While the kinetic parameters of the archaeal EctC enzyme resemble those of its bacterial counterpart from *H. elongata* [165], their enzyme activity profile in response to salt is strikingly different. As outlined above, the *H. elongata* enzyme is strongly dependent on high salinity, while the activity of the *N. maritimus* SCM1 ectoine synthase is restricted to a narrow range of salt concentrations [92].

The ectoine synthase can also be exploited to produce non-natural compatible solutes. Witt et al. [181] demonstrated that L-glutamine can be used as an alternative substrate to DABA by the *H. elongata* EctC enzyme, albeit with a very low catalytic efficiency. In this reaction, L-glutamine is converted into the cyclic condensation product 5-amino-3,4-dihydro-2H-pyrrole-2-carboxylate (ADPC). ADPC is a synthetic compatible solute as it enhances bacterial growth under salt stress conditions and also stabilizes enzymes against denaturation caused by repeated cycles of freezing and thawing [181]. The EctC-catalyzed formation of ADPC is reversible, with the equilibrium of this reaction lying largely on the site of the hydrolytic product L-glutamine. The *H. elongata* EctC enzyme is also able to hydrolyze the synthetic ectoine analogs [143] homoectoine [(*S*)-4,5,6,7-tetrahydro-2-methyl-1H-(1,3)-diazepine-4-carboxylic acid], and DL-DHMICA [(*RS*)-4,5-dihydro-2-methyl-imidazole-4-carboxylic acid], whereas its hydrolytic activity for ectoine was found to be negligible [181].

The ectoine synthase belongs to the functionally diverse superfamily of cupin proteins [182,183], and it contains a characteristic cupin domain comprising two conserved motifs [176]. Most members of this protein superfamily are metal-dependent enzymes, and highly conserved residues that are derived from both conserved cupin motifs usually anchor and position the metal cofactor in the active site [182]. Like other cupins [182,183], studies with the *S. alaskensis* EctC enzyme revealed that it is promiscuous with respect to the divalent metal used in enzyme catalysis, but Fe^{2+} is the most-likely biochemically relevant cofactor for the EctC-catalyzed enzyme reaction [176].

The crystal structure of the *S. alaskensis* EctC protein (Figure 3B) has been elucidated at a resolution of 1.2 Å (PDB accession codes 5BXX and 5BY5) [176] and exhibits an overall barrel-type fold typical for cupins [182,183]. While the crystal structures of the *S. alaskensis* ectoine synthase are of high resolution, they unfortunately lack the catalytically important metal, and contain neither the substrate *N*-γ-ADABA nor the reaction product ectoine. Bioinformatics and site-directed mutagenesis identified the most likely residues involved in the binding of the catalytically important metal by the *S. alaskensis* ectoine synthase. The corresponding three residues (Glu^{57}, Tyr^{85}, His^{93}) of the *S. alaskensis* EctC protein are evolutionarily highly conserved among a large group of EctC-type proteins. Their side chains protrude into the lumen of the cupin barrel (Figure 3B) [176], the location at which the cyclo-condensation of the *N*-γ-ADABA substrate to ectoine will take place [182,183]. The *S. alaskensis* EctC protein is a head-to-tail dimer; the dimer interface is formed by two anti-parallel β-sheets present near the N- and C-termini of each monomer, stabilizing interactions that thus occurs twice within the EctC dimer assembly (Figure 3B).

5.2.4. Ectoine Hydroxylase EctD

A substantial number of the ectoine producers additionally synthesize 5-hydroxyectoine [92,93,98] through a position- and stereo-specific hydroxylation of ectoine (Figure 2). Bursy et al. [79,98] elucidated the biochemical basis for the formation of 5-hydroxyectoine through studies with the purified ectoine hydroxylases (EctD; EC 1.14.11.55) from the moderate halophile *S. salexigens* (taxonomically now reclassified as *Virgibacillus salexigens*) and the soil bacterium *S. coelicolor*. This biochemical analysis and subsequent structural work [177,184] revealed that EctD is a member of the superfamily of non-heme Fe(II)-containing and 2-oxoglutarate-dependent dioxygenases [185]. The O_2-dependent hydroxylation of the substrate ectoine is accompanied by the oxidative decarboxylation of 2-oxoglutarate to form succinate and CO_2, while the iron cofactor acts as a catalyst for the activation of molecular oxygen [186] (Figure 2). Therefore, the catalytic activity of the EctD enzyme is strongly dependent on the presence of molecular oxygen [92,93,177,184]. 5-hydroxyectoine produced in vivo by *S. parvulus* is known to have the (4*S*,5*S*) stereo-chemical configuration [90], and the very same configuration is also found in the reaction product formed in vitro by the purified *V. salexigens* EctD enzyme as analyzed by one-dimensional ^{1}H-NMR spectroscopy [98].

To date, nine ectoine hydroxylases have been biochemically characterized; eight of these originate from various, mostly extremophilic, bacteria (*V. salexigens*, *S. coelicolor*, *S. alaskensis*, *Paenibacillus lautus*, *P. stutzeri*, *Alkalilimnicola ehrlichii*, *A. cryptum*, *H. elongata*) [93,184], and one of the studied enzymes was derived from the archaeon *N. maritimus* SCM1 [92]. The EctD-containing microorganisms live in ecophysiologically rather different habitats, but the biochemical properties of the studied ectoine hydroxylases are all very similar. Their enzyme activities are not strongly dependent on salts, and their pH (between 7.5 and 8) and temperature optima (between 32 and 40 °C) range within narrow windows. The apparent kinetic parameters of these enzymes for the substrate ectoine (K_m values between 6 and 10 mM) and the co-substrate 2-oxoglutarate (K_m values between 3 and 5 mM) are similar, and their catalytic efficiencies (k_{cat}/K_m) vary only between 0.12 and 1.5 mM^{-1} s^{-1} [92,93,184]. Hence, ectoine hydroxylases possess rather moderate affinities for their substrate ectoine, a property that is potentially connected with the fact that the accumulation of ectoine to a substantial intracellular level via de novo synthesis typically precedes the production of 5-hydroxyectoine [79,98,122,123]. Although all ectoine hydroxylases studied to date possess similar kinetic parameters, it should be noted that the in vivo performance of these enzymes can differ substantially when they are expressed in an *E. coli*-based synthetic cell factory that imports externally provided ectoine via the osmotically induced ProP and ProU osmolyte import systems [187–189], hydroxylates it, and then excretes the newly formed 5-hydroxyectoine almost quantitatively into the growth medium [151]. These differences in performance might stem from differences in the production levels or the stability of the recombinant proteins in the heterologous host, or the properties of the *E. coli* cytoplasm is not optimal for the enzymatic activities of the various EctD proteins. Such differences in the in vivo performance of ectoine

hydroxylases with seemingly similar in vitro kinetic parameters need to be carefully considered when such enzymes are used in heterologous microbial cell factories for the biotechnological production of 5-hydroxyectoine [116].

Among the four enzymes involved in ectoine/5-hydroxyectoine biosynthesis [164–166], the ectoine hydroxylase is certainly the best studied [92,93,177,184,186]. A substantial number of EctD enzymes have been biochemically assessed that were derived from physiologically and taxonomically distinct groups of microorganisms [92,93]. Furthermore, the structure/function relationship of this enzyme has been studied by site-directed mutagenesis, by molecular dynamics simulations and finally via crystal structure analysis [93,177,184,186]. Together, these studies have led to a detailed understanding of the EctD-mediated enzyme reaction [186] and illuminated the architecture of the active site [177]. Crystal structures of *V. salexigens* without any substrates or products [184], and that of *S. alaskensis* with various ligands [177] have been reported.

The ectoine hydroxylase is a dimer in solution and in the crystal structure. The dimer interface of the swapped head-to-tail dimeric structure is primarily formed through interactions by loop areas pointing from one monomer towards the other (Figure 3C). bona fide EctD-type proteins can be distinguished from other members of the broadly distributed non-heme Fe(II)-containing and 2-oxoglutarate-dependent dioxygenases superfamily through an evolutionarily highly conserved signature sequence consisting of a continuous stretch of 17 amino acids (F-x-W-H-S-D-F-E-T-W-H-x-E-D-G-M/L-P) [177,184]. When the signature amino acid sequence is viewed in the context of the EctD crystal structure, this segment of the EctD polypeptide chain is important from a structural point of view, as it forms one side of the cupin barrel (Figure 3C). In addition, it also contains five residues involved in the binding of the iron catalyst, the co-substrate 2-oxoglutarate, and the reaction-product 5-hydroxyectoine [177,184].

In their excellent and widely appreciated overview on ectoines as stress protectants and commercially interesting compounds, Pastor et al. [91] suggest that 5-hydroxyectoine may also be formed by first converting the EctA-formed *N*-γ-acetyl-2,4-diaminobutyrate (Figure 2) into 3-hydroxy-*N*-γ-acetyl-2,4-diaminobutyrate, which is proposed to be subsequently cyclized to 5-hydroxyectoine. In this envisioned pathway, the activity of EctC is circumvented by an unknown enzyme and the existence of an additional unknown enzyme is invoked that would cyclize the linear 3-hydroxy-*N*-γ-acetyl-2,4-diaminobutyrate molecule to 5-hydroxyectoine [80]. This proposal for an alternative route for the formation of 5-hydroxyectoine is primarily based on the properties of a particular *ectC* mutant (*ectC*:*Tn*1732; strain CHR63) of *C. salexigens* [120] in which, quite surprisingly, both ectoine and 5-hydroxyectoine were still detected [179]. There have been no follow-up studies on this hypothetical 5-hydroxyectoine biosynthetic route since it was originally proposed by Canovas et al., in 1999 [179]. Synthesis of ectoine and 5-hydroxyectoine in the *ectC* mutant may be a particular feature of the studied *C. salexigens* genetic background [120,179], or the fact that *C. salexigens* is also able to catabolize ectoines [80,190] and may thus use some of the degradative enzymes (see Section 7) to partially restore ectoine/5-hydroxyectoine production.

We suggest that the envisioned EctC- and EctD-independent route for the synthesis of 5-hydroxyectoine [91] is of no physiological relevance in natural settings of osmotically stressed wild-type 5-hydroxyectoine-producing microorganisms. To avoid confusion, this hypothetical pathway should, in our view, not be presented in the literature [80,91] as a true alternative to the biochemically and structurally buttressed direct and stereo-specific hydroxylation of ectoine by the ectoine hydroxylase EctD [92,93,98,177] until it is further substantiated by molecular and biochemical evidence.

5.2.5. Specialized Aspartokinase Ask_Ect

The precursor for ectoine synthesis (Figure 2), L-aspartate-β-semialdehyde, is a central metabolic hub in microorganisms from which a branched network of various biosynthetic pathways diverges [167]. L-aspartate-β-semialdehyde is synthesized through the sequential enzymatic reactions of an aspartokinase (Ask; EC 2.7.2.4) and a L-aspartate-semialdehyde-dehydrogenase (Asd; EC 1.2.1.11). Ask synthesizes L-4-aspartyl-β-phosphate via an ATP-dependent phosphorylation of L-aspartate, which is

then in turn reduced to L-aspartate-β-semialdehyde by the Asd enzyme in an NADPH-dependent reaction (Figure 2). To avoid a wasteful production of the energy-rich intermediate L-4-aspartyl-β-phosphate, the enzymatic activities of aspartokinases are usually regulated by feedback inhibition and the expression of the corresponding *ask* gene is also often subjected to sophisticated transcriptional regulation [167]. Since major production routes of biotechnologically interesting antibiotics and commercially used amino acids (e.g., L-lysine) branch off from L-aspartate-β-semialdehyde as the initial metabolite, aspartokinases are often targeted in genetic engineering approaches to relieve their feedback inhibition. This leads to an increased cellular L-aspartate-β-semialdehyde pool and thereby fosters the flow of this precursor into biosynthetic pathways of interest [152,191]. When applied to the heterologous production of ectoine in *E. coli,* a bacterium that does not naturally synthesize ectoine [187], the yield was indeed improved by co-expressing a feedback-resistant aspartokinase (LysC) derived from *Corynebacterium glutamicum* together with the ectoine biosynthetic genes obtained from *Marinococcus halophilus* [191]. Such feedback-resistant aspartokinases have also been employed in the design of engineered synthetic microbial cell factories, thereby resulting in enhanced production of ectoines [152,153,155].

Because the feedback-control of Ask enzyme activity could potentially lead to a bottleneck in ectoine biosynthesis [191], the report of Reshetnikow et al. [168] that the osmotically inducible ectoine biosynthetic gene cluster of *M. alcaliphilum* was co-transcribed with a gene encoding an aspartokinase was of considerable interest. This finding indicated that the enzyme encoded by this particular *ask* gene could play a specialized role in ectoine biosynthesis. Indeed, it was observed in subsequent studies [93] that a considerable number of ectoine/5-hydroxyectoine biosynthetic gene clusters include an additional paralogous *ask* gene (referred to in the following as *ask_ect*) [122] (see Section 5.3).

A comprehensive cohesion group analysis of aspartokinases revealed that the Ask_Ect enzymes form a distinct sub-cluster among the large aspartokinase enzyme family, and that those residues implicated in participating in the feedback control of various Ask enzymes are not conserved in the Ask_Ect group [167]. Stöveken et al. [122] purified such an Ask_Ect enzyme from the ectoine/5-hydroxyectoine-producing plant-root-associated bacterium *P. stutzeri* A1501 and benchmarked its biochemical properties against those of the biosynthetic standard aspartokinase (Ask_LysC) present in this bacterium as well. Both enzymes possess similar kinetic parameters, but exhibit significant differences with regard to the allosteric control by biosynthetic products derived from L-aspartate. Ask_LysC was inhibited by L-threonine alone and in a concerted fashion by L-threonine and L-lysine, whereas Ask_Ect showed inhibition only by L-threonine. Moreover, the inhibiting effect by L-threonine on the latter enzyme was significantly reduced when the enzyme activity assay was carried out in presence of 650 mM NaCl or KCl [122].

An *E. coli* strain carrying the plasmid-based *ectABCD-ask_ect* gene cluster from *P. stutzeri* A1501 produced substantially more (about 5-fold) ectoine/5-hydroxyectoine than a strain expressing the same gene cluster without the *ask_ect* gene [122]. Taken together, these findings suggest that the *ask_ect* gene encodes an aspartokinase with a specialized role for the biosynthesis of ectoine and 5-hydroxyectoine. The frequent co-expression of this gene with osmotically inducible *ect* gene clusters [93,122,168] (Figure 4 and Section 6.3) will ensure an optimal supply of the precursor L-aspartate-β-semialdehyde under osmotic stress conditions. However, it should be noted that the majority of ectoine/5-hydroxyectoine-producing bacteria do not contain such a specialized Ask_Ect enzyme (Figure 5), indicating that they may use different strategies to maintain their L-aspartate-β-semialdehyde pools at high enough cellular levels to support their large-scale ectoine/5-hydroxyectoine biosynthetic activities under high-salinity growth conditions.

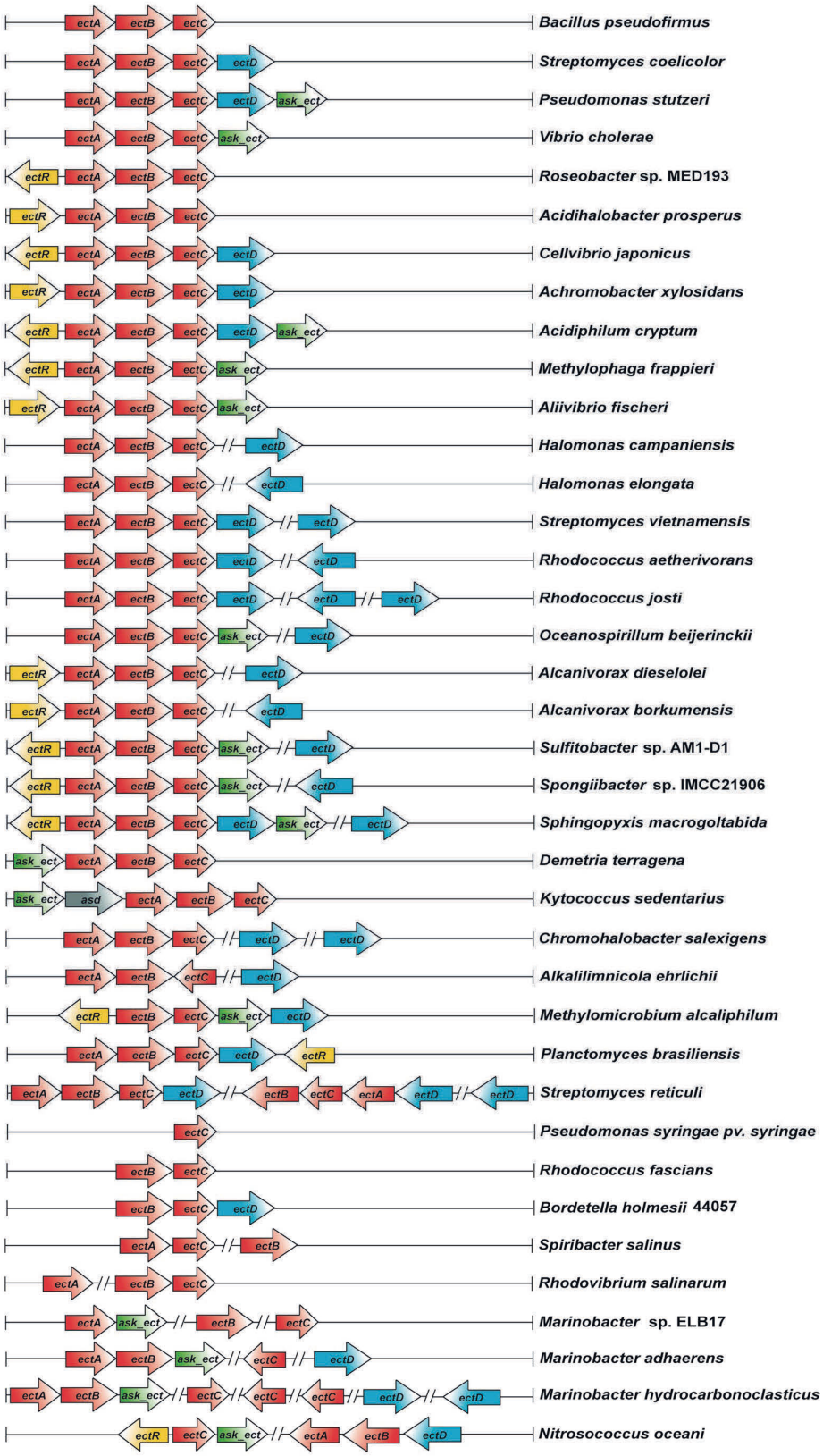

Figure 4. Diversity of the genetic organization of ectoine and 5-hydroxyectoine biosynthetic gene clusters in microbial genomes.

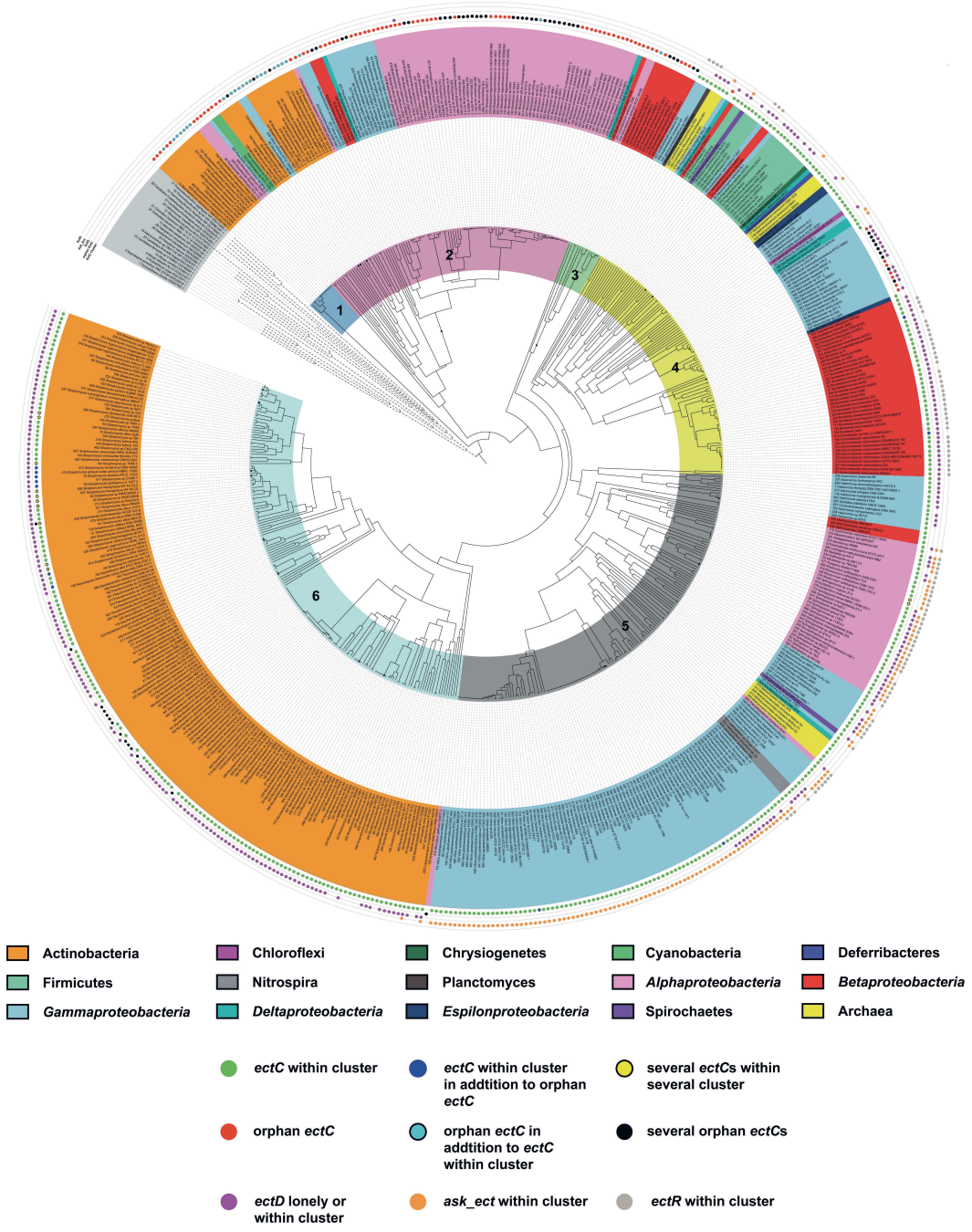

Figure 5. Phylogenomics of the ectoine synthase. The amino acid sequences of 582 EctC-type proteins were retrieved from microorganisms with fully sequenced genomes, aligned with MAFFT [192] and then used for a clade analysis using the iTOL software [193]. The tree was rooted with a number of microbial cupin-type proteins, a superfamily of proteins [182,183] to which the EctC protein also belongs [176]. The phylogenetic affiliation of the various EctC proteins is depicted in different colors shown in the outer ring, and the color code is explained in the figure. Different groups (1 to 6) in which the EctC-type proteins can be clustered are depicted in the inner colored circle. The dots in the outmost 5 rings depict (from the inside to the outside) if the EctC protein is encoded within an *ect* biosynthetic gene cluster, if the EctC protein is an orphan, if the pertinent EctC-containing microorganism also possesses the ectoine hydroxylase EctD, if the specialized aspartokinases Ask_Ect is part of the *ect* cluster, or if the *ect* gene cluster is affiliated with a gene encoding the EctR regulatory protein.

5.2.6. Adjusting Central Carbon Metabolism to the Drain Exerted by Ectoine Biosynthesis

Under osmotic stress conditions, ectoines can be accumulated through synthesis to exceedingly high intracellular concentrations [91,94], and the degree of the imposed osmotic stress dictates their pool size. There seems to be a linear relationship between the external osmolarity/salinity and the amounts of the produced ectoines [116–118]. As a consequence, the microbial cell has to sensitively adjust its metabolism to constraints imposed by high-level synthesis of the nitrogen-rich ectoine/5-hydroxyectoine molecules (Figure 1B), which will impose a serious drain of available carbon- and nitrogen-sources. Hence, it is necessary to understand the interplay of the carbon and nitrogen supplies for the production of ectoines in greater detail [194]. Their synthesis burdens the assimilation of nitrogen via the glutamine synthetase pathway and central metabolic routes by recruiting TCA-cycle intermediates—in particular, oxaloacetate and acetyl-CoA [195–197]. Consequently, anaplerotic routes have to be engaged to replenish the TCA cycle for routine central carbon metabolism and at the same time an increased flux of metabolites into the ectoine/5-hydroxyectoine biosynthetic pathway has to be ensured. Genome-scale modeling and integrative systems biology approaches have recently provided insights into how this is accomplished by *C. salexigens* [196] and *H. elongata* [197]. These studies paint a complex picture of the involved metabolic changes and highlight the considerable metabolic and energetic burden [24,37,106] that osmotically stressed cells face when they try to alleviate osmotically imposed constraints on growth through the synthesis of stress-relieving ectoines [194–197]. This aspect is not only important for a full understanding of the cells' behavior under osmotic stress conditions, but is also a pre-requisite to further improvement of the high-yield production of ectoines by natural and synthetic microbial cell factories.

6. Genetics and Phylogenomics of Ectoine and 5-Hydroxyectoine Biosynthetic Genes

1. Genetic Organization of the Ectoine/5-Hydroxyectoine Biosynthetic Gene Clusters

The description of the *ectABC* genes in *M. halophilus* [95], along with that of the *ectABCD* locus in *Streptomyces chrysomallus* [96], provided the primers for a molecular analysis of the ectoine/5-hydroxyectoine biosynthetic genes. Studies on *C. salexigens* [97] and *S. salexigens* [98] subsequently demonstrated that the *ectD* gene was not necessarily part of the *ectABC* gene cluster but could be encoded somewhere else in the genome, with *C. salexigens* possessing even two *ectD*-type genes [80,97] (Figure 4). Previous genome assessments [91–93,99], and our current own comprehensive database searches (see Section 6.3), revealed an evolutionarily rather conserved genetic configuration of the ectoine/5-hydroxyectoine biosynthetic genes in many bacterial and some archaeal genomes. In some notable cases, several copies of complete ectoine/5-hydroxyectoine biosynthetic gene clusters are even present that might have arisen either through gene duplication or lateral gene transfer. *Streptomyces reticuli* is an example where two copies of the *ectABCD* gene clusters are present, and an additional copy of an *ectD*-type can even be found in the genome of this actinobacterium. The occurrence of multiple copies of *ectD*-type genes in the same genome is not unusual (Figure 4).

As highlighted in Figure 4, the *ectABC* and *ectABCD* gene clusters build a conserved backbone in most ectoine/5-hydroxyectoine producers that can additionally be genetically configured with the gene (*ask_ect*) for the specialized aspartokinases and/or the gene (*ectR*) for a MarR-type regulator, EctR (see Section 5.2) [91–93,99,122,168,198]. In practically all ectoine/5-hydroxyectoine gene clusters inspected by us, we found that the gene for the second enzyme (L-aspartate-β-semialdehye-dehydrogenase, Asd) involved in providing the ectoine biosynthetic precursor L-aspartate-β-semialdehyde is absent (Figures 2 and 4). The notable exception to this rule is the *ect* gene cluster from the marine actinobacterium and opportunistic pathogen *Kytococcus sedentarius* where *ask_ect* and *asd* are encoded up-stream of the *ectABC* operon (Figure 4).

In addition to the evolutionarily conserved *ectABC/ectD* gene arrangement, substantially re-arranged configurations of the *ect* genes can be found in a sizable number of microorganisms (Figure 4). There can be a re-arrangement of individual genes within the *ect* cluster, but there are also

cases where individual *ect* genes have been separated from each other, or where multiple copies of the same gene (e.g., *ectC*) are present at various locations within the genome (Figure 4).

Many representatives with re-arranged or disentangled *ect* biosynthetic genes live in marine ecosystems [199]. Given the re-arrangement of the canonical *ect* gene configuration in these bacteria, one wonders if they are capable of ectoine/5-hydroxyectoine production. One representative of this group of microorganisms is the gammaproteobacterium *Spiribacter salinus*, an ecophysiologically successful and abundant inhabitant of hypersaline ecosystems [200]. In its genome, *ectAB* and a separate *ectC* gene can be found (Figure 4); despite this non-canonical arrangement of the *ect* biosynthetic genes, a recent study demonstrated the production of ectoine in *S. salinus* in response to increases in the external salinity [199].

6.2. Regulation of ect Gene Expression

It is fitting from the main physiological function of ectoines as osmostress protectants that the transcription of the corresponding biosynthetic genes is under osmotic control. Indeed, studies with reporter gene fusions and Northern-blot analysis have demonstrated that this is the case in both Gram-negative and Gram-positive bacteria. However, the way osmotic stress is sensed by the bacterial cell and the way the gleaned information is processed to trigger enhanced *ect* transcription is far from understood. As a matter of fact, the literature pertinent to this topic is plagued with a considerable over-interpretation of preliminary findings.

Northern-blot analysis of osmotically stressed *V.* (*Salibacillus*) *salexigens* cells proved that transcription of the *ectABC* genes, and of the separately encoded *ectD* gene, is strongly enhanced in high-salinity growth media. Primer extension analysis pinpointed a single *ectABC* promoter that resembles in its sequence typical SigA-type promoters [98], the housekeeping sigma factor of Bacilli [201]. Transcription of the *ectABC* genes from *V. pantothenticus* was found to be responsive both to increases in osmolarity and to decreases (but not to increases) in growth temperature [77]. In this Gram-positive bacterium, transcription of the gene for the ectoine/5-hydroxyectoine transporter EctT followed the same pattern of gene expression, and primer extension analysis demonstrated that this response is mediated by a single SigB-type promoter [78]; SigB is the general stress-responsive alternative sigma factor in Bacilli [202] and salt and temperature stress are major inducers of the SigB-regulon in *B. subtilis* [203]. The dependence of the *V. pantothenticus ectT* gene on SigB was verified in a *sigB* mutant of *B. subtilis* [78], but the implicated dependence of *ectABC* transcription on SigB activity in *V. pantothenticus* was not experimentally tested [77].

When the DNA sequence of the first ever cloned *ectABC* gene cluster was reported by Louis and Galinski [95], these authors proposed that its expression was mediated by a single SigB-dependent promoter positioned upstream of *ectA*. Because *M. halophilus* is a Gram-positive bacterium, this was a reasonable assumption, but no experimental evidence for the involvement of SigB was provided in this study [95]. However, in view of the fact that *E. coli* does not possess SigB and that SigB-dependent promoters differ substantially from the consensus sequence of promoters recognized by the house keeping sigma factor RpoD or the general stress alternative sigma factor RpoS of *E. coli* [204,205], it was rather surprising that the introduction of the *M. halophilus* recombinant *ect* genes into this Gram-negative host bacterium led to an osmostress-responsive production of ectoine [95]. Bestvater and Galinski [206] subsequently rationalized this finding by invoking the fortuitous existence of stationary-phase/general stress-type RpoS-dependent promoters in front of the *M. halophilus ectABC* genes. If these types of promoters exist, they certainly cannot have any physiological relevance in the authentic *M. halophilus* host because Gram-positive bacteria do not possess RpoS-type alternative sigma factors [205]. Hence, the dependence of the *M. halophilus ectABC* gene cluster on SigB awaits experimental verification.

In *H. elongata*, the industrially used bacterium for the production of ectoines [86,91,94], two promoters preceding the *ectABC* genes and an additional promoter present in front of *ectC* were mapped by RACE-PCR [158]. Based upon DNA-sequence inspection, Schwibbert et al. [158] suggested that the

promoter exclusively driving *ectC* transcription was recognized by the alternative transcription factor Sig-54, a sigma factor that is frequently involved in regulating the expression of genes involved in physiological processes connected to nitrogen metabolism. However, it is not obvious to us what the function of this internal promoter within the *H. elongata ect* gene cluster might be; its implicated dependence on Sig-54 activity was not verified experimentally [158]. One of the two promoters present in front of *ectA* was described by Schwibbert et al. [158] as a promoter recognized by the housekeeping sigma factor RpoD (Sig-70); the distal located promoter was deemed to be dependent or the stationary-phase/general stress sigma factor RpoS (Sig-38). While the putative RpoS-dependent promoter of the *H. elongata ect* gene cluster exhibited features found in some other osmotically regulated RpoS-dependent promoters from *E. coli* [207,208], the *H. elongata* promoter nevertheless deviates considerably (in particular in the spacing of the -10 and -35 regions) from typical RpoS-type promoters [130,131,205]. Osmoregulation of either the proposed RpoD- or RpoS-dependent *H. elongata ect* promoters was not studied in any detail, nor was the involvement of RpoS in *ect* gene expression verified by mutant analysis [158].

The importance of a careful genetic analysis is exemplified by data reported on the apparent complex transcriptional control of the *ectABC* genes from *C. salexigens*, a salt-tolerant bacterium closely related to *H. elongata* [80,118]. S1 mRNA protection assays suggested the existence of four promoters driving *ectABC* transcription, three of which were deemed by Calderon et al. [118] to be osmotically responsive. When a *ectA-lacZ* reporter fusion expressed from the three promoters mapped in front of *ectA* was introduced into *E. coli*, expression of the reporter fusion was linearly dependent on the osmotic strength of the growth medium and its activity increased strongly in stationary phase. One (P*ectA*-3) of the suggested promoters of the *C. salexigens* biosynthetic *ect* gene cluster [118] resembled, with respect to certain features of the -10 and -35 regions, osmoregulated *E. coli* promoters that are dependent on the alternative sigma-factor RpoS [130,131,205,207,208]. Since the activity of above described *ectA-lacZ* reporter fusion carrying all three promoters was reduced by about 50% in an *E. coli rpoS* mutant, Calderon et al. [118] ascribed an important role to this alternative sigma-factor for the direct transcriptional regulation of the *C. salexigens ect* gene cluster in the heterologous *E. coli* host. However, subsequent follow-up studies by the same laboratory showed that the observed effect of RpoS was indirect [209]; in other words, the initially envisioned direct effect of RpoS on the proposed *C. salexigens* P*ectA*-3 promoters does not exist.

In studying the interplay between iron homeostasis and the salt stress response of *C. salexigens*, Argandona et al. [135] found that the amount and relative proportion of ectoine and 5-hydroxyectoine was affected by excess iron in the growth medium. These authors ascribed an activator function of the Fur regulatory protein for the transcription of the ectoine biosynthetic genes, and through in silico inspection of the *ect* regulatory region, noted the presence of several potential Fur DNA-binding boxes overlapping two of the putative *ect* promoters. In quantitative RT-PCR experiments, they observed a drastic fall in the *ectA* transcript in a *fur* mutant [135], consistent with previous *ectA-lacZ* transcriptional reporter fusion studies that revealed a down-regulation of *ect* expression in *C. salexigens* wild-type cells grown at high salinity in the presence of excess iron [118]. However, the data reported by Argandona et al. [135] on the suggested direct interaction of the Fur protein with the *ect* regulatory region and the proposed activator function of the Fur regulatory protein are hard to reconcile with the findings of these authors that there was no real difference in ectoine/hydroxyectoine content between the *C. salexigens* wild-type and its isogenic *fur* mutant [135]. Hence, the inferred interaction of Fur with the *ect* promoter region and the role of Fur as an activator of *ect* transcription [135] awaits verification through DNA-binding studies and mutational analysis.

The S1 mRNA protection data reported by Calderon et al. [118] also suggested the existence of a heat-shock (RpoH; Sig-32)-dependent promoter (PectB) that is positioned upstream of the *C. salexigens ectB* gene. The physiological rationale for producing a separate *ectB-ectC* transcript under heat-shock conditions is not immediately apparent but reporter gene fusion studies showed enhanced expression of a *PectB-lacZ* reporter fusion at high temperature (40 °C) [118]. However, a molecular analysis that

would identify this promoter as a direct target for RNA-polymerase complexed with the alternative sigma factor RpoH was not performed.

We generally consider the assignment of putative *ect* promoters that are in their core exclusively based on DNA-sequence gazing as unreliable, and we caution against the over-interpretation of such suggestions in published reports. In our view, reliable data on the transcriptional regulation of *ect* genes can only be attained through site-directed mutagenesis of the proposed promoter(s) and, if an alternative sigma factor is invoked in their transcriptional activity, through studies with appropriate mutant strains (if at all possible) in the authentic ectoine/5-hydroxyectoine producer bacterium.

DNA sequence inspection can readily overlook the true osmotically controlled promoter(s) of *ect* biosynthetic genes, as these might deviate considerably from the consensus sequences one might look for. In a recent report, Czech et al. [116] studied the osmostress-responsive transcription of the *ect* biosynthetic genes from the plant-root-associated Gram-negative bacterium *P. stutzeri* A1501 in heterologous *E. coli* host strains. While the *ect* promoter possesses a good match (TTGAGA) to the consensus sequence (TTGACA) of the -35 element of Sig-70-type *E. coli* promoters [204], its highly G/C-rich -10 sequence (TACCCT) [116] deviates strikingly from the A/T-rich consensus sequence (TATAAT) of these types of promoters. Furthermore, the spacing of the -10 and -35 elements of the *ect* promoter with a length of 18 bp was sub-optimal for Sig-70-type *E. coli* promoters [204]. Osmostress-responsive promoters with such G/C-rich -10 elements and sub-optimal spacer length have previously been described both in *E. coli* and *B. subtilis* [84], but no *ect* promoter has been reported with such an unusual configuration in its -10 region. This prompted the study of the salient features of this promoter through *lacZ* reporter gene studies and extensive site-directed mutagenesis experiments [116]. The transcriptional activity of a wild-type *ect-lacZ* reporter fusion, when introduced into *E. coli*, proved to be linearly dependent on the external salinity and responded to true osmotic cues, as both ionic (NaCl, KCl) and non-ionic (suchrose, lactose) osmolytes triggered similar increases in promoter activity [116]. Osmotic induction of the *ect-lacZ* reporter fusion required the establishment of an osmotically active trans-membrane gradient, as high concentration of membrane-permeable glycerol did not trigger enhanced *ect* promoter activity [116].

Site-directed mutagenesis studies proved that the *P. stutzeri ect* promoter was critically dependent for its activity on the function of the *E. coli* house-keeping Sig-70 transcription factor. Furthermore, point mutations rendering its -35 and -10 regions, or that of the spacer length, towards a closer match to the consensus sequence, conferred drastic changes in gene expression. Typically, the activity of the mutant *ect* promoters rose substantially under both non-salt and salt-stress conditions [116]. Studies with *E. coli* mutants with defects in *hns*, *rpoS*, *ompR*, or *cya*, genes that have been implicated in osmoregulation of various *E. coli* genes demonstrated that the *P. stutzeri ect* promoter operates in its osmotic control completely independently of these important transcription factors [116].

None of the 18 variants of the *P. stutzeri ect* promoter constructed by site-directed mutagenesis lost osmotic control altogether; surprisingly, this was even true for an *ect* promoter variant that was synthetically adjusted to the complete consensus sequence of Sig-70 *E. coli* promoters [116]. Hence, one can conclude from this study that (i) the deviations of the *P. stutzeri ect* promoter from the consensus sequence serve to keep promoter activity low when the cell does not have to rely on the synthesis of ectoines, while simultaneously allowing strong osmotic induction of *ect* transcription when the cell physiologically needs these cytoprotectants for its adjustment to the adverse environmental conditions; and that (ii) a determinant for osmotic control must be present outside the particular sequence of the -10 and -35 regions and of the spacer that separates them. Osmotic control of the *P. stutzeri ect* promoter was traced through deletion analysis to a 116-bp DNA fragment [116]. Hence, despite the fact that *E. coli* does not synthesize ectoines naturally [187], the *P. stutzeri ect* promoter retained its exquisitely sensitive osmotic control in the heterologous host bacterium, indicating that osmoregulation of this promoter is an inherent feature of the rather small regulatory region per se. It is not yet clear yet how this can be accomplished mechanistically, but Czech et al. [116] speculated that RNA polymerase alone, perhaps in response to changes in osmotically triggered changes in DNA supercoiling [210], and in combination

with changes in the intracellular ion pool (in particular the pair of K^+ and L-glutamate) [207,208,211] and the size of the compatible solute pool [212,213], might afford osmoregulation of *ect* expression. It is currently difficult to grasp intuitively that the exquisitely sensitive osmotic control of the *ect* promoter and the tuning of its strength via incremental increases in sustained osmotic stress can be explained by this molecular mechanism alone. It will be a challenge to experimentally verify or refute this model through in vivo or in vitro studies.

A highly interesting finding with respect to the genetic control of *ect* genes is the report of Mustakhimov et al. [198], who studied these biosynthetic genes in the halotolerant methanotroph *M. alcaliphilum* 20Z. These authors detected a gene (*ectR*) positioned upstream of the *ectABC-ask_ect-ectD* gene cluster (Figure 4) that encodes a MarR-type regulator, a super-family of widely distributed transcription factors [214]. Primer extension analysis showed that the osmoregulated *ect* genes of *M. alcaliphilum* 20Z are expressed from two closely spaced promoters. Through foot-printing analysis, Mustakhimov et al. [198] found that EctR binds a homodimeric protein to a region overlapping the -10 region of the promoter most distal to the beginning of the *ectA* gene. EctR acts as a repressor of *ect* expression in *M. alcaliphilum* 20Z but notably, salt-stress responsive induction of the *ect* gens still occurred in an *ectR* mutant strain [198]. Hence, EctR is certainly not solely responsible for osmotic induction of the *ect* genes. Interestingly, EctR controls the transcription of its own gene in *M. alcaliphilum* 20Z [198].

In the methanol-utilizing bacterium *M. alcalica*, EctR served as a repressor for the ectoine biosynthetic gene cluster as well [215], and in the methylotroph *Methylophaga thalassica*, the purified EctR protein interacted in DNA-band shift assays with a region carrying the two promoters of the *ect* biosynthetic genes. However, in contrast to the situation in *M. alcaliphilum* 20Z, no auto-regulation of *ectR* transcription was found [99]. In both *M. alcaliphilum* 20Z and *M. thalassica*, the level of the *ectR* transcript increased upon osmotic up-shock and a complex array of three intertwined promoters was found to direct the transcription of the *M. thalassica ectR* gene [215].

All currently available data point to the function of EctR as a repressor of ectoine biosynthesis genes. Unfortunately, the cellular or environmental cues to which this interesting regulatory protein reacts are not known. It seems possible that EctR responds to changes in the ionic/osmotic strength of the cytoplasm. Such a mechanism has been proposed for the BusR regulatory protein, which regulates the expression of an operon (*busAA-busAB*), encoding an ABC-type compatible solute import system in *Lactococcus lactis* [216,217], and for the CosR regulator controlling (among other genes) genes for ectoine biosynthesis and compatible solute import in *Vibrio cholerae* [218]. Our database searches (see Section 6.3) revealed that *ectR*-type genes are found in close proximity to *ect* biosynthetic genes in 19% (97 out of 510) of putative ectoines producers and that all of the *ectR*-harboring microorganisms belong to members of the *Alphaproteobacteria*, *Betaproteobacteria*, and *Gammaproteobacteria* (Figure 5). Previous phylogenetic analysis of EctR-type proteins conducted by Reshetnikov et al. [99] and Mustakhimov et al. [215] showed that they form a specific phylogenetic subgroup with in the very large superfamily of MarR-type transcriptional regulators [214]. Like other MarR-type regulatory proteins, EctR is predicted to contain a winged-helix-turn-helix DNA-binding motive, and the EctR operator sequence in *M. alcaliphilum* 20Z, as revealed by DNA-foot-printing analysis, comprises a pseudo-palindromic highly A/T-rich DNA-sequence composed of two eight-bp half-sites separated by two bp [198,215].

In the context of discussions on the genetic control of the ectoine/5-hydroxyectoine biosynthetic genes, it is noteworthy that in *S. coelicolor*, GlnR—a major regulator for nitrogen metabolism—serves as a negative regulator for *ect* gene expression [219]. In our phylogenomic analysis (Figure 5), and in contrast to the distribution of *ectR*, we found no *glnR*- or *cosR*-type regulatory genes in close association with any ectoine/5-hydroxyectoine biosynthetic gene cluster. However, a possible genetic or physiological link of ectoine/5-hydroxyectoine biosynthesis to the overall nitrogen control in microbial cells [194] is an interesting aspect for future studies, given that ectoines are nitrogen-rich compounds (Figure 1B).

The genetic control of *ect* gene expression is embedded in the overall osmostress adjustment response of cells using the *salt-out* strategy (Figure 1A). Frequently, the size of the ectoine/5-hydroxyectoine pool is substantially reduced when other compatible solutes (e.g., glycine betaine) are imported from the growth medium. This effect can be traced through reporter fusion studies to a dampening influence of the imported solutes on the strength of *ect* transcription [116,118,206]. However, there is also a report in the literature that claims an inducing effect of imported ectoines on the transcription of the *ectABCD* gene cluster from *Streptomyces rimosus* C-2012 under salt stress conditions [220]. However, such an effect, to the best of our knowledge, has not been observed in any other microorganism in which the regulation of *ect* gene expression has been studied.

The dampening effect of imported compatible solutes on *ect* transcription is not unique to this particular type of promoter(s), as the activity of many osmostress responsive promoters is down-regulated when externally provided compatible solutes are accumulated [84,212,213]. Hence, it seems plausible that newly synthesized ectoines will influence *ect* promoter activity when the cellular pools of these compatible solutes rise in response to increased osmotic stress. This regulatory effect might provide the cell with a homeostatic system not to wastefully overproduce ectoines when it has attained osmotic equilibrium and it might be a contributing factor to the striking linear relationship between *ect* expression and the external salinity observed in several microorganisms [116,117]. It is currently not known whether the dampening effects of imported osmostress protectants on the strength of *ect* transcription are directly exerted via an influence on the activity of RNA-polymerase or its ability to productively interact with the *ect* promoter, or whether the effects are somehow indirectly caused by the weakened osmotic stress perceived by the microbial cell [84].

6.3. Phylogenomics of ect Genes

While the EctA (L-2,4-diaminobutyrate acetyltransferase) and EctB (L-2,4-diaminobutyrate transaminase) enzymes have close paralogs related in their amino acid sequences and function in microbial biosynthetic pathways not related to ectoine biosynthesis, the ectoine synthase (EctC) can be regarded as a diagnostic enzyme for ectoine producers. However, microorganisms have been discovered, which either possess EctC-related proteins but lack the *ectAB* genes or possess solitary *ectC*-type genes in addition to a canonical *ectABC* gene cluster [93,176,221]. Hence, when EctC is used as the search query to assess the phylogenomics of microbial ectoine producers, it is critical to inspect the gene neighborhood of each retrieved *ectC* hit. Likewise, *bona fide* ectoine hydroxylases (EctD) need to be distinguished from related 2-oxoglutarate-dependent dioxygenases with different enzymatic functions, as EctD proteins are often miss-annotated in genome sequences either as proline- or phytanoyl-hydroxylases. True EctD proteins (see Section 5.2.4) can be distinguished from the other members of the non-heme Fe(II)-containing and 2-oxoglutarate-dependent dioxygenase enzyme super-family [182] by a highly conserved consensus sequence motif harboring residues critical for substrate binding and enzyme catalysis [177,184].

We used the Integrated Microbial Genomes and Microbiomes (IMG/M) database of the Joint Genomics Institute (JGI) of the US Department of Energy (http://img.jgi.doe.gov/cgi-bin/w/main.cgi) [222] for our new database searches to identify putative producers of ectoines, since the web-tools of this Internet portal allow a simple evaluation of the gene neighborhood of the gene(s) of interest. For our analysis, we used the amino acid sequence of the EctC protein from *V. salexigens* as the search query, since this particular ectoine synthase has been intensively characterized by both enzymatic and structural approaches [93,177]. At the time of our search (13 November 2017) the IMG/M database contained 56,624 bacterial and 1325 archaeal genomes; from this data set we identified 4493 bacterial and 20 archaeal EctC-type proteins. It should be noted that the IMG/M database, like other microbial genome databases, is skewed with respect to the types of microorganisms covered because sequences of certain microbial species/strains are strongly overrepresented. For instance, in the dataset of 4493 bacterial genomes containing *ectC*-type genes, 1215 *Vibrio* species/strains (with 443 *V. cholerae* strains alone) and 511 *Streptomyces* isolates are represented.

When only considering fully sequenced microbial genomes, our final dataset contained 499 bacterial and 11 archaeal species/strains that collectively possessed 582 predicted EctC-type proteins. We inspected these genome sequences for the presence of other ectoine biosynthesis related genes (*ectAB*, *ectD, ask_ect, ectR*) in the neighborhood of *ectC* or elsewhere. We retrieved the 582 EctC-related protein sequences, aligned them using the MAFFT multiple amino acid sequence alignment server (https://mafft.cbrc.jp/alignment/server/) [192], and then conducted a clade analysis of the putative ectoine synthase proteins using bioinformatics resources provided by the Interactive Tree of Life (iTOL software) (https://itol.embl.de/) [193] (Figure 5). We have rooted the EctC-protein based tree with out-group sequences of several microbial cupin-type proteins [182,183] not involved in ectoine biosynthesis, as the EctC synthase belongs to this protein superfamily [176]. In Figure 5, we highlight not only the taxonomic affiliation of the microorganisms from which we retrieved the particular EctC sequence, but also the presence of the ectoine hydroxylase EctD [96–98], that of the specialized aspartokinases Ask_Ect [122,166,168], and that of the regulatory protein EctR [99,198,215]. Data from this analysis of the genetic configuration of ectoine/5-hydroxyectoine biosynthetic genes (*ectABC/ectD*) in 510 completely sequenced bacterial and archaeal genomes of predicted ectoine/5-hydroxyectoine producers and additional genes involved in providing the ectoine biosynthetic precursor L-aspartate-β-semialdehyde (*ask_ect*) or in the transcriptional control of *ect* gene expression (*ectR*) are summarized in Table 1.

Table 1. Analysis of the genetic neighborhood of the 582 EctC-type proteins obtained through genome database analysis.

Gene	*ectC* (in Total)	*ectC* (within *ect* Cluster)	*ectC* (Solitary)	*ectD* (within *ect* Cluster)	*ectD* (Separated from *ect* Cluster)	*ask_ect* (within *ect* Cluster)	*ectR*
Abundance	582	437	145	259	68	133	97

EctC-type proteins are phylogenetically associated with ten bacterial (including five subphyla of the *Proteobacteria*) and two archaeal phyla. In this clade analysis, EctC proteins that are encoded within true *ect* gene clusters follow, in general, the taxonomic affiliation of the predicted ectoine-producing microorganism. In those few cases where this is not the case, their position in the EctC-derived protein sequence clade can probably be explained by lateral gene transfer events (Figure 5). The EctC protein tree is dominated by ectoine synthases originating from *Actinobacteria* and from *Alphaproteobacteria*, *Betaproteobacteria*, and *Gammaproteobacteria*, which together make up 91% of our dataset. EctC proteins from members of the other EctC-containing ten bacterial phyla or subphyla (*Firmicutes*, *Delta-* and *Epsilonproteobacteria, Nitrospirae, Planctomycetes, Chrysiogenetes, Deferribacteres, Chloroflexi, Cyanobacteria*, and *Spirochaetes*) are only scarcely represented (Figure 5). Because of the existing bias of available genome sequences in databases, it is too early to conclude how much of the apparent incidence of ectoine synthesis actually differs between these phyla or arises from insufficient representation of some phyla in the IMG/M database.

Lateral gene transfer is a major driver of microbial evolution [223,224] and has in particular shaped the genome of Archaea that acquired many genes from bacterial donors [225]. This is also evident for the rare cases where EctC-type proteins have been detected in Archaea [92]. In our dataset, 11 archaeal EctC protein sequences cluster in three different locations in the tree. These genomes represent members of two archaeal phyla, the *Thaumarchaeota* and *Euryarchaeota* (Figure 5). All 11 archaeal representatives in our dataset possess a complete *ectABC* gene cluster. The EctC proteins of the three marine representatives of the *Thaumarchaeota* (all strains of *Nitrosopumilus* sp.) cluster with that of the marine bacterium *Planctomyces brasiliensis* (Figure 5). In contrast to the joint clustering of the EctC proteins from the three *Thaumarchaeota*, the eight EctC proteins from the *Euryachaeota* are present in two different segments of the phylogenomic EctC protein tree. Three EctC proteins from various *Methanobacterium formicicum* strains are part of a cluster of EctC proteins present in strictly

anaerobic members of rather heterogeneous bacterial taxa that comprise representatives of the phyla *Chrysiogenetes*, *Deferribacteres*, and *Deltaproteobacteria* (Figure 5).

In our dataset, 437 microbial genomes contained the *ectC* gene in the immediate vicinity of other *ect* genes; 76 genomes contained only *ectC* (e.g., *Pseudomonas fluorescens* L228, *Burkholderia multivorans* CEPA 002), and in 11 genomes, a complete set of ectoine biosynthetic genes was present, in addition to a single orphan *ectC* (e.g., *Rhizobium gallicum*, *Mycobacterium abscessus* FLAC 0046). Another subgroup of the inspected genomes contained several orphan *ectC* genes but no complete *ect* gene cluster (31 genomes) (e.g., *Pseudomonas syringae* pv. syringae B301D, *Burkholderia cepacia*). Interestingly, some bacteria contained several complete *ect* biosynthetic gene clusters (e.g., *S. reticuli*, *Streptomyces flavogriseus*, Rhodovulum sulfidophilum DSM 1374). From this extended phylogenomic analysis, it is apparent that the vast majority (75%) of *ectC*-containing genomes contain a complete set of ectoine biosynthetic genes. Most orphan *ectC* gene products cluster close to the root of the tree, possibly indicating early evolutionary states (Figure 5). In a notable number of instances, microorganisms carrying both solitary *ectC* genes and additional *ect* gene clusters, or even several copies of complete *ect* gene clusters were detected. This leaves 76 genomes in our dataset, which contain exclusively solitary *ectC* genes.

Solitary *ectC* genes were first discovered in the context of a genome-driven investigation of compatible solute synthesis in the plant pathogen *Pseudomonas syringae* pv. syringae B728a [221]. This bacterium does not produce ectoine naturally under laboratory conditions, as it lacks the *ectAB* genes. However, when surface-sterilized leaves of its host plant *Syringa vulgaris* were added to high-salinity grown cultures, ectoine production was observed, indicating that the plant provides the substrate (*N*-γ-ADABA) (Figure 2) for the EctC ectoine synthase, and that the solitary EctC-type protein *P. syringae* pv. syringae B728a was functional [221]. Indeed, heterologous expression of the solitary *ectC* gene from *P. syringae* pv. syringae B728a in an *ectC* mutant of *H. elongata*, led to ectoine production. However, while externally provided *N*-γ-ADABA was readily imported by *P. syringae* pv. syringae B728a, the expected ectoine formation was not observed [221]. Hence, this dataset is, in its core, not yet conclusive. Previous database searches have already indicated that the existence of solitary EctC-type proteins is not an isolated incident in *P. syringae* pv. syringae B728a [92,176]; we detected their presence in 13% out of the studied 457 genomes (Table 1).

EctC-type proteins can be assigned to six major clusters of sequence similarity. The three most basal of these clusters contain most of the proteins from orphan *ectC* genes, while the three others contain all EctC proteins encoded by *ect* gene clusters and only a few by isolated genes (Figure 5). The most basal major cluster (group 1) exclusively represents EctC-like proteins from various strains of *M. abscessus,* which may not be true ectoine synthases because the same strains also contain paralogs of more conventional EctC proteins. The next two major clusters (groups 2 and 3) correspond to most other organisms containing orphan *ectC* genes and comprise mostly members of the *Alphaproteobacteria*, notable groups of *Actinobacteria*, *Betaproteobacteria* and *Gammaproteobacteria*, together with two strains affiliated with the *Cyanobacteria* and two with the *Deltaproteobacteria* (Figure 5). It is currently not clear whether the solitary EctC proteins are remnants of a previously intact ectoine biosynthetic route, whether they were recruited by the EctAB proteins to form the ectoine biosynthetic pathway as we know it today (Figure 2), or whether they have evolved a new enzymatic function that nevertheless might allow in a side-reaction the cyclization of the *N*-γ-ADABA molecule to ectoine. However, the placement of the orphan EctC protein from *P. syringae* [221] in group 2 (Figure 5) suggests that these proteins might represent catalytically competent ectoine synthases. Still, careful genetic and biochemical analysis will be required in the future to establish the true function of these solitary EctC-type proteins.

The major group 4 contains mainly EctC proteins from *Firmicutes*, marine *Gamma-* and *Betaproteobacteria*, together with rare orthologs from the *Planctomycetes*, *Spirochaetes*, *Delta-* and *Epsilonproteobacteria*, *Chrysiogenetes*, *Chloroflexi*, *Deferribacteres* and two archaeal groups comprising the *Nitrosopumilus* and *Methanobacterium* strains. Group 5 contains the proteins from mostly marine *Alphaproteobacteria*, *Betaproteobacteria* and *Gammaproteobacteria*, including many members of the

Roseobacteriales, *Halomonadadales* and *Vibrionales*, together with one spirochaete, one sulfate-reducing *Deltaproteobacterium*, three *Leptospirillum* strains affiliated to the *Nitrospirae* and the remaining *ect* gene clusters containing archaeal species representing five members of the *Methanosarcinales*. Finally, group 6 represents exclusively terrestrial *Actinobacteria*, with the exception of one basal EctC sequence from a strain of the alphaproteobacterium *R. gallicum* (Figure 5).

The formation of 5-hydroxyectoine depends on the prior synthesis of ectoine and is catalyzed in a position- and stereo-specific reaction by the ectoine hydroxylase (EctD) [98,177]. The *ectD* gene can be found in one of two different genetic contexts: (i) it either can be present in the vicinity of other *ect* biosynthetic genes, or (ii) it can be encoded somewhere else in the genome of a predicted ectoine producer [96–98]. In our dataset of 510 predicted ectoine producers, 314 (62%) possess an *ectD* gene; in 259 genomes, *ectD* is part of the biosynthetic gene cluster, and 68 *ectD* genes are found outside of the *ect* gene cluster (Figures 4 and 5). Some organisms (20 genome sequences) possess an external *ectD* gene, in addition to the *ectD* gene encoded in the *ect* gene cluster. Since the EctD enzyme is a member of the non-heme-containing, iron(II)- and 2-oxoglutarate-dependend dioxygenase enzyme superfamily [177,185], all predicted 5-hydroxyectoine producers are either aerobic or, at least, oxygen-tolerant microorganisms. This can be nicely observed in those Archaea that are predicted to synthesize ectoine either alone or in combination with 5-hydroxyectoine. In the strictly anaerobic methanogenic Archaea belonging to the genera *Methanosaeta* and *Metanobacterium*, only an *ectABC* cluster can be found, while in the oxygen-dependent nitrifying Archaea of the genus *Nitrosopumilus*, *ectABCD* gene clusters are present [92] (Figure 5).

As outlined above, some *ectABC(D)* gene clusters are associated with a gene (*ask_ect*) encoding a specialized aspartokinase [122,166–168]. We assessed the phylogenetic occurrence of the Ask_Ect (Figure 5) and the genetic organization of its structural gene within the context of the *ect* biosynthetic genes (Figure 4). In our dataset of 510 putative producers of ectoines, 133 ectoine/5-hydroxyectoine biosynthetic gene clusters contained the gene for the specialized aspartokinase. These gene clusters are primarily found in *Alphaproteobacteria* and *Gammaproteobacteria* (Figure 5).

Ectoine producers can populate ecological niches with rather different attributes. This is actually not surprising, because microorganisms will experience increases in the environmental osmolarity not only in marine and high-saline surroundings (e.g., open ocean waters, marine sediments, salterns, brines), but also, for instance, when the soil slowly dries out. If one views the putative ectoine/5-hydroxyectoine producers in an ecophysiological context, many marine and terrestrial microorganisms are represented, as are some bacteria that live associated with plants or animals. Among the latter group of microbes, bacteria are found that are beneficial to plant growth (e.g., many *Rhizobium*, *Sinorhizobium* or *Bradyrhizobium* strains), others are formidable plant pathogens (e.g., many *Pseudomonas syringae* pathovars). Likewise, some of the putative ectoine/5-hydroxyectoine producers are human or animal pathogens (e.g., *V. cholerae*, *M. abscessus, B. cepacia, B. parapertussis,* or *Bordetella bronchioseptica*). Some ectoine producers are also found among microorganisms that live in rather specialized habitats. A striking example is the gammaproteobacterium *Teredinibacter turnerae*, an intracellular endosymbiont in the gills of *Lyrodus pedicellatus*, commonly known as shipworms. This mollusk digests wood immersed in salt water, a catabolic process that relies on cellulases produced by *T. turnerae* [226]. Interestingly, ectoine/5-hydroxyectoine producers are also found in a few representatives of the phylogenetically deep-branching phylum *Planctomycetes*, microorganisms with highly interesting cell biology that are widely distributed in marine and terrestrial habitats. Physiological studies with slight halophilic representative of the genus *Planctomyces*, *P. brasiliensis* (recently re-classified as *Rubinisphaera brasiliensis*) and *Planctomyces maris* (recently re-classified as *Gimesia maris*) showed that ectoine and 5-hydroxyectoine play major roles in osmostress adaptation [227]. Attesting to the metabolic flexibility of these microorganisms under severe osmotic stress conditions, non-nitrogen-containing compatible solutes (e.g., sucrose and glucosylglycerate) are produced when nitrogen becomes limiting [227].

Ectoine/5-hydroxyectoine producers are also found in ecosystems whose salinity is not particularly high; one example is *A. cryptum*, a heterotrophic alphaproteobacterium that thrives in acidic, metal-rich environments, but which is not known to tolerate high concentrations of salt [180]. One also needs to keep in mind that taxonomically closely related microorganisms can rely, as far as the accumulation of ectoines is concerned, on the accumulation of different types of compatible solutes. This is exemplified by studies with the marine predatory heterotrophic myxobacteria *Enhygromyxa salina* SWB007 and *Plesiocystis pacifica* SIR-1 [228]. While *P. pacifica* SIR-1 relied on the accumulation of amino acids for its osmostress adjustment process, *E. salina* SWB007 employed, besides glycine betaine, 5-hydroxyectoine as its dominant compatible solute under high-salinity growth conditions. Accordingly, no ectoine/5-hydroxyectoine biosynthetic genes were found in the genome sequence of *P. pacifica* SIR-1, while an *ect_ask-ectABCD* gene cluster was present in the genome sequence of *E. salina* SWB007. This ectoine/5-hydroxyectoine biosynthetic gene cluster is also associated with a copy of the *ectR* regulatory gene [228].

While the *ect* genes are widely distributed in ecophysiologically different types of microorganisms, there is evidence in certain groups of ectoine/5-hydroxyectoine producers for ecotype diversification. For instance, ectoine/5-hydroxyectoine biosynthetic genes were found not only in the archaeon *N. maritimus* strain SCM1 [92] but are also present in the draft genomes of halotolerant *Nitrosopumilus* species populating brine-seawater interfaces, whereas they are not present in genomes of *Nitrosopumilus* species enriched from low-salinity estuary and costal environments [229]. The clearest evidence reported to date for an association of ectoine biosynthesis with microbial niche diversification stems from a comprehensive phylogenomic analysis of *Rhodobacteraceae* [230]. These *Alphaproteobacteria* are metabolically highly versatile and are key players in global biogeochemical cycling [231,232]. Based upon the analysis of 106 genome sequences, Simon et al. [230] found that during the evolution of this group of microorganisms several shifts between marine and non-marine habitats occurred and signature changes in genomic content reflect the different ecosystem populated by members of the *Rhodobacteraceae*. During this process, marine *Rhodobacteraceae* gained the genes for ectoine synthesis and that for the production of the compatible solute carnitine, and they also acquired the ability to import this latter osmostress protectant [230]. In a study addressing the phylogeny of the ectoine biosynthetic genes in aerobic, moderate halophilic methylotrophic bacteria, Reshetnikov et al. [99] found that the amino acid sequence relationship of the ectoine biosynthetic proteins did not strictly correlate with the phylogenetic affiliation of the studied methylotrophic species and strains, thereby suggesting that the ability to synthesize ectoine most likely results from lateral gene transfer events. Such gene transfer events are clearly manifested when one views the position of the EctC proteins from Archaea within the clade analysis of ectoine synthases present in Bacteria (Figure 5) [92].

7. Scavenging Ectoines as Stress Protectants from Environmental Sources

Ectoines are produced and accumulated in high-osmolarity-stressed microorganisms to exceedingly high cellular levels [91,94]. They are released from these producers through the transient opening of mechanosensitive channels during osmotic down-shocks, through secretion, by decomposing microbial cells attacked by phages or toxins, or through the predatory activity of microorganisms and eukaryotic cells [233]. Hence, it is not surprising that environmentally compatible solutes, including ectoines, have been detected in different ecosystems [234–239]. As a result, the presence of cell-free ectoines provides new opportunities for microorganisms living in the same habitat as the ectoine producers by allowing them to ameliorate osmotic or temperature stress through import of these compatible solutes.

Transport systems for compatible solutes are ubiquitous in microorganisms, and these are typically osmotically regulated both at the level of transport activity and in the transcriptional response of their structural genes [2,6,10,240–242]. The activity regulation of osmolyte transporters provides the cell with a practically instantaneous adjustment response to osmotic up-shift [240,242–246] that, depending on the severity, can strongly impair growth [247]. The transcriptional induction of the transporter genes will then provide enhanced transport capacity for osmostress protectants to permit

growth under sustained osmotically unfavorable conditions [2,84,85]. Hence, uptake systems for compatible solutes [1–3,241], or for their biosynthetic precursors (e.g., choline for the synthesis of glycine betaine) [171,248], are integral parts of the overall osmostress adjustment strategy of many microbial cells (Figure 1A). They typically possess K_m values in the low µM range, thereby allowing the recovery of stress protective solutes from scarce environmental sources. Often, a given microbial cell possesses several osmostress protectant uptake systems, which frequently differ in their substrate profile and mode in which the transport process is energized [10,84,85,240,249], thereby providing additional flexibility to the osmotically challenged cell.

Ectoine/5-hydroxyectoine transport systems involved in alleviating osmotic or temperature stress have been characterized in various Gram-negative and Gram-positive bacteria. These importers belong to four different transporter families: (i) binding protein-dependent ABC transporters [250,251] that use ATP to fuel substrate translocation across the cytoplasmic membrane (e.g., the ProU system from *E. coli*, the OusB system from *Erwinia chrysanthemi,* the OpuC transporter from *B. subtilis* and the ProU system from *Vibrio anguillarum*) [121,187,252,253], (ii) members of the Major Facilitator Family (MFS) [254] that are dependent on the proton motif force (e.g., the ProP and OusA system from *E. coli* and *E. chrysanthemi*, respectively) [243,255], (iii) members of the Betaine-Choline-Carnitine Transporters (BCCT) [241] that are energized either by proton or sodium gradients (e.g., the OpuD transporter from *B. subtilis,* EctT from *V. pantothenticus*, EctM from *M. halophilus,* EctP and LcoP from *C. glutamicum*) [78,256–259], and (iv) members of the periplasmic binding protein-dependent tripartite ATP independent periplasmic transporter family (TRAP-T) [160] that are energized by proton or sodium gradients (e.g., the TeaABC system from *H. elongata*) [161]. Often, transporters used for the import of ectoines exhibit broad substrate specificity (e.g., the ProU and ProP systems from *E. coli* and the OpuC transporter from *B. subtilis*) [84,85,188,189], but dedicated importers for these compounds are also known (e.g., the TeaABC system from *H. elongata* and the EctT transporter from *V. pantothenticus*) [78,161].

In the context of osmostress-responsive transporters for ectoine/5-hydroxyectoine, it is important to note that some compatible solute transporters (e.g., BCCT- and TRAP-types) import substantial amounts of Na^+ into the cell, along with the stress-relieving substrate. For instance, the glycine betaine transporter BetP from *C. glutamicum*, the biochemically and structurally best-studied transporter of the BCCT family [241], to which the ectoine/5-hydroxyectoine transporter EctT, EctM, EctP, and LcoP also belong [78,257–259], has a stoichiometry of two Na^+ ions per imported glycine betaine molecule [241,245,246,260]. Since substantial compatible solute pools are generated through transport, effective export systems for the co-transported cytotoxic Na^+ ions are key players in the overall osmostress adjustment strategy of microorganisms using the *salt-out* strategy (Figure 1A).

High-resolution crystal structures of the TeaA periplasmic ligand-binding protein, in complex with either ectoine (PDB accession code 2VPN) or 5-hydroxyectoine (PDB accession code 2VPO), have been determined [261]. The crystal structure of another ectoine-binding protein (OpuCC) (PDB accession code 3PPR) has also been reported [262]. OpuCC is the extracellular solute receptor of the promiscuous, osmotically inducible OpuC ABC transporter from *B. subtilis* [84,85]. In contrast to the high affinity TeaABC system [261], OpuC imports ectoine only in a side reaction (the K_i of ectoine import via OpuC is about 1.5 mM) [252] and thus will not play a decisive role for ectoine import in natural settings of *B. subtilis* where ectoines will only be present in very low concentrations [234–237].

8. Ectoines as Nutrients

1. Physiology

A hallmark of microorganisms is their enormous metabolic potential. There is essentially no compound synthesized by microorganisms that cannot be catabolized, either by the producer cell itself or by other microorganisms living in the same habitat. This is also true for the nitrogen-rich ectoine/5-hydroxyectoine molecules (Figure 1B); their use as sole carbon, nitrogen and energy sources

has been demonstrated for different microbial species [74,158,190,263–266]. Environmental ectoines have been detected in various ecosystems [234–237,239], and their presence provides new opportunities for microbial ectoine consumers living in habitats that are also populated by ectoine producers. Ectoine-catabolizing microorganisms can scavenge these valuable compounds from the environment through high-affinity, substrate-induced transport systems such as the ABC-system EhuABCD or the TRAP transporter UehABC [263,265,267,268]. Since ectoines are unlikely to be continuously present in a given habitat, it makes physiologically sense for nutrient-limited microorganisms to exert a tight transcriptional control over ectoine/5-hydroxyectoine importer and catabolic genes. We will address below the taxonomic affiliation of ectoine consumers, the catabolic route for ectoines, transport systems for their acquisition, and the genetics underlying the transcriptional control of ectoine/5-hydroxyectoine import and degradation gene clusters.

8.2. Genetics and Phylogenomics of Ectoine Catabolic Genes

While the use of ectoines as nutrients has been known about for quite some time [74,190,263–266], inroads into a molecular and biochemical understanding of ectoine/5-hydroxyectoine catabolism have only been made recently. In a pioneering study, Jebbar et al. [265] used a proteomics approach to identify proteins induced in cells of the symbiotic plant-root-associated soil bacterium *Sinorhizobium meliloti* grown in the presence of ectoine. The protein products of eight ectoine-induced genes were identified by mass-spectrometry, and their genes co-localized in the same gene cluster together with several other genes whose products had not been detected by proteomics (Figure 6A) [265]. This gene cluster is carried by the pSymB mega-plasmid of *S. meliloti*. Four of the nine ectoine-inducible genes encode the components of a binding-protein-dependent ABC-transporter (EhuABCD; *ehu*: *e*ctoine-*h*ydroxyectoine-*u*ptake) and form an operon with five additional genes (*eutABCDE; eut*: *e*ctoine *ut*ilization) predicted to encode enzymes for ectoine/5-hydroxyectoine catabolism. The entire *ehuABCD-eutABCDE* gene cluster is preceded by a gene encoding a member of the GntR superfamily of transcriptional regulators [269] (Figure 6A), a regulatory gene that is now known as *enuR* (*e*ctoine *nu*trient *r*egulator) [270]. Divergently oriented from the *S. meliloti ehuABCD-eutABCDE* operon was an additional regulatory gene (*asnC*) encoding a member of the AsnC/Lrp family of the *feast-and-famine* DNA-binding proteins [271–273] and three ectoine-inducible genes functionally annotated as an aminotransferase, an oxidoreductase, and a succinate semialdehyde dehydrogenase (Figure 6A) [265]. Using an *ehuAB-uidA* transcriptional reporter system, enhanced expression of the reporter fusion was observed when either ectoine or 5-hydroxyectoine was present in the growth medium, but neither glycine betaine nor high salinity triggered enhanced gene expression [265]. Hence, the *ehuABCD-eutABCDE* operon is substrate inducible, as expected for a catabolic system. Building on these findings in *S. meliloti* [265], related ectoine/5-hydroxyectoine import and catabolic gene clusters were identified and experimentally studied in *H. elongata* [158] and the marine bacterium *Ruegeria pomeroyi* DSS-3 [263]. For *H. elongata* [158], a genetic nomenclature different from those used for the annotation of the ectoine/5-hydroxyectoine catabolic genes in *S. meliloti* and *R. pomeroyi* was used; in Figure 6A we have compared the corresponding gene organization in these three organisms to minimize confusion that can be caused by the different annotation of the *H. elongata* genes.

In this figure, we have also included the genetic organization of the ectoine catabolic genes from *C. salexigens*, a gammaproteobacterium taxonomically closely related to *H. elongata*, in which ectoine/5-hydroxyectoine synthesis has been studied in quite some detail [80,194] and in which catabolism of these compounds has also been physiologically assessed [266]. An inspection of the ectoine/5-hydroxyectoine catabolic and importer gene clusters from these four organisms reveals a considerable variation in genetic organization and gene content (Figure 6A). For instance, while the *S. meliloti* gene cluster encodes an ABC import system (EhuABCD) for ectoines [265,267], that of *R. pomeroyi* DSS-3 possesses a TRAP transporter (UehABC) for their uptake [263,268]. In contrast, the *H. elongata* and *C. salexigens* catabolic gene clusters lack genes for an import

system for ectoines altogether (Figure 6A), but they both possess genes for UehABC-related ectoine/5-hydroxyectoine-specific import systems (TeaABC) [161,261] somewhere else in their genomes [263,270]. It is, however, not clear whether the TeaABC transporter serves for the acquisition of ectoines as nutrients since the transcription of the *teaABC* operon is osmotically inducible in *H. elongata* [161].

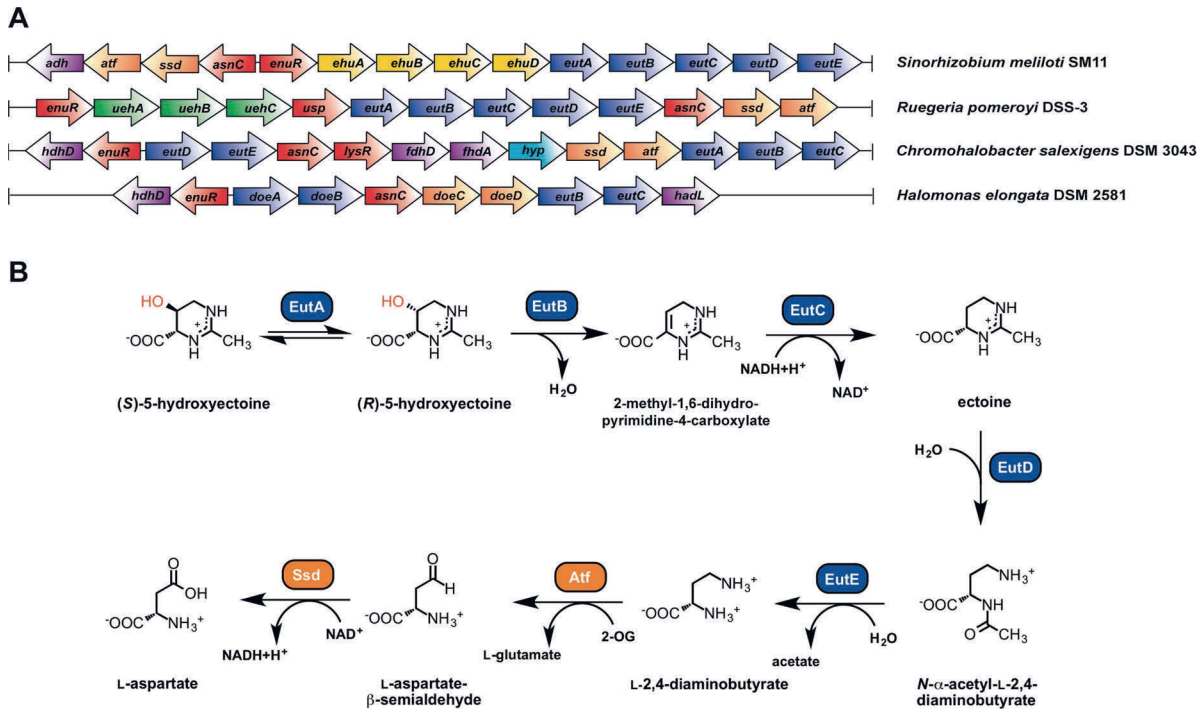

Figure 6. Genetics and catabolic pathways for the utilization of ectoine and 5-hydroxyectoine as nutrients. (**A**) Genetic organization of the ectoine/5-hydroxyectoine-catabolic gene cluster in *Sinorhizobium meliloti* SM11 [265], *Ruegeria pomeroyi* DSS-3 [263,270], *Halomonas elongata* DSM 258 [158] and *Chromohalobacter salexigens* DSM 3043 (predicted from the genome sequence) [274]. In addition to the transporter and catabolic genes discussed in the main text, some of these gene clusters contain genes with yet undefined roles in ectoine catabolism. Their gene products have bioinformatically predicted functions as alcohol dehydrogenase (*adh*), hydroxyacid dehydrogenase (*hdhD*), formate dehydrogenases (*fdhD*, *fdhA*), haloacid dehalogenase (*hadL*), transcriptional regulator (*lysR*) and a hypothetical protein (*hyp*). (**B**) Predicted pathway for the catabolism of ectoine and its derivative 5-hydroxyectoine in *R. pomeroyi* DSS-3. The EutABC-enzymes are predicted to convert 5-hydroxyectoine in a three-step reaction into ectoine. The ectoine ring is subsequently hydrolyzed by the EutD enzyme, resulting in the production of *N*-α-ADABA, an intermediate, which is then further catabolized to L-aspartate by the EutE, Atf and Ssd enzymes. These data were compiled from the literature [158,263,270]. The ectoine-derived metabolites *N*-α-ADABA and L-2,4-diaminobutyrate (DABA) serve as inducers for the transcriptional control of the ectoine/5-hydroxyectoine import and catabolic gene clusters by the EnuR regulatory protein [270].

Using the ectoine hydrolase (EutD), a key enzyme of ectoine catabolism (Figure 6B) [158,263], as a search query for the analysis of 32,523 bacterial and 654 archaeal genomes, 539 EutD orthologes were found [263]. Inspection of the *eutD* gene neighborhoods then revealed a diverse genetic organization and gene content of the ectoine/5-hydroxyectoine import and catabolic gene clusters on a broad scale [158,263]. This stands in contrast to the rather stable and evolutionarily conserved genetic organization of the ectoine/5-hydroxyectoine biosynthetic genes as an *ectABC/ectD*-type operon (Figure 4A). Strikingly, while microbial ectoine/5-hydroxyectoine producers can be found in ten bacterial and two archaeal phyla (Figure 5), ectoine consumers are taxonomically restricted to the

phylum of *Proteobacteria* [263]. In the particular dataset of the 539 *eutD*-containing microbial genomes inspected by Schulz et al. [263], 58% belong to the *Alphaproteobacteria*, 15% were from *Betaproteobacteria,* 27% were from *Gammaproteobacteria*, and there was only a single representative (*Desulfovibrio bastinii* DSM 16055) from the *Deltaproteobacteria*.

Interestingly, among the 539 predicted ectoine/5-hydroxyectoine consumers, 100 microorganisms are predicted to synthesize ectoines as well [263]. The simultaneous presence of ectoine/5-hydroxyectoine biosynthetic and catabolic genes in a given microorganism will require a careful genetic and physiological wiring of these physiologically and biochemically conflicting processes (see Section 7.5) in order to avoid a futile cycle (see Section 7.5). One of the organisms capable of ectoine synthesis and degradation is *H. elongata*, and in the context of its genome annotation and analysis of ectoine synthesis and catabolism, Schwibbert et al. [158] suggested that the ability to both synthesize and degrade ectoines might aid the *H. elongata* cell to physiologically navigate osmotic downshifts. If this hypothesis holds true, then it can only apply to situations where the environmental osmolarity is decreased rather slowly, since mechanosensitive channels (genes for these safety-valves are present in *H. elongata*) (Figure 1A) will otherwise open within milliseconds during harsh osmotic downshifts to reduce the ectoine pool rapidly [11]. Furthermore, Schwibbert et al. [158] calculated that a futile cycle of simultaneous synthesis and degradation of ectoine would saddle the metabolism of *H. elongata* under already energetically and physiologically challenging osmotic conditions [37,106,197] with the expenditure of two additional ATP molecules per turn of ectoine synthesis. Microorganisms capable of both ectoine synthesis and catabolism are quite prevalent in nature; in the dataset of Schulz et al. [263], about 19% of ectoine/5-hydroxyectoine producers were also able to degrade these compounds. It will thus be of considerable interest to learn in future studies how these types of microbes can avoid wasteful futile cycles under steady-state high osmolarity growth conditions.

8.3. Transporters for the Scavenging of Ectoines for Their Use as Nutrients

Ectoines present in the environment occur at very low concentrations [234–239]; hence, high-affinity transporters are required for their recovery and use as nutrients. The EhuABCD ABC transporter from *S. meliloti* and the UehABC TRAP transporter from *R. pomeroyi* are uptake systems whose main function is the scavenging of ectoines for nutritional purposes [263,265,267,268]. The transcription of the underlying structural genes is substrate inducible, but they are not osmotically induced. Although the Ehu and Ueh systems belong to different transporter families (ABC and TRAP transporters, respectively) [160,250,251], they are both dependent on a periplasmic substrate-binding protein (EhuB and UehA, respectively) [267,268]. These binding proteins trap ectoines that have passed the outer membrane via passive diffusion (probably via general porins) with high affinity in the periplasm and deliver them to the core components of the Ehu and Ueh transporters present in the inner membrane for energy-dependent translocation into the cytoplasm. Ligand-binding studies with the purified EhuB and UehA proteins revealed their high affinity for ectoine and 5-hydroxyectoine; EhuB has apparent K_d values of 1.6 µM for ectoine and 0.5 µM for 5-hydroxyectoine [265,267], while UehA exhibits apparent K_d values of 1.4 µM for ectoine and 1.1 µM for 5-hydroxyectoine [268]. Crystallographic studies of the EhuB (PDB accession codes 2Q88 and 2Q89) [267] and UehA (PDB accession code 3FXB) [268] proteins in complex with ectoines revealed the details of the architecture of a ligand-binding site for these compatible solutes, thereby providing further insights into the structural principles of substrate recognition and binding of organic osmolytes that are preferentially excluded from protein surfaces [60–62].

Similar design principles for trapping the ectoine ligand were observed in the crystal structure of the binding protein (TeaA) of the TeaABC TRAP transporter from *H. elongata* [261], a system that primarily serves for the acquisition of ectoines when they are used as osmostress protectants and as a recovery system for newly synthesized ectoines that are leaked or actively excreted from the *H. elongata* producer cell [161]. Crystal structures of the TeaA protein in complex with either ectoine (PDB accession code 2VPN) or 5-hydroxyectoine (PDB accession code 2VPO) have been determined [261]. This protein

has K_d values of 0.2 µM for ectoine and 3.8 µM for 5-hydroxyectoine, respectively [261]. Interestingly, the crystal structures of the UehA and TeaA ligand-binding sites are virtually superimposable [261,268], despite the fact that the TeaABC and UehABC TRAP-type transporters serve different physiological functions. Hence, nature has taken a proven transporter module for the import of ectoines and endowed the transcription of the underlying structural genes with regulatory patterns that allow the transporter either to serve in osmostress protection (TeaABC) [161], or to enable the feeding on ectoines (UehABC) [263,270].

As indicated above, the TeaABC-type transporter might not only serve in osmostress protection, but might also function in the acquisition of ectoines as nutrients. While genes for Ehu-type (370 genomes out of a dataset of 539 ectoine degraders) and Ueh-type (48 genomes out of a dataset of 539 ectoine degraders) transporters are widely affiliated with the corresponding catabolic gene clusters, there is a substantial group of ectoine consumers (122 representatives) that lack transporter genes in the immediate vicinity of the catabolic gene cluster [263]. Since ectoines need to be imported before they can be consumed, it is obvious that transporter genes for these compounds must be encoded somewhere else in the genomes. Perhaps additional transporters for the acquisition of ectoines as nutrients might await discovery. Notably, a sub-group (23 representatives) of predicted ectoine consumers lacking genes for transporters in the vicinity of the catabolic genes possesses genes for TeaABC-type transporters somewhere else in their genome sequence [263], and *H. elongata* is a representative of this group [158,161]. Because mutants with inactivated *ectABC* and *teaABC* genes are available [94,158,161], *H. elongata* would be well-suited to testing the idea [263] that the osmoregulated TeaABC-type transporter might also be involved in the uptake of ectoines when these are consumed.

8.4. Biochemistry of Ectoine/5-Hydroxyectoine Catabolism

Building on the data reported by Jebbar et al. [265] on the identification of ectoine-inducible proteins in *S. meliloti*, Schwibbert et al. [158] made the first concrete proposal for the degradation pathway of ectoine using the blueprint of the *H. elongata* genome sequence. According to this proposal, ectoine degradation begins with the enzymatic opening of the ectoine ring by the ectoine hydrolase (DoeA/EutD; EC 3.5.4.44) to form *N*-α-acetyl-L-2,4-diaminobutyrate (*N*-α-ADABA) as a key intermediate which is further catabolized by the *N*-α-acetyl-L-2,4-diaminobutyrate deacetylase (DoeB/EutE; EC 3.5.1.125) to acetate and DABA. The DoeD/Atf enzyme then converts DABA to L-aspartate-β-semialdehyde and L-glutamate by a transamination reaction; this enzyme belongs to the family of acetyl ornithine aminotransferases. The DoeC/Ssd enzyme then further oxidizes the L-aspartate-β-semialdehyde formed by the DoeD/Atf enzyme to L-aspartate, an important intermediate in central metabolism; the DoeC/Ssd protein is an enzyme related to known succinate semialdehyde dehydrogenases (Figure 6B). Notably, this proposal for ectoine catabolism [158,263] traces the ectoine biosynthetic route (Figure 2) backwards but the types of enzymes involved in the anabolic and catabolic routes are obviously different.

Heterologous expression of the *H. elongata* ectoine hydrolase (DoeA/EutD) in *E. coli* showed that it converts ectoine into both the alpha- and gamma-isomers of ADABA in a 2:1 ratio [158], with *N*-γ-ADABA being the main substrate for the ectoine synthase EctC (Figure 2). Since *N*-γ-ADABA does not seem to be a substrate for the DoeB/EutE enzyme (Figure 6B) [158], it is currently not clear if the formation of *N*-α-ADABA and *N*-γ-ADABA by the ectoine hydrolase (DoeA/EutD) is a specific feature of those microorganisms capable of both synthesizing and catabolizing ectoine (note that *H. elongata* possesses both pathways [158]). Otherwise the formation of *N*-γ-ADABA by the ectoine hydrolase could be rather wasteful, unless the EutE enzyme (Figure 6B) is able to transform both *N*-α-ADABA and *N*-γ-ADABA into DABA.

Examining the ectoine/5-hydroxyectoine catabolic pathway in *R. pomeroyi* DSS-3, Schulz et al. [263] concurred with the proposal by Schwibbert et al. [158] with respect to the degradation route of ectoine to L-aspartate, but they additionally made a proposal for the conversion of 5-hydroxyectoine into ectoine. The removal of the 5-hydroxyl group from the ectoine ring is envisioned as a three-step enzymatic

process that involves the EutABC proteins (Figure 6B). The first step in this reaction is the steric inversion of the hydroxy group by the racemase EutA, converting the native (*S*)-5-hydroxyectoine conformation to the (*R*)-5-hydroxyectoine enantiomer to fit the stereochemical requirements of the next enzyme, EutB (Figure 6B). The EutB enzyme belongs to the family of threonine dehydratases and might be a pyridoxal-5^{0}-phosphate (PLP) dependent enzyme which eliminates a water molecule from the 5-(*R*)-hydroxyectoine enantiomer. The predicted reaction product of EutB is 2-methyl-1,6-dihydropyrimidine-4-carboxylate, which is proposed to be reduced to ectoine by the EutC enzyme, a protein that is thought to serve in a NADH-dependent reduction as an ectoine dehydrogenase (Figure 6B) [263].

We stress here that the envisioned conversion of 5-hydroxectoine to ectoine and its further catabolism to L-aspartate as suggested by Schwibbert et al. [158] and Schulz et al. [263] have not been biochemically evaluated, with the exception of the preliminary assessment of the opening of the ectoine ring by the ectoine hydrolase from *H. elongata* in cells of a heterologous host bacterium [158]. Furthermore, the rather varied gene content of ectoine/5-hydroxyectoine catabolic gene clusters (Figure 6A) [158,263] suggests that variations of the 5-hydroxyectoine to ectoine to L-aspartate catabolic route are likely to exist in microorganisms. In particular, many of these gene clusters lack a homolog of the *eutA* gene. It is also possible that some microorganisms can catabolize ectoine, but cannot use 5-hydroxyectoine as a nutrient, as suggested by the inspection of the gene content of a substantial number of ectoine catabolic gene clusters [263].

8.5. Genetic Regulation of Ectoine/5-Hydroxyectoine Catabolism

As expected for a catabolic system, the ectoine/5-hydroxyectoine import and catabolic gene clusters of *S. meliloti* and of *R. pomeroyi* DSS-3 are substrate inducible [263,265,268,270]. Detailed genetic studies with this system in *R. pomeroyi* DSS-3 revealed that an external supply of either ectoine or 5-hydroxyectoine triggers enhanced import of these compounds and strongly increases the transcription of the *uehABC-usp-eutABCDE-asnC-ssd-atf* gene cluster, forming a 13.5 Kbp poly-cistronic mRNA [268,270]. However, neither ectoine nor 5-hydroxyectoine serve as the true inducers for the de-repression of the transcription of this operon; instead two intermediates in ectoine catabolism, *N*-α-ADABA and DABA (Figure 6B), serve as the physiologically relevant inducers [270]. These compounds are recognized by EnuR, a member of the MocR/GabR sub-group of the large GntR superfamily of transcriptional regulators [275,276]. The *enuR* structural gene (*enuR*: *e*ctoine *n*utrient *u*tilization *r*egulator) is positioned upstream of the *uehABC-usp-eutABCDE-asnC-ssd-atf* gene cluster (Figure 6A) and is expressed from a separate non-ectoine responsive promoter in *R. pomeroyi* DSS-3 [270]. This situation is apparently different from that observed in *S. meliloti* where substrate induction of *enuR* transcription was reported [277]. The EnuR protein appears to play an important role in controlling the transcription of ectoine/5-hydroxyectoine import and catabolic gene clusters in many microorganisms. In the dataset of 539 putative microbial ectoine consumers analyzed by Schulz et al. [270], 456 ectoine/5-hydroxyectoine catabolic gene clusters were associated with an *enuR* gene.

MocR/GabR-type transcriptional regulators are widely distributed in microorganisms [275,276], but are clearly an understudied sub-group of the GntR super-family [269]. The best-studied representative of the MocR/GabR group is the GabR regulator from *B. subtilis* that serves to control genes involved in the metabolism of γ-aminobutyrate (GABA) [278]. The GabR protein is a head-to-tail swapped dimer with an N-terminal DNA reading head containing a winged helix-turn-helix DNA binding motif that is connected via a long flexible linker region to a large carboxy-terminal effector binding/dimerization domain [279]. This latter domain, structurally related to aminotransferases of type-1 fold, contains a covalently bound PLP molecule. However, the C-terminal domain of GabR does not perform a full aminotransferase reaction; instead, a partial aminotransferase reaction occurs [279–283]. In this chemical sequence of events, the co-factor PLP binds to the side-chain of a particular Lys residue of GabR, yielding a Schiff base and thereby resulting in the formation of an

internal aldimine [173]. Subsequently, the system-specific low-molecular mass effector molecule GABA binds to the PLP molecule, which then leads to the detachment of the PLP molecule from the Lys residue of GabR and the formation of an PLP:GABA complex, the external aldimine [173,279–282]. This sequence of events triggers a conformational change of the GabR dimer [279,282], which in turn dictates the DNA-binding activity of the regulatory protein to function either as an activator of the *gabTD* metabolic operon, or as a repressor of its own structural gene (*gabR*) [278].

A homology model of the EnuR dimer based on the crystal structure from the *B. subtilis* GabR regulatory protein [279] is shown in Figure 7A. The EnuR protein from *R. pomeroyi* DSS-3, as heterologously produced (in *E. coli*) and purified by affinity chromatography, has a striking yellow color [263] and possesses spectroscopic properties resembling those of PLP-containing enzymes [173,284,285]. Modeling studies identified Lys^{302} in the EnuR aminotransferase domain as the PLP-binding residue. Its substitution by a His residue (EnuR*) via site-directed mutagenesis leads to loss of the yellow color exhibited by the EnuR wild-type protein in solution and alters its authentic spectroscopic properties. When the *enuR** gene was expressed in a *R. pomeroyi* DSS-3 wild-type strain (*enuR*$^+$), the EnuR* protein conferred a dominant negative phenotype. In other words: the EnuR* protein abrogated the ability of *R. pomeroyi* DSS-3 to use ectoines as nutrients, since its DNA-binding to the cognate operator sequence cannot be relieved in vivo [270]. These combined genetic and biochemical data unambiguously show that the PLP molecule covalently attached to Lys^{302} is critical for the regulatory function of EnuR. EnuR acts as a repressor for the ectoine/5-hydroxyectoine uptake and catabolic genes of *R. pomeroyi* DSS-3 and *S. meliloti* since an *enuR* gene disruption mutation leads to de-repression of the corresponding gene clusters [270,277]. However, since some MocR/GabR-type transcriptional regulators can act both as repressors and activators [278], it remains to be seen in future studies if EnuR possesses these two types of regulatory attributes as well. Operator sequences for EnuR-type proteins have been deduced through bioinformatics in many microorganisms [276] and DNA fragments of *R. pomeroyi* DSS-3 and *S. meliloti* containing these in silico predicted sequences are recognized and stably bound by purified EnuR proteins from the corresponding bacteria [270,277]. In DNA-band-shift assays with the EnuR protein from *R. pomeroyi* DSS-3, specific DNA:EnuR complexes began to form at concentrations of EnuR as low as 75 nM [270].

The chemistry underlying the reaction between the Lys-bound PLP cofactor in MocR/GabR-type regulators and the system-specific inducer requires a primary amino group [278,279,282,283]. Although an external supply of ectoine or 5-hydroxyectoine induces the transcription of the ectoine/5-hydroxyectoine uptake and catabolic gene cluster [263,270], neither of these compounds possesses such a primary amino group (Figure 1B). Consequently, the purified and PLP-containing EnuR protein from *R. pomeroyi* DSS-3 did not bind these two ectoines [270].

It seemed logical that the system-specific inducer molecule that will interact with the Lys^{302} bound PLP co-factor is generated through the metabolism of ectoines. Indeed, several ectoine-derived metabolites possess primary amino groups (Figure 6B). Microscale thermophoresis (MST) experiments revealed that *N*-α-ADABA serves as the primary system-specific inducer for EnuR; it is bound by the EnuR-PLP protein with a K_d value of about 1.7 μM. In Figure 7C we provide a scheme for the binding of the PLP molecule to EnuR/Lys^{302} to form the internal aldemine, the subsequent reaction of the inducer *N*-α-ADABA with the covalently bound PLP molecule and the subsequent formation of the PLP:*N*-α-ADABA complex, the external aldimine [270]. Additional binding studies showed that DABA also interacts with the purified EnuR protein in a Lys^{302}- and PLP-dependent fashion, but the binding constant (K_d about 457 μM) for this reaction is about 270-fold reduced in comparison with the K_d value of *N*-α-ADABA [270]. As a consequence, substantial DABA concentrations (30 mM) were required to displace in vitro the EnuR protein (also referred to in the literature as EhuR or EutR [276,277]) in DNA band-shift assays from its DNA target sequence at the ectoine/5-hydroxyectoine gene cluster of *S. meliloti* [277].

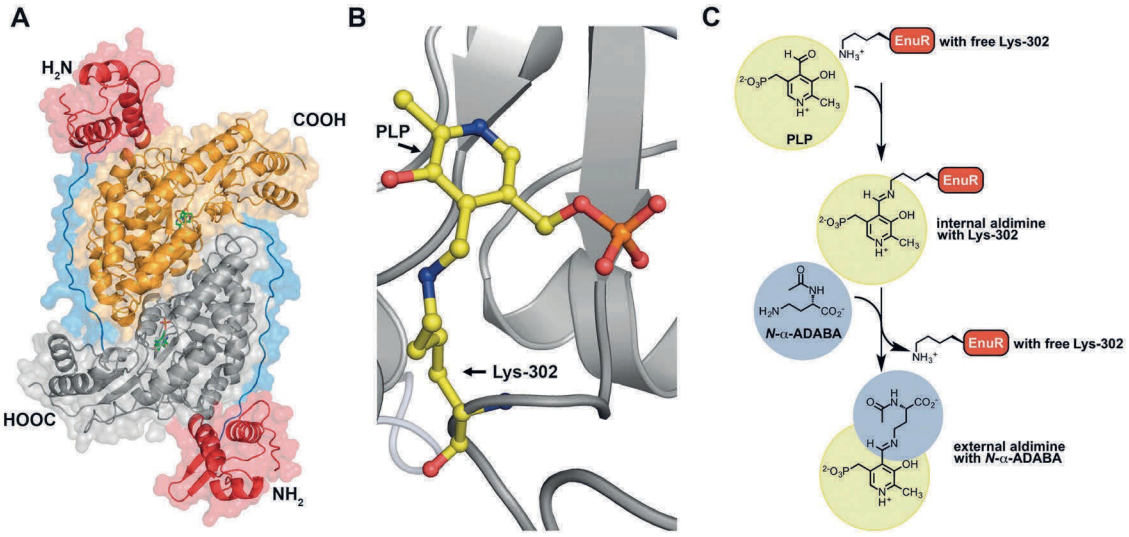

Figure 7. EnuR, a PLP-containing transcriptional regulator of ectoine/5-hydroxyectoine gene clusters. (**A**) in silico model of the predicted *Ruegeria pomeroyi* DSS-3 EnuR dimer that was derived from the crystallographic structure of the *Bacillus subtilis* GabR (PDB accession code 4N0B) [279]. The EnuR model was built with the SWISS-MODEL web server (https://swissmodel.expasy.org/) [286] and visualized using the PyMOL Molecular Graphics System suit (https://pymol.org/2/) [287]. The C-terminal aminotransferase-domains of the EnuR dimer are shown in grey/yellow, the N-terminal DNA-binding domains are represented in red and the flexible linkers connecting these domains are depicted in blue. Each monomer contains a PLP molecule covalently bound via an Schiff base to Lys^{302} in the aminotransferase domain [263,270]. This internal aldimine [173] is depicted in (**B**) in a close-up view. (**C**) Model for the chemistry underlying binding and release of the inducer *N*-α-ADABA to the PLP-cofactor bound to Lys^{302} of the EnuR regulator. In the first step, PLP is covalently bound by the side-chain of Lys^{302} and thus forms an internal aldimine [173]. Upon binding of the inducer *N*-α-ADABA to PLP, PLP is released from Lys^{302} and an external aldimine [173] is formed. This sequence of events is envisioned to trigger a conformational change in EnuR, thereby altering its DNA-binding properties. This scheme for inducer binding by EnuR is based upon detailed biochemical and structural analysis of the *B. subtilis* GabR regulator that uses GABA as its inducer [279–283].

Apart from the high affinity of EnuR for *N*-α-ADABA, this compound has the additional advantage of being an ectoine-catabolism-specific metabolite (Figure 6B), whereas DABA also occurs as an intermediate in other metabolic and biosynthetic processes in microorganisms, including the biosynthesis of ectoine (Figure 2). Taken together, the pairing of the EnuR repressor with its covalently attached PLP co-factor and ectoine-derived metabolites (*N*-α-ADABA and DABA) establishes a sensitive intracellular trigger to relieve EnuR-mediated repression of the ectoine/5-hydroxyectoine catabolic gene cluster [270]. The finding that the isomer of the inducer *N*-α-ADABA, *N*-γ-ADABA, the main substrate for the ectoine synthase (Figure 2), is not recognized by the PLP-bound EnuR regulatory protein [270] is a physiologically highly relevant result. It is of critical importance for the group of microorganisms that are capable of both ectoine synthesis and catabolism in order to avoid a wasteful futile cycle. However, the report by Schwibbert et al. [158] that the ectoine hydrolase of *H. elongata* can generate both *N*-α- and *N*-γ-ADABA molecules raises questions about the ability of microorganisms to establish a strict genetic separation of ectoine synthesis and catabolic pathways.

Many ectoine/5-hydroxyectoine uptake and catabolic gene clusters (494 representatives from a dataset of 539 ectoine consumers [263,270]) contain an *asnC* gene. It encodes a member of the broadly distributed AsnC/Lrp-family of transcriptional regulators that can wrap DNA into nucleosome-like structures and frequently respond in their DNA-binding properties to low-molecular mass effector molecules generated through metabolism (e.g., amino acids) [271,272,288]. In many cases,

these proteins respond to feast-and-famine situations, and thereby permit the efficient exploitation of sudden burst in the supply of nutrients. Studies with *asnC* mutants from the ectoine/5-hydroxyectoine uptake and catabolic gene cluster of *R. pomeroyi* DSS-3 revealed a clear activating influence on the transcription of this operon and the ability of *R. pomeroyi* DSS-3 to use ectoine as sole carbon source was abolished in the *asnC* mutant strain [270]. It is currently unclear as to which metabolite or cellular cue AsnC responds, but given the reported data for the effector molecules of EnuR (*N*-α-ADABA and DABA) [270], we would not be surprised if this regulator uses intermediates or end-products of ectoine degradation (Figure 6B) to alter its DNA-binding activity. Preliminary DNA-binding studies with the AsnC homolog (referred to as DoeX) from *H. elongata* showed that it binds to DNA segments in the proposed regulatory region of the ectoine catabolic gene cluster [158]. Relevant for an understanding of the role played by AsnC is the fact that feast-and-famine type DNA-binding proteins can work in concert with other regulatory proteins [289], a facet in gene regulation that is probably highly relevant for the large group of microbial ectoine consumers that possess both EnuR and AsnC (85% of the 539 predicted ectoine consumers in the dataset of Schulz et al. [263,270]).

Two-component regulatory systems (TCS) are major sensor devices through which microbial cells monitor either extra- or intracellular changes [290]. Most TCS consist of a cytoplasmic membrane-embedded histidine kinase and a cytoplasmic response regulator. Upon detection of a specific signal, the histidine kinase auto-phosphorylates using ATP as phosphor donor; it then transfers the phosphoryl group to the response regulator, which will communicate with the transcriptional apparatus of the cell to alter, in many cases, gene expression [290]. Transposon mutagenesis of *R. pomeroyi* DSS-3 revealed the involvement of such a system, NtrYX [291], in the genetic control of its ectoine/5-hydroxyectoine catabolic gene cluster [270]. The NtrX response regulator is an unusual member of the NtrC-family and its cognate sensor kinase NtrY is a protein with four predicted transmembrane regions and a large, 161-amino-acids-long, extra-cytoplasmic domain. The NtrYX TCS has been implicated in a variety of cellular functions in various microorganisms, including the control of catabolic genes for nitrogen-containing compounds [291–293]. Genetic inactivation of *R. pomeroyi* DSS-3 *ntrYX* genes renders this bacterium unable to use ectoine as the sole carbon source [270]. Hence, the NtrYX TCS functions as a positive regulatory device for ectoine catabolism. However, it is currently unknown whether the NtrY sensor kinase recognizes externally provided ectoine directly and what the target sequences for the NtrX response regulator in the large *uehABC-usp-eutABCDE-asnC-ssd-atf* operon are. While *enuR* and *asnC* genes are widely distributed among all branches of ectoine degrading *Proteobacteria*, the *ntrYX* genes are only found in ectoine-consuming members of the *Alphaproteobacteria* [263,270].

Genetic studies addressing the transcriptional regulation of ectoine/5-hydroxyectoine uptake and catabolism in the marine proteobacterium *R. pomeroyi* DSS-3 have significantly advanced the understanding of the genetic wiring of this process [270]. In the dataset reported by Schulz et al. [263,270], 45% of the 539 inspected genome sequences of predicted ectoine consumers possess all three regulatory systems (EnuR, AsnC, NtrYX) that we have described in some detail in this overview. Hence, it is highly likely that their intricate interplay will set the genetic regulation of ectoine/5-hydroxyectoine catabolism in many different microbial species and strains. On the other hand, the report by Schulz et al. [270] also revealed considerable variations in terms of the presence of the *enuR*, *asnC*, and *ntrYX* genes in a given bacterium, suggesting that variants of the regulatory circuit discovered in *R. pomeroyi* DSS-3 exist.

While these studies already paint a rather complex picture of the genetic control of microbial ectoine/5-hydroxyectoine catabolism [270], the recent discovery of a regulatory small trans-acting RNA controlling ectoine catabolic genes in the *S. meliloti* strain Sm2B3001 [294] already adds a new dimension to this process. Transcription of the gene for this small non-coding RNA (NfeR1; Nodule formation efficiency RNA) is stimulated by high osmolarity, and lack of the NfeR1 RNA altered the expression of an array of salt-responsive genes in this symbiotic bacterium. Notably, under high-salinity growth conditions, the level of the *eutAED* mRNA is down-regulated in a NfeR1 RNA-dependent

fashion [294]. However, the details of this interesting regulatory circuit, its physiological consequences, and its possible wider occurrence in ectoine-consuming microorganisms need to be further explored.

9. Ectoines in Eukarya: A Recent Discovery

Ectoines have so far been considered as compatible solutes exclusively synthesized and used as stress protectants by members of the Bacteria, and by a few Archaea [91–94]. Recent studies with halophilic protists now change this picture substantially [104], since ectoine/5-hydroxyectoine biosynthetic genes have been detected in *Halocafeteria seosinensis* [100,101] and ectoine production has been directly observed in *Schmidingerothrix salinarum* [102]. *H. seosinensis* is a heterotrophic, borderline extreme halophilic nano-flagelate that actively ingests bacteria as its food source; 18S rRNA-based phylogenetic analysis placed this protist into the stramenophile linage, and it was taxonomically positioned into the order *Bicosoecida* [295]. *S. salinarum* is a bacteriovorous heterotroph as well; it is a halotolerant ciliate and a member of the order *Stichotrichia* [296].

Marine and hypersaline habitats are populated not only by a physiologically and taxonomically diverse group of Bacteria and Archaea [23,297] but halophilic protists are also ecophysiologically critical inhabitants of these challenging ecosystems [103]. These unicellular eukaryotes serve crucial roles as primary producers and decomposers in these habitats, and some of them exert a major influence on the abundance of microorganisms and the release of bacteria-derived metabolites into the environment through their bacterivorous activity. However, their salt-stress adaptation strategy has largely been neglected [103].

In their studies on the genome sequence of *H. seosinensis* and its salt-stress-responsive transcriptional profile, Harding et al. [100,101] discovered the presence and the salt-stress responsive induction of ectoine/5-hydroxyectoine biosynthetic and *ask_ect* genes. Since *H. seosinensis* is a heterotroph feeding on microorganisms living in its habitat, the detection of DNA sequences related to microbial genes is at least initially of some concern. The misinterpretation of these sequences as being of eukaryotic origin can seriously compromise assembly into DNA scaffolds of the eukaryotic genome sequence and the interpretation of biological findings [298]. In the case of *H. seosinensis*, at least for the *ectABCD* and *ask_ect* genes, one can exclude this complication, since each of these genes harbors spliceosomal introns [100,101], genetic elements that are not found in Bacteria and Archaea [299]. The *H. seosinensis* ectoine/5-hydroxyectoine biosynthetic enzymes possess N-terminal mitochondrial targeting signals, while their bacterial and archaeal counterparts are all cytoplasmic enzymes [165]. This observation suggests that the production of these compatible solutes might occur in the mitochondria of the protists, cell compartments in which the biosynthetic precursors (Glu and Asp) of ectoines are synthesized using intermediates of the Krebs cycle [101].

In extended database searches of eukaryotic genomes, Harding et al. [101] discovered *ectA*- and *ectC*-related sequences in previously reported transcriptional profiles of other protists and in various other Eukarya. This includes even the deuterostome animals *Branchiostoma floridae* and *Saccoglossus kowalevskii*. *B. floridae* is a lancelet, modern survivors of an ancient chordate lineage [300], while *S. kowalevskii* belongs to the hemicordate phylum, marine invertebrates that are taxonomically classified together with the Chordata as Deuterostomia [301]. Experimental proof that the protist *H. seosinensis*, or for that matter any other *ect* gene-containing eukaryote, actually produces ectoines is missing in the interesting report of Harding et al. [101]. This important gap has now been closed by a comprehensive study conducted by Weinisch et al. [102], in which the salt-stress-dependent synthesis of ectoine was directly demonstrated by ^{1}H-NMR spectroscopy in the halophilic heterotrophic ciliate *S. salinarum*. Since no genome sequence of *S. salinarum* is currently publicly available, the genetic organization of the ectoine biosynthetic genes remains to be determined. Interestingly, *S. salinarum* is also able to import ectoine and can derive osmostress protection from this process [102].

Detailed phylogenetic considerations reported by Harding et al. [100,101] on the *H. seosinensis* *ectABC-ectD* genes lead to the conclusion that they might have been acquired via lateral gene transfer from a prokaryote and were subsequently genetically adjusted to the transcriptional and translational

apparatus of the new eukaryotic host. Considering that both *H. seosinensis* and *S. salinarum* are predatory protists [103], this is a plausible evolutionary scenario, particularly since many microbial ectoine/5-hydroxyectoine producers are inhabitants of high-saline ecosystems (Figure 5) [91–94]. It is well established that Eukarya can acquire novel metabolic traits and stress resistance determinants by stealing pre-formed gene clusters from microorganisms [302]. Since ectoines are potent protectants against osmotic, desiccation, and temperature stress, it is highly likely that the acquisition of *ect* genes by *H. seosinensis* and *S. salinarum* from their microbial food prey [100,101,104] will provide a distinct growth and survival advantage to these eukaryotic cells in their physiologically challenging high-salinity habitats [103].

Another interesting finding related to the synthesis of ectoines by Eukarya stems from a recent study by Landa et al. [303], in which the remodeling of the transcriptional profile of *R. pomeroyi* DSS-3 co-cultured with the diatom *Thalassiosira pseudonana* was assessed. The observed gene expression pattern indicates that, in addition to dihydroxypropanesulfonate, xylose, and glycolate, ectoine also fueled carbon and energy metabolism of the heterotroph *R. pomeroyi*. In view of the findings on the substrate-induction of the ectoine/5-hydroxyectoine uptake and catabolic genes [263,265,270], the report by Landa et al. [303] implies that the diatom produces and releases ectoine/5-hydroxyectoine that are then detected by the prokaryotic partner and exploited as a nutrient [263,270]. This interpretation rests on the assumption that the culture of *T. pseudonana* used in this study [303] is truly axenic. The finding of Landa et al. [303] and the genetic data on the transcriptional induction of the ectoine/5-hydroxyectoine uptake and catabolic gene cluster by intermediates in ectoine degradation (Figures 6 and 7) [263,270] have broader implications. Members of the metabolically and ecophysiologically versatile *Roseobacter* clade are not only found as widespread free-living members of marine habitats, but also associate closely with the cells of diverse phytoplankton groups in the ocean [230,232]. Hence ectoines could play an important role in establishing and maintaining ecophysiological relevant food webs in various ecological niches.

10. Conclusions and Perspectives

The data presented here provide the most comprehensive study to date on the phylogenomics of the ectoine (*ectABC*) and 5-hydroxyectoine (*ectD*) biosynthetic gene clusters, and the genes functionally associated with them, with respect to the production (*ask_ect*) of their biosynthetic precursor or the transcriptional regulation (*ectR*) of their structural genes (Figure 5). This data set can therefore serve as a reference point for the distribution of the *ect* genes in future studies, as new genome sequences of Bacteria and Archaea are determined at an ever-increasing pace. Despite the existing bias of the available genome sequences in databases, one can conclude from our phylogenomic analysis that the taxonomic affiliation of presumed ectoine/5-hydroxyectoine producers is dominated by representatives of the *Actinobacteria* and members from the *Alphaproteobacteria*, *Betaproteobacteria*, and *Gammaproteobacteria*, which together make up 91% of our dataset. Although some ectoine/5-hydroxyectoine producers are found among members of the Archaea, we conclude that the synthesis of ectoines is primarily a bacterial trait, since available evidence (Figure 5) points to the transmission of the *ectABC/ectD* genes via lateral gene transfer into the genomes of a restricted number of Archaea from members of the Bacteria [92]. This evolutionarily important process [223–225,302] is in all likelihood also responsible for the acquisition of *ect* biosynthetic genes by unicellular Eukarya that live in high-saline habitats [100–102]. This recent finding opens new avenues of research, and follow-up studies might hold surprising discoveries. Our overview on the phylogenomics of *ectABC* and *ectD* biosynthetic genes can also aid the further development and biotechnological exploitation of natural and synthetic microbial cell factories for ectoines, commercially high-value natural products [86,91,94,145,146,148], since there are many microorganisms with different life-styles to choose from (Figure 5).

The accumulation of ectoines by high-osmolarity/salinity stressed cells through synthesis and import [1] has a major influence on the hydration status of the cytoplasm, and hence on cell

volume and turgor [2,10,108–111] and their function-preserving attributes [91,94,105,145–147] will also likely contribute to the ability of the cell to strive under osmotically challenging growth conditions. An understanding of the role of ectoines as highly effective microbial osmostress protectants therefore seems rather straightforward. However, it is not clear yet how the thermoprotective effects of ectoines [77–79,97,121] are achieved on a biochemical and molecular level. While the portrayal of ectoines as chemical chaperones is suggestive, the molecular mechanisms underpinning the function-preserving characteristics of these compounds do not necessarily need to be the same at high and low growth temperatures. From the perspective of basic science, and with respect to practical applications, studies addressing the function of ectoines as thermolytes might prove to be highly rewarding.

The core of the ectoine/5-hydroxyectoine biosynthetic route and the properties of the involved enzymes (Figure 2) are now reasonably well understood, but nevertheless require further focused efforts to attain a detailed structure/function description of each of the involved biocatalysts. This has already been accomplished in quite some detail for the ectoine hydroxylase (EctD) through biochemical, structural, site-directed mutagenesis, and modeling approaches [93,177,186]. Ectoine/5-hydroxyectoine producers live in ecophysiological varied and often stressful habitats that might require evolutionary adaptation of the underlying biosynthetic enzymes. The phylogenomic data (Figure 5) might therefore serve as a guide to choosing those ectoine biosynthetic enzymes that are best suited for structural approaches. Our extended overview of the genetic context of *ectC* genes underscored recent reports on the widespread occurrence of solitary EctC-type proteins [92,93]. Their biochemical properties and potential physiological function [221] are so far unresolved and certainly should be a topic for future studies.

From the view of basic science, the understanding of the genetic and physiological regulatory circuits controlling *ect* gene expression in response to environmental and cellular cues is a pressing issue. There is no consistent picture of how this is accomplished, and the literature on this topic is plagued with claims that are not sufficiently substantiated by experimental data. In the bacteria studied so far, transcription of the ectoine/5-hydroxyectoine biosynthetic genes is under osmotic control, fully consistent with the major physiological function of these potent osmostress protectants. However, the underlying genetic regulatory mechanisms might differ in different microbial species and might entail promoters that operate independently of specific regulatory proteins [116], while others might be dependent on such transcription factors (e.g., RpoS; SigB) [77,78]. Most interesting is the association of the *ect* genes in many *Proteobacteria* with a gene (*ectR*) that encodes a member of the MarR super-family of transcriptional regulators (Figure 5). So far, EctR has only been functionally studied in a few aerobic, moderately halophilic methylotrophic bacteria (*M. alcaliphilum* 20Z, *M. alcalica, M. thalassica*), where it serves as a repressor of *ect* gene expression [99,198,215], but does not seem to be critical for their osmostress-responsive transcription [198]. The environmental or cellular cues to which EctR responds in its DNA-binding activity are unknown and hence our understanding of the role of this intriguing regulatory protein in controlling *ect* gene expression is rather incomplete.

The widespread occurrence of ectoine/5-hydroxyectoine producers in terrestrial and marine habitats (Figure 5) also leads to the presence of cell-free ectoines in natural ecosystems when these cells are osmotically down-shocked or when they lyse [233]. The recovery of ectoines by microorganisms from environmental sources via high affinity transport systems will aid these bacteria in their attempts to withstand osmotic and temperature extremes. These transporters are of ecophysiological importance not only for the acquisition of ectoines, where they act as stress protectants, but they also seem to serve as recycling systems for newly synthesized ectoines that are either leaked or actively excreted from the producer cells [161,304]. Continued efforts are required to understand the physiological relevance and molecular underpinning of this latter process [161,304,305], and to further enhance our understanding of the structure/function relationship of ectoine/5-hydroxyectoine importers [241,261,267,268]. Furthermore, new selection or screening procedures might lead to the identification of additional members (and perhaps also novel types) of transporters for ectoines.

Ectoine/5-hydroxyectoine import systems (e.g., EhuABCD, UehABC) also play a crucial role in scavenging these compounds from scarce environmental sources, where these nitrogen-rich molecules (Figure 1B) are used as nutrients. Consistent with their important contribution to ectoine/5-hydroxyectoine catabolism, the transcription of the *ehu* and *ueh* structural genes is substrate-inducible but is not subjected to osmotic control [265,267,268,270]. In contrast to the already rather well studied ectoine/5-hydroxyectoine biosynthetic genes, an understanding of the biochemistry of the catabolic enzymes is in its infancy. Although experimentally testable proposals for the catabolism of 5-hydroxyectoine and ectoine have been made (Figure 6B) [158,263], the inspection of the corresponding gene clusters not only revealed a considerable variation in their genetic organization but also in their gene content (Figure 6A) [158,263,270]. This variation suggests that alternatives (or additions) to the proposed catabolic pathways might exist in microorganisms.

Recent studies on the genetics of the transcriptional control of ectoine/5-hydroxyectoine utilization genes paint a rather complex picture of this process [270], but they have already uncovered a central role of the MocR/GabR-type EnuR regulator and its ectoine-derived inducers *N*-α-ADABA and DABA [270,277]. Nevertheless, further in-depth studies are required to elucidate the complete regulatory circuit controlling import and catabolism of ectoines and to illuminate the role played by the feast-and-famine regulator AsnC and the NtrYX two-component regulatory system [270]. Although about 45% of the genomes of the 539 predicted ectoine/5-hydroxyectoine consumers simultaneously possess the EnuR, AsnC, and NtrYX regulatory systems implicated in controlling ectoine/5-hydroxyectoine catabolic genes [270], there is again a considerable variation in their phylogenetic distribution, suggesting that differently configured regulatory circuits control the catabolism of ectoines in different microorganisms.

The recent discovery of ectoine/5-hydroxyectoine biosynthetic genes in the halophilic protist *H. seosinensis* [100,101] and the salt-stress-responsive production and import of ectoine in *S. salinarum* [102] came at a considerable surprise for scholars of microbial osmostress response systems [104]. The data reported by Harding et al. [100,101] suggest the presence of ectoine/5-hydroxyectoine biosynthetic genes in Eukarya other than *H. seosinensis* and *S. salinarum*. As a case in point, the re-programming and induction of ectoine/5-hydroxyectoine uptake and catabolic genes in the marine bacterium *R. pomeroyi* in a co-culture with the diatom *T. pseudonana* [303] strongly suggest that this eukaryote produces and releases ectoines, because enhanced expression of these genes by *R. pomeroyi* DSS-3 is strictly dependent on ectoine-derived metabolites [270,277]. Taken together, these findings underscore the importance of ectoines not only as effective stress- and cytoprotectants but also suggest an important function of these nitrogen-rich compounds as mediators of ecophysiologically important food webs. Ectoines will remain a fascinating research topic for many years to come, both from the perspective of basic science and applied approaches.

Acknowledgments: We greatly appreciate the expert help of Vickie Koogle in the language editing of our manuscript. Work in the laboratory of E.B. at the University of Marburg on the synthesis and degradation of compatible solutes is supported by the Deutsche Forschungsgemeinschaft (DFG) through the SFB 987 and by the LOEWE-Center for Synthetic Microbiology. We thank Stefanie Kobus of the Center of Structural Studies (CSS) at the Heinrich-Heine University of Düsseldorf (Germany) for her focused efforts and expert help in the determination of crystal structures of ectoine/5-hydroxyectoine biosynthetic enzymes and components of ectoine transporters. E.B. thanks Joeren Dickschat (University of Bonn, Germany) for fruitful collaborations on the synthesis and catabolism of ectoines. L.C. is a member of the International Max Planck Research School on Environmental, Cellular and Molecular Microbiology (IMPRS-Mic Marburg) and gratefully acknowledges its financial support.

Author Contributions: L.C. and E.B. wrote the manuscript with input from the other authors.

Conflicts of Interest: The authors declare no conflict of interest.

References

1. Kempf, B.; Bremer, E. Uptake and synthesis of compatible solutes as microbial stress responses to high osmolality environments. *Arch. Microbiol.* **1998**, *170*, 319–330. [CrossRef] [PubMed]

2. Bremer, E.; Krämer, R. Coping with osmotic challenges: Osmoregulation through accumulation and release of compatible solutes. In *Bacterial Stress Responses*; Storz, G., Hengge-Aronis, R., Eds.; ASM Press: Washington, DC, USA, 2000; pp. 79–97.
3. Wood, J.M.; Bremer, E.; Csonka, L.N.; Krämer, R.; Poolman, B.; van der Heide, T.; Smith, L.T. Osmosensing and osmoregulatory compatible solute accumulation by bacteria. *Comp. Biochem. Physiol. A Mol. Integr. Physiol.* **2001**, *130*, 437–460. [CrossRef]
4. Csonka, L.N. Physiological and genetic responses of bacteria to osmotic stress. *Microbiol. Rev.* **1989**, *53*, 121–147. [PubMed]
5. Roesser, M.; Müller, V. Osmoadaptation in bacteria and archaea: Common principles and differences. *Environ. Microbiol.* **2001**, *3*, 743–754. [CrossRef] [PubMed]
6. Wood, J.M. Osmosensing by bacteria: Signals and membrane-based sensors. *Microbiol. Mol. Biol. Rev.* **1999**, *63*, 230–262. [CrossRef] [PubMed]
7. Ball, P. Water is an active matrix of life for cell and molecular biology. *Proc. Natl. Acad. Sci. USA* **2017**, *114*, 13327–13335. [CrossRef] [PubMed]
8. De Lima Alves, F.; Stevenson, A.; Baxter, E.; Gillion, J.L.; Hejazi, F.; Hayes, S.; Morrison, I.E.; Prior, B.A.; McGenity, T.J.; Rangel, D.E.; et al. Concomitant osmotic and chaotropicity-induced stresses in *Aspergillus wentii*: Compatible solutes determine the biotic window. *Curr. Genet.* **2015**, *61*, 457–477. [CrossRef] [PubMed]
9. Van den Berg, J.; Boersma, A.J.; Poolman, B. Microorganisms maintain crowding homeostasis. *Nat. Rev. Microbiol.* **2017**, *15*, 309–318. [CrossRef] [PubMed]
10. Wood, J.M. Bacterial osmoregulation: A paradigm for the study of cellular homeostasis. *Annu. Rev. Microbiol.* **2011**, *65*, 215–238. [CrossRef] [PubMed]
11. Booth, I.R. Bacterial mechanosensitive channels: Progress towards an understanding of their roles in cell physiology. *Curr. Opin. Microbiol.* **2014**, *18*, 16–22. [CrossRef] [PubMed]
12. Whatmore, A.M.; Reed, R.H. Determination of turgor pressure in *Bacillus subtilis*: A possible role for K^+ in turgor regulation. *J. Gen. Microbiol.* **1990**, *136*, 2521–2526. [CrossRef] [PubMed]
13. Deng, Y.; Sun, M.; Shaevitz, J.W. Direct measurement of cell wall stress stiffening and turgor pressure in live bacterial cells. *Phys. Rev. Lett.* **2011**, *107*, 158101. [CrossRef] [PubMed]
14. Cayley, D.S.; Guttman, H.J.; Record, M.T., Jr. Biophysical characterization of changes in amounts and activity of *Escherichia coli* cell and compartment water and turgor pressure in response to osmotic stress. *Biophys. J.* **2000**, *78*, 1748–1764. [CrossRef]
15. Rojas, E.R.; Huang, K.C. Regulation of microbial growth by turgor pressure. *Curr. Opin. Microbiol.* **2017**, *42*, 62–70. [CrossRef] [PubMed]
16. Levina, N.; Totemeyer, S.; Stokes, N.R.; Louis, P.; Jones, M.A.; Booth, I.R. Protection of *Escherichia coli* cells against extreme turgor by activation of MscS and MscL mechanosensitive channels: Identification of genes required for mscs activity. *EMBO J.* **1999**, *18*, 1730–1737. [CrossRef] [PubMed]
17. Hoffmann, T.; Boiangiu, C.; Moses, S.; Bremer, E. Responses of *Bacillus subtilis* to hypotonic challenges: Physiological contributions of mechanosensitive channels to cellular survival. *Appl. Environ. Microbiol.* **2008**, *74*, 2454–2460. [CrossRef] [PubMed]
18. Cetiner, U.; Rowe, I.; Schams, A.; Mayhew, C.; Rubin, D.; Anishkin, A.; Sukharev, S. Tension-activated channels in the mechanism of osmotic fitness in *Pseudomonas aeruginosa*. *J. Gen. Physiol.* **2017**, *149*, 595–609. [CrossRef] [PubMed]
19. Reuter, M.; Hayward, N.J.; Black, S.S.; Miller, S.; Dryden, D.T.; Booth, I.R. Mechanosensitive channels and bacterial cell wall integrity: Does life end with a bang or a whimper? *J. R. Soc. Interface* **2014**, *11*, 20130850. [CrossRef] [PubMed]
20. Cox, C.D.; Bavi, N.; Martinac, B. Bacterial mechanosensors. *Annu. Rev. Physiol.* **2018**, *80*, 71–93. [CrossRef] [PubMed]
21. Calamita, G. The *Escherichia coli* aquaporin-Z water channel. *Mol. Microbiol.* **2000**, *37*, 254–262. [CrossRef] [PubMed]
22. Jiang, J.; Daniels, B.V.; Fu, D. Crystal structure of AqpZ tetramer reveals two distinct Arg-189 conformations associated with water permeation through the narrowest constriction of the water-conducting channel. *J. Biol. Chem.* **2006**, *281*, 454–460. [CrossRef] [PubMed]

23. Ventosa, A.; Nieto, J.J.; Oren, A. Biology of moderately halophilic aerobic bacteria. *Microbiol. Mol. Biol. Rev.* **1998**, *62*, 504–544. [PubMed]
24. Oren, A. Life at high salt concentrations, intracellular KCl concentrations, and acidic proteomes. *Front. Microbiol.* **2013**, *4*, 315. [CrossRef] [PubMed]
25. Galinski, E.A.; Trüper, H.G. Microbial behaviour in salt-stressed ecosystems. *FEMS Microbiol. Rev.* **1994**, *15*, 95–108. [CrossRef]
26. Buda, R.; Liu, Y.; Yang, J.; Hegde, S.; Stevenson, K.; Bai, F.; Pilizota, T. Dynamics of *Escherichia coli's* passive response to a sudden decrease in external osmolarity. *Proc. Natl. Acad. Sci. USA* **2016**, *113*, E5838–E5846. [CrossRef] [PubMed]
27. Bialecka-Fornal, M.; Lee, H.J.; Phillips, R. The rate of osmotic downshock determines the survival probability of bacterial mechanosensitive channel mutants. *J. Bacteriol.* **2015**, *197*, 231–237. [CrossRef] [PubMed]
28. Egan, A.J.; Cleverley, R.M.; Peters, K.; Lewis, R.J.; Vollmer, W. Regulation of bacterial cell wall growth. *FEBS J.* **2017**, *284*, 851–867. [CrossRef] [PubMed]
29. Typas, A.; Banzhaf, M.; Gross, C.A.; Vollmer, W. From the regulation of peptidoglycan synthesis to bacterial growth and morphology. *Nat. Rev. Microbiol.* **2012**, *10*, 123–136. [CrossRef] [PubMed]
30. Rasmussen, T. How do mechanosensitive channels sense membrane tension? *Biochem. Soc. Trans.* **2016**, *44*, 1019–1025. [CrossRef] [PubMed]
31. Booth, I.R.; Blount, P. The MscS and MscL families of mechanosensitive channels act as microbial emergency release valves. *J. Bacteriol.* **2012**, *194*, 4802–4809. [CrossRef] [PubMed]
32. Pliotas, C.; Naismith, J.H. Spectator no more, the role of the membrane in regulating ion channel function. *Curr. Opin. Struct. Biol.* **2017**, *45*, 59–66. [CrossRef] [PubMed]
33. Coquelle, N.; Talon, R.; Juers, D.H.; Girard, E.; Kahn, R.; Madern, D. Gradual adaptive changes of a protein facing high salt concentrations. *J. Mol. Biol.* **2010**, *404*, 493–505. [CrossRef] [PubMed]
34. Talon, R.; Coquelle, N.; Madern, D.; Girard, E. An experimental point of view on hydration/solvation in halophilic proteins. *Front. Microbiol.* **2014**, *5*, 66. [CrossRef] [PubMed]
35. Tadeo, X.; Lopez-Mendez, B.; Trigueros, T.; Lain, A.; Castano, D.; Millet, O. Structural basis for the aminoacid composition of proteins from halophilic archea. *PLoS Biol.* **2009**, *7*, e1000257. [CrossRef] [PubMed]
36. Oren, A. Thermodynamic limits to microbial life at high salt concentrations. *Environ. Microbiol.* **2011**, *13*, 1908–1923. [CrossRef] [PubMed]
37. Oren, A. Bioenergetic aspects of halophilism. *Microbiol. Mol. Biol. Rev.* **1999**, *63*, 334–348. [PubMed]
38. Youssef, N.H.; Savage-Ashlock, K.N.; McCully, A.L.; Luedtke, B.; Shaw, E.I.; Hoff, W.D.; Elshahed, M.S. Trehalose/2-sulfotrehalose biosynthesis and glycine-betaine uptake are widely spread mechanisms for osmoadaptation in the *Halobacteriales*. *ISME J.* **2014**, *8*, 636–649. [CrossRef] [PubMed]
39. Deole, R.; Challacombe, J.; Raiford, D.W.; Hoff, W.D. An extremely halophilic proteobacterium combines a highly acidic proteome with a low cytoplasmic potassium content. *J. Biol. Chem.* **2013**, *288*, 581–588. [CrossRef] [PubMed]
40. Kokoeva, M.V.; Storch, K.F.; Klein, C.; Oesterhelt, D. A novel mode of sensory transduction in archaea: Binding protein-mediated chemotaxis towards osmoprotectants and amino acids. *EMBO J.* **2002**, *21*, 2312–2322. [CrossRef] [PubMed]
41. Becker, E.A.; Seitzer, P.M.; Tritt, A.; Larsen, D.; Krusor, M.; Yao, A.I.; Wu, D.; Madern, D.; Eisen, J.A.; Darling, A.E.; et al. Phylogenetically driven sequencing of extremely halophilic archaea reveals strategies for static and dynamic osmo-response. *PLoS Genet.* **2014**, *10*, e1004784. [CrossRef] [PubMed]
42. Lippert, K.; Galinski, E.A.; Truper, H.G. Biosynthesis and function of trehalose in *Ectothiorhodospira halochloris*. *Antonie Leeuwenhoek* **1993**, *63*, 85–91. [CrossRef] [PubMed]
43. Vaidya, S.; Dev, K.; Sourirajan, A. Distinct osmoadaptation strategies in the strict halophilic and halotolerant bacteria isolated from Lunsu salt water body of North West Himalayas. *Curr. Microbiol.* **2018**. [CrossRef] [PubMed]
44. Yancey, P.H.; Clark, M.E.; Hand, S.C.; Bowlus, R.D.; Somero, G.N. Living with water stress: Evolution of osmolyte systems. *Science* **1982**, *217*, 1214–1222. [CrossRef] [PubMed]
45. Burg, M.B.; Ferraris, J.D. Intracellular organic osmolytes: Function and regulation. *J. Biol. Chem.* **2008**, *283*, 7309–7313. [CrossRef] [PubMed]
46. Gunde-Cimerman, N.; Plemenitas, A.; Oren, A. Strategies of adaptation of microorganisms of the three domains of life to high-salt concentrations. *FEMS Microbiol. Rev.* **2018**, in press. [CrossRef] [PubMed]

47. Le Rudulier, D.; Strom, A.R.; Dandekar, A.M.; Smith, L.T.; Valentine, R.C. Molecular biology of osmoregulation. *Science* **1984**, *224*, 1064–1068. [CrossRef] [PubMed]
48. Brown, A.D. Microbial water stress. *Bacteriol. Rev.* **1976**, *40*, 803–846. [PubMed]
49. Gilles, R. "Compensatory" organic osmolytes in high osmolarity and dehydration stresses: History and perspectives. *Comp. Biochem. Physiol. A Physiol.* **1997**, *117*, 279–290. [CrossRef]
50. Yancey, P.H. Organic osmolytes as compatible, metabolic and counteracting cytoprotectants in high osmolarity and other stresses. *J. Exp. Biol.* **2005**, *208*, 2819–2830. [CrossRef] [PubMed]
51. Holtmann, G.; Bremer, E. Thermoprotection of *Bacillus subtilis* by exogenously provided glycine betaine and structurally related compatible solutes: Involvement of opu transporters. *J. Bacteriol.* **2004**, *186*, 1683–1693. [CrossRef] [PubMed]
52. Hoffmann, T.; Bremer, E. Protection of *Bacillus subtilis* against cold stress via compatible-solute acquisition. *J. Bacteriol.* **2011**, *193*, 1552–1562. [CrossRef] [PubMed]
53. Caldas, T.; Demont-Caulet, N.; Ghazi, A.; Richarme, G. Thermoprotection by glycine betaine and choline. *Microbiology* **1999**, *145*, 2543–2548. [CrossRef] [PubMed]
54. Diamant, S.; Eliahu, N.; Rosenthal, D.; Goloubinoff, P. Chemical chaperones regulate molecular chaperones in vitro and in cells under combined salt and heat stresses. *J. Biol. Chem.* **2001**, *276*, 39586–39591. [CrossRef] [PubMed]
55. Da Costa, M.S.; Santos, H.; Galinski, E.A. An overview of the role and diversity of compatible solutes in *Bacteria* and *Archaea*. *Adv. Biochem. Eng. Biotechnol.* **1998**, *61*, 117–153. [PubMed]
56. Martins, L.O.; Huber, R.; Huber, H.; Stetter, K.O.; da Costa, M.S.; Santos, H. Organic solutes in hyperthermophilic archaea. *Appl. Environ. Microbiol.* **1997**, *63*, 896–902. [PubMed]
57. Santos, H.; da Costa, M.S. Compatible solutes of organisms that live in hot saline environments. *Environ. Microbiol.* **2002**, *4*, 501–509. [CrossRef] [PubMed]
58. Yancey, P.H. Compatible and counteracting solutes: Protecting cells from the Dead Sea to the deep sea. *Sci. Prog.* **2004**, *87*, 1–24. [CrossRef] [PubMed]
59. Arakawa, T.; Timasheff, S.N. The stabilization of proteins by osmolytes. *Biophys. J.* **1985**, *47*, 411–414. [CrossRef]
60. Auton, M.; Rösgen, J.; Sinev, M.; Holthauzen, L.M.; Bolen, D.W. Osmolyte effects on protein stability and solubility: A balancing act between backbone and side-chains. *Biophys. Chem.* **2011**, *159*, 90–99. [CrossRef] [PubMed]
61. Bolen, D.W.; Baskakov, I.V. The osmophobic effect: Natural selection of a thermodynamic force in protein folding. *J. Mol. Biol.* **2001**, *310*, 955–963. [CrossRef] [PubMed]
62. Street, T.O.; Bolen, D.W.; Rose, G.D. A molecular mechanism for osmolyte-induced protein stability. *Proc. Natl. Acad. Sci. USA* **2006**, *103*, 13997–14002. [CrossRef] [PubMed]
63. Bourot, S.; Sire, O.; Trautwetter, A.; Touze, T.; Wu, L.F.; Blanco, C.; Bernard, T. Glycine betaine-assisted protein folding in a *lysA* mutant of *Escherichia coli*. *J. Biol. Chem.* **2000**, *275*, 1050–1056. [CrossRef] [PubMed]
64. Ignatova, Z.; Gierasch, L.M. Inhibition of protein aggregation in vitro and in vivo by a natural osmoprotectant. *Proc. Natl. Acad. Sci. USA* **2006**, *103*, 13357–13361. [CrossRef] [PubMed]
65. Stadmiller, S.S.; Gorensek-Benitez, A.H.; Guseman, A.J.; Pielak, G.J. Osmotic shock induced protein destabilization in living cells and its reversal by glycine betaine. *J. Mol. Biol.* **2017**, *429*, 1155–1161. [CrossRef] [PubMed]
66. Harishchandra, R.K.; Wulff, S.; Lentzen, G.; Neuhaus, T.; Galla, H.J. The effect of compatible solute ectoines on the structural organization of lipid monolayer and bilayer membranes. *Biophys. Chem.* **2010**, *150*, 37–46. [CrossRef] [PubMed]
67. Smiatek, J.; Harishchandra, R.K.; Galla, H.J.; Heuer, A. Low concentrated hydroxyectoine solutions in presence of DPPC lipid bilayers: A computer simulation study. *Biophys. Chem.* **2013**, *180–181*, 102–109. [CrossRef] [PubMed]
68. Record, M.T., Jr.; Courtenay, E.S.; Cayley, S.; Guttman, H.J. Biophysical compensation mechanisms buffering *E. coli* protein-nucleic acid interactions against changing environments. *Trends Biochem. Sci.* **1998**, *23*, 190–194. [CrossRef]
69. Record, M.T., Jr.; Courtenay, E.S.; Cayley, D.S.; Guttman, H.J. Responses of *E. coli* to osmotic stress: Large changes in amounts of cytoplasmic solutes and water. *Trends Biochem. Sci.* **1998**, *23*, 143–148. [CrossRef]

70. Tatzelt, J.; Prusiner, S.B.; Welch, W.J. Chemical chaperones interfere with the formation of scrapie prion protein. *EMBO J.* **1996**, *15*, 6363–6373. [PubMed]
71. Kolp, S.; Pietsch, M.; Galinski, E.A.; Gutschow, M. Compatible solutes as protectants for zymogens against proteolysis. *Biochim. Biophys. Acta* **2006**, *1764*, 1234–1242. [CrossRef] [PubMed]
72. Lippert, K.; Galinski, E.A. Enzyme stabilization by ectoine-type compatible solutes: Protection against heating, freezing and drying. *Appl. Micro Biotechnol.* **1992**, *37*, 61–65. [CrossRef]
73. Knapp, S.; Ladenstein, R.; Galinski, E.A. Extrinsic protein stabilization by the naturally occurring osmolytes beta-hydroxyectoine and betaine. *Extremophiles* **1999**, *3*, 191–198. [CrossRef] [PubMed]
74. Manzanera, M.; Garcia de Castro, A.; Tondervik, A.; Rayner-Brandes, M.; Strom, A.R.; Tunnacliffe, A. Hydroxyectoine is superior to trehalose for anhydrobiotic engineering of *Pseudomonas putida* KT2440. *Appl. Environ. Microbiol.* **2002**, *68*, 4328–4333. [CrossRef] [PubMed]
75. Manzanera, M.; Vilchez, S.; Tunnacliffe, A. High survival and stability rates of *Escherichia coli* dried in hydroxyectoine. *FEMS Microbiol. Lett.* **2004**, *233*, 347–352. [CrossRef] [PubMed]
76. Chattopadhyay, M.K.; Kern, R.; Mistou, M.Y.; Dandekar, A.M.; Uratsu, S.L.; Richarme, G. The chemical chaperone proline relieves the thermosensitivity of a *dnaK* deletion mutant at 42 °C. *J. Bacteriol.* **2004**, *186*, 8149–8152. [CrossRef] [PubMed]
77. Kuhlmann, A.U.; Bursy, J.; Gimpel, S.; Hoffmann, T.; Bremer, E. Synthesis of the compatible solute ectoine in *Virgibacillus pantothenticus* is triggered by high salinity and low growth temperature. *Appl. Environ. Microbiol.* **2008**, *74*, 4560–4563. [CrossRef] [PubMed]
78. Kuhlmann, A.U.; Hoffmann, T.; Bursy, J.; Jebbar, M.; Bremer, E. Ectoine and hydroxyectoine as protectants against osmotic and cold stress: Uptake through the SigB-controlled betaine-choline- carnitine transporter-type carrier EctT from *Virgibacillus pantothenticus*. *J. Bacteriol.* **2011**, *193*, 4699–4708. [CrossRef] [PubMed]
79. Bursy, J.; Kuhlmann, A.U.; Pittelkow, M.; Hartmann, H.; Jebbar, M.; Pierik, A.J.; Bremer, E. Synthesis and uptake of the compatible solutes ectoine and 5-hydroxyectoine by *Streptomyces coelicolor* A3(2) in response to salt and heat stresses. *Appl. Environ. Microbiol.* **2008**, *74*, 7286–7296. [CrossRef] [PubMed]
80. Vargas, C.; Argandona, M.; Reina-Bueno, M.; Rodriguez-Moya, J.; Fernandez-Aunion, C.; Nieto, J.J. Unravelling the adaptation responses to osmotic and temperature stress in *Chromohalobacter salexigens*, a bacterium with broad salinity tolerance. *Saline Syst.* **2008**, *4*, 14. [CrossRef] [PubMed]
81. Malin, G.; Lapidot, A. Induction of synthesis of tetrahydropyrimidine derivatives in *Streptomyces* strains and their effect on *Escherichia coli* in response to osmotic and heat stress. *J. Bacteriol.* **1996**, *178*, 385–395. [CrossRef] [PubMed]
82. Tschapek, B.; Pittelkow, M.; Sohn-Bosser, L.; Holtmann, G.; Smits, S.H.; Gohlke, H.; Bremer, E.; Schmitt, L. Arg149 is involved in switching the low affinity, open state of the binding protein *Af* ProX into its high affinity, closed state. *J. Mol. Biol.* **2011**, *411*, 36–52. [CrossRef] [PubMed]
83. Lamosa, P.; Burke, A.; Peist, R.; Huber, R.; Liu, M.Y.; Silva, G.; Rodrigues-Pousada, C.; LeGall, J.; Maycock, C.; Santos, H. Thermostabilization of proteins by diglycerol phosphate, a new compatible solute from the hyperthermophile *Archaeoglobus fulgidus*. *Appl. Environ. Microbiol.* **2000**, *66*, 1974–1979. [CrossRef] [PubMed]
84. Hoffmann, T.; Bremer, E. Management of osmotic stress by *Bacillus subtilis*: Genetics and physiology. In *Stress and Environmental Regulation of Gene Expression and Adaptation in Bacteria*; de Bruijn, F.J., Ed.; Wiley-Blackwell Publishers: Hoboken, NJ, USA, 2016; Volume 1, pp. 657–676.
85. Hoffmann, T.; Bremer, E. Guardians in a stressful world: The Opu family of compatible solute transporters from *Bacillus subtilis*. *Biol. Chem.* **2017**, *398*, 193–214. [CrossRef] [PubMed]
86. Lentzen, G.; Schwarz, T. Extremolytes: Natural compounds from extremophiles for versatile applications. *Appl. Microbiol. Biotechnol.* **2006**, *72*, 623–634. [CrossRef] [PubMed]
87. Roberts, M.F. Osmoadaptation and osmoregulation in archaea: Update 2004. *Front. BioSci.* **2004**, *9*, 1999–2019. [CrossRef] [PubMed]
88. Galinski, E.A.; Pfeiffer, H.P.; Trüper, H.G. 1,4,5,6-tetrahydro-2-methyl-4-pyrimidinecarboxylic acid. A novel cyclic amino acid from halophilic phototrophic bacteria of the genus *Ectothiorhodospira*. *Eur. J. Biochem.* **1985**, *149*, 135–139. [CrossRef] [PubMed]
89. Inbar, L.; Lapidot, A. The structure and biosynthesis of new tetrahydropyrimidine derivatives in actinomycin D producer *Streptomyces parvulus*. Use of ^{13}C- and ^{15}N-labeled L-glutamate and ^{13}C and ^{15}N NMR spectroscopy. *J. Biol. Chem.* **1988**, *263*, 16014–16022. [PubMed]

90. Inbar, L.; Frolow, F.; Lapidot, A. The conformation of new tetrahydropyrimidine derivatives in solution and in the crystal. *Eur. J. Biochem.* **1993**, *214*, 897–906. [CrossRef] [PubMed]
91. Pastor, J.M.; Salvador, M.; Argandona, M.; Bernal, V.; Reina-Bueno, M.; Csonka, L.N.; Iborra, J.L.; Vargas, C.; Nieto, J.J.; Canovas, M. Ectoines in cell stress protection: Uses and biotechnological production. *Biotechnol. Adv.* **2010**, *28*, 782–801. [CrossRef] [PubMed]
92. Widderich, N.; Czech, L.; Elling, F.J.; Könneke, M.; Stöveken, N.; Pittelkow, M.; Riclea, R.; Dickschat, J.S.; Heider, J.; Bremer, E. Strangers in the archaeal world: Osmostress-responsive biosynthesis of ectoine and hydroxyectoine by the marine thaumarchaeon *Nitrosopumilus maritimus*. *Environ. Microbiol.* **2016**, *18*, 1227–1248. [CrossRef] [PubMed]
93. Widderich, N.; Höppner, A.; Pittelkow, M.; Heider, J.; Smits, S.H.; Bremer, E. Biochemical properties of ectoine hydroxylases from extremophiles and their wider taxonomic distribution among microorganisms. *PLoS ONE* **2014**, *9*, e93809. [CrossRef] [PubMed]
94. Kunte, H.J.; Lentzen, G.; Galinski, E. Industrial production of the cell protectant ectoine: Protection, mechanisms, processes, and products. *Curr. Biotechnol.* **2014**, *3*, 10–25. [CrossRef]
95. Louis, P.; Galinski, E.A. Characterization of genes for the biosynthesis of the compatible solute ectoine from *Marinococcus halophilus* and osmoregulated expression in *Escherichia coli*. *Microbiology* **1997**, *143*, 1141–1149. [CrossRef] [PubMed]
96. Prabhu, J.; Schauwecker, F.; Grammel, N.; Keller, U.; Bernhard, M. Functional expression of the ectoine hydroxylase gene (*thpD*) from *Streptomyces chrysomallus* in *Halomonas elongata*. *Appl. Environ. Microbiol.* **2004**, *70*, 3130–3132. [CrossRef] [PubMed]
97. Garcia-Estepa, R.; Argandona, M.; Reina-Bueno, M.; Capote, N.; Iglesias-Guerra, F.; Nieto, J.J.; Vargas, C. The *ectD* gene, which is involved in the synthesis of the compatible solute hydroxyectoine, is essential for thermoprotection of the halophilic bacterium *Chromohalobacter salexigens*. *J. Bacteriol.* **2006**, *188*, 3774–3784. [CrossRef] [PubMed]
98. Bursy, J.; Pierik, A.J.; Pica, N.; Bremer, E. Osmotically induced synthesis of the compatible solute hydroxyectoine is mediated by an evolutionarily conserved ectoine hydroxylase. *J. Biol. Chem.* **2007**, *282*, 31147–31155. [CrossRef] [PubMed]
99. Reshetnikov, A.S.; Khmelenina, V.N.; Mustakhimov, I.I.; Kalyuzhnaya, M.; Lidstrom, M.; Trotsenko, Y.A. Diversity and phylogeny of the ectoine biosynthesis genes in aerobic, moderately halophilic methylotrophic bacteria. *Extremophiles* **2011**, *15*, 653–663. [CrossRef] [PubMed]
100. Harding, T.; Roger, A.J.; Simpson, A.G.B. Adaptations to high salt in a halophilic protist: Differential expression and gene acquisitions through duplications and gene transfers. *Front. Microbiol.* **2017**, *8*, 944. [CrossRef] [PubMed]
101. Harding, T.; Brown, M.W.; Simpson, A.G.; Roger, A.J. Osmoadaptative strategy and its molecular signature in obligately halophilic heterotrophic protists. *Genome Biol. Evol.* **2016**, *8*, 2241–2258. [CrossRef] [PubMed]
102. Weinisch, L.; Kuhner, S.; Roth, R.; Grimm, M.; Roth, T.; Netz, D.J.A.; Pierik, A.J.; Filker, S. Identification of osmoadaptive strategies in the halophile, heterotrophic ciliate *Schmidingerothrix salinarum*. *PLoS Biol.* **2018**, *16*, e2003892. [CrossRef] [PubMed]
103. Harding, T.; Simpson, A.G.B. Recent advances in halophilic protozoa research. *J. Eukaryot. Microbiol.* **2018**. [CrossRef] [PubMed]
104. Czech, L.; Bremer, E. With a pinch of extra salt—Did predatory protists steal genes from their food? *PLoS Biol.* **2018**, *16*, e2005163. [CrossRef] [PubMed]
105. Zaccai, G.; Bagyan, I.; Combet, J.; Cuello, G.J.; Deme, B.; Fichou, Y.; Gallat, F.X.; Galvan Josa, V.M.; von Gronau, S.; Haertlein, M.; et al. Neutrons describe ectoine effects on water H-bonding and hydration around a soluble protein and a cell membrane. *Sci. Rep.* **2016**, *6*, 31434. [CrossRef] [PubMed]
106. Dötsch, A.; Severin, J.; Alt, W.; Galinski, E.A.; Kreft, J.U. A mathematical model for growth and osmoregulation in halophilic bacteria. *Microbiology* **2008**, *154*, 2956–2969. [CrossRef] [PubMed]
107. Held, C.; Neuhaus, T.; Sadowski, G. Compatible solutes: Thermodynamic properties and biological impact of ectoines and prolines. *Biophys. Chem.* **2010**, *152*, 28–39. [CrossRef] [PubMed]
108. Eiberweiser, A.; Nazet, A.; Kruchinin, S.E.; Fedotova, M.V.; Buchner, R. Hydration and ion binding of the osmolyte ectoine. *J. Phys. Chem. B* **2015**, *119*, 15203–15211. [CrossRef] [PubMed]

109. Hahn, M.B.; Solomun, T.; Wellhausen, R.; Hermann, S.; Seitz, H.; Meyer, S.; Kunte, H.J.; Zeman, J.; Uhlig, F.; Smiatek, J.; et al. Influence of the compatible solute ectoine on the local water structure: Implications for the binding of the protein G5P to DNA. *J. Phys. Chem. B* **2015**, *119*, 15212–15220. [CrossRef] [PubMed]
110. Smiatek, J. Osmolyte effects: Impact on the aqueous solution around charged and neutral spheres. *J. Phys. Chem. B* **2014**, *118*, 771–782. [CrossRef] [PubMed]
111. Smiatek, J.; Harishchandra, R.K.; Rubner, O.; Galla, H.J.; Heuer, A. Properties of compatible solutes in aqueous solution. *Biophys. Chem.* **2012**, *160*, 62–68. [CrossRef] [PubMed]
112. Malin, G.; Iakobashvili, R.; Lapidot, A. Effect of tetrahydropyrimidine derivatives on protein-nucleic acids interaction. Type II restriction endonucleases as a model system. *J. Biol. Chem.* **1999**, *274*, 6920–6929. [CrossRef] [PubMed]
113. Lapidot, A.; Ben-Asher, E.; Eisenstein, M. Tetrahydropyrimidine derivatives inhibit binding of a Tat-like, arginine-containing peptide, to HIV TAR RNA in vitro. *FEBS Lett.* **1995**, *367*, 33–38. [CrossRef]
114. Kurz, M. Compatible solute influence on nucleic acids: Many questions but few answers. *Saline Syst.* **2008**, *4*, 6. [CrossRef] [PubMed]
115. Barth, S.; Huhn, M.; Matthey, B.; Klimka, A.; Galinski, E.A.; Engert, A. Compatible-solute-supported periplasmic expression of functional recombinant proteins under stress conditions. *Appl. Environ. Microbiol.* **2000**, *66*, 1572–1579. [CrossRef] [PubMed]
116. Czech, L.; Poehl, S.; Hub, P.; Stoeveken, N.; Bremer, E. Tinkering with osmotically controlled transcription allows enhanced production and excretion of ectoine and hydroxyectoine from a microbial cell factory. *Appl. Environ. Microbiol.* **2108**, *84*, e01772-17. [CrossRef] [PubMed]
117. Kuhlmann, A.U.; Bremer, E. Osmotically regulated synthesis of the compatible solute ectoine in *Bacillus pasteurii* and related *Bacillus* spp. *Appl. Environ. Microbiol.* **2002**, *68*, 772–783. [CrossRef] [PubMed]
118. Calderon, M.I.; Vargas, C.; Rojo, F.; Iglesias-Guerra, F.; Csonka, L.N.; Ventosa, A.; Nieto, J.J. Complex regulation of the synthesis of the compatible solute ectoine in the halophilic bacterium *Chromohalobacter salexigens* DSM 3043T. *Microbiology* **2004**, *150*, 3051–3063. [CrossRef] [PubMed]
119. Göller, K.; Ofer, A.; Galinski, E.A. Construction and characterization of an NaCl sensitive mutant of *Halomonas elongata* impaired in ectoine biosynthesis. *FEMS Microbiol. Lett.* **1998**, *161*, 293–300. [CrossRef]
120. Canovas, D.; Vargas, C.; Iglesias-Guerra, F.; Csonka, L.N.; Rhodes, D.; Ventosa, A.; Nieto, J.J. Isolation and characterization of salt-sensitive mutants of the moderate halophile *Halomonas elongata* and cloning of the ectoine synthesis genes. *J. Biol. Chem.* **1997**, *272*, 25794–25801. [CrossRef] [PubMed]
121. Ma, Y.; Wang, Q.; Xu, W.; Liu, X.; Gao, X.; Zhang, Y. Stationary phase-dependent accumulation of ectoine is an efficient adaptation strategy in *Vibrio anguillarum* against cold stress. *Microbiol. Res.* **2017**, *205*, 8–18. [CrossRef] [PubMed]
122. Stöveken, N.; Pittelkow, M.; Sinner, T.; Jensen, R.A.; Heider, J.; Bremer, E. A specialized aspartokinase enhances the biosynthesis of the osmoprotectants ectoine and hydroxyectoine in *Pseudomonas stutzeri* A1501. *J. Bacteriol.* **2011**, *193*, 4456–4468. [CrossRef] [PubMed]
123. Seip, B.; Galinski, E.A.; Kurz, M. Natural and engineered hydroxyectoine production based on the *Pseudomonas stutzeri ectABCD-ask* gene cluster. *Appl. Environ. Microbiol.* **2011**, *77*, 1368–1374. [CrossRef] [PubMed]
124. Saum, S.H.; Müller, V. Salinity-dependent switching of osmolyte strategies in a moderately halophilic bacterium: Glutamate induces proline biosynthesis in *Halobacillus halophilus*. *J. Bacteriol.* **2007**, *189*, 6968–6975. [CrossRef] [PubMed]
125. Saum, S.H.; Müller, V. Regulation of osmoadaptation in the moderate halophile *Halobacillus halophilus*: Chloride, glutamate and switching osmolyte strategies. *Saline Syst.* **2008**, *4*, 4. [CrossRef] [PubMed]
126. Cheng, X.; Guinn, E.J.; Buechel, E.; Wong, R.; Sengupta, R.; Shkel, I.A.; Record, M.T. Basis of protein stabilization by K glutamate: Unfavorable interactions with carbon, oxygen groups. *Biophys. J.* **2016**, *111*, 1854–1865. [CrossRef] [PubMed]
127. Diehl, R.C.; Guinn, E.J.; Capp, M.W.; Tsodikov, O.V.; Record, M.T., Jr. Quantifying additive interactions of the osmolyte proline with individual functional groups of proteins: Comparisons with urea and glycine betaine, interpretation of *m*-values. *Biochemistry* **2013**, *52*, 5997–6010. [CrossRef] [PubMed]
128. Cayley, S.; Lewis, B.A.; Record, M.T., Jr. Origins of the osmoprotective properties of betaine and proline in *Escherichia coli* K-12. *J. Bacteriol.* **1992**, *174*, 1586–1595. [CrossRef] [PubMed]

129. Tao, P.; Li, H.; Yu, Y.; Gu, J.; Liu, Y. Ectoine and 5-hydroxyectoine accumulation in the halophile *Virgibacillus halodenitrificans* PDB-F2 in response to salt stress. *Appl. Microbiol. Biotechnol.* **2016**, *100*, 6779–6789. [CrossRef] [PubMed]
130. Klauck, E.; Typas, A.; Hengge, R. The sigmaS subunit of RNA polymerase as a signal integrator and network master regulator in the general stress response in *Escherichia coli*. *Sci. Prog.* **2007**, *90*, 103–127. [PubMed]
131. Hengge-Aronis, R. Back to log phase: Sigma S as a global regulator in the osmotic control of gene expression in *escherichia coli*. *Mol. Microbiol.* **1996**, *21*, 887–893. [CrossRef] [PubMed]
132. Tanne, C.; Golovina, E.A.; Hoekstra, F.A.; Meffert, A.; Galinski, E.A. Glass-forming property of hydroxyectoine is the cause of its superior function as a dessication protectant. *Front. Microbiol.* **2014**, *5*, 150. [CrossRef] [PubMed]
133. Borges, N.; Ramos, A.; Raven, N.D.; Sharp, R.J.; Santos, H. Comparative study of the thermostabilizing properties of mannosylglycerate and other compatible solutes on model enzymes. *Extremophiles* **2002**, *6*, 209–216. [CrossRef] [PubMed]
134. Van-Thuoc, D.; Hashim, S.O.; Hatti-Kaul, R.; Mamo, G. Ectoine-mediated protection of enzyme from the effect of pH and temperature stress: A study using *Bacillus halodurans* xylanase as a model. *Appl. Microbiol. Biotechnol.* **2013**, *97*, 6271–6278. [CrossRef] [PubMed]
135. Argandona, M.; Nieto, J.J.; Iglesias-Guerra, F.; Calderon, M.I.; Garcia-Estepa, R.; Vargas, C. Interplay between iron homeostasis and the osmotic stress response in the halophilic bacterium *Chromohalobacter salexigens*. *Appl. Environ. Microbiol.* **2010**, *76*, 3575–3589. [CrossRef] [PubMed]
136. Scoma, A.; Boon, N. Osmotic stress confers enhanced cell integrity to hydrostatic pressure but impairs growth in *Alcanivorax borkumensis* SK2. *Front. Microbiol.* **2016**, *7*, 729. [CrossRef] [PubMed]
137. Kish, A.; Griffin, P.L.; Rogers, K.L.; Fogel, M.L.; Hemley, R.J.; Steele, A. High-pressure tolerance in *Halobacterium salinarum* NCR-1 and other non-piezophilic prokaryotes. *Extremophiles* **2012**, *16*, 355–361. [CrossRef] [PubMed]
138. Schröter, M.A.; Meyer, S.; Hahn, M.B.; Solomun, T.; Sturm, H.; Kunte, H.J. Ectoine protects DNA from damage by ionizing radiation. *Sci. Rep.* **2017**, *7*, 15272. [CrossRef] [PubMed]
139. Hahn, M.B.; Meyer, S.; Schröter, M.A.; Kunte, H.J.; Solomun, T.; Sturm, H. DNA protection by ectoine from ionizing radiation: Molecular mechanisms. *Phys. Chem. Chem. Phys.* **2017**, *19*, 25717–25722. [CrossRef] [PubMed]
140. Meyer, S.; Schröter, M.A.; Hahn, M.B.; Solomun, T.; Sturm, H.; Kunte, H.J. Ectoine can enhance structural changes in DNA in vitro. *Sci. Rep.* **2017**, *7*, 7170. [CrossRef] [PubMed]
141. Buenger, J.; Driller, H. Ectoine: An effective natural substance to prevent UVA-induced premature photoaging. *Skin Pharmacol. Physiol.* **2004**, *17*, 232–237. [CrossRef] [PubMed]
142. Bünger, J.; Degwert, J.; Driller, H. The protective function of compatible solute ectoine on skin cells and its biomolecules with respect to uv-radiation, immunosuppression and membrane damage. *IFSCC Mag.* **2001**, *4*, 1–6.
143. Schnoor, M.; Voss, P.; Cullen, P.; Boking, T.; Galla, H.J.; Galinski, E.A.; Lorkowski, S. Characterization of the synthetic compatible solute homoectoine as a potent PCR enhancer. *Biochem. Biophys. Res. Commun.* **2004**, *322*, 867–872. [CrossRef] [PubMed]
144. Wedeking, A.; Hagen-Euteneuer, N.; Gurgui, M.; Broere, R.; Lentzen, G.; Tolba, R.H.; Galinski, E.; van Echten-Deckert, G. A lipid anchor improves the protective effect of ectoine in inflammation. *Curr. Med. Chem.* **2014**, *21*, 2565–2572. [CrossRef] [PubMed]
145. Graf, R.; Anzali, S.; Buenger, J.; Pfluecker, F.; Driller, H. The multifunctional role of ectoine as a natural cell protectant. *Clin. Dermatol.* **2008**, *26*, 326–333. [CrossRef] [PubMed]
146. Jorge, C.D.; Borges, N.; Bagyan, I.; Bilstein, A.; Santos, H. Potential applications of stress solutes from extremophiles in protein folding diseases and healthcare. *Extremophiles* **2016**, *20*, 251–259. [CrossRef] [PubMed]
147. Bownik, A.; Stepniewska, Z. Ectoine as a promising protective agent in humans and animals. *Arch. Ind. Hig. Toksikol.* **2016**, *67*, 260–265. [CrossRef] [PubMed]
148. Strong, P.J.; Kalyuzhnaya, M.; Silverman, J.; Clarke, W.P. A methanotroph-based biorefinery: Potential scenarios for generating multiple products from a single fermentation. *Bioresour. Technol.* **2016**, *215*, 314–323. [CrossRef] [PubMed]

149. Cantera, S.; Munoz, R.; Lebrero, R.; Lopez, J.C.; Rodriguez, Y.; Garcia-Encina, P.A. Technologies for the bioconversion of methane into more valuable products. *Curr. Opin. Biotechnol.* **2018**, *50*, 128–135. [CrossRef] [PubMed]
150. Vyrides, I.; Stuckey, D.C. Compatible solute addition to biological systems treating waste/wastewater to counteract osmotic and other environmental stresses: A review. *Crit. Rev. Biotechnol.* **2017**, *37*, 865–879. [CrossRef] [PubMed]
151. Czech, L.; Stöveken, N.; Bremer, E. EctD-mediated biotransformation of the chemical chaperone ectoine into hydroxyectoine and its mechanosensitive channel-independent excretion. *Microb. Cell Fact.* **2016**, *15*, 126. [CrossRef] [PubMed]
152. Becker, J.; Schafer, R.; Kohlstedt, M.; Harder, B.J.; Borchert, N.S.; Stöveken, N.; Bremer, E.; Wittmann, C. Systems metabolic engineering of *Corynebacterium glutamicum* for production of the chemical chaperone ectoine. *Microb. Cell Fact.* **2013**, *12*, 110. [CrossRef] [PubMed]
153. Ning, Y.; Wu, X.; Zhang, C.; Xu, Q.; Chen, N.; Xie, X. Pathway construction and metabolic engineering for fermentative production of ectoine in *Escherichia coli*. *Metabol. Eng.* **2016**, *36*, 10–18. [CrossRef] [PubMed]
154. Rodriguez-Moya, J.; Argandona, M.; Iglesias-Guerra, F.; Nieto, J.J.; Vargas, C. Temperature- and salinity-decoupled overproduction of hydroxyectoine by *Chromohalobacter salexigens*. *Appl. Environ. Microbiol.* **2013**, *79*, 1018–1023. [CrossRef] [PubMed]
155. Perez-Garcia, F.; Ziert, C.; Risse, J.M.; Wendisch, V.F. Improved fermentative production of the compatible solute ectoine by *Corynebacterium glutamicum* from glucose and alternative carbon sources. *J. Biotechnol.* **2017**, *258*, 59–69. [CrossRef] [PubMed]
156. Chen, W.; Zhang, S.; Jiang, P.X.; Yao, J.; He, Y.Z.; Chen, L.C.; Gui, X.W.; Dong, Z.Y.; Tang, S.Y. Design of an ectoine-responsive arac mutant and its application in metabolic engineering of ectoine biosynthesis. *Metabol. Eng.* **2015**, *30*, 149–155. [CrossRef] [PubMed]
157. Chen, W.C.; Hsu, C.C.; Lan, J.C.; Chang, Y.K.; Wang, L.F.; Wei, Y.H. Production and characterization of ectoine using a moderately halophilic strain *Halomonas salina* BCRC17875. *J. BioSci. Bioeng.* **2018**. [CrossRef] [PubMed]
158. Schwibbert, K.; Marin-Sanguino, A.; Bagyan, I.; Heidrich, G.; Lentzen, G.; Seitz, H.; Rampp, M.; Schuster, S.C.; Klenk, H.P.; Pfeiffer, F.; et al. A blueprint of ectoine metabolism from the genome of the industrial producer *Halomonas elongata* DSM 2581T. *Environ. Microbiol.* **2011**, *13*, 1973–1994. [CrossRef] [PubMed]
159. Sauer, T.; Galinski, E.A. Bacterial milking: A novel bioprocess for production of compatible solutes. *Biotechnol. Bioeng.* **1998**, *57*, 306–313. [CrossRef]
160. Rosa, L.T.; Bianconi, M.E.; Thomas, G.H.; Kelly, D.J. Tripartite ATP-independent periplasmic (TRAP) tansporters and tripartite tricarboxylate transporters (TTT): From uptake to pathogenicity. *Front. Cell. Infect. Microbiol.* **2018**, *8*, 33. [CrossRef] [PubMed]
161. Grammann, K.; Volke, A.; Kunte, H.J. New type of osmoregulated solute transporter identified in halophilic members of the bacteria domain: TRAP transporter TeaABC mediates uptake of ectoine and hydroxyectoine in *Halomonas elongata* DSM 2581(T). *J. Bacteriol.* **2002**, *184*, 3078–3085. [CrossRef] [PubMed]
162. Cyplik, P.; Piotrowska-Cyplik, A.; Marecik, R.; Czarny, J.; Drozdzynska, A.; Chrzanowski, L. Biological denitrification of brine: The effect of compatible solutes on enzyme activities and fatty acid degradation. *Biodegradation* **2012**, *23*, 663–672. [CrossRef] [PubMed]
163. Liu, M.; Peng, Y.; Wang, S.; Liu, T.; Xiao, H. Enhancement of anammox activity by addition of compatible solutes at high salinity conditions. *Bioresour. Technol.* **2014**, *167*, 560–563. [CrossRef] [PubMed]
164. Peters, P.; Galinski, E.A.; Trüper, H.G. The biosyntheis of ectoine. *FEMS Microbiol. Lett.* **1990**, *71*, 157–162. [CrossRef]
165. Ono, H.; Sawada, K.; Khunajakr, N.; Tao, T.; Yamamoto, M.; Hiramoto, M.; Shinmyo, A.; Takano, M.; Murooka, Y. Characterization of biosynthetic enzymes for ectoine as a compatible solute in a moderately halophilic eubacterium, *Halomonas elongata*. *J. Bacteriol.* **1999**, *181*, 91–99. [PubMed]
166. Reshetnikov, A.S.; Khmelenina, V.N.; Mustakhimov, I.I.; Trotsenko, Y.A. Genes and enzymes of ectoine biosynthesis in halotolerant methanotrophs. *Methods Enzymol.* **2011**, *495*, 15–30. [PubMed]
167. Lo, C.C.; Bonner, C.A.; Xie, G.; D'Souza, M.; Jensen, R.A. Cohesion group approach for evolutionary analysis of aspartokinase, an enzyme that feeds a branched network of many biochemical pathways. *Microbiol. Mol. Biol. Rev.* **2009**, *73*, 594–651. [CrossRef] [PubMed]

168. Reshetnikov, A.S.; Khmelenina, V.N.; Trotsenko, Y.A. Characterization of the ectoine biosynthesis genes of haloalkalotolerant obligate methanotroph "*Methylomicrobium alcaliphilum* 20z". *Arch. Microbiol.* **2006**, *184*, 286–297. [CrossRef] [PubMed]
169. Nyyssölä, A.; Kerovuo, J.; Kaukinen, P.; von Weymarn, N.; Reinikainen, T. Extreme halophiles synthesize betaine from glycine by methylation. *J. Biol. Chem.* **2000**, *275*, 22196–22201. [CrossRef] [PubMed]
170. Boch, J.; Kempf, B.; Schmid, R.; Bremer, E. Synthesis of the osmoprotectant glycine betaine in *Bacillus subtilis*: Characterization of the *gbsAB* genes. *J. Bacteriol.* **1996**, *178*, 5121–5129. [CrossRef] [PubMed]
171. Lamark, T.; Kaasen, I.; Eshoo, M.W.; Falkenberg, P.; McDougall, J.; Strom, A.R. DNA sequence and analysis of the *bet* genes encoding the osmoregulatory choline-glycine betaine pathway of *Escherichia coli*. *Mol. Microbiol.* **1991**, *5*, 1049–1064. [CrossRef] [PubMed]
172. Salvi, F.; Wang, Y.F.; Weber, I.T.; Gadda, G. Structure of choline oxidase in complex with the reaction product glycine betaine. *Acta Crystallogr. D Biol. Crystallogr.* **2014**, *70*, 405–413. [CrossRef] [PubMed]
173. Oliveira, E.F.; Cerqueira, N.M.; Fernandes, P.A.; Ramos, M.J. Mechanism of formation of the internal aldimine in pyridoxal 5^{0}-phosphate-dependent enzymes. *J. Am. Chem. Soc.* **2011**, *133*, 15496–15505. [CrossRef] [PubMed]
174. Vetting, M.W.; de Carvalho, L.P.S.; Yu, M.; Hegde, S.S.; Magnet, S.; Roderick, S.L.; Blanchard, J.S. Structure and functions of the GNAT superfamily of acetyltransferases. *Arch. Biochem. Biophys.* **2005**, *433*, 212–226. [CrossRef] [PubMed]
175. Mustakhimov, I.I.; Rozova, O.N.; Reshetnikov, A.S.; Khmelenina, V.N.; Murrell, J.C.; Trotsenko, Y.A. Characterization of the recombinant diaminobutyric acid acetyltransferase from *Methylophaga thalassica* and *Methylophaga alcalica*. *FEMS Microbiol. Lett.* **2008**, *283*, 91–96. [CrossRef] [PubMed]
176. Widderich, N.; Kobus, S.; Höppner, A.; Ricela, R.; Seubert, A.; Dickschat, J.S.; Heider, J.; Smits, S.H.J.; Bremer, E. Biochemistry and crystal structure of the ectoine synthase: A metal-containing member of the cupin superfamily. *PLoS ONE* **2016**, *11*, e0151285. [CrossRef] [PubMed]
177. Höppner, A.; Widderich, N.; Lenders, M.; Bremer, E.; Smits, S.H.J. Crystal structure of the ectoine hydroxylase, a snapshot of the active site. *J. Biol. Chem.* **2014**, *289*, 29570–29583. [CrossRef] [PubMed]
178. Garcia-Estepa, R.; Canovas, D.; Iglesias-Guerra, F.; Ventosa, A.; Csonka, L.N.; Nieto, J.J.; Vargas, C. Osmoprotection of *Salmonella enterica* serovar Typhimurium by *N*-γ-acetyldiaminobutyrate, the precursor of the compatible solute ectoine. *Syst. Appl. Microbiol.* **2006**, *29*, 626–633. [CrossRef] [PubMed]
179. Canovas, D.; Borges, N.; Vargas, C.; Ventosa, A.; Nieto, J.J.; Santos, H. Role of *N*-γ-acetyldiaminobutyrate as an enzyme stabilizer and an intermediate in the biosynthesis of hydroxyectoine. *Appl. Environ. Microbiol.* **1999**, *65*, 3774–3779. [PubMed]
180. Moritz, K.D.; Amendt, B.; Witt, E.M.H.J.; Galinski, E.A. The hydroxyectoine gene cluster of the non-halophilic acidophile *Acidiphilium cryptum*. *Extremophiles* **2015**, *19*, 87–99. [CrossRef] [PubMed]
181. Witt, E.M.; Davies, N.W.; Galinski, E.A. Unexpected property of ectoine synthase and its application for synthesis of the engineered compatible solute ADPC. *Appl. Microbiol. Biotechnol.* **2011**, *91*, 113–122. [CrossRef] [PubMed]
182. Dunwell, J.M.; Purvis, A.; Khuri, S. Cupins: The most functionally diverse protein superfamily? *Phytochemistry* **2004**, *65*, 7–17. [CrossRef] [PubMed]
183. Dunwell, J.M.; Culham, A.; Carter, C.E.; Sosa-Aguirre, C.R.; Goodenough, P.W. Evolution of functional diversity in the cupin superfamily. *Trends Biochem. Sci.* **2001**, *26*, 740–746. [CrossRef]
184. Reuter, K.; Pittelkow, M.; Bursy, J.; Heine, A.; Craan, T.; Bremer, E. Synthesis of 5-hydroxyectoine from ectoine: Crystal structure of the non-heme iron(II) and 2-oxoglutarate-dependent dioxygenase EctD. *PLoS ONE* **2010**, *5*, e10647. [CrossRef] [PubMed]
185. Clifton, I.J.; McDonough, M.A.; Ehrismann, D.; Kershaw, N.J.; Granatino, N.; Schofield, C.J. Structural studies on 2-oxoglutarate oxygenases and related double-stranded beta-helix fold proteins. *J. Inorg. Biochem.* **2006**, *100*, 644–669. [CrossRef] [PubMed]
186. Widderich, N.; Pittelkow, M.; Hoppner, A.; Mulnaes, D.; Buckel, W.; Gohlke, H.; Smits, S.H.; Bremer, E. Molecular dynamics simulations and structure-guided mutagenesis provide insight into the architecture of the catalytic core of the ectoine hydroxylase. *J. Mol. Biol.* **2014**, *426*, 586–600. [CrossRef] [PubMed]
187. Jebbar, M.; Talibart, R.; Gloux, K.; Bernard, T.; Blanco, C. Osmoprotection of *Escherichia coli* by ectoine: Uptake and accumulation characteristics. *J. Bacteriol.* **1992**, *174*, 5027–5035. [CrossRef] [PubMed]

188. Lucht, J.M.; Bremer, E. Adaptation of *Escherichia coli* to high osmolarity environments: Osmoregulation of the high-affinity glycine betaine transport system ProU. *FEMS Microbiol. Rev.* **1994**, *14*, 3–20. [CrossRef] [PubMed]
189. MacMillan, S.V.; Alexander, D.A.; Culham, D.E.; Kunte, H.J.; Marshall, E.V.; Rochon, D.; Wood, J.M. The ion coupling and organic substrate specificities of osmoregulatory transporter ProP in *Escherichia coli*. *Biochim. Biophys. Acta* **1999**, *1420*, 30–44. [CrossRef]
190. Rodriguez-Moya, J.; Argandona, M.; Reina-Bueno, M.; Nieto, J.J.; Iglesias-Guerra, F.; Jebbar, M.; Vargas, C. Involvement of EupR, a response regulator of the NarL/FixJ family, in the control of the uptake of the compatible solutes ectoines by the halophilic bacterium *Chromohalobacter salexigens*. *BMC Microbiol.* **2010**, *10*, 256. [CrossRef] [PubMed]
191. Bestvater, T.; Louis, P.; Galinski, E.A. Heterologous ectoine production in *Escherichia coli:* By-passing the metabolic bottle-neck. *Saline Syst.* **2008**, *4*, 12. [CrossRef] [PubMed]
192. Kuraku, S.; Zmasek, C.M.; Nishimura, O.; Katoh, K. aLeaves facilitates on-demand exploration of metazoan gene family trees on MAFFT sequence alignment server with enhanced interactivity. *Nucleic Acids Res.* **2013**, *41*, W22–W28. [CrossRef] [PubMed]
193. Letunic, I.; Bork, P. Interactive tree of life (iTOL) v3: An online tool for the display and annotation of phylogenetic and other trees. *Nucleic Acids Res.* **2016**, *44*, W242–W245. [CrossRef] [PubMed]
194. Salar-Garcia, M.J.; Bernal, V.; Pastor, J.M.; Salvador, M.; Argandona, M.; Nieto, J.J.; Vargas, C.; Canovas, M. Understanding the interplay of carbon and nitrogen supply for ectoines production and metabolic overflow in high density cultures of *Chromohalobacter salexigens*. *Microb. Cell Fact.* **2017**, *16*, 23. [CrossRef] [PubMed]
195. Pastor, J.M.; Bernal, V.; Salvador, M.; Argandona, M.; Vargas, C.; Csonka, L.; Sevilla, A.; Iborra, J.L.; Nieto, J.J.; Canovas, M. Role of central metabolism in the osmoadaptation of the halophilic bacterium *Chromohalobacter salexigens*. *J. Biol. Chem.* **2013**, *288*, 17769–17781. [CrossRef] [PubMed]
196. Piubeli, F.; Salvador, M.; Argandona, M.; Nieto, J.J.; Bernal, V.; Pastor, J.M.; Canovas, M.; Vargas, C. Insights into metabolic osmoadaptation of the ectoines-producer bacterium *Chromohalobacter salexigens* through a high-quality genome scale metabolic model. *Microb. Cell Fact.* **2018**, *17*, 2. [CrossRef] [PubMed]
197. Kindzierski, V.; Raschke, S.; Knabe, N.; Siedler, F.; Scheffer, B.; Pfluger-Grau, K.; Pfeiffer, F.; Oesterhelt, D.; Marin-Sanguino, A.; Kunte, H.J. Osmoregulation in the halophilic bacterium *Halomonas elongata*: A case study for integrative systems biology. *PLoS ONE* **2017**, *12*, e0168818. [CrossRef] [PubMed]
198. Mustakhimov, I.I.; Reshetnikov, A.S.; Glukhov, A.S.; Khmelenina, V.N.; Kalyuzhnaya, M.G.; Trotsenko, Y.A. Identification and characterization of EctR1, a new transcriptional regulator of the ectoine biosynthesis genes in the halotolerant methanotroph *Methylomicrobium alcaliphilum* 20Z. *J. Bacteriol.* **2010**, *192*, 410–417. [CrossRef] [PubMed]
199. Leon, M.J.; Hoffmann, T.; Sanchez-Porro, C.; Heider, J.; Ventosa, A.; Bremer, E. Compatible solute synthesis and import by the moderate halophile *Spiribacter salinus*: Physiology and genomics. *Front. Microbiol.* **2018**, *9*, 108. [CrossRef] [PubMed]
200. Leόn, M.J.; Fernandez, A.B.; Ghai, R.; Sanchez-Porro, C.; Rodriguez-Valera, F.; Ventosa, A. From metagenomics to pure culture: Isolation and characterization of the moderately halophilic bacterium *Spiribacter salinus* gen. nov., sp. nov. *Appl. Environ. Microbiol.* **2014**, *80*, 3850–3857.
201. Haldenwang, W.G. The sigma factors of *Bacillus subtilis*. *Microbiol. Rev.* **1995**, *59*, 1–30. [PubMed]
202. Hecker, M.; Pane-Farre, J.; Völker, U. SigB-dependent general stress response in *Bacillus subtilis* and related gram-positive bacteria. *Annu. Rev. Microbiol.* **2007**, *61*, 215–236. [CrossRef] [PubMed]
203. Nannapaneni, P.; Hertwig, F.; Depke, M.; Hecker, M.; Mäder, U.; Völker, U.; Steil, L.; van Hijum, S.A. Defining the structure of the general stress regulon of *Bacillus subtilis* using targeted microarray analysis and random forest classification. *Microbiology* **2012**, *158*, 696–707. [CrossRef] [PubMed]
204. Feklistov, A.; Sharon, B.D.; Darst, S.A.; Gross, C.A. Bacterial sigma factors: A historical, structural, and genomic perspective. *Annu. Rev. Microbiol.* **2014**, *68*, 357–376. [CrossRef] [PubMed]
205. Typas, A.; Becker, G.; Hengge, R. The molecular basis of selective promoter activation by the sigmaS subunit of RNA polymerase. *Mol. Microbiol.* **2007**, *63*, 1296–1306. [CrossRef] [PubMed]
206. Bestvater, T.; Galinski, E.A. Investigation into a stress-inducible promoter region from *Marinococcus halophilus* using green fluorescent protein. *Extremophiles* **2002**, *6*, 15–20. [CrossRef] [PubMed]
207. Gralla, J.D.; Huo, Y.X. Remodeling and activation of *Escherichia coli* RNA polymerase by osmolytes. *Biochemistry* **2008**, *47*, 13189–13196. [CrossRef] [PubMed]

208. Gralla, J.D.; Vargas, D.R. Potassium glutamate as a transcriptional inhibitor during bacterial osmoregulation. *EMBO J.* **2006**, *25*, 1515–1521. [CrossRef] [PubMed]
209. Salvador, M.; Argandona, M.; Pastor, J.M.; Bernal, V.; Canovas, M.; Csonka, L.N.; Nieto, J.J.; Vargas, C. Contribution of RpoS to metabolic efficiency and ectoines synthesis during the osmo- and heat-stress response in the halophilic bacterium *Chromohalobacter salexigens*. *Environ. Microbiol. Rep.* **2015**, *7*, 301–311. [CrossRef] [PubMed]
210. Higgins, C.F.; Dorman, C.J.; Stirling, D.A.; Waddell, L.; Booth, I.R.; May, G.; Bremer, E. A physiological role for DNA supercoiling in the osmotic regulation of gene expression in *S. typhimurium* and *E. coli*. *Cell* **1988**, *52*, 569–584. [CrossRef]
211. Booth, I.R.; Higgins, C.F. Enteric bacteria and osmotic stress: Intracellular potassium glutamate as a secondary signal of osmotic stress? *FEMS Microbiol. Rev.* **1990**, *6*, 239–246. [CrossRef] [PubMed]
212. Hoffmann, T.; Wensing, A.; Brosius, M.; Steil, L.; Völker, U.; Bremer, E. Osmotic control of *opuA* expression in *Bacillus subtilis* and its modulation in response to intracellular glycine betaine and proline pools. *J. Bacteriol.* **2013**, *195*, 510–522. [CrossRef] [PubMed]
213. Hoffmann, T.; Bleisteiner, M.; Sappa, P.K.; Steil, L.; Mader, U.; Volker, U.; Bremer, E. Synthesis of the compatible solute proline by *Bacillus subtilis*: Point mutations rendering the osmotically controlled *proHJ* promoter hyperactive. *Environ. Microbiol.* **2017**, *19*, 3700–3720. [CrossRef] [PubMed]
214. Deochand, D.K.; Grove, A. MarR family transcription factors: Dynamic variations on a common scaffold. *Crit. Rev. Biochem. Mol. Biol.* **2017**, *52*, 595–613. [CrossRef] [PubMed]
215. Mustakhimov, I.I.; Reshetnikov, A.S.; Fedorov, D.N.; Khmelenina, V.N.; Trotsenko, Y.A. Role of RctR as transcriptional regulator of ectoine biosynthesis genes in *Methylophaga thalassica*. *Biochem. Biokhimiia* **2012**, *77*, 857–863. [CrossRef] [PubMed]
216. Romeo, Y.; Bouvier, J.; Gutierrez, C. Osmotic regulation of transcription in *Lactococcus lactis*: Ionic strength-dependent binding of the BusR repressor to the *busA* promoter. *FEBS Lett.* **2007**, *581*, 3387–3390. [CrossRef] [PubMed]
217. Romeo, Y.; Obis, D.; Bouvier, J.; Guillot, A.; Fourcans, A.; Bouvier, I.; Gutierrez, C.; Mistou, M.Y. Osmoregulation in *Lactococcus lactis*: BusR, a transcriptional repressor of the glycine betaine uptake system BusA. *Mol. Microbiol.* **2003**, *47*, 1135–1147. [CrossRef] [PubMed]
218. Shikuma, N.J.; Davis, K.R.; Fong, J.N.C.; Yildiz, F.H. The transcriptional regulator, CosR, controls compatible solute biosynthesis and transport, motility and biofilm formation in *Vibrio cholerae*. *Environ. Microbiol.* **2013**, *15*, 1387–1399. [CrossRef] [PubMed]
219. Shao, Z.; Deng, W.; Li, S.; He, J.; Ren, S.; Huang, W.; Lu, Y.; Zhao, G.; Cai, Z.; Wang, J. GlnR-mediated regulation of *ectABCD* transcription expands the role of the GlnR regulon to osmotic stress management. *J. Bacteriol.* **2015**, *197*, 3041–3307. [CrossRef] [PubMed]
220. Sadeghi, A.; Soltani, B.M.; Nekouei, M.K.; Jouzani, G.S.; Mirzaei, H.H.; Sadeghizadeh, M. Diversity of the ectoines biosynthesis genes in the salt tolerant *Streptomyces* and evidence for inductive effect of ectoines on their accumulation. *Microbiol. Res.* **2014**, *169*, 699–708. [CrossRef] [PubMed]
221. Kurz, M.; Burch, A.Y.; Seip, B.; Lindow, S.E.; Gross, H. Genome-driven investigation of compatible solute biosynthesis pathways of *Pseudomonas syringae* pv. syringae and their contribution to water stress tolerance. *Appl. Environ. Microbiol.* **2010**, *76*, 5452–5462. [CrossRef] [PubMed]
222. Chen, I.A.; Markowitz, V.M.; Chu, K.; Palaniappan, K.; Szeto, E.; Pillay, M.; Ratner, A.; Huang, J.; Andersen, E.; Huntemann, M.; et al. IMG/M: Integrated genome and metagenome comparative data analysis system. *Nucleic Acids Res.* **2017**, *45*, D507–D516. [CrossRef] [PubMed]
223. Soucy, S.M.; Huang, J.; Gogarten, J.P. Horizontal gene transfer: Building the web of life. *Nat. Rev. Genet.* **2015**, *16*, 472–482. [CrossRef] [PubMed]
224. Treangen, T.J.; Rocha, E.P.C. Horizontal transfer, not duplication, drives the expansion of protein families in prokaryotes. *PLoS Genet.* **2011**, *7*, e1001284. [CrossRef] [PubMed]
225. Wagner, A.; Whitaker, R.J.; Krause, D.J.; Heilers, J.H.; van Wolferen, M.; van der Does, C.; Albers, S.V. Mechanisms of gene flow in archaea. *Nat. Rev. Microbiol.* **2017**, *15*, 492–501. [CrossRef] [PubMed]
226. Yang, J.C.; Madupu, R.; Durkin, A.S.; Ekborg, N.A.; Pedamallu, C.S.; Hostetler, J.B.; Radune, D.; Toms, B.S.; Henrissat, B.; Coutinho, P.M.; et al. The complete genome of *Teredinibacter turnerae* T7901: An intracellular endosymbiont of marine wood-boring bivalves (shipworms). *PLoS ONE* **2009**, *4*, e6085. [CrossRef] [PubMed]

227. Ferreira, C.; Soares, A.R.; Lamosa, P.; Santos, M.A.; da Costa, M.S. Comparison of the compatible solute pool of two slightly halophilic planctomycetes species, *Gimesia maris* and *Rubinisphaera brasiliensis*. *Extremophiles* **2016**, *20*, 811–820. [CrossRef] [PubMed]
228. Amiri Moghaddam, J.; Boehringer, N.; Burdziak, A.; Kunte, H.J.; Galinski, E.A.; Schäberle, T.F. Different strategies of osmoadaptation in the closely related marine myxobacteria *Enhygromyxa salina* SWB007 and *Plesiocystis pacifica* SIR-1. *Microbiology* **2016**, *162*, 641–661. [CrossRef] [PubMed]
229. Qin, W.; Heal, K.R.; Ramdasi, R.; Kobelt, J.N.; Martens-Habbena, W.; Bertagnolli, A.D.; Amin, S.A.; Walker, C.B.; Urakawa, H.; Konneke, M.; et al. *Nitrosopumilus maritimus* gen. nov., sp. nov., *Nitrosopumilus cobalaminigenes* sp. nov., *Nitrosopumilus oxyclinae* sp. nov., and *Nitrosopumilus ureiphilus* sp. Nov., four marine ammonia-oxidizing archaea of the phylum thaumarchaeota. *Int. J. Syst. Evol. Microbiol.* **2017**, *67*, 5067–5079. [CrossRef] [PubMed]
230. Simon, M.; Scheuner, C.; Meier-Kolthoff, J.P.; Brinkhoff, T.; Wagner-Döbler, I.; Ulbrich, M.; Klenk, H.P.; Schomburg, D.; Petersen, J.; Göker, M. Phylogenomics of *Rhodobacteraceae* reveals evolutionary adaptation to marine and non-marine habitats. *ISME J.* **2017**, *11*, 1483–1499. [CrossRef] [PubMed]
231. Wagner-Döbler, I.; Biebl, H. Environmental biology of the marine *Roseobacter* lineage. *Annu. Rev. Microbiol.* **2006**, *60*, 255–280. [CrossRef] [PubMed]
232. Luo, H.; Moran, M.A. Evolutionary ecology of the marine *Roseobacter* clade. *Microbiol. Mol. Biol. Rev.* **2014**, *78*, 573–587. [CrossRef] [PubMed]
233. Welsh, D.T. Ecological significance of compatible solute accumulation by micro-organisms: From single cells to global climate. *FEMS Microbiol. Rev.* **2000**, *24*, 263–290. [CrossRef] [PubMed]
234. Warren, C. Do microbial osmolytes or extracellular depolymerization products accumulate as soil dries? *Soil Biol. Biochem.* **2016**, *98*, 54–63. [CrossRef]
235. Warren, C.R. Quaternary ammonium compounds can be abundant in some soils and are taken up as intact molecules by plants. *New Phytol.* **2013**, *198*, 476–485. [CrossRef] [PubMed]
236. Warren, C.R. Response of osmolytes in soil to drying and rewetting. *Soil Biol. Biochem.* **2014**, *70*, 22–32. [CrossRef]
237. Bouskill, N.J.; Wood, T.E.; Baran, R.; Hao, Z.; Ye, Z.; Bowen, B.P.; Lim, H.C.; Nico, P.S.; Holman, H.Y.; Gilbert, B.; et al. Belowground response to drought in a tropical forest soil. II. Change in microbial function impacts carbon composition. *Front. Microbiol.* **2016**, *7*, 323. [CrossRef] [PubMed]
238. Bouskill, N.J.; Wood, T.E.; Baran, R.; Ye, Z.; Bowen, B.P.; Lim, H.; Zhou, J.; Nostrand, J.D.; Nico, P.; Northen, T.R.; et al. Belowground response to drought in a tropical forest soil. I. Changes in microbial functional potential and metabolism. *Front. Microbiol.* **2016**, *7*, 525. [CrossRef] [PubMed]
239. Mosier, A.C.; Justice, N.B.; Bowen, B.P.; Baran, R.; Thomas, B.C.; Northen, T.R.; Banfield, J.F. Metabolites associated with adaptation of microorganisms to an acidophilic, metal-rich environment identified by stable-isotope-enabled metabolomics. *mBio* **2013**, *4*, e00484-12. [CrossRef] [PubMed]
240. Poolman, B.; Spitzer, J.J.; Wood, J.M. Bacterial osmosensing: Roles of membrane structure and electrostatics in lipid-protein and protein-protein interactions. *Biochim. Biophys. Acta* **2004**, *1666*, 88–104. [CrossRef] [PubMed]
241. Ziegler, C.; Bremer, E.; Krämer, R. The BCCT family of carriers: From physiology to crystal structure. *Mol. Microbiol.* **2010**, *78*, 13–34. [CrossRef] [PubMed]
242. Krämer, R. Bacterial stimulus perception and signal transduction: Response to osmotic stress. *Chem. Rec.* **2010**, *10*, 217–229. [CrossRef] [PubMed]
243. Culham, D.E.; Shkel, I.A.; Record, M.T., Jr.; Wood, J.M. Contributions of coulombic and Hofmeister effects to the osmotic activation of *Escherichia coli* transporter ProP. *Biochemistry* **2016**, *55*, 1301–1313. [CrossRef] [PubMed]
244. Gul, N.; Schuurman-Wolters, G.; Karasawa, A.; Poolman, B. Functional characterization of amphipathic alpha-helix in the osmoregulatory ABC transporter OpuA. *Biochemistry* **2012**, *51*, 5142–5152. [CrossRef] [PubMed]
245. Perez, C.; Faust, B.; Mehdipour, A.R.; Francesconi, K.A.; Forrest, L.R.; Ziegler, C. Substrate-bound outward-open state of the betaine transporter BetP provides insights into Na^+ coupling. *Nat. Commun.* **2014**, *5*, 4231. [CrossRef] [PubMed]
246. Perez, C.; Koshy, C.; Yildiz, O.; Ziegler, C. Alternating-access mechanism in conformationally asymmetric trimers of the betaine transporter BetP. *Nature* **2012**, *490*, 126–130. [CrossRef] [PubMed]

247. Hahne, H.; Mäder, U.; Otto, A.; Bonn, F.; Steil, L.; Bremer, E.; Hecker, M.; Becher, D. A comprehensive proteomics and transcriptomics analysis of *Bacillus subtilis* salt stress adaptation. *J. Bacteriol.* **2010**, *192*, 870–882. [CrossRef] [PubMed]
248. Kappes, R.M.; Kempf, B.; Kneip, S.; Boch, J.; Gade, J.; Meier-Wagner, J.; Bremer, E. Two evolutionarily closely related ABC transporters mediate the uptake of choline for synthesis of the osmoprotectant glycine betaine in *Bacillus subtilis*. *Mol. Microbiol.* **1999**, *32*, 203–216. [CrossRef] [PubMed]
249. Morbach, S.; Krämer, R. Body shaping under water stress: Osmosensing and osmoregulation of solute transport in bacteria. *ChemBioChem* **2002**, *3*, 384–397. [CrossRef]
250. Rice, A.J.; Park, A.; Pinkett, H.W. Diversity in ABC transporters: Type I, II and III importers. *Crit. Rev. Biochem. Mol. Biol.* **2014**, *49*, 426–437. [CrossRef] [PubMed]
251. Ter Beek, J.; Guskov, A.; Slotboom, D.J. Structural diversity of ABC transporters. *J. Gen. Physiol.* **2014**, *143*, 419–435. [CrossRef] [PubMed]
252. Jebbar, M.; von Blohn, C.; Bremer, E. Ectoine functions as an osmoprotectant in *Bacillus subtilis* and is accumulated via the ABC-transport system OpuC. *FEMS Microbiol. Lett.* **1997**, *154*, 325–330. [CrossRef]
253. Choquet, G.; Jehan, N.; Pissavin, C.; Blanco, C.; Jebbar, M. OusB, a broad-specificity ABC-type transporter from *Erwinia chrysanthemi*, mediates uptake of glycine betaine and choline with a high affinity. *Appl. Environ. Microbiol.* **2005**, *71*, 3389–3398. [CrossRef] [PubMed]
254. Yan, N. Structural biology of the major facilitator superfamily transporters. *Annu. Rev. Biophys.* **2015**, *44*, 257–283. [CrossRef] [PubMed]
255. Gloux, K.; Touze, T.; Pagot, Y.; Jouan, B.; Blanco, C. Mutations of *ousA* alter the virulence of *Erwinia chrysanthemi*. *Mol. Plant. Microbe Interact.* **2005**, *18*, 150–157. [CrossRef] [PubMed]
256. Kappes, R.M.; Kempf, B.; Bremer, E. Three transport systems for the osmoprotectant glycine betaine operate in *Bacillus subtilis*: Characterization of OpuD. *J. Bacteriol.* **1996**, *178*, 5071–5079. [CrossRef] [PubMed]
257. Vermeulen, V.; Kunte, H.J. *Marinococcus halophilus* DSM 20408T encodes two transporters for compatible solutes belonging to the betaine-carnitine-choline transporter family: Identification and characterization of ectoine transporter EctM and glycine betaine transporter BetM. *Extremophiles* **2004**, *8*, 175–184. [CrossRef] [PubMed]
258. Steger, R.; Weinand, M.; Krämer, R.; Morbach, S. LcoP, an osmoregulated betaine/ectoine uptake system from *Corynebacterium glutamicum*. *FEBS Lett.* **2004**, *573*, 155–160. [CrossRef] [PubMed]
259. Peter, H.; Weil, B.; Burkovski, A.; Kramer, R.; Morbach, S. *Corynebacterium glutamicum* is equipped with four secondary carriers for compatible solutes: Identification, sequencing, and characterization of the proline/ectoine uptake system, ProP, and the ectoine/proline/glycine betaine carrier, EctP. *J. Bacteriol.* **1998**, *180*, 6005–6012. [PubMed]
260. Perez, C.; Koshy, C.; Ressl, S.; Nicklisch, S.; Krämer, R.; Ziegler, C. Substrate specificity and ion coupling in the Na^+/betaine symporter BetP. *EMBO J.* **2011**, *30*, 1221–1229. [CrossRef] [PubMed]
261. Kuhlmann, S.I.; Terwisscha van Scheltinga, A.C.; Bienert, R.; Kunte, H.J.; Ziegler, C. 1.55 a structure of the ectoine binding protein TeaA of the osmoregulated TRAP-transporter TeaABC from *Halomonas elongata*. *Biochemistry* **2008**, *47*, 9475–9485. [CrossRef] [PubMed]
262. Du, Y.; Shi, W.W.; He, Y.X.; Yang, Y.H.; Zhou, C.Z.; Chen, Y. Structures of the substrate-binding protein provide insights into the multiple compatible solute binding specificities of the *Bacillus subtilis* ABC transporter OpuC. *Biochem. J.* **2011**, *436*, 283–289. [CrossRef] [PubMed]
263. Schulz, A.; Stöveken, N.; Binzen, I.M.; Hoffmann, T.; Heider, J.; Bremer, E. Feeding on compatible solutes: A substrate-induced pathway for uptake and catabolism of ectoines and its genetic control by EnuR. *Environ. Microbiol.* **2017**, *19*, 926–946. [CrossRef] [PubMed]
264. Galinski, E.A.; Herzog, R.M. The role of trehalose as a substitute for nitrogen-containing compatible solutes (*Ectothiorhodospira halochloris*). *Arch. Microbiol.* **1990**, *153*, 607–613. [CrossRef]
265. Jebbar, M.; Sohn-Bosser, L.; Bremer, E.; Bernard, T.; Blanco, C. Ectoine-induced proteins in *Sinorhizobium meliloti* include an ectoine ABC-type transporter involved in osmoprotection and ectoine catabolism. *J. Bacteriol.* **2005**, *187*, 1293–1304. [CrossRef] [PubMed]
266. Vargas, C.; Jebbar, M.; Carrasco, R.; Blanco, C.; Calderon, M.I.; Iglesias-Guerra, F.; Nieto, J.J. Ectoines as compatible solutes and carbon and energy sources for the halophilic bacterium *Chromohalobacter salexigens*. *J. Appl. Microbiol.* **2006**, *100*, 98–107. [CrossRef] [PubMed]

267. Hanekop, N.; Höing, M.; Sohn-Bösser, L.; Jebbar, M.; Schmitt, L.; Bremer, E. Crystal structure of the ligand-binding protein EhuB from *Sinorhizobium meliloti* reveals substrate recognition of the compatible solutes ectoine and hydroxyectoine. *J. Mol. Biol.* **2007**, *374*, 1237–1250. [CrossRef] [PubMed]
268. Lecher, J.; Pittelkow, M.; Zobel, S.; Bursy, J.; Bonig, T.; Smits, S.H.; Schmitt, L.; Bremer, E. The crystal structure of UehA in complex with ectoine—A comparison with other TRAP-T binding proteins. *J. Mol. Biol.* **2009**, *389*, 58–73. [CrossRef] [PubMed]
269. Rigali, S.; Derouaux, A.; Giannotta, F.; Dusart, J. Subdivision of the helix-turn-helix GntR family of bacterial regulators in the FadR, HutC, MocR, and YtrA subfamilies. *J. Biol. Chem.* **2002**, *277*, 12507–12515. [CrossRef] [PubMed]
270. Schulz, A.; Hermann, L.; Freibert, S.-A.; Bönig, T.; Hoffmann, T.; Riclea, R.; Dickschat, J.S.; Heider, J.; Bremer, E. Transcriptional regulation of ectoine catabolism in response to multiple metabolic and environmnetal cues. *Environ. Microbiol.* **2017**, *19*, 4599–4619. [CrossRef] [PubMed]
271. Kumarevel, T.; Nakano, N.; Ponnuraj, K.; Gopinath, S.C.; Sakamoto, K.; Shinkai, A.; Kumar, P.K.; Yokoyama, S. Crystal structure of glutamine receptor protein from *Sulfolobus tokodaii* strain 7 in complex with its effector L-glutamine: Implications of effector binding in molecular association and DNA binding. *Nucleic Acids Res.* **2008**, *36*, 4808–4820. [CrossRef] [PubMed]
272. Shrivastava, T.; Ramachandran, R. Mechanistic insights from the crystal structures of a feast/famine regulatory protein from *Mycobacterium tuberculosis* h37rv. *Nucleic Acids Res.* **2007**, *35*, 7324–7335. [CrossRef] [PubMed]
273. Yokoyama, K.; Ishijima, S.A.; Clowney, L.; Koike, H.; Aramaki, H.; Tanaka, C.; Makino, K.; Suzuki, M. Feast/famine regulatory proteins (FFRPs): *Escherichia coli* LRP, AsnC and related archaeal transcription factors. *FEMS Microbiol. Rev.* **2006**, *30*, 89–108. [CrossRef] [PubMed]
274. Copeland, A.; O'Connor, K.; Lucas, S.; Lapidus, A.; Berry, K.W.; Detter, J.C.; Del Rio, T.G.; Hammon, N.; Dalin, E.; Tice, H.; et al. Complete genome sequence of the halophilic and highly halotolerant *Chromohalobacter salexigens* type strain (1H11^{T}). *Stand. Genom. Sci.* **2011**, *5*, 379–388. [CrossRef] [PubMed]
275. Bramucci, E.; Milano, T.; Pascarella, S. Genomic distribution and heterogeneity of MocR-like transcriptional factors containing a domain belonging to the superfamily of the pyridoxal-5^{0}-phosphate dependent enzymes of fold type I. *Biochem. Biophys. Res. Commun.* **2011**, *415*, 88–93. [CrossRef] [PubMed]
276. Suvorova, I.; Rodionov, D. Comparitive genomics of pyridoxal 5^{0}-phosphate-dependent transcription factor regulons in *Bacteria*. *Microb. Genom.* **2016**, *2*, e000047. [PubMed]
277. Yu, Q.; Cai, H.; Zhang, Y.; He, Y.; Chen, L.; Merritt, J.; Zhang, S.; Dong, Z. Negative regulation of ectoine uptake and catabolism in *Sinorhizobium meliloti*: Characterization of the EhuR gene. *J. Bacteriol.* **2017**, *199*, e00119-16. [CrossRef] [PubMed]
278. Belitsky, B.R. *Bacillus subtilis* GabR, a protein with DNA-binding and aminotransferase domains, is a PLP-dependent transcriptional regulator. *J. Mol. Biol.* **2004**, *340*, 655–664. [CrossRef] [PubMed]
279. Edayathumangalam, R.; Wu, R.; Garcia, R.; Wang, Y.; Wang, W.; Kreinbring, C.A.; Bach, A.; Liao, J.; Stone, T.A.; Terwilliger, T.C.; et al. Crystal structure of *Bacillus subtilis* GabR, an autorepressor and transcriptional activator of *gabT*. *Proc. Natl. Acad. Sci. USA* **2013**, *110*, 17820–17825. [CrossRef] [PubMed]
280. Okuda, K.; Ito, T.; Goto, M.; Takenaka, T.; Hemmi, H.; Yoshimura, T. Domain characterization of *Bacillus subtilis* GabR, a pyridoxal 5^{0}-phosphate-dependent transcriptional regulator. *J. Biochem.* **2015**, *158*, 225–234. [CrossRef] [PubMed]
281. Okuda, K.; Kato, S.; Ito, T.; Shiraki, S.; Kawase, Y.; Goto, M.; Kawashima, S.; Hemmi, H.; Fukada, H.; Yoshimura, T. Role of the aminotransferase domain in *Bacillus subtilis* GabR, a pyridoxal 5^{0}-phosphate-dependent transcriptional regulator. *Mol. Microbiol.* **2015**, *95*, 245–257. [CrossRef] [PubMed]
282. Park, S.A.; Park, Y.S.; Lee, K.S. Crystal structure of the C-terminal domain of *Bacillus subtilis* GabR reveals a closed conformation by gamma-aminobutyric acid binding, inducing transcriptional activation. *Biochem. Biophys. Res. Commun.* **2017**, *487*, 287–291. [CrossRef] [PubMed]
283. Wu, R.; Sanishvili, R.; Belitsky, B.R.; Juncosa, J.I.; Le, H.V.; Lehrer, H.J.; Farley, M.; Silverman, R.B.; Petsko, G.A.; Ringe, D.; et al. Plp and GABA trigger GabR-mediated transcription regulation in *Bacillus subtilis* via external aldimine formation. *Proc. Natl. Acad. Sci. USA* **2017**, *114*, 3891–3896. [CrossRef] [PubMed]

284. Steffen-Munsberg, F.; Vickers, C.; Kohls, H.; Land, H.; Mallin, H.; Nobili, A.; Skalden, L.; van den Bergh, T.; Joosten, H.J.; Berglund, P.; et al. Bioinformatic analysis of a PLP-dependent enzyme superfamily suitable for biocatalytic applications. *Biotechnol. Adv.* **2015**, *33*, 566–604. [CrossRef] [PubMed]
285. Phillips, R.S. Chemistry and diversity of pyridoxal-5^{0}-phosphate dependent enzymes. *Biochim. Biophys. Acta* **2015**, *1854*, 1167–1174. [CrossRef] [PubMed]
286. Biasini, M.; Bienert, S.; Waterhouse, A.; Arnold, K.; Studer, G.; Schmidt, T.; Kiefer, F.; Cassarino, T.G.; Bertoni, M.; Bordoli, L.; et al. SWISS-MODEL: Modelling protein tertiary and quaternary structure using evolutionary information. *Nucleic Acids Res.* **2014**, *42*, W252–W258. [CrossRef] [PubMed]
287. Delano, W.L. *The PyMol Molecular Graphics System*; Delano Scientific: San Carlos, CA, USA, 2002.
288. Dey, A.; Shree, S.; Pandey, S.K.; Tripathi, R.P.; Ramachandran, R. Crystal structure of *Mycobacterium tuberculosis* H37Rv AldR (Rv2779c), a regulator of the *ald* gene: DNA-binding, and identification of small-molecule inhibitors. *J. Biol. Chem.* **2016**, *291*, 11967–11980. [CrossRef] [PubMed]
289. Kamensek, S.; Browning, D.F.; Podlesek, Z.; Busby, S.J.; Zgur-Bertok, D.; Butala, M. Silencing of DNase colicin e8 gene expression by a complex nucleoprotein assembly ensures timely colicin induction. *PLoS Genet.* **2015**, *11*, e1005354. [CrossRef] [PubMed]
290. Zschiedrich, C.P.; Keidel, V.; Szurmant, H. Molecular mechanisms of two-component signal transduction. *J. Mol. Biol.* **2016**, *428*, 3752–3775. [CrossRef] [PubMed]
291. Fernandez, I.; Cornaciu, I.; Carrica, M.D.; Uchikawa, E.; Hoffmann, G.; Sieira, R.; Marquez, J.A.; Goldbaum, F.A. Three-dimensional structure of full-length NtrX, an unusual member of the NtrC family of response regulators. *J. Mol. Biol.* **2017**, *429*, 1192–1212. [CrossRef] [PubMed]
292. Bonato, P.; Alves, L.R.; Osaki, J.H.; Rigo, L.U.; Pedrosa, F.O.; Souza, E.M.; Zhang, N.; Schumacher, J.; Buck, M.; Wassem, R.; et al. The NtrY-NtrX two-component system is involved in controlling nitrate assimilation in *Herbaspirillum seropedicae* strain SmR1. *FEBS J.* **2016**, *283*, 3919–3930. [CrossRef] [PubMed]
293. Calatrava-Morales, N.; Nogales, J.; Ameztoy, K.; van Steenbergen, B.; Soto, M.J. The NtrY/NtrX system of *Sinorhizobium meliloti* GR4 regulates motility, EPS I production and nitrogen metabolism but is dispensable for symbiotic nitrogen fixation. *Mol. Plant. Microbe Interact.* **2017**, *30*, 566–577. [CrossRef] [PubMed]
294. Robledo, M.; Peregrina, A.; Millan, V.; Garcia-Tomsig, N.I.; Torres-Quesada, O.; Mateos, P.F.; Becker, A.; Jimenez-Zurdo, J.I. A conserved alpha-proteobacterial small RNA contributes to osmoadaptation and symbiotic efficiency of rhizobia on legume roots. *Environ. Microbiol.* **2017**, *19*, 2661–2680. [CrossRef] [PubMed]
295. Park, J.S.; Cho, B.C.; Simpson, A.G.B. *Halocafeteria seosinensis* gen. et. sp. nov. (bicosoecida), a halophilic bacterivorous nanoflagellate isolated from a solar saltern. *Extremophiles* **2006**, *10*, 493–504. [CrossRef] [PubMed]
296. Foissner, W.; Filker, S.; Stoeck, T. *Schmidingerothrix salinarum* nov spec. is the molecular sister of the large oxytrichid clade (ciliophora, hypotricha). *J. Eukary Microbiol.* **2014**, *61*, 61–74. [CrossRef] [PubMed]
297. Ventosa, A.; de la Haba, R.R.; Sanchez-Porro, C.; Papke, R.T. Microbial diversity of hypersaline environments: A metagenomic approach. *Curr. Opin. Microbiol.* **2015**, *25*, 80–87. [CrossRef] [PubMed]
298. Moreira, D.; Lopez-Garcia, P. Protist evolution: Stealing genes to gut it out. *Curr. Biol.* **2017**, *27*, R223–R225. [CrossRef] [PubMed]
299. Rogozin, I.B.; Carmel, L.; Csuros, M.; Koonin, E.V. Origin and evolution of spliceosomal introns. *Biol. Direct* **2012**, *7*, 11. [CrossRef] [PubMed]
300. Putnam, N.H.; Butts, T.; Ferrier, D.E.K.; Furlong, R.F.; Hellsten, U.; Kawashima, T.; Robinson-Rechavi, M.; Shoguchi, E.; Terry, A.; Yu, J.K.; et al. The amphioxus genome and the evolution of the chordate karyotype. *Nature* **2008**, *453*, 1064–1071. [CrossRef] [PubMed]
301. Simakov, O.; Kawashima, T.; Marletaz, F.; Jenkins, J.; Koyanagi, R.; Mitros, T.; Hisata, K.; Bredeson, J.; Shoguchi, E.; Gyoja, F.; et al. Hemichordate genomes and deuterostome origins. *Nature* **2015**, *527*, 459–465. [CrossRef] [PubMed]
302. Husnik, F.; McCutcheon, J.P. Functional horizontal gene transfer from bacteria to eukaryotes. *Nat. Rev. Microbiol.* **2018**, *16*, 67–79. [CrossRef] [PubMed]

303. Landa, M.; Burns, A.S.; Roth, S.J.; Moran, M.A. Bacterial transcriptome remodeling during sequential co-culture with a marine dinoflagellate and diatom. *ISMEJ* **2017**, *11*, 2677–2690. [CrossRef] [PubMed]
304. Hoffmann, T.; von Blohn, C.; Stanek, A.; Moses, S.; Barzantny, S.; Bremer, E. Synthesis, release, and recapture of the compatible solute proline by osmotically stressed *Bacillus subtilis* cells. *Appl. Environ. Microbiol.* **2012**, *78*, 5753–5762. [CrossRef] [PubMed]
305. Börngen, K.; Battle, A.R.; Möker, N.; Morbach, S.; Marin, K.; Martinac, B.; Krämer, R. The properties and contribution of the *Corynebacterium glutamicum* MscS variant to fine-tuning of osmotic adaptation. *Biochim. Biophys. Acta* **2010**, *1798*, 2141–2149. [CrossRef] [PubMed]

6.4.2 The ups and downs of ectoine: structural enzymology of a major microbial stress protectant and versatile nutrient (2020)

Biol. Chem. 2020; 401(12): 1443-1468 doi: 10.1515/hsz-2020-0223

Lucas Hermann, Christopher-Nils Mais, Laura Czech, Sander H.J. Smits, Gert Bange* and Erhard Bremer*

The ups and downs of ectoine: structural enzymology of a major microbial stress protectant and versatile nutrient

The following review article “The ups and downs of ectoine: structural enzymology of a major microbial stress protectant and versatile nutrient” was published in Biological Chemistry in 2020 after a peer-reviewing process. Prof. E. Bremer and I wrote the text with contributions of C. N. Mais, L. Czech, S. H. J. Smits and G. Bange. The bioinformatic analyses were performed by me and I prepared all figures in the publication with contributions by L. Czech. All authors helped in finalizing the manuscript.

Review

Lucas Hermann, Christopher-Nils Mais, Laura Czech, Sander H.J. Smits, Gert Bange* and Erhard Bremer*

The ups and downs of ectoine: structural enzymology of a major microbial stress protectant and versatile nutrient

https://doi.org/10.1515/hsz-2020-0223
Received June 18, 2020; accepted July 22, 2020; published online August 27, 2020

Abstract: Ectoine and its derivative 5-hydroxyectoine are compatible solutes and chemical chaperones widely synthesized by *Bacteria* and some *Archaea* as cytoprotectants during osmotic stress and high- or low-growth temperature extremes. The function-preserving attributes of ectoines led to numerous biotechnological and biomedical applications and fostered the development of an industrial scale production process. Synthesis of ectoines requires the expenditure of considerable energetic and biosynthetic resources. Hence, microorganisms have developed ways to exploit ectoines as nutrients when they are no longer needed as stress protectants. Here, we summarize our current knowledge on the phylogenomic distribution of ectoine producing and consuming microorganisms. We emphasize the structural enzymology of the pathways underlying ectoine biosynthesis and consumption, an understanding that has been achieved only recently. The synthesis and degradation pathways critically differ in the isomeric form of the key metabolite *N*-acetyldiaminobutyric acid (ADABA). *γ*-ADABA serves as preferred substrate for the ectoine synthase, while the α-ADABA isomer is produced by the ectoine hydrolase as an intermediate in catabolism. It can serve as internal inducer for the genetic control of ectoine catabolic genes via the GabR/MocR-type regulator EnuR. Our review highlights the importance of structural enzymology to inspire the mechanistic understanding of metabolic networks at the biological scale.

Keywords: chemical chaperones; compatible solutes; enzymes; gene regulation; microbial physiology; osmotic stress; structural analysis.

Lucas Hermann, Christopher-Nils Mais, and Laura Czech contributed equally to this article.

***Corresponding authors: Gert Bange**, Center for Synthetic Microbiology (SYNMIKRO) & Faculty of Chemistry, Philipps-University Marburg, Hans-Meerwein Str. 6, D-35043 Marburg, Germany; and **Erhard Bremer**, Department of Biology, Laboratory for Microbiology, Philipps-University Marburg, Karl-von Frisch Str. 8, D-35043 Marburg, Germany; Center for Synthetic Microbiology (SYNMIKRO), Philipps University Marburg, Hans-Meerwein Str. 6, D-35043 Marburg, Germany, E-mail: gert.bange@synmikro.uni-marburg.de (Gert Bange); bremer@staff.uni-marburg.de (Erhard Bremer)

Lucas Hermann, Department of Biology, Laboratory for Microbiology, Philipps-University Marburg, Karl-von Frisch Str. 8, D-35043 Marburg, Germany; Biochemistry and Synthetic Biology of Microbial Metabolism Group, Max Planck Institute for Terrestrial Microbiology, Karl-von Frisch Str. 10, D-35043 Marburg, Germany, E-mail: lucas.hermann@biologie.uni-marburg.de. https://orcid.org/0000-0001-6684-1644

Christopher-Nils Mais, Center for Synthetic Microbiology (SYNMIKRO) & Faculty of Chemistry, Philipps-University Marburg, Hans-Meerwein Str. 6, D-35043 Marburg, Germany, E-mail: cn.mais@staff.uni-marburg.de

Laura Czech, Department of Biology, Laboratory for Microbiology, Philipps-University Marburg, Karl-von Frisch Str. 8, D-35043 Marburg, Germany; Center for Synthetic Microbiology (SYNMIKRO) & Faculty of Chemistry, Philipps-University Marburg, Hans-Meerwein Str. 6, D-35043 Marburg, Germany, E-mail: czechla@staff.uni-marburg.de

Sander H.J. Smits, Center for Structural Studies, Heinrich Heine University Düsseldorf, Universitätsstr. 1, D-40225 Düsseldorf, Germany; Institute of Biochemistry, Heinrich Heine University Düsseldorf, Universitätsstr. 1, D-40225 Düsseldorf, Germany, E-mail: sander.smits@uni-duesseldorf.de

Introduction: managing water stress

Changes in the environmental osmolarity, a parameter to which most microorganisms are frequently exposed (Gunde-Cimerman et al. 2018; Kempf and Bremer 1998; Roeßler and Müller 2001), impinge on hydration of the cytoplasm, magnitude of turgor, growth and cellular survival (Bremer and Krämer 2019; Wood 2011). Microorganisms lack the ability to actively pump water across the cytoplasmic membrane to counteract water fluxes in or out of the cell that are triggered by increases or decreases in the

external osmolarity. Hence, as water passes along pre-existing osmotic gradients through the semi-permeable cytoplasmic membrane, bacterial cells have to counteract hypo- and hyper-osmotic challenges through an active, yet indirect, water-management to avoid dehydration under hyper-osmotic circumstances and cell rupture under hypo-osmotic conditions. Directing and scaling these water fluxes is key for the cellular osmostress response of microorganisms (Bremer and Krämer 2019; Wood 2011).

Upon sudden exposure to hypo-osmotic circumstances, microorganisms reduce the osmotic potential of their cytoplasm through the transient opening of mechanosensitive channels. Consequently, ions and metabolites are rapidly jettisoned, thereby curbing water influx, an undue increase in turgor and in extreme cases cell rupture is avoided (Booth 2014). Conversely, when microorganisms face hyper-osmotic surroundings, they initially accumulate potassium ions, and on a longer time scale, a particular class of physiologically compliant organic osmolytes, the compatible solutes (Brown 1976). This adjustment strategy to acute and sustained osmotic stress, often referred to as the "salt-out" response, aims at avoiding a long-lasting increase in the ionic strength of the cytoplasm to maintain the functionality of the cell's constituents and biochemical activities (Galinski and Trüper 1994; Gunde-Cimerman et al. 2018; Kempf and Bremer 1998). Collectively, the accumulation of compatible solutes prevents dehydration of the cytoplasm, an undue increase in molecular crowding, and a drop in turgor to non-physiologically adequate values (Bremer and Krämer 2019; van den Berg et al. 2017; Wood 2011) (Figure 1).

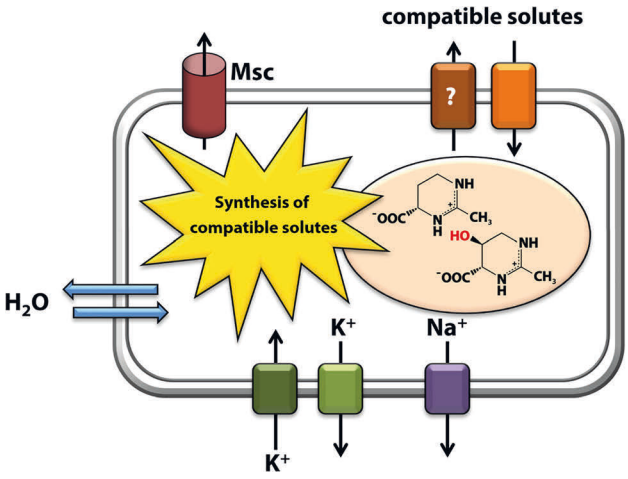

Figure 1: The core of the salt-out osmostress response. Shown are the systems that mediate cellular import of K^+ under acute osmotic stress as an immediate adjustment response and those that allow it extrusion once the cell begins with the import and/or synthesis of compatible solutes (e.g., ectoine and its derivative 5-hydroxyectoine) (Bremer and Krämer 2019; Wood 2011). Cells also seem to possess efflux systems for compatible solutes, probably a measure to fine-tune turgor when the cell elongates and doubles its volume prior to division (Czech et al. 2016; Vandrich et al. 2020). Cells maintain very low intracellular Na^+ concentration through dedicated export systems as this ion, in contrast to K^+, is cytotoxic (Danchin and Nikel 2019). Overall, cells that use the *salt-out* osmostress response, in contrast to those that use high concentrations of K^+/Cl^- to balance the osmotic gradient (the *salt-in* response) (Gunde-Cimerman et al. 2018), strive to prevent the development of a long-lasting high-ionic strength cytoplasm. The accumulation of compatible solutes is a key component of the acclimatization to both acute and sustained high osmolarity surroundings by microbial cells (Bremer and Krämer 2019; Wood 2011). The designation Msc represents MscS- and MscL-type mechanosensitive channels serving as safety valves for the rapid release of ions and organic solutes upon sudden osmotic down-shocks (Booth 2014).

Compatible solutes are operationally defined as highly water-soluble organic molecules that can be accumulated by both pro- and eukaryotic cells to exceedingly high intracellular levels without impairing the physiology and biochemistry of the cell (Brown 1976; Yancey 2005). The cytoprotective effects of compatible solutes are routinely interpreted in the framework of the 'preferential exclusion model' (Arakawa and Timasheff 1985; Bolen and Baskakov 2001), which proposes that these molecules are preferentially excluded from the protein backbone (Street et al. 2006; Capp et al. 2009; Cayley and Record 2003; Zaccai et al. 2016). This physico-chemical property of compatible solutes generates a thermodynamic driving force for proteins to minimize their exposed surface in order to keep the uneven distribution of compatible solutes in the cell water at a minimum. Hence, compatible solutes act against the denatured state and thereby promote the correct folding and appropriate hydration of proteins (Bolen and Baskakov 2001). Maintaining functionality of macromolecules through compatible solutes cannot only be observed *in vitro* for isolated proteins (Lippert and Galinski 1992), but most importantly also *in vivo* (Barth et al. 2000; Bourot et al. 2000; Caldas et al. 1999; Ignatova and Gierasch 2006; Stadmiller et al. 2017). These solutes also protect the functionality of other macromolecules (e.g., nucleic acids) and cellular compartments (e.g., membranes) (Hahn et al. 2017, 2020; Harishchandra et al. 2010, 2011; Herzog et al. 2019; Kurz 2008). Accordingly, compatible solutes can also be addressed as 'chemical chaperones' (Chattopadhyay et al. 2004; Diamant et al. 2001). The physico-chemical characteristics of compatible solutes and their high water-solubility make them ideally suited as osmostress protectants as they can be accumulated to high cytoplasmic pools, a process occurring in tune with the degree of the imposed osmotic stress onto the microbial cell (Czech et al. 2018b; Kuhlmann and Bremer 2002).

Microorganisms synthesize or import a great variety of compatible solutes (da Costa et al. 1998; Gunde-Cimerman et al. 2018; Kempf and Bremer 1998; Klähn and Hagemann 2011; Roeßler and Müller 2001). However, those that are synthesized by members of the *Bacteria* belong only to a restricted number of chemical classes: quaternary amines (e.g., glycine betaine), amino acids (e.g., L-proline), amino acid derivatives (e.g., ectoine), sugars (e.g., trehalose), and polyoles (e.g., glycerol, glucosylglycerol). Here, we focus on ectoine and its derivative 5-hydroxyectoine (Figure 1), cytoprotectants that are among the most widely synthesized compatible solutes in the microbial world (Czech et al. 2018a; da Costa et al. 1998; Galinski and Trüper 1994).

Ectoines: broadly synthesized and highly effective microbial cytoprotectants

The tetrahydropyrimidines ectoine [(4*S*)-2-methyl-1,4,5,6-tetrahydropyrimidine-4-carboxylic acid] and its derivative 5-hydroxyectoine [(4*S*,5*S*)-2-methyl-5-hydroxy-1,4,5,6-tetrahydropyrimidine-4-carboxylic acid] stand out from other compatible solutes due to their excellent cytoprotective attributes. In addition, numerous biotechnological and biomedical applications for these compounds have been developed (Becker and Wittmann 2020; Czech et al. 2018a; Jorge et al. 2016; Kunte et al. 2014; Pastor et al. 2010). Ectoine was originally discovered by Galinski et al. (1985) in the halophilic phototrophic bacterium *Ectothiorhodospira halochloris* (Galinski et al. 1985; Schuh et al. 1985), followed by the discovery of its derivative 5-hydroxyectoine just a few years later in the soil bacterium *Streptomyces parvulus* (Inbar and Lapidot 1988). Ectoines are zwitter-ions in solutions of neutral pH. They are highly soluble in water [up to 4 M at 20 °C and up to 6 M at 4 °C (Schuh et al. 1985; Zaccai et al. 2016)], and affect the hydrogen bonding network of water on a local scale (Sahle et al. 2018). Molecular dynamics simulations and dielectric relaxation spectra predict strong hydrogen bonds formed between water and ectoine and 5-hydroxyectoine (i.e., seven and nine water molecules, respectively) (Eiberweiser et al. 2015; Smiatek et al. 2012).

Synthesis and import of ectoines contribute greatly to osmotic stress resistance in many microorganisms as their accumulation averts water loss and provides functional protection of cellular constituents and biosynthetic processes (Czech et al. 2018a; Galinski and Trüper 1994; Gunde-Cimerman et al. 2018; Kunte et al. 2014; Leon et al. 2018; Pastor et al. 2010; Reshetnikov et al. 2011a; Schwibbert et al. 2011). Moreover, ectoines can also serve as cytoprotectants for either cold- or heat-challenged cells (Bursy et al. 2008; Garcia-Estepa et al. 2006; Kuhlmann et al. 2008a, 2011; Malin and Lapidot 1996; Ma et al. 2017). However, the molecular underpinnings for their function as thermoprotectants are less well-understood; these probably depend on the chemical chaperone properties of ectoines. For instance, ectoines might stabilize a selected set of proteins crucial for temperature stress resistance or preserve vital biosynthetic processes (Bayles et al. 2000; Biran et al. 2018; Zhao et al. 2019). 5-Hydroxyectoine is also an excellent desiccation protectant (Manzanera et al. 2004), an attribute that probably depends on its enhanced ability to produce glasses in comparison with ectoine (Tanne et al. 2014).

Organisms that produce both ectoine and 5-hydroxyectoine often accumulate a mixture of these solutes, even though the ratio of the two ectoines can vary between species (Bursy et al. 2008; Czech et al. 2016; Pastor et al. 2010; Stöveken et al. 2011; Tao et al. 2016). Moreover, some microorganisms accumulate higher amounts of 5-hydroxectoine when they enter stationary growth phase (Saum and Müller 2008; Schiraldi et al. 2006; Seip et al. 2011; Tao et al. 2016). This observation points to superior stress-relieving properties of 5-hydroxyectoine for cells when nutrients become limiting, growth slows down, and cells face a multitude of new challenges (Hengge-Aronis 2002).

Phylogenomic distribution of ectoine-producing microorganisms among *Bacteria*

Although initially widely considered as rarely occurring microbial compatible solutes, the discovery of the ectoine (*ectABC*) (Louis and Galinski 1997) and 5-hydroxyectoine (*ectD*) biosynthetic genes (Bursy et al. 2007; Garcia-Estepa et al. 2006; Prabhu et al. 2004), coupled with an ever increasing availability of genome sequences, revealed the wide distribution of ectoines in members of the *Bacteria*. However, their occurrence in *Archaea* is restricted (Czech et al. 2018a; Kunte et al. 2014; Pastor et al. 2010; Widderich et al. 2016a) (Figure 2). Building on recent searches of the IMG/MER database of microbial genomes and metagenomic assemblies (Chen et al. 2019), and considering only fully sequenced bacterial and archaeal genomes (Czech et al. 2018a; Mais et al. 2020), the distribution of the ectoine biosynthetic genes in 8 850 fully sequenced genomes (8557 *Bacteria* and 293 *Archaea*) was assessed (Figure 2). In this dataset, 665 predicted ectoine producers originated from *Bacteria* while 11 representatives belong to

the *Archaea* (Supplementary Figure S1). This corresponds to an occurrence of ectoine biosynthetic genes in approximately 7.5% of all queried 8 850 fully sequenced microbial genomes. These numbers are for obvious reasons only fleeting snapshots. Given that incompletely sequenced microbial genomes and metagenomic sequences were not taken into account, it is highly likely that the number of microbial ectoine producers will considerably exceed the number derived from the inspection of only fully sequenced microbial genomes (Mais et al. 2020). Studies on the taxonomic affiliation of ectoine-synthesizing microorganisms revealed their presence in 10 bacterial and two archaeal phyla (Figure 2). This analysis also illustrates that the *ect* genes are not evenly distributed among members of the *Bacteria*: 38% are present in Actinobacteria, 6% are found in Bacilli, and 53% occur collectively in the *α*-, *β*-, and *γ*-Proteobacteria.

While ectoine producers are often referred to in the literature as either halophilic or at least halotolerant bacteria, a closer analysis of the habitats of the 676 ectoine synthesizing microorganisms shows that 7% are associated with habitats exhibiting extreme conditions, 18% are associated with marine habitats, 27% are found in terrestrial habitats, 38% represent microbes associated with various types of hosts, and 8% are even found in freshwater ecosystems (Mais et al. 2020). These numbers illustrate that microorganisms with rather different physiological attributes and growth characteristics can take advantage of ectoine synthesis to cope with environmental constrains (Supplementary Figure S1).

Phylogenomic distribution of ectoine-producing microorganisms in *Archaea*

It is well-known that many halophilic *Archaea* primarily use the salt-in osmostress response. They accumulate molar concentrations of potassium chloride on a permanent basis to balance the steep osmotic gradient across their cytoplasmic membrane. This strategy necessitated, on an evolutionarily timescale, the adjustment of the amino acid composition of the entire proteome in order to keep proteins soluble and functional (Gunde-Cimerman et al. 2018). However, there are also many *Archaea* that use the salt-out response when they adjust to high salinity/osmolarity environments and they synthesize a variety of compatible solutes, some of which also serve as excellent

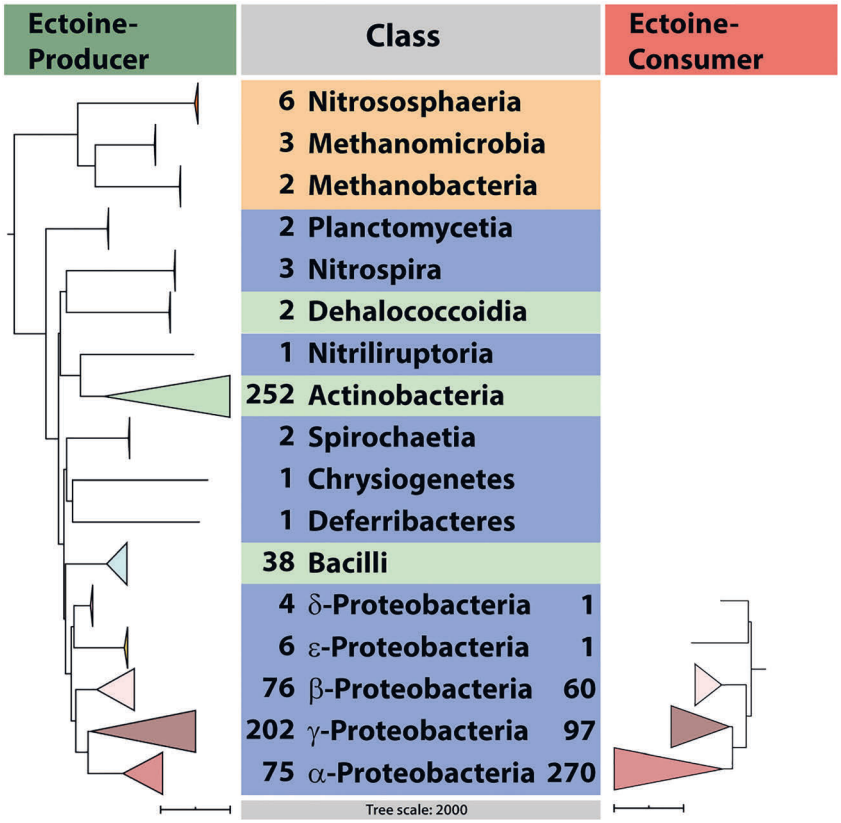

Figure 2: Phylogenetic distribution of ectoine-producing and ectoine–consuming microorganisms. The phylogenomic association of ectoine-producing and ectoine-consuming microorganisms was built on a recently reported data-set (Mais et al. 2020). In this dataset, 665 bacterial and 11 archaeal ectoine-producing microorganisms, and 429 ectoine consuming bacteria are represented. Collectively, in these 1105 microorganisms, 96 bacteria are found that both synthesize and consume ectoine. Ectoine producers were identified in the database search through the presence of the signature gene (*ectC*) for the ectoine synthase when juxtapositioned to other ectoine biosynthetic genes (*ectAB*) (Czech et al. 2018a, 2019a). Ectoine consuming bacteria were identified through the presence of juxtapositioned genes (*eutD*/*eutE*) for the central catabolic enzyme bi-module, the ectoine hydrolase (EutD) and the DABA-deacetylase (EutE) (Mais et al. 2020). For the studied 1105 microorganisms, 16S-rRNA data were collected and represented as collapsed clades. The scale is given as the number of changes between the corresponding DNA-sequences.

thermoprotectants (Müller et al. 2005; Roeßler and Müller 2001). Hence, the finding that some *Archaea* can synthesize ectoine (or 5-hydroxyectoine) is in principle per se not surprising (Widderich et al. 2016a).

Those *Archaea* that contain ectoine biosynthetic genes belong to the phyla of the Euryarchaeota and the Thaumarchaeota. Ectoine/5-hydroxyectoine production was experimentally verified in the Thamuarchaeon *Nitrosopumilus maritimus* (Widderich et al. 2016a). When one considers the ecophysiology of ectoine-producing *Archaea* identified in the previous database analysis in greater detail, one finds interesting environmental constrains that impinge on the ability to synthesize 5-hydroxyectoine, as the ectoine hydroxylase EctD is an oxygen-requiring enzyme (Bursy et al. 2007; Höppner et al. 2014; Widderich et al. 2014a). Accordingly, *ectD* is absent from the strict anaerobic Euryarchaeota, while it can be found in oxygen-tolerant nitrifying *Thaumarchaeota* (Widderich et al. 2016a). Interestingly, from the 81 *Thaumarchaeota* analyzed by Ren et al. (2019), only seven representatives possessed ectoine/5-hydroxyectoine biosynthetic genes and all of these archaea inhabit shallow ocean waters. In contrast, none of the *Thaumarchaeota* living either in deep ocean waters or in terrestrial habitats possessed ectoine biosynthetic genes (Ren et al. 2019).

Previously reported data suggest that *Archaea* containing ectoine biosynthetic genes probably have acquired them via horizontal gene transfer events (Widderich et al. 2014a, 2016a), a major driver of microbial evolution (Treangen and Rocha 2011). This conclusion was based on the finding of the signature enzyme of the ectoine biosynthetic route, the ectoine synthase EctC, in distant clades for the archaeal EctC proteins, while those derived from *Bacteria* consistently followed the phylogenetic association of the bacteria from which they were derived (Widderich et al. 2016a). We reinvestigated this issue by examining those EctC-containing *Archaea* whose genome sequences are currently available in the database of the National Center for Biotechnology Information (NCBI). Among the represented 1762 archaeal genomes, 40 presumably ectoine-producing *Archaea* were found: 10 were representatives of the *Thaumarchaeota*, 29 were *Euryarchaeota*, and a single representative of the *Crenarchaeota* was represented (Figure 3A). The phylogenomic uneven distribution of *ectC* is highlighted by the fact that among the 1762 archaeal genomes available through the NCBI database, 1155 originate from *Eury-achaeota*, yet only 29 genomes contained ectoine biosynthetic genes. This skewed distribution is also found for the *Thaumarchaeota* (10 *ectC*-containing genome sequences out of 128 database entries) and for the *Crenarchaeota* just a single *ectC*-containing genome sequence was detected out of 124 represented genomes.

We aligned the amino acid sequences of the aforementioned 40 archaeal EctC proteins with 591 bacterial EctC proteins and visualized the resulting data set through an EctC-based tree using bioinformatic resources provided by the iTOL suit (Letunic and Bork 2016). With a few exceptions, the bacterial EctC proteins followed in this type of analysis the taxonomic association of those microorganisms from which they were derived (Figure 3B). However, this was not true for the archaeal EctC proteins as these were present in three major, yet separate clusters (and five addition positions). Notably, two separate clusters of *Euryarchaeota* were present and that of the Thaumarchaeota even contained an EctC protein from the Euryarchaeon *Methanophagales* (Figure 3B). Although this type of analysis certainly does not formally prove the involvement of gene transfer events, horizontal gene transfer seems a plausible scenario for the evolution of those *Archaea* containing *ect* gene clusters. It is well known that transfer of bacterial genes into *Archaea* significantly contributed to the development and expansion of this major domain of life (Wang et al. 2019).

Biochemistry and structural biology of ectoine biosynthesis

The overall route and enzymes for the synthesis of ectoine and 5-hydroxyectoine are known for some time (Bursy et al. 2007; Ono et al. 1999; Peters et al. 1990; Reshetnikov et al. 2011b) (Figure 4). Biosynthesis of ectoines is an energy-demanding process. Calculations by A. Oren (1999) suggest that the production of just a single ectoine molecule requires the expenditure of about 40 ATP equivalents. This calculation considers the entire production route of ectoine in cells growing heterotrophically with glucose at the sole carbon and energy source. The metabolism of glucose would otherwise yield 38 ATP-equivalents and two additional ATP-equivalents have to be spent to produce a single ectoine molecule from the biosynthetic precursor L-asparate-β-semialdehyde via the EctABC enzymes (Oren 1999). Hence, in these calculations, the vast majority of the spent ATP equivalents are required for the synthesis of the ectoine precursor L-asparate-β-semialdehyde. Energetic calculations based on a theoretical metabolic network analysis of *Halomonas elongata* suggest that either (i) an energetically neutral or (ii) an even one ATP-generating route can also be considered (Schwibbert et al. 2011). By growing *H. elongata* continuously in a calorimeter with

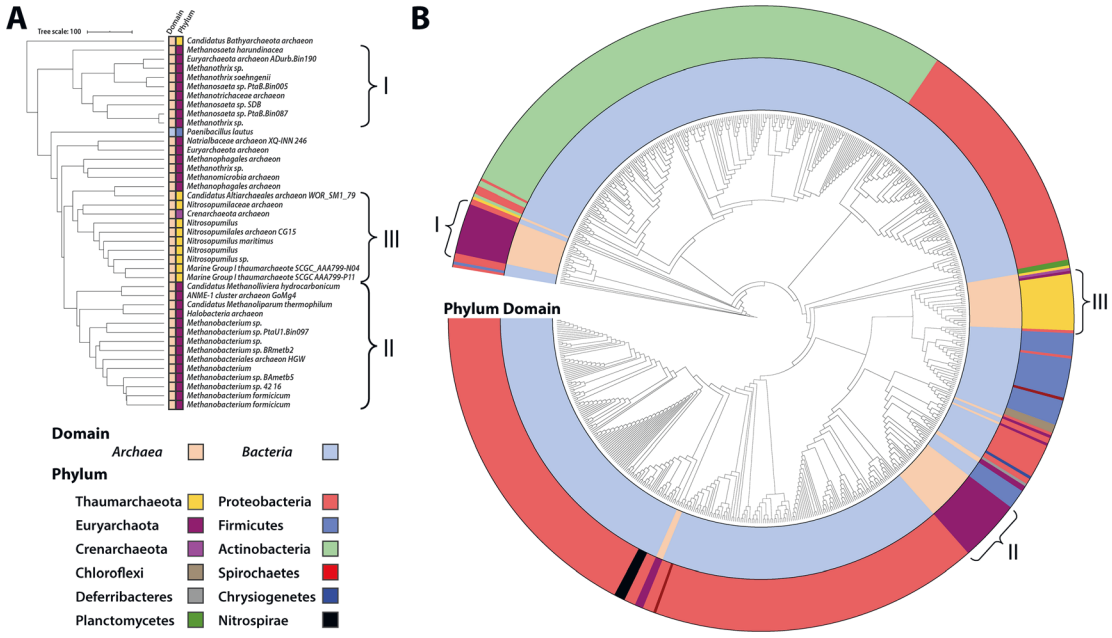

Figure 3: Phylogenetic analysis of EctC-type proteins. (A) 40 EctC-type proteins from *Archaea* were identified in the NCBI database using the EctC ectoine synthase from *Paenibacillus* lautus as the search query. The amino acid sequences of these proteins were aligned using Clustal O (Sievers et al. 2011) and the data from this alignment are graphically represented using the iTOL tool (Letunic and Bork 2016). Phylogenetic affiliations of microorganisms to different phyla are shown by color-code as listed in the figure. The scale of the tree is given as amino acid changes between the sequences. (B) The 40 archaeal EctC-type proteins found in the NCBI database were added to the previously assembled dataset of EctC-type proteins by Czech et al. (2018). The protein sequences were aligned with Clustal O (Sievers et al. 2011) and graphically represented with the iTOL tool (Letunic and Bork 2016). Phylogenetic affiliations of microorganisms to different domains and phyla are shown by color-code as listed at the bottom of the Figure. For simplicity, the names of the *ectC*-possessing microorganisms were left out.

glucose as the carbon and energy source, an approximately 100% efficiency for the conversion of the substrate glucose into ectoine was achievable (Maskow and Babel 2001).

Great strides have recently been made in our understanding of this biosynthetic process through a detailed biochemical and structural analysis of all enzymes involved in ectoine/5-hydroxyectoine production. In the following sections, we summarize our structural and biochemical understanding of the enzymes forming the biosynthetic pathway for ectoine and its derivative 5-hydroxyectoine (Figure 4, left side).

Making the precursor for ectoine biosynthesis

L-aspartate-β-semialdehyde is a central metabolic hub that feeds a branched network for the biosynthesis of several amino acids, the production of crucial components of the peptidoglycan and of the spore coat, and the synthesis of antibiotics (Lo et al. 2009). L-aspartate-β-semialdehyde is also the precursor for the synthesis of ectoine (Ono et al. 1999; Peters et al. 1990) (Figure 4). Two enzymes are involved in L-aspartate-β-semialdehyde production from L-glutamate, the aspartate kinase (Ask) (EC 2.7.2.4) and the aspartate-semialdehyde-dehydrogenase (Asd) (EC 1.2.1.11). Ask catalyzes the ATP-dependent phosphorylation of L-Aspartate to yield ADP and L-aspartyl-β-phosphate, the latter of which then undergoes a reductive dephosphorylation in a NADP-dependent reaction to form L-aspartate-β-semialdehyde (Figure 4).

We know of only one ectoine/5-hydroxyectoine biosynthetic gene cluster in which genes for Ask and Asd enzymes are jointly present (Czech et al. 2018a; Widderich et al. 2014a). This gene cluster (*ask_ect-asd-ectABCD*) is found in *Kytococcus sedentarius*, a marine, strictly aerobic Gram-positive bacterium (Sims et al. 2009). Using molecular modeling, we have visualized the overall fold of the *K. sedentarius* Ask and Asd enzymes using the crystal structure of the Ask protein from *Synechocystis* sp. PCC 6803 (PDB accession code: 3L76) and that of the Asd protein from *Mycobacterium tuberculosis* (PDB accession code: 3TZ6) as templates (Robin et al. 2010; Vyas et al. 2012). The Ask_Ect and Asd proteins from *K. sedentarius* are both predicted to form homo-dimers (Figure 5).

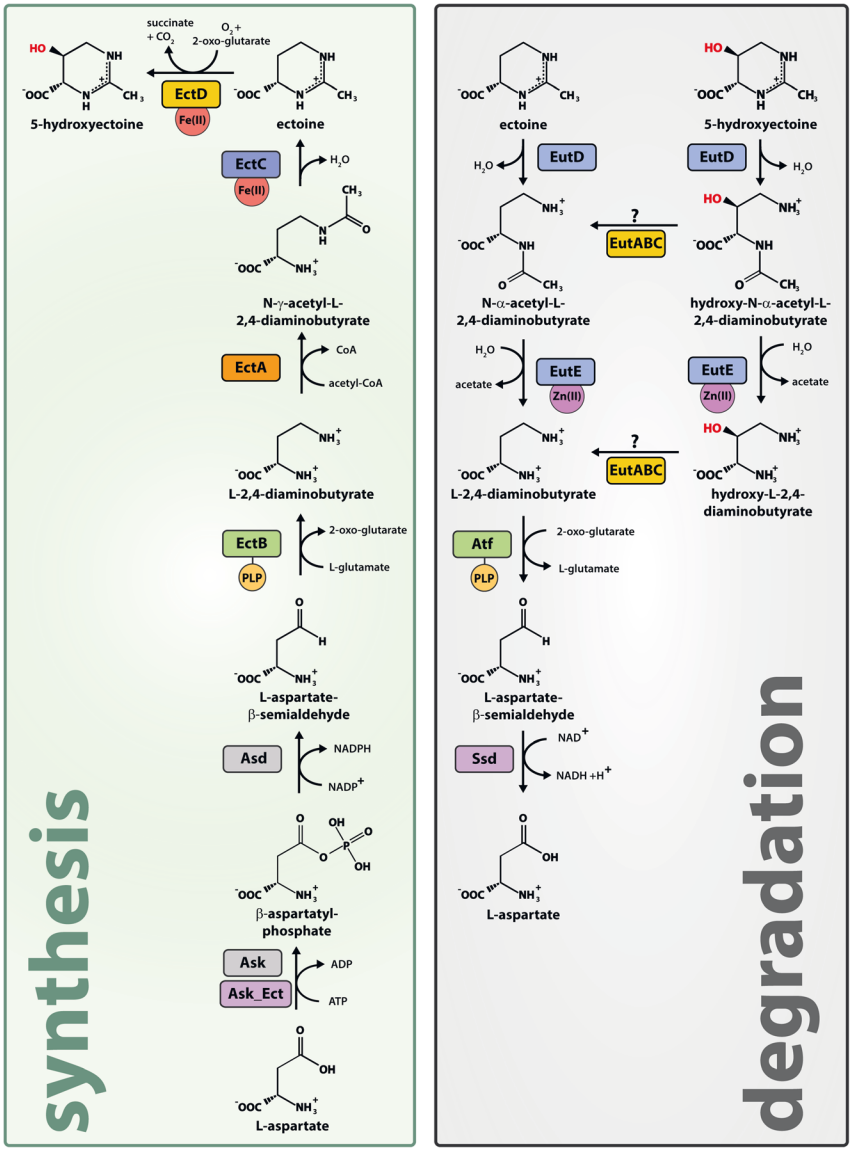

Figure 4: Ectoine metabolism. The green and grey boxes show the pathways enabling biosynthesis and degradation of ectoine/5-hydroxyectoine, respectively. Both can be thought as opposites of one another. Note: The biosynthesis pathway employs γ-ADABA as unique intermediate, while the degradation pathway relies on the α-ADABA. As discussed in the text, the latter isomer is critical for the genetic regulation of ectoine metabolism.

While a gene for Asd is typically absent from *ect* biosynthetic gene clusters, many contain a gene for a specialized aspartokinase (Ask_Ect) (Czech et al. 2018a; Lo et al. 2009; Reshetnikov et al. 2006; Widderich et al. 2014a). Within the super-family of aspartokinases, Ask_Ect-type enzymes form a separate branch and its representatives are mainly found in the Alpha-, Gamma- and Delta-Proteobacteria (Lo et al. 2009). Aspartokinases are enzymes with a complex allosteric activity control (Lo et al. 2009), and this is also true for Ask_Ect (Stöveken et al. 2011). A considerable number of microorganisms contain genes for multiple aspartokinases, and as exemplified by Ask_Ect, some of which then serve specialized biosynthetic routes (Lo et al. 2009). Often, multiple *ask* genes present in a given bacterium are also subject to different types of genetic regulation thereby tying enhanced synthesis of specialized Ask enzymes to the needs of the particular biosynthetic route they assist (Lo et al. 2009).

In an assessment of the gene content of 582 *ect* biosynthetic gene clusters, 23% (133) possessed an associated *ask_ect* gene (Czech et al. 2018a). It thus appears that while a specialized aspartokinase seems to be beneficial for ectoine/5-hydroxyectoine production (Bestvater et al. 2008; Stöveken et al. 2011), its presence is certainly not a pre-requisite to achieve adequate osmostress-protective levels of ectoines through synthesis. However, as *ask_ect* genes are co-expressed along with the ectoine/5-hydroxyectoine biosynthetic genes, osmotically stressed cells will ramp-up the production of this specialized aspartokinases enabling them to seemingly avoid a

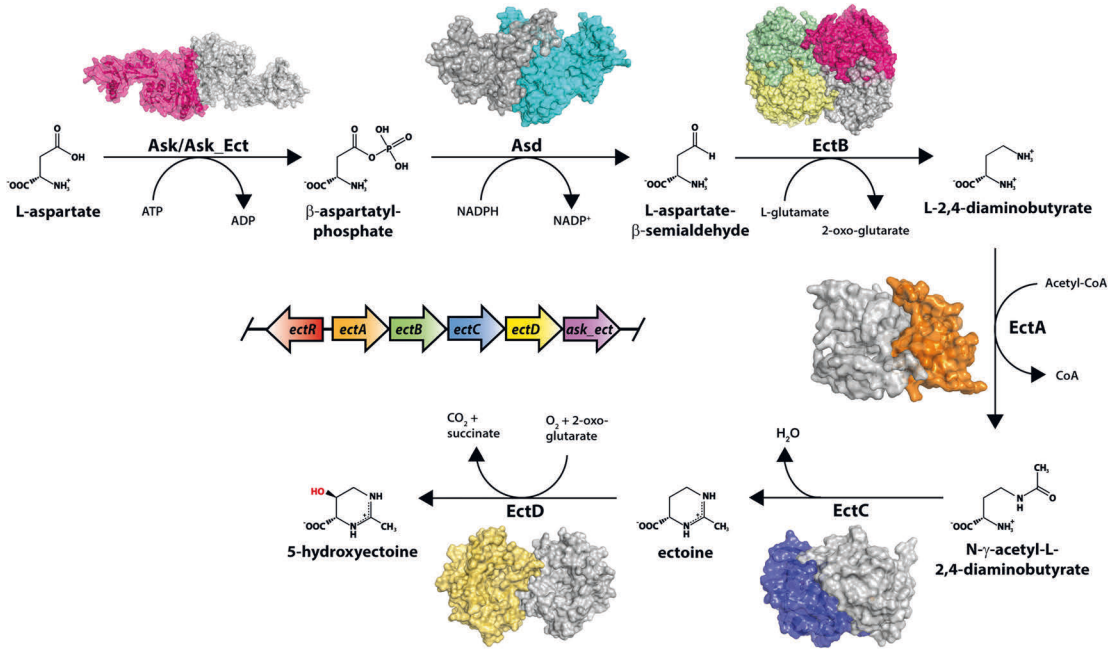

Figure 5: Structural enzymology of ectoine/5-hydroxyectoine biosynthesis. L-aspartate is transformed to ß-aspartylphosphate by either a general aspartokinase (Ask), or a specialized aspartokinases (Ask_Ect) (Stöveken et al. 2011). The shown structure of the Ask_Ect from *K. sedentarius*, a marine actinobacterium and opportunistic pathogen (Sims et al. 2009), was modeled on a crystallized aspartate kinase from *Synechocystis* sp. PCC 6803 (PDB: 3L76) (Robin et al. 2010). The intermediate ß-aspartylphosphate is then further transformed to L-aspartate-ß-semialdehyde by an aspartate semialdehyde dehydrogenase (Asd). The Asd protein originating from the *ect* cluster of *K. sedentarius* was modeled on the aspartate semialdehyde dehydrogenase from *M. tuberculosis* (PDB: 3TZ6) (Vyas et al. 2012). The ectoine/5-hydroxyectoine biosynthetic gene cluster (*ask_ect-asd-ectABCD*) from *K. sedentarius* is the only one of which we are aware in which the genes for the two enzymes required for the synthesis of the ectoine biosynthetic precursor, L-aspartate-ß-semialdehyde, are jointly present. L-2,4-diaminobutyric acid (DABA) aminotransferase EctB: (PDB: 6RL5); DABA-acetyltransferase EctA (PDB: 6SLL); ectoine synthase EctC (PDB: 5ONM), ectoine hydroxylase EctD (PDB: 4Q5O). Details on the features of these crystal structures are given in Table 1. In the middle of the figure, the genetic organization of the *ect* gene cluster from *Acidiphilium cryptum* is shown (Moritz et al. 2015). The *ectR* gene (shown in red) encodes a MarR-type repressor protein (EctR) that is involved in the transcriptional control of a considerable number of ectoine biosynthetic gene clusters (Czech et al. 2018a; Mustakhimov et al. 2010).

metabolic bottleneck for the supply of the ectoine biosynthetic precursor L-aspartate-β-semialdehyde (Figure 5). Indeed, the productivity of a heterologous *Escherichia coli* cell factory carrying the *Pseudomonas stutzeri* A1501 *ectABCD-ask_ect* operon cluster was notably higher when the *ask_ect* gene was present on the recombinant plasmid (Stöveken et al. 2011). Such a beneficial effect on ectoine production had also been seen when the *Marinococcus halophilus ectABC* genes were co-expressed in *E. coli* along with the gene for a feed-back resistant Ask_LysC enzyme derived from *Corynebacterium glutamicum* (Bestvater et al. 2008). A feed-back resistant Ask_LysC is also part of the genomic chassis of the current ectoine-producing champion (65 g L^{-1}), a synthetic cell factory of the industrial workhorse *C. glutamicum* (Becker et al. 2013; Giesselmann et al. 2019).

The Ask_Ect enzyme from the plant roots associated bacterium *P. stutzeri* A1501 is so far the only representative of this specialized group of aspartokinases that has been studied biochemically at any level of detail (Stöveken et al. 2011). The Ask_Ect enzyme and that of the only other aspartokinase (Ask_LysC) present in from *P. stutzeri* A1501 possess an amino acid sequence identity of 25% and display a different domain organization, thereby reflecting membership of the two Ask proteins in different subgroups of the Ask enzyme superfamily (Lo et al. 2009). When biochemically benchmarked against each other, comparable kinetic parameters for the two enzymes were found, both with respect to the K_m and V_{max} values for their substrates L-aspartate and ATP (e.g., the K_m for L-aspartate were about 22 mM for Ask_Lys and 30 mM for the Ask_Ect enzyme; the corresponding V_{max} values were about 5 U mg^{-1} and about 7 U mg^{-1}, respectively) (Stöveken et al. 2011). These enzyme activities are comparable to those of other biochemically characterized microbial aspartokinases (Lo et al. 2009).

Most notably were the differences in the allosteric control of Ask_LysC and Ask_Ect. Ask_LysC was feed-back inhibited by L-threonine and in a concerted fashion by L-threonine and L-lysine, while Ask_Ect was only inhibited by L-threonine. The two enzymes additionally differed in their allosteric control when they were assayed in the presence of high concentrations of salts (KCl, NaCl). High salt concentrations reduced the allosteric inhibition Ask_Ect by L-threonine, as the IC_{50} value was increased from 3.6 to 18.7 mM and 13.5 mM in the presence of 650 mM NaCl or KCl, respectively (Stöveken et al. 2011). This behavior of the Ask_Ect enzyme might be relevant under temporary suddenly increased ionic strength conditions in the cytoplasm of osmotically stressed ectoine-producing cells. Remarkably, the feed-back inhibition of Ask-LysC enzyme activity by either L-threonine alone, or a combination of L-threonine and L-lysine, was not influenced by high concentrations of either KCl or NaCl (Stöveken et al. 2011).

The L-2,4-diaminobutyrate transaminase: EctB

The first step of ectoine biosynthesis is catalyzed by the L-2,4-diaminobutyrate transaminase, EctB (EC 2.6.1.76) (Figure 4). EctB uses L-glutamate as the amino donor and L-aspartate-β-semialdehyde as the acceptor molecule to form 2-oxoglutarate and diamino-butyric acid (DABA), the latter serving as substrate for EctA (Hillier et al. 2020; Ono et al. 1999; Reshetnikov et al. 2011b; Richter et al. 2019) (Figure 4). EctB enzymes belong to the pyridoxal-5′-phosphate (PLP)-dependent transaminases (also referred to in the literature as aminotransferases) (Steffen-Munsberg et al. 2015), with the γ-aminobutyrate transaminase (GABA-TA) being the closest homologue (Bruce et al. 2012; Richter et al. 2019). Indeed, EctB from the thermotolerant Gram-positive bacterium *Paenibacillus lautus* possesses a residual GABA-TA activity (Richter et al. 2019). Structural, computational and biochemical analysis of EctB proteins from the Gram-negative bacterium *Chromohalobacter salexigens* and from *P. lautus*, show that the protein forms tetramers (Hillier et al. 2020; Richter et al. 2019) (Figure 5). Earlier biochemical studies on the *H. elongata* and *Methylomicrobium alcaliphilum* EctB enzymes suggested that these proteins form hexamers (Ono et al. 1999; Reshetnikov et al. 2006, 2011b). In the structure of the *C. salexigens* EctB tetramer (Table 1) (Figure 6A), each of the monomers carries a PLP molecule covalently attached to a Lys residue (Hillier et al. 2020) (Supplementary Figure S2). PLP is critical for enzyme function as substitution of this Lys residue with amino acid residues unable to covalently bind PLP yielded enzymatically inactive variants of the *P. lautus* EctB protein (Richter et al. 2019).

Structural analysis of *C. salexigens* EctB also revealed the molecular determinants required for the interactions of the monomers in the tetrameric assembly, including the positioning of a gating loop that aids the proper formation of the active site of the neighboring monomer (Hillier et al. 2020) (Supplementary Figure S2). Transaminases are known to possess two binding pockets for the amino donor and the acceptor molecule that are required for catalytic

Table 1: Structures of ectoine and 5-hydroxyectoine biosynthetic enzymes.

Enzyme (EC number)	Ligand	PDB accession	Resolution	Organism	References
EctA	apo	6SLK	2.2 Å	*P. lautus*	(Richter et al. 2020)
(2.3.1.178)	CoA	6SK1	1.5 Å	*P. lautus*	(Richter et al. 2020)
	DABA – CoA	6SLL	1.2 Å	*P. lautus*	(Richter et al. 2020)
	DABA	6SL8	1.5 Å	*P. lautus*	(Richter et al. 2020)
	N-γ-ADABA	6SJY	2.2 Å	*P. lautus*	(Richter et al. 2020)
EctB (2.6.1.76)	PLP	6RL5	2.5 Å	*C. salexigens*	(Hillier et al. 2020)
EctC (4.2.1.108)	apo; semi-closed	5BXX	2.0 Å	*S. alaskensis*	(Widderich et al. 2016b)
	1,2-Propanediol; open	5BY5	1.2 Å	*S. alaskensis*	(Widderich et al. 2016b)
	Fe(III)	5ONM	1.52 Å	*P. lautus*	(Czech et al. 2019a)
	Fe(III); *N*-γ-ADABA	5ONN	1.4 Å	*P. lautus*	(Czech et al. 2019a)
	Fe(III); ectoine	5ONO	2.5 Å	*P. lautus*	(Czech et al. 2019a)
EctD	Fe(III)	3EMR	1.9 Å	*V. salexigens*	(Reuter et al. 2010)
(1.14.11.55)	apo	4MHR	2.1 Å	*S. alaskensis*	(Höppner et al. 2014)
	Fe(III)	4MHU	2.6 Å	*S. alaskensis*	(Höppner et al. 2014)
	Fe(III); 2-oxoglutarat; 5-hydroxyectoine	4Q5O	1.6 Å	*S. alaskensis*	(Höppner et al. 2014)

The abbreviations used are: CoA: Coenzyme A; DABA: diaminobutyric acid; *N*-γ-ADABA: *N*-γ-acetyl-diaminobutyric acid; PLP: pyridoxal-5-phosphate.

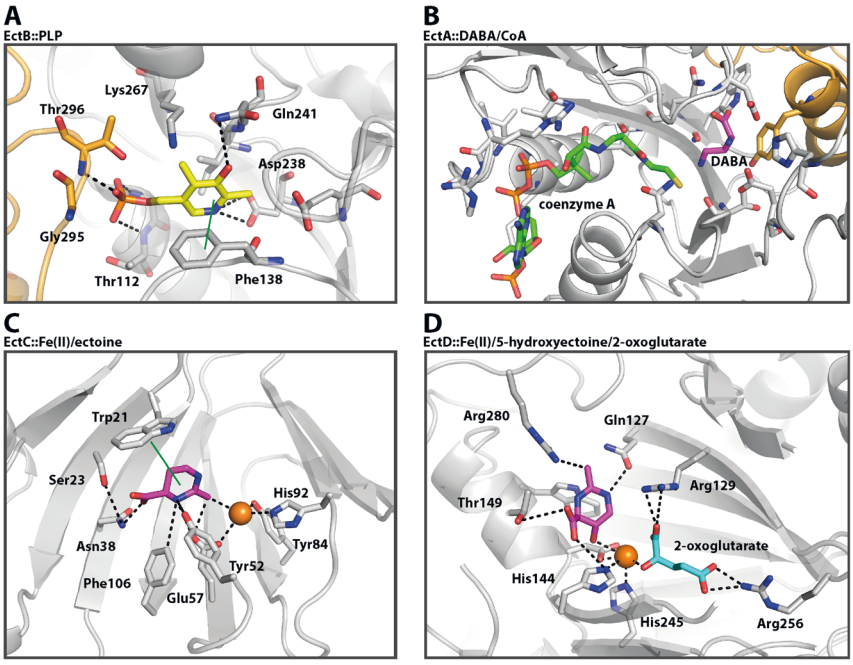

Figure 6: Structural views into the active sites of ectoine/5-hydroxyectoine biosynthetic enzymes. (A) The crystal structure of the dimeric EctB enzyme from *C. salexigens* was solved in complex with the cofactor PLP (yellow sticks) which is tightly coordinated by amino acid residues originating from both monomers, highlighted as orange (monomer 1) and grey sticks (monomer 2) (PDB: 6RL5) (Hillier et al. 2020). (B) The EctA enzyme from *P. lautus* was crystallized in complex with DAB (PDB: 6SL8) and CoA (PDB: 6SK1). An overlay of both structures with CoA depicted as green and DAB as pink sticks is shown. The DAB binding site also involves a Tyr-residue from the second monomer (shown as an orange stick) (Richter et al. 2020). (C) The ectoine synthase EctC from *P. lautus* is shown in complex with ectoine (pink sticks); the amino acid residues involved in ectoine and iron binding are shown as sticks and iron is represented by an orange sphere (PDB: 5ONO) (Czech et al. 2019a). (D) The ectoine hydroxylase, EctD, from *S. alaskensis* is depicted in complex with the reaction production 5-hydroxyectoine (pink sticks) and the co-substrate 2-oxoglutarate (blue sticks). Amino acids involved in ligand binding are shown as grey sticks, and the iron catalyst is represented by an orange sphere (PDB: 4Q5O) (Höppner et al. 2014).

activity (Steffen-Munsberg et al. 2015). The crystal structure of the *C. salexigens* EctB protein provides the first detailed description of the architecture of these binding sites of L-2,4-diaminobutyrate transaminase that are involved in ectoine production (Hillier et al. 2020). However, so far crystal structures in complex with the substrates (L-glutamate as the amino donor and L-aspartate-β-semialdehyde as the amino acceptor), or the reaction products (2-oxoglutarate and DABA) are not available. Such structures are highly desirable as they should further strengthen our understanding of the catalytic activity of EctB.

The diaminobutyrate acetyltransferase: EctA

The second step in ectoine biosynthesis is catalyzed by L-2,4-diaminobutuyrate acetyltransferase (EC 2.3.1.178), EctA (Figure 4). This enzyme catalyzes the acetylation of L-2,4-diaminobutyric acid (DABA) into *N*-γ-acetyl-L-2,4-diaminobutyric acid (*N*-γ-ADABA) in an acetyl-CoA-dependent manner. EctA belongs to the GCN5-related *N*-acetyltransferases (GNAT) (Salah Ud-Din et al. 2016; Vetting et al. 2005). High-resolution X-ray structures of the dimeric EctA from *P. lautus* in its apo-, substrate, and co-substrate-bound forms have recently been reported, and a crystal structure trapping the reaction product of EctA, *N*-γ-ADABA, has also been obtained (Richter et al. 2020) (Table 1). These crystal structures, combined with biochemical analysis, clarified the entire reaction mechanism catalyzed by the EctA enzyme. The enzyme activity of the homodimeric *P. lautus* EctA protein (Figure 5) is highly region-specific as it produces exclusively *N*-γ-ADABA but not the isomer *N*-α-ADABA (Richter et al. 2020), a crucial metabolite formed during ectoine catabolism (see below).

In the apo-form of the enzyme, the binding sites for the substrate DABA and the co-substrate acetyl-CoA are present in an "open" conformation. In this structure, there is a surface-exposed extended tunnel in which acetyl-CoA will bind, and a deep cavity in which DABA will be bound (Supplementary Figure S3). In the secondary complexes of the *P. lautus* EctA protein [*Pl*EctA::CoA and *Pl*EctB::DABA] (Figure 6B), the chemical groups of the substrate and of the co-substrate involved in the acetylation reaction point towards each other. A structure with *N*-γ-ADABA was also captured (Richter et al. 2020) (Supplementary Figure S3). While keeping in mind that crystal structures only provide snapshots of "trapped states" of proteins, the superimposable positions of DABA and *N*-γ-ADABA in the active site suggest that the backbone of the EctA protein and the amino acid side chains relevant for substrate, co-substrate and product binding do not move substantially during enzyme catalysis. An overlay of the *Pl*EctA::DABA and *Pl*EctA::CoA structures revealed a distance of less than 3 Å between the sulfur atom of the CoA molecule and the

reactive nitrogen in the γ-position of DABA. Hence, these two crystal structures probably represent stages of the L-2,4-diaminobutuyrate acetyltransferase prior to catalysis (Richter et al. 2020). Because acetyl-CoA is highly reactive, the non-reactive CoA was purposely used in the crystallization of EctA. However, when the thiol hydrogen of CoA was substituted *in silico* with an acetyl group, it became clear how close the reactive groups of acetyl-CoA and DABA are juxtapositioned just before the transfer of the acetyl group to DABA occurs (Supplementary Figure S3). Collectively, the obtained five crystal structures of the *P. lautus* EctA protein (Table 1) allowed the rendering of a movie capturing the various enzymatic steps of the L-2,4-diaminobutuyrate acetyltransferase conducted between the binding of the substrate and co-substrate and the formation of the reaction product (Richter et al. 2020).

The ectoine synthase: EctC

The ectoine synthase EctC (EC 4.2.1.108) uses the EctA-produced *N*-γ-ADABA to synthesize ectoine in an iron-dependent cyclo-condensation reaction in which a water molecule is eliminated (Czech et al. 2019a; Widderich et al. 2016b) (Figure 4). Specifically, EctC cyclizes the linear *N*-γ-ADABA molecule through a nucleophilic attack on the alpha amino nitrogen positioned at the terminal carbonyl group of the substrate (Czech et al. 2019a; Ono et al. 1999; Witt et al. 2011). High-resolution crystal structures of EctC proteins from the cold-adapted bacterium *Sphingopyxis alaskensis* and the thermotolerant bacterium *P. lautus*, have been reported in the absence or presence of various ligands (Czech et al. 2019a; Widderich et al. 2016b) (Table 1). The crystal structures of the EctC protein from both microorganisms show that the ectoine synthase belongs to the cupin super-family (Figure 5). These type of proteins are characterized by barrel-like structures in which the catalytically important residues protrude into the lumen of the barrel (Dunwell et al. 2004) (Supplementary Figure S4). Most of these proteins contain catalytically important divalent transition state metals (e.g., iron, copper, zinc, manganese, cobalt, nickel), allowing the imposition of different types of chemical reactions onto a common structural fold (Dunwell et al. 2004). The EctC protein forms homodimers with a 'head-to-tail' configuration through backbone-contacts and weak hydrophobic interactions mediated by two beta-sheets within each monomer (Widderich et al. 2016b; Czech et al. 2019a). Crystal structures of *P. lautus* EctC in its iron-bound, iron- and substrate (*N*-γ-ADABA)-bound and in the presence of its reaction product ectoine (Figure 6C) have been determined (Table 1) (Supplementary Figure S4), which enabled reconstruction of its catalytic cycle (Czech et al. 2019a). The *N*-γ-ADABA substrate appears in these structures an in extended configuration, rather than in a pre-bent form that would facilitate the EctC-mediated cyclo-condensation reaction (Czech et al. 2019a) (Figure 5). Residues critical for iron coordination, *N*-γ-ADABA- and ectoine-binding are evolutionarily highly conserved, and their mutation leads to EctC variants with only residual catalytic activity (Czech et al. 2019a; Widderich et al. 2016b).

In a slow side-reaction, EctC can also produce the synthetic compatible solute 5-amino-3,4-dihydro-2H-pyrrole-2-carboxylate (ADPC) by cyclic condensation of glutamine (Witt et al. 2011). Import of ADPC by an osmotically sensitive *H. elongata* mutant affords osmostress resistance. ADPC also possesses effective chemical chaperone activity for a model enzyme subjected to denaturing repeated freeze-thaw cycles (Witt et al. 2011). Of note is also that the substrate for the ectoine synthase, *N*-γ-ADABA, is an osmostress protectant and function-preserving compatible solute in its own right (Canovas et al. 1999).

EctC can be regarded as the signature enzyme for ectoine biosynthesis, because EctB-related transaminases and EctA-related acetyl-transferases have counterparts in other metabolic pathways of microbes. Database searches using EctC as the query protein can thus be used to identify *bona fide* ectoine biosynthetic gene clusters with confidence (Czech et al. 2018a; Leon et al. 2018; Widderich et al. 2014a). However, EctC-type proteins can also be found in microorganisms either lacking the *ectAB* genes or containing *ectC*-type gene copies in addition to complete *ectABC(D)* operons. Orphan *ectC*-type genes were first identified in the plant pathogen *Pseudomonas syringae* pv. *syringae* (Kurz et al. 2010). In an EctC-based phylogenetic tree, the orphan EctC-type proteins are found in a separate group located at the root of the tree representing a taxonomically rather heterogeneous assemblage of microorganisms (Czech et al. 2018a). *bona fide* EctC proteins and their orphan counterparts share considerable amino acid sequence identity (around 40%) with essentially all amino acid residues critical for substrate and metal binding being conserved. However, the physiological role of orphan EctC-type proteins awaits biochemical clarification.

The ectoine hydroxylase: EctD

EctD (EC 1.14.11.55) catalyzes the iron-dependent hydroxylation of ectoine into its 5-hydroxylated counterpart using molecular oxygen and 2-oxoglutarate as the substrates. In addition to 5-hydroxyectoine, EctD also forms CO_2 and

succinate as products during catalysis (Figure 4). EctD proteins form 'head-to-tail' arranged homo-dimers in solution (Figure 5) and in various crystal structures (Table 1) (Höppner et al. 2014; Reuter et al. 2010; Widderich et al. 2014a). Crystal structures of the ectoine hydroxylase from the salt-tolerant bacterium *Virgibacillus salexigens* and the cold-adapted marine bacterium *S. alaskensis* in its apo-form, and various ligands have been reported (Höppner et al. 2014; Reuter et al. 2010). One of these structures jointly contained the iron catalyst, the co-substrate 2-oxoglutarate, and the reaction product 5-hydroxyectoine (Figure 6D). Collectively, the crystallographic analysis, coupled with site-directed mutagenesis and molecular dynamics simulations, exposed an intricate network of interactions between the enzyme and its ligands that ensures the placing of ectoine within the active site such that its hydroxylation can occur in a precise position- and stereo-specific manner (Höppner et al. 2014).

The overall fold of EctD consists of a double-stranded β-sheet core surrounded and stabilized by a number of α-helices (Supplementary Figure S5). This core, also known as the jelly role or cupin fold (Aik et al. 2012; Hangasky et al. 2013; Islam et al. 2018), is formed by two four-stranded anti-parallel β-sheets that are arranged in the form of a *β*-sandwich. The two monomers in the EctD dimer assembly interact via amino acid residues located in extended loop areas (Höppner et al. 2014). These structural characteristics also assign EctD to the cupin super-family (Höppner et al. 2014; Reuter et al. 2010). Ectoine hydroxylases contain an evolutionarily highly conserved signature sequence consisting of a continuous stretch of 17 amino acids (F-X-W-H-S-D-F-E-T-W-H-X-E-D-G-M/L-P). This segment is structurally and functionally important as it spans an extended α-helix and a linked short β-sheet lining one side of the cupin barrel. It harbors five residues involved in the binding of the iron catalysts, the co-substrate 2-oxoglutarate, and the reaction product 5-hydroxyectoine (Höppner et al. 2014; Reuter et al. 2010; Widderich et al. 2014a). Furthermore, it can be used as a signature sequence to distinguish *bona fide* ectoine hydroxylases from other members of the widely distributed non-heme-containing iron (II) and 2-oxoglutarate-dependent family dioxygenases, as *bona fide* ectoine hydroxylases are often miss-annotated in microbial genome sequences as phytanoly-CoA dioxygenases.

EctD belongs to the sub-family of non-heme-containing iron (II) and 2-oxoglutarate-dependent dioxygenases (Aik et al. 2012; Dunwell et al. 2004; Hangasky et al. 2013; Islam et al. 2018). These types of enzymes carry out a remarkably broad range of oxidative reactions on a variety of substrates, yet common enzyme reaction mechanisms are observed. Most of these types of dioxygenases couple a two-electron oxidation of their substrates with the chemical reactivity of oxygen and 2-oxoglutarate (Hangasky et al. 2013; Herr and Hausinger 2018; Islam et al. 2018). The ectoine hydroxylase adheres to this general reaction scheme (Widderich et al. 2014b) and seems to closely follow in its catalytic cycle that of the biochemically and structurally intensively studied archetypical non-heme-containing iron (II) and 2-oxoglutarate-dependent dioxygenase, the taurine dioxygenase TauD (Proshlyakov et al. 2017).

Within the cupin domain of EctD, the iron atom coordinates through two conserved histidines and an aspartate (Höppner et al. 2014; Reuter et al. 2010) (Figure 6D). These residues belong to the structurally conserved *H-X-(D/E)…H* motif, the so-called '2-His-1-carboxylate facial triad', forming a type of mononuclear iron center found in many members of the dioxygenase superfamily (Aik et al. 2012; Hangasky et al. 2013). The 2-oxoidic group of the co-substrate 2-oxoglutarate locates in close vicinity to the iron catalysts (Höppner et al. 2014) (Supplementary Figure S6). The 5-hydroxyectoine molecule found in the *S. alaskensis* EctD structure (PDB: 4Q5O) (Table 1) is bound slightly above the three residues forming the iron binding site with its hydroxyl group at C-5 in the heteropyrimidine ring pointing towards the iron catalysts. It is also positioned in close vicinity of the co-substrate 2-oxoglutarate, thereby resembling its expected orientation in the active site cavity after the enzymatic hydroxylation of ectoine by EctD (Höppner et al. 2014).

The EctD-mediated hydroxylation of ectoine occurs in a precise position and stereospecific manner yielding exclusively, both *in vivo* and *in vitro*, (4*S*,5*S*)-2-methyl-5-hydroxy-1,4,5,6-tetrahydropyrimidine-4-carboxylic acid (=5-hydroxyectoine) (Bursy et al. 2007; Czech et al. 2016; Inbar and Lapidot 1988; Inbar et al. 1993). So far, nine ectoine hydroxylases have been characterized biochemically, including enzymes from various extremophilic *Bacteria* and also one protein from a marine archaeon (*Nitrosopumilus maritimus*) (Bursy et al. 2007; Reuter et al. 2010; Widderich et al. 2014a, 2016a). These enzymes seemed to possess similar kinetic parameters, but the subsequent optimization of assay conditions for individual enzymes revealed significant differences in their catalytic efficiency (Czech et al. 2019b). This aspect becomes important when the catalytic efficiency and robustness of ectoine hydroxylases are benchmarked against each other when EctD enzymes are used in chemical biology approaches to hydroxylate substrates other than ectoine (Czech et al. 2016, 2019b; Galinski et al. 2009; Hara et al. 2019).

As a mark of their evolutionary history, many enzymes exhibit a certain degree of substrate ambiguity. This

metabolic profile, also referred to as underground metabolism, can be exploited by microbial cells to develop novel functions (D'Ari and Casadesus 1998; Jensen 1976). Recent studies have already exploited the substrate promiscuity of the EctD enzyme towards ectoine-related substrates; e. g., aiming at the selective hydroxylation of L-proline and of the synthetic ectoine derivative homoectoine (Czech et al. 2019b; Galinski et al. 2009; Hara et al. 2019). Hence, ectoine hydroxylases have already found interesting uses in chemical biology.

Catabolism of ectoine and 5-hydroxyectoine

Ecophysiological role of ectoines as nutrients

Synthesis of compatible solutes such as the ectoines requires considerable biosynthetic and energetic resources (Oren 1999) (see above). It is thus not surprising that microorganisms have found ways to re-use these compounds when they are no longer needed as osmostress protectants (Welsh 2000). Compatible solutes are released into the environment through the transient opening of mechanosensitive channels when producer cells are subjected to a rapid osmotic down-shift (Booth 2014). Microorganisms also excrete compatible solutes under steady-state high osmolarity growth conditions, perhaps in an effort to fine-tune turgor (Czech et al. 2016, 2018b; Grammann et al. 2002; Hoffmann et al. 2012; Lamark et al. 1992; Vandrich et al. 2020). An ecophysiologically important process for the release of compatible solutes into the environment is also cell lysis; e.g., after the attack of ectoine producers by lytic phages (Van Goethem et al. 2019). Combined, these processes can shape the ecophysiology of microbial communities and the high turn-over of compatible solutes in the soil indicates their rapid re-use in natural settings (Warren 2019).

Use of ectoines as nutrients has been described for various microorganisms (Reshetnikov et al. 2020; Schulz et al. 2017b; Schwibbert et al. 2011; Vargas et al. 2006). Indeed, free ectoines have been found in various ecosystems; e.g., in the soil and in the effluent of an acid mine (Bouskill et al. 2016; Mosier et al. 2013). Since compatible solutes are present in the environment in very low concentrations, high affinity transporters are needed to scavenge them for their use as nutrients. So far, two substrate-inducible uptake systems for environmental ectoines have been studied that supply these nitrogen-rich molecules (Figure 1) to the cell for catabolism. These are EhuABCD and UehABC, representatives of binding-protein-dependent ABC-transporters (Ehu) and tripartite ATP-independent periplasmic transporters (TRAP-T) (Ueh), respectively (Hanekop et al. 2007; Jebbar et al. 2005; Lecher et al. 2009) (Supplementary Figure S6). EhuB and UehA, the periplasmic high-affinity substrate-binding proteins have been crystalized in the presence of ectoines, thereby revealing the molecular determinants for the efficient capturing of environmental ectoines by transporters (Hanekop et al. 2007; Lecher et al. 2009) (Supplementary Figure S6). The osmotically inducible TeaABC transporter form *H. elongata*, a system closely related to the TRAP-T UehABC system from *Ruegeria pomeroyi*, not only serves for the import of ectoines as osmostress protectants and as a recycling systems for newly synthesized and excreted ectoines (Grammann et al. 2002; Kuhlmann et al. 2008b; Vandrich et al. 2020) but it might also be used for their acquisition as nutrients (Schwibbert et al. 2011).

Phylogenomics of ectoine and hydroxyectoine catabolic genes

Building on the inspection of 8557 bacterial and 293 archaeal completely sequenced genomes, Mais et al. (2020) recently identified 429 potential ectoine/5-hydroxyectoine consumers (Mais et al. 2020) (Figure 2). These were recognized through the presence of adjacent genes (*eutD*/*eutE*) for the ectoine hydrolase (EutD) (EC 3.5.4.44) and the *N*-acetyl-2,4-diaminobutyric acid (*α*-ADABA) deacetylase (EutE) (EC 3.5.1.125). These two proteins form the central enzyme bi-module for the catabolism of ectoines (Mais et al. 2020; Reshetnikov et al. 2020; Schulz et al. 2017b; Schwibbert et al. 2011) (Figure 4). None of the potential ectoine/5-hydroxyectoine consumers belong to the domain of the *Archaea*, and those found in the *Bacteria* are all members of the super-phylum of the Proteobacteria (Figure 2). The data on the predicted ectoine/5-hydroxyectoine consumers compiled by Mais et al. (2020) are constrained by the used database search criterion [adjacently located *eutD-eutE* genes] and thereby miss the detection of those ectoine/5-hydroxyectoine catabolic gene clusters in which these two genes are not juxtapositioned; e.g., those from *M. alcaliphilum* (Figure 7A) and related species (Reshetnikov et al. 2020). Given that ectoine/5-hydroxyectoine catabolic gene clusters are quite variable in gene order and content (Figure 7A), microorganisms that consume ectoines might occur more frequently than suggested (Mais et al. 2020).

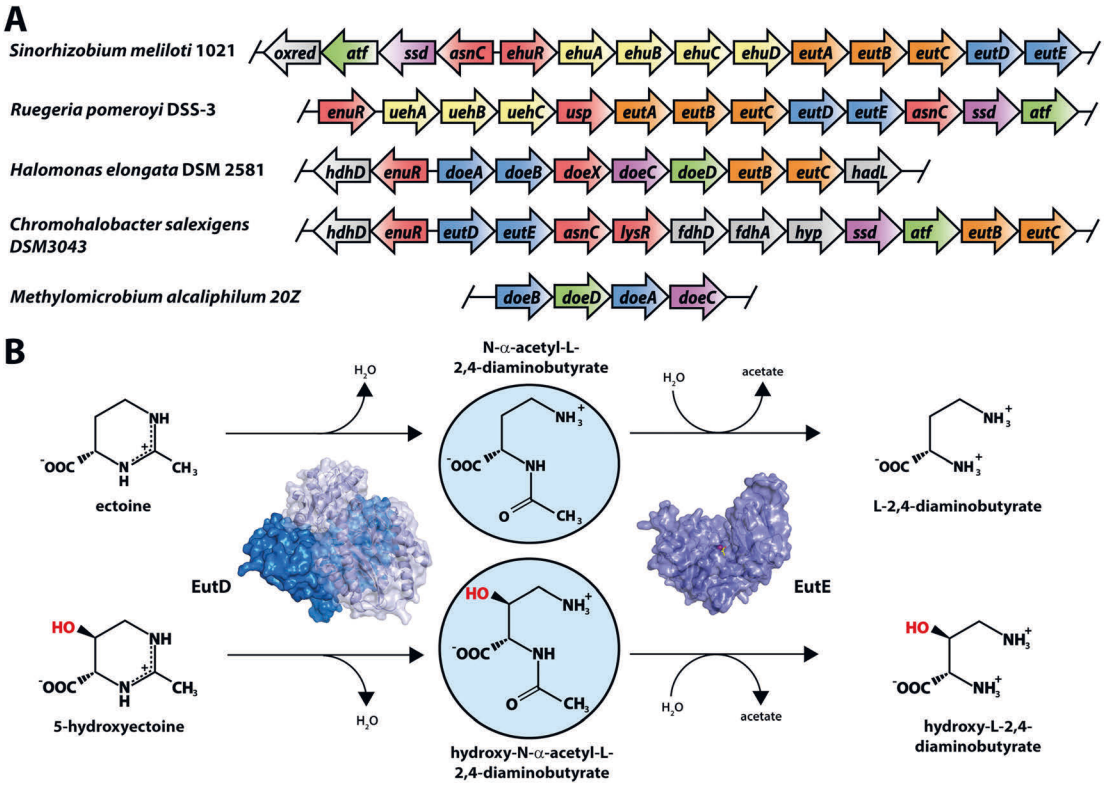

Figure 7: Genetic organization and structural enzymology of ectoine catabolism. (A) Schematic illustration of the ectoine catabolic gene clusters from *S. meliloti* (Jebbar et al. 2005), *H. elongata* (Schwibbert et al. 2011), *C. salexigens* (Vargas et al. 2006), *R. pomeroyi* (Schulz et al. 2017b) and *M. alcaliphilum* (Reshetnikov et al. 2020). (B) Pathway for the catabolism of ectoine via *N*-α-acetyl-L-2,4-diaminobutyrate to L-2,4-diaminobutyrate and for the degradation of 5-hydroxyectoine via hydroxy-*N*-α-acetyl-L-2,4-diaminobutyrat to hydroxy-L-2,4-diaminobutyrate. EutD: ectoine/5-hydroxyectoine hydrolase; EutE: *N*-α-acetyl-L-2,4-diaminobutyrate/hydroxy-*N*-α-acetyl-L-2,4-diaminobutyrat deacetylase. The crystal structures of the *H. elongata* EutD protein in complex with ectoine and the Glu-255-ADABA adduct (PDB: 6TWK) was used to visualize the dimeric protein assembly. The crystal structure of the *R. pomeroyi* EutE ADABA deacetylase in complex with the reaction products DABA and acetate (PDB: 6TWM) was used to visualize the monomeric protein. Mais et al. (2020) reported all mentioned crystal structures of the EutD and EutE proteins and details on the features of these crystal structures are given in Table 2.

Bacteria that can both synthesize and catabolize ectoine (Figure 2) represent a minority (9.5%) among the analyzed microorganisms, as most can either only synthesize or only consume ectoines. A closer inspection of the phylogenetic association of those bacteria capable to produce and to consume ectoines revealed that they are primarily represented in members of the Oceanospirillales, Vibrionales, and Rhodobacteriales (Supplementary Figure S1). Hence, a substantial fraction (41%) of bacteria predicted to produce and consume ectoines, live in marine habitats.

Genetics of ectoine and 5-hydroxyectoine degradation

An inroad into a molecular understanding of ectoine catabolism was provided by a pioneering proteomics study conducted by Jebbar et al. (2005) focusing on ectoine-inducible proteins from the plant roots-associated bacterium *Sinorhizobium meliloti* (Jebbar et al. 2005). These data promoted the identification of orthologous genes in other ectoine-consuming microorganisms; e.g., *H. elongata*, *C. salexigens*, *R. pomeroyi*, and *M. alcaliphilum* (Reshetnikov et al. 2020; Schulz et al., 2017b; Schwibbert et al. 2011; Vargas et al. 2006). In contrast to the core ectoine biosynthetic genes (*ectABC*) that are mainly found in an evolutionarily conserved operon (Czech et al. 2018a), those encoding ectoine/5-hydroxyectoine catabolic genes are highly variable with respect to both gene order and content (Jebbar et al. 2005; Reshetnikov et al. 2020; Schulz et al. 2017b; Schwibbert et al. 2011; Vargas et al. 2006) (Figure 7A).

The following basic information can be gleaned from the inspection of the various catabolic gene clusters: (i) Most of these clusters are rather large, while that from *M. alcaliphilum* seems to represent a minimal catabolic module (Reshetnikov et al. 2020). For the large gene cluster

from *R. pomeroyi*, co-transcription of the various genes (13.5 kbp) has been demonstrated (Schulz et al. 2017b); (ii) Not even the gene clusters from the phylogenetically very closely related species *H. elongata* and *C. salexigens* are identical (Copeland et al. 2011; Schwibbert et al. 2011); (iii) Some of the four large gene clusters contain genes not present in all of them; (iv) Only the gene clusters from *S. meliloti* and *R. pomeroyi* contain genes for ectoine/5-hydroxyectoine-specific transporters but the two encoded systems belong to different transporter families (Hanekop et al. 2007; Lecher et al. 2009); (v) The number and types of regulatory proteins differ between the various gene clusters (Figure 6A).

Structural enzymology of ectoine and 5-hydroxyectoine degradation

Concerted ectoine degradation by the EutD/EutE hydrolase-deacetylase complex

Organisms able to degrade ectoine, employ two enzymes, the ectoine hydrolase EutD and the *N*-acetyl-L-2,4-diaminobutyrate deacetylase EutE (Mais et al. 2020) [also referred to as DoeA and DoeB, respectively (Schwibbert et al. 2011)] (Figure 7B). These two enzymes degrade ectoine/5-hydroxyectoine into acetate and diaminobutyric acid (DABA). The resulting EutD/EutE enzyme reaction product DABA can then be further metabolized to L-aspartate by the Atf aminotransferase and the Ssd dehydrogenase (Schulz et al. 2017b; Schwibbert et al. 2011) (Figure 4). Importantly, α-ADABA, but not the major EctC substrate γ-ADABA, is the central intermediate of the concerted reactions of the ectoine hydrolase EutD and the deacetylase EutE (Mais et al. 2020). This is physiologically important, as α-ADABA, but not γ-ADABA, serves as internal inducer for ectoine/5-hydroxyectoine catabolic gene clusters regulated by the widely distributed EnuR repressor protein (Schulz et al. 2017a).

In the following sections, we summarize our structural and biochemical understanding of the enzymes making-up the pathway for the degradation of ectoines (Figure 4, *right side*).

The ectoine hydrolase: EutD

EutD (EC 3.5.4.44) reversibly catalyzes the initial step of ectoine degradation, which is the opening of the heteropyrimidine ring (Figure 7B). High-resolution crystal structures of the apo, substrate- and product-bound states of the EutD protein from *H. elongata* (*He*EutD) have been solved (Mais et al. 2020) (Table 2). These structures show that EutD forms a highly intertwined homodimer (Figure 7B) with both active sites being approximately 30 Å apart from each other (Mais et al. 2020) (Supplementary Figure S7). Each EutD monomer can be subdivided into a α-helical N-terminal domain and a C-terminal domain exhibiting a typical pita-bread fold (Bazan et al. 1994), consisting of two antiparallel β-sheets. The active site of EutD is accommodated in the center of these β-sheets, with the N-terminal domain of the opposing chain forming a lid on top of the active site. This pita-bread fold is well known from the related protein family of M24 amino-peptidases, whose enzyme activity typically depends on two highly coordinated metals (Rawlings and Barrett 1993). However, in the case of the EutD hydrolase, no metals are incorporated in the active site, as residues not suitable for metal ion coordination have replaced most of those residues typically involved in metal-coordination in M24-type amino-peptidases (Rawlings and Barrett 1993). Instead, the active site of EutD has evolved to specifically accommodate the cyclic substrate ectoine (Mais et al. 2020) (Figure 8A).

Structural analysis of the EutD homodimer in the presence of its ectoine substrate showed the ectoine substrate in one active site and the α-ADABA product covalently bound to a conserved glutamate in the other (Figure 8A,B). In the ectoine-bound active site, a water molecule hydrogen-bonded to His-238, can be found in a distance of 4 Å to the methyl group-bearing carbon of ectoine (Figure 8A). This water molecule, activated by its coordinating histidine residue might perform a nucleophilic attack on the ectoine molecule, leading to the cleavage of the heteropyrimidine ring. The EutD-mediated ring cleavage results in α-ADABA, which is covalently linked to the carboxyl side chain of Glu-255 in the other active site of the EutD homodimer. Moreover, the Glu-255-α-ADABA adduct is stabilized in the EutD active site by interactions with His-238 and Asp-338 in the active site of monomer_II (Figure 8B). Thus, structural analysis supported by mutational analysis visualized the catalytic mechanism by which EutD cleaves the ectoines ring resulting in the formation of an unusual covalent EutD-α-ADABA intermediate (Figure 8B).

The structural analysis of the ectoine hydrolase also shows that both active sites within the EutD homodimer signal their catalytic progress to each other. This communication is enabled by Tyr-52 at the N-terminus of one monomer, which protrudes into the active site of the other (and *vice versa*) to sense the catalytic state of the partnering

Table 2: Structures of ectoine and 5-hydroxyectoine degrading enzymes.

Enzyme (EC number)	Ligand	PDB accession	Resolution	Organism	References
EutD (3.5.4.44)	apo	6TWJ	2.2 Å	*H. elongata*	(Mais et al. 2020)
	ectoine; Glu255-ADABA	6TWK	2.3 Å	*H. elongata*	(Mais et al. 2020)
	N-α-ADABA; Glu255-ADABA	6YO9	2.4 Å	*H. elongata*	(Mais et al. 2020)
EutE (3.5.1.125)	apo	6TWL	2.0 Å	*R. pomeroyi*	(Mais et al. 2020)
	DABA, acetate	6TWM	2.5 Å	*R. pomeroyi*	(Mais et al. 2020)

The abbreviations used are: *N*-α-acetyl-L-2,4-diaminobutyric acid (*N*-α-ADABA); L-2,4-diaminobutyric acid (DABA).

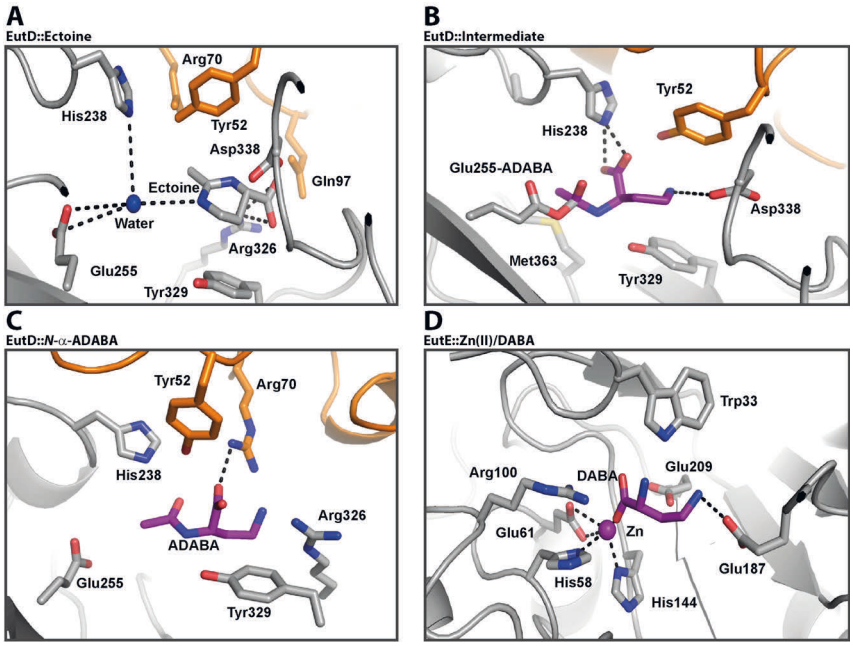

Figure 8: Structural views into the active sites of ectoine/5-hydroxyectoine degrading enzymes. (A) Architecture of the *H. elongata* ectoine/5-hydroxyectoine hydrolase (EutD). The active site_I of the dimeric EutD enzyme is shown in complex with ectoine. EutD accommodates a catalytically active water molecule by hydrogen bonds to His-238. The substrate ectoine is kept in place by hydrogen bonds to Arg-326 (PDB: 6TWK). (B) A view into the active site_II of the *H. elongata* EutD protein subsequent to ectoine hydrolysis and formation of the Glu-255-ADABA adduct. This covalent intermediate is tethered via an orthoester-like bond to the amino acid side chain of Glu-255 (PDB: 6TWK). (C) In the backward reaction of the *H. elongata* EutD enzyme (α-ADABA was provided during crystallization), the Glu-255-ADABA adduct is found in one active site of the dimer (not shown), and the second active site contains a free ADABA molecule. ADABA is coordinated by hydrogen bonds to Arg-70 (PDB: 6YO9). (D) Architecture of the *R. pomeroyi* ADABA deacetylase (EutE) active site in complex with the reaction product DABA. Crystals of EutE were grown in the presence of the EutD reaction product α-ADABA. The active site of EutE harbors a zinc-ion bound to Glu-61, His-58 and His-144. DABA coordinates to the zinc metal and hydrogen bonds to Glu-178 (PDB: 6TWM). Mais et al. (2020) reported the crystal structures of the EutD and EutE proteins.

monomer in the EutD homodimer assembly (Figure 8A–C). Superimposition of the two active sites of the EutD homodimer revealed a noticeable movement of the loop harboring Tyr-52. This movement of the "signaling loop", in turn, leads to other conformational changes in the N-terminal domain of the ectoine hydrolase (Mais et al. 2020). It can thus be imagined that the way in which the two EutD catalytic sites communicate through structural changes will aid cooperativity during the catalytic cycle (Figure 8A–C). The critical role of Tyr-52 for the communication of the two active sites in the EutD homodimer is supported by the finding that substituting Tyr-52 by alanine abolishes enzymatic activity of the ectoine hydrolase (Mais et al. 2020).

The crystal structure of EutD obtained in the presence of its reaction product α-ADABA (Figure 4) showed the same Glu-255-α-ADABA adduct observed when ectoine was supplied as the substrate (Figure 8B), while the other active site contained a free α-ADABA molecule (Figure 8C). In this crystal structure, α-ADABA is primarily hydrogen-bonded to Arg-70 from the N-terminal domain of the opposing EutD chain (Mais et al. 2020). Collectively, these two structures further supported the reversible character of the EutD-mediated cleavage of ectoine. Reversibility of the EutD-mediated reaction seems to be the reason why efficient ectoine degradation can only occur in the presence of EutE, which deacetylates α-ADABA irreversibly.

The *N*-acetyl-L-2,4-diaminobutyrate deacetylase: EutE

The *N*-acetyl-L-2,4-diaminobutyrate deacetylase EutE (EC 3.5.1.125) converts α-ADABA into DABA (Mais et al. 2020;

Schulz et al. 2017b; Schwibbert et al. 2011) (Figure 4). Biochemical analysis of the *R. pomeroyi* EutE enzyme demonstrated that EutE exclusively processes *N*-α-ADABA in an highly efficient manner, while its isomer γ-ADABA, the substrate of the ectoine synthase (Czech et al. 2019a), cannot be deacetylated (Mais et al. 2020) (Figure 8C) (Supplementary Figure S8). These data are consistent with reports on the properties of the corresponding *H. elongata* enzyme (Schwibbert et al. 2011).

Crystal structures of EutE from *R. pomeroyi* are available in the apo state and bound to its products DABA and acetate (Table 2) (Mais et al. 2020), revealing structural homology to asparto-acylases (Le Coq et al. 2008). Conserved features among these types of enzymes are the crescent-like shape with two distinct subdomains (Figure 7B) and a zinc-binding site formed one Glu and two His residues (Figure 8D) (Mais et al. 2020). The products of *N*-α-ADABA deacetylation, DABA and acetate, both coordinate the central zinc-atom in the active site of the EutE enzyme with their carboxyl moieties. Comparison of the EutE crystal structure to asparto-acylases, which have been crystalized in presence of a substrate-mimic (Le Coq et al. 2008), as well as mutational analysis of EutE, hint that Arg-111 is most likely hydrogen bonding the second carboxyl moiety of *N*-α-ADABA, while Asp-195 hydrogen bonds the amine group, thus fixating the substrate in the enzyme reaction chamber. During the hydrolysis of *N*-α-ADABA, which proceeds via a tetrahedral transition state, the guanidinium moiety of Arg-100 (Figure 8D) further compensates the emerging negative charge (Mais et al. 2020).

We would like to note that EutE forms stable hexamers in solution when substrates, products and the catalytically essential zinc ion are absent (Mais et al. 2020). However, our crystallographic analysis did not support such a ternary assembly as all crystallographic contacts appear of non-biologically relevant nature. Therefore, we suggested that the active form of EutE is a monomer (Mais et al. 2020). Whether the observed EutE hexamer in solution is of functional relevance or simply a concentration artifact remains to be determined.

Heterologous production of the EutD hydrolase from *R. pomeroyi* and *M. alcaliphilum* in *E. coli* in the presence of ectoine yielded exclusively *N*-α-ADABA and, when the *Rp*EutD enzyme was exposed *in vivo* to 5-hydroxyectoine, also hydroxy-*N*-α-ADABA (Mais et al. 2020; Reshetnikov et al. 2020). In contrast, the heterologous production of the EutD (DoeA) hydrolase from *H. elongata* seemingly yielded both α- and γ-ADABA, with the apparent use of *N*-γ-ADABA for a new round of ectoine synthesis via EctC in *H. elongata* (Schwibbert et al. 2011). Hence, the catalytic profile of the ectoine hydrolase from *M. alcaliphilum* and *H. elongata* seem to differ, despite the fact that both extremophiles can consume and produce ectoine (Reshetnikov et al. 2020; Schwibbert et al., 2011).

Topology of the ectoine/5-hydroxyectoine catabolic route

In a study that specifically addressed the catabolism of 5-hydroxyectoine, Schulz et al. (2017) suggested that the use of this compound as nutrient would require the initial removal of the hydroxyl group by the EutABC enzymes to form ectoine (Schulz et al. 2017a,b). Consistent with this hypothesis was the finding that an *eutABC* deletion of the *R. pomeroyi* catabolic gene cluster abolished the use of 5-hydroxyectoine but not that of ectoine (Schulz et al. 2017b). However, the finding of Mais et al. (2020) that the *Rp*EutD hydrolase can also open the heteropyrimidine ring of 5-hydroxyectoine to form hydroxy-*N*-α-ADABA (Figure 8B) requires a re-interpretation of the data reported by Schulz et al. (2017). Rather than being initially involved in removing the hydroxyl group from the 5-hydroxyectoine ring, the growth defect of the *R. pomeroyi eutABC* deletion mutant on 5-hydroxyectoine as the carbon source suggests now a role of either all, or at least some, of the EutABC proteins in the down-stream metabolic procession of the EutD- or EutD/EutE-formed metabolites (Figure 4).

The EutABC enzymes are currently annotated in the *R. pomeroyi* genome sequence as Asp/Glu/hydantoine racemase (EutA), as L-threonine ammonia lyase (EutB), and as ornithine cyclodeaminase (EutC) (Moran et al. 2004). Hence, the EutB/EutC enzymes might contribute at the level of the hydroxy-*N*-α-ADABA intermediate to the catabolism of 5-hydroxyectoine (Figure 4). EutB shares significant homology to the PLP-dependent group of threonine dehydratases. Hence, it seems possible that EutB removes the hydroxyl moiety from hydroxy-*N*-α-ADABA, and this novel intermediate could then be reduced by EutC in a NADPH-dependent manner to yield *N*-α-ADABA. *N*-α-ADABA would then serve as a *bona-fide* substrate for the EutE deacetylase (Figure 4). Interestingly, a pair of functionally related enzymes (BhcB and BhcD) operates in a similar manner in the widely distributed β-hydroxyaspartate pathway of microorganisms (Schada von Borzyskowski et al. 2019). The role of EutA in such a scheme remains uncertain and different entry points of the EutABC enzymes into the overall 5-hydroxyectoine catabolic rout remain a possibility (Figure 4). Notably, there exist a considerable number of ectoine/5-hydroxyectoine catabolic gene clusters that lack *eutA* (Mais et al. 2020; Schulz

et al. 2017b), indicating the ectoine/5-hydroxyectoine catabolic route might not be identical in microorganisms consuming ectoines.

Genetic regulation of ectoine metabolism - lessons from structural enzymology?

Reflecting the major function of ectoines as osmostress protectants, the transcription of *ect* biosynthetic gene clusters is typically strongly up-regulated when cells experience either sudden or sustained high osmolarity (Czech et al., 2018a; Kunte et al. 2014; Pastor et al. 2010). However, the molecular underpinnings of the signal transduction process that emanates from the increase in the environmental osmolarity and eventually determines the transcriptional activity of promoters for ectoine biosynthetic genes has largely remained enigmatic [for references and a critical discussion of the literature related this issue see (Czech et al. 2018a)].

Data from the detailed molecular analysis of the *ect* promoter from the plant roots-associated bacterium *P. stutzeri* A1501 are however noteworthy in this context (Czech et al. 2018b). Transcriptional activity, and hence ectoine production, of this *ect* promoter is linearly dependent on the degree of the imposed osmotic stress, implying that the cell can detect and react to incremental increases in environmental osmolarity. This transcription pattern of the *P. stutzeri ect* promoter was fully replicated in the non ectoine producing surrogate host bacterium *E. coli*. Furthermore, osmotic induction was still preserved when the G/C-rich -10 region of the *ect* promoter was mutated to a perfect sigma-70-type promoter that is typically A/T-rich (Czech et al. 2018b). Taken together, these data suggest that osmotic regulation seems to be an inherent feature of the promoter elements, the spacer and flanking regions.

However, in some organisms regulatory proteins have been shown to be involved in the regulation of the ectoine biosynthetic genes, such as the MarR-type regulators EctR from *M. alcaliphilum* (Mustakhimov et al. 2010) or CosR from *Vibrio cholera* (Gregory et al. 2019, 2020; Shikuma et al. 2013). Interestingly, for CosR ionic strength has been proposed as the key factor determining its DNA-binding activity (Shikuma et al. 2013). In the case of EctR, its genetic inactivation increased *ect* transcription notably but osmoregulation of this gene cluster was maintained (Mustakhimov et al. 2010). However, it remains unknown, which factors trigger EctR binding and release from the DNA. In *Streptomyces coelicolor* the global regulator for nitrogen metabolism, GlnR, also serves as a repressor for the expression of the ectoine/5-hydroxyectoine biosynthetic genes (Shao et al. 2015). This finding, links the genetic control of nitrogen metabolism in *Streptomycetes* with the regulation of a gene cluster encoding the enzymes for the synthesis of the nitrogen-rich ectoines (Bursy et al. 2008; Kol et al. 2010).

In contrast to osmotic control the biosynthetic gene clusters (Czech et al. 2018a), expression of the catabolic gene clusters [at least for the two that have been studied in more detail (e.g., *S. meliloti* and *R. pomeroyi*)], is substrate inducible. Their transcription is strongly up-regulated when ectoines are present in the growth medium (Jebbar et al. 2005; Schulz et al. 2017a; Yu et al. 2017) but ectoines are not the true inducers (see below) (Schulz et al. 2017a). Most inspected ectoine/5-hydroxyectoine catabolic gene clusters [456 out of 539 (Schulz et al. 2017a);] contain a gene encoding a member (EhuR/EnuR) of the MocR/GabR-family of transcriptional regulators (Tramonti et al. 2018). Detailed studies on the EhuR/EnuR regulatory proteins from *S. meliloti* and *R. pomeroyi* identified the degradation intermediates *N*-α-ADABA and DABA as system-specific inducers and ligands for EhuR/EnuR (Schulz et al. 2017a; Yu et al. 2017). MocR/GabR-type regulators typically consist of a N-terminal winged-helix-turn-helix DNA-reading head connected via a long and highly flexible linker to a C-terminal aminotransferase domain of fold I (Edayathumangalam et al. 2013; Tramonti et al. 2018). The aminotransferase domain does not possess enzymatic function; instead the chemistry of a covalently bound PLP in a reaction with a systems-specific low-molecular-weight effector molecule triggers a conformational change affecting DNA binding (Edayathumangalam et al. 2013; Frezzini et al. 2020; Tramonti et al. 2018; Wu et al. 2017).

In EnuR, the PLP cofactor is covalently bound to Lys-302 forming an internal aldimine. The formation of the intermediate of ectoine degradation *N*-α-ADABA in cells catabolizing ectoine results in the binding of *N*-α-ADABA, or DABA, to PLP thereby forming an external aldimine (Schulz et al. 2017a). These chemical reactions trigger a conformational change of the EnuR regulator, and concurrently relieves the transcriptional repression of the ectoine/5-hydroxyectoine catabolic gene cluster. The replacement of Lys-302 with an amino acid residue to which PLP cannot be covalently attached transforms the mutant EnuR protein into a super-repressor that no longer responds to its ectoine-derived internal inducers (Schulz et al. 2017a). Physiologically important is the fact that in contrast to the specific ectoine metabolite *N*-α-ADABA, *N*-γ-ADABA, the major substrate of the ectoine synthase EctC (Czech et al. 2019a), does not serve as an inducer of the catabolic genes (Schulz et al. 2017a).

It has recently been found that the hydroxylated forms of *N*-α-ADABA and DABA are selectively generated during the EutD-mediated hydrolysis of 5-hydroxyectoine (Mais et al. 2020) (Figure 4). Because external 5-hydroxyectoine is a strong inducer of the *R. pomeroyi* ectoine/5-hydroxyectoine catabolic genes (Schulz et al. 2017a), it seems plausible that hydroxy-*N*-α-ADABA and hydroxy-DABA will also serve as internal inducers for the EnuR repressor.

Many ectoine/5-hydroxyectoine catabolic gene clusters also contain a gene (*asnC*/*doeX*) (Figure 7A) for a member of the feast and famine family of transcriptional regulators (Schulz et al. 2017a; Schwibbert et al. 2011; Yokoyama et al. 2006). These types of proteins can wrap DNA into nucleosome-like structures and frequently respond in their DNA-binding activity to low-molecular weight effector molecules (e.g., amino acids) (Dey et al. 2016; Kumarevel et al. 2008; Shrivastava and Ramachandran 2007). Schwibbert et al. (2011) showed that such an AsnC-type protein (referred to by these authors as DeoX) targets DNA sequences located at or in the vicinity of the promoter for the *H. elongata* ectoine/5-hydroxyectoine catabolic gene cluster (Schwibbert et al. 2011). Notably, AsnC serves as an activator for the *R. pomeroyi* import and catabolic gene cluster and its loss abolished the use of ectoine as sole carbon but not as sole nitrogen source (Schulz et al. 2017a). Details of the structure and genetic mode of action of the DoeX- and AsnC-type proteins still need to be worked out and their effector molecule(s) must be identified. An educated guess would suggest that these regulatory proteins would bind either ectoines or metabolites derived from them as effectors.

Perspectives and open questions

Marking the 35th anniversary of the seminal discovery of the major microbial cytoprotectant ectoine (Galinski et al. 1985) and the detection of its derivative 5-hydroxyectoine just a few years later (Inbar and Lapidot 1988), a complete structural view and an in-depth biochemical understanding of the ectoine/5-hydroxyectoine biosynthetic route is now available (Figure 5). Not only are ectoines excellent cytoprotectants (Czech et al. 2018a; Pastor et al. 2010) but these natural products are also of considerable commercial value (Becker and Wittmann 2020; Kunte et al. 2014). Innovative uses of laboratory evolution experiments, site-directed mutagenesis, exploits of ectoine-responsive biosensors (Chen et al. 2015), and synthetic microbiology approaches (Giesselmann et al. 2019) should aid further improvements in the productivity of synthetic or natural cell factories for ectoine and 5-hydroxyectoine. The changes resulting from such experiments can then be correlated to specific changes in either regulatory DNA sequences or features of the ectoine/5-hydroxyectoine biosynthetic enzymes, to further illuminate the salient genetic and biochemical features of the ectoine/5-hydroxyectoine biosynthetic route required for the optimal synthesis of these commercially valuable compounds.

The actual mechanism of osmosensing and the molecular biology allowing osmotically stressed microbial cells to transform this environmental cue into enhanced promoter activity of ectoine biosynthetic genes is only rudimentarily comprehended. Is osmotic control of *ect* transcription mediated by specific regulatory proteins, or is this an intrinsic property of the given promoter and its flanking region? Contributors to this latter regulatory modus might be changes in DNA-topology under osmotic stress conditions (Higgins et al. 1988) and altered interaction of RNA-polymerase with -10 and -35 promoter regions in a crowded cytoplasm with changing solvation attributes when the external osmolarity is raised (Cagliero and Jin 2012; Cayley et al. 1991; Gralla and Huo 2008; Record et al. 1998; van den Berg et al. 2017). The mode of action of transcriptional regulators (e.g., EctR, CosR, GlnR, AphA, OpaR, EupR, and alternative sigma factors) that have been implicated in the control of *ect* promoter activity in various bacteria certainly deserve future study and scrutiny (Calderon et al. 2004; Gregory et al. 2019, 2020; Kuhlmann et al. 2011; Mustakhimov et al. 2010; Rodriguez-Moya et al. 2010; Schwibbert et al. 2011; Shao et al. 2015; Shikuma et al. 2013).

Biosynthesis and the ecophysiology of ectoines have been actively studied for a considerable time but the uses of these cytoprotectants as nutrients have only come recently into focus (Jebbar et al. 2005; Reshetnikov et al. 2020; Schulz et al. 2017b; Schwibbert et al. 2011; Vargas et al. 2006). A major advance has now been achieved through the structural analysis of the EutD/EutE hydrolase/deacetylase enzyme bi-module that opens the heteropyrimidine ring of ectoine and 5-hydroxyectoine and processes the formed *N*-α-ADABA and hydroxy-*N*-α-ADABA for further catabolism (Mais et al. 2020) (Figures 4 and 7B). The intermediate *N*-α-ADABA, and presumably also hydroxy-*N*-α-ADABA, serve as high-affinity internal inducers for the EnuR repressor, thereby triggering substrate-mediated induction of ectoine/5-hydroxectoine catabolic gene clusters (Schulz et al. 2017a). Further molecular and biochemical studies should now advance our understanding of this interesting PLP-dependent MocR/GabR-type repressor (Tramonti et al. 2018).

While the recent biochemical and structural analysis of the ectoine/5-hydroxyectoine hydrolase (EutD) and the *N*-α-ADABA-deacetylase (EutE) is a major advance, important questions remain with respect to those enzymes (EutABC) operating down-stream of the EutD/EutE enzyme bi-module (Figure 4). The elucidation of the function of these enzymes, and hence the clarification of the topology of the ectoine/5-hydroxyectoine degradation pathway as a whole, requires a concerted biochemical and physiological approach that needs to be supported by studies using well defined single gene deletion mutant strains. The synthesis and degradation routes of ectoines can be viewed as opposing pathways; yet they share a number of common intermediates (Figure 4). While the ability to synthesize or consume ectoines is clearly separated in most bacteria (Supplementary Figure S1), there is an interesting group of microorganisms that can do both (Reshetnikov et al. 2020; Schwibbert et al. 2011; Vargas et al. 2006). These latter organisms are faced with a potentially wasteful futile cycle. How does the cell balance the two physiological tasks at hand, osmostress protection and nutrient utilization, under osmotic steady-state growth conditions? Can it take a physiological advantage from a continuously running synthesis - degradation process (Reshetnikov et al. 2020; Schwibbert et al. 2011)?

The ecophysiological importance of ectoines for microbial assemblages and biofilms has only recently gained increased attention. For instance, transcription of the ectoine biosynthetic genes and corresponding transport systems were strongly induced when biofilms of *Sphingomonas* sp. LH128 (reclassified as *Novosphingobium* sp.) were subjected to an osmotic up-shock (Fida et al. 2012). This finding points to a role of ectoines in protecting cells encased in biofilms, multi-cellular assemblages strained and architecturally shaped by osmotic forces (Rubinstein et al. 2012; Seminara et al. 2012; Yan et al. 2017). In the pathogens *Vibrio cholerae* and *Vibrio parahaemolyticus* (and taxonomically related species) the genetic control of ectoine biosynthesis, compatible solute import, and biofilm formation is embedded in complex regulatory circuits that also involve quorum-sensing-type transcriptional regulators (Gregory et al. 2019, 2020; Shikuma et al. 2013). Dissecting these regulatory processes will open exciting entire new avenues for research. Released/actively secreted ectoines might also become a public good for microbial communities, as has been found for glycine betaine in the case of *V. cholerae* (Kapfhammer et al. 2005).

The unexpected discovery of ectoine/5-hydroxy ectoine-producing ciliates and micro-algae and the way in which these eukaryotic cells interact with bacteria paves the way for studies addressing the role of these cytoprotectants in the framework of microbial ecology (Fenizia et al. 2020; Harding et al. 2016; Landa et al. 2017; Weinisch et al. 2019). It is of interest to note in this context that the plant roots-associated bacterium *S. meliloti* performs chemotaxis towards the plant-produced compatible solute proline betaine and other types of quaternary ammonium compounds (e.g., glycine betaine) found in root exudates (Shrestha et al. 2018; Webb et al. 2017). Hence, one might ask if environmental ectoines might serve as chemo-attractants when microorganisms seek them out either as stress protectants or nutrients.

And finally, what are the molecular and physicochemical mechanisms when ectoines are used either as cold- or heat-stress protectants (Bursy et al. 2008; Garcia-Estepa et al. 2006; Kuhlmann et al. 2008a, 2011; Ma et al. 2017)? Are the principles underlying thermoprotection by ectoines different from those that govern their function as osmostress protectants, or are there mechanistically unifying underpinnings?

Acknowledgments: Long-term financial support for our studies on ectoines was provided by the Deutsche Forschungsgemeinschaft (DFG) in the framework of the Collaborative Research Center 987 (SFB 987), and via the Center for Synthetic Microbiology (SYNMIKRO) (Philipps-University Marburg). The Center for Structural Studies at the Heinrich-Heine University Düsseldorf was also funded by the DFG (Grant No. 417919780). L.C. gratefully acknowledges the receipt of a Ph.D. fellowship from the International Max Planck Research School for Environmental, Cellular and Molecular Microbiology (IMPRS-Mic; Marburg). We greatly value the expert help of Vickie Koogle in the language editing of our manuscript.
Author contribution: All the authors have accepted responsibility for the entire content of this submitted manuscript and approved submission.
Research funding: This research was funded by the Deutsche Forschungsgemeinschaft, and Philipps-Universität Marburg.
Conflict of interest statement: The authors declare no conflicts of interest regarding this article.

References

Aik, W., McDonough, M.A., Thalhammer, A., Chowdhury, R., and Schofield, C.J. (2012). Role of the jelly-roll fold in substrate binding by 2-oxoglutarate oxygenases. Cur. Opin. Struc. Biol. 22: 691–700.

Arakawa, T., and Timasheff, S.N. (1985). The stabilization of proteins by osmolytes. Biophys. J. 47: 411–414.

Barth, S., Huhn, M., Matthey, B., Klimka, A., Galinski, E.A., and Engert, A. (2000). Compatible-solute-supported periplasmic expression of functional recombinant proteins under stress conditions. Appl. Environ. Microbiol. 66: 1572–1579.

Bayles, D.O., Tunick, M.H., Foglia, T.A., and Miller, A.J. (2000). Cold shock and its effect on ribosomes and thermal tolerance in *Listeria monocytogenes*. Appl. Environ. Microbiol. 66: 4351–4355.

Bazan, J.F., Weaver, L.H., Roderick, S.L., Huber, R., and Matthews, B.W. (1994). Sequence and structure comparison suggest that methionine aminopeptidase, prolidase, aminopeptidase P, and creatinase share a common fold. Proc. Natl. Acad. Sci. U.S.A. 91: 2473–2477.

Becker, J., Schäfer, R., Kohlstedt, M., Harder, B.J., Borchert, N.S., Stöveken, N., Bremer, E., and Wittmann, C. (2013). Systems metabolic engineering of *Corynebacterium glutamicum* for production of the chemical chaperone ectoine. Microb. Cell Fact. 12: 110.

Becker, J., and Wittmann, C. (2020). Microbial production of extremolytes - high-value active ingredients for nutrition, health care, and well-being. Curr. Opin. Biotechnol. 65: 118–128.

Bestvater, T., Louis, P., and Galinski, E.A. (2008). Heterologous ectoine production in *Escherichia coli:* by-passing the metabolic bottle-neck. Saline Syst. 4: 12.

Biran, D., Rotem, O., Rosen, R., and Ron, E.Z. (2018). Coping with high temperature: a unique regulation in *A. tumefaciens*. Curr. Top. Microbiol. Immunol. 418: 185–194.

Bolen, D.W., and Baskakov, I.V. (2001). The osmophobic effect: natural selection of a thermodynamic force in protein folding. J. Mol. Biol. 310: 955–963.

Booth, I.R. (2014). Bacterial mechanosensitive channels: progress towards an understanding of their roles in cell physiology. Curr. Opin. Microbiol. 18: 16–22.

Bourot, S., Sire, O., Trautwetter, A., Touze, T., Wu, L.F., Blanco, C., and Bernard, T. (2000). Glycine betaine-assisted protein folding in a *lysA* mutant of *Escherichia coli*. J. Biol. Chem. 275: 1050–1056.

Bouskill, N.J., Wood, T.E., Baran, R., Ye, Z., Bowen, B.P., Lim, H., Zhou, J., Nostrand, J.D., Nico, P., Northen, T.R., et al. (2016). Belowground response to drought in a tropical forest soil. I. changes in microbial functional potential and metabolism. Front. Microbiol. 7: 525.

Bremer, E., and Krämer, R. (2019). Responses of microorganisms to osmotic stress. Annu. Rev. Microbiol. 73: 313–314.

Brown, A.D. (1976). Microbial water stress. Bacteriol. Rev. 40: 803–846.

Bruce, H., Nguyen Tuan, A., Mangas Sanchez, J., Leese, C., Hopwood, J., Hyde, R., Hart, S., Turkenburg, J.P., and Grogan, G. (2012). Structures of a γ-aminobutyrate (GABA) transaminase from the s-triazine-degrading organism *Arthrobacter aurescens* TC1 in complex with PLP and with its external aldimine PLP-GABA adduct. Acta Crystallogr. Sect. F Struct. Biol. Cryst. Commun. 68: 1175–1180.

Bursy, J., Kuhlmann, A.U., Pittelkow, M., Hartmann, H., Jebbar, M., Pierik, A.J., and Bremer, E. (2008). Synthesis and uptake of the compatible solutes ectoine and 5-hydroxyectoine by *Streptomyces coelicolor* A3(2) in response to salt and heat stresses. Appl. Environ. Microbiol. 74: 7286–7296.

Bursy, J., Pierik, A.J., Pica, N., and Bremer, E. (2007). Osmotically induced synthesis of the compatible solute hydroxyectoine is mediated by an evolutionarily conserved ectoine hydroxylase. J. Biol. Chem. 282: 31147–31155.

Cagliero, C., and Jin, D.J. (2012). Dissociation and re-association of RNA polymerase with DNA during osmotic stress response in *Escherichia coli*. Nucleic Acids Res. 41: 315–326.

Caldas, T., Demont-Caulet, N., Ghazi, A., and Richarme, G. (1999). Thermoprotection by glycine betaine and choline. Microbiology 145: 2543–2548.

Calderon, M.I., Vargas, C., Rojo, F., Iglesias-Guerra, F., Csonka, L.N., Ventosa, A., and Nieto, J.J. (2004). Complex regulation of the synthesis of the compatible solute ectoine in the halophilic bacterium *Chromohalobacter salexigens* DSM 3043T. Microbiology 150: 3051–3063.

Canovas, D., Borges, N., Vargas, C., Ventosa, A., Nieto, J.J., and Santos, H. (1999). Role of *N*-γ-acetyldiaminobutyrate as an enzyme stabilizer and an intermediate in the biosynthesis of hydroxyectoine. Appl. Environ. Microbiol. 65: 3774–3779.

Capp, M.W., Pegram, L.M., Saecker, R.M., Kratz, M., Riccardi, D., Wendorff, T., Cannon, J.G., and Record, M.T., Jr. (2009). Interactions of the osmolyte glycine betaine with molecular surfaces in water: thermodynamics, structural interpretation, and prediction of m-values. Biochemistry 48: 10372–10379.

Cayley, S., Lewis, B.A., Guttman, H.J., and Record, M.T., , Jr. (1991). Characterization of the cytoplasm of *Escherichia coli* K-12 as a function of external osmolarity. Implications for protein-DNA interactions *in vivo*. J. Mol. Biol. 222: 281–300.

Cayley, S., and Record, M.T. , Jr. (2003). Roles of cytoplasmic osmolytes, water, and crowding in the response of *Escherichia coli* to osmotic stress: biophysical basis of osmoprotection by glycine betaine. Biochemistry 42: 12596–12609.

Chattopadhyay, M.K., Kern, R., Mistou, M.Y., Dandekar, A.M., Uratsu, S.L., and Richarme, G. (2004). The chemical chaperone proline relieves the thermosensitivity of a *dnaK* deletion mutant at 42 degrees C. J. Bacteriol. 186: 8149–8152.

Chen, I.A., Chu, K., Palaniappan, K., Pillay, M., Ratner, A., Huang, J., Huntemann, M., Varghese, N., White, J.R., Seshadri, R., et al. (2019). IMG/M v.5.0: an integrated data management and comparative analysis system for microbial genomes and microbiomes. Nucleic Acids Res. 47: D666–D677.

Chen, W., Zhang, S., Jiang, P.X., Yao, J., He, Y.Z., Chen, L.C., Gui, X.W., Dong, Z.Y., and Tang, S.Y. (2015). Design of an ectoine-responsive AraC mutant and its application in metabolic engineering of ectoine biosynthesis. Metab. Eng. 30: 149–155.

Copeland, A., O'Connor, K., Lucas, S., Lapidus, A., Berry, K.W., Detter, J.C., Del Rio, T.G., Hammon, N., Dalin, E., Tice, H., et al. (2011). Complete genome sequence of the halophilic and highly halotolerant *Chromohalobacter salexigens* type strain (1H11(T)). Stand. Genomic Sci. 5: 379–388.

Czech, L., Hermann, L., Stöveken, N., Richter, A.A., Höppner, A., Smits, S.H.J., Heider, J., and Bremer, E. (2018a). Role of the extremolytes ectoine and hydroxyectoine as stress protectants and nutrients: genetics, phylogenomics, biochemistry, and structural analysis. Genes 9: 177.

Czech, L., Höppner, A., Kobus, S., Seubert, A., Riclea, R., Dickschat, J.S., Heider, J., Smits, S.H.J., and Bremer, E. (2019a). Illuminating the catalytic core of ectoine synthase through structural and biochemical analysis. Sci. Rep. 9: 364.

Czech, L., Poehl, S., Hub, P., Stoeveken, N., and Bremer, E. (2018b). Tinkering with osmotically controlled transcription allows enhanced production and excretion of ectoine and

hydroxyectoine from a microbial cell factory. Appl. Environ. Microbiol. 84: e01772-17.

Czech, L., Stöveken, N., and Bremer, E. (2016). EctD-mediated biotransformation of the chemical chaperone ectoine into hydroxyectoine and its mechanosensitive channel-independent excretion. Microb. Cell Fact. 15: 126.

Czech, L., Wilcken, S., Czech, O., Linne, U., Brauner, J., Smits, S.H.J., Galinski, E.A., and Bremer, E. (2019b). Exploiting substrate promiscuity of ectoine hydroxylase for regio- and stereoselective modification of homoectoine. Front. Microbiol. 10: 2745.

D'Ari, R., and Casadesus, J. (1998). Underground metabolism. Bioessays 20: 181–186.

da Costa, M.S., Santos, H., and Galinski, E.A. (1998). An overview of the role and diversity of compatible solutes in *Bacteria* and *Archaea*. Adv. Biochem. Eng. Biotechnol. 61: 117–153.

Danchin, A., and Nikel, P.I. (2019). Why nature chose potassium. J. Mol. Evol. 87: 271–288.

Dey, A., Shree, S., Pandey, S.K., Tripathi, R.P., and Ramachandran, R. (2016). Crystal structure of *Mycobacterium tuberculosis* H37Rv AldR (rv2779c), a regulator of the *ald* gene: DNA-binding, and identification of small-molecule inhibitors. J. Biol. Chem. 291: 11967–11980.

Diamant, S., Eliahu, N., Rosenthal, D., and Goloubinoff, P. (2001). Chemical chaperones regulate molecular chaperones i*n vitro* and in cells under combined salt and heat stresses. J. Biol. Chem. 276: 39586–39591.

Dunwell, J.M., Purvis, A., and Khuri, S. (2004). Cupins: the most functionally diverse protein superfamily? Phytochemistry 65: 7–17.

Edayathumangalam, R., Wu, R., Garcia, R., Wang, Y., Wang, W., Kreinbring, C.A., Bach, A., Liao, J., Stone, T.A., Terwilliger, T.C., et al. (2013). Crystal structure of *Bacillus subtilis* GabR, an autorepressor and transcriptional activator of *gabT*. Proc. Natl. Acad. Sci. U.S.A. 110: 17820–17825.

Eiberweiser, A., Nazet, A., Kruchinin, S.E., Fedotova, M.V., and Buchner, R. (2015). Hydration and ion binding of the osmolyte ectoine. J. Phys. Chem. B 119: 15203–15211.

Fenizia, S., Thume, K., Wirgenings, M., and Pohnert, G. (2020). Ectoine from bacterial and algal origin Is a compatible solute in microalgae. Mar. Drugs 18, https://doi.org/10.3390/md18010042.

Fida, T.T., Breugelmans, P., Lavigne, R., Coronado, E., Johnson, D.R., van der Meer, J.R., Mayer, A.P., Heipieper, H.J., Hofkens, J., and Springael, D. (2012). Exposure to solute stress affects genome-wide expression but not the polycyclic aromatic hydrocarbon-degrading activity of *Sphingomonas* sp. strain LH128 in biofilms. Appl. Environ. Microbiol. 78: 8311–8320.

Frezzini, M., Narzi, D., Sciolari, A.M., Guidoni, L., and Pascarella, S. (2020). Molecular dynamics of an asymmetric form of GabR, a bacterial transcriptional regulator. Biophys. Chem. 262: 106380.

Galinski, E.A., Pfeiffer, H.P., and Trüper, H.G. (1985). 1,4,5,6-Tetrahydro-2-methyl-4-pyrimidinecarboxylic acid. A novel cyclic amino acid from halophilic phototrophic bacteria of the genus *Ectothiorhodospira*. Eur. J. Biochem. 149: 135–139.

Galinski, E.A., Stein, M., Ures, A., and Schwarz, T. (2009). *Stereo-specific hydroxylation* (International patent application WO 2009/059783 A1).

Galinski, E.A., and Trüper, H.G. (1994). Microbial behaviour in salt-stressed ecosystems. FEMS Microbiol. Rev. 15: 95–108.

Garcia-Estepa, R., Argandona, M., Reina-Bueno, M., Capote, N., Iglesias-Guerra, F., Nieto, J.J., and Vargas, C. (2006). The *ectD* gene, which is involved in the synthesis of the compatible solute hydroxyectoine, is essential for thermoprotection of the halophilic bacterium *Chromohalobacter salexigens*. J. Bacteriol. 188: 3774–3784.

Giesselmann, G., Dietrich, D., Jungmann, L., Kohlstedt, M., Jeon, E.J., Yim, S.S., Sommer, F., Zimmer, D., Muhlhaus, T., Schroda, M., et al. (2019). Metabolic engineering of *Corynebacterium glutamicum* for high-level ectoine production - design, combinatorial assembly and implementation of a transcriptionally balanced heterologous ectoine pathway. Biotechnol. J. 14: e201800417.

Gralla, J.D., and Huo, Y.X. (2008). Remodeling and activation of *Escherichia coli* RNA polymerase by osmolytes. Biochemistry 47: 13189–13196.

Grammann, K., Volke, A., and Kunte, H.J. (2002). New type of osmoregulated solute transporter identified in halophilic members of the bacteria domain: TRAP transporter TeaABC mediates uptake of ectoine and hydroxyectoine in *Halomonas elongata* DSM 2581(T). J. Bacteriol. 184: 3078–3085.

Gregory, G.J., Morreale, D.P., and Boyd, E.F. (2020). CosR is a global regulator of the osmotic stress response with widespread distribution among bacteria. Appl. Environ. Microbiol. 86: e00120-20. https://doi.org/10.1128/AEM.00120-20.

Gregory, G.J., Morreale, D.P., Carpenter, M.R., Kalburge, S.S., and Boyd, E.F. (2019). Quorum sensing regulators AphA and OpaR control expression of the operon responsible for biosynthesis of the compatible solute ectoine. Appl. Environ. Microbiol. 85: e01543-19.

Gunde-Cimerman, N., Plemenitas, A., and Oren, A. (2018). Strategies of adaptation of microorganisms of the three domains of life to high salt concentrations. FEMS Microbiol. Rev. 42: 353–375.

Hahn, M.B., Meyer, S., Schroter, M.A., Kunte, H.J., Solomun, T., and Sturm, H. (2017). DNA protection by ectoine from ionizing radiation: molecular mechanisms. Phys. Chem. Chem. Phys. 19: 25717–25722.

Hahn, M.B., Smales, G.J., Seitz, H., Solomun, T., and Sturm, H. (2020). Ectoine interaction with DNA: influence on ultraviolet radiation damage. Phys. Chem. Chem. Phys. 22: 6984–6992.

Hanekop, N., Höing, M., Sohn-Bösser, L., Jebbar, M., Schmitt, L., and Bremer, E. (2007). Crystal structure of the ligand-binding protein EhuB from *Sinorhizobium meliloti* reveals substrate recognition of the compatible solutes ectoine and hydroxyectoine. J. Mol. Biol. 374: 1237–1250.

Hangasky, J.A., Taabazuing, C.Y., Valliere, M.A., and Knapp, M.J. (2013). Imposing function down a (cupin)-barrel: secondary structure and metal stereochemistry in the alphaKG-dependent oxygenases. Metallomics 5: 287–301.

Hara, R., Nishikawa, T., Okuhara, T., Koketsu, K., and Kino, K. (2019). Ectoine hydroxylase displays selective trans-3-hydroxylation activity towards L-proline. Appl. Microbiol. Biotechnol. 103: 5689–5698.

Harding, T., Brown, M.W., Simpson, A.G., and Roger, A.J. (2016). Osmoadaptative strategy and its molecular signature in obligately halophilic heterotrophic protists. Genome Biol. Evol. 8: 2241–2258.

Harishchandra, R.K., Sachan, A.K., Kerth, A., Lentzen, G., Neuhaus, T., and Galla, H.J. (2011). Compatible solutes: ectoine and hydroxyectoine improve functional nanostructures in artificial lung surfactants. Biochim. Biophys. Acta 1808: 2830–2840.

Harishchandra, R.K., Wulff, S., Lentzen, G., Neuhaus, T., and Galla, H.J. (2010). The effect of compatible solute ectoines on the structural organization of lipid monolayer and bilayer membranes. Biophys. Chem. 150: 37–46.

Hengge-Aronis, R. (2002). Signal transduction and regulatory mechanisms involved in control of the sigma(S) (RpoS) subunit of RNA polymerase. Microbiol. Mol. Biol. Rev. 66: 373–395.

Herr, C.Q., and Hausinger, R.P. (2018). Amazing diversity in biochemical roles of Fe(II)/2-oxoglutarate oxygenases. Trends Biochem. Sci. 43: 517–532.

Herzog, M., Dwivedi, M., Kumar Harishchandra, R., Bilstein, A., Galla, H.J., and Winter, R. (2019). Effect of ectoine, hydroxyectoine and beta-hydroxybutyrate on the temperature and pressure stability of phospholipid bilayer membranes of different complexity. Colloids Surf. B Biointerfaces 178: 404–411.

Higgins, C.F., Dorman, C.J., Stirling, D.A., Waddell, L., Booth, I.R., May, G., and Bremer, E. (1988). A physiological role for DNA supercoiling in the osmotic regulation of gene expression in *S. typhimurium* and *E. coli*. Cell 52: 569–584.

Hillier, H.T., Altermark, B., and Leiros, I. (2020). The crystal structure of the tetrameric DABA-aminotransferase EctB, a rate-limiting enzyme in the ectoine biosynthesis pathway. FEBS J. in press, https://doi.org/10.1111/febs.15265.

Hoffmann, T., von Blohn, C., Stanek, A., Moses, S., Barzantny, S., and Bremer, E. (2012). Synthesis, release, and recapture of the compatible solute proline by osmotically stressed *Bacillus subtilis* cells. Appl. Environ. Microbiol. 78: 5753–5762.

Höppner, A., Widderich, N., Lenders, M., Bremer, E., and Smits, S.H.J. (2014). Crystal structure of the ectoine hydroxylase, a snapshot of the active site. J. Biol. Chem. 289: 29570–29583.

Ignatova, Z., and Gierasch, L.M. (2006). Inhibition of protein aggregation *in vitro* and *in vivo* by a natural osmoprotectant. Proc. Nat. Acad. Sci. USA. 103: 13357–13361.

Inbar, L., Frolow, F., and Lapidot, A. (1993). The conformation of new tetrahydropyrimidine derivatives in solution and in the crystal. Eur. J. Biochem. 214: 897–906.

Inbar, L., and Lapidot, A. (1988). The structure and biosynthesis of new tetrahydropyrimidine derivatives in actinomycin D producer *Streptomyces parvulus*. Use of ^{13}C- and ^{15}N-labeled L-glutamate and ^{13}C and ^{15}N NMR spectroscopy. J. Biol. Chem. 263: 16014–16022.

Islam, M.S., Leissing, T.M., Chowdhury, R., Hopkinson, R.J., and Schofield, C.J. (2018). 2-Oxoglutarate-dependent oxygenases. Annu. Rev. Biochem. 87: 585–620.

Jebbar, M., Sohn-Bösser, L., Bremer, E., Bernard, T., and Blanco, C. (2005). Ectoine-induced proteins in *Sinorhizobium meliloti* include an ectoine ABC-type transporter involved in osmoprotection and ectoine catabolism. J. Bacteriol. 187: 1293–1304.

Jensen, R.A. (1976). Enzyme recruitment in evolution of new function. Annu. Rev. Microbiol. 30: 409–425.

Jorge, C.D., Borges, N., Bagyan, I., Bilstein, A., and Santos, H. (2016). Potential applications of stress solutes from extremophiles in protein folding diseases and healthcare. Extremophiles 20: 251–259.

Kapfhammer, D., Karatan, E., Pflughoeft, K.J., and Watnick, P.I. (2005). Role for glycine betaine transport in *Vibrio cholerae* osmoadaptation and biofilm formation within microbial communities. Appl. Environ. Microbiol. 71: 3840–3847.

Kempf, B., and Bremer, E. (1998). Uptake and synthesis of compatible solutes as microbial stress responses to high osmolality environments. Arch. Microbiol. 170: 319–330.

Klähn, S., and Hagemann, M. (2011). Compatible solute biosynthesis in cyanobacteria. Env. Microbiol. 13: 551–562.

Kol, S., Merlo, M.E., Scheltema, R.A., de Vries, M., Vonk, R.J., Kikkert, N.A., Dijkhuizen, L., Breitling, R., and Takano, E. (2010). Metabolomic characterization of the salt stress response in *Streptomyces coelicolor*. Appl. Environ. Microbiol. 76: 2574–2581.

Kuhlmann, A.U., and Bremer, E. (2002). Osmotically regulated synthesis of the compatible solute ectoine in *Bacillus pasteurii* and related *Bacillus* spp. Appl. Environ. Microbiol. 68: 772–783.

Kuhlmann, A.U., Bursy, J., Gimpel, S., Hoffmann, T., and Bremer, E. (2008a). Synthesis of the compatible solute ectoine in *Virgibacillus pantothenticus* is triggered by high salinity and low growth temperature. Appl. Environ. Microbiol. 74: 4560–4563.

Kuhlmann, A.U., Hoffmann, T., Bursy, J., Jebbar, M., and Bremer, E. (2011). Ectoine and hydroxyectoine as protectants against osmotic and cold stress: uptake through the SigB-controlled betaine-choline- carnitine transporter-type carrier EctT from *Virgibacillus pantothenticus*. J. Bacteriol. 193: 4699–4708.

Kuhlmann, S.I., Terwisscha van Scheltinga, A.C., Bienert, R., Kunte, H.J., and Ziegler, C. (2008b). 1.55 A structure of the ectoine binding protein TeaA of the osmoregulated TRAP-transporter TeaABC from *Halomonas elongata*. Biochemistry 47: 9475–9485.

Kumarevel, T., Nakano, N., Ponnuraj, K., Gopinath, S.C., Sakamoto, K., Shinkai, A., Kumar, P.K., and Yokoyama, S. (2008). Crystal structure of glutamine receptor protein from *Sulfolobus tokodaii* strain 7 in complex with its effector L-glutamine: implications of effector binding in molecular association and DNA binding. Nucleic Acids Res. 36: 4808–4820.

Kunte, H.J., Lentzen, G., and Galinski, E. (2014). Industrial production of the cell protectant ectoine: protection, mechanisms, processes, and products. Cur. Biotechnol. 3: 10–25.

Kurz, M. (2008). Compatible solute influence on nucleic acids: many questions but few answers. Saline Syst. 4: 6.

Kurz, M., Burch, A.Y., Seip, B., Lindow, S.E., and Gross, H. (2010). Genome-driven investigation of compatible solute biosynthesis pathways of *Pseudomonas syringae* pv. syringae and their contribution to water stress tolerance. Appl. Environ. Microbiol. 76: 5452–5462.

Lamark, T., Styrvold, O.B., and Strom, A.R. (1992). Efflux of choline and glycine betaine from osmoregulating cells of *Escherichia coli*. FEMS Microbiol. Lett. 75: 149–154.

Landa, M., Burns, A.S., Roth, S.J., and Moran, M.A. (2017). Bacterial transcriptome remodeling during sequential co-culture with a marine dinoflagellate and diatom. ISME J. 11: 2677–2690.

Le Coq, J., Pavlovsky, A., Malik, R., Sanishvili, R., Xu, C., and Viola, R.E. (2008). Examination of the mechanism of human brain aspartoacylase through the binding of an intermediate analogue. Biochemistry 47: 3484–3492.

Lecher, J., Pittelkow, M., Zobel, S., Bursy, J., Bonig, T., Smits, S.H., Schmitt, L., and Bremer, E. (2009). The crystal structure of UehA in complex with ectoine- a comparison with other TRAP-T binding proteins. J. Mol. Biol. 389: 58–73.

Leon, M.J., Hoffmann, T., Sanchez-Porro, C., Heider, J., Ventosa, A., and Bremer, E. (2018). Compatible solute synthesis and import by the moderate halophile *Spiribacter salinus*: physiology and genomics. Front. Microbiol. 9: 108.

Letunic, I., and Bork, P. (2016) Intreactive tree of life (iTOL) v3. An online tool for the display and annotation of phylogenetic and other tress. Nucleic Acids Res. 44: W242–W245.

Lippert, K., and Galinski, E.A. (1992). Enzyme stabilization by ectoine-type compatible solutes: protection against heating, freezing and drying. Appl. Microb. Biotechnol. 37: 61–65.

Lo, C.C., Bonner, C.A., Xie, G., D'Souza, M., and Jensen, R.A. (2009). Cohesion group approach for evolutionary analysis of aspartokinase, an enzyme that feeds a branched network of many biochemical pathways. Microbiol. Mol. Biol. Rev. 73: 594–651.

Louis, P., and Galinski, E.A. (1997). Characterization of genes for the biosynthesis of the compatible solute ectoine from *Marinococcus halophilus* and osmoregulated expression in *Escherichia coli*. Microbiology 143: 1141–1149.

Ma, Y., Wang, Q., Xu, W., Liu, X., Gao, X., and Zhang, Y. (2017). Stationary phase-dependent accumulation of ectoine is an efficient adaptation strategy in *Vibrio anguillarum* against cold stress. Microbiol. Res. 205: 8–18.

Mais, C. -N., Hermann, L., Altegoer, F., Seubert, A., Richter, A.A., Wernersbach, I., Czech, L., Bremer, E., and Bange, G. (2020). Degradation of the microbial stress protectants and chemical chaperones ectoine and hydroxyectoine by a bacterial hydrolase-deacetylase complex. J. Biol. Chem. 295: 9087–9104.

Malin, G., and Lapidot, A. (1996). Induction of synthesis of tetrahydropyrimidine derivatives in *Streptomyces* strains and their effect on *Escherichia coli* in response to osmotic and heat stress. J. Bacteriol. 178: 385–395.

Manzanera, M., Vilchez, S., and Tunnacliffe, A. (2004). High survival and stability rates of *Escherichia coli* dried in hydroxyectoine. FEMS Microbiol. Lett. 233: 347–352.

Maskow, T., and Babel, W. (2001). Calorimetrically obtained information about the efficiency of ectoine synthesis from glucose in *Halomonas elongata*. Biochim. Biophys. Acta 1527: 4–10.

Moran, M.A., Buchan, A., Gonzalez, J.M., Heidelberg, J.F., Whitman, W.B., Kiene, R.P., Henriksen, J.R., King, G.M., Belas, R., Fuqua, C., et al. (2004). Genome sequence of *Silicibacter pomeroyi* reveals adaptations to the marine environment. Nature 432: 910–913.

Moritz, K.D., Amendt, B., Witt, E.M.H.J., and Galinski, E.A. (2015). The hydroxyectoine gene cluster of the non-halophilic acidophile *Acidiphilium cryptum*. Extremophiles 19: 87–99.

Mosier, A.C., Justice, N.B., Bowen, B.P., Baran, R., Thomas, B.C., Northen, T.R., and Banfield, J.F. (2013). Metabolites associated with adaptation of microorganisms to an acidophilic, metal-rich environment identified by stable-isotope-enabled metabolomics. mBio 4: e00484-12.

Mustakhimov, I.I, Reshetnikov, A.S., Glukhov, A.S., Khmelenina, V.N., Kalyuzhnaya, M.G., and Trotsenko, Y.A. (2010). Identification and characterization of EctR1, a new transcriptional regulator of the ectoine biosynthesis genes in the halotolerant methanotroph *Methylomicrobium alcaliphilum* 20Z. J. Bacteriol. 192: 410–417.

Müller, V., Spanheimer, R., and Santos, H. (2005) Stress response by solute accumulation in archaea. Curr. Opin. Microbiol. 8: 729–736.

Ono, H., Sawada, K., Khunajakr, N., Tao, T., Yamamoto, M., Hiramoto, M., Shinmyo, A., Takano, M., and Murooka, Y. (1999). Characterization of biosynthetic enzymes for ectoine as a compatible solute in a moderately halophilic eubacterium, *Halomonas elongata*. J. Bacteriol. 181: 91–99.

Oren, A. (1999). Bioenergetic aspects of halophilism. Microbiol. Mol. Biol. Rev. 63: 334–348.

Pastor, J.M., Salvador, M., Argandona, M., Bernal, V., Reina-Bueno, M., Csonka, L.N., Iborra, J.L., Vargas, C., Nieto, J.J., and Canovas, M. (2010). Ectoines in cell stress protection: uses and biotechnological production. Biotechnol. Adv. 28: 782–801.

Peters, P., Galinski, E.A., and Trüper, H.G. (1990). The biosyntheis of ectoine. FEMS Microbiol. Lett. 71: 157–162.

Prabhu, J., Schauwecker, F., Grammel, N., Keller, U., and Bernhard, M. (2004). Functional expression of the ectoine hydroxylase gene (*thpD*) from *Streptomyces chrysomallus* in *Halomonas elongata*. Appl. Environ. Microbiol. 70: 3130–3132.

Proshlyakov, D.A., McCracken, J., and Hausinger, R.P. (2017). Spectroscopic analyses of 2-oxoglutarate-dependent oxygenases: TauD as a case study. J. Biol. Inorg. Chem. 22: 367–379.

Rawlings, N.D., and Barrett, A.J. (1993). Evolutionary families of peptidases. Biochem. J. 290: 205–218.

Record, M.T. , Jr., Courtenay, E.S., Cayley, S., and Guttman, H.J. (1998). Biophysical compensation mechanisms buffering *E. coli* protein-nucleic acid interactions against changing environments. Trends Biochem. Sci. 23: 190–194.

Ren, M., Feng, X., Huang, Y., Wang, H., Hu, Z., Clingenpeel, S., Swan, B.K., Fonseca, M.M., Posada, D., Stepanauskas, R., et al. (2019). Phylogenomics suggests oxygen availability as a driving force in Thaumarchaeota evolution. ISME J. 13: 2150–2161.

Reshetnikov, A.S., Khmelenina, V.N., Mustakhimov, , II, Kalyuzhnaya, M., Lidstrom, M., and Trotsenko, Y.A. (2011a). Diversity and phylogeny of the ectoine biosynthesis genes in aerobic, moderately halophilic methylotrophic bacteria. Extremophiles 15: 653–663.

Reshetnikov, A.S., Khmelenina, V.N., Mustakhimov, I.I., and Trotsenko, Y.A. (2011b). Genes and enzymes of ectoine biosynthesis in halotolerant methanotrophs. Methods Enzymol. 495: 15–30.

Reshetnikov, A.S., Khmelenina, V.N., and Trotsenko, Y.A. (2006). Characterization of the ectoine biosynthesis genes of haloalkalotolerant obligate methanotroph *"Methylomicrobium alcaliphilum* 20Z*"*. Arch. Microbiol. 184: 286–297.

Reshetnikov, A.S., Rozova, O.N., Trotsenko, Y.A., But, S.Y., Khmelenina, V.N., and Mustakhimov, I.I. (2020). Ectoine degradation pathway in halotolerant methylotrophs. PloS One 15: e0232244.

Reuter, K., Pittelkow, M., Bursy, J., Heine, A., Craan, T., and Bremer, E. (2010). Synthesis of 5-hydroxyectoine from ectoine: crystal structure of the non-heme iron(II) and 2-oxoglutarate-dependent dioxygenase EctD. PloS One 5: e10647.

Richter, A.A., Kobus, S., Czech, L., Hoeppner, A., Zarzycki, J., Erb, T.J., Lauterbach, L., Dickschat, J.S., Bremer, E., and Smits, S.H.J. (2020). The architecture of the diaminobutyrate acetyltransferase active site provides mechanistic insight into the biosynthesis of the chemical chaperone ectoine. J. Biol. Chem. 295: 2822–2838.

Richter, A.A., Mais, C.-N., Czech, L., Geyer, K., Hoeppner, A., Smits, A.H.J., Erb, T.J., and Bremer, E. (2019). Biosynthesis of the stress-protectant and chemical chaperone ectoine: biochemistry of the transaminase EctB. Front. Microbiol. 10: 2811.

Robin, A.Y., Cobessi, D., Curien, G., Robert-Genthon, M., Ferrer, J.L., and Dumas, R. (2010). A new mode of dimerization of allosteric enzymes with ACT domains revealed by the crystal structure of the aspartate kinase from *Cyanobacteria*. J. Mol. Biol. 399: 283–293.

Rodriguez-Moya, J., Argandona, M., Reina-Bueno, M., Nieto, J.J., Iglesias-Guerra, F., Jebbar, M., and Vargas, C. (2010). Involvement of EupR, a response regulator of the NarL/FixJ family, in the control of the uptake of the compatible solutes ectoines by the halophilic bacterium *Chromohalobacter salexigens*. BMC Microbiol. 10: 256.

Roeßler, M., and Müller, V. (2001). Osmoadaptation in bacteria and archaea: common principles and differences. Env. Microbiol. 3: 743–754.

Rubinstein, S.M., Kolodkin-Gal, I., McLoon, A., Chai, L., Kolter, R., Losick, R., and Weitz, D.A. (2012). Osmotic pressure can regulate matrix gene expression in *Bacillus subtilis*. Mol. Microbiol. 86: 426–436.

Sahle, C.J., Schroer, M.A., Jeffries, C.M., and Niskanen, J. (2018). Hydration in aqueous solutions of ectoine and hydroxyectoine. Phys. Chem. Chem. Phys. 20: 27917–27923.

Salah Ud-Din, A.I., Tikhomirova, A., and Roujeinikova, A. (2016). Structure and functional diversity of GCN5-related N-acetyltransferases (GNAT). Int. J. Mol. Sci. 17: 1018.

Saum, S.H., and Müller, V. (2008). Growth phase-dependent switch in osmolyte strategy in a moderate halophile: ectoine is a minor osmolyte but major stationary phase solute in *Halobacillus halophilus*. Env. Microbiol. 10: 716–726.

Schada von Borzyskowski, L., Severi, F., Kruger, K., Hermann, L., Gilardet, A., Sippel, F., Pommerenke, B., Claus, P., Cortina, N.S., Glatter, T., et al. (2019). Marine Proteobacteria metabolize glycolate via the beta-hydroxyaspartate cycle. Nature 575: 500–504.

Schiraldi, C., Maresca, C., Catapano, A., Galinski, E.A., and De Rosa, M. (2006). High-yield cultivation of *Marinococcus* M52 for production and recovery of hydroxyectoine. Res. Microbiol. 157: 693–699.

Schuh, W., Puff, H., Galinski, E.A., and Trüper, H.G. (1985). Die Kristallstruktur des Ectoin, einer neuen osmoregulatorisch wirksamen Aminosäure. Z. Naturforsch. 40c: 780–784.

Schulz, A., Hermann, L., Freibert, S.-A., Bönig, T., Hoffmann, T., Riclea, R., Dickschat, J.S., Heider, J., and Bremer, E. (2017a). Transcriptional regulation of ectoine catabolism in response to multiple metabolic and environmental cues. Env. Microbiol. 19: 4599–4619.

Schulz, A., Stöveken, N., Binzen, I.M., Hoffmann, T., Heider, J., and Bremer, E. (2017b). Feeding on compatible solutes: a substrate-induced pathway for uptake and catabolism of ectoines and its genetic control by EnuR. Environ. Microbiol. 19: 926–946.

Schwibbert, K., Marin-Sanguino, A., Bagyan, I., Heidrich, G., Lentzen, G., Seitz, H., Rampp, M., Schuster, S.C., Klenk, H.P., Pfeiffer, F., et al. (2011). A blueprint of ectoine metabolism from the genome of the industrial producer *Halomonas elongata* DSM 2581 T. Env. Microbiol. 13: 1973–1994.

Seip, B., Galinski, E.A., and Kurz, M. (2011). Natural and engineered hydroxyectoine production based on the *Pseudomonas stutzeri ectABCD-ask* gene cluster. Appl. Environ. Microbiol. 77: 1368–1374.

Seminara, A., Angelini, T.E., Wilking, J.N., Vlamakis, H., Ebrahim, S., Kolter, R., Weitz, D.A., and Brenner, M.P. (2012). Osmotic spreading of *Bacillus subtilis* biofilms driven by an extracellular matrix. Proc. Natl. Acad. Sci. U.S.A. 109: 1116–1121.

Shao, Z., Deng, W., Li, S., He, J., Ren, S., Huang, W., Lu, Y., Zhao, G., Cai, Z., and Wang, J. (2015). GlnR-mediated regulation of *ectABCD* transcription expands the role of the GlnR regulon to osmotic stress management. J. Bacteriol. 197: 3041–3307.

Shikuma, N.J., Davis, K.R., Fong, J.N.C., and Yildiz, F.H. (2013). The transcriptional regulator, CosR, controls compatible solute biosynthesis and transport, motility and biofilm formation in *Vibrio cholerae*. Env. Microbiol. 15: 1387–1399.

Shrestha, M., Compton, K.K., Mancl, J.M., Webb, B.A., Brown, A.M., Scharf, B.E., and Schubot, F.D. (2018). Structure of the sensory domain of McpX from *Sinorhizobium meliloti*, the first known bacterial chemotactic sensor for quaternary ammonium compounds. Biochem. J. 475: 3949–3962.

Shrivastava, T., and Ramachandran, R. (2007). Mechanistic insights from the crystal structures of a feast/famine regulatory protein from *Mycobacterium tuberculosis* H37Rv. Nucleic Acids Res. 35: 7324–7335.

Sims, D., Brettin, T., Detter, J.C., Han, C., Lapidus, A., Copeland, A., Glavina Del Rio, T., Nolan, M., Chen, F., Lucas, S., et al. (2009). Complete genome sequence of *Kytococcus sedentarius* type strain (541). Stand. Genomic Sci. 1: 12–20.

Sievers, F., Wilm, A., Dineen, D., Gibson, T.J., Karplus, K., LI, W., Lopez, R., McWilliam, H., Remmert, M., Söding, J., et al. (2011) Fast, scalable generation of high-quality protein multiple sequence alingmnets using Clustal Omega. Mol. Syst. Biol. 7: 539.

Smiatek, J., Harishchandra, R.K., Rubner, O., Galla, H.J., and Heuer, A. (2012). Properties of compatible solutes in aqueous solution. Biophys. Chem. 160: 62–68.

Stadmiller, S.S., Gorensek-Benitez, A.H., Guseman, A.J., and Pielak, G.J. (2017). Osmotic shock induced protein destabilization in living cells and its reversal by glycine betaine. J. Mol. Biol. 429: 1155–1161.

Steffen-Munsberg, F., Vickers, C., Kohls, H., Land, H., Mallin, H., Nobili, A., Skalden, L., van den Bergh, T., Joosten, H.J., Berglund, P., et al. (2015). Bioinformatic analysis of a PLP-dependent enzyme superfamily suitable for biocatalytic applications. Biotechnol. Advances 33: 566–604.

Stöveken, N., Pittelkow, M., Sinner, T., Jensen, R.A., Heider, J., and Bremer, E. (2011). A specialized aspartokinase enhances the biosynthesis of the osmoprotectants ectoine and hydroxyectoine in *Pseudomonas stutzeri* A1501. J. Bacteriol. 193: 4456–4468.

Street, T.O., Bolen, D.W., and Rose, G.D. (2006). A molecular mechanism for osmolyte-induced protein stability. Proc. Natl. Acad. Sci. U.S.A. 103: 13997–14002.

Tanne, C., Golovina, E.A., Hoekstra, F.A., Meffert, A., and Galinski, E.A. (2014). Glass-forming property of hydroxyectoine is the cause of its superior function as a dessication protectant. Front. Microbiol. 5: 150.

Tao, P., Li, H., Yu, Y., Gu, J., and Liu, Y. (2016). Ectoine and 5-hydroxyectoine accumulation in the halophile *Virgibacillus halodenitrificans* PDB-F2 in response to salt stress. Appl. Microbiol. Biotechnol. 100: 6779–6789.

Tramonti, A., Nardella, C., di Salvo, M.L., Pascarella, S., and Contestabile, R. (2018). The MocR-like transcription factors: pyridoxal 5'-phosphate-dependent regulators of bacterial metabolism. FEBS J. 285, 3925–3944.

Treangen, T.J., and Rocha, E.P.C. (2011). Horizontal transfer, not duplication, drives the expansion of protein families in prokaryotes. PLoS Genet. 7: e1001284.

van den Berg, J., Boersma, A.J., and Poolman, B. (2017). Microorganisms maintain crowding homeostasis. Nat. Rev. Microbiol. 15: 309–318.

Van Goethem, M.W., Swenson, T.L., Trubl, G., Roux, S., and Northen, T.R. (2019). Characteristics of wetting-induced bacteriophage blooms in biological soil crust. mBio 10: e02287-19.

Vandrich, J., Pfeiffer, F., Alfaro-Espinoza, G., and Kunte, H.J. (2020). Contribution of mechanosensitive channels to osmoadaptation and ectoine excretion in *Halomonas elongata*. Extremophiles 24: 421–432.

Vargas, C., Jebbar, M., Carrasco, R., Blanco, C., Calderon, M.I., Iglesias-Guerra, F., and Nieto, J.J. (2006). Ectoines as compatible solutes and carbon and energy sources for the halophilic bacterium *Chromohalobacter salexigens*. J. Appl. Microbiol. 100: 98–107.

Vetting, M.W., LP, S.d.C., Yu, M., Hegde, S.S., Magnet, S., Roderick, S.L., and Blanchard, J.S. (2005). Structure and functions of the GNAT superfamily of acetyltransferases. Arch. Biochem. Biophys. 433: 212–226.

Vyas, R., Tewari, R., Weiss, M.S., and Karthikeyan, S. (2012). Structures of ternary complexes of aspartate-semialdehyde dehydrogenase (Rv3708c) from *Mycobacterium tuberculosis* H37Rv. Acta Crystallogr. D Biol. Crystallogr. 68: 671–679.

Wang, B., Qin, W., Ren, Y., Zhou, X., Jung, M.-Y., Han, P., Eloe-Fadrosh, E.A., Li, M., Zhen, Y., Lu, L., et al. (2019) Expansion of *Thaumarchaeota* habitat range is correlated with horizontal transfer of ATPase operons. ISME J. 13: 3057–3079.

Warren, C. (2019). Isotope pool dilution reveals rapid turnover of small quaternary ammonium compounds. Soil Biol. Biochem. 131: 90–99.

Webb, B.A., Karl Compton, K., Castaneda Saldana, R., Arapov, T.D., Keith Ray, W., Helm, R.F., and Scharf, B.E. (2017). *Sinorhizobium meliloti* chemotaxis to quaternary ammonium compounds is mediated by the chemoreceptor McpX. Mol. Microbiol. 103: 333–346.

Weinisch, L., Kirchner, I., Grimm, M., Kuhner, S., Pierik, A.J., Rossello-Mora, R., and Filker, S. (2019). Glycine betaine and ectoine are the major compatible solutes used by four different halophilic heterotrophic ciliates. Microb. Ecol. 77: 317–331.

Welsh, D.T. (2000). Ecological significance of compatible solute accumulation by micro-organisms: from single cells to global climate. FEMS Microbiol. Rev. 24: 263–290.

Widderich, N., Czech, L., Elling, F.J., Könneke, M., Stöveken, N., Pittelkow, M., Riclea, R., Dickschat, J.S., Heider, J., and Bremer, E. (2016a). Strangers in the archaeal world: osmostress-responsive biosynthesis of ectoine and hydroxyectoine by the marine thaumarchaeon *Nitrosopumilus maritimus*. Env. Microbiol. 18: 1227–1248.

Widderich, N., Höppner, A., Pittelkow, M., Heider, J., Smits, S.H., and Bremer, E. (2014a). Biochemical properties of ectoine hydroxylases from extremophiles and their wider taxonomic distribution among microorganisms. PloS One 9: e93809.

Widderich, N., Kobus, S., Höppner, A., Ricela, R., Seubert, A., Dickschat, J.S., Heider, J., Smits, S.H.J., and Bremer, E. (2016b). Biochemistry and crystal structure of the ectoine synthase: a metal-containing member of the cupin superfamily. PloS One 11: e0151285.

Widderich, N., Pittelkow, M., Höppner, A., Mulnaes, D., Buckel, W., Gohlke, H., Smits, S.H., and Bremer, E. (2014b). Molecular dynamics simulations and structure-guided mutagenesis provide insight into the architecture of the catalytic core of the ectoine hydroxylase. J. Mol. Biol. 426: 586–600.

Witt, E.M., Davies, N.W., and Galinski, E.A. (2011). Unexpected property of ectoine synthase and its application for synthesis of the engineered compatible solute ADPC. Appl. Microbiol. Biotechnol. 91: 113–122.

Wood, J.M. (2011). Bacterial osmoregulation: a paradigm for the study of cellular homeostasis. Annu. Rev. Microbiol. 65: 215–238.

Wu, R., Sanishvili, R., Belitsky, B.R., Juncosa, J.I., Le, H.V., Lehrer, H.J., Farley, M., Silverman, R.B., Petsko, G.A., Ringe, D., et al. (2017). PLP and GABA trigger GabR-mediated transcription regulation in *Bacillus subtilis* via external aldimine formation. Proc. Natl. Acad. Sci. U.S.A. 114: 3891–3896.

Yan, J., Nadell, C.D., Stone, H.A., Wingreen, N.S., and Bassler, B.L. (2017). Extracellular-matrix-mediated osmotic pressure drives *Vibrio cholerae* biofilm expansion and cheater exclusion. Nat. Commun. 8: 327.

Yancey, P.H. (2005). Organic osmolytes as compatible, metabolic and counteracting cytoprotectants in high osmolarity and other stresses. J. Exp. Biol. 208: 2819–2830.

Yokoyama, K., Ishijima, S.A., Clowney, L., Koike, H., Aramaki, H., Tanaka, C., Makino, K., and Suzuki, M. (2006). Feast/famine regulatory proteins (FFRPs): *Escherichia coli* Lrp, AsnC and related archaeal transcription factors. FEMS Microbiol. Rev. 30: 89–108.

Yu, Q., Cai, H., Zhang, Y., He, Y., Chen, L., Merritt, J., Zhang, S., and Dong, Z. (2017). Negative regulation of ectoine uptake and catabolism in *Sinorhizobium meliloti*: characterization of the EhuR gene. J. Bacteriol. 199: e00119-16.

Zaccai, G., Bagyan, I., Combet, J., Cuello, G.J., Deme, B., Fichou, Y., Gallat, F.X., Galvan Josa, V.M., von Gronau, S., Haertlein, M., et al. (2016). Neutrons describe ectoine effects on water H-bonding and hydration around a soluble protein and a cell membrane. Sci. Rep. 6: 31434.

Zhao, L., Vecchi, G., Vendruscolo, M., Korner, R., Hayer-Hartl, M., and Hartl, F.U. (2019). The Hsp70 chaperone system stabilizes a thermosensitive subproteome in *E. coli*. Cell Rep. 28: 1335–45. e1336.

Supplementary material: The online version of this article offers supplementary material (https://doi.org/10.1515/hsz-2020-0223).

The ups and downs of ectoine: structural enzymology of a major microbial stress protectant and versatile nutrient

Lucas Hermann, Christopher-Nils Mais, Laura Czech, Sander H.J. Smits, Gert Bange and Erhard Bremer

Supplementary material

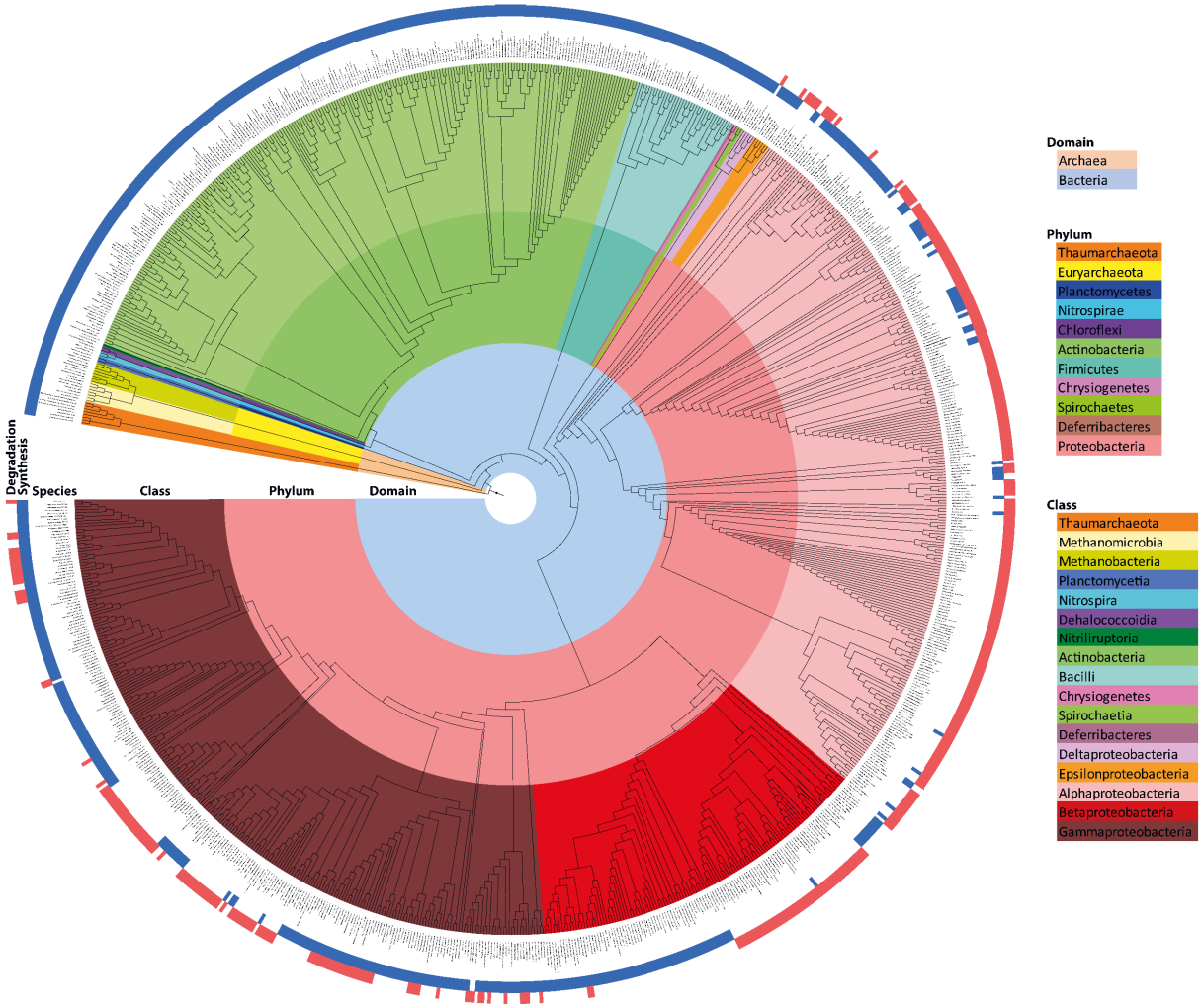

Supplementary Figure S1: Phylogenetic tree of microorganisms predicted to synthesize and/or to degrade ectoines.

Based on previous database searches by Czech et al. (2018) and Mais et al. (2020), fully sequenced genomes of *Bacteria* (8 557) and *Archaea* (293) deposited in the IMG/MER database (Chen et al., 2019) was searched from potential ectoine synthesizing microorganisms and those that are predicted to consume ectoine. The presence of gene (*ectC*) for the ectoine synthase (EctC) in the context of the other genes (*ectBA*) involved in ectoine synthesis (Czech et al., 2018) is marked with a blue square. The ability to degrade ectoines (Mais et al., 2020) was predicted by the co-adjacent genes for the ectoine utilization bi-module EutD/EutE, and is marked with a red square next to the respective microorganism. In this way, 676 microorganisms were predicted to synthesize ectoine, while 429 bacteria are predicted to consume ectoine. In this dataset, there are 96 microorganisms represented that are predicted to both synthesize and catabolize ectoine (Mais et al., 2020). A manually curated 16S rRNA-based phylogenetic tree was established by aligning the 16S rRNA DNA sequences with Clustal O (Sievers et al., 2011) and graphically represented with the iTOL tool (Letunic and Bork, 2016). Phylogenetic affiliations of microorganisms to domains, phyla and class are shown by color-code as listed in the figure.

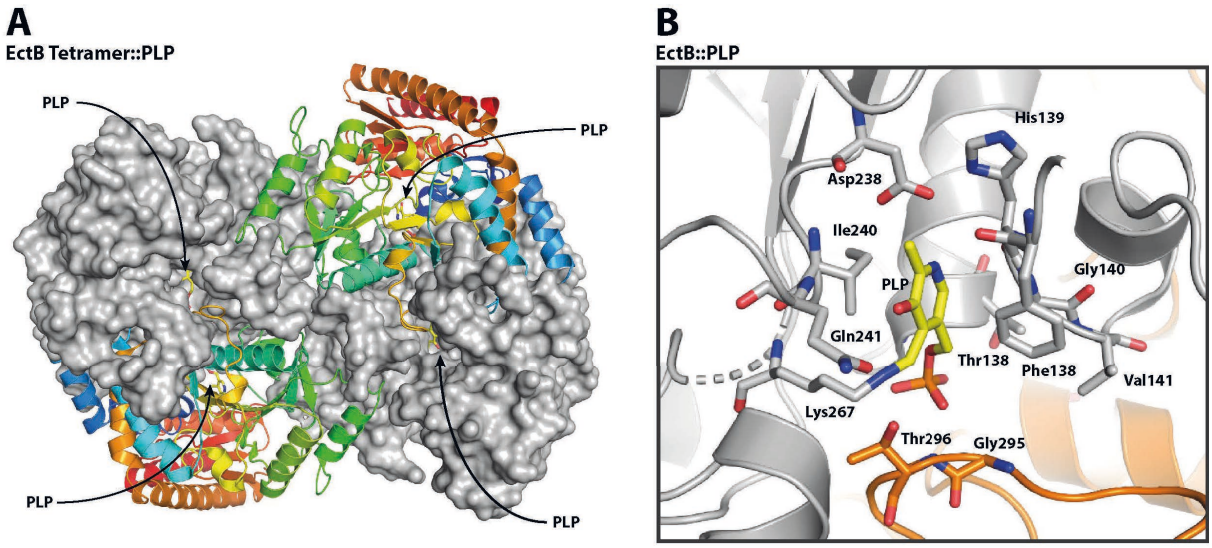

Supplementary Figure S2: Crystal structure of the L-2,4-diaminobutyrate transaminase EctB from *Chromohalobacter salexigens* in complex with pyridoxal-5'-phosphate (PLP).

Overview of the EctB tetramer with pyridoxal-5'-phosphate (PLP) bound in the active site of each monomer [PDB accession code: 6RL5] (Hillier et al., 2020). Two oft he EctB monomers are shown in cartoon representation with a rainbow coloring from carboxy-terminus to amino-terminus, while the two other monomers in the tetrameric assembly are depicted in surfaces representation modus. (B) Architecture of the active site of EctB with the covalently bound PLP (shown as yellow sticks) and amino acid residues highlights that are presumably involved in the enzyme reaction catalyzed by the EctB L-2,4-diaminobutyrate transaminase. Crystallographic data deposited in the PDB-file 6RL5 were used to render this cartoon using PyMol (Delano, 2002).

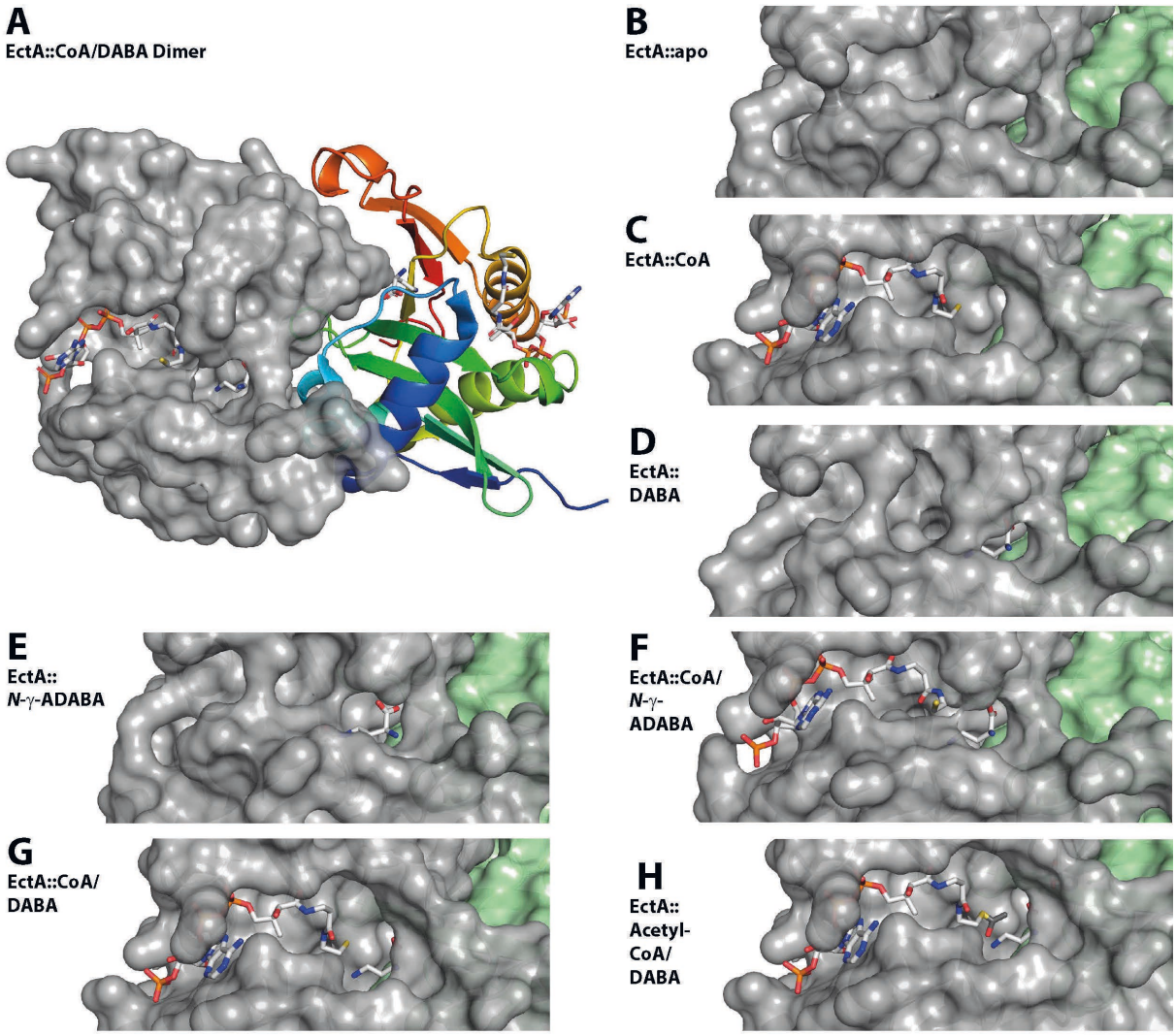

Supplementary Figure S3: A structural view of the reaction steps of the EctA diaminobuytrate acetyltransferase from *Paenibacillus lautus*.

This figure represents crystal structure of the EctA diaminobuytrate acetyltransferase from the thermotolerant bacterium *Paenibacillus lautus* in its apo, substrate- and enzyme reaction product-bound forms (Richter et al., 2020). (A) Overview of the EctA-dimer in complex with CoA and DABA [PDB accession code: 6SLL]. One of the monomers is shown in a cartoon representation with a rainbow coloring from carboxy-terminus to amino-terminus, while the second monomer is depicted in surfaces representation modus. (B) The empty binding sites for the substrates acetyl-CoA and DABA in the apo-form of EctA is shown [PDB accession code: 6SLK]. (C) Crystal structure of EctA in complex with CoA [PDB accession code: 6SK1]. (D) Crystal structure of EctA in complex with DABA [PDB accession code: 6SL8]. (E) Crystal structure of EctA in complex with γ-ADABA [PDB accession code: 6SJY]. (F) Crystal structure of EctA in complex with DABA and CoA [PDB accession code: 6SLL]. (G) γ-ADABA and CoA bound in the active sites of EctA [PDB accession code: 6SJY]. (H) Crystal structure of EctA in complex with DABA and CoA in which with an acetyl-group was added *in-silico* to the CoA sulfur to mimic the architecture of the EctA active site prior to enzyme catalysis. This picture

was generated by using the crystal structure of EctA in complex with DABA and CoA [PDB accession code: 6SLL] a the template. Crystallographic data deposited in the indicated PDB-files were used to render each cartoon by using PyMol (Delano, 2002). The depicted EctA dimers are depicted in surfaces representation modus; one monomer of EctA is depicted in grey, and the second monomer is depicted in green.

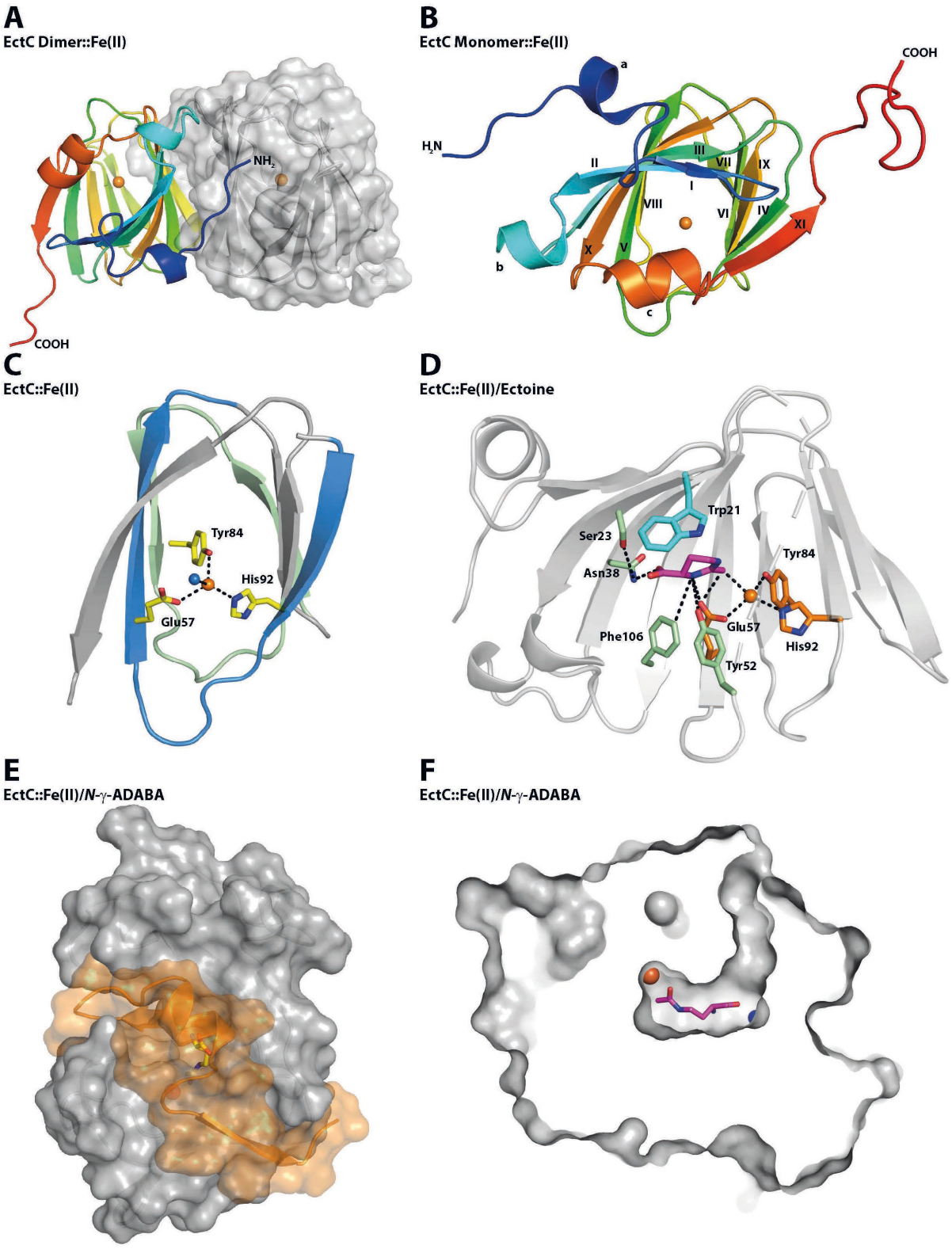

Supplementary Figure S4: Structural insights of the ectoine synthase EctC from *Paenibacillus lautus*. (A) The *Paenibacillus lautus* ectoine synthase (*Pl*EctC) (Czech et al., 2019) is a dimer present in a head-to-tail configuration with the iron catalyst (red sphere) bound in each monomer. The first monomer is shown in cartoon representation with a rainbow coloring from carboxy-terminus to amino-terminus, while the second monomer is depicted in surfaces representation modus [PDB accession code: 5ONM].

(B) The *Pl*EctC monomer in complex with iron is shown in a side-view with a rainbow-coloring from amino- to carboxy-terminus. The β-strands are labeled by roman numbers, and the three α-helices are marked by letters (a, b and c). (C) Close-up view of the iron-binding site of the *Pl*EctC protein (PDB code 5ONM). The iron (red sphere) is coordinated by the side-chains of Glu-57, Tyr-84, and His-92 and a localized water molecule (blue sphere); it has a distance of 2.9 Å to the iron atom. The two conserved cupin-motifs include those residues that coordinate the metal ion and are highlighted as part of the overall fold of the protein *Pl*EctC. (D) Iron (red sphere) and ectoine (gray sticks) bound in the catalytic core of the *Pl*EctC protein [PDB accession code: 5ONO]. The side-chains of the iron coordinating amino acids are depicted in orange, while the ectoine coordinating side-chains are shown in green. The side-chain of the catalytically relevant residue Trp-21 is shown in cyan. (E) Surface representation of the (*Pl*)EctC crystal structure with *N*-γ-ADABA [PDB accession code: 5ONN] in which the lid region (Czech et al., 2019; Widderich et al., 2016) is highlighted in orange; *N*-γ-ADABA is shown as yellow sticks and the iron atom is represented as a red sphere. (F) Cross-section through the catalytic core of the (*Pl*)EctC::Fe/*N*-γ-ADABA crystal structure [PDB accession code: 5ONN] with the entry tunnel for the *N*-γ-ADABA substrate. The positions of the catalytically important iron atom (red sphere) and a water molecule (blue sphere) are indicated. Crystallographic data deposited in the indicated PDB-files were used to render each cartoon by using PyMol (Delano, 2002).

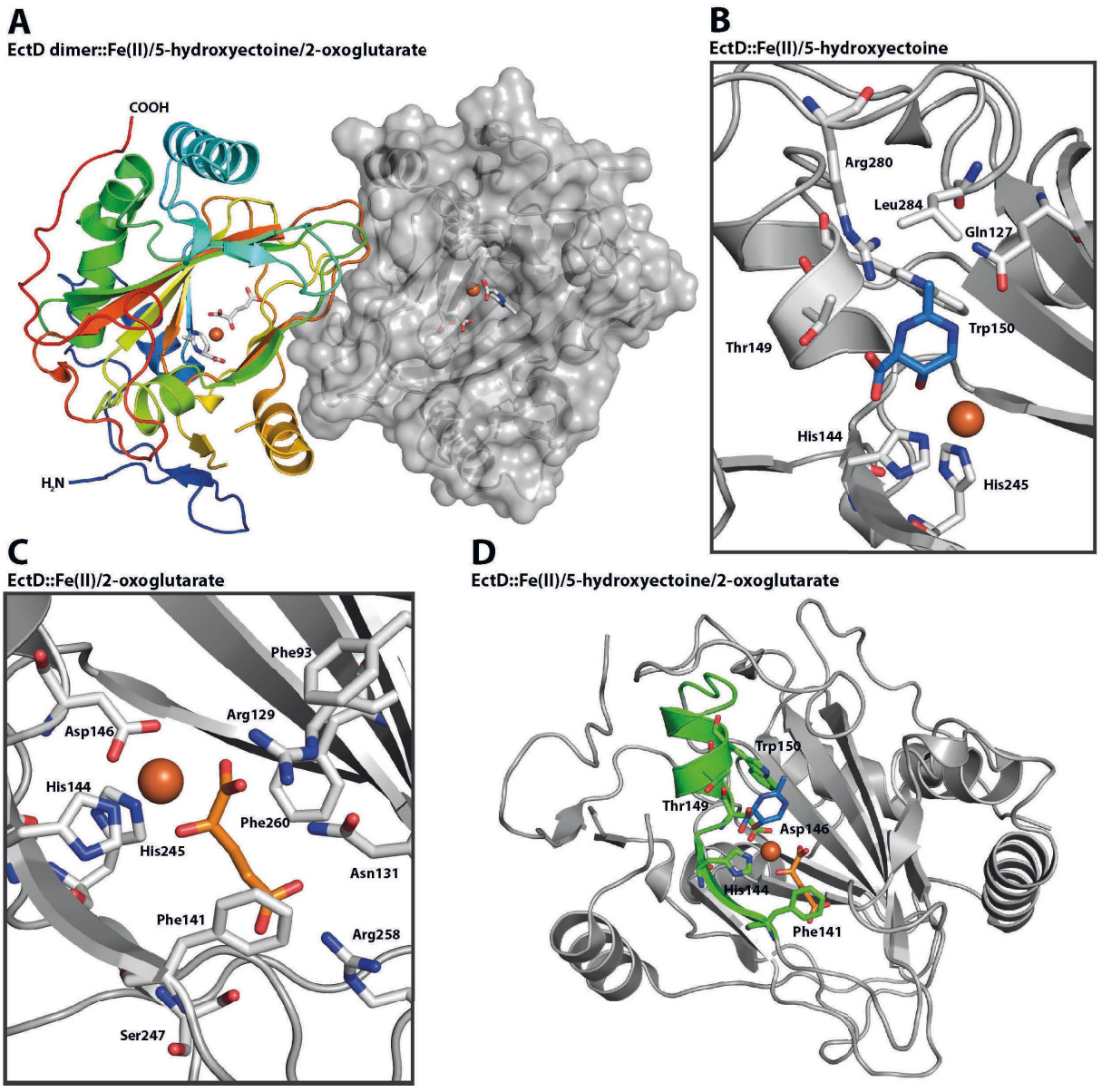

Supplementary Figure S5: Crystal structures of the ectoine hydroxylase EctD from *Sphingopyxis alaskensis*.

(A) Overview of the *Sphingopyxis alaskensis* (*Sa*) dimer. One monomer is shown in cartoon representation with a rainbow coloring from carboxy-terminus to amino-terminus while the second monomer is depicted in surfaces representation modus. Both Monomers have iron (orange sphere), 5-hydroxyectoine and 2-oxoglutarate bound in their active site [PDB accession code: 4Q5O]. (B) 5-hydroxyectoine (blue sticks) and iron (orange sphere) coordination in the catalytic center of the *Sa*EctD protein [PDB accession code: 4Q5O]. (C) 2-oxoglutarate (orange sticks) and iron (orange sphere) coordination in the catalytic center of the *Sa*EctD [PDB accession code: 4Q5O]. (D) The ectoine hydroxylase signature sequence motif (green) shown in the *Sa*EctD structure [PDB accession code: 4Q5O]. The side chains of the amino acids of the sequence motif coordinating ectoine (blue sticks), 2-oxogflutarate (orange sticks) and iron (orange sphere) are highlighted. Crystallographic data deposited

in the PDB-file 4Q5O (Höppner et al., 2014) were used to render each cartoon by using PyMol (Delano, 2002).

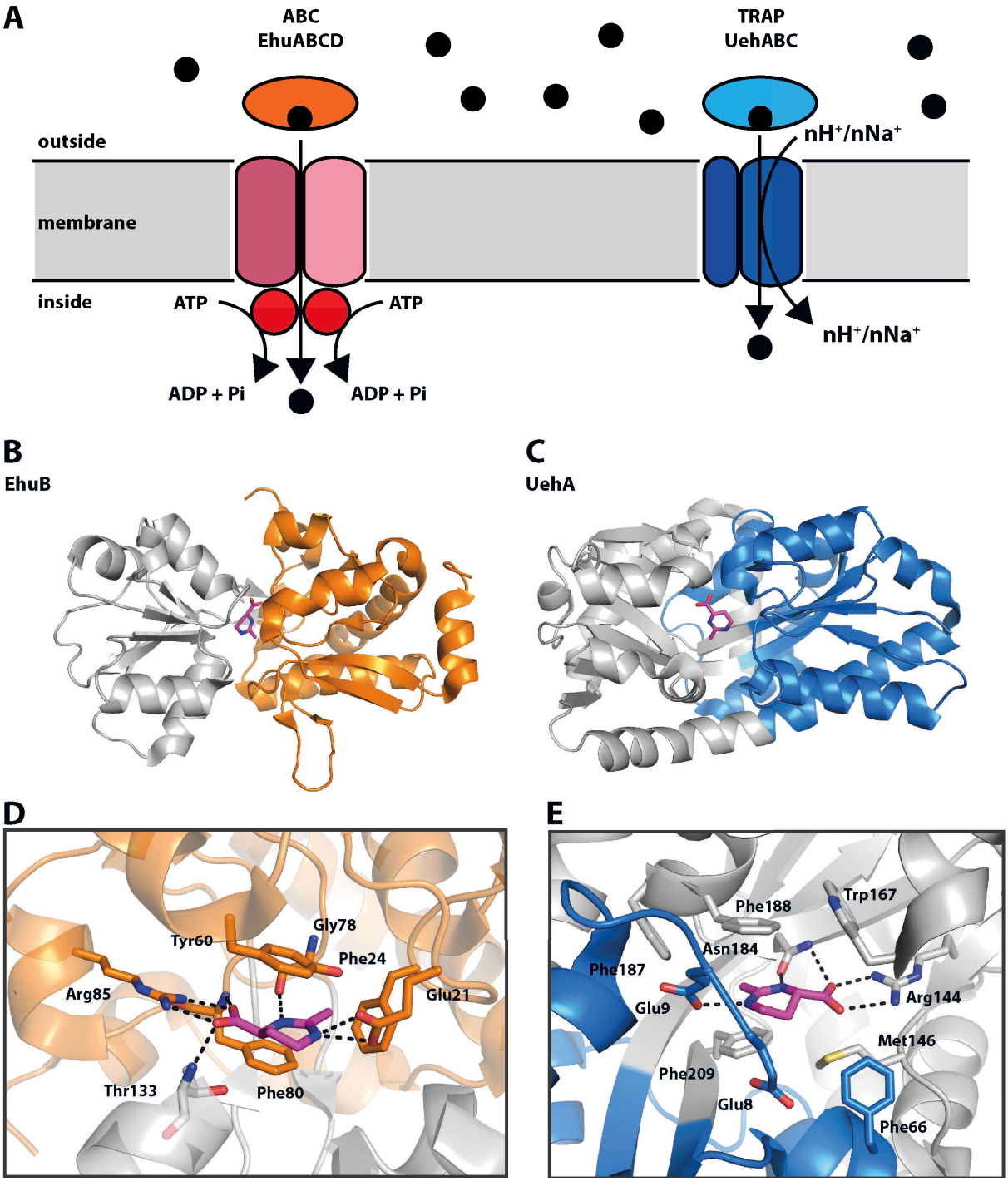

Supplementary Figure S6: ABC- and TRAP-type transporters used for the scavenging of ectoine and 5-hydroxyectoine when they are used as nutrients.

The EhuABCD system from *Sinorhizobium meliloti* is an ATP-binding-cassette (ABC) type transporter (Jebbar et al., 2005), while the UehABC system from *Ruegeria pomeroyi* is a member of the Tripartite ATP-independent periplasmic (TRAP) transporter family (Schulz et al., 2017b). The EhuB and UehA proteins are the extracellular substrate-binding proteins of these transporters; these have been crystalized in the presence of ectoine (Lecher et al., 2009; Hanekop et al., 2007). The transcription of the genes encoding the EhuABCD and UehABC importers is strongly induced when ectoine or 5-hydroxyectoine

is present in the growth medium, thereby reflecting the function of these transport systems for the acquisition of ectoines for use as nutrients (Jebbar et al., 2005; Schulz et al., 2017a; Lecher et al., 2009). (A) Schematic overview on the subunit composition of the EhuABCD and UehABC system. The transport activity of the Ehu transporter is fueled by ATP-hydrolysis, while that of the Ueh system is energized either by a proton (H^+) or a sodium (Na^+) gradient. (B and C) Overall fold of the EhuB [PDB accession code: 2Q88] (Hanekop et al., 2007) and UehA [PDB accession code: 3FXB] (Lecher et al., 2009) substrate binding proteins cyrstalized in the presence of ectoine. The two domains in EhuB and UehA are highlighted in grey/orange (B) and grey/blue (C), respectively. The bound ectoine ligand is shown as pink sticks. (D, E) Zoom into the ligand-binding site of EhuB (D) and UehA (E) and. All residues involved in ectoine binding are depicted as sticks; the ectoine ligand is shown in pink sticks. Crystallographic data deposited in the indicated PDB-files were used to render each cartoon by using PyMol (Delano, 2002).

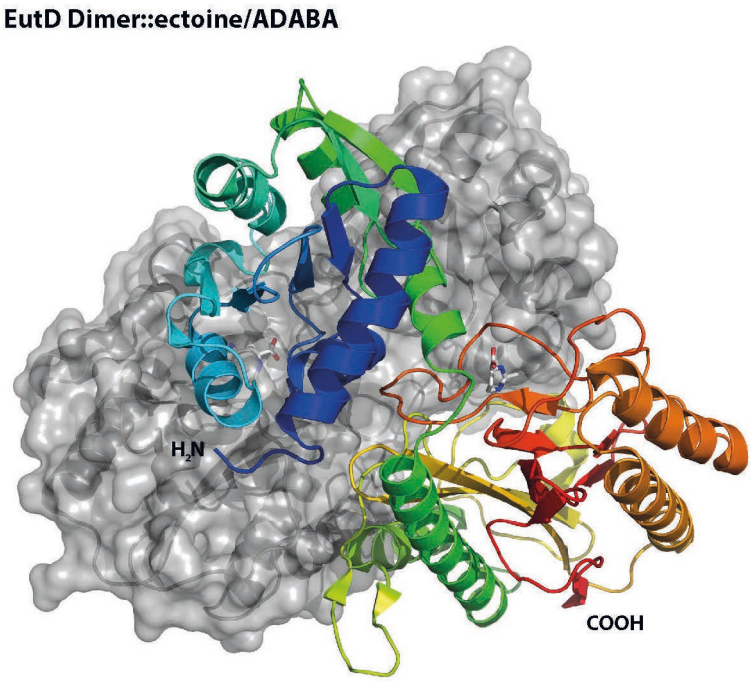

Supplementary Figure S7: Overview of the dimer of the ectoine/5-hydroxyectoine hydrolase EutD from *Halomonas elongata* [PDB accession code: 6TWK]. Monomer_1 is shown in cartoon representation with a rainbow coloring from the carboxy-terminus to the amino-terminus while monomer_2 is depicted in surfaces representation modus. In the active site of monomer I the substrate, ectoine, of the enzyme is bound, while in the active site of monomer II the reaction product, *N*-α-ADABA, of the ectoine hydrolase is present (Mais et al., 2020). Crystallographic data deposited in the indicated PDB-file were used to render each cartoon by using PyMol (Delano, 2002).

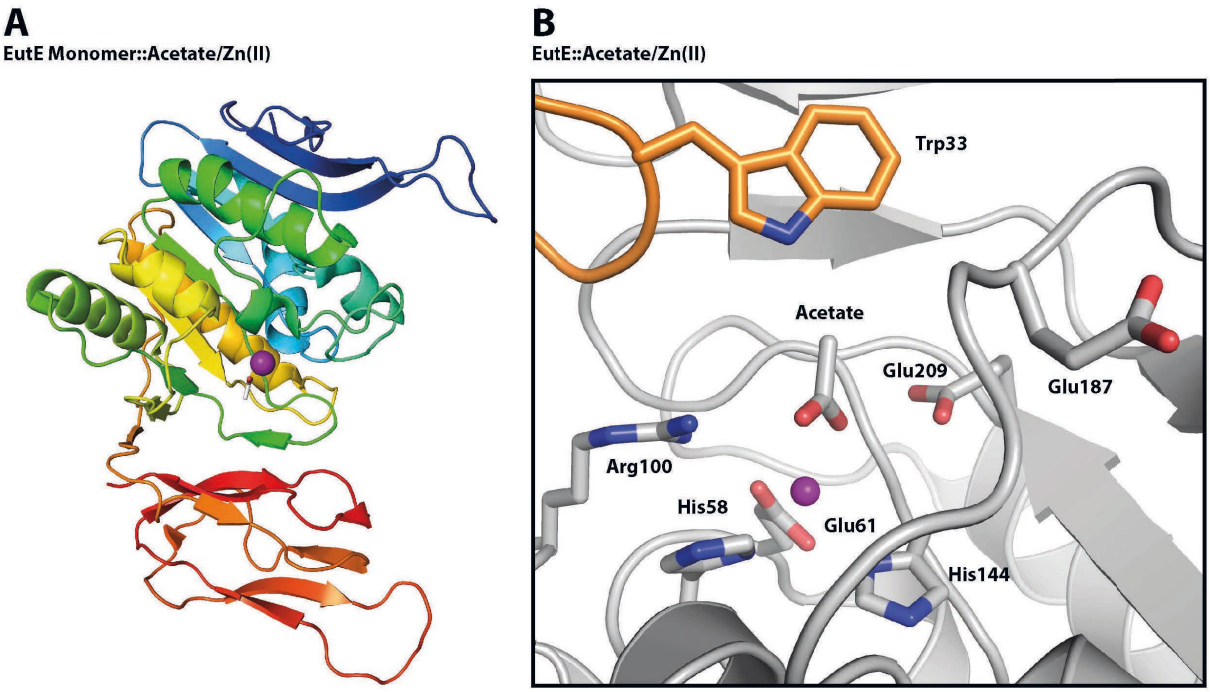

Supplementary Figure S8: Structural overviews of the *N*-α-ADABA deacetylase EutE from *Ruegeria pomeroyi.*

(A) The EutE protein is a *N*-acetyl-diaminobutyrate deacetylase (Mais et al., 2020). An overview of the monomeric *Ruegeria pomeroyi* (*Rp*) EutE protein is shown in cartoon representation with a rainbow coloring from carboxy-terminus to amino-terminus. In this crystal structure, the catalytically critical zinc ion (purple sphere) and the reaction product, acetate (sticks), of the (*Rp*)EutE protein is present in the active site [PDB accession code: 6TWM] (Mais et al., 2020). (B) A view into the active site of the (*Rp*)EutE protein with bound zinc (purple sphere) and acetate (sticks) [PDB accession code: 6TWM]. Crystallographic data deposited in the indicated PDB-file were used to render each cartoon by using PyMol (Delano, 2002).

References

Chen, I.A., Chu, K., Palaniappan, K., Pillay, M., Ratner, A., Huang, J., Huntemann, M., Varghese, N., White, J.R., Seshadri, R., Smirnova, T., Kirton, E., Jungbluth, S.P., Woyke, T., Eloe-Fadrosh, E.A., Ivanova, N.N. and Kyrpides, N.C. (2019). IMG/M v.5.0: an integrated data management and comparative analysis system for microbial genomes and microbiomes. Nucleic Acids Res. *47*, D666-D677.

Czech, L., Hermann, L., Stöveken, N., Richter, A.A., Höppner, A., Smits, S.H.J., Heider, J. and Bremer, E. (2018). Role of the extremolytes ectoine and hydroxyectoine as stress protectants and nutrients: genetics, phylogenomics, biochemistry, and structural analysis. Genes (Basel) *9*, 177.

Czech, L., Höppner, A., Kobus, S., Seubert, A., Riclea, R., Dickschat, J.S., Heider, J., Smits, S.H.J. and Bremer, E. (2019). Illuminating the catalytic core of ectoine synthase through structural and biochemical analysis. Sci. Rep. *9*, 364.

Delano, W.L. (2002). The *PyMol* molecular graphics system. Delano Scientific, San Carlos, CA, USA.

Hanekop, N., Höing, M., Sohn-Bösser, L., Jebbar, M., Schmitt, L. and Bremer, E. (2007). Crystal structure of the ligand-binding protein EhuB from *Sinorhizobium meliloti* reveals substrate recognition of the compatible solutes ectoine and hydroxyectoine. J. Mol. Biol. *374*, 1237-1250.

Hillier, H.T., Altermark, B. and Leiros, I. (2020). The crystal structure of the tetrameric DABA-aminotransferase EctB, a rate-limiting enzyme in the ectoine biosynthesis pathway. FEBS J., (in press) (doi: 10.1111/febs. 15265).

Höppner, A., Widderich, N., Lenders, M., Bremer, E. and Smits, S.H.J. (2014). Crystal structure of the ectoine hydroxylase, a snapshot of the active site. J. Biol. Chem. *289*, 29570-29583.

Jebbar, M., Sohn-Bösser, L., Bremer, E., Bernard, T. and Blanco, C. (2005). Ectoine-induced proteins in *Sinorhizobium meliloti* include an ectoine ABC-type transporter involved in osmoprotection and ectoine catabolism. J. Bacteriol. *187*, 1293-1304.

Lecher, J., Pittelkow, M., Zobel, S., Bursy, J., Bonig, T., Smits, S.H., Schmitt, L. and Bremer, E. (2009). The crystal structure of UehA in complex with ectoine-A comparison with other TRAP-T binding proteins. J. Mol. Biol. *389*, 58-73.

Letunic, I. and Bork, P. (2016). Interactive tree of life (iTOL) v3: an online tool for the display and annotation of phylogenetic and other trees. Nucleic Acids Res. *44*, W242-W245.

Mais, C.-N., Hermann, L., Altegoer, F., Seubert, A., Richter, A.A., Wernersbach, I., Czech, L., Bremer, E. and Bange, G. (2020). Degradation of the microbial stress protectants and chemical chaperones ectoine and hydroxyectoine by a bacterial hydrolase-deacetylase complex. J. Biol. Chem. (in press) (doi: 10.1074/jbc.RA 120.012722).

Richter, A.A., Kobus, S., Czech, L., Hoeppner, A., Zarzycki, J., Erb, T.J., Lauterbach, L., Dickschat, J.S., Bremer, E. and Smits, S.H.J. (2020). The architecture of the diaminobutyrate acetyltransferase active site provides mechanistic insight into the biosynthesis of the chemical chaperone ectoine. J. Biol. Chem. *295*, 2822-2838.

Schulz, A., Hermann, L., Freibert, S.-A., Bönig, T., Hoffmann, T., Riclea, R., Dickschat, J.S., Heider, J. and Bremer, E. (2017a). Transcriptional regulation of ectoine catabolism in response to multiple metabolic and environmental cues. Env. Microbiol. *19*, 4599-4619.

Schulz, A., Stöveken, N., Binzen, I.M., Hoffmann, T., Heider, J. and Bremer, E. (2017b). Feeding on compatible solutes: a substrate-induced pathway for uptake and catabolism of ectoines and its genetic control by EnuR. Environ. Microbiol. *19*, 926-946.

Sievers, F., Wilm, A., Dineen, D., Gibson, T.J., Karplus, K., Li, W., Lopez, R., McWilliam, H., Remmert, M., Soding, J., Thompson, J.D. and Higgins, D.G. (2011). Fast, scalable generation of high-quality protein multiple sequence alignments using Clustal Omega. Mol. Syst. Biol. *7*, 539.

Widderich, N., Kobus, S., Höppner, A., Ricela, R., Seubert, A., Dickschat, J.S., Heider, J., Smits, S.H.J. and Bremer, E. (2016). Biochemistry and crystal structure of the ectoine synthase: a metal-containing member of the cupin superfamily. PLoS One *11*, e0151285.

7 Discussion and Perspectives

The tetrahydropyrimidines ectoine and 5-hydroxyectoine were shown in recent years, to not only be exquisite “extremolytes” but ubiquitously used compatible solutes, present in all three domains of life, and used by microorganisms in a wide variety of habitats. As they are produced in up to molar intracellular concentrations, ectoines are frequently set free and can be detected in samples from various natural settings. Ectoine and 5-hydroxyectoine are valuable compounds, for practical purposes as well as energetically in terms of their biochemical production. Therefore, it is of no surprise, that nature came up with a way to recycle them. A vast group of bacteria can import, break down, and use the energy, carbon, and nitrogen sources, provided by ectoines. Although recent findings show that not only one type of ectoine catabolic pathway seem to exist, one type of pathway is the most intensively researched one. In this type of pathway, the central building block is the EutDE enzyme-bi-module which can break down the ring structure of both ectoines. As we could show, the so generated breakdown products of ectoine and 5-hydroxyectoine, α-ADABA and hydroxy-α-ADABA, are the key inducers for the central regulator of ectoine catabolism. The GntR-type regulator EnuR makes use of a highly ligand-specific sensory mechanism to detect α-ADABA and hydroxy-α-ADABA. Upon contact with a ligand, a PLP molecule covalently bound in the aminotransferase domain of EnuR performs the switch from an internal to an external aldimine, exchanging its bond to a lysine residue of the EnuR molecule to a free amino group of the ligand. Research included in this work illuminates the biochemical underpinnings of ectoine catabolism, its regulation as well as the distribution of this trait among bacteria.

7.1 The marine *Roseobacter*-group, *Ruegeria pomeroyi* and insights into metabolism

Ruegeria pomeroyi DSS-3 was the first sequenced species of the metabolically versatile and abundant marine *Roseobacter* clade (Moran *et al.*, 2004) and is the model organism of this clade which most of the research since then was focused on. First described as *Silicibacter pomeroyi* (Gonzalez *et al.*, 2003) but later on reclassified as a species of the *Ruegeria* genus (Yi *et al.*, 2007), *R. pomeroyi* is a versatile, heterotrophic, Gram-negative, marine, α-*Proteobacterium* (Moran *et al.*, 2004). It is able to use a variety of biochemical compounds as nutrients, which enables this specie to inhabit a ubiquitous niche in the generally highly competitive habitat of the world’s oceans (Moran *et al.*, 2004). The importance of marine microorganisms for the world ecosystems is evident as they are key drivers of global biochemical cycles such as carbon (Jiao and Zheng, 2011), nitrogen, and sulfur (Karl and Church, 2014). Marine phytoplankton are key species in fixing CO_2 in the upper ocean via photosynthesis, producing large quantities of organic matter (Jiao *et al.*, 2010), making oceans a major carbon reservoir and CO_2

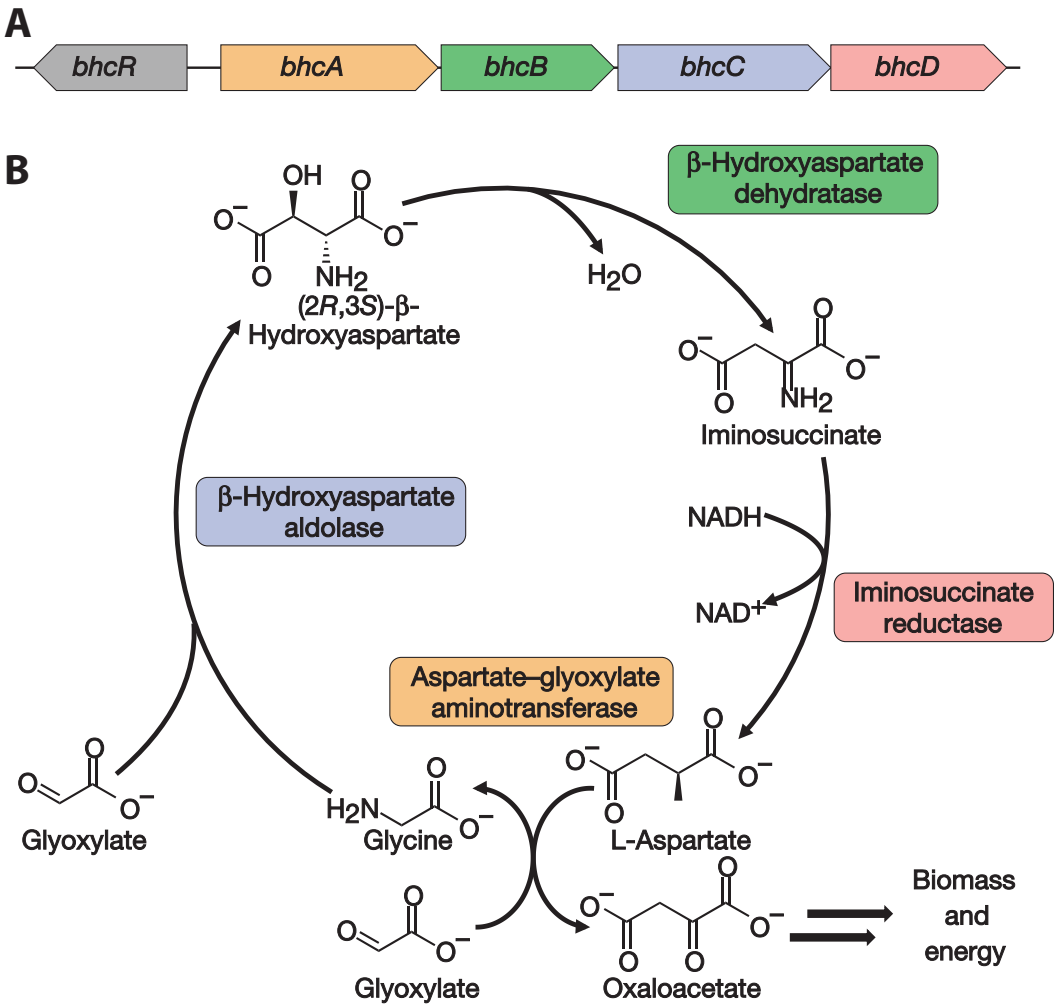

Figure 9: The β-hydroxyaspartate pathway. A) Genetic structure of the *bhc* gene cluster in *P. denitrificans* and *R. pomeroyi*. B) Reaction sequence and net balance of the β-hydroxyaspartate pathway. Image taken from (von Borzyskowski *et al.*, 2019).

sink. Heterotrophic organisms (e.g. bacterioplankton) are able to recycle this organic matter as carbon and energy sources, returning valuable nutrients to the phototrophic community (Christie-Oleza *et al.*, 2017; Kaur *et al.*, 2018). As the *Roseobacter* clade, to which *R. pomeroyi* belongs, is an integral part of bacterioplankton, accounting for up to 20% of the sea surface bacterioplankton in surface waters (Wagner-Dobler and Biebl, 2006), many aspects of *R. pomeroyi*'s metabolic potential attracted research in the microbial sciences.

A biochemical pathway which only little research was focused on in the nearly past 60 years is the β-hydroxyaspartate cycle (Figure 9). Nevertheless, the starting point of this pathway, glycolate is one of the most abundant sources of organic carbon in the ocean. Many *Proteobacteria* like *R. pomeroyi* are able to assimilate glyoxylate via the β-hydroxyaspartate cycle (BHAC). Overall, the BHAC enables the direct production of oxaloacetate from glyoxylate through only four enzymatic steps, representing the most efficient glyoxylate assimilation route described to date. Analysis of marine metagenomes shows that the BHAC is globally distributed and on average 20-fold more abundant than

the glycerate pathway, and actively transcribed in a phytoplankton bloom, suggesting a previously undescribed trophic interaction between autotrophic phytoplankton and heterotrophic bacterioplankton (von Borzyskowski *et al.*, 2019).

One key focus of research in this field over recent years was the ability of microorganisms like *R. pomeroyi* to produce and also degrade the compatible solute dimethyl sulfoniopropionate (DMSP) (Reisch *et al.*, 2013; Bullock *et al.*, 2017; Williams *et al.*, 2019). DMSP is frequently produced by marine phytoplankton, macroalgae, and reef building corals as an anti-stress molecule (Kiene *et al.*, 2000; Raina *et al.*, 2010; Bullock *et al.*, 2017). Dimethyl sulfide (DMS) produced in DMSP degradation is associated with the "smell of the seaside", fish, and used by a variety of animals as a navigation clue (Ishida, 1996; Nevitt and Bonadonna, 2005). As this active greenhouse gas forms condensation nuclei, it has also been proposed as promoting cloud formation (Charlson *et al.*, 1987). Therefore, DMSP degradation by marine bacteria like *R. pomeroyi* might play a role in climate and weather events (Charlson *et al.*, 1987; Kiene and Bates, 1990), although the actual significance of its participation in this process is still unclear (Hoffmann *et al.*, 2016). *R. pomeroyi* is also able to oxidize DMS to dimethylsulfoxide (DMSO) (Lidbury *et al.*, 2016), a process providing a major sink of DMS in marine surface waters and an important feature of the global sulfur cycle (Wang *et al.*, 2021). Strikingly, *R. pomeroyi* possesses four different DMSP degrading enzymes, three DMSP lyases (DddP, DddQ and DddW) as well as a DMSP demethylase DmdA (Todd *et al.*, 2012). Whether *R. pomeroyi* cleaves or demethylates DMSP is a decision process regulated by the level of salinity of the environment (Salgado et al., 2014). *R. pomeroyi* uses its elaborate genetic build up as a specialist of DMSP metabolism to interact intensively with phytoplankton species like cyanobacteria (Kaur *et al.*, 2018), especially in algal blooms, and changes its biochemical pathways towards a cooperative lifestyle, including quorum-sensing molecule production (Johnson *et al.*, 2016).

Next to DMSP metabolism, other substances which can be degraded and re-used by *R. pomeroyi* have been extensively investigated. These include monophosphates (Sebastian and Ammerman, 2011) and polyphosphates (Achbergerová and Nahálka, 2014), purines like xanthine (Cunliffe, 2015), the osmoprotectant Trimethylamine-*N*-oxide (TMAO) (Lidbury *et al.*, 2014; Li *et al.*, 2015), dimethylamines (Lidbury *et al.*, 2017) polyamines like spermidine and putrescine (Mou *et al.*, 2010), polycyclic aromatic hydrocarbons like pyrene (Zada *et al.*, 2021) and Dihydroxypropanesulfonate (DHPS) (Chen *et al.*, 2021). *R. pomeroyi* is able to oxidize carbon monoxide (Cunliffe, 2013) and some *R. pomeroyi* ecotypes can also respirate nitrate can dwell on in its highly competitive habitat. To scavenge them, *R. pomeroyi* not only uses high affinity transport systems (Christie-Oleza *et al.*, 2012; Sun *et al.*, 2012; Durham *et al.*, 2017), but also uses biological warfare to increase its chances. Algicidal lactones are produced by *R. pomeroyi* and can be used to fend of competitor bacterial species (Sharpe *et al.*, 2020) and might play an increased role in the fading of algal

blooms to scavenge the intracellular constituents of algae (Riclea *et al.*, 2012). Such a Jekyll-and-Hyde switch of a symbiotic to an opportunistic pathogenic lifestyle in the closely related *Roseobacter* species *Phaeobacter gallaeciensis* has been observed (Seyedsayamdost *et al.*, 2011). Although *R. pomeroyi* does not possess the roseobacticides produced by *P. gallaeciensis* their role can possibly be taken over by the lactones produced by *R. pomeroyi*. All these aspects play part in the niche adaptation eagerly performed by *Roseobacter*-species (Christie-Oleza *et al.*, 2012; Simon *et al.*, 2017).

7.2 Ectoines, their prevalence, and uptake by microorganisms

The tetrahydropyrimidines ectoine [(4*S*)-2-methyl-1,4,5,6-tetrahydropyrimidine-4-carboxylic acid] and its derivative 5-hydroxyectoine [(4*S,*5*S*)-2-methyl-5-hydroxy-1,4,5,6-tetrahydropyrimidine-4-carboxylic acid] are excellent cytoprotectants (Pastor *et al.*, 2010; Czech *et al.*, 2018b) and can be synthesized and/or imported by a great number of microorganisms (Galinski and Truper, 1994; Pastor *et al.*, 2010; Reshetnikov *et al.*, 2011b; Schwibbert *et al.*, 2011; Kunte *et al.*, 2014; Czech *et al.*, 2018b; Gunde-Cimerman *et al.*, 2018; Leon *et al.*, 2018). These osmotically active substances can not only function as protectants against increased osmolarity of the environment, but also be used by cold- or heat-challenged cells against these dangers (Malin and Lapidot, 1996; Garcia-Estepa *et al.*, 2006a; Bursy *et al.*, 2008; Kuhlmann *et al.*, 2008a; Kuhlmann *et al.*, 2011; Ma *et al.*, 2017). Many organisms even accumulate both ectoines in a mixture with changing ratios (Schiraldi *et al.*, 2006; Saum and Muller, 2007; Bursy *et al.*, 2008; Saum and Muller, 2008; Pastor *et al.*, 2010; Seip *et al.*, 2011; Stöveken *et al.*, 2011; Czech *et al.*, 2016; Tao *et al.*, 2016). The wide distribution of the biosynthetic genes for ectoines (*ectABCD*) in members of the *Bacteria* and in some *Archaea* has been established over the recent years (Pastor *et al.*, 2010; Kunte *et al.*, 2014; Widderich *et al.*, 2016c; Czech *et al.*, 2018b; Hermann *et al.*, 2020; Mais *et al.*, 2020). In these analysis up to 7.5% of all 8,850 fully sequenced microbial genomes have the genetic setup of ectoine producers, spanning ten bacterial and two archaeal phyla (Hermann *et al.*, 2020). Organisms which overall use these substances might even be in a much larger number as exemplified by microalgae that are able to import ectoines (Harding *et al.*, 2016; Landa *et al.*, 2017; Weinisch *et al.*, 2019; Fenizia *et al.*, 2020). Ecological niches in which ectoines are used are not only limited to environments with extreme salt concentrations but also marine and terrestrial habitats, as well as microbes associated in a symbiotic relationship with a host (Hermann *et al.*, 2020).This widespread usage of ectoines and the very substantial intracellular concentrations of ectoines which can be achieved (Pastor *et al.*, 2010; Kunte *et al.*, 2014) also explains why ectoines can be found in various environmental settings (Mosier *et al.*, 2013; Warren, 2013, 2014; Bouskill *et al.*, 2016b; Bouskill *et al.*, 2016a; Warren, 2016). Ectoines are introduced into these environments either after an osmotic down-shock in which ectoine producing organisms rapidly and unselectively open mechanosensitive channels (Reuter *et al.*, 2014; Booth *et al.*, 2015) or when cells actively excrete these

compounds, a process potentially allowing a more fine-tuned control of the osmoadaptation (Lamark *et al.*, 1992; Grammann *et al.*, 2002; Kuhlmann *et al.*, 2008a; Czech *et al.*, 2016; Hoffmann and Bremer, 2016; Czech *et al.*, 2018a; Vandrich *et al.*, 2020). Another factor is the death and degradation of bacterial cells, which could set ectoines free; a process supported by interbacterial-warfare (Granato *et al.*, 2019), predators of bacteria (Williams *et al.*, 2016) or the lytic effect of a phages, the most abundant biological entity on earth (Young, 1992; Fuhrman, 1999; Weinbauer, 2004; Suttle, 2007)

As the synthesis of ectoines is an energetically expensive process (Oren, 1999; Hermann *et al.*, 2020), microorganisms are keen to rather take up free ectoines from environmental sources (Welsh, 2000). Since compatible solutes in the environment are generally in very low concentrations, their uptake must be facilitated by high affinity transporters. Examples of such transporter systems which have been investigated and characterized are the Tripartite ATP-independent periplasmic (TRAP) transporter TeaABC from *H. elongata* (Grammann *et al.*, 2002; Tetsch and Kunte, 2002), the betaine-choline-carnitine transporter-type carrier EctT from *Virgibacillus pantothenticus* (Kuhlmann *et al.*, 2011), as well as the binding-protein-dependent ABC-transporter EhuABCD from *Sinorhizobium meliloti* (Jebbar *et al.*, 2005; Hanekop *et al.*, 2007) and the TRAP-transporter UehABC from *R. pomeroyi* (Lecher *et al.*, 2009). Nevertheless, not all of these transport systems are actually used to collect ectoines as cytoprotectants. *R. pomeroyi* for example, although possessing the UehABC transport system cannot use ectoines as a protectant against increased salinity (Schulz *et al.*, 2017b).

7.3 Ectoines as nutrients

As described above, synthesis of compatible solutes such as ectoines is an energetically expensive process for cells (Oren, 1999). The high turn-over rate of compatible solutes indicates their rapid re-use in nature, affording the low concentrations of ectoines measured in nature (Warren, 2020). Additionally to re-using compatible solutes as stress protectants, microorganisms also came up with mechanisms to recycle them as nutrients (Welsh, 2000). Especially the two nitrogen atoms fixed in ectoines are an attempting resource as nitrogen is often growth limiting, for example in marine habitats (Vitousek and Howarth, 1991; Howarth and Marino, 2006). As *R. pomeroyi* belongs to the heterotrophic and metabolically versatile *Roseobacter*-clade, it is an organism especially keen on this kind of metabolical traits, as exemplified above for the metabolism of the compatible solutes DMSP and TMAO. Ectoines are also subject to bacterial consumption, as first detected in *Ectothiorhodospora halochloris* (Galinski and Herzog, 1990). Early physiological research on ectoine metabolism was carried out in *Rhizobium leguminosarum* (Talibart *et al.*, 1994) and *Pseudomonas putida* (Manzanera *et al.*, 2002). The first molecular understanding of the enzymes involved in ectoine catabolism stem from research on the plant roots-associated bacterium *S. meliloti.* In this organism ectoine-inducible proteins could be found in a proteomics study (Jebbar *et al.*, 2005). In addition to *S. meliloti,* genes

involved in ectoine catabolism were also investigated in *H. elongata, Chromohalobacter salexigens*, *R. pomeroyi*, and *Methylomicrobium alcaliphilum* (also referred to as *Methylotuvimicrobium alcaliphilum*) (Vargas *et al.*, 2006; Schwibbert *et al.*, 2011; Schulz *et al.*, 2017a; Reshetnikov *et al.*, 2020). As described in a biochemical and structural study included in this work, organisms able to degrade ectoine, employ two enzymes, the ectoine hydrolase EutD and the *N*-α-acetyl-L-2,4-diaminobutyrate deacetylase EutE (Mais *et al.*, 2020) [also referred to as DoeA and DoeB, respectively (Schwibbert *et al.*, 2011)]. These two enzymes degrade ectoine/5-hydroxyectoine into acetate and diaminobutyric acid (DABA). The resulting EutD/EutE enzyme reaction product DABA can then be further metabolized to L-aspartate by the Atf aminotransferase and the Ssd dehydrogenase and the product L-aspartate might finally fuel the TCA-cycle (Schwibbert *et al.*, 2011; Schulz *et al.*, 2017a). However, in the previous studies misconceptions about the mechanism of ectoine catabolism were introduced which could be clarified in this work. Especially the functioning of the central enzymes EutD and EutE could be characterized and previously proposed hypothesis about properties of these enzymes (Schulz *et al.*, 2017a) could be reevaluated.

7.4 Structural insight in the ectoine hydrolase EutD

EutD reversibly catalyzes the initial step of ectoine degradation, which is the opening of the heteropyrimidine ring (Mais *et al.*, 2020). High-resolution crystal structures of the apo (PDB: 6TWJ), substrate- (PDB:6TWK) and product-bound (PDB: 6YO9) states of the EutD protein from *H. elongata* (*He*EutD) have been solved (Mais *et al.*, 2020). These structures show that EutD forms a highly intertwined homodimer (Mais *et al.*, 2020) (Figure 9). Each EutD monomer consists of an α-helical N-terminal domain and a C-terminal domain exhibiting a typical pita-bread fold (Bazan *et al.*, 1994), consisting of two antiparallel β-sheets and harboring the active site of EutD. The N-terminal domain of the opposing chain forms a lid on top of this active site. This kind of protein structure is highly similar to the related protein family of M24 amino peptidases, whose enzyme activity typically depends on two highly coordinated metals (Rawlings and Barrett, 1993). In contrast, in the case of the EutD no metals are incorporated in the active site, as residues not suitable for metal ion coordination have replaced most of those residues typically involved in metal-coordination in M24-type amino-peptidases (Rawlings and Barrett, 2013). The active site of EutD has evolved to specifically accommodate the cyclic substrate ectoine without an additional specific co-factor (Mais *et al.*, 2020). Another example of this process is the ribosome-biogenesis factor Ebp1 (also Arx1), an ancient M24-amino-peptidase in which the substrate-binding pocket is maintained, but the zinc-ion binding site evolved into a ribosome-biogenesis factor (Kowalinski *et al.*, 2007). The only amino acid left in the active site, which in other aminopeptidases coordinates the metal ion is Glu255. Nevertheless, in EutD this highly conserved amino acid was found to be the ‘anchor’ of the α-ADABA intermediate, which is

covalently attached to this residue via an orthoester bond. While covalently bonded reaction intermediates with cysteines or lysines are rather frequently described (Heine *et al.*, 2001), this is a unique example of a covalent intermediate involving a glutamate-bond.

Intriguingly, the EutD homodimer crystallized in the presence of its ectoine substrate harbors the ectoine substrate in one active site and an α-ADABA product covalently bound to the conserved glutamate (Glu255) in the other. In the ectoine-bound active site, a water molecule hydrogen-bonded to His238, can be found close to the methyl group-bearing carbon of ectoine. This water molecule, activated by its coordinating histidine residue might perform a nucleophilic attack on the ectoine molecule, leading to the cleavage of the heteropyrimidine ring. The EutD-mediated ring cleavage results in α-ADABA, which then covalently binds the carboxyl side chain of Glu255. As the N-terminus of one monomer protrudes into the active site of the other monomer (and *vice versa*) a tyrosine residue (Tyr52) might facilitate a sort of communication between both monomers in order to signal their catalytic progress to each other. Superimposition of the two active sites of the EutD homodimer revealed a noticeable movement of the "signaling loop" harboring Tyr52. This movement of the "signaling loop" in turn, leads to other conformational changes in the N-terminal domain of the ectoine hydrolase (Mais *et al.*, 2020). Thus, it can be imagined that the way in which the two EutD catalytic sites communicate through structural changes will aid cooperativity during the catalytic cycle and forms some sort of "pumping-mechanism". The critical role of Tyr52 for the communication of the two active sites in the EutD homodimer is supported by the finding that substituting Tyr52 by alanine abolishes enzymatic activity of the ectoine hydrolase (Mais *et al.*, 2020). The signaling loop could potentially also interact with EutE, the next enzyme of the pathway, which seems to be needed to release α-ADABA from the active site of EutD.

The crystal structure of EutD obtained in the presence of its reaction product α-ADABA showed the same Glu255-α-ADABA adduct observed when ectoine was supplied as the substrate, while the other active site contained a free α-ADABA molecule. In this crystal structure, α-ADABA is primarily hydrogen-bonded to Arg70 from the N-terminal domain of the opposing EutD chain (Mais *et al.*, 2020). Collectively, these two structures further supported the reversible character of the EutD-mediated cleavage of ectoine. Reversibility of the EutD-mediated reaction seems to be the reason why efficient ectoine degradation can only occur in the presence of EutE, which efficiently deacetylates α-ADABA irreversibly.

7.5 Structural insights in the *N*-α-acetyl-L-2,4-diaminobutyrate deacetylase EutE

The *N*-α-acetyl-L-2,4-diaminobutyrate deacetylase EutE converts α-ADABA into DABA (Schwibbert *et al.*, 2011; Schulz *et al.*, 2017a; Mais *et al.*, 2020) and is also needed for EutD to perform its ring-opening function (Mais *et al.*, 2020). The enzyme shares high structural and sequence similarity to the

aspartodeacylase (AAC) family, which is conserved across all kingdoms of life (Makarova *et al.*, 1999). Biochemical analysis of the *R. pomeroyi* EutE enzyme demonstrated that EutE exclusively processes α-ADABA in a highly efficient manner, while its isomer γ-ADABA, the substrate of the ectoine synthase (Czech *et al.*, 2019), cannot be deacetylated (Mais *et al.*, 2020). These data are consistent with reports on the properties of the corresponding *H. elongata* enzyme (Schwibbert *et al.*, 2011). EutE forms stable hexamers in solution when substrates, products and the catalytically essential zinc ion are absent (Mais *et al.*, 2020). Nevertheless, this ternary assembly could not be supported by the crystallographic data suggesting the active form of EutE to be a monomer (Figure 10) (Mais *et al.*, 2020). Whether the observed EutE hexamer in solution is of functional relevance or simply an artifact remains to be determined.

Crystal structures of EutE from *R. pomeroyi* are available in the apo state (PDB: 6TWL) and bound to its products DABA and acetate (PDB: 6TWM) (Mais *et al.*, 2020), revealing structural homology to aspartodeacylases (Le Coq *et al.*, 2008). Aspartodeacylases in general are crescent-like shaped enzymes with two subdomains and one active site. In the latter they possess a zinc-binding site constituted by a glutamate and two histidine residues (Mais *et al.*, 2020). The products of α-ADABA deacetylation, DABA and acetate, both coordinate the central zinc-atom in the active site of the EutE enzyme with their carboxyl moieties. Comparison of the EutE crystal structure to aspartodeacylases, which have been crystalized in presence of a substrate-mimic (*N*-phosphonomethyl-L-aspartate) (Le Coq *et al.*, 2008), as well as mutational analysis of EutE, indicate Arg111 is to form the hydrogen bond with the second carboxyl moiety of α-ADABA, and Asp195 to hydrogen-bond the amine group. During the hydrolysis of α-ADABA, which proceeds via a tetrahedral transition state, the guanidinium moiety of Arg100 further compensates the emerging negative charge (Mais *et al.*, 2020).

A recent bioinformatic study found that this type of ADABA-deacetylases might not be the only type of ADABA-deacetylase involved in the catabolism of ectoines (Hermann, 2022). As the enzyme previously identified as EutE (DoeB) in *M. alcaliphilum* 20Z (from now on referred to as HipO) only has a minimal sequence identity to EutE (DoeB) from *H. elongata*, this identification might not hold true. The enzyme is also ascribed to a different type of protein family as EutE and annotated not as an aspartoacylase but as a hippurate hydrolase. Protein modelling using the alphafold2 facility (Jumper *et al.*, 2021) suggests a different type of structural build-up to this protein. Experimental data in *M. alcaliphilum* 20Z supported the functioning of "HipO" as an ADABA-deacetylase indicating that actually two independent types of ADABA-deacetylases might exist (Hermann, 2022).

7.6 The EutDE-bi-module and topology of the ectoine catabolic pathway

Intriguingly, *in-vitro* biochemical data and heterologous expression in *E. coli*, of only EutD from *R. pomeroyi* did not suffice to open the ectoine molecules. However, when EutD and EutE together

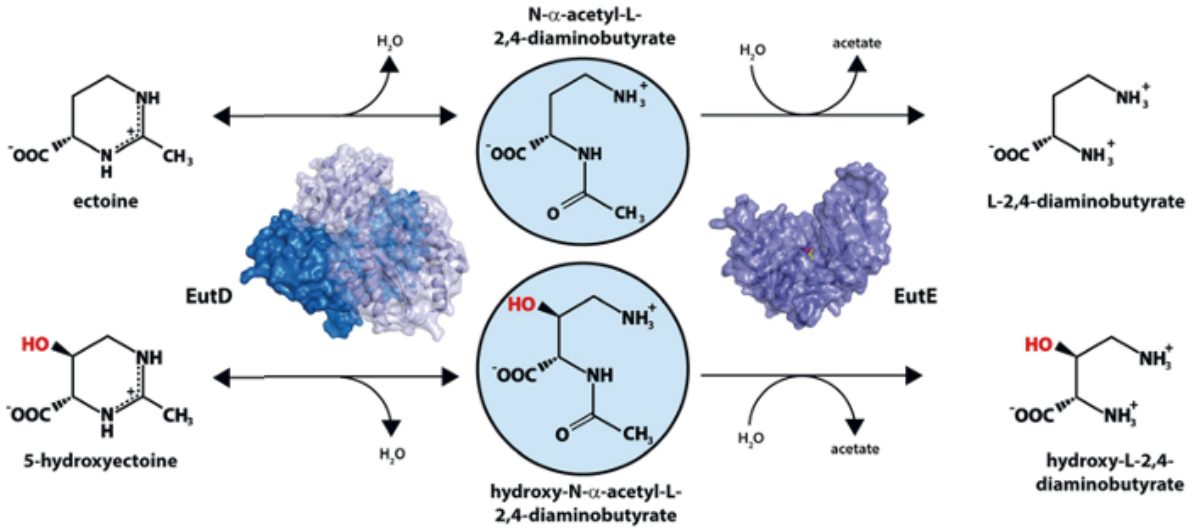

Figure 10: Pathway for the catabolism of ectoine via α-ADABA to DABA and for the degradation of 5-hydroxyectoine via hydroxy-α-ADABA to hydroxy-DABA. EutD: ectoine/5-hydroxyectoine hydrolase; EutE: *N*-α-acetyl-L-2,4-diaminobutyrate/hydroxy-*N*-α-acetyl-L-2,4-diaminobutyrat deacetylase. The crystal structures of the H. elongata EutD protein in complex with ectoine and the Glu-255-ADABA adduct (PDB: 6TWK) was used to visualize the dimeric protein assembly. The crystal structure of the *R. pomeroyi* EutE ADABA deacetylase in complex with the reaction products DABA and acetate (PDB: 6TWM) was used to visualize the monomeric protein. Image taken from (Hermann *et al.*, 2020).

were set to this task, the ectoine as well as the hydroxyectoine ring could be readily cleaved, indicating that both enzymes need to work jointly (Mais *et al.*, 2020). A per-se non-functioning of the EutD-enzyme can be ruled-out in this case, as the sole EutD-enzyme was able to diminish α-ADABA and produce ectoine when added to a sample of α-ADABA. Therefore, EutD alone actually catalyzes the reverse reaction attributed to it. Co-expression of EutD and EutE in contrast could readily degrade ectoines, indicating that EutE is needed to give the EutD-mediated ring-cleavage its physiologically assigned direction. Heterologous production of the EutD hydrolase from *R. pomeroyi* and *M. alcaliphilum* in *Escherichia coli* in the presence of ectoine yielded exclusively α-ADABA and, when the *Rp*EutD enzyme was exposed *in vivo* to 5-hydroxyectoine, also hydroxy-α-ADABA (Mais *et al.*, 2020; Reshetnikov *et al.*, 2020). In contrast, the heterologous production of the EutD (DoeA) hydrolase from *H. elongata* seemingly yielded both α- and γ-ADABA, with the apparent use of γ-ADABA for a new round of ectoine synthesis via EctC in *H. elongata* (Schwibbert *et al.*, 2011). Hence, the catalytic profile of the ectoine hydrolase from *M. alcaliphilum* and *H. elongata* seem to differ, despite the fact, that both extremophiles can consume and produce ectoine (Schwibbert *et al.*, 2011; Reshetnikov *et al.*, 2020). α-ADABA, but not γ-ADABA, serves as the internal inducer for ectoine/5-hydroxyectoine catabolic gene clusters regulated by the widely distributed EnuR repressor protein (Schulz *et al.*, 2017b). This is of special physiological importance in microorganisms like *H. elongata* which can synthesize as well as degrade ectoines. Otherwise newly synthesized ectoine in osmoadaptation would

immediately be subject to degradation again, increasing the energetic costs tremendously. As previously described (Figure 8), Schulz *et al.* (2017) suggested that the use of this compound as a nutrient would require the initial removal of the hydroxyl group by the EutABC enzymes to form ectoine (Schulz *et al.*, 2017b; Schulz *et al.*, 2017a). Consistent with this hypothesis was the finding that an *eutABC* deletion of the *R. pomeroyi* catabolic gene cluster abolished the use of 5-hydroxyectoine but not that of ectoine (Schulz *et al.*, 2017b). Nevertheless, regarding the finding of Mais *et al.* (2020) that the EutD hydrolase can also open the heteropyrimidine ring of 5-hydroxyectoine to form hydroxy-α-ADABA rather suggests a role of the EutABC enzymes in the down-stream procession of the EutD- or EutD/EutE-formed metabolites, presumably converting hydroxy-DABA to DABA, as hydroxy-DABA could be detected in high concentrations in intracellular samples of the targeted metabolic analysis of *R. pom*eroyi cells grown on 5-hydroxyectoine.

7.7 EnuR and regulation of ectoine catabolism

The reason ectoine catabolic genes were first detected is that their transcription is strongly up-regulated when ectoines are present in the growth medium (Jebbar *et al.*, 2005; Schulz *et al.*, 2017a; Yu *et al.*, 2017), in contrast to the osmotically controlled ectoine-biosynthetic gene clusters (Czech *et al.*, 2018a). Nevertheless, ectoines are not the true inducers of ectoine catabolism (Schulz *et al.*, 2017b). Most inspected ectoine/5-hydroxyectoine catabolic gene clusters contain a gene encoding a member (EhuR/EnuR) (Schulz *et al.*, 2017b) of the MocR/GabR-family of transcriptional regulators (Tramonti *et al.*, 2018). In this family of MocR/GabR-type regulators EnuR/EhuR-type proteins form a clade well separated from other sub-groups of MocR/GabR-type transcription factors (Pascarella, 2019). Nevertheless, as the other members of this family of proteins, EnuR possesses a DNA-binding domain connected via a long flexible linker to an aminotransferase domain (Edayathumangalam *et al.*, 2013; Tramonti *et al.*, 2018) (Figure 11). The aminotransferase domain does not actually perform an enzymatic reaction (Edayathumangalam *et al.*, 2013; Wu *et al.*, 2017; Tramonti *et al.*, 2018; Frezzini *et al.*, 2020). In general, this class of enzymes rather possesses a PLP molecule covalently bound to a highly conserved lysine residue (Lys302 in *R. pomeroyi*). In EnuR, the PLP cofactor is covalently bound to Lys302, forming an internal aldimine as mass spectrometric data could show (Hermann *et al.*, 2021). As studied in detail for the *B. subtilis* GabR protein, a reaction of the covalently bound PLP molecule drives the transition of an internal to an external aldimine (Edayathumangalam *et al.*, 2013; Okuda *et al.*, 2015a; Okuda *et al.*, 2015b; Park *et al.*, 2017; Wu *et al.*, 2017; Tramonti *et al.*, 2018). For the PLP driven reaction the system-specific low-molecular-weight effector molecule forming needs a primary amino group to form the external aldimine. The degradation products of both ectoines (α-ADABA and hydroxy-α-ADABA), but not ectoine or 5-hydroxyectoine themselves, possess such a primary amino group.

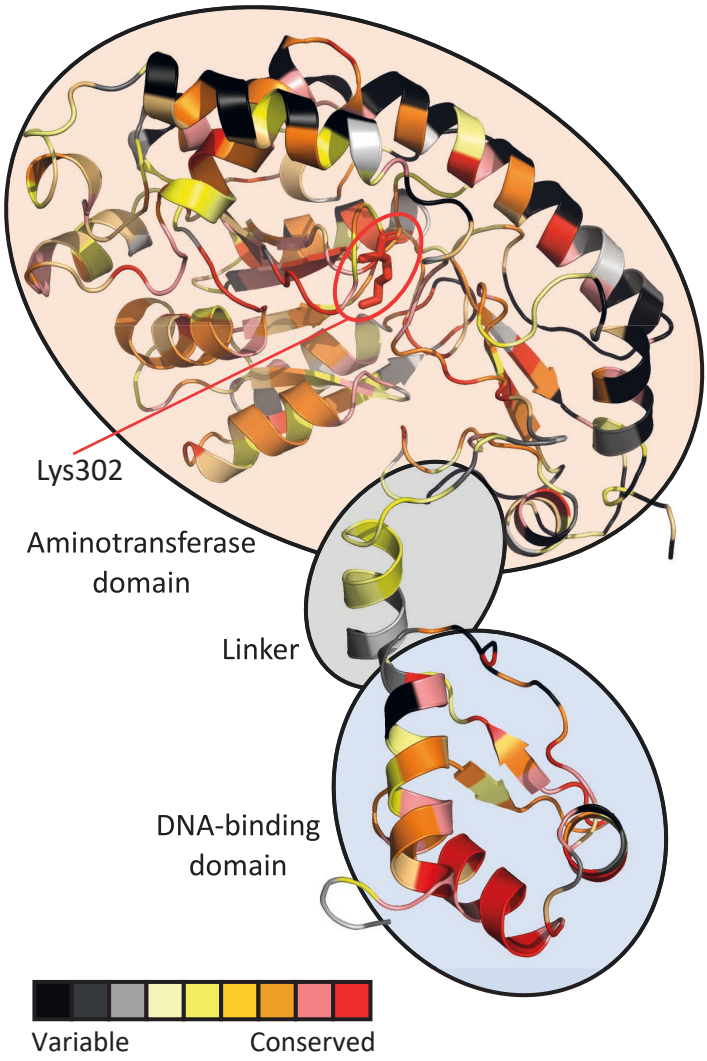

Figure 11: A model of the *R. pomeroyi* DSS-3 EnuR protein, each amino acid in this model is color coded by its degree of conservation in EnuR-type proteins. An amino acid sequence alignment of 278 EnuR-type proteins was used to calculate the conservation at each position of the protein chain. The predicted domain-organization of EnuR with its N-terminal DNA-reading head containing a winged-helix-turn-helix motif, the flexible linker region, and the C-terminal ATD containing the Lys residue (Lys302) to which the PLP cofactor is covalently attached, is indicated. Image taken from (Hermann *et al.*, 2021).

Studies on the EhuR/EnuR regulatory proteins from *S. meliloti* and *R. pomeroyi* identified the degradation intermediates α-ADABA and DABA as the system-specific inducers and ligands for the repressor of ectoine catabolism (Schulz *et al.*, 2017b; Yu *et al.*, 2017). Spectroscopic and mutagenesis studies have previously suggested that the EnuR repressor from *R. pomeroyi* DSS-3 contains PLP as a cofactor that is covalently attached to the side chain of Lys302 (Schulz *et al.*, 2017b). The mass-spectrometry data reported here corroborate now these previous reports. The presence of the Lys302-bound PLP cofactor is crucial for the induction process, as a mutant (Lys302His) (EnuR*) unable to incorporate PLP into EnuR functions as a constitutive repressor leading to the inability of *R. pomeroyi* DSS3 to use ectoines as nutrients (Schulz *et al.*, 2017b). The central role of this residue for the

functioning of the EnuR repressor from *R. pomeroyi* DSS-3 is reflected in the strict conservation of the corresponding lysine residue in each of the 278 EnuR-type proteins inspected by us (Hermann *et al.*, 2021). The replacement of this Lys302 with a histidine residue to which PLP cannot covalently attach, transforms the mutant EnuR protein into a super-repressor that no longer responds to its ectoine-derived internal inducers (Schulz *et al.*, 2017b). Also, this mutant protein loses the strong yellow color provided by the PLP molecule (Schulz *et al.*, 2017b; Hermann *et al.*, 2021). Physiologically important is the fact that in contrast to the specific ectoine metabolite α-ADABA, γ-ADABA, the major substrate of the ectoine synthase EctC (Czech *et al.*, 2019), does not serve as an inducer of the catabolic genes (Schulz *et al.*, 2017b). The hydroxylated forms of α-ADABA and DABA are selectively generated during the EutD-mediated hydrolysis of 5-hydroxyectoine (Mais *et al.*, 2020) (Figure 10), fit extraordinary well in the PLP-bound aminotransferase domain of EnuR (Figure 12) and as measured for hydroxy-α-ADABA possess high affinity towards the aminotransferase of EnuR. Combined, these traits might explain why externally provided 5-hydroxyectoine is a strong inducer of the *R. pomeroyi* ectoine/5-hydroxyectoine catabolic genes (Schulz *et al.*, 2017b). As indicated by the research included in this work, the four compounds metabolically derived from ectoine/5-hydroxyectoine (DABA, hydroxy-DABA, α-ADABA, and hydroxy-α-ADABA) serve as internal inducers for the EnuR repressor (Hermann *et al.*, 2021), although the role of hydroxy-DABA remains unclear as this compound is currently not available in quantities suitable for ligand-binding experiments. α-ADABA and DABA have been shown to serve as ligands for the *R. pomeroyi* DSS-3 EnuR protein (Schulz *et al.*, 2017b) and DABA has also been shown to serve such a role for EhuR from *S. meliloti* (Yu *et al.*, 2017). Hydroxy-α-ADABA interacts in a high affinity process with EnuR with a K_d-value of 0.43 ± 0.2 μM^{-1}, an about five-fold improved affinity compared with α-ADABA (K_d of 2.55 ± 0.5 μM^{-1}). On the other hand, the *R. pomeroyi* DSS-3 EnuR protein binds DABA with a K_d-value of about 460 μM^{-1} (Schulz *et al.*, 2017b). Hence, the affinities of EnuR for the primary, EutD-mediated hydrolysis products of ectoine and 5-hydroxyectoine, are about 180- and 1000-fold higher than those for DABA.

Although the central ectoine/5-hydroxyectoine catabolic enzymes, the hydrolase EutD and the deacetylase EutE, operate as a bi-module (Mais *et al.*, 2020), α-ADABA and hydroxy-α-ADABA, are actually present in the cell and are not immediately deacetylated to produce the medium-affinity inducers DABA and hydroxy-DABA. Through targeted metabolic analysis of cultures grown either in the presence of ectoine or 5-hydroxyectoine, considerable amounts of DABA, α-ADABA and hydroxy-α-ADABA, could be detected. Sizable amounts of the inducer DABA were also detected in cells grown on 5-hydroxyectoine, while hydroxy-DABA was found only in rather low concentrations. The substantial amounts of DABA in the cytoplasm of cells of these latter cultures indicate that hydroxy-DABA is rapidly converted into DABA, a finding that needs to be taken into account for further studies on the

enzymology of the ectoine/5-hydroxyectoine catabolic route (Schwibbert *et al.*, 2011; Hermann *et al.*, 2020; Mais *et al.*, 2020; Reshetnikov *et al.*, 2020).

Our docking experiments with EnuR involving α-ADABA and hydroxy-α-ADABA as ligands do not capture the chemical interconversion of the internal to the external aldimine crucial for the change in the DNA-binding properties of MocR/GabR-type regulators (Edayathumangalam *et al.*, 2013; Okuda *et al.*, 2015a; Park *et al.*, 2017; Wu *et al.*, 2017; Tramonti *et al.*, 2018). The unconstrained docking experiments position the primary nitrogen group present in both inducers in close distance, 3 Å for hydroxy-α-ADABA and 2.6 Å for α-ADABA, to the PLP cofactor with which they must interact. These distances are well suited for a chemical reaction between the bound PLP and the inducers. Most of the EnuR residues predicted by our modeling studies to interact with hydroxy-α-ADABA or α-ADABA are either completely or functionally conserved in the 278 EnuR-type proteins onto which our analysis relied.

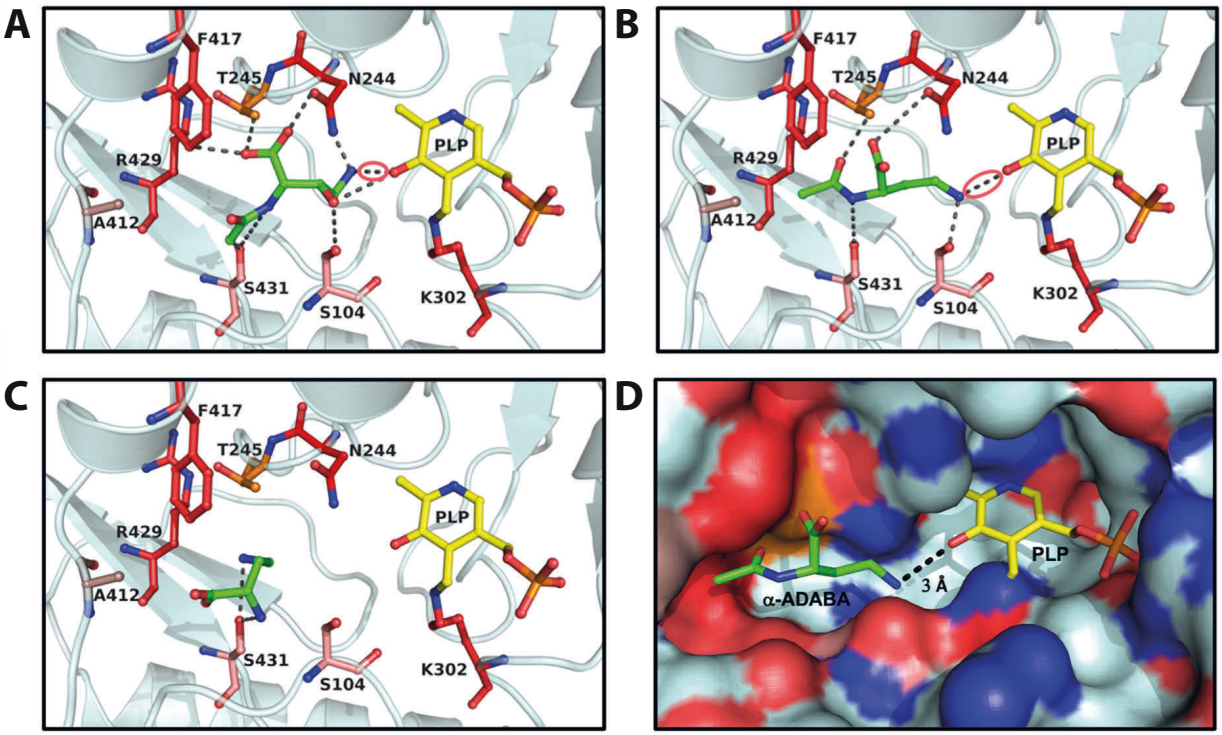

Figure 12: Structural views into the inducer binding sites of EnuR. Docking models of the ectoine/5-hydroxyectoine derived inducers (green) (A) hydroxy-α-ADABA, (B) α -ADABA, and (C) DABA docked into the presumed EnuR ligand binding cavity. The ligands and EnuR amino acid residues predicted to be involved in inducer-binding are displayed as sticks. The protein backbone is shown in cyan for the EnuR protein and the PLP cofactor covalently attached to the sidechain of Lys302 in EnuR is depicted in yellow. The aldimine bonds formed by the chemical interaction of the inducers and PLP in the process of the external aldimine (Tramonti *et al.*, 2018) are indicated by red circles in (B, C). (D) Surface representation of the EnuR ligand and PLP cofactor binding cavity with the predicted position of the α-ADABA molecule. Positively and negatively charged segments of the binding cavity are labeled in blue and red, respectively. Figure taken from (Hermann *et al.*, 2021).

The isomer of α-ADABA, γ-ADABA, is enzymatically generated during ectoine biosynthesis and serves as the substrate for the ectoine synthase EctC (Czech *et al.*, 2019). It does not serve as an inducer for EnuR (Schulz *et al.*, 2017b). Consistent with previous ligand-binding experiments, we were unable to place γ-ADABA into the presumed inducer-binding site of EnuR in our docking experiments. Assuming the core of the γ-ADABA molecule would localize in the same manner in the EnuR ligand-binding cavity as its isomer α-ADABA, so that its primary amino group would be positioned towards the PLP cofactor, the carboxyl moiety of γ-ADABA would be placed too close to the side chain of Asn244. This would likely lead to a sterical clash, and binding of γ-ADABA should thereby prevented, or at least be strongly disfavored. Collectively, these are physiologically important findings as the central intermediate in ectoine synthesis, γ-ADABA, can consequently not trigger ectoine catabolism in those microorganisms capable to both synthesize and degrade ectoines (Schwibbert *et al.*, 2011; Czech *et al.*, 2018b; Hermann *et al.*, 2020; Mais *et al.*, 2020).

Many ectoine/5-hydroxyectoine catabolic gene clusters also contain a gene (*asnC*/*doeX*) for a member of the feast and famine family of transcriptional regulators (Yokoyama *et al.*, 2006; Schwibbert *et al.*, 2011; Schulz *et al.*, 2017b; Schulz *et al.*, 2017a). These proteins can wrap DNA into nucleosome-like structures and frequently respond in their DNA-binding activity to low-molecular weight effector molecules like amino acids (Shrivastava and Ramachandran, 2007; Kumarevel *et al.*, 2008; Dey *et al.*, 2016). Schwibbert *et al.* (2011) showed that such a protein targets DNA sequences in the promoter region of the *H. elongata* ectoine/5-hydroxyectoine catabolic gene cluster (Schwibbert *et al.*, 2011). Notably, AsnC serves as an activator for the *R. pomeroyi* import and catabolic gene cluster and its loss abolishes the use of ectoine as sole carbon but not as sole nitrogen source (Schulz *et al.*, 2017b). Details of the structure and genetic mode of action of the DoeX- and AsnC-type proteins still need to be worked out and their effector molecules have not yet been identified.

Two-component regulatory systems such as NtrYX serve as major signaling devices through which information about changes in the environment are detected, processed, and transmitted to the microbial cell to change gene expression or behavior (Zschiedrich *et al.*, 2016). The NtrYX system consists of a membrane-bound histidine kinase (NtrY) that co-operates with the NtrX response regulator. It has been implicated in a number of biologically quite varied cellular processes in *Alphaproteobacteria* [for a recent description of the NtrYX system and additional references see (Fernandez *et al.*, 2017)], most notably in the metabolism and assimilation of nitrogen-containing compounds (Pawlowski *et al.*, 1991; Carrica Mdel *et al.*, 2012; Cheng *et al.*, 2014; Bonato *et al.*, 2016; Calatrava-Morales *et al.*, 2017). Our data now also subscribe such a function to the NtrYX system of *R. pomeroyi* with respect to the catabolism of the nitrogen-rich hydroxyectoine and ectoine molecules. We do not know whether these effects are mediated through direct interactions of the unusual NtrC-type NtrX response regulator (Zschiedrich *et al.*, 2016; Fernandez *et al.*, 2017) with the regulatory

region present in front of the *R. pomeroyi* hydroxyectoine/ectoine-uptake and catabolic gene cluster, or whether they are mediated indirectly through a so far undisclosed regulatory circuit (e.g. by controlling the expression of *asnC* or AsnC activity). The *ntrYX* genes are only found in the alphaproteobacterial species among the presumed hydroxyectoine/ectoine consumers. Since *ntrYX* genes are present in virtually every alphaproteobacterial species, including those not degrading ectoines, this appears to be phylum-specific regulatory trait to link hydroxyectoine/ectoine degradation to the cellular nitrogen status.

Recapitulated, in the absence of ectoines, the *R. pomeroyi* DSS-3 importer and catabolic gene cluster is expressed at a very low level (Schulz *et al.*, 2017b). Nevertheless, this basal level of transcription is sufficient to allow import of trace amounts of ectoines via the high affinity TRAP-type UehABC uptake system from *R. pomeroyi* DSS-3 (Lecher *et al.*, 2009). However, a low-level ectoine concentration can still be detected under these conditions by *R. pomeroyi* (Lecher *et al.*, 2009) and, consequently, as soon as traces of ectoines are present in the habitat (Mosier *et al.*, 2013; Warren, 2014, 2016), microorganisms will import these compounds through high-affinity transport systems such as the TRAP-transporters UehABC or TeaABC (Grammann *et al.*, 2002; Kuhlmann *et al.*, 2008b; Lecher *et al.*, 2009; Schulz *et al.*, 2017a). After the initial import of ectoines, their catabolism will set in at a low level, thereby forming limited pools of especially the high-affinity EnuR inducers α-ADABA and hydroxy-α-ADABA. Their interactions with the covalently bound PLP cofactor will relieve EnuR-mediated repression of the transcriptional activity of the substrate-inducible promoter. Consequently, enhanced and subsequently sustained increased expression of the ectoine/5-hydroxyectoine importer and catabolic gene cluster will ensue and thereby promote increased import and catabolism of ectoines. As the inducers α-ADABA, hydroxy-α-ADABA, DABA and hydroxy-DABA are early intermediates in the catabolism of ectoines (Schwibbert *et al.*, 2011; Yu *et al.*, 2017; Hermann *et al.*, 2020; Mais *et al.*, 2020) they will inevitably disappear from the cell when the environmental supply of ectoines has been exhausted. EnuR will consequently resume its repressor function.

7.8 Perspectives and open questions

Ectoine and its derivative 5-hydroxyectoine are widely synthesized compatible solutes, used by a large number of microorganisms in their stress responses (Czech *et al.*, 2018b; Hermann *et al.*, 2020). Cases in which ectoines are employed by microbes are extremes in growth-temperature, hydrostatic pressure, freezing, desiccation and the denaturation of macromolecules by ions and urea (Caldas *et al.*, 1999; Diamant *et al.*, 2001; Holtmann and Bremer, 2004; Manzanera *et al.*, 2004; Yancey, 2005; Hoffmann and Bremer, 2011). Of special importance is the useage of ectoines as osmoprotectants, a trait, not exclusively, but effectively used by microorganisms confronted with a highly elevated

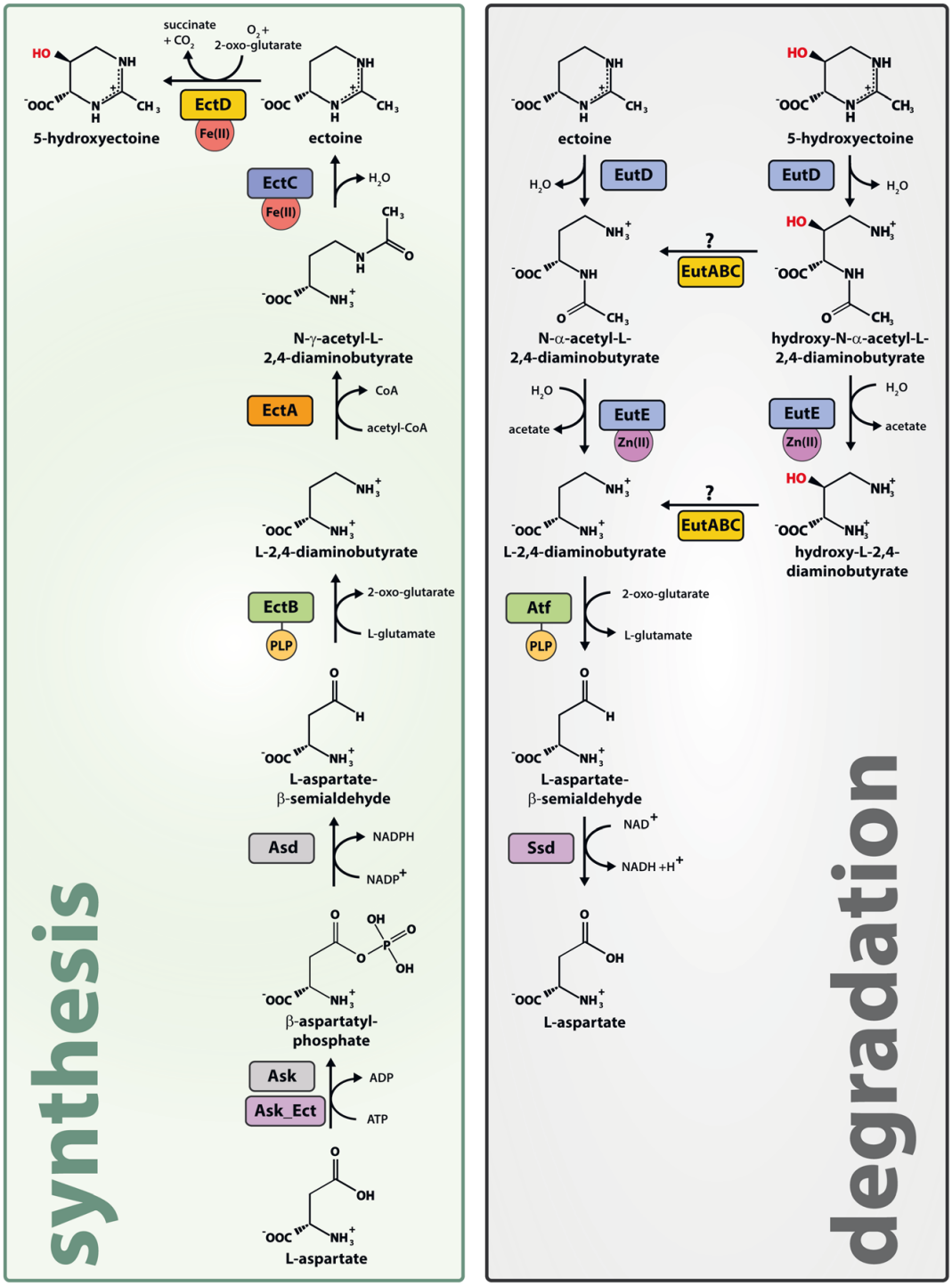

Figure 13: Ectoine metabolism. The green and grey boxes show the pathways enabling biosynthesis and degradation of ectoine/ 5-hydroxyectoine, respectively. Both can be thought as opposites of one another. Note: The biosynthesis pathway employs γ-ADABA as unique intermediate, while the degradation pathway relies on α-ADABA. Figure taken from (Hermann *et al.*, 2020).

osmolarity in their respective environments (Czech *et al.*, 2018b). These cytoprotective effects of ectoines led to early and intensive research on ectoines, their biosynthesis, and the way the accomplish these cytoprotective effects. Alltogether, this research led to distinguished insights in the biosynthesis of ectoines. Not only biochemically, but also structurally, most questions concerning ectoine

biosynthesis could be solved in recent years (Figure 13) (Czech *et al.*, 2018b; Hermann *et al.*, 2020). Questions remaining on the part of the biosynthesis of ectoines from today's point of view are either concerning small details (e.g. a substrate-bound form of EctA), or tackle far deeper questions (e.g. the regulatory mechanisms of osmoprotection and the actual signal triggering these responses). Concerning the regulatory mechanisms of ectoine biosynthesis, progress in recent years includes a better understanding of the promoters and regulatory proteins involved. The *ect* promoter of *P. stutzeri* A1501 itself, its promoter elements, the spacer, and the flanking regions seem to be solely responsible for osmoprotection (Czech *et al.*, 2018a). Additionally, several regulatory proteins were shown to be involved in ectoine biosynthesis, as the global regulator of nitrogen metabolism, GlnR (Shao *et al.*, 2015), the ionic strength dependent CosR (Shikuma *et al.*, 2013; Gregory *et al.*, 2019; Gregory *et al.*, 2020) and EctR, often associated with *ect* genes (Mustakhimov *et al.*, 2009; Czech, 2019). The overall interplay and significance of all these factors remain to be clarified. Also, frequently new organisms producing ectoines are identified and bioengineering methods to produce ectoines are developed, for recent examples see (Cantera *et al.*, 2020; Pérez *et al.*, 2021; Kang *et al.*, 2022; Sattar *et al.*, 2022).

The degradation of ectoines, in contrast, is a research field which developed in far fewer years (Jebbar *et al.*, 2005; Vargas *et al.*, 2006; Schwibbert *et al.*, 2011; Schulz *et al.*, 2017a; Reshetnikov *et al.*, 2020) and far more questions remain to be solved. Important findings included in this dissertation are the structural and biochemical analysis of the EutDE bi-module that opens the ectoine rings (Mais *et al.*, 2020), as well as the EnuR repressor detecting the so generated α-ADABA and especially hydroxy-α-ADABA with high affinity to trigger induction of catabolic genes for ectoines (Hermann *et al.*, 2021). Unsolved issues in the catabolism of ectoines include:

- The mechanisms of the EutABC enzymes involved in 5-hydroxyectoine metabolism. These enzymes are annotated as Asp/Glu/hydantoine racemase (EutA), as L-threonine ammonia lyase (EutB), and as ornithine cyclodeaminase (EutC) (Moran *et al.*, 2004). Especially the role of EutA remains a mystery, as the *eutA* gene is only scarcely associated with the *eutBC* genes and ectoine/5-hydroxyectoine catabolic gene clusters in general (Hermann *et al.*, 2020; Mais *et al.*, 2020).
- Many microorganisms, not exclusively belonging to the *Proteobacteria*, possess a different type of α-ADABA-deacetylase, namely an enzyme annotated as a hippurate hydrolase (Hermann, 2022). What are the biochemical differences between both enzymes and what advantages could each enzyme afford its host?
- The AsnC protein, belonging to the feast and famine family of transcriptional regulators, presumably forms oktamers like the closely related Lrp proteins (Kumarevel *et al.*, 2008; Dey *et al.*, 2016). Do these oktamers also wrap DNA to activate gene expression? In *H. elongata*

AsnC (DoeX) binds upstream of the ectoine catabolic operon presumably to perform this exact task (Schwibbert *et al.*, 2011). Does the same mechanism apply when the ectoine catabolic gene is split in two parts with different orientations as exemplified in *S. meliloti*? As proteins related to AsnC detect low molecular ligands to activate gene expression, are the ligands in this case ectoine and 5-hydroxyectoine or degradation products thereof?

- Like AsnC, the two-component system NtrYX is also needed to activate gene expression of ectoine-/ 5-hydroxyectoine catabolic genes. In which way does NtrX interact with the ectoine-/ 5-hydroxyectoine catabolic genes? And which signal does the NtrY protein sense? NtrY possesses a large extracytoplasmic domain. Could this domain be used to sense ectoines in the environment? Or are the overall tasks of these proteins far more global, generally sensing nitrogen occurrences in the environment as exemplified by the closely related NtrBC system (Zhang and Rainey, 2008)?
- Several aspects of the mechanisms of EnuR also remain unclear. Although several crystals of EnuR could be produced (unpublished data), no crystal structure could be solved yet. Presumably either the flexible linker or the PLP in the aminotransferase domain produce too much disorder, could a tethering of the PLP with borohydride to produce an apo-form solve this problem? Although two binding sites could be detected (Schulz *et al.*, 2017b), the actual binding mechanism of EnuR to them remains unclear. RNAse-footprinting and detailed mutagenetic analysis would be needed to decipher the role each binding site plays.

Overall, the ecophysiological role of ectoines, their biosynthetic genes, and transporters gained importance in recent years, as they were identified in more and more cases. Microbial assemblages and biofilms are examples (Fida *et al.*, 2012; Rubinstein *et al.*, 2012; Seminara *et al.*, 2012; Yan *et al.*, 2017). Released/actively secreted ectoines might also become a public good for microbial communities, as exemplified by glycine betaine in the case of *V. cholerae* (Kapfhammer *et al.*, 2005). The unexpected discovery of ectoine/5-hydroxyectoine-producing ciliates and micro-algae and the way in which these eukaryotic cells interact with bacteria paves the way for studies addressing the role of these cytoprotectants in the framework of microbial ecology (Harding *et al.*, 2016; Landa *et al.*, 2017; Weinisch *et al.*, 2019; Fenizia *et al.*, 2020). It is of interest to note in this context that the plant roots-associated bacterium *S. meliloti* caries out chemotaxis towards the plant-produced compatible solute proline betaine and other types of quaternary ammonium compounds (e.g. glycine betaine) found in root exudates (Webb *et al.*, 2017). Hence, one might ask if environmental ectoines serve as chemo-attractants when microorganisms seek them out either as stress protectants or nutrients.

As ectoines are identified as of key importance in more and more scenarios, their recycling as nutrients gains importance and can shape architecture and composition of microbial communities (Landa *et al.*, 2017). Therefore, the main results of this work, the structure-based mechanisms of the

enzyme core essential for the catabolism of ectoine and 5-hydroxyectoine and the key molecular underpinnings of transcriptional regulation performed by EnuR, will presumably gain importance in the future as well.

8 References

1. **Achbergerová, L., and Nahálka, J.** (2014) Degradation of polyphosphates by polyphosphate kinases from *Ruegeria pomeroyi*. *Biotechnol Lett* 36:2029-2035.
2. **Aik, W., McDonough, M.A., Thalhammer, A., Chowdhury, R., and Schofield, C.J.** (2012) Role of the jelly-roll fold in substrate binding by 2-oxoglutarate oxygenases. *Curr Opin Struct Biol* 22:691-700.
3. **Arakawa, T., and Timasheff, S.N.** (1985) Calculation of the partial specific volume of proteins in concentrated salt and amino acid solutions. *Methods Enzymol* 117:60-65.
4. **Auton, M., Rösgen, J., Sinev, M., Holthauzen, L.M., and Bolen, D.W.** (2011) Osmolyte effects on protein stability and solubility: A balancing act between backbone and side-chains. *Biophys Chem* 159:90-99.
5. **Ball, P.** (2017) Water is an active matrix of life for cell and molecular biology. *Proc Natl Acad Sci USA* 114:13327-13335.
6. **Barth, S., Huhn, M., Matthey, B., Klimka, A., Galinski, E.A., and Engert, A.** (2000) Compatible-solute-supported periplasmic expression of functional recombinant proteins under stress conditions. *Appl Environ Microbiol* 66:1572-1579.
7. **Bartnicki-Garcia, S.** (1968) Cell wall chemistry, morphogenesis, and taxonomy of fungi. *Annu Rev Microbiol* 22:87-108.
8. **Bazan, J., Weaver, L., Roderick, S., Huber, R., and Matthews, B.** (1994) Sequence and structure comparison suggest that methionine aminopeptidase, prolidase, aminopeptidase P, and creatinase share a common fold. *Proc Natl Acad Sci USA* 91:2473-2477.
9. **Becker, E.A., Seitzer, P.M., Tritt, A., Larsen, D., Krusor, M., Yao, A.I., Wu, D., Madern, D., Eisen, J.A., Darling, A.E., and Facciotti, M.T.** (2014) Phylogenetically driven sequencing of extremely halophilic archaea reveals strategies for static and dynamic osmo-response. *PLoS Genet* 10:e1004784.
10. **Becker, J., Schäfer, R., Kohlstedt, M., Harder, B.J., Borchert, N.S., Stöveken, N., Bremer, E., and Wittmann, C.** (2013) Systems metabolic engineering of *Corynebacterium glutamicum* for production of the chemical chaperone ectoine. *Microb Cell Fact* 12:110.
11. **Bestvater, T., Louis, P., and Galinski, E.A.** (2008) Heterologous ectoine production in *Escherichia coli:* By-passing the metabolic bottle-neck. *Saline Systems* 4:12.
12. **Bolen, D.W., and Baskakov, I.V.** (2001) The osmophobic effect: Natural selection of a thermodynamic force in protein folding. *J Mol Biol* 310:955-963.
13. **Bonato, P., Alves, L.R., Osaki, J.H., Rigo, L.U., Pedrosa, F.O., Souza, E.M., Zhang, N., Schumacher, J., Buck, M., Wassem, R., and Chubatsu, L.S.** (2016) The NtrY-NtrX two-component system is involved in controlling nitrate assimilation in *Herbaspirillum seropedicae* strain SmR1. *FEBS J* 283:3919-3930.
14. **Booth, I.R.** (2014) Bacterial mechanosensitive channels: Progress towards an understanding of their roles in cell physiology. *Curr Opin Microbiol* 18:16-22.
15. **Booth, I.R., Miller, S., Muller, A., and Lehtovirta-Morley, L.** (2015) The evolution of bacterial mechanosensitive channels. *Cell Calcium* 57:140-150.
16. **Booth, I.R., Edwards, M.D., Black, S., Schumann, U., and Miller, S.** (2007a) Mechanosensitive channels in bacteria: Signs of closure? *Nat Rev Microbiol* 5:431-440.
17. **Booth, I.R., Edwards, M.D., Black, S., Schumann, U., Bartlett, W., Rasmussen, T., Rasmussen, A., and Miller, S.** (2007b) Physiological analysis of bacterial mechanosensitive channels. *Methods Enzymol* 428:47-61.
18. **Borges, N., Ramos, A., Raven, N.D., Sharp, R.J., and Santos, H.** (2002) Comparative study of the thermostabilizing properties of mannosylglycerate and other compatible solutes on model enzymes. *Extremophiles* 6:209-216.
19. **Bouskill, N.J., Wood, T.E., Baran, R., Ye, Z., Bowen, B.P., Lim, H., Zhou, J., Nostrand, J.D., Nico, P., Northen, T.R., Silver, W.L., and Brodie, E.L.** (2016a) Belowground response to drought in a

tropical forest soil. I. Changes in microbial functional potential and metabolism. *Front Microbiol* 7:525.

20. **Bouskill, N.J., Wood, T.E., Baran, R., Hao, Z., Ye, Z., Bowen, B.P., Lim, H.C., Nico, P.S., Holman, H.Y., Gilbert, B., Silver, W.L., Northen, T.R., and Brodie, E.L.** (2016b) Belowground response to drought in a tropical forest soil. II. Change in microbial function impacts carbon composition. *Front Microbiol* 7:323.
21. **Bremer, E., and Krämer, R.** (eds) (2000) Coping with osmotic challenges: Osmoregulation through accumulation and release of compatible solutes in bacteria. Washington DC: ASM PRess.
22. **Brown, A.D.** (1976) Microbial water stress. *Bacteriol Rev* 40:803-846.
23. **Bruce, H., Nguyen Tuan, A., Mangas Sánchez, J., Leese, C., Hopwood, J., Hyde, R., Hart, S., Turkenburg, J.P., and Grogan, G.** (2012) Structures of a γ-aminobutyrate (GABA) transaminase from the S-triazine-degrading organism *Arthrobacter aurescens* TC1 in complex with PLP and with its external aldimine PLP-GABA adduct. *Acta Cryst F* 68:1175-1180.
24. **Bullock, H.A., Luo, H., and Whitman, W.B.** (2017) Evolution of dimethylsulfoniopropionate metabolism in marine phytoplankton and bacteria. *Front Microbiol* 8:637.
25. **Burg, M.B., and Ferraris, J.D.** (2008) Intracellular organic osmolytes: Function and regulation. *J Biol Chem* 283:7309-7313.
26. **Bursy, J., Pierik, A.J., Pica, N., and Bremer, E.** (2007) Osmotically induced synthesis of the compatible solute hydroxyectoine is mediated by an evolutionarily conserved ectoine hydroxylase. *J Biol Chem* 282:31147-31155.
27. **Bursy, J., Kuhlmann, A.U., Pittelkow, M., Hartmann, H., Jebbar, M., Pierik, A.J., and Bremer, E.** (2008) Synthesis and uptake of the compatible solutes ectoine and 5-hydroxyectoine by *Streptomyces coelicolor* A3(2) in response to salt and heat stresses. *Appl Environ Microbiol* 74:7286-7296.
28. **Calamita, G.** (2000) The *Escherichia coli* aquaporin-Z water channel. *Mol Microbiol* 37:254-262.
29. **Calatrava-Morales, N., Nogales, J., Ameztoy, K., van Steenbergen, B., and Soto, M.J.** (2017) The NtrY/NtrX system of *Sinorhizobium meliloti* GR4 regulates motility, EPS I production, and nitrogen metabolism but is dispensable for symbiotic nitrogen fixation. *Mol Plant Microbe Interact* 30:566-577.
30. **Caldas, T., Demont-Caulet, N., Ghazi, A., and Richarme, G.** (1999) Thermoprotection by glycine betaine and choline. *Microbiol* 145 2543-2548.
31. **Canovas, D., Borges, N., Vargas, C., Ventosa, A., Nieto, J.J., and Santos, H.** (1999) Role of N-gamma-acetyldiaminobutyrate as an enzyme stabilizer and an intermediate in the biosynthesis of hydroxyectoine. *Appl Environ Microbiol* 65:3774-3779.
32. **Canovas, D., Vargas, C., Iglesias-Guerra, F., Csonka, L.N., Rhodes, D., Ventosa, A., and Nieto, J.J.** (1997) Isolation and characterization of salt-sensitive mutants of the moderate halophile *Halomonas elongata* and cloning of the ectoine synthesis genes. *J Biol Chem* 272:25794-25801.
33. **Cánovas, D., Vargas, C., Ventosa, A., and Nieto, J.J.** (1997) Salt-sensitive and auxotrophic mutants of *Halomonas elongata* and *H. meridiana* by use of hydroxylamine mutagenesis. *Curr Microbiol* 34:85-90.
34. **Cantera, S., Phandanouvong-Lozano, V., Pascual, C., García-Encina, P.A., Lebrero, R., Hay, A., and Muñoz, R.** (2020) A systematic comparison of ectoine production from upgraded biogas using *Methylomicrobium alcaliphilum* and a mixed haloalkaliphilic consortium. *Waste Management* 102:773-781.
35. **Carrica Mdel, C., Fernandez, I., Marti, M.A., Paris, G., and Goldbaum, F.A.** (2012) The NtrY/X two-component system of *Brucella* spp. acts as a redox sensor and regulates the expression of nitrogen respiration enzymes. *Mol Microbiol* 85:39-50.
36. **Castle, A., Macnab, R., and Shulman, R.** (1986) Coupling between the sodium and proton gradients in respiring *Escherichia coli* cells measured by 23Na and 31P nuclear magnetic resonance. *J Biol Chem* 261:7797-7806.

37. **Cayley, S., Lewis, B.A., and Record, M.T., Jr.** (1992) Origins of the osmoprotective properties of betaine and proline in *Escherichia coli* K-12. *J Bacteriol* 174:1586-1595.
38. **Chandler, D.** (2005) Interfaces and the driving force of hydrophobic assembly. *Nature* 437:640-647.
39. **Charlson, R.J., Lovelock, J.E., Andreae, M.O., and Warren, S.G.** (1987) Oceanic phytoplancton, atmospheric sulphur, cloud albedo and climate. *Nature* 326:655-661.
40. **Chen, W., Zhang, S., Jiang, P., Yao, J., He, Y., Chen, L., Gui, X., Dong, Z., and Tang, S.Y.** (2015) Design of an ectoine-responsive AraC mutant and its application in metabolic engineering of ectoine biosynthesis. *Metab Eng* 30:149-155.
41. **Chen, W.C., Hsu, C.C., Lan, J.C., Chang, Y.K., Wang, L.F., and Wei, Y.H.** (2018) Production and characterization of ectoine using a moderately halophilic strain *Halomonas salina* BCRC17875. *J Biosci Bioeng* 125:578-584.
42. **Chen, X., Liu, L., Gao, X., Dai, X., Han, Y., Chen, Q., and Tang, K.** (2021) Metabolism of chiral sulfonate compound 2, 3-dihydroxypropane-1-sulfonate (DHPS) by *Roseobacter* bacteria in marine environment. *Environ Int* 157:106829.
43. **Cheng, X., Guinn, E.J., Buechel, E., Wong, R., Sengupta, R., Shkel, I.A., and Record, M.T., Jr.** (2016) Basis of protein stabilization by K glutamate: Unfavorable interactions with carbon, oxygen groups. *Biophys J* 111:1854-1865.
44. **Cheng, Z., Lin, M., and Rikihisa, Y.** (2014) *Ehrlichia chaffeensis* proliferation begins with NtrY/NtrX and PutA/GlnA upregulation and CtrA degradation induced by proline and glutamine uptake. *mBio* 5:e02141.
45. **Christie-Oleza, J.A., Piña-Villalonga, J.M., Bosch, R., Nogales, B., and Armengaud, J.** (2012) Comparative proteogenomics of twelve *Roseobacter* exoproteomes reveals different adaptive strategies among these marine bacteria. *Mol Cell Proteom* 11.
46. **Christie-Oleza, J.A., Sousoni, D., Lloyd, M., Armengaud, J., and Scanlan, D.J.** (2017) Nutrient recycling facilitates long-term stability of marine microbial phototroph–heterotroph interactions. *Nat Microbiol* 2:1-10.
47. **Clifton, I.J., McDonough, M.A., Ehrismann, D., Kershaw, N.J., Granatino, N., and Schofield, C.J.** (2006) Structural studies on 2-oxoglutarate oxygenases and related double-stranded beta-helix fold proteins. *J Inorg Biochem* 100:644-669.
48. **Commichau, F.M., Gibhardt, J., Halbedel, S., Gundlach, J., and Stülke, J.** (2018) A delicate connection: c-di-AMP affects cell integrity by controlling osmolyte transport. *Trends Microbiol* 26:175-185.
49. **Coquelle, N., Talon, R., Juers, D.H., Girard, E., Kahn, R., and Madern, D.** (2010) Gradual adaptive changes of a protein facing high salt concentrations. *J Mol Biol* 404:493-505.
50. **Crick, F.H.** (1968) The origin of the genetic code. *J Mol Biol* 38:367-379.
51. **Csonka, L.N.** (1989) Physiological and genetic responses of bacteria to osmotic stress. *Microbiol Rev* 53:121-147.
52. **Culham, D.E., Marom, D., Boutin, R., Garner, J., Ozturk, T.N., Sahtout, N., Tempelhagen, L., Lamoureux, G., and Wood, J.M.** (2018) Dual role of the C-terminal domain in osmosensing by bacterial osmolyte transporter ProP. *Biophys J* 115:2152-2166.
53. **Cunliffe, M.** (2013) Physiological and metabolic effects of carbon monoxide oxidation in the model marine bacterioplankton *Ruegeria pomeroyi* DSS-3. *Appl Microbiol Biotechnol* 79:738-740.
54. **Cunliffe, M.** (2015) Purine catabolic pathway revealed by transcriptomics in the model marine bacterium *Ruegeria pomeroyi* DSS-3. *FEMS Microbiol Ecol* 92.
55. **Czech, L.** (2019) The stress-protectants and chemical chaperones ectoine and hydroxyectoine: Enzymes, importer, exporter and transcriptional regulation. *Dissertation, Philipps-Universität Marburg*.
56. **Czech, L., Stöveken, N., and Bremer, E.** (2016) EctD-mediated biotransformation of the chemical chaperone ectoine into hydroxyectoine and its mechanosensitive channel-independent excretion. *Microb Cell Fact* 15:126.

57. **Czech, L., Poehl, S., Hub, P., Stöveken, N., and Bremer, E.** (2018a) Tinkering with osmotically controlled transcription allows enhanced production and excretion of ectoine and hydroxyectoine from a microbial cell factory. *Appl Environ Microbiol* 84:e01772-01717.
58. **Czech, L., Hermann, L., Stöveken, N., Richter, A.A., Hoeppner, A., Smits, S.H.J., Heider, J., and Bremer, E.** (2018b) Role of the extremolytes ectoine and hydroxyectoine as stress protectants and nutrients: Genetics, phylogenomics, biochemistry, and structural snalysis. *Genes* 9:177.
59. **Czech, L., Hoeppner, A., Kobus, S., Seubert, A., Riclea, R., Dickschat, J.S., Heider, J., Smits, S.H., and Bremer, E.** (2019) Illuminating the catalytic core of ectoine synthase through structural and biochemical analysis. *Sci Rep* 9:1-21.
60. **da Costa, M.S., Santos, H., and Galinski, E.A.** (1998) An overview of the role and diversity of compatible solutes in Bacteria and Archaea. *Adv Biochem Eng Biotechnol* 61:117-153.
61. **Deole, R., Challacombe, J., Raiford, D.W., and Hoff, W.D.** (2013) An extremely halophilic proteobacterium combines a highly acidic proteome with a low cytoplasmic potassium content. *J Biol Chem* 288:581-588.
62. **Dey, A., Shree, S., Pandey, S.K., Tripathi, R.P., and Ramachandran, R.** (2016) Crystal structure of *Mycobacterium tuberculosis* H37Rv AldR (Rv2779c), a regulator of the *ald* gene: DNA binding and identification of small molecule inhibitors. *J Biol Chem* 291:11967-11980.
63. **Diamant, S., Eliahu, N., Rosenthal, D., and Goloubinoff, P.** (2001) Chemical chaperones regulate molecular chaperones i*n vitro* and in cells under combined salt and heat stresses. *J Biol Chem* 276:39586-39591.
64. **Diehl, R.C., Guinn, E.J., Capp, M.W., Tsodikov, O.V., and Record, M.T., Jr.** (2013) Quantifying additive interactions of the osmolyte proline with individual functional groups of proteins: Comparisons with urea and glycine betaine, interpretation of m-values. *Biochem* 52:5997-6010.
65. **Dotsch, A., Severin, J., Alt, W., Galinski, E.A., and Kreft, J.U.** (2008) A mathematical model for growth and osmoregulation in halophilic bacteria. *Microbiol Mol Biol Rev* 154:2956-2969.
66. **Dumetz, A.C., Snellinger-O'brien A, M., Kaler, E.W., and Lenhoff, A.M.** (2007) Patterns of protein protein interactions in salt solutions and implications for protein crystallization. *Protein Sci* 16:1867-1877.
67. **Dunwell, J.M., Purvis, A., and Khuri, S.** (2004) Cupins: The most functionally diverse protein superfamily? *Phytochemistry* 65:7-17.
68. **Durham, B.P., Dearth, S.P., Sharma, S., Amin, S.A., Smith, C.B., Campagna, S.R., Armbrust, E.V., and Moran, M.A.** (2017) Recognition cascade and metabolite transfer in a marine bacteria-phytoplankton model system. *Environ Microbiol* 19:3500-3513.
69. **Edayathumangalam, R., Wu, R., Garcia, R., Wang, Y., Wang, W., Kreinbring, C.A., Bach, A., Liao, J., Stone, T.A., Terwilliger, T.C., Hoang, Q.Q., Belitsky, B.R., Petsko, G.A., Ringe, D., and Liu, D.** (2013) Crystal structure of *Bacillus subtilis* GabR, an autorepressor and transcriptional activator of *gabT*. *Proc Natl Acad Sci USA* 110:17820-17825.
70. **Eiberweiser, A., Nazet, A., Kruchinin, S.E., Fedotova, M.V., and Buchner, R.** (2015) Hydration and ion binding of the osmolyte ectoine. *J Phys Chem B* 119:15203-15211.
71. **Fenizia, S., Thume, K., Wirgenings, M., and Pohnert, G.** (2020) Ectoine from bacterial and algal origin is a compatible solute in microalgae. *Mar Drugs* 18:42.
72. **Fernandez, I., Cornaciu, I., Carrica, M.D., Uchikawa, E., Hoffmann, G., Sieira, R., Marquez, J.A., and Goldbaum, F.A.** (2017) Three-dimensional structure of full-length NtrX, an unusual member of the NtrC family of response regulators. *J Mol Biol* 429:1192-1212.
73. **Fida, T.T., Breugelmans, P., Lavigne, R., Coronado, E., Johnson, D.R., van der Meer, J.R., Mayer, A.P., Heipieper, H.J., Hofkens, J., and Springael, D.** (2012) Exposure to solute stress affects genome-wide expression but not the polycyclic aromatic hydrocarbon-degrading activity of *Sphingomonas* sp. strain LH128 in biofilms. *Appl Environ Microbiol* 78:8311-8320.
74. **Fischer, K.E., and Bremer, E.** (2012) Activity of the osmotically regulated *yqiHIK* promoter from *Bacillus subtilis* is controlled at a distance. *J Bacteriol* 194:5197-5208.

75. **Frezzini, M., Narzi, D., Sciolari, A.M., Guidoni, L., and Pascarella, S.** (2020) Molecular dynamics of an asymmetric form of GabR, a bacterial transcriptional regulator. *Biophys Chem* 262:106380.
76. **Friis, N.** (1975) Some recommendations concerning primary isolation of *Mycoplasma suipneumoniae* and *Mycoplasma flocculare* a survey. *Nord Vet Med* 27:337.
77. **Fuhrman, J.A.** (1999) Marine viruses and their biogeochemical and ecological effects. *Nature* 399:541-548.
78. **Galinski, E.A., and Herzog, R.M.** (1990) The role of trehalose as a substitute for nitrogen-containing compatible colutes (*Ectothiorhodospira halochloris*). *Arch Microbiol* 153:607-613.
79. **Galinski, E.A., and Oren, A.** (1991) Isolation and structure determination of a novel compatible solute from the moderately halophilic purple sulfur bacterium *Ectothiorhodospira marismortui*. *Eur J Biochem* 198:593-598.
80. **Galinski, E.A., and Truper, H.G.** (1994) Microbial behavior in salt-stressed ecosystems. *FEMS Microbiol Rev* 15:95-108.
81. **Galinski, E.A., Pfeiffer, H.P., and Truper, H.G.** (1985) 1,4,5,6-Tetrahydro-2-methyl-4-pyrimidinecarboxylic acid. A novel cyclic amino acid from halophilic phototrophic bacteria of the genus *Ectothiorhodospira*. *Eur J Biochem* 149:135-139.
82. **Garcia-Estepa, R., Argandona, M., Reina-Bueno, M., Capote, N., Iglesias-Guerra, F., Nieto, J.J., and Vargas, C.** (2006a) The *ectD* gene, which is involved in the synthesis of the compatible solute hydroxyectoine, is essential for thermoprotection of the halophilic bacterium *Chromohalobacter salexigens*. *J Bacteriol* 188:3774-3784.
83. **Garcia-Estepa, R., Canovas, D., Iglesias-Guerra, F., Ventosa, A., Csonka, L.N., Nieto, J.J., and Vargas, C.** (2006b) Osmoprotection of *Salmonella enterica serovar* Typhimurium by Ngamma-acetyldiaminobutyrate, the precursor of the compatible solute ectoine. *Syst Appl Microbiol* 29:626-633.
84. **Gilbert, W.** (1986) Origin of life: The RNA world. *Nature* 319:618-618.
85. **Gonzalez, J.M., Covert, J.S., Whitman, W.B., Henriksen, J.R., Mayer, F., Scharf, B., Schmitt, R., Buchan, A., Fuhrman, J.A., Kiene, R.P., and Moran, M.A.** (2003) *Silicibacter pomeroyi* sp. nov. and *Roseovarius nubinhibens* sp. nov., dimethylsulfoniopropionate-demethylating bacteria from marine environments. *Int J Syst Evol Microbiol* 53:1261-1269.
86. **Gouesbet, G., Trautwetter, A., Bonnassie, S., Wu, L.F., and Blanco, C.** (1996) Characterization of the *Erwinia chrysanthemi* osmoprotectant transporter gene *ousA*. *J Bacteriol* 178:447-455.
87. **Grabber, J.H.** (2005) How do lignin composition, structure, and cross-linking affect degradability? A review of cell wall model studies. *Crop Sci* 45:820-831.
88. **Graeme-Cook, K.A., May, G., Bremer, E., and Higgins, C.F.** (1989) Osmotic regulation of porin expression: A role for DNA supercoiling. *Mol Microbiol* 3:1287-1294.
89. **Graf, R., Anzali, S., Buenger, J., Pfluecker, F., and Driller, H.** (2008) The multifunctional role of ectoine as a natural cell protectant. *Clin Dermatol* 26:326-333.
90. **Gralla, J.D., and Vargas, D.R.** (2006) Potassium glutamate as a transcriptional inhibitor during bacterial osmoregulation. *In* EMBO J, pp.1515-1521.
91. **Grammann, K., Volke, A., and Kunte, H.J.** (2002) New type of osmoregulated solute transporter identified in halophilic members of the bacteria domain: TRAP transporter TeaABC mediates uptake of ectoine and hydroxyectoine in *Halomonas elongata* DSM 2581(T). *J Bacteriol* 184:3078-3085.
92. **Granato, E.T., Meiller-Legrand, T.A., and Foster, K.R.** (2019) The evolution and ecology of bacterial warfare. *Curr Biol* 29:R521-R537.
93. **Gregory, G.J., Morreale, D.P., and Boyd, E.F.** (2020) CosR is a global regulator of the osmotic stress response with widespread distribution among bacteria. *Appl Environ Microbiol* 86:e00120-00120.
94. **Gregory, G.J., Morreale, D.P., Carpenter, M.R., Kalburge, S.S., and Boyd, E.F.** (2019) Quorum sensing regulators AphA and OpaR control expression of the operon responsible for biosynthesis of the compatible solute ectoine. *Appl Environ Microbiol* 85:01543-01519.

95. **Gunde-Cimerman, N., Plemenitas, A., and Oren, A.** (2018) Strategies of adaptation of microorganisms of the three domains of life to high salt concentrations. *FEMS Microbiol Rev* 42:353-375.
96. **Gundlach, J., Commichau, F.M., and Stülke, J.** (2018) Perspective of ions and messengers: An intricate link between potassium, glutamate, and cyclic di-AMP. *Curr Genet* 64:191-195.
97. **Hahn, M.B., Meyer, S., Schröter, M.A., Kunte, H.J., Solomun, T., and Sturm, H.** (2017) DNA protection by ectoine from ionizing radiation: Molecular mechanisms. *Phys Chem Chem Phys* 19:25717-25722.
98. **Hahn, M.B., Solomun, T., Wellhausen, R., Hermann, S., Seitz, H., Meyer, S., Kunte, H.J., Zeman, J., Uhlig, F., Smiatek, J., and Sturm, H.** (2015) Influence of the compatible solute ectoine on the local water structure: Implications for the binding of the protein G5P to DNA. *J Phys Chem B* 119:15212-15220.
99. **Hanekop, N., Höing, M., Sohn-Bösser, L., Jebbar, M., Schmitt, L., and Bremer, E.** (2007) Crystal structure of the ligand-binding protein EhuB from *Sinorhizobium meliloti* reveals substrate recognition of the compatible solutes ectoine and hydroxyectoine. *J Mol Biol* 374:1237-1250.
100. **Hangasky, J.A., Taabazuing, C.Y., Valliere, M.A., and Knapp, M.J.** (2013) Imposing function down a (cupin)-barrel: Secondary structure and metal stereochemistry in the alphaKG-dependent oxygenases. *Metallomics* 5:287-301.
101. **Harding, T., Brown, M.W., Simpson, A.G., and Roger, A.J.** (2016) Osmoadaptative strategy and its molecular signature in obligately halophilic heterotrophic protists. *Genome Biol Evol* 8:2241-2258.
102. **Harishchandra, R.K., Wulff, S., Lentzen, G., Neuhaus, T., and Galla, H.J.** (2010) The effect of compatible solute ectoines on the structural organization of lipid monolayer and bilayer membranes. *Biophys Chem* 150:37-46.
103. **Heine, A., DeSantis, G., Luz, J.G., Mitchell, M., Wong, C.-H., and Wilson, I.A.** (2001) Observation of covalent intermediates in an enzyme mechanism at atomic resolution. *Science* 294:369-374.
104. **Held, C., Neuhaus, T., and Sadowski, G.** (2010) Compatible solutes: Thermodynamic properties and biological impact of ectoines and prolines. *Biophys Chem* 152:28-39.
105. **Hermann, L.** (2022) Ectoine metabolism: A diverse field with differing modes. In *Unpublished manuscript*.
106. **Hermann, L., Mais, C.N., Czech, L., Smits, S.H.J., Bange, G., and Bremer, E.** (2020) The ups and downs of ectoine: Structural enzymology of a major microbial stress protectant and versatile nutrient. *Biol Chem* 401:1443-1468.
107. **Hermann, L., Dempwolff, F., Steinchen, W., Freibert, S.-A., Smits, S.H.J., Seubert, A., and Bremer, E.** (2021) The MocR/GabR ectoine and hydroxyectoine catabolism regulator EnuR: Inducer and DNA binding. *Front Microbiol* 12.
108. **Higgins, C.F.** (1992) ABC transporters: From microorganisms to man. *Annu Rev Cell Biol* 8:67-113.
109. **Higgins, C.F., Dorman, C.J., Stirling, D.A., Waddell, L., Booth, I.R., May, G., and Bremer, E.** (1988) A physiological role for DNA supercoiling in the osmotic regulation of gene expression in *S. typhimurium* and *E. coli*. *Cell* 52:569-584.
110. **Hill, A.E., Shachar-Hill, B., and Shachar-Hill, Y.** (2004) What are aquaporins for? *J Membr Biol* 197:1-32.
111. **Hillier, H.T., Altermark, B., and Leiros, I.** (2020) The crystal structure of the tetrameric DABA-aminotransferase EctB, a rate-limiting enzyme in the ectoine biosynthesis pathway. *FEBS J* 287:4641-4658.
112. **Hoeppner, A., Widderich, N., Lenders, M., Bremer, E., and Smits, S.H.** (2014) Crystal structure of the ectoine hydroxylase, a snapshot of the active site. *J Biol Chem* 289:29570-29583.
113. **Hoffmann, E.H., Tilgner, A., Schrödner, R., Bräuer, P., Wolke, R., and Herrmann, H.** (2016) An advanced modeling study on the impacts and atmospheric implications of multiphase dimethyl sulfide chemistry. *Proc Natl Acad Sci USA* 113:11776-11781.

114. **Hoffmann, T., and Bremer, E.** (2011) Protection of *Bacillus subtilis* against cold stress via compatible-solute acquisition. *J Bacteriol* 193:1552-1562.
115. **Hoffmann, T., and Bremer, E.** (eds) (2016) Management of osmotic stress by *Bacillus subtilis*: Genetics and physiology. Hoboken, NJ, USA: John Wiley & Sons, Inc.
116. **Hoffmann, T., and Bremer, E.** (2017) Guardians in a stressful world: The Opu family of compatible solute transporters from *Bacillus subtilis*. *Biol Chem* 398:193-214.
117. **Hoffmann, T., Boiangiu, C., Moses, S., and Bremer, E.** (2008) Responses of *Bacillus subtilis* to hypotonic challenges: Physiological contributions of mechanosensitive channels to cellular survival. *Appl Environ Microbiol* 74:2454-2460.
118. **Hoffmann, T., Warmbold, B., Smits, S.H.J., Tschapek, B., Ronzheimer, S., Bashir, A., Chen, C., Rolbetzki, A., Pittelkow, M., Jebbar, M., Seubert, A., Schmitt, L., and Bremer, E.** (2018) Arsenobetaine: An ecophysiologically important organoarsenical confers cytoprotection against osmotic stress and growth temperature extremes. *Environ Microbiol* 20:305-323.
119. **Holtmann, G., and Bremer, E.** (2004) Thermoprotection of *Bacillus subtilis* by exogenously provided glycine betaine and structurally related compatible solutes: Involvement of Opu transporters. *J Bacteriol* 186:1683-1693.
120. **Howarth, R.W., and Marino, R.** (2006) Nitrogen as the limiting nutrient for eutrophication in coastal marine ecosystems: Evolving views over three decades. *Limnol Oceanogr* 51:364-376.
121. **Inbar, L., and Lapidot, A.** (1988) The structure and biosynthesis of new tetrahydropyrimidine derivatives in actinomycin D producer *Streptomyces parvulus*. Use of ^{13}C- and ^{15}N-labeled L-glutamate and ^{13}C and ^{15}N NMR spectroscopy. *J Biol Chem* 263:16014-16022.
122. **Inbar, L., Frolow, F., and Lapidot, A.** (1993) The conformation of new tetrahydropyrimidine derivatives in solution and in the crystal. *Eur J Biochem* 214:897-906.
123. **Iorio, M., Davatgarbenam, S., Serina, S., Criscenzo, P., Zdouc, M.M., Simone, M., Maffioli, S.I., Ebright, R.H., Donadio, S., and Sosio, M.** (2021) Blocks in the pseudouridimycin pathway unlock hidden metabolites in the *Streptomyces producer* strain. *Sci Rep* 11:5827.
124. **Ishida, M.L., Assumpcao, M.C., Machado, H.B., Benelli, E.M., Souza, E.M., and Pedrosa, F.O.** (2002) Identification and characterization of the two-component NtrY/NtrX regulatory system in *Azospirillum brasilense*. *Braz J Med Biol Res* 35:651-661.
125. **Ishida, Y.** (1996) 30 years of research on dimethylsulfoniopriopionate. *In* Biological and environmental chemistry of DMSP and related sulfonium compounds: Springer, pp.1-12.
126. **Islam, M.S., Leissing, T.M., Chowdhury, R., Hopkinson, R.J., and Schofield, C.J.** (2018) 2-Oxoglutarate-dependent oxygenases. *Annu Rev Biochem* 87:585-620.
127. **Jebbar, M., Talibart, R., Gloux, K., Bernard, T., and Blanco, C.** (1992) Osmoprotection of *Escherichia coli* by ectoine: Uptake and accumulation characteristics. *J Bacteriol* 174:5027-5035.
128. **Jebbar, M., Sohn-Bösser, L., Bremer, E., Bernard, T., and Blanco, C.** (2005) Ectoine-induced proteins in *Sinorhizobium meliloti* include an ectoine ABC-type transporter involved in osmoprotection and ectoine catabolism. *J Bacteriol* 187:1293-1304.
129. **Jiang, H., Dong, H., Yu, B., Liu, X., Li, Y., Ji, S., and Zhang, C.L.** (2007) Microbial response to salinity change in Lake Chaka, a hypersaline lake on Tibetan plateau. *Environ Microbiol* 9:2603-2621.
130. **Jiao, N., and Zheng, Q.** (2011) The microbial carbon pump: From genes to ecosystems. *Appl Environ Microbiol* 77:7439-7444.
131. **Jiao, N., Herndl, G.J., Hansell, D.A., Benner, R., Kattner, G., Wilhelm, S.W., Kirchman, D.L., Weinbauer, M.G., Luo, T., and Chen, F.** (2010) Microbial production of recalcitrant dissolved organic matter: Long-term carbon storage in the global ocean. *Nat Rev Microbiol* 8:593-599.
132. **Johnson, W.M., Soule, M.C.K., and Kujawinski, E.B.** (2016) Evidence for quorum sensing and differential metabolite production by a marine bacterium in response to DMSP. *ISME J* 10:2304-2316.

133. **Jorge, C.D., Borges, N., Bagyan, I., Bilstein, A., and Santos, H.** (2016) Potential applications of stress solutes from extremophiles in protein folding diseases and healthcare. *Extremophiles* 20:251-259.
134. **Jumper, J., Evans, R., Pritzel, A., Green, T., Figurnov, M., Ronneberger, O., Tunyasuvunakool, K., Bates, R., Zidek, A., Potapenko, A., Bridgland, A., Meyer, C., Kohl, S.A.A., Ballard, A.J., Cowie, A., Romera-Paredes, B., Nikolov, S., Jain, R., Adler, J., Back, T., Petersen, S., Reiman, D., Clancy, E., Zielinski, M., Steinegger, M., Pacholska, M., Berghammer, T., Bodenstein, S., Silver, D., Vinyals, O., Senior, A.W., Kavukcuoglu, K., Kohli, P., and Hassabis, D.** (2021) Highly accurate protein structure prediction with AlphaFold. *Nature* 596:583-589.
135. **Kang, J.Y., Lee, B., Kim, J.A., Kim, M.-S., and Kim, C.H.** (2022) Identification and characterization of an ectoine biosynthesis gene cluster from *Aestuariispira ectoiniformans* sp. nov., isolated from seawater. *Microbiological Research* 254:126898.
136. **Kapfhammer, D., Karatan, E., Pflughoeft, K.J., and Watnick, P.I.** (2005) Role for glycine betaine transport in *Vibrio cholerae* osmoadaptation and biofilm formation within microbial communities. *Appl Environ Microbiol* 71:3840-3847.
137. **Karl, D.M., and Church, M.J.** (2014) Microbial oceanography and the Hawaii Ocean Time-series programme. *Nat Rev Microbiol* 12:699-713.
138. **Kaur, A., Hernandez-Fernaud, J.R., Aguilo-Ferretjans, M.D.M., Wellington, E.M., and Christie-Oleza, J.A.** (2018) 100 Days of marine *Synechococcus-Ruegeria pomeroyi* interaction: A detailed analysis of the exoproteome. *Environ Microbiol* 20:785-799.
139. **Kempf, B., and Bremer, E.** (1998) Uptake and synthesis of compatible solutes as microbial stress responses to high-osmolality environments. *Arch Microbiol* 170:319-330.
140. **Kiene, R.P., and Bates, T.S.** (1990) Biological removal of dimethyl sulphide from sea water. *Nature* 345:702-705.
141. **Kiene, R.P., Linn, L.J., and Bruton, J.A.** (2000) New and important roles for DMSP in marine microbial communities. *J Sea Res* 43:209-224.
142. **Kindzierski, V., Raschke, S., Knabe, N., Siedler, F., Scheffer, B., Pflüger-Grau, K., Pfeiffer, F., Oesterhelt, D., Marin-Sanguino, A., and Kunte, H.J.** (2017) Osmoregulation in the halophilic bacterium *Halomonas elongata*: A case study for integrative systems biology. *PLoS One* 12:e0168818.
143. **Klauck, E., Typas, A., and Hengge, R.** (2007) The sigmaS subunit of RNA polymerase as a signal integrator and network master regulator in the general stress response in *Escherichia coli*. *Sci Prog* 90:103-127.
144. **Kloda, A., and Martinac, B.** (2001) Mechanosensitive channel of *Thermoplasma*, the cell wall-less archaea. *Cell Biochem Biophys* 34:321-347.
145. **Knapp, S., Ladenstein, R., and Galinski, E.A.** (1999) Extrinsic protein stabilization by the naturally occurring osmolytes beta-hydroxyectoine and betaine. *Extremophiles* 3:191-198.
146. **Kowalinski, E., Bange, G., Bradatsch, B., Hurt, E., Wild, K., and Sinning, I.** (2007) The crystal structure of Ebp1 reveals a methionine aminopeptidase fold as binding platform for multiple interactions. *FEBS Lett* 581:4450-4454.
147. **Kuhlmann, A.U., and Bremer, E.** (2002) Osmotically regulated synthesis of the compatible solute ectoine in *Bacillus pasteurii* and related *Bacillus* spp. *Appl Environ Microbiol* 68:772-783.
148. **Kuhlmann, A.U., Bursy, J., Gimpel, S., Hoffmann, T., and Bremer, E.** (2008a) Synthesis of the compatible solute ectoine in *Virgibacillus pantothenticus* is triggered by high salinity and low growth temperature. *Appl Environ Microbiol* 74:4560-4563.
149. **Kuhlmann, A.U., Hoffmann, T., Bursy, J., Jebbar, M., and Bremer, E.** (2011) Ectoine and hydroxyectoine as protectants against osmotic and cold stress: Uptake through the SigB-controlled betaine-choline- carnitine transporter-type carrier EctT from *Virgibacillus pantothenticus*. *J Bacteriol* 193:4699-4708.
150. **Kuhlmann, S.I., Terwisscha van Scheltinga, A.C., Bienert, R., Kunte, H.J., and Ziegler, C.** (2008b) 1.55 A structure of the ectoine binding protein TeaA of the osmoregulated TRAP-transporter TeaABC from *Halomonas elongata*. *Biochem* 47:9475-9485.

151. **Kum, E., and Ince, E.** (2021) Genome-guided investigation of secondary metabolites produced by a potential new strain *Streptomyces* BA2 isolated from an endemic plant rhizosphere in Turkey. *Arch Microbiol*.
152. **Kumarevel, T., Nakano, N., Ponnuraj, K., Gopinath, S.C., Sakamoto, K., Shinkai, A., Kumar, P.K., and Yokoyama, S.** (2008) Crystal structure of glutamine receptor protein from *Sulfolobus tokodaii* strain 7 in complex with its effector L-glutamine: Implications of effector binding in molecular association and DNA binding. *Nucleic Acids Res* 36:4808-4820.
153. **Kunte, H.J., Lentzen, G., and A Galinski, E.** (2014) Industrial production of the cell protectant ectoine: Protection mechanisms, processes, and products. *Curr Biotechnol* 3:10-25.
154. **Kurz, M.** (2008) Compatible solute influence on nucleic acids: Many questions but few answers. *Saline Systems* 4:6.
155. **Lamark, T., Styrvold, O.B., and Strom, A.R.** (1992) Efflux of choline and glycine betaine from osmoregulating cells of *Escherichia coli*. *FEMS Microbiol Lett* 75:149-154.
156. **Landa, M., Burns, A.S., Roth, S.J., and Moran, M.A.** (2017) Bacterial transcriptome remodelling during sequential co-culture with a marine dinoflagellate and diatome. *ISME J* 11:2677-2690.
157. **Le Coq, J., Pavlovsky, A., Malik, R., Sanishvili, R., Xu, C., and Viola, R.E.** (2008) Examination of the mechanism of human brain aspartoacylase through the binding of an intermediate analogue. *Biochem* 47:3484-3492.
158. **Lecher, J., Pittelkow, M., Zobel, S., Bursy, J., Bonig, T., Smits, S.H., Schmitt, L., and Bremer, E.** (2009) The crystal structure of UehA in complex with ectoine - a comparison with other TRAP-T binding proteins. *J Mol Biol* 389:58-73.
159. **Lee, C., Kang, H.J., Von Ballmoos, C., Newstead, S., Uzdavinys, P., Dotson, D.L., Iwata, S., Beckstein, O., Cameron, A.D., and Drew, D.** (2013) A two-domain elevator mechanism for sodium/proton antiport. *Nature* 501:573-577.
160. **Lentzen, G., and Schwarz, T.** (2006) Extremolytes: Natural compounds from extremophiles for versatile applications. *Appl Microbiol Biotechnol* 72:623-634.
161. **Leon, M.J., Hoffmann, T., Sanchez-Porro, C., Heider, J., Ventosa, A., and Bremer, E.** (2018) Compatible solute synthesis and import by the moderate halophile *Spiribacter salinus*: Physiology and genomics. *Front Microbiol* 9:108.
162. **Levina, N., Totemeyer, S., Stokes, N.R., Louis, P., Jones, M.A., and Booth, I.R.** (1999) Protection of *Escherichia coli* cells against extreme turgor by activation of MscS and MscL mechanosensitive channels: Identification of genes required for MscS activity. *EMBO J* 18:1730-1737.
163. **Li, C.-Y., Chen, X.-L., Shao, X., Wei, T.-D., Wang, P., Xie, B.-B., Qin, Q.-L., Zhang, X.-Y., Su, H.-N., Song, X.-Y., Shi, M., Zhou, B.-C., Zhang, Y.-Z., and Stock, A.M.** (2015) Mechanistic insight into trimethylamine *N*-oxide recognition by the marine bacterium *Ruegeria pomeroyi* DSS-3. *J Bacteriol* 197:3378-3387.
164. **Lidbury, I., Murrell, J.C., and Chen, Y.** (2014) Trimethylamine *N*-oxide metabolism by abundant marine heterotrophic bacteria. *Proc Natl Acad Sci USA* 111:2710-2715.
165. **Lidbury, I., Mausz, M.A., Scanlan, D.J., and Chen, Y.** (2017) Identification of dimethylamine monooxygenase in marine bacteria reveals a metabolic bottleneck in the methylated amine degradation pathway. *ISME J* 11:1592-1601.
166. **Lidbury, I., Krober, E., Zhang, Z., Zhu, Y., Murrell, J.C., Chen, Y., and Schafer, H.** (2016) A mechanism for bacterial transformation of dimethylsulfide to dimethylsulfoxide: A missing link in the marine organic sulfur cycle. *Environ Microbiol* 18:2754-2766.
167. **Lippert, K., and Galinski, E.A.** (1992) Enzyme stabilization by ectoine-type compatible solutes - protection against heating, freezing and drying. *Appl Microbiol Biotechnol* 37:61-65.
168. **Lo, C.-J., Leake, M.C., and Berry, R.M.** (2006) Fluorescence measurement of intracellular sodium concentration in single *Escherichia coli* cells. *Biophys J* 90:357-365.

169. **Lo, C.C., Bonner, C.A., Xie, G., D'Souza, M., and Jensen, R.A.** (2009) Cohesion group approach for evolutionary analysis of aspartokinase, an enzyme that feeds a branched network of many biochemical pathways. *Microbiol Mol Biol Rev* 73:594-651.
170. **Louis, P., and Galinski, E.A.** (1997) Characterization of genes for the biosynthesis of the compatible solute ectoine from *Marinococcus halophilus* and osmoregulated expression in *Escherichia coli*. *Microbiol* 143 (Pt 4):1141-1149.
171. **Lucht, J.M., and Bremer, E.** (1994) Adaptation of *Escherichia coli* to high osmolarity environments: Osmoregulation of the high-affinity glycine betaine transport system ProU. *FEMS Microbiol Rev* 14:3-20.
172. **Ma, Y., Wang, Q., Xu, W., Liu, X., Gao, X., and Zhang, Y.** (2017) Stationary phase-dependent accumulation of ectoine is an efficient adaptation strategy in *Vibrio anguillarum* against cold stress. *Microbiol Res* 205:8-18.
173. **Mais, C.N., Hermann, L., Altegoer, F., Seubert, A., Richter, A.A., Wernersbach, I., Czech, L., Bremer, E., and Bange, G.** (2020) Degradation of the microbial stress protectants and chemical chaperones ectoine and hydroxyectoine by a bacterial hydrolase-deacetylase complex. *J Biol Chem* 295:9087-9104.
174. **Makarova, K.S., Aravind, L., and Koonin, E.V.** (1999) A superfamily of archaeal, bacterial, and eukaryotic proteins homologous to animal transglutaminases. *Protein Sci* 8:1714-1719.
175. **Malin, G., and Lapidot, A.** (1996) Induction of synthesis of tetrahydropyrimidine derivatives in *Streptomyces* strains and their effect on *Escherichia coli* in response to osmotic and heat stress. *J Bacteriol* 178:385-395.
176. **Manzanera, M., Vilchez, S., and Tunnacliffe, A.** (2004) High survival and stability rates of *Escherichia coli* dried in hydroxyectoine. *FEMS Microbiol Lett* 233:347-352.
177. **Manzanera, M., Garcia de Castro, A., Tondervik, A., Rayner-Brandes, M., Strom, A.R., and Tunnacliffe, A.** (2002) Hydroxyectoine is superior to trehalose for anhydrobiotic engineering of *Pseudomonas putida* KT2440. *Appl Environ Microbiol* 68:4328-4333.
178. **Margolin, W.** (2009) Sculpting the bacterial cell. *Curr Biol* 19:R812-R822.
179. **Mazzarello, P.** (1999) A unifying concept: The history of cell theory. *Nat Cell Biol* 1:E13-E15.
180. **Megaw, J., Kelly, S.A., Thompson, T.P., Skvortsov, T., and Gilmore, B.F.** (2019) Profiling the microbial community of a Triassic halite deposit in Northern Ireland: An environment with significant potential for biodiscovery. *FEMS Microbiol Lett* 366.
181. **Meyer, S., Schröter, M.A., Hahn, M.B., Solomun, T., Sturm, H., and Kunte, H.J.** (2017) Ectoine can enhance structural changes in DNA in vitro. *Sci Rep* 7:7170.
182. **Mheen, T.-I., and Kwon, T.-W.** (1984) Effect of temperature and salt concentration on kimchi fermentation. *Korean J Food Sci Technol* 16:443-450.
183. **Moran, M.A., Buchan, A., Gonzalez, J.M., Heidelberg, J.F., Whitman, W.B., Kiene, R.P., Henriksen, J.R., King, G.M., Belas, R., Fuqua, C., Brinkac, L., Lewis, M., Johri, S., Weaver, B., Pai, G., Eisen, J.A., Rahe, E., Sheldon, W.M., Ye, W., Miller, T.R., Carlton, J., Rasko, D.A., Paulsen, I.T., Ren, Q., Daugherty, S.C., Deboy, R.T., Dodson, R.J., Durkin, A.S., Madupu, R., Nelson, W.C., Sullivan, S.A., Rosovitz, M.J., Haft, D.H., Selengut, J., and Ward, N.** (2004) Genome sequence of *Silicibacter pomeroyi* reveals adaptations to the marine environment. *Nature* 432:910-913.
184. **Moritz, K.D., Amendt, B., Witt, E.M., and Galinski, E.A.** (2015) The hydroxyectoine gene cluster of the non-halophilic acidophile *Acidiphilium cryptum*. *Extremophiles* 19:87-99.
185. **Mosier, A.C., Justice, N.B., Bowen, B.P., Baran, R., Thomas, B.C., Northen, T.R., and Banfield, J.F.** (2013) Metabolites associated with adaptation of microorganisms to an acidophilic, metal-rich environment identified by stable-isotope-enabled metabolomics. *mBio* 4:e00484-00412.
186. **Mou, X., Sun, S., Rayapati, P., and Moran, M.A.** (2010) Genes for transport and metabolism of spermidine in *Ruegeria pomeroyi* DSS-3 and other marine bacteria. *Aquat Microb Ecol* 58:311-321.

187. **Mustakhimov, I., Reshetnikov, A.S., Khmelenina, V.N., and Trotsenko, Y.A.** (2009) EctR - A novel transcriptional regulator of ectoine biosynthesis genes in the haloalcaliphilic methylotrophic bacterium *Methylophaga alcalica*. *Dokl Biochem Biophys* 429:305-308.
188. **Mustakhimov, I., Rozova, O.N., Reshetnikov, A.S., Khmelenina, V.N., Murrell, J.C., and Trotsenko, Y.A.** (2008) Characterization of the recombinant diaminobutyric acid acetyltransferase from *Methylophaga thalassica* and *Methylophaga alcalica*. *FEMS Microbiol Lett* 283:91-96.
189. **Mustakhimov, I., Reshetnikov, A.S., Glukhov, A.S., Khmelenina, V.N., Kalyuzhnaya, M.G., and Trotsenko, Y.A.** (2010) Identification and characterization of EctR1, a new transcriptional regulator of the ectoine biosynthesis genes in the halotolerant methanotroph *Methylomicrobium alcaliphilum* 20Z. *J Bacteriol* 192:410-417.
190. **Nagarajavel, V., Madhusudan, S., Dole, S., Rahmouni, A.R., and Schnetz, K.** (2007) Repression by binding of H-NS within the transcription unit. *J Biol Chem* 282:23622-23630.
191. **Nevitt, G.A., and Bonadonna, F.** (2005) Sensitivity to dimethyl sulphide suggests a mechanism for olfactory navigation by seabirds. *Biol Lett* 1:303-305.
192. **Ning, Y., Wu, X., Zhang, C., Xu, Q., Chen, N., and Xie, X.** (2016) Pathway construction and metabolic engineering for fermentative production of ectoine in *Escherichia coli*. *Metab Eng* 36:10-18.
193. **Okuda, K., Ito, T., Goto, M., Takenaka, T., Hemmi, H., and Yoshimura, T.** (2015a) Domain characterization of *Bacillus subtilis* GabR, a pyridoxal 5'-phosphate-dependent transcriptional regulator. *J Biochem* 158:225-234.
194. **Okuda, K., Kato, S., Ito, T., Shiraki, S., Kawase, Y., Goto, M., Kawashima, S., Hemmi, H., Fukada, H., and Yoshimura, T.** (2015b) Role of the aminotransferase domain in *Bacillus subtilis* GabR, a pyridoxal 5'-phosphate-dependent transcriptional regulator. *Mol Microbiol* 95:245-257.
195. **Ono, H., Sawada, K., Khunajakr, N., Tao, T., Yamamoto, M., Hiramoto, M., Shinmyo, A., Takano, M., and Murooka, Y.** (1999) Characterization of biosynthetic enzymes for ectoine as a compatible solute in a moderately halophilic eubacterium, *Halomonas elongata*. *J Bacteriol* 181:91-99.
196. **Oren, A.** (1999) Bioenergetic aspects of halophilism. *In* Microbiol Mol Biol Rev, pp.334-348.
197. **Oren, A.** (2011) Thermodynamic limits to microbial life at high salt concentrations. *Environ Microbiol* 13:1908-1923.
198. **Oren, A.** (2013) Life at high salt concentrations, intracellular KCl concentrations, and acidic proteomes. *Front Microbiol* 4:315.
199. **Oren, A., Heldal, M., and Norland, S.** (1997) X-ray microanalysis of intracellular ions in the anaerobic halophilic eubacterium *Haloanaerobium praevalens*. *Can J Microbiol* 43:588-592.
200. **Park, S.A., Park, Y.S., and Lee, K.S.** (2017) Crystal structure of the C-terminal domain of Bacillus subtilis GabR reveals a closed conformation by gamma-aminobutyric acid binding, inducing transcriptional activation. *Biochem Biophys Res Commun* 487:287-291.
201. **Pascarella, S.** (2019) Computational classification of MocR transcriptional regulators into subgroups as a support for experimental and functional characterization. *Bioinformation* 15:151-159.
202. **Pastor, J.M., Salvador, M., Argandona, M., Bernal, V., Reina-Bueno, M., Csonka, L.N., Iborra, J.L., Vargas, C., Nieto, J.J., and Canovas, M.** (2010) Ectoines in cell stress protection: Uses and biotechnological production. *Biotechnol Adv* 28:782-801.
203. **Pastor, J.M., Bernal, V., Salvador, M., Argandona, M., Vargas, C., Csonka, L., Sevilla, A., Iborra, J.L., Nieto, J.J., and Canovas, M.** (2013) Role of central metabolism in the osmoadaptation of the halophilic bacterium Chromohalobacter salexigens. *J Biol Chem* 288:17769-17781.
204. **Paulino, C., and Kuhlbrandt, W.** (2014) pH- and sodium-induced changes in a sodium/proton antiporter. *eLife* 3:e01412.

205. **Pawlowski, K., Klosse, U., and de Bruijn, F.J.** (1991) Characterization of a novel *Azorhizobium caulinodans* ORS571 two-component regulatory system, NtrY/NtrX, involved in nitrogen fixation and metabolism. *Mol Gen Genet* 231:124-138.
206. **Pérez, V., Moltó, J.L., Lebrero, R., and Muñoz, R.l.** (2021) Ectoine production from biogas in waste treatment facilities: A techno-economic and sensitivity analysis. *ACS Sustain Chem Eng* 9:17371–17380.
207. **Perez-Garcia, F., Ziert, C., Risse, J.M., and Wendisch, V.F.** (2017) Improved fermentative production of the compatible solute ectoine by *Corynebacterium glutamicum* from glucose and alternative carbon sources. *J Biotechnol* 258:59-68.
208. **Peters, P., Galinski, E.A., and Trüper, H.G.** (1990) The biosyntheis of ectoine. *FEMS Microbiol Lett* 71:157-162.
209. **Piubeli, F., Salvador, M., Argandona, M., Nieto, J.J., Bernal, V., Pastor, J.M., Canovas, M., and Vargas, C.** (2018) Insights into metabolic osmoadaptation of the ectoines-producer bacterium *Chromohalobacter salexigens* through a high-quality genome scale metabolic model. *Microb Cell Fact* 17:2.
210. **Prabhu, J., Schauwecker, F., Grammel, N., Keller, U., and Bernhard, M.** (2004) Functional expression of the ectoine hydroxylase gene (*thpD*) from *Streptomyces chrysomallus* in *Halomonas elongata*. *Appl Environ Microbiol* 70:3130-3132.
211. **Raina, J.-B., Dinsdale, E.A., Willis, B.L., and Bourne, D.G.** (2010) Do the organic sulfur compounds DMSP and DMS drive coral microbial associations? *Trends Microbiol* 18:101-108.
212. **Rajkumari, K., Kusano, S., Ishihama, A., Mizuno, T., and Gowrishankar, J.** (1996) Effects of H-NS and potassium glutamate on sigma(S)- and sigma(70)-directed transcription in vitro from osmotically regulated P1 and P2 promoters of proU in *Escherichia coli*. *J Bacteriol* 178:4176-4181.
213. **Rawlings, N.D., and Barrett, A.J.** (1993) Evolutionary families of peptidases. *Biochem* 290:205-218.
214. **Rawlings, N.D., and Barrett, A.J.** (2013) Introduction: Metallopeptidases and their clans. *In* Handbook of Proteolytic Enzymes: Elsevier, pp.325-370.
215. **Ray, S., Kassan, A., Busija, A.R., Rangamani, P., and Patel, H.H.** (2016) The plasma membrane as a capacitor for energy and metabolism. *Am J Physiol Cell Physiol* 310:C181-192.
216. **Reisch, C.R., Crabb, W.M., Gifford, S.M., Teng, Q., Stoudemayer, M.J., Moran, M.A., and Whitman, W.B.** (2013) Metabolism of dimethylsulphoniopropionate by *Ruegeria pomeroyi* DSS-3. *Mol Microbiol* 89:774-791.
217. **Reshetnikov, A.S., Khmelenina, V.N., and Trotsenko, Y.A.** (2006) Characterization of the ectoine biosynthesis genes of haloalkalotolerant obligate methanotroph "*Methylomicrobium alcaliphilum* 20Z". *Arch Microbiol* 184:286-297.
218. **Reshetnikov, A.S., Khmelenina, V.N., Mustakhimov, II, and Trotsenko, Y.A.** (2011a) Genes and enzymes of ectoine biosynthesis in halotolerant methanotrophs. *Methods Enzymol* 495:15-30.
219. **Reshetnikov, A.S., Khmelenina, V.N., Mustakhimov, II, Kalyuzhnaya, M., Lidstrom, M., and Trotsenko, Y.A.** (2011b) Diversity and phylogeny of the ectoine biosynthesis genes in aerobic, moderately halophilic methylotrophic bacteria. *Extremophiles* 15:653-663.
220. **Reshetnikov, A.S., Rozova, O.N., Trotsenko, Y.A., But, S.Y., Khmelenina, V.N., and Mustakhimov, II** (2020) Ectoine degradation pathway in halotolerant methylotrophs. *PLoS One* 15:e0232244.
221. **Reuter, K., Pittelkow, M., Bursy, J., Heine, A., Craan, T., and Bremer, E.** (2010) Synthesis of 5-hydroxyectoine from ectoine: Crystal structure of the non-heme iron(II) and 2-oxoglutarate-dependent dioxygenase EctD. *PLoS One* 5:e10647.
222. **Reuter, M., Hayward, N.J., Black, S.S., Miller, S., Dryden, D.T., and Booth, I.R.** (2014) Mechanosensitive channels and bacterial cell wall integrity: Does life end with a bang or a whimper? *J R Soc Interface* 11:20130850.

223. **Richter, A.A., Mais, C.-N., Czech, L., Geyer, K., Hoeppner, A., Smits, S.H., Erb, T.J., Bange, G., and Bremer, E.** (2019) Biosynthesis of the stress-protectant and chemical chaperon ectoine: Biochemistry of the transaminase EctB. *Front Microbiol* 10:2811.
224. **Richter, A.A., Kobus, S., Czech, L., Hoeppner, A., Zarzycki, J., Erb, T.J., Lauterbach, L., Dickschat, J.S., Bremer, E., and Smits, S.H.** (2020) The architecture of the diaminobutyrate acetyltransferase active site provides mechanistic insight into the biosynthesis of the chemical chaperone ectoine. *J Bacteriol* 295:2822-2838.
225. **Riclea, R., Gleitzmann, J., Bruns, H., Junker, C., Schulz, B., and Dickschat, J.S.** (2012) Algicidal lactones from the marine *Roseobacter* clade bacterium *Ruegeria pomeroyi*. *Beilstein J Org Chem* 8:941-950.
226. **Ridley, R.T.** (1986) To be taken with a pinch of salt: The destruction of Carthage. *Class Philol* 81:140-146.
227. **Roberts, K.B.** (2004) Urinary tract infection treatment and evaluation: Update. *Pediatr Infect Dis J* 23:1163-1164.
228. **Robin, A.Y., Cobessi, D., Curien, G., Robert-Genthon, M., Ferrer, J.-L., and Dumas, R.** (2010) A new mode of dimerization of allosteric enzymes with ACT domains revealed by the crystal structure of the aspartate kinase from Cyanobacteria. *J Mol Biol* 399:283-293.
229. **Roda, A., Yong Cong, M., Donner, B., Dickens, K., Howe, A., Sharma, S., and Smith, T.** (2018) Designing a trapping strategy to aid Giant African Snail (*Lissachatina fulica*) eradication programs. *PLoS One* 13:e0203572.
230. **Rodriguez-Moya, J., Argandona, M., Iglesias-Guerra, F., Nieto, J.J., and Vargas, C.** (2013) Temperature- and salinity-decoupled overproduction of hydroxyectoine by *Chromohalobacter salexigens*. *Appl Environ Microbiol* 79:1018-1023.
231. **Rodriguez-Moya, J., Argandona, M., Reina-Bueno, M., Nieto, J.J., Iglesias-Guerra, F., Jebbar, M., and Vargas, C.** (2010) Involvement of EupR, a response regulator of the NarL/FixJ family, in the control of the uptake of the compatible solutes ectoines by the halophilic bacterium *Chromohalobacter salexigens*. *BMC Microbiol* 10:256.
232. **Roesser, M., and Müller, V.** (2001) Osmoadaptation in bacteria and archaea: Common principles and differences. *Environ Microbiol* 3:743-754.
233. **Rojas, E.R., and Huang, K.C.** (2018) Regulation of microbial growth by turgor pressure. *Curr Opin Microbiol* 42:62-70.
234. **Rojas, E.R., Huang, K.C., and Theriot, J.A.** (2017) Homeostatic cell growth is accomplished mechanically through membrane tension inhibition of cell-wall synthesis. *Cell Syst* 5:578-590 e576.
235. **Romaniuk, J.A., and Cegelski, L.** (2015) Bacterial cell wall composition and the influence of antibiotics by cell-wall and whole-cell NMR. *Philos Trans R Soc Lond B Biol Sci* 370:20150024.
236. **Romeo, Y., Bouvier, J., and Gutierrez, C.** (2007) Osmotic regulation of transcription in *Lactococcus lactis*: Ionic strength-dependent binding of the BusR repressor to the *busA* promoter. *FEBS Lett* 581:3387-3390.
237. **Romeo, Y., Obis, D., Bouvier, J., Guillot, A., Fourcans, A., Bouvier, I., Gutierrez, C., and Mistou, M.Y.** (2003) Osmoregulation in *Lactococcus lactis*: BusR, a transcriptional repressor of the glycine betaine uptake system BusA. *Mol Microbiol* 47:1135-1147.
238. **Rubinstein, S.M., Kolodkin-Gal, I., McLoon, A., Chai, L., Kolter, R., Losick, R., and Weitz, D.A.** (2012) Osmotic pressure can regulate matrix gene expression in *Bacillus subtilis*. *Mol Microbiol* 86:426-436.
239. **Salar-Garcia, M.J., Bernal, V., Pastor, J.M., Salvador, M., Argandona, M., Nieto, J.J., Vargas, C., and Canovas, M.** (2017) Understanding the interplay of carbon and nitrogen supply for ectoines production and metabolic overflow in high density cultures of *Chromohalobacter salexigens*. *Microb Cell Fact* 16:23.
240. **Sankaran, N.** (2016) The RNA world at thirty: A look back with its author. *J Mol Evol* 83:169-175.

241. **Santos, H., and da Costa, M.S.** (2002) Compatible solutes of organisms that live in hot saline environments. *Environ Microbiol* 4:501-509.
242. **Sattar, O.I.A., Abuseada, H.H., Emara, M.S., and Rabee, M.** (2022) Green electrochemical and chromatographic quantifications of the extremolyte ectoine in halophilic bacterial cultures and related pharmaceutical preparations. *J Pharm Biomed Anal*:114680.
243. **Saum, S.H., and Muller, V.** (2007) Salinity-dependent switching of osmolyte strategies in a moderately halophilic bacterium: Glutamate induces proline biosynthesis in *Halobacillus halophilus*. *J Bacteriol* 189:6968-6975.
244. **Saum, S.H., and Muller, V.** (2008) Growth phase-dependent switch in osmolyte strategy in a moderate halophile: Ectoine is a minor osmolyte but major stationary phase solute in *Halobacillus halophilus*. *Environ Microbiol* 10:716-726.
245. **Schiraldi, C., Maresca, C., Catapano, A., Galinski, E.A., and De Rosa, M.** (2006) High-yield cultivation of *Marinococcus* M52 for production and recovery of hydroxyectoine. *Res Microbiol* 157:693-699.
246. **Schnoor, M., Voss, P., Cullen, P., Boking, T., Galla, H.J., Galinski, E.A., and Lorkowski, S.** (2004) Characterization of the synthetic compatible solute homoectoine as a potent PCR enhancer. *Biochem Biophys Res Commun* 322:867-872.
247. **Schroter, M.A., Meyer, S., Hahn, M.B., Solomun, T., Sturm, H., and Kunte, H.J.** (2017) Ectoine protects DNA from damage by ionizing radiation. *Sci Rep* 7:15272.
248. **Schulz, A., Stöveken, N., Binzen, I.M., Hoffmann, T., Heider, J., and Bremer, E.** (2017a) Feeding on compatible solutes: A substrate-induced pathway for uptake and catabolism of ectoines and its genetic control by EnuR. *Environ Microbiol* 19:926-946.
249. **Schulz, A., Hermann, L., Freibert, S.-A., Bönig, T., Hoffmann, T., Riclea, R., Dickschat, J.S., Heider, J., and Bremer, E.** (2017b) Transcriptional regulation of ectoine catabolism in response to multiple metabolic and environmental cues. *Environ Microbiol* 19:4599-4619.
250. **Schuster, C.F., Bellows, L.E., Tosi, T., Campeotto, I., Corrigan, R.M., Freemont, P., and Grundling, A.** (2016) The second messenger c-di-AMP inhibits the osmolyte uptake system OpuC in *Staphylococcus aureus*. *Sci Signal* 9:ra81.
251. **Schweikhard, E.S., Kuhlmann, S.I., Kunte, H.J., Grammann, K., and Ziegler, C.M.** (2010) Structure and function of the universal stress protein TeaD and its role in regulating the ectoine transporter TeaABC of *Halomonas elongata* DSM 2581(T). *Biochem* 49:2194-2204.
252. **Schwibbert, K., Marin-Sanguino, A., Bagyan, I., Heidrich, G., Lentzen, G., Seitz, H., Rampp, M., Schuster, S.C., Klenk, H.P., Pfeiffer, F., Oesterhelt, D., and Kunte, H.J.** (2011) A blueprint of ectoine metabolism from the genome of the industrial producer *Halomonas elongata* DSM 2581 T. *Environ Microbiol* 13:1973-1994.
253. **Scoma, A., and Boon, N.** (2016) Osmotic stress confers enhanced cell integrity to hydrostatic pressure but impairs growth in *Alcanivorax borkumensis* SK2. *Front Microbiol* 7:729.
254. **Sebastian, M., and Ammerman, J.W.** (2011) Role of the phosphatase PhoX in the phosphorus metabolism of the marine bacterium *Ruegeria pomeroyi* DSS-3. *Environ Microbiol Rep* 3:535-542.
255. **Seip, B., Galinski, E.A., and Kurz, M.** (2011) Natural and engineered hydroxyectoine production based on the *Pseudomonas stutzeri ectABCD-ask* gene cluster. *Appl Environ Microbiol* 77:1368-1374.
256. **Seminara, A., Angelini, T.E., Wilking, J.N., Vlamakis, H., Ebrahim, S., Kolter, R., Weitz, D.A., and Brenner, M.P.** (2012) Osmotic spreading of *Bacillus subtilis* biofilms driven by an extracellular matrix. *Proc Natl Acad Sci USA* 109:1116-1121.
257. **Severin, J., Wohlfarth, A., and Galinski, E.A.** (1992) The predominant role of recently discovered tetrahydropyrimidines for the osmoregulation of halophilic eubactreia. *J Gen Microbiol* 138:1629-1638.
258. **Seyedsayamdost, M.R., Case, R.J., Kolter, R., and Clardy, J.** (2011) The Jekyll-and-Hyde chemistry of Phaeobacter gallaeciensis. *Nat Chem* 3:331-335.

259. **Shao, Z., Deng, W., Li, S., He, J., Ren, S., Huang, W., Lu, Y., Zhao, G., Cai, Z., and Wang, J.** (2015) GlnR-mediated regulation of *ectABCD* transcription expands the role of the GlnR regulon to osmotic stress management. *J Bacteriol* 197:3041-3047.
260. **Sharpe, G.C., Gifford, S.M., Septer, A.N., and Tullman-Ercek, D.** (2020) A model *Roseobacter*, *Ruegeria pomeroyi* DSS-3, employs a diffusible killing mechanism to eliminate competitors. *mSystems* 5:e00443-00420.
261. **Shikuma, N.J., Davis, K.R., Fong, J.N., and Yildiz, F.H.** (2013) The transcriptional regulator, CosR, controls compatible solute biosynthesis and transport, motility and biofilm formation in *Vibrio cholerae*. *Environ Microbiol* 15:1387-1399.
262. **Shrivastava, T., and Ramachandran, R.** (2007) Mechanistic insights from the crystal structures of a feast/famine regulatory protein from *Mycobacterium tuberculosis* H37Rv. *Nucleic Acids Res* 35:7324-7335.
263. **Shrivastava, T., Kumar, S., and Ramachandran, R.** (2004) Cloning, expression, purification and crystallization of a transcriptional regulatory protein (Rv3291c) from *Mycobacterium tuberculosis* H37Rv. *Acta Cryst D* 60:1874-1876.
264. **Simon, M., Scheuner, C., Meier-Kolthoff, J.P., Brinkhoff, T., Wagner-Döbler, I., Ulbrich, M., Klenk, H.P., Schomburg, D., Petersen, J., and Göker, M.** (2017) Phylogenomics of *Rhodobacteraceae* reveals evolutionary adaptation to marine and non-marine habitats. *ISME J* 11:1483-1499.
265. **Sims, D., Brettin, T., Detter, J.C., Han, C., Lapidus, A., Copeland, A., Glavina Del Rio, T., Nolan, M., Chen, F., Lucas, S., Tice, H., Cheng, J.F., Bruce, D., Goodwin, L., Pitluck, S., Ovchinnikova, G., Pati, A., Ivanova, N., Mavrommatis, K., Chen, A., Palaniappan, K., D'Haeseleer, P., Chain, P., Bristow, J., Eisen, J.A., Markowitz, V., Hugenholtz, P., Schneider, S., Goker, M., Pukall, R., Kyrpides, N.C., and Klenk, H.P.** (2009) Complete genome sequence of *Kytococcus sedentarius* type strain (541). *Stand Genomic Sci* 1:12-20.
266. **Smiatek, J.** (2014) Osmolyte effects: Impact on the aqueous solution around charged and neutral spheres. *J Phys Chem B* 118:771-782.
267. **Smiatek, J., Harishchandra, R.K., Galla, H.J., and Heuer, A.** (2013) Low concentrated hydroxyectoine solutions in presence of DPPC lipid bilayers: A computer simulation study. *Biophys Chem* 180-181:102-109.
268. **Smiatek, J., Harishchandra, R.K., Rubner, O., Galla, H.J., and Heuer, A.** (2012) Properties of compatible solutes in aqueous solution. *Biophys Chem* 160:62-68.
269. **Steger, R., Weinand, M., Kramer, R., and Morbach, S.** (2004) LcoP, an osmoregulated betaine/ectoine uptake system from *Corynebacterium glutamicum*. *FEBS Lett* 573:155-160.
270. **Stöveken, N., Pittelkow, M., Sinner, T., Jensen, R.A., Heider, J., and Bremer, E.** (2011) A specialized aspartokinase enhances the biosynthesis of the osmoprotectants ectoine and hydroxyectoine in *Pseudomonas stutzeri* A1501. *J Bacteriol* 193:4456-4468.
271. **Street, T.O., Bolen, D.W., and Rose, G.D.** (2006) A molecular mechanism for osmolyte-induced protein stability. *Proc Natl Acad Sci USA* 103:13997-14002.
272. **Strong, P.J., Kalyuzhnaya, M., Silverman, J., and Clarke, W.P.** (2016) A methanotroph-based biorefinery: Potential scenarios for generating multiple products from a single fermentation. *Bioresour Technol* 215:314-323.
273. **Sun, L., Curson, A.R., Todd, J.D., and Johnston, A.W.** (2012) Diversity of DMSP transport in marine bacteria, revealed by genetic analyses. *Biogeochemistry* 110:121-130.
274. **Sutherland, L., Cairney, J., Elmore, M.J., Booth, I.R., and Higgins, C.F.** (1986) Osmotic regulation of transcription: Induction of the *proU* betaine transport gene is dependent on accumulation of intracellular potassium. *J Bacteriol* 168:805-814.
275. **Suttle, C.A.** (2007) Marine viruses—major players in the global ecosystem. *Nat Rev Microbiol* 5:801-812.
276. **Tadeo, X., Lopez-Mendez, B., Trigueros, T., Lain, A., Castano, D., and Millet, O.** (2009) Structural basis for the aminoacid composition of proteins from halophilic archea. *PLoS Biol* 7:e1000257.

277. **Takekawa, N., Imada, K., and Homma, M.** (2020) Structure and energy-conversion mechanism of the bacterial Na(+)-driven flagellar motor. *Trends Microbiol* 28:719-731.
278. **Talibart, R., Jebbar, M., Gouesbet, G., Himdi-Kabbab, S., Wroblewski, H., Blanco, C., and Bernard, T.** (1994) Osmoadaptation in rhizobia: Ectoine-induced salt tolerance. *J Bacteriol* 176:5210-5217.
279. **Talon, R., Coquelle, N., Madern, D., and Girard, E.** (2014) An experimental point of view on hydration/solvation in halophilic proteins. *Front Microbiol* 5:66.
280. **Tanghe, A., Van Dijck, P., and Thevelein, J.M.** (2006) Why do microorganisms have aquaporins? *Trends Microbiol* 14:78-85.
281. **Tanne, C., Golovina, E.A., Hoekstra, F.A., Meffert, A., and Galinski, E.A.** (2014) Glass-forming property of hydroxyectoine is the cause of its superior function as a dessication protectant. *Front Microbiol* 5:150.
282. **Tanveer, F., Shehroz, M., Ali, M., Xie, Y., Abbasi, R., Shinwari, Z.K., and Yasmin, A.** (2021) Genome sequence analysis and bioactivity profiling of marine-derived actinobacteria, *Brevibacterium luteolum*, and *Cellulosimicrobium funkei*. *Arch Microbiol*.
283. **Tao, P., Li, H., Yu, Y., Gu, J., and Liu, Y.** (2016) Ectoine and 5-hydroxyectoine accumulation in the halophile *Virgibacillus halodenitrificans* PDB-F2 in response to salt stress. *Appl Microbiol Biotechnol* 100:6779-6789.
284. **Tatzelt, J., Prusiner, S.B., and Welch, W.J.** (1996) Chemical chaperones interfere with the formation of scrapie prion protein. *EMBO J* 15:6363-6373.
285. **Tetsch, L., and Kunte, H.J.** (2002) The substrate-binding protein TeaA of the osmoregulated ectoine transporter TeaABC from *Halomonas elongata*: Purification and characterization of recombinant TeaA. *FEMS Microbiol Lett* 211:213-218.
286. **Thompson, T.P., Kelly, S.A., Skvortsov, T., Plunkett, G., Ruffell, A., Hallsworth, J.E., Hopps, J., and Gilmore, B.F.** (2021) Microbiology of a NaCl stalactite 'salticle'in Triassic halite. *Environ Microbiol*.
287. **Todd, J.D., Kirkwood, M., Newton-Payne, S., and Johnston, A.W.** (2012) DddW, a third DMSP lyase in a model *Roseobacter* marine bacterium, *Ruegeria pomeroyi* DSS-3. *ISME J* 6:223-226.
288. **Tong, H., Hu, Q., Zhu, L., and Dong, X.** (2019) Prokaryotic aquaporins. *Cells* 8.
289. **Tramonti, A., Nardella, C., di Salvo, M.L., Pascarella, S., and Contestabile, R.** (2018) The MocR-like transcription factors: Pyridoxal 5'-phosphate-dependent regulators of bacterial metabolism. *FEBS J* 285:3925-3944.
290. **Vaidya, S., Dev, K., and Sourirajan, A.** (2018) Distinct osmoadaptation strategies in the strict halophilic and halotolerant bacteria isolated from Lunsu salt water body of North West Himalayas. *Curr Microbiol* 75:888-895.
291. **van den Berg, J., Boersma, A.J., and Poolman, B.** (2017) Microorganisms maintain crowding homeostasis. *Nat Rev Microbiol* 15:309-318.
292. **Van-Thuoc, D., Hashim, S.O., Hatti-Kaul, R., and Mamo, G.** (2013) Ectoine-mediated protection of enzyme from the effect of pH and temperature stress: A study using *Bacillus halodurans* xylanase as a model. *Appl Microbiol Biotechnol* 97:6271-6278.
293. **Vandrich, J., Pfeiffer, F., Alfaro-Espinoza, G., and Kunte, H.J.** (2020) Contribution of mechanosensitive channels to osmoadaptation and ectoine excretion in *Halomonas elongata*. *Extremophiles* 24:421-432.
294. **Vargas, C., Argandona, M., Reina-Bueno, M., Rodriguez-Moya, J., Fernandez-Aunion, C., and Nieto, J.J.** (2008) Unravelling the adaptation responses to osmotic and temperature stress in *Chromohalobacter salexigens*, a bacterium with broad salinity tolerance. *Saline Systems* 4:14.
295. **Vargas, C., Jebbar, M., Carrasco, R., Blanco, C., Calderon, M.I., Iglesias-Guerra, F., and Nieto, J.J.** (2006) Ectoines as compatible solutes and carbon and energy sources for the halophilic bacterium *Chromohalobacter salexigens*. *J Appl Microbiol* 100:98-107.
296. **Vellai, T., Takács, K., and Vida, G.** (1998) A new aspect to the origin and evolution of eukaryotes. *J Mol Evol* 46:499-507.

297. **Venkataraman, R., and Sreenivasan, A.** (1954) Studies on the red halophilic bacteria from salted fish and salt. In *Proc Indian Acad Sci B - Biol Sci*: Springer, pp.17-23.
298. **Vetting, M.W., LP, S.d.C., Yu, M., Hegde, S.S., Magnet, S., Roderick, S.L., and Blanchard, J.S.** (2005) Structure and functions of the GNAT superfamily of acetyltransferases. *Arch Biochem Biophys* 433:212-226.
299. **Vitousek, P.M., and Howarth, R.W.** (1991) Nitrogen limitation on land and in the sea: how can it occur? *Biogeochemistry* 13:87-115.
300. **von Borzyskowski, L.S., Severi, F., Krüger, K., Hermann, L., Gilardet, A., Sippel, F., Pommerenke, B., Claus, P., Cortina, N.S., and Glatter, T.** (2019) Marine Proteobacteria metabolize glycolate via the β-hydroxyaspartate cycle. *Nature* 575:500-504.
301. **Vyas, R., Tewari, R., Weiss, M.S., and Karthikeyan, S.** (2012) Structures of ternary complexes of aspartate-semialdehyde dehydrogenase (Rv3708c) from *Mycobacterium tuberculosis* H37Rv. *Acta Cryst D* 68:671-679.
302. **Wagner-Dobler, I., and Biebl, H.** (2006) Environmental biology of the marine *Roseobacter* lineage. *Annu Rev Microbiol* 60:255-280.
303. **Walz, T., Hirai, T., Murata, K., Heymann, J.B., Mitsuoka, K., Fujiyoshi, Y., Smith, B.L., Agre, P., and Engel, A.** (1997) The three-dimensional structure of aquaporin-1. *Nature* 387:624-627.
304. **Wang, X.J., Zhang, N., Teng, Z.J., Wang, P., Zhang, W.P., Chen, X.L., Zhang, Y.Z., Chen, Y., Fu, H.H., and Li, C.Y.** (2021) Structural and mechanistic insights into dimethylsulfoxide formation through dimethylsulfide oxidation. *Front Microbiol* 12:735793.
305. **Warren, C.R.** (2013) Quaternary ammonium compounds can be abundant in some soils and are taken up as intact molecules by plants. *New Phytol* 198:476-485.
306. **Warren, C.R.** (2014) Response of osmolytes in soil to drying and rewetting. *Soil Biol Biochem* 70:22-32.
307. **Warren, C.R.** (2016) Do microbial osmolytes or extracellular depolymerisation products accumulate as soil dries? *Soil Biol Biochem* 98:54-63.
308. **Webb, B.A., Karl Compton, K., Castañeda Saldaña, R., Arapov, T.D., Keith Ray, W., Helm, R.F., and Scharf, B.E.** (2017) *Sinorhizobium meliloti* chemotaxis to quaternary ammonium compounds is mediated by the chemoreceptor McpX. *Mol Microbiol* 103:333-346.
309. **Wedeking, A., Hagen-Euteneuer, N., Gurgui, M., Broere, R., Lentzen, G., Tolba, R.H., Galinski, E., and van Echten-Deckert, G.** (2014) A lipid anchor improves the protective effect of ectoine in inflammation. *Curr Med Chem* 21:2565-2572.
310. **Weinbauer, M.G.** (2004) Ecology of prokaryotic viruses. *FEMS Microbiol Rev* 28:127-181.
311. **Weinisch, L., Kirchner, I., Grimm, M., Kühner, S., Pierik, A.J., Rossello-Mora, R., and Filker, S.** (2019) Glycine betaine and ectoine are the major compatible solutes used by four different halophilic heterotrophic Ciliates. *Microb Ecol* 77:317-331.
312. **Welsh, D.T.** (2000) Ecological significance of compatible solute accumulation by microorganisms: From single cells to global climate. *FEMS Microbiol Rev* 24:263-290.
313. **Whatmore, A.M., and Reed, R.H.** (1990) Determination of turgor pressure in *Bacillus subtilis*: A possible role for K+ in turgor regulation. *J Gen Microbiol* 136:2521-2526.
314. **Widderich, N., Bremer, E., and Smits, S.H.J.** (2016a) The ectoine hydroxylase: A nonheme-containing iron(II) and 2-oxoglutarate-dependent dioxygenase. *Encycl Inorg Bioinorg Chem*.
315. **Widderich, N., Hoeppner, A., Pittelkow, M., Heider, J., Smits, S.H., and Bremer, E.** (2014) Biochemical properties of ectoine hydroxylases from extremophiles and their wider taxonomic distribution among microorganisms. *PLoS One* 9:e93809.
316. **Widderich, N., Kobus, S., Hoeppner, A., Riclea, R., Seubert, A., Dickschat, J.S., Heider, J., Smits, S.H., and Bremer, E.** (2016b) Biochemistry and crystal structure of ectoine synthase: A metal-containing member of the cupin superfamily. *PLoS One* 11:e0151285.
317. **Widderich, N., Czech, L., Elling, F.J., Konneke, M., Stöveken, N., Pittelkow, M., Riclea, R., Dickschat, J.S., Heider, J., and Bremer, E.** (2016c) Strangers in the archaeal world: Osmostress-responsive biosynthesis of ectoine and hydroxyectoine by the marine thaumarchaeon *Nitrosopumilus maritimus*. *Environ Microbiol* 18:1227-1248.

318. **Widmer, R., and Stadtherr, R.** (1961) Post-planting weed control in garden chrysanthemums. *Weeds* 9:204-208.
319. **Wiggins, P.M.** (1990) Role of water in some biological processes. *Microbiol Rev* 54:432-449.
320. **Williams, B.T., Cowles, K., Bermejo Martinez, A., Curson, A.R.J., Zheng, Y., Liu, J., Newton-Payne, S., Hind, A.J., Li, C.Y., Rivera, P.P.L., Carrion, O., Liu, J., Spurgin, L.G., Brearley, C.A., Mackenzie, B.W., Pinchbeck, B.J., Peng, M., Pratscher, J., Zhang, X.H., Zhang, Y.Z., Murrell, J.C., and Todd, J.D.** (2019) Bacteria are important dimethylsulfoniopropionate producers in coastal sediments. *Nat Microbiol* 4:1815-1825.
321. **Williams, H.N., Lymperopoulou, D.S., Athar, R., Chauhan, A., Dickerson, T.L., Chen, H., Laws, E., Berhane, T.-K., Flowers, A.R., and Bradley, N.** (2016) *Halobacteriovorax,* an underestimated predator on bacteria: Potential impact relative to viruses on bacterial mortality. *ISME J* 10:491-499.
322. **Williams, T.J., Allen, M.A., DeMaere, M.Z., Kyrpides, N.C., Tringe, S.G., Woyke, T., and Cavicchioli, R.** (2014) Microbial ecology of an Antarctic hypersaline lake: Genomic assessment of ecophysiology among dominant haloarchaea. *ISME J* 8:1645-1658.
323. **Witt, E.M., Davies, N.W., and Galinski, E.A.** (2011) Unexpected property of ectoine synthase and its application for synthesis of the engineered compatible solute ADPC. *Appl Microbiol Biotechnol* 91:113-122.
324. **Wood, J.M.** (2011) Bacterial osmoregulation: A paradigm for the study of cellular homeostasis. *Annu Rev Microbiol* 65:215-238.
325. **Wu, R., Sanishvili, R., Belitsky, B.R., Juncosa, J.I., Le, H.V., Lehrer, H.J., Farley, M., Silverman, R.B., Petsko, G.A., Ringe, D., and Liu, D.** (2017) PLP and GABA trigger GabR-mediated transcription regulation in *Bacillus subtilis* via external aldimine formation. *Proc Natl Acad Sci USA* 114:3891-3896.
326. **Xu, J., and Johnson, R.C.** (1997) Cyclic AMP receptor protein functions as a repressor of the osmotically inducible promoter *proP* P1 in *Escherichia coli*. *J Bacteriol* 179:2410-2417.
327. **Yan, J., Nadell, C.D., Stone, H.A., Wingreen, N.S., and Bassler, B.L.** (2017) Extracellular-matrix-mediated osmotic pressure drives *Vibrio cholerae* biofilm expansion and cheater exclusion. *Nat Commun* 8:327.
328. **Yancey, P.H.** (2005) Organic osmolytes as compatible, metabolic and counteracting cytoprotectants in high osmolarity and other stresses. *J Exp Biol* 208:2819-2830.
329. **Yi, H., Lim, Y.W., and Chun, J.** (2007) Taxonomic evaluation of the genera *Ruegeria* and *Silicibacter*: A proposal to transfer the genus *Silicibacter* Petursdottir and Kristjansson 1999 to the genus *Ruegeria* Uchino *et al*. 1999. *Int J Syst Evol Microbiol* 57:815-819.
330. **Yokoyama, K., Ishijima, S.A., Clowney, L., Koike, H., Aramaki, H., Tanaka, C., Makino, K., and Suzuki, M.** (2006) Feast/famine regulatory proteins (FFRPs): *Escherichia coli* Lrp, AsnC and related archaeal transcription factors. *FEMS Microbiol Rev* 30:89-108.
331. **Young, K.D.** (2006) The selective value of bacterial shape. *Microbiol Mol Biol Rev* 70:660-703.
332. **Young, R.** (1992) Bacteriophage lysis: Mechanism and regulation. *Microbiol Rev* 56:430-481.
333. **Youssef, N.H., Savage-Ashlock, K.N., McCully, A.L., Luedtke, B., Shaw, E.I., Hoff, W.D., and Elshahed, M.S.** (2014) Trehalose/2-sulfotrehalose biosynthesis and glycine-betaine uptake are widely spread mechanisms for osmoadaptation in the *Halobacteriales*. *ISME J* 8:636-649.
334. **Yu, Q., Cai, H., Zhang, Y., He, Y., Chen, L., Merritt, J., Zhang, S., and Dong, Z.** (2017) Negative regulation of ectoine uptake and catabolism in *Sinorhizobium meliloti*: Characterization of the EhuR gene. *J Bacteriol* 199.
335. **Zaccai, G., Bagyan, I., Combet, J., Cuello, G.J., Deme, B., Fichou, Y., Gallat, F.X., Galvan Josa, V.M., von Gronau, S., Haertlein, M., Martel, A., Moulin, M., Neumann, M., Weik, M., and Oesterhelt, D.** (2016) Neutrons describe ectoine effects on water H-bonding and hydration around a soluble protein and a cell membrane. *Sci Rep* 6:31434.
336. **Zada, S., Zhou, H., Xie, J., Hu, Z., Ali, S., Sajjad, W., and Wang, H.** (2021) Bacterial degradation of pyrene: Biochemical reactions and mechanisms. *Int Biodeterior Biodegradation* 162:105233.

337. **Zhang, X.-X., and Rainey, P.B.** (2008) Dual involvement of CbrAB and NtrBC in the regulation of histidine utilization in *Pseudomonas fluorescens* SBW25. *Genetics* 178:185-195.
338. **Ziegler, C., Bremer, E., and Kramer, R.** (2010) The BCCT family of carriers: From physiology to crystal structure. *Mol Microbiol* 78:13-34.
339. **Zschiedrich, C.P., Keidel, V., and Szurmant, H.** (2016) Molecular mechanisms of two-component signal transduction. *J Mol Biol* 428:3752-3775.

10 Danksagung

Mein Dank gilt zuallererst dem Betreuer dieser Doktorarbeit, Prof. Erhard Bremer. Seinem hingebungsvollen, langjährigen Einsatz, auch über seine Emeritierung hinaus, habe ich sehr viel zu Verdanken. Nicht nur konnte er mich in dieser Zeit in den „mikrobiologischen Untergrund“ einführen, insbesondere sein Interesse an meinen Ideen, und deren konstruktive Bearbeitung waren mir eine Hilfe. Auch wusste ich, dass ich mich bei jeglichen „Problemos“ bei ihm melden konnte und man gemeinsam eine Lösung finden konnte.

Zudem möchte ich mich sehr bei Prof. Tobias Erb für die zeitweise Übernahme meiner Anstellung, die Kooperation zu BhcR und die Übernahme des Zweitgutachtens dieser Arbeit bedanken. Auch Prof. Uwe Maier und Prof. Ulrich Mösch bin ich für Ihren Einsatz als Prüfer dieser Dissertation zu großem Dank verpflichtet!

Mein Dank gilt auch meinen Kooperationspartnern in verschiedensten Projekten in den vergangenen Jahren. Gert Bange und Christoper-Nils Mais mit denen wir zusammen den Kern des Ectoin-Abbaus aufklären konnten, Francesca Severi und insbesondere Lennart Schada von Borzyskowski, die mich auf ihre Reise in den Bha-Pathway mitnahmen, Andreas Seubert für seine große Hilfe Ectoin-Metabolite zu detektieren, Sven-Andreas Freibert für seine Hilfe zur MST, Wieland Steinchen für seine fast schon unvorhergesehene Hilfe, Sander Smits für seine Docking-Experimente, und auch Pietro Giammarinaro sowie Elizaveta Krol für ihre Hilfsbereitschaft.

Sehr dankbar bin ich auch allen Bremerlingen! Tamara und Laura C als Vorbilder in verschiedensten Hinsichten, Bianca die mir wirklich geholfen hat auch mal auf die Bremse, bzw. die Kaffeemaschine zu drücken, Laura T, Christine, Doreen, Alex, Daniela, Svenja und Nelli, sowie Felix, der die Hinterbliebenen nochmal aufgemischt hat. Mein Dank gilt auch Annika Bamberger und Deborah Trummel, von deren Bachelorarbeiten auch ich viel lernen konnte. Jutta, die gute Seele der Arbeitsgruppe, mit der es immer eine Freude war, das Labor zu teilen. Jochen, mit dem ich auch sehr viel Freude hatte und mit dem man auch (oder grade auch) in den chaotischsten Situationen noch sehr viel Lachen konnte.

Meiner Familie, Mama, Papa, Oma, Hannah und allen die da noch zugehören, meinen Freunden in Marburg, Moischt und Westerwald, und vor allem Jette werde ich sowieso nicht genug danken können. Trotzdem:

Danke!